Value Addition of Unripe 'Nendran' Banana (*Musa* (AAB) cv. Nendran) and Exploration of its Phytoconstituents

by

Raveena Natakkakath Kaliyathan

Enrollment No:10BB18A39036

A thesis submitted to the

Academy of Scientific and Innovative Research

for the award of the degree of

DOCTOR OF PHILOSOPHY

in

SCIENCE

Under the supervision of

Dr. Reshma M V

CSIR – National Institute for Interdisciplinary Science and Technology (CSIR-NIIST)
Thiruvananthapuram-695 019

Academy of Scientific and Innovative Research
AcSIR Headquarters, CSIR-HRDC Campus
Sector 19, Kamla Nehru Nagar,
Ghaziabad, U.P. – 201 002, India

September - 2024

राष्ट्रीय अंतर्विषयी विज्ञान तथा प्रौद्योगिकी संस्थान
वैज्ञानिक तथा औद्योगिक अनुसंधान परिषद् | विज्ञान तथा प्रौद्योगिकी मंत्रालय, भारत सरकार
इंडस्ट्रियल इस्टेट पी.ओ., पाप्पनंकोड, तिरुवनंतपुरम, भारत-695 019

CSIR-NATIONAL INSTITUTE FOR INTERDISCIPLINARY SCIENCE AND TECHNOLOGY (CSIR-NIIST)
Council of Scientific & Industrial Research | Ministry of Science and Technology, Govt. of India
Industrial Estate P.O., Pappanamcode, Thiruvananthapuram, India-695 019

CERTIFICATE

This is to certify that the work incorporated in this Ph.D. thesis entitled, "**Value Addition of Unripe 'Nendran' Banana (*Musa* (AAB) cv. Nendran) and Exploration of its Phytoconstituents**", submitted by **Ms. Raveena Natakkakath Kaliyathan** to the Academy of Scientific and Innovative Research (AcSIR) in fulfillment of the requirements for the award of the Degree of **Doctor of Philosophy in Science**, embodies original research work carried out by the student. We certify that this work has not been submitted to any other University or Institution in part or whole for the award of any degree or diploma. Research materials obtained from different sources and used in this research work have been duly acknowledged in the thesis. Images, illustrations, figures, tables, etc., used in the thesis from other sources have also been duly cited and acknowledged.

10/09/2024

Raveena Natakkakath Kaliyathan

10/09/24

Dr. Reshma M V
(Supervisor)

Tel : 91 471 2515226 | 2515234 | E-mail : director@niist.res.in | Website : http://niist.res.in

STATEMENTS OF ACADEMIC INTEGRITY

I **Raveena Natakkakath Kaliyathan**, a Ph.D. student of the Academy of Scientific and Innovative Research (AcSIR) with Registration No. **I0BB18A39036** hereby undertake that the thesis entitled **"Value Addition of Unripe 'Nendran' Banana (*Musa* (AAB) cv. Nendran) and Exploration of its Phytoconstituents"** has been prepared by me and that the document reports original work carried out by me and is free of any plagiarism in compliance with the UGC Regulations on "Promotion of Academic Integrity and Prevention of Plagiarism in Higher Educational Institutions (2018)" and the CSIR Guidelines for "Ethics in Research and in Governance (2020)".

Raveena 10/09/2024

Raveena Natakkakath Kaliyathan

10/09/2024

Thiruvananthapuram

It is hereby certified that the work done by the student, under my supervision, is plagiarism free in accordance with the UGC Regulations on "*Promotion of Academic Integrity and Prevention of Plagiarism in Higher Educational Institutions* (2018)" and the CSIR guidelines for "*Ethics in Research and in Governance* (2020)".

10/09/2024

Dr. Reshma M V

10/09/2024

Thiruvananthapuram

ACKNOWLEDGEMENTS

In my life journey, one of the best decisions I have taken so far was choosing to pursue a Ph.D. The journey has been transformative, challenging, exciting, and inspirational in many ways. This journey has helped me to expand the boundaries of my knowledge, sharpen my critical thinking, improve my skills, and taught me that challenges are the fuelling force for victories. I am indebted to many people who stood with me in all the challenges and I would like to extend my sincere gratitude and appreciation to all those who made this Ph.D. thesis possible.

First and foremost, I would like to extend my sincere gratitude to my supervisor, ***Dr. Reshma M. V.****, for her guidance, advice, and unwavering support throughout my Ph.D. journey. From the beginning, she believed in my potential, inspiring me and encouraging me every step of the way. As a botany graduate, I was unfamiliar with many terms in food science, but ma'am introduced me to this fascinating field of food science and opened my eyes to the world of phytochemistry. Her passion for research and deep commitment to societal welfare have left a lasting impression on me. When I was pursuing my degree, I dreamed of conducting research that would be beneficial to society. That dream became a reality through the development and technology transfer of 'banana grit' during my thesis work—an achievement made possible by her dedication to societal impact. Ma'am provided unwavering personal care and support. Words cannot fully express the depth of my gratitude and love for her. She is truly a gem of a person; I could not have imagined having a better advisor and mentor in my life.*

I heartfully acknowledge and extend my heartfelt thanks to ***Dr. Ravi Shankar L****., (DAC member), for his unconditional support and guidance for the phytochemical isolation studies. In fact, the isolation of bioactive molecules from the starchy matrix of bananas was really a tough job, and I have experienced so many challenges and failures during the study. But sir gave me the motivation and support to continue the work and he generously devoted his valuable time for the structure elucidation of the isolated compounds. During the journey, we could isolate 'glucocerebrosides', which was the first report of that molecule from the Musa species, thrilling and unforgettable days in my Ph.D. I took this opportunity to thank Dr. Ravi*

Shankar L. for his constant support, guidance, and patience throughout my thesis and for inspiring me to do more.

I sincerely thank ***Dr. C. Anandharamakrishnan*** *and* ***Dr. A. Ajayaghosh****, present and former Director of the CSIR-National Institute for Interdisciplinary Science and Technology, Thiruvananthapuram, for providing me with the necessary facilities for carrying out the work.*

I am grateful to ***Dr. P. Jayamurthy, Dr. V. Karunakaran, Dr. C. H. Suresh****, and* ***Dr. R. Luxmi Varma****, present and former AcSIR coordinators for all their help in the timely completion of the course-works and other AcSIR requirements.*

My sincere thanks to ***Sri V. V. Venugopalan****, and* ***Dr. K. G. Raghu****, present and former Head of the Agro-processing and Technology Division (APTD), for allowing me to use the facilities available in the department.*

I am extremely grateful to my Doctoral Advisory Committee members (DAC) ***Dr. Priya S., Dr. Ravi Shankar L., Dr. Vasanth Raghavan K.****, and* ***Dr. Dileep Kumar B S*** *(former DAC Member) for their timely suggestions, insights, and discussions during the DAC meetings, which greatly helped to improve my thesis work. Special thanks to Dr. Priya for her guidance in the cell culture studies.*

I take this opportunity to thank ***Dr. Rajkumar G****. (Head, Plant Systematics and Evolutionary Science Division, JNTBGRI, Palode) for the authentication of samples and for helping me with herbarium deposition. I am also indebted to team '****Madras Diabetes Research Foundation (MDRF)****' for conducting the clinical GI-GL studies.*

I am thankful to all the ***scientists*** *and* ***technical staff*** *at APTD for all their support. I owe a huge depth of gratitude to all my teachers who paved the passion for research in my mind with their knowledge and guidance. I want to extend my gratitude towards* ***Mr. Pratheesh*** *and* ***Mr. Sreejith****, the technical staff of APTD, for their support and help during the pilot plant operation, administrative works, and bulk preparation of samples for the studies.*

My sincere thanks to all the staff members in the administration, IT lab, KRC, canteen, HLS, security, and the scientists at CSIR-NIIST for their cooperation and support. I thank Mr. Merin Santhosh and Ms. Aswathy at the AcSIR office for their humble nature and for helping with the academic documentation.

I also take this opportunity to thank my friends, especially present and former members of team RMV and RSL for all the help received. Special thanks to ***Nagaraja Ingaladal*** *and* ***Sornarani Rajan*** *for their immense support during the phytochemical exploration studies. I express my sincere thanks to* ***Anjali Krishna T U, Parveen Aysha, Akshaya****, and* ***Shagana****, who were with me during the initial phase of the journey and helped me in setting up the lab. Further, I would like to thank my friends* ***Athira A.S., Gopika Biju, Diya Mallick, Gopika G., Haritha,*** *and* ***Anjali*** *for their friendship, special care, helping hands, and for creating a wonderful lab atmosphere. Special thanks to* ***Adarsh P, Dr. Jesmina, Nandhu Lal, Anusha, Anagha Nair, Dr. Taniya, Dr. Veena, Dr. Arun, Abhi, Krishna Kumar, Harikrishnan, Anoop, Lijoy, Roopasree,*** *and* ***Anirudh*** *for their supporting hands, friendship and invaluable help always extended. Thank you,* ***Theertha Anilkumar*** *and* ***Arya****, for always being there for me, 'my home away from the home'. A heartfelt thanks to* ***Sheela Aunty*** *and her family for providing a happy and safe stay in their house.*

*I am also indebted to the Council of Scientific and Industrial Research (****CSIR)****, New Delhi, India for financial assistance in the form of the research fellowship (JRF & SRF) and the Academy of Scientific and Innovative Research (****AcSIR****), India, is duly acknowledged for enrolling me in their Ph.D. program and the reviewers for their time, patience, and invaluable insights in reviewing my thesis.*

Last but certainly not least, I owe my deepest gratitude to my family for their unwavering support and understanding of my goals and aspirations. Your love and encouragement have always been my greatest strength. Even though we have faced some of the most challenging days together, the way you have overcome everything continues to inspire me every day. I want to take this opportunity to thank my beloved parents, ***Nandanan P.*** *and* ***Rathnavalli N. K****., who have been my pillars of strength, my first teachers, my inspiration, and my role models. Without their patience, sacrifices, faith in my potential, and endless love, I would not have been able to accomplish all that I have or become the person I am today. I also extend my heartfelt thanks to my sister****, Naveena N. K.****, and my brother-in-law,* ***Vipin P****., for always standing by me, encouraging me to follow my dreams, and managing everything in my absence. Special thanks to my dear nieces,* ***Aishwarya*** *and* ***Anelkka****, for being a constant source of joy and happiness in my life. I also take this opportunity to thank* ***Dr. Sreejith Padmanabhan****, spine surgeon,*

Yenepoya Spinal Clinic, Mangalore, for giving me a new life, without his care, I wouldn't be where I am today.

Finally, I thank ***God almighty*** *for guiding me through every step of this incredible journey. Living with sixteen screws and two titanium rods in my spine has not been easy, but his grace and strength sustained me through the challenges, kept me focused on my goal and helped me to reach this important milestone in my academic life.*

Mother Nature, I am humbled before your miracles!

Once again, thank you everyone!

Thiruvananthapuram **Raveena Natakkakath Kaliyathan**

Dedicated to my parents, my pillars of strength.

"No one has ever inspired and supported me the way you have!"

CONTENTS

ABBREVIATIONS

%	Percentage
$[2M+Na]^+$	[2Molecular ion +Na]$^+$
$[M + H]^+$	[Molecular ion + H]$^+$
$[M + Na]^+$	[Molecular ion + Na]$^+$
$[M\text{-glucose-OH}]^+$	[Molecular ion-glucose-OH]$^+$
$[M\text{-OH}]^+$	[Molecular ion-OH]$^+$
°	Degree
°C	Degree Celsius
µg	Microgram
µg/mL	Microgram per milliliter
µL	Microliter
µm	Micrometer
µM	Micromolar
^{13}C NMR	Carbon NMR
1D	One dimensional
^{1}H NMR	Proton NMR
2D	Two-dimensional NMR
^{31}P	Phosphorous NMR
3D	Three-dimensional
AACC	American Association of Cereal Chemists
ACN	Acetonitrile
Al	Aluminum
ALA	Alpha-linolenic acid
AMG	Amyloglucosidase
AMT	Acetonitrile:methanol:tetrahydrofuran
ANOVA	Analysis of variance
AOAC	Association of Official Analytical Collaboration
APEDA	Agricultural and Processed Food Products Export Development Authority
As	Arsenic

ASG	Acyl steryl glycosides
ASP	Aspartic acid
ASPNET	Asia and Pacific Network
ATP	Adenosine-5'-triphosphate
AUC	Area under the curve
B	Boron
Ba	Barium
BAPNET	Banana Asia and Pacific Network
BCA	Bicinchoninic acid
BG	Banana grit
BG-CHL	BG chloroform extract
Bi	Bismuth
BMI	Body mass index
BOPP	Biaxially oriented polypropylene
BP-CHL-GC-1	Banana peel-chloroform extract-glucocerebroside-1
BP-CHL-GC-2	Banana peel-chloroform extract-glucocerebroside-2
BP-GC-TT-15-18	Banana peel-glucocerebroside-test tube-5-18
BP-GC-TT-19-23	Banana peel-glucocerebroside-test tube-19-23
BP-GC-TT-24-26	Banana peel-glucocerebroside-test tube-24-26
BPM	Banana peel methanol extract
BP-MeOH-GC-1	Banana peel-methanol extract-glucocerebroside-1
BP-MeOH-GC-2	Banana peel-methanol extract-glucocerebroside-2
BRS	Banana Research Station
BSA	Bovine serum albumin
BUP	Boiled unripe plantain
BUPC	Boiled unripe plantain crisps
C	Carbon
C_∞	Maximum hydrolysis extent
Ca	Calcium
CAS No.	Chemical Abstracts Service Number
CCK	Cholecystokinin
CD	Crohn's disease
Cd	Cadmium

CD_3OD	Deuterated methanol
$CDCl_3$	Deuterated chloroform
CFU	Colony-forming units
$CHCl_3$	Chloroform
CIAT	International Center for Tropical Agriculture
CIRAD	Centre de Coopération Internationale en Recherche Agronomique pour le Développement
CISH	Central Institute for Subtropical Horticulture
cm	Centimeter
CM	Chloroform-methanol
Co	Cobalt
COSY	Correlation spectroscopy
COX-2	Cyclooxygenase-2
Cr	Chromium
Cs	Cesium
CSIR	Council of Scientific and Industrial Research
CTRI	Clinical Trials Registry India
Cu	Copper
CVD	Cardiovascular disease
d	Doublet
DAD	Diode Array Detector
dd	Double doublet
DEPT	Distortionless enhancement by polarization transfer
DG	Director General
DGDG	Digalactosyldiacylglycerol
DMEM	Dulbecco's Modified Eagle Medium
DMSO	Dimethyl sulfoxide
DP	Degree of polymerization
dw	Dry weight
E. coli	*Escherichia coli*
EC_{50}	Free-radical scavenging activity
eGI	Estimated glycaemic index
ELISA	Enzyme-linked immunosorbent assay

EtOAc	Ethyl acetate
F-6-P	Fructose-6-phosphate
FAO	Food and Agriculture Organization
FBS	Fetal bovine serum
Fe	Iron
FFAR2	Free fatty acid receptors 2
FFAR3	Free fatty acid receptors 3
FG	Free glucose
FOS	Fructooligosaccharides
fw	Fresh weight
FYM	Farmyard manure
g	Gram
g/L	Gram per liter
G_{120}	Glucose released at 120 minutes
G_{20}	Glucose released at 20 minutes
G-6-P	Glucose-6-phosphate
G6P-DH	Glucose-6-phosphate dehydrogenase
Ga	Gallium
GALT	Gut-associated lymphoid tissue
GC	Glucocerebroside
GC-MS	Gas chromatography- mass spectrometry
GIFSA	Glycemic Index Foundation of South Africa
GI-GL	Glycemic index and glycemic load
GIP	Gastric inhibitory polypeptide
GLP-1	Glucagon-like peptide 1
GLUT2	Glucose transporter 2
GOD-POD	Glucose oxidase-peroxidase
GOS	Galactooligosaccharides
GPCRs	G protein coupled receptors
H	Hydrogen
H_2SO_4	Sulphuric acid
H_{90}	Percentage of starch hydrolysis at 90 minutes
HbA1c	Glycated hemoglobin

HCl	Hydrochloric acid
HCT-116	Human colorectal carcinoma cell line
HI	Hydrolysis index
HIV	Human immunodeficiency virus
HK	Hexokinase
HMBC	Heteronuclear multiple bond correlation
Hon.	Honourable
HPLC	High-performance liquid chromatography
HPLC-ESI-QTOF-MS/MS	High-performance liquid chromatography coupled with electrospray ionization-quadrupole-time of flight-mass spectrometry
HR-ESI-MS	High-Resolution Electrospray Ionization Mass Spectrometry
HSQC	Heteronuclear single quantum coherence
HT-29	Human colon adenocarcinoma cell line
Hz	Hertz
IBD	Inflammatory bowel disease
IC_{50}	Half-maximal inhibitory concentration
ICAR-NRCB	Indian Council of Agricultural Research-National Research Centre for Banana
ICP-MS	Inductively coupled plasma mass spectrometry
IFN-γ	Interferon-gamma
IgE	Immunoglobulin E
IgG/HRP	Immunoglobulin G conjugated with horseradish peroxidase enzyme
IIHR	Indian Institute of Horticultural Research
IITA	International Institute of Tropical Agriculture
IL-10	Interleukin 10
IL-13	Interleukin-13
IL-1α	Interleukin-1alpha
IL-1β	Interleukin-1beta
IL-6	Interleukin-6
In	Indium
INIBAP	International Network for the Improvement of Banana and Plantain
iNOS	Inducible nitric oxide synthase
ISO	International Organization for Standardization

J	Coupling constant
Jak1/Tyk2	Janus kinases/tyrosine kinase 2
K	Potassium
k	Kinetic constant
K-ACHDF	Available carbohydrates assay kit
K-DSTRS	Digestible and resistant starch assay kit
K-FRU	Fructan assay kit
K-FRUHK	Fructan HK kit
kg	Kilogram
Kg/m^2	Kilogram per square meter
kHz	Kilohertz
K-TDFR	Total dietary fiber assay kit
L	Liter
LDL	Low-density lipoprotein
LDPE	Low-density polyethylene
Li	Lithium
LMICs	Low- and middle-income countries
LPS	Lipopolysaccharide
m	Multiplet
M	Molar
m/z	Mass-to-charge ratio
MAP	Modified atmosphere packaging
MCF-7 cell line	Michigan Cancer Foundation-7 cell line
MCP-1	Monocyte chemoattractant protein-1
MDA-MB-231 cell line	M.D. Anderson-Metastasis Breast cancer-231 cell line
MDRF	Madras Diabetes Research Foundation
MeOH	Methanol
MES	2-(N-morpholino)ethanesulfonic acid
Mg	Magnesium
mg	Milligram
mg GAE/g	Milligram gallic acid equivalent per gram
mg QE/g	Milligram quercetin equivalent per gram
mg/mL	Milligram per milliliter

MGA	Maltase-glucoamylase
MGDG	Monogalactosyldiacylglycerol
MHz	Megahertz
mL	Milliliter
Mm	Micromolar
mmol/L	Millimoles per liter
Mn	Manganese
mRNA	Messenger ribonucleic acid
MS	Mass spectrometry
MS/MS	Tandem mass spectrometry
mTorr	Millitorr
MTT	3-(4,5-dimethylthiazol-2-yl)-2,5-diphenyl tetrazolium bromide
Na^+/K^+-ATPase	Sodium-potassium adenosine triphosphatase
Na_2CO_3	Sodium carbonate
Na_2SO_4	Sodium sulfate
$NADP^+$	Nicotinamide-adenine dinucleotide phosphate
NADPH	Nicotinamide-adenine dinucleotide phosphate hydrogen
$NaHCO_3$	Sodium bicarbonate
$NaNO_2$	Sodium nitrite
NCCS	National Centre for Cell Science
NF-κB	Nuclear factor-kappa B
NH	Amide
NHB	National horticulture board
Ni	Nickel
NIIST	National Institute of Interdisciplinary Science and Technology
NKT cells	Natural killer T cells
nm	Nanometer
NMR	Nuclear magnetic resonance
NO	Nitric oxide
NPK	Nitrogen-phosphorous-potassium
OD	Optical density
OD/mg	Optical density per milligram
OH	Hydroxy

PAA/AMG	α-amylase and amyloglucosidase
PAHBAH	P-hydroxybenzoic acid hydrazide
Pb	Lead
PBS	Phosphate buffered saline
PDA	Photo Diode Array
PET	Polyester
PGI	Phosphoglucose isomerase
PGPR	Plant Growth Promoting Rhizobacteria
pH	Potential of hydrogen
PIC	Protease inhibitor cocktail
pNPG	*p*-nitrophenyl-α-D-glucopyranoside
PPARγ	Peroxisome proliferator-activated receptor gamma
ppm	Parts per million
Pvt. Ltd.	Private Limited
PYY	Peptide YY
QuEChERS	Quick, easy, cheap, effective, rugged, and safe
R^2	Coefficient of determination
RAW 264.7 cell line	Ralph, rAschke, Watson 264.7 cell line
Rb	Rubidium
RDS	Rapidly digestible starch
Rf	Retention factor
RIPA	Radioimmunoprecipitation assay
rpm	Revolutions per minute
RRP	Ripe raw plantain
RS	Resistant starch
RTC	Ready-to-cook
RTE	Ready-to-eat
RTR	Ready-to-reconstitute
s	Singlet
SCFA	Short chain fatty acids
SCORAD	Scoring Atopic Dermatitis
SD	Standard deviation
SDS	Slowly digestible starch

Se	Selenium
SEM	Standard error of the mean
SGLT1	Sodium-dependent glucose transporter
sn	Unimolecular nucleophilic substitution
SPME	Solid-Phase Microextraction
SPSS	Statistical Package for the Social Sciences
Sr	Strontium
SR-B1	Scavenger receptor class B1
STAT3	Signal transducer and activator of transcription 3
TBGT	Herbarium of Jawaharlal Nehru Tropical Botanic Garden and Research Institute
TBRI	Taiwan Banana Research Institute
TCC	Total carotenoid content
TDF	Total dietary fiber
TDS	Total digestible starch
TFC	Total flavonoid content
TG	Total glucose portion
Th1	Type 1 helper
THF	Tetrahydrofuran
Ti	Titanium
TLC	Thin-layer chromatography
TLR4	Toll-like receptor 4
TMB	3,3′,5,5′-Tetramethylbenzidine
TNAU	Tamil Nadu Agricultural University
TNF-α	Tumour necrosis factor-alpha
TPC	Total phenol content
TRIS	Tris(hydroxymethyl)aminomethane
TS	Total starch
U	Units
U/mL	Units per milliliter
UC	Ulcerative colitis
UN	United Nations
USA	United States of America

UV-VIS	Ultraviolet-visible
V	Vanadium
v/v	Volume/volume
VFPCK	Vegetable and Fruit Promotion Council Keralam
wb	Wet basis
WHO	World Health Organization
Zn	Zinc
α	Alpha
α-amylase	Alpha-amylase
α-carotene	Alpha-carotene
α-cryptoxanthin	Alpha-cryptoxanthin
α-glucosidase	Alpha-glucosidase
α-linolenic acid	Alpha-linolenic acid
β-amylase	Beta-amylase
β-carotene	Beta-carotene
β-cryptoxanthin	Beta-cryptoxanthin
β-glycoside	Beta-glycoside
β-sitosterol	Beta-sitosterol
δ	Chemical shifts
μL	Microliter
ω	Omega

LIST OF TABLES

LIST OF FIGURES

LIST OF SCHEMES

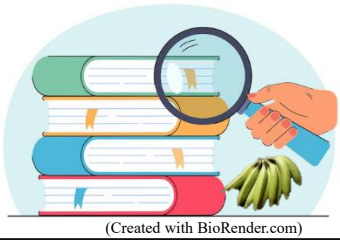

Chapter 1

Introduction and Review of Literature

1.1. Introduction

Banana, belonging to the genus *Musa* of the Musaceae family, is an important crop cultivated in over 130 countries, primarily in tropical and subtropical regions. Bananas are the fifth most important global crop in economic value, following coffee, cereals, sugar, and cacao (Pereira & Maraschin, 2015; B. Singh et al., 2016). India is the largest producer of bananas globally, followed by China, Brazil, Ecuador, Philippines, Indonesia, Costa Rica, Mexico, Thailand, and Colombia (*APEDA, 2022*, n.d.). The international banana trade, valued at over US$45 billion, significantly impacts the economies of many countries. In 2023, global banana exports reached around 19.20 million tonnes, with India leading in banana production (*FAOSTAT*, n.d.).

Bananas are thought to have first appeared around 10,000 years ago in South-East Asia and are thought to have first cultivated around 8,000 B.C. in the Kuk Valley of New Guinea. From there, it migrated across the South Pacific and Southeast Asia, eventually reaching the Philippines and spreading out in all directions throughout the tropical regions (Denham et al., 2003). Within the first two millennia following their domestication, bananas were brought to Australia, Indonesia, India, and Malaysia by traders and travellers. According to Buddhist scriptures, traders traveling through the Malaysian region tasted bananas and brought them to India. According to literature, edible bananas are believed to have evolved from wild species through parthenocarpy and seed suppression. These hybrids can be diploid, triploid, or tetraploid, and possess A and B genomes. The A-genome originated from *Musa acuminata* (AA), while the B-genome came from *Musa balbisiana* (BB) (Osuji et al., 1997). Human intervention resulted in the creation of hybrids between *M. acuminate* and *M. balbisiana* (Lejju et al., 2006). Currently, more than 1000 varieties of bananas with different ploidy are cultivated around the globe and the plant morphology, fruit size and taste, and insect and disease resistance vary with cultivar (Pereira & Maraschin, 2015). The *Musa* subgroups Sucrier (AA), Adukkan (AB), Poomkali (AB), Njalipoovan (AB) and Ney Poovan (AB) are the popular diploid varieties. Cavendish (AAA), Red banana (AAA), Robusta (AAA), Mysore (AAB), Poovan (AAB), Nendran (AAB), Plantain (AAB), Terra (AAB), Figo (ABB), Peyan (ABB), Pisang Awak (ABB), Karpooravalli (ABB), and Saba (BBB) are some of the popular triploid

cultivars. Champa Nasik (AAAA) and Goldfinger (AAAB) are the tetraploid varieties of banana cultivated (Pereira & Maraschin, 2015). Bananas are predominantly produced in Asia, Latin America, and Africa. Banana cultivars are of main two types: dessert type and cooking type (plantain), and some cultivars are of dual purpose (*FAO-Banana Facts*, n.d.).

Bananas are one of the most widely produced, traded, and consumed fruits globally. With over 1,000 varieties, bananas provide essential nutrients to people all over the globe. The Cavendish variety with an estimated annual yield of 50 million tonnes accounts for half of the global banana production and is the most commercially traded variety also. In many of the developing, low-income countries bananas are of great significance by serving as a staple food for households and a cash crop for income generation. Additionally, Bananas with year-round fruiting, bridge the 'hunger gap' between harvests, contributing significantly to food and income security in developing countries (*FAO-Banana Facts*, n.d.). In Africa, they provide over 25% of carbohydrate needs for more than 70 million people, with the world's highest per capita consumption at over 250 kg (Talengera, 2007). The ripe bananas are widely consumed and also used for the preparation of value-added products like jam, jelly, purees, wine, cake, yogurt, beverages, etc.

On dry weight (dw) basis, the pulp of unripe bananas contains up to 70-80% starch. Due to the high starch content unripe bananas are primarily used for producing banana flour and also for the preparation of bread, pasta, and cookies as a substitute for wheat flour (Bezerra et al., 2013; da Mota et al., 2000; Fida et al., 2020; Giraldo-Gómez et al., 2019; Khoza et al., 2021; Kumar et al., 2019; Nimsung et al., 2007; Suntharalingam & Ravindran, 1993). At the green stage, bananas are distinguished by their elevated resistant starch (RS) content. RS gets fermented in the large intestine by gut microbiota, and serves as a substrate for probiotic bacteria growth, making it a recognized prebiotic food. Additionally, RS exhibits low postprandial glycemic response, hypocholesterolemic effects, and aids in mineral absorption (Lockyer & Nugent, 2017). In addition to the nutritional benefits, banana is a rich source of phytochemicals including phenolics, flavonoids, anthocyanins, carotenoids, sterols and triterpenes, steryl glycosides, diarylheptanoids, phytoalexins, indoles, and biogenic amines which were of great therapeutic relevance. The phytochemicals associated with bananas are attributed with a broad range of pharmacological benefits such as anti-diabetic, antioxidant, anti-inflammatory, anti-microbial, and anthelminthic (Afzal et al., 2022, 2022; Lopes et al., 2020; Pereira & Maraschin, 2015; B. Singh et al., 2016). Moreover, bananas boast a rich mineral profile, including potassium, magnesium, phosphorus, sodium, iron, calcium, and

manganese (B. Singh et al., 2016). Further, the presence of a notable amount of dietary fiber makes bananas a good prebiotic source (Anyasi et al., 2013).

Despite the nutritional richness, unripe banana is an underutilized matrix. Beyond traditional weaning foods, there are no novel products derived from unripe bananas with innovative applications in the market. The 'Nendran' banana variety (*Musa* (AAB) cv. Nendran), widely cultivated in South India, holds popularity for its versatile uses. In its unripe state, 'Nendran' bananas are commonly utilized in culinary practices and for preparing banana chips. Understanding the potential and current scenario of underutilization, this thesis aims to spotlight the potential of unripe banana pulp as a novel alternative to traditional cereal-based diets. With a focus on gut health and general well-being, we aim for the extensive characterization of its bioactive compounds, nutrient evaluation, studies on process-induced changes in the RS content, and quantification of its bioactive carbohydrates.

Banana peel, the primary waste product generated by banana processing industries, also holds untapped potential. The UN 2030 agenda for sustainable development calls for actions focused on eliminating waste and maximizing food resources. In line with this, the thesis also explores the potent bioactive compounds in banana peel and its value addition potential.

1.2. Review of Literature

1.2.1. Banana cultivation and production statistics

Bananas are fast-growing, monocotyledonous herbaceous plants that can reach heights of up to 15 meters. After planting, the crop can be harvested within 12 to 15 months, and September to April is the main harvesting season. The bunches mature within 90 to 150 days after flowering, depending on the variety, soil quality, weather conditions, and elevation (*NHB-BANANA*, n.d.). A temperature range of 15 ºC to 35 ºC and a relative humidity of 75-85% are ideal for banana growth. Temperatures below 12 ºC can cause chilling injury, and wind speeds exceeding 80 km/hour can damage the crop. They can be grown from sea level to an elevation of 2000 meters above mean sea level. At higher altitudes, a few varieties such as the 'Hill banana' are only cultivated. Bananas grow best in soil with a pH between 6.5 and 7.5, adequate fertility and moisture. Soil with a calcareous nature and salinity is unsuitable for banana cultivation (*NHB-BANANA*, n.d.).

In 2020, the global production of bananas and plantains reached 155.2 million tonnes from 8.72 million hectares. With 33.06 million tonnes produced over 9.24 lakh hectares, India

accounts for 19.37% of global banana production and stands as the largest producer of bananas in the world (*APEDA, 2022*, n.d.). India and China together contributed to 28% of the global production. (Bonavita, n.d.). Apart from India, the major banana-producing countries are China, Brazil, Philippines, Ecuador, Indonesia, Mexico, Guatemala, and Colombia. In the list, Indonesia and Guatemala recorded the highest productivity at nearly 50 tonnes per hectare. The Asian region, led by India, Indonesia, China, and the Philippines, boasts the highest area, production, and productivity, contributing over 60% of global banana production (*Banana Market Review*, n.d.; Bonavita, n.d.).

For the last one decade, India has been the largest producer of bananas in the world. After the 1990s, due to the expansion of the area under cultivation and through the adoption of scientific practices, India showed a significant increase in banana production (*APEDA, 2022*, n.d.; *NHB-BANANA*, n.d.; Bonavita, n.d.). India accounts for 0.3% of the global banana export market, ranking as the 21st largest exporter. The country's banana exports are valued at approximately US$ 90 million, with an export volume of 1,81,000 tonnes (*APEDA, 2022*, n.d.; Bonavita, n.d.).

In India, bananas are cultivated mainly in the states of Andhra Pradesh, Tamil Nadu, Maharashtra, Gujarat, Karnataka, Uttar Pradesh, Kerala, Madhya Pradesh, Bihar, West Bengal, Assam, and Odisha. The northeastern states are biodiversity hotspots of bananas (*Horticulture :: Fruits :: Banana*, n.d.; *NHB-BANANA*, n.d.). Important cultivars in India include Red banana, Grand Naine, Robusta, Nyali, Karpurvalli, Safed Velchi, Rasthali, Nendran, Monthan, Karthali, Poovan, Basrai, Ardhapuri, and Dwarf Cavendish etc. (*NHB-BANANA*, n.d.). The major banana-producing belts and the important varieties of bananas cultivated in India are listed in Table 1.1.

Table 1.1. Major banana-producing belts and varieties cultivated in India (Source: NHB, http://nhb.gov.in/report_files/banana/BANANA.htm)

States	Growing belt	Varieties
Andhra Pradesh	East Godavari, West Godavari,Kurnool, Cuddapah	Thellachakrakeli, Karpoora Poovan, Robusta, Rasthali, Amritpant, Dwarf Cavendish, Chakrakeli, Monthan, and Yenagu Bontha
Assam	Goalpara, Nagaon, Sonitpur, foothills of Garo hills	Chini Champa, Malbhog, Borjahaji (Robusta), Honda, Manjahaji, Chinia (Manohar), Kanchkol, Bhimkol, Jatikol, Digjowa, Kulpait, Bharat Moni, Jahaji (Dwarf Cavendish)
Gujarat	Surat, Vadodara, Anand, Kheda, Junagadh, Narmada, Bharuch	Dwarf Cavendish, Lacatan, Harichal (Lokhandi), Gandevi Selection, Basrai, Robusta, G-9, Harichal, Shrimati
Jharkhand	Ranchi, Sahebganj	Basrai, Singapuri
Karnataka	Bangalore, Chitradurga, Shioroga, Hassan, Chikka Mangloor	Dwarf Cavendish, Robusta, Rasthali, Poovan, Monthan, Elakkibale
Kerala	Thiruvananthapuram, Kollam, Pathanamthitta, Alappuzha, Kottayam, Idukki, Ernakulam, Malappuram, Thrissur, Kozhikode, Wayanad, Kannur, Palakkad, Kasargod	Nendran, Palayankodan (Poovan), Rasthali, Monthan, Red Banana, Robusta
Madhya Pradesh	Khargaon, Badwani, Dhar, Khandwa	Basrai
Maharashtra	Jalgaon, Ahmednagar, Buldhana, Pune, Wardha, Dhule, Nanded, Parbani, Nandurbar, Satara, Sangli, Osmanabad, Buldhana, Akola, Yeothmal, Amravati, Thane, Kulara, Alibag	Dwarf Cavendish, Basrai, Robusta, Lal Velchi, Safed Velchi, Rajeli Nendran, Grand Naine, Shreemanti, Red Banana
Orissa	Ganjam, Puri, Khurda, Gajpati, Cuttack, Dhenkanal, Angul, Sundargarh, Sambalpur, Bargarh, Deogarh, Koraput, Keonjhar, Raygada, Mayurbhanj	Dwarf Cavendish, Robusta, Champa, Patkapura (Rasthali)
Tamil Nadu	Thoothukudi, Tiruchirapalli, Coimbatore, Tirunelveli, Karur, Erode, Kanniyakumari	Virupakshi, Robusta, Red Banana, Poovan, Rasthali, Nendran, Monthan, Karpuravalli, Sakkai, Peyan, Matti
West Bengal	Hooghly, Nadia, North 24 Parganas	Champa, Mortman, Dwarf Cavendish, Giant Governor, Kanthali, Singapuri

Andhra Pradesh (17.64%), Maharashtra (12.77%), Gujarat (11.81%), Tamil Nadu (11.78%), and Uttar Pradesh (10.24%) are the top banana-producing states in India (Fig 1.1.) and Kerala stands in the 11th position. In Kerala and Tamil Nadu, more than 15 varieties of banana are grown commercially whereas the monoclonal cultivation of Grand Naine is common in states like Gujarat and Maharashtra (*APEDA, 2022*, n.d.).

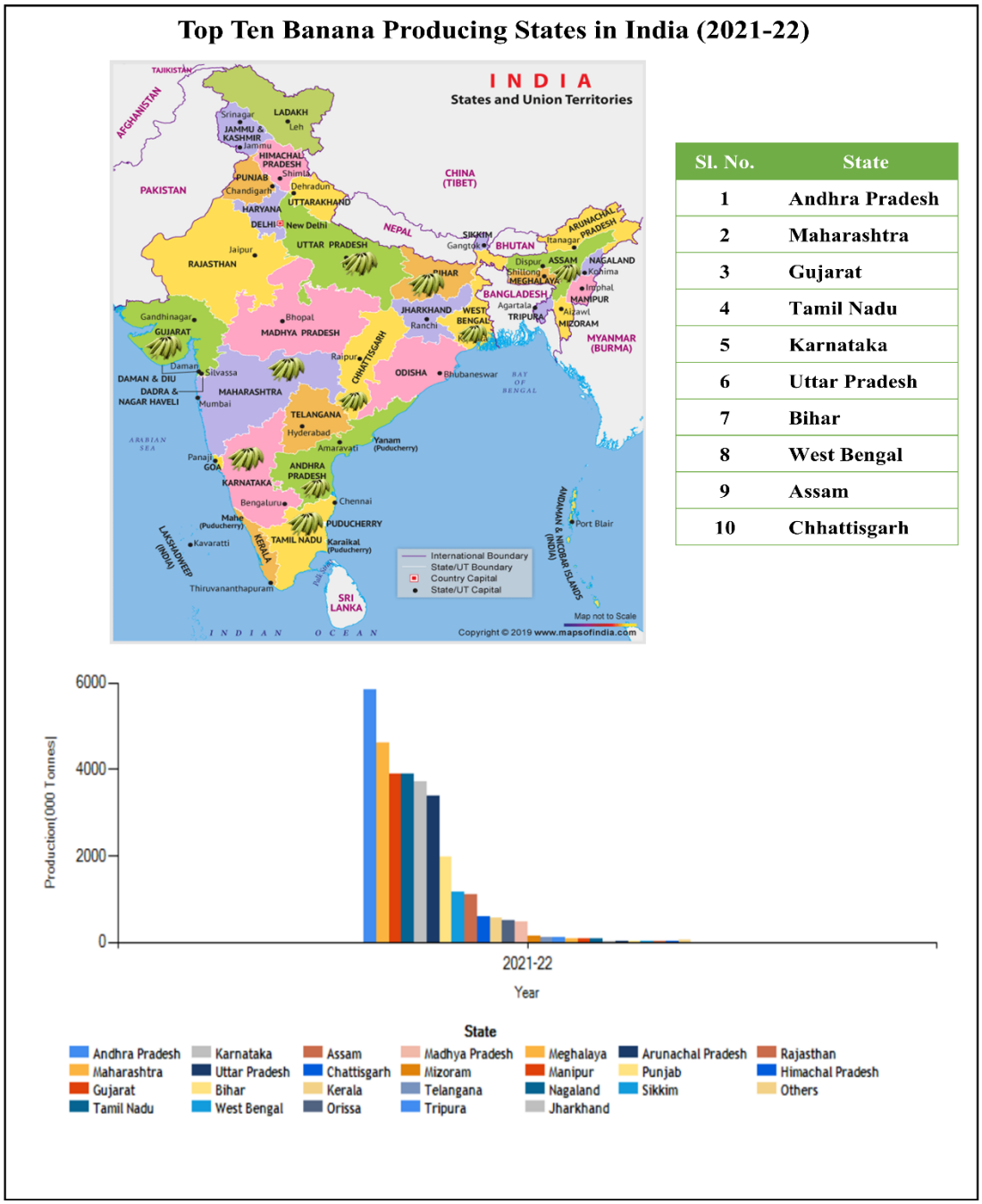

Fig. 1.1. Top ten banana-producing states in India (Source: APEDA, https://agriexchange.apeda.gov.in/India%20Production/India_Productions.aspx?cat=fruit&hscode=1042)

According to the Department of Economics and Statistics, Govt. of Kerala, in the year 2019-20, the area under banana cultivation in Kerala was 60678 hectares with a production of 548425 tonnes. Wayanad, Palakkad, and Malappuram were the top three banana-producing districts in Kerala (DES,Government of Kerala, n.d.). Banana varieties commonly cultivated in Kerala include Nendran, Kannankaya, Chingampazhati, Kappa, Rasakadali, Malayannan, and Robusta (Fig. 1.2.).

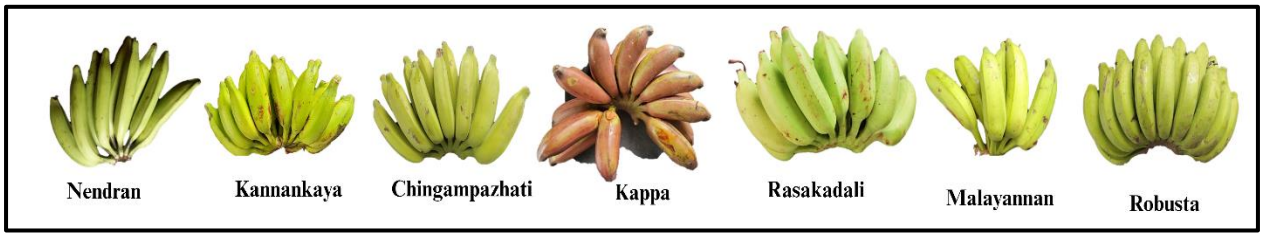

Fig. 1.2. Banana varieties cultivated in Kerala

1.2.2. Significance of banana-postharvest use of pulp and peel

Studies demonstrate that bananas are the storehouse of numerous bioactive components with health benefits and the physicochemical and phytochemical makeup of different banana types varies significantly. Bananas are rich sources of starch, fibers, and important phytonutrients, including vitamins and phenolic compounds. Additionally, it has a notable mineral composition comprising iron, copper, zinc, manganese, sodium, potassium, calcium, phosphorus, and magnesium (Forster et al., 2003; Lim et al., 2007). Studies also prove that banana fruit is a good source of vitamin C, vitamin A, vitamin E, thiamine, and riboflavin (Nadeeshani et al., 2021; Wall, 2006). The chemical and nutrient composition of ripe banana fruits of eight selected banana varieties of Kerala was studied by Siji & Nandini (2017). They found the Nendran variety has the highest carbohydrate content (41.33 g/100g), while Poovan has the highest protein content (1.37 g/100g). Mineral content in banana varieties ranges from 0.17g to 0.70g/100g, with Rasakadali and Nendran showing the highest sodium (0.26 g/100g) and potassium (0.55 g/100g) levels, respectively (Siji & Nandini, 2017). Nadeeshani et al., 2021 analyzed the nutritional composition of five banana varieties commonly cultivated in Sri Lanka. The studied banana cultivars had total carbohydrate values of 13.46-26.46%, protein levels of 0.14–0.2%, and dietary fiber contents of 1.97-2.49%. Linoleic, palmitic, α-linolenic, oleic, palmitoleic, stearic, and myristic acids were the main fatty acids found. Among the banana varieties examined, Kolikuttu stood out for its higher dietary fiber, protein, thiamine, and riboflavin content. Variety Ambul kesel was found to have the highest vitamin C content among the varieties studied (Nadeeshani et al., 2021).

Due to nutrient richness and versatility in consumption, both ripe and unripe bananas were used for the preparation of various products. Ripe banana fruits were used for the preparation of yogurt, cake, ice cream, bread, wine, baby food, puree, and bakery products (R. Singh et al., 2018). Green bananas are used for the preparation of chips and banana flour (R. Singh et al., 2018). Banana flour contains 70-80% starch and hence it has been incorporated into various food items such as pasta, bread, cookies, and biscuits to increase its functional properties (Anyasi et al., 2013; Dibakoane et al., 2023). Recently, several researchers added unripe banana starch and flour for the preparation of different foods such as cookies (Aparicio-Saguilán et al., 2007), pasta (Agama-Acevedo et al., 2009; Biernacka et al., 2020; Oupathumpanont & Wisansakkul, 2021; Ovando-Martinez et al., 2009; Zandonadi et al., 2012; Zheng et al., 2016), and noodles (Ritthiruangdej et al., 2011; Saifullah et al., 2009) with enhanced functional properties. Banana flour incorporated edible films showed enhanced film strength, higher film elastic modulus, and tensile strength (Sothornvit & Pitak, 2007). The raw banana powder as a weaning food for babies occupies a special place in the commercial market and it is marketed by various industries such as Baby Vita, Slurrp Farma, Dr. Food, Staple green, etc.

Similarly, banana peel is also utilized to improve the nutritional and physicochemical properties of various products. Recent research has shown that mature banana (*Nanica cavendish*) peel can be used to make gluten-free Rissol, while the peel of *Musa cavendish* can be incorporated into bakery products and pasta. Furthermore, *Musa balbisiana* peel powder has been used to enhance the sensory and nutritional quality of chicken sausage (Gomes et al., 2022; Segura-Badilla et al., 2022; Zaini et al., 2020). Nida et al. (2023) utilized it to prepare 3D-printed food package casings and apart from the food sector, the banana peel has also found applications in wastewater treatment, biofuel production, bioplastic, and nanocellulose (Alzate Acevedo et al., 2021; Nida et al., 2023). Notably, banana peels find applications across various industries, including cosmetics, medicine, food processing, beverages, textiles, energy production, paper manufacturing, bio-absorbents, biofuel production, and agriculture (Bhavani et al., 2023).

1.2.3. Phytochemicals reported in bananas and their associated health benefits

Due to the incredible therapeutic potential such as anti-inflammatory, anti-cancer, anti-viral, and antioxidant properties bioactive compounds or plant secondary metabolites are of great significance to mankind. There are mainly six classes of bioactive compounds reported from bananas. It includes carotenoids, flavonoids, biogenic amines, phenolic compounds, organic acids, and phytosterols (Fig. 1.3.) (Pereira & Maraschin, 2015; B. Singh et al., 2016).

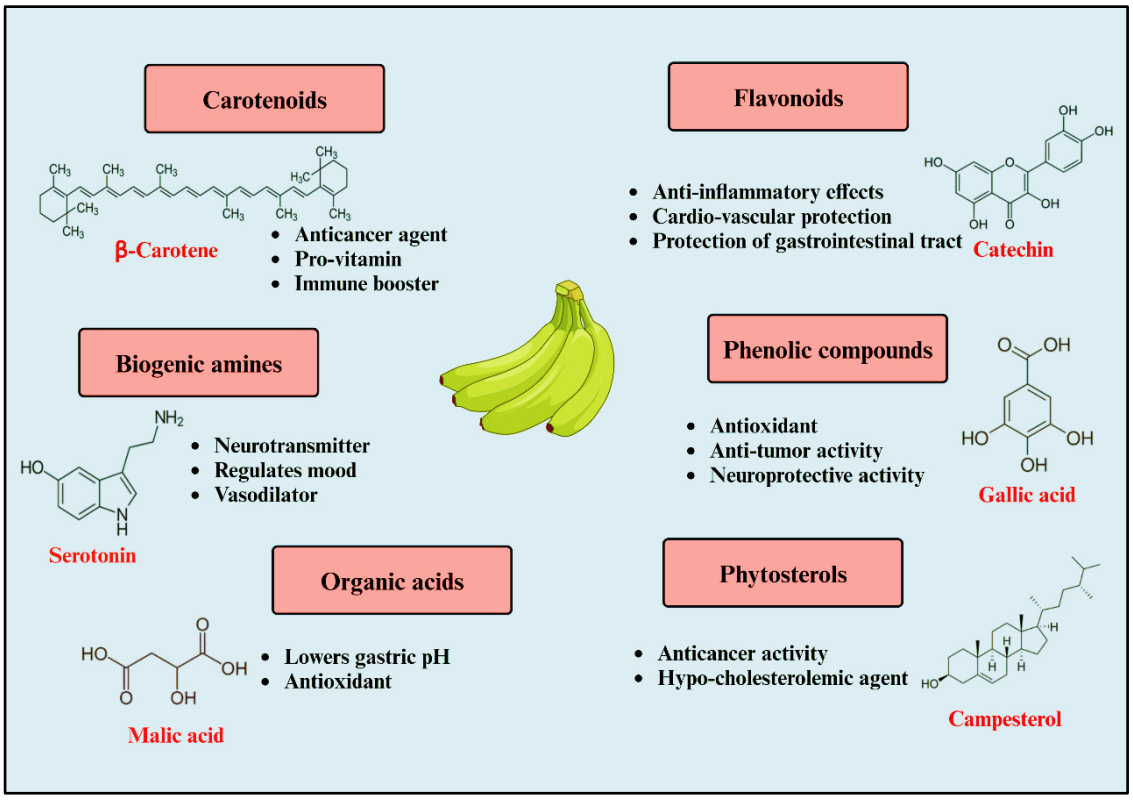

Fig. 1.3. Major classes of bioactive compounds reported from banana (Created with BioRender.com)

Polyphenols, the most abundant bioactive compounds, which impart the astringent taste to bananas, well known for their potent antioxidant, anti-tumor, anti-bacterial, anti-viral, anti-inflammatory and vasodilation properties (Anyasi et al., 2013; De Bruyne et al., 1999; Haslam, 1996; Lairon & Amiot, 1999; B. Singh et al., 2016). In 2006, Mattila and his team conducted a comprehensive study on the content of total phenolic acids in *Musa sapientum* banana through high-performance liquid chromatography (HPLC) and found the total phenolic acids as aglycones in *Musa sapientum* species of banana was 25.4 mg/100 g fresh weight (fw) (Mattila et al., 2006). Bennet et al., 2010 analyzed the phenolics in the fruit pulp of *Musa acuminata* Juss. cultivars and identified condensed tannins, catechin, gallocatechin, delphidin, and epicatechin in the matrix (Bennett et al., 2010).

The total phenol content (TPC) of pulps and peels from eight Malaysian banana cultivars was examined by Sulaiman et al. (2011). The fresh pulps of the Raja cultivar exhibited the highest TPC content (Sulaiman et al., 2011). Through High-performance liquid chromatography coupled with electrospray ionization-quadrupole-time of flight-mass spectrometry (HPLC-ESI-QTOF-MS/MS) analysis 24 phenolic compounds including ferulic acid, caffeic acid, *p*-coumaroyl glycolic acid, cyanidin 3,5-*O*-diglucoside, myricetin 3-*O*-rutinoside, umbelliferone, etc. were tentatively characterized in the ethanol extract of Australian grown bananas (Bashmil et al., 2021). The organic acids reported from bananas include citric, malic, lactic, and acetic acid (Lopes et al., 2020; B. Singh et al., 2016).

Several pharmacological studies revealed that bananas were beneficial and efficient in treating gastrointestinal tract disorders. Pannangpetch et al. (2001) investigated the gastro-protective activities of two banana cultivars grown and consumed in Northeastern Thailand: "Palo" (*Musa paradisiaca*) and "Hom" (*Musa sapientum* Linn.). The results showed that rats treated with extracts of Palo or Horn bananas at a dose of 1 g/kg/day for 3 days had significantly shorter gastric lesions compared to the control group (Pannangpetch et al., 2001). The anti-ulcerogenic action of bananas appears to be due to their ability to stimulate the growth of gastric mucosa (Best et al., 1984). In a study by Lewis and co-workers in 1999, an active anti-ulcerogenic ingredient was extracted from unripe plantain through sequential solvent extraction method and identified it as the flavonoid leucocyanidin (Lewis et al., 1999). Studies by Prabha et al., 2011 also indicated the presence of leucocyanidin in the unripe pulp of *Musa sapientum* species (Prabha et al., 2011). According to research, bananas can help in treating hyperlipidemia and several atherosclerotic conditions also. Hypolipidemic activities, such as a decrease in the concentrations of free fatty acids, cholesterol, phospholipids, and triglycerides in the kidney, liver, and blood serum were observed in male rats upon treatment with flavonoid-rich extract of unripe banana (*Musa paradisiaca*) (Krishnan & Vijayalakshmi, 2005; Vijayakumar et al., 2009).

Carotenoids are another class of molecules that is abundant in banana. Carotenoids are well known for having many physiological properties that contribute to health, including provitamin A and their activity as antioxidants, particularly in scavenging singlet oxygen. Carotenoids identified in bananas were α-carotene, β-carotene, lutein, isolutein, violaxanthin, α-cryptoxanthin, auroxanthin, β-cryptoxanthin, and neoxanthin (Lopes et al., 2020; B. Singh et al., 2016). Another interesting class of compound reported from bananas is biogenic amines. Amination of aldehydes and ketones or decarboxylation of amino acids results in the formation

of biogenic amines. These compounds are found to have an impact on our mood, ability to concentrate, and emotional stability. In 1959, a study on physiologically active biogenic amines in common fruits and vegetables revealed the presence of norepinephrine, dopamine, and serotonin in both the pulp and peel of bananas (Udenfriend et al., 1959).

Phytosterols are another class of molecule abundant in banana. Villaverde et al., (2013) identified the following phytosterols campesterol, cycloeucalenone, cycloartenol, cycloeucalenol, stigmasterol, and β-Sitosterol in *Musa balbisiana* and *Musa acuminata* cultivars (Villaverde et al., 2013). Two new steryl glycosides, myo-inosityl-β-D-glucoside, and sitosterol gentiobioside, two new acyl steryl glycosides, sitoindoside-III and sitoindoside-IV, and β-sitosterol were identified in the unripe pulp of *Musa paradisiaca* (Ghosal, 1985). Among these, steryl glucosides gained special attention due to their pharmacological actions, which included anti-inflammatory, anti-cancer, and hepatoprotective qualities (Oliveira et al., 2006). In the lipophilic extract of dwarf Cavendish bananas, Olivera et al. (2006) identified campesterol, stigmasterol, sitosterol, and fatty acids, including palmitic, stearic, linoleic, linolenic, 22-hydroxydocosanoic, 24-hydroxytetracosanoic, and 26-hydroxyhexacosanoic acids (Oliveira et al., 2006). In addition to steroids, they have also reported the α-hydroxy fatty acids and ω-hydroxy fatty acids in these extracts (Oliveira et al., 2006). Vilela *et al.* reported sterols such as β-sitosterol, campesterol, and stigmasterol from the ripe pulp of ten *Musa* species (Vilela et al., 2014). These diverse arrays of phytochemicals belonging to different classes indicate the potent health benefits of banana consumption.

1.2.4. Starch

1.2.4.1. Starch-structure, composition, and properties

Starch (CAS No. 9005-25-8) is the predominant carbohydrate reserve in plants, the most abundant carbohydrate molecule on earth after cellulose, and is the weaning food for a growing plant embryo; this molecule is critical for the existence of life on earth. In one way or the other, the life and livelihood of humans depend upon starch molecules. Starch comprises two kinds of homo-polymer (glucans) of α-D-glucose units, i.e., amylose and amylopectin. The amylopectin consists of α-(1,4) linked glucose units along with intense branching, which occurs by the formation of α-(1,6) linkages by the glucose chains at intervals of 10 nm along the axis of the molecule. The glucose units are joined by α-(1,4) glycosidic linkages to create linear chains ‘amylose’ with limited branching point at α-1,6 position (Durrani & Donald, 1995). The length of the glucose chain was considered as the degree of polymerization (DP). Amylose is

typically 500–5000 DP and contains <1% branch linkages (α-1,6 linkages) with an average molecular weight of 10^5-10^6 Daltons. In contrast, amylopectin has a DP ranging from 5000 to 50000, with a high branching pattern, and a molecular weight of 10^7-10^9 Daltons (Regina et al., 2010). The amylose and amylopectin are arranged in a semi-crystalline structure in the matrix of the starch granule. The starch matrix consists of alternating amorphous and crystalline areas formed by the amylose and amylopectin units, respectively (P. J. Jenkins et al., 1993). The amylopectin's branched design enables nearby chains to create double helices, which then fit into crystalline lamellae, with the branch points located in the non-crystalline lamellae. The alternating crystalline and amorphous lamellae result in the formation of the semi-crystalline matrix of starch granules (Seung, 2020). Starch normally contains about 20-30% amylose and 70-80% amylopectin. The amylose and amylopectin ratio varies from species to species, and the starch properties, such as water absorption, pasting, gelatinization, and retrogradation, also vary accordingly (Marichelvam et al., 2019). Starch granules with high amylose content absorb limited water content during cooking, in contrast, starch granules with high amylopectin content (waxy starches) have very low resistance to breakdown during processing, giving high viscosity, and enable expansion in snacks (Biliaderis, 1991).

Starch from different botanical sources was found to have different crystalline patterns and thus exhibit specific X-ray diffraction patterns accordingly. Based on X-ray diffraction patterns starch was generally classified into three crystalline structures: type-A, type-B, and type-C (Tester et al., 2004). The glucose helixes are densely packed in A-type crystalline and B-type crystalline starch, on the other hand, has less dense packing, which allows water molecules to move freely between the branches. The combination of A and B-type crystallinity forms the C-type crystalline starch (Dome et al., 2020). In C-type crystals, the starch granule core is formed by a B-type structure and surrounded by A-type crystals. A-type crystalline structure is mainly found in rice, wheat, and maize. The dense packing in A-type crystals prevents chemical reactions such as acid hydrolysis. Starch with high amylose content exhibits B-type crystalline structure e.g., starches extracted from potatoes, canna, banana, and sago. Starch extracted from peas, beans, some bananas, and cassava exhibits a C-type crystalline structure (Dome et al., 2020).

Starch swelling, gelatinization, retrogradation, and gelation were the significant physicochemical properties associated with starch. Starch is insoluble in water below its gelatinization temperature. Since water diffuses and absorbs into the amorphous portions of starch, it causes slight swelling of starch in cold water; however, this swelling can be reversed

by drying. However, during heating, as temperature increases, a point is reached where granule swelling becomes irreversible. At this point the the granules lose their structural integrity and keep expanding, leaking amylose into the aqueous intergranular phase. As a result, the viscosity increases significantly. The term 'gelatinization' is used to describe the collective processes of swelling and hydration, solubilization of starch molecules, and disintegration of granular structure (Biliaderis, 1991). the parameters like type of starch, heating temperature, presence of other solutes, and agitation imparted during heating will affect the gelatinization process (Biliaderis, 1991). For gelatinization to initiate at least 50 °C temperature and more than 25% water content is required (Tako et al., 2014). The presence of solutes, lipids, or proteins raises gelatinization temperature and slows retrogradation. The amylose/amylopectin ratio greatly influences these processes. Amylose recrystallizes faster than amylopectin, requiring stronger conditions for gelatinization and faster retrogradation (Perin & Murano, 2017).

Upon cooling of the heated starch solution, gelatinized dispersion in the form of a loose paste or a gel will be formed depending on the concentration of starch. Further, the chains of swollen granules, through hydrogen bonding, form a three-dimensional dimensional network that will be immersed in a continuous matrix of entangled amylose molecules. This complex polymer blend solidifies into 'gel'. These gels are in a non-equilibrium state, and during storage, they undergo further aggregation and recrystallization. These crystals then gradually increase rigidity, and phase separation from the solvent occurs. This process was termed syneresis. The term 'retrogradation' was used to indicate the re-association of disaggregated amylopectin and amylose chains in a gelatinized state to form ordered structures. Retrogradation is the primary reason for the staling of baked products such as bread (Biliaderis, 1991; Perin & Murano, 2017). Gelatinization and retrogradation are directly correlated with starch digestibility. Completely gelatinized starch will be digested and absorbed in the small intestine and retrograded starch shows resistance to digestion (Wang et al., 2015).

1.2.4.2. Starch digestion in humans

Starch digestion begins in the mouth with the action of the enzyme salivary α-amylase (ptyalin), which is aided by chewing and starch hydration. Once the food reaches the stomach, the acidic gastric environment quickly deactivates the enzyme. Digestion continues in the duodenum, where pancreatic α-amylase further breaks down starch into maltose, maltotriose, and α-limit dextrins, which cannot be absorbed directly. The enzymes maltase-glucoamylase (MGA) and sucrose-isomaltase in the brush border of the small intestine then convert these products into glucose. Undigested starch passes from the small intestine to the large intestine,

where probiotic microorganisms ferment it (Fig. 1.4.) (H. N. Englyst & Cummings, 1985; J. Singh et al., 2010).

Enteroendocrine cells scattered throughout the gastrointestinal tract produce various hormones that influence functions related to digestion, including secretion, motility, absorption, and digestion. The duodenum and jejunum produce cholecystokinin (CKK), which stimulates pancreatic secretion and gallbladder contraction. The glucagon-like peptide 1 (GLP-1) is released by intestinal L-cells, while gastric inhibitory polypeptide (GIP) is released by K cells in the duodenum and jejunum. These hormones stimulate insulin secretion, reduce the secretion of glucagon, and slow down gastric emptying (Li et al., 2023).

The resealed glucose is absorbed through two main transport systems: sodium-dependent glucose transporter 1 (SGLT1) and glucose transporter 2 (GLUT2). SGLT1, located on the brush border of enterocytes, uses the sodium gradient, maintained by Na^+/K^+-ATPase, to actively transport glucose into the cells. Glucose then exits the enterocytes into the bloodstream via GLUT2, which is found in the basolateral membrane (Perin & Murano, 2017).

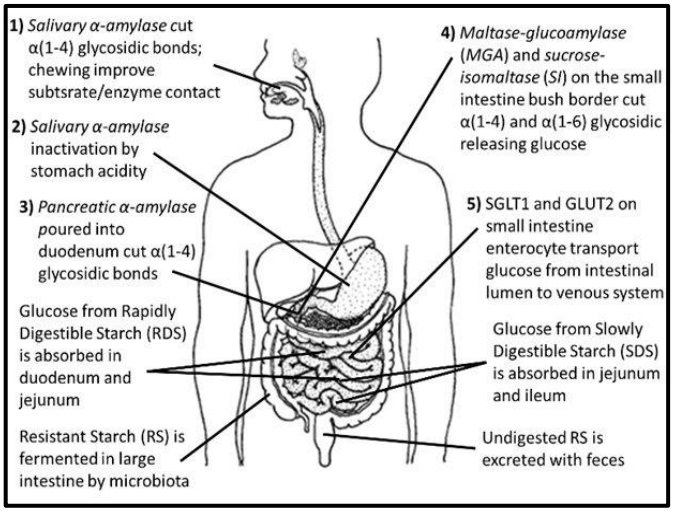

Fig. 1.4. Starch digestion in humans (Source: Perin & Murano, 2017, https://doi.org/10.1177/1934578X1701200606)

1.2.5. Glycemic index and glycemic load (GI-GL)

The term GI was coined by Jenkins and his colleagues in 1981, and GI remains a relevant topic still. The GI concept was developed to rank or classify carbohydrate-rich foods in the diet based on their postprandial glycemic response. GI measures the rise in blood glucose levels after consuming a 50 g carbohydrate portion of a test food, expressed as a percentage of the response to the same amount of carbohydrate from a standard food (glucose or white bread) consumed by the same individual (Augustin et al., 2015; D. J. Jenkins et al., 1981; Joint, 1998).

GI of a food is evaluated through clinical as well as *in vitro* studies. In simpler terms, GI is a measurement of a food's ability to raise blood sugar levels in relation to a similar quantity of a reference food. The *in vitro* and *in vivo* assessment of starch digestibility and the factors influencing it gained a great attraction since starch digestibility has been associated with the GI of food.

Since GI is an indication of post-prandial glucose response, it is used to assess the nutritional quality of food. A GI value of 55 or less makes a food a low GI food; if it is 56 to 69, it is termed as mid-range GI and a value more than 70 indicates a high GI food (Fig. 1.5.) (D. J. Jenkins et al., 1981). The product of the food's GI value and the amount of available carbohydrates in grams per serving is the food's GL (Kim, 2020). GL is calculated by multiplying the food's carbohydrate content in a specified serving size by its GI value, then dividing the result by 100 (Foster-Powell et al., 2002). A GL value of 10 or below is categorized as low, 11-19 as medium, and 20 or above as high (Fig. 1.5.) (Foster-Powell et al., 2002; Carneiro & Leloup, 2020).

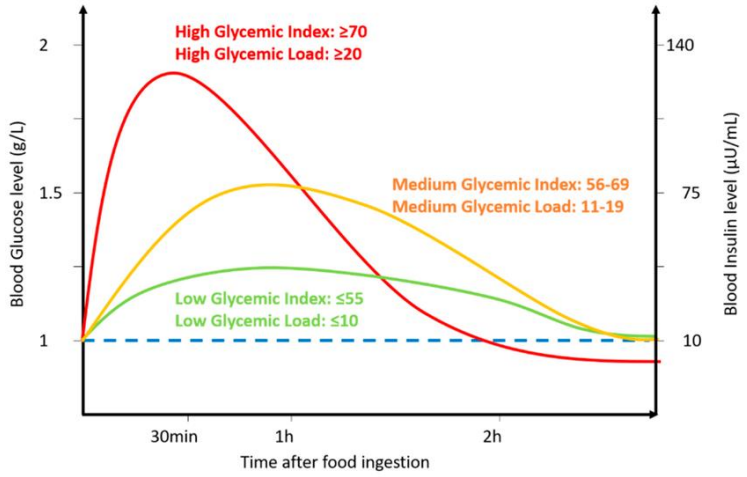

Fig.1.5. Impact of different GI-GL category foods on blood glucose level (Source: Carneiro & Leloup, 2020, https://doi.org/10.3390/nu12102989)

Clinical studies have demonstrated that low GI diets improve glycemic control, serum lipids, and cardiovascular risk factors, potentially aiding weight loss. Epidemiological studies associate low GI diets with reduced risks of diabetes, cardiovascular diseases, and certain cancers. Clinical trials further support the benefits of low GI and GL diets in enhancing glycemic control and lowering cardiovascular disease (CVD) risk factors in type 2 diabetes mellitus (Augustin et al., 2015). The portion size of foods consumed is important for managing blood glucose and for losing or maintaining weight. However, the utility of GI needs to be

balanced with the basic nutrition principles for a range of healthful foods and moderation of foods with few nutrients (Gray & Threlkeld, 2015).

1.2.6. Countries with regulations on GI-food labelling

Even though the GI labelling of food provides potential benefits for consumers managing their blood glucose levels, currently, very few countries have regulations regarding the use of GI on food labels. A comprehensive literature review was conducted using PubMed with the keywords "GI food labelling," "GI logos," and "GI endorsement," and also visiting food regulatory authority sites and general Google search. Australia was the first country to introduce GI labeling of food products. In 2001, the Australian government, in collaboration with the University of Sydney, launched the GI Symbol Program, which allowed food manufacturers to voluntarily display the low GI symbol on their products (Fig. 1.6.). In 2007 New Zealand also adopted Australia's GI symbol in food labelling (*GI Foundation*, n.d.). The GI Symbol was registered by the University of Sydney and licensed to the GI Foundation. The University of Sydney, Diabetes Australia, and the Juvenile Diabetes Research Foundation Australia are the three partners of this non-profit organization (*GI Foundation*, n.d.).

The GI Foundation of South Africa (GIFSA), established in 1999, also introduced GI labelling on food and beverage products in 2011. The GIFSA endorsement logo categorizes food into, frequent food (GI: 0-40), often food (GI: 40-55), active food (GI: 56-70), and exercise food (GI >70) (Fig. 1.6.). Along with GI, the food must also meet specific requirements of fat, dietary fiber, carbohydrate, sugar, sodium, protein, and alcohol content to fall into each category (*GIFSA*, n.d.). Low GI claims in Singapore are subject to particular guidelines provided by Singapore's Healthier Choice Symbol (Fig. 1.6.) (*Healthier Choice Symbol*, n.d.). In India, the Food Safety and Standards Authority of India (FSSAI) permits the use of low GI claims in the nutrient labelling of food but no GI symbol has been implemented so far (*FSSAI, 2019*, n.d.). Although voluntary claims are permitted, there are no national regulations in China specifically pertaining to GI. GI claims are accepted in the USA even if they are not strictly controlled since they are thought to be covered by general food labelling laws. Current food laws prohibit GI claims in both the European Union and Canada (Barclay et al., 2021).

These inconsistent food regulations around the world highlight the need for standardization and the creation of global standards for GI claims in food, which would benefit people with diabetes and other lifestyle diseases (Barclay et al., 2021).

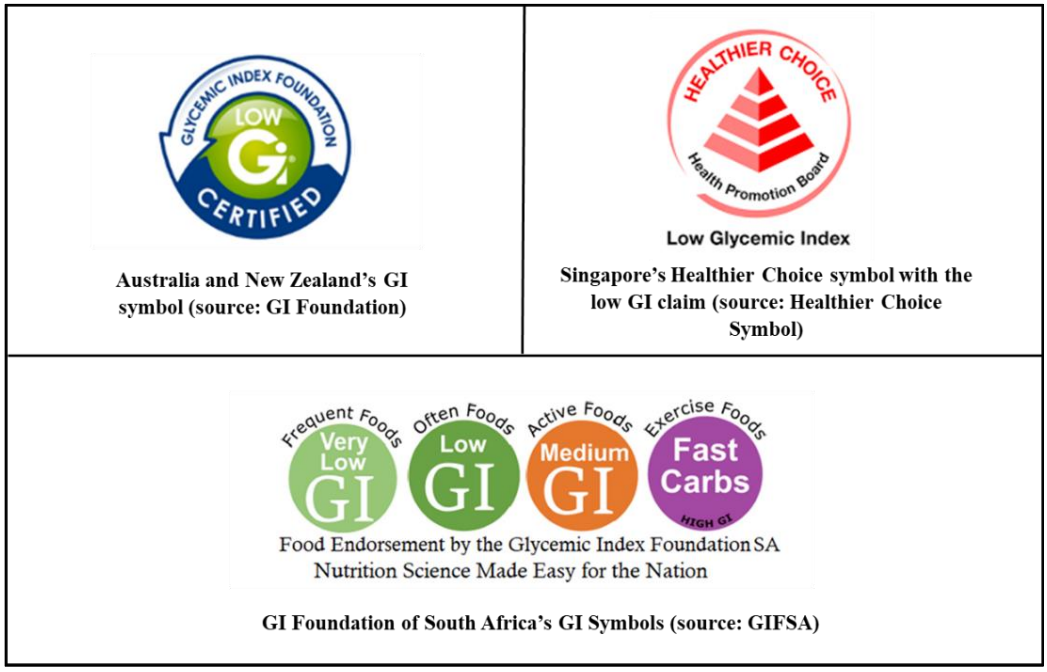

Fig. 1.6. International GI symbols (Source: Barclay et al., 2022, https://doi.org/10.3390/nu13093244)

1.2.7. *In vitro* GI-GL studies

The determination of the GI of food through clinical studies involves extensive and expensive procedures and it also has great ethical concerns. Therefore, the measurement of starch digestibility *in vitro* and the prediction of GI was introduced.

The first effort to determine *in vitro* starch digestibility was done by Southgate in 1969. His two publications in the same year dealt with the determination of available and unavailable carbohydrates in the food matrix using enzymes amyloglucosidase and pullulanase (Southgate, 1969a, 1969b). This method was highly criticized since the starch digestion was incomplete, and later in 1982, Englyst and his co-workers (H. Englyst et al., 1982) introduced a more efficient method for complete hydrolysis of starch with enzymes α-amylase, pullulanase, and amyloglucosidase and further determination of non-starch polysaccharides through gas chromatography technique. One significant drawback of this method was the initial heating step of samples at 100 °C, contradicting the normal physiological conditions. Hence in 1986, Berry introduced a modified method of Englyst et al. (1982) where the initial heating step was eliminated, and the shaking water bath facility cooperated to mimic the physiological conditions more accurately (Berry, 1986). The long experimental time was the major drawback of this procedure.

In the year 1992, another significant contribution was made by Englyst and his team. They developed an *in vitro* digestion method that can differentiate the starch fractions of the food

matrix into rapidly digestible starch (RDS), slowly digestible starch (SDS), and RS. As the name indicates, these fractions show various degrees of hydrolysis during enzyme incubation. RDS is the amount of starch digested by enzymes within 20 minutes of digestion and SDS is the amount of starch that can be completely digested within 20 minutes to 120 minutes. The portion of starch that was not hydrolyzed even after 120 minutes of amylase and pullulanase treatment is termed RS (H. N. Englyst et al., 1992). Compared to B-type starches, which typically contain a significant proportion of RS, type-A starches have higher amounts of RDS and SDS fractions (Lehmann & Robin, 2007). SDS provides various health advantages by helping to stabilize and maintain blood glucose levels and has a moderate impact on GI. Whereas RS imparts health benefits mainly through the short chain fatty acids (SCFA) produced through the fermentation of RS by probiotics in the large intestine (Bojarczuk et al., 2022; Lehmann & Robin, 2007). The Englyst 1992 method got wide acceptance, and later methods for *in vitro* assessment of starch digestibility were a modification of this basic method.

In 1994 Granfeldt et al. introduced the term hydrolysis index (HI) for measuring starch hydrolysis rate. The HI was the ratio between the area under the starch hydrolysis curve for test food and the for a reference food which was expressed in percentage, which in turn used to predict the GI of food (Granfeldt et al., 1994). In 1997 another approach was put forward by Goni and others, they introduced a mathematical first-order reaction kinetic equation ($C = C_{\infty}(1 - e^{-kt})$) for the prediction of HI and, thereby prediction of GI (Goñi et al., 1997). This method of GI prediction acquired wide acceptance and is still used for the prediction of GI of starchy food matrices.

Currently, there are many *in vitro* starch digestion methods that were the modification of Englyst's method. These methods include three basic digestion phases of oral, gastric, and intestinal digestion processes, but differ in the way of implementation of the physiological conditions. It includes variations in the duration of digestion time, choice of enzymes, incubation temperature, pH, and mode of execution (McCleary et al., 2020; Ren et al., 2016; Tudorică et al., 2002; Urooj & Puttraj, 1999).

While Englyst's method followed a 2-hour digestion protocol, the method put forward by McCleary et al., 2020 employs a digestion time of 4 hours, which is the average time of residence of food in the human small intestine. In addition to RDS, SDS, and RS they have introduced a new term 'total digestible starch' (TDS) to refer to all starch that is digested within four hours. Whereas RS is starch that is not digested in a period of four hours or less (McCleary et al., 2020). Based on this method they have developed kits for the rapid

assessment of RDS, SDS, TDS, and RS fractions of samples (*Digestible and Resistant Starch Assay Kit*, n.d.).

Recently, INFOGEST , an international network of researchers focused on improving the understanding of food digestion and the nutritional value of foods put forward a static *in vitro* simulation of gastrointestinal food digestion involving oral, gastric, and intestinal phases for evaluating the GI, and nutrient bioavailability (Brodkorb et al., 2019). A schematic representation of major milestones in the assessment of *in vitro* starch digestibility and estimation of GI is represented in Fig. 1.7.

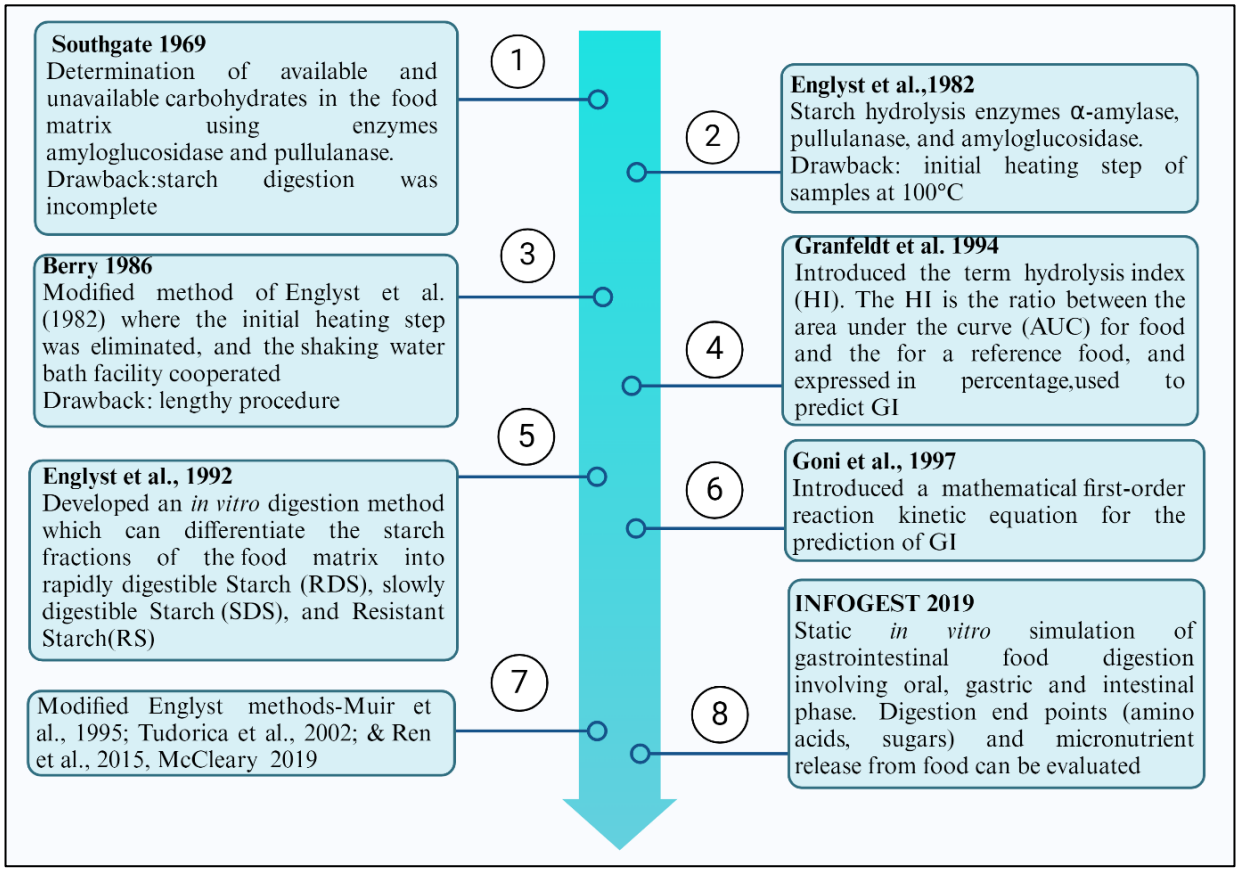

Fig. 1.7. Major milestones in the assessment of *in vitro* starch digestibility and estimation of GI (Created with BioRender.com)

1.2.8. Resistant starch (RS)

1.2.8.1. RS-structure and classification

Englyst and his team in 1982 introduced the term RS to represent the starch fraction which exhibited resistance to digestion. In physiological conditions, Since RS cannot be absorbed or digested in the small intestine, it passes to the large intestine where it is fermented by bacteria (H. Englyst et al., 1982). Many investigations have been conducted to understand the structural

features of RS. According to the studies of Tharanathan, 2002, RS is a linear α-1,4 linked glucans chain derived from the retrogradation of amylose fractions. This compact structure will be the factor that limits the accessibility of digestive enzymes to RS (Tharanathan, 2002). Similarly high amylose starch shows high resistance to digestion and more susceptible to retrogradation and favors resistance to enzymatic digestion (Nugent, 2005).

In 1992, Englyst and coworkers classified RS into further subgroups. They divided RS into three subcategories as physically inaccessible starch (RS1), resistant starch granules (RS2), and retrograded starch (RS3). RS1 includes starch which becomes inaccessible for enzymes due to the structure of the seed, the presence of an intact cell wall, etc. The food matrix and protein encasements provide a barrier that prevents enzymes from physically accessing RS1. Examples include unmilled or partly milled seeds, grains etc. The second category (RS2) holds starch showing resistance to digestion due to the peculiar nature crystalline nature of granules, type B crystallinity, as seen in raw potato and banana. High amylose starch also belongs to RS2 category. RS3 includes cooked and cooled starches, the retrograded starches, which are present in bread and cornflakes (H. N. Englyst et al., 1992). The cooling process causes the starch molecules to realign and recrystallize, enhancing their resistance to degradation by enzymes. The main food sources of RS3 are cooked and cooled potatoes, pasta, and rice.

Later Nugent (2005) introduced a new classification system of RS with four subcategories: RS1, RS2, RS3 & RS4. This system closely resembles Englyst's classification (1992) but introduced an additional category RS4 to include starches that were chemically modified to obtain resistance to digestion. Here chemical cross-linking agents are used for attributing the compact structure to starch, e.g. esterified starch (Nugent, 2005). Further, in 2017 Lockyer and Nugent introduced one more additional category RS5 in the RS classification system (Fig. 1.8.). RS5 comprises starch containing amylose-lipid complex and exhibits great resistance to digestion. The amylose-lipid complexes formation is influenced by various parameters such as the length of the starch chain, the kind of fat, water content, the degree of polymerisation, amylose to lipid concentration, and the processing method (Andriani et al., 2021). The RS content of RS1, RS2, and RS3 was found to vary greatly with cooking, processing, and other treatments and RS5 has more thermal stability (Lockyer & Nugent, 2017).

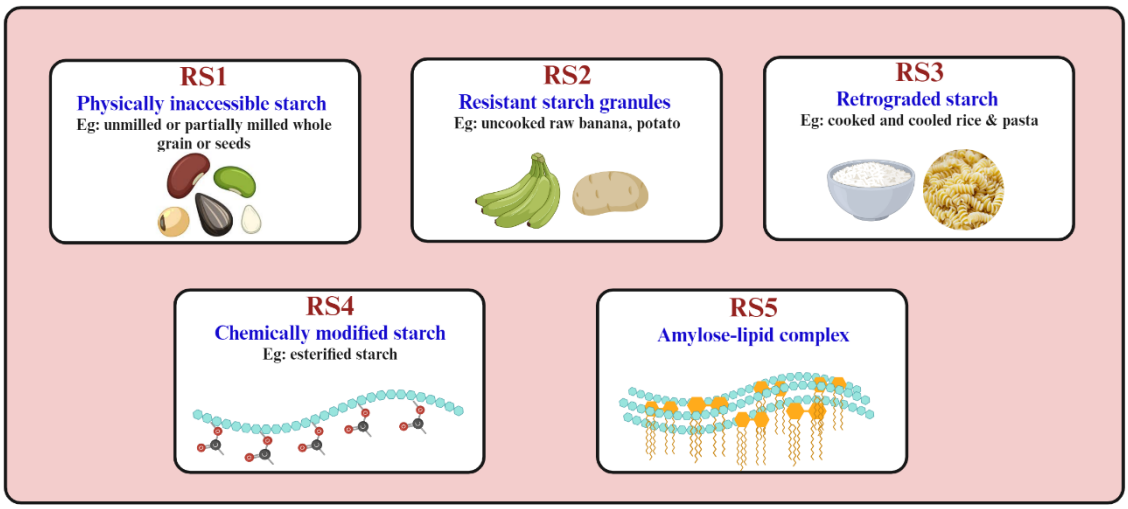

Fig. 1.8. RS classification (Created with BioRender.com)

1.2.8.2. RS and health benefits

RS has gained a great interest in the food industry due to its associated numerous health benefits including improved intestinal health, glycemic balance, lipid metabolism, body weight management, diabetes, obesity, and lipid disorders (Fig. 1.9.).

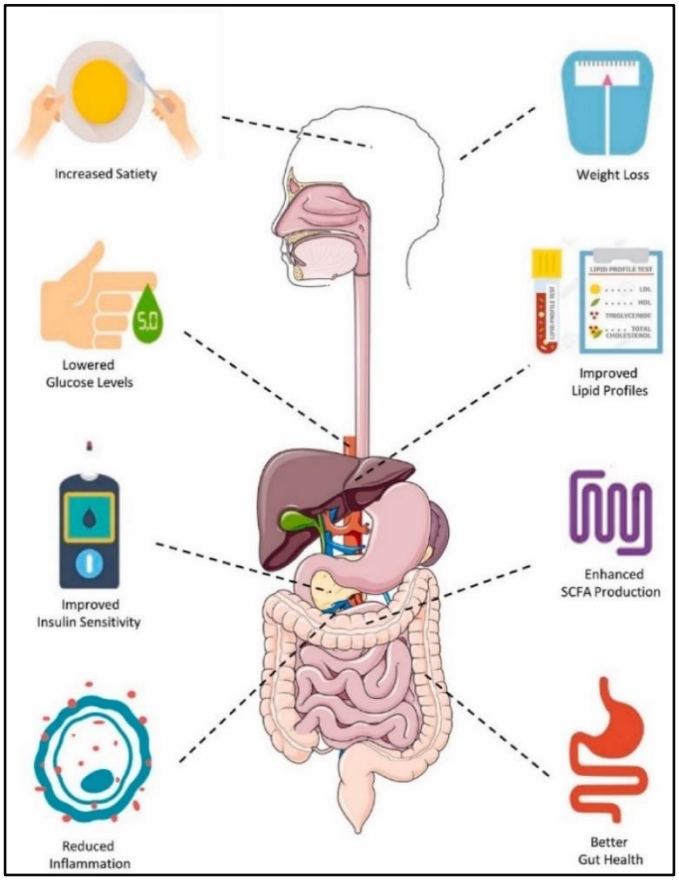

Fig. 1.9. Health benefits of RS (Source: *Guo, J* et al., 2022, https://doi.org/10.1016/j.jafr.2022.100380)

The main physiological potential of RS is attributed to the production of SCFA by fermentation of RS by gut bacteria. *Bacteroidetes* and *Firmicutes* phyla are the primary RS fermenters. SCFAs such as acetate, propionate, and butyrate were produced by fermentation which have several physiological and metabolic impacts on humans as well as promote the growth of the probiotics (Guo et al., 2022). These SCFA are the prime energy source for the colonocyte and they act as growth factors to the healthy epithelium. Butyrate is predominantly produced by *Firmicutes* and propionate mainly by *Bacteroidetes* phylum (Chen et al., 2024). The SCFAs not only lower the risk of gastrointestinal diseases but also play crucial roles as activators for G protein-coupled receptors (GPCRs) engaged in immune system modulation (Segain et al., 2000; Smith et al., 2013). Activated GPCR coupled free fatty acid receptors 2 and 3 (FFAR2, FFAR3) enhance the secretion of GLP-1 and peptide YY (PYY) from intestinal L cells and improve insulin secretion and sensitivity thereby exerting beneficial effects in subjects with diabetes and obesity by providing satiety (Tolhurst et al., 2012).

Among the SCFA produced butyrate plays a crucial role in maintaining colon health. Butyrate lowers the risk factors that lead to the development of colorectal cancer and intestinal inflammation (Brouns et al., 2002). It also helps in the reduction of the luminal pH, which in turn helps to inhibit the growth of pathogenic microorganisms and also helps in increasing the absorption of nutrients (Chen et al., 2024). By suppressing the production of pro-inflammatory cytokines like tumour necrosis factor- α (TNF-α), and modulating the gut-associated lymphoid tissue (GALT), an integral part of the human immune system, butyrate demonstrates anti-inflammatory properties (Chen et al., 2024; Cummings et al., 2004; Lockyer & Nugent, 2017; Segain et al., 2000). SCFA, such as acetate plays a crucial role in lipid biosynthesis and cholesterol synthesis and they show anti-inflammation properties by modulating the anti-inflammatory cytokine interleukin 10 (IL-10) level (LeBlanc et al., 2017; Topping et al., 2003). Propionate is involved in gluconeogenesis, associated with the inhibition of cholesterol synthesis, indicating potential cardioprotective benefit, and also regulates satiety hormones (Canfora et al., 2015). It also has a role in hepatic glucose production regulation and exerts anti-inflammation potential by inhibiting the nuclear factor-kappa B (NF-κB) pathway (Chen et al., 2024).

1.2.8.3. Effect of RS on mineral absorption

The effect of RS on mineral absorption was well explored. In comparison to a completely digestible starch meal, a meal containing 16.4% RS increased the apparent absorption of calcium and iron in research carried out by Morais et al. in 1996 on infant pigs (Morais et al.,

1996). Clinical studies by Trinidad and team (1996) proved that the SCFAs propionate and acetate were found to enhance calcium absorption in the distal colon of humans (Trinidad et al., 1996).

1.2.8.4. RS and hypocholesterolemic effects

The hypocholesterolemic effects of RS were also well explored. RS was found to be more effective than cholestyramine in lowering lipid levels in rats. Feeding studies in rats demonstrated that the RS fractions of beans increased hepatic mRNA levels, sterol excretions, and decreased blood cholesterol in rats. The administration of bean starch to rats resulting in elevated levels of hepatic scavenger receptor class B1 (SR-B1) and cholesterol 7-α-hydroxylase mRNA suggested that RS had a reducing effect on blood cholesterol. Additionally, the bean starches enhanced the concentration of SCFA in the cecum and decreased serum and total cholesterol levels (Younes et al., 1995).

1.2.8.5. RS and hypoglycemic effect

Another significant attribute of RS is its hypoglycemic effect. The best way for diabetes management is to keep post-prandial glycemia low; hence food rich in RS content is the best option for the diabetic population (Chen et al., 2024). The effect of RS on post-prandial plasma concentrations of glucose was investigated in 10 healthy young males by Raben et al. in 1994. The test meal given to the participants was 50 g of pre-gelatinized starch (0% RS) or 50 g of raw potato starch (54% RS). It was found that after the RS-rich meal, post-prandial plasma concentrations of glucose were significantly lower compared with after the RS-less meal. This implies the significance of RS in the reduction of post-prandial glycemia and increased satiety (Raben et al., 1994). Following a 10-week intervention, the RS-fed group showed a significant decrease in fasting blood glucose, triglyceride, low-density lipoprotein levels, and the area under the glucose curve as compared to the control group. The relative abundance of beneficial *Bacteroidetes, Lactobacillus, Lachnospiraceae*, and *Faecalibaculum*, and a lower ratio of *Firmicutes* to *Bacteroidetes* was also observed (Chang et al., 2024)

1.2.9. Banana starch and its significance

The crystallinity of banana starch varies with varieties. Varieties like Nangka, Ambon, Kepok, and Kapas exhibit B-type crystallinity (Marta et al., 2019), whereas varieties like Pisang Awak, Dwarf Red, and Cavendish exhibit C-type crystallinity (Bi et al., 2017). The granular morphology of banana starch also varies with varieties. Scanning electron microscopy analysis of Kapas starch showed elongated granules and Kepok, Ambon, and Nangka varieties exhibited round morphology (Marta et al., 2019). Starch granules of two banana varieties (Hom

Khieo & Namwa) cultivated in Thailand showed elongated and round-shaped granules with B-type crystalline structure (Thanyapanich et al., 2021).

The RS in bananas is mainly composed of RS2, which is resistant to digestion due to its crystalline structure (Faisant et al., 1995). RS2 was found to decline by food processing and cooking methods (Yi et al., 2021). The RS content of banana flour can vary depending on the processing method and the banana cultivar used. Studies in the *Musa acuminata* subgroup Cavendish showed that air velocity during the drying process has a major impact on the RS content. The RS content of green banana flour dried at higher air velocities was found to be higher when the air temperature was below the gelatinization temperature. They showed an RS content ranging from 40.90% to 58.50% based on variations in drying conditions (Tribess et al., 2009). Both flour and starch prepared from the unripe plantain bananas of the variety Terra (*Musa paradisiaca*) showed an RS content of 49% and 50% respectively (Pelissari et al., 2012). Studies by Das et al., 2022 showed that the intrinsic RS content of bananas can be increased from 38.50% to 68.99% through amylopullulanase treatments (Das et al., 2022). A study on unripe banana flour from 12 commercial samples across five Brazilian states revealed RS content variation from 4% to 62% (Hoffmann Sardá et al., 2016). Banana flour of the 'Mountain' variety exhibited 25% RS with tray drying and 37% with freeze drying (Ahmed et al., 2020). Disaggregation of starch molecules during freeze-drying will put them on a rigidity angle hence the content of the non-digestible portion increases (Kaur et al., 2020). Khawas and Deka's (2017) study found that treatment with debranching enzyme pullulanase and hydrothermal procedure can improve the RS yield from culinary bananas kachkal (*Musa* ABB). The RS content increased from 12.3 to 26.4% as a result of three cycles of continuous autoclaving and cooling (hydrothermal) followed by storage at -20 ºC. Likewise, using the debranching enzyme and subsequently retrograding at -20 ºC resulted in a 31.2% increase in the RS yield (Khawas & Deka, 2017).

The effect of banana flour in the glycemic response of the individual was investigated by researchers. The effect of banana ripening on the postprandial blood glucose and insulin responses was studied in ten type 2 diabetic subjects. On different days, they were fed with three meals: 40 g of white bread, 120 g of overripe banana, and 120 g of underripe banana. Compared to white bread (181 ± 45 mmol/L) the mean postprandial blood glucose response area of under-ripe bananas (62 ± 17 mmol/L) and over-ripe bananas (106 ± 17 mmol/L) was significantly lower. Even though the insulin response of the three meals was similar, the GI of the under-ripe (43 ± 10) and over-ripe bananas (74 ± 9) differed greatly. Authors suggest

that the low GI of under-ripe bananas may be ascribed to the high RS content (Hermansen et al., 1992). A study by Oladele and Williamson., 2014 evaluated the impact of RS in three plantain (*Musa* AAB) products i.e., boiled unripe plantain crisps (BUPC), boiled unripe plantain (BUP), and ripe raw plantain (RRP) on glycemic response of ten healthy volunteers. The study used white bread as reference and the obtained GI values for the samples BUP, BUPC, RRP, and white bread were 44.9, 55, 38, and 71.4 respectively (Oladele & Williamson, 2016). Another study reported the GI value of mature ripe banana varieties. The GI values of Mysore, Gros Michel, Silk, and Pisang Awak were 61 ± 6, 67 ± 7, 61 ± 5, and 69 ± 9, respectively through clinical studies using bread as reference food (Hettiaratchi et al., 2011). *In vitro* studies demonstrated that the supplementation of 50% unripe banana flour was found to decrease the estimated GI of cookies (GI=98.6) compared to the control cookies (GI=116.8) (Agama-Acevedo et al., 2012).

1.2.10. Prebiotic potential of banana pulp

Both *in vitro* and *in vivo* studies have demonstrated that banana starch promotes the growth of beneficial gut microbiota. The ratio of *Firmicutes* to *Bacteroidete*s is crucial for maintaining gut health. *Bacteroidetes* can help reduce obesity, enhance glucose regulation, and prevent inflammation-related diseases (Wu et al., 2019). The impact of green banana flour consumption on symptoms associated with obesity in rats fed with high-fat diets was examined by Rosado et al. in 2021. According to the study, green banana flour reduced inflammation and enhanced the metabolic status, adipose tissue remodeling, and gut microbiota composition of obese mice. In mice fed with a diet supplemented with unripe banana flour, the population of bacteroidetes (22-29%) in the gut was higher than the population of firmicutes (22-23%) (Rosado et al., 2021). *In vitro* studies showed that supplementation of banana flour in some of the probiotic foods helps in maintaining the viability of the probiotics. Fermented milk containing unripe banana flour maintained the viability of *Streptococcus thermophilus, Lactobacillus acidophilus*, and *Bifidobacterium lactis* (Batista et al., 2017) These microbes play a vital role in gut health by producing increased acetate, propionate, and butyrate levels. In a recent study, yogurt mixed with unripe banana flour preserved the viability of *Lactobacillus delbrueckii subsp. Bulgaricus* and *Streptococcus thermophilus* (Costa et al., 2023).

Apart from RS, banana is a good source of dietary fiber, fructooligosaccharides (FOS), and Inulin (Anyasi et al., 2013). Since banana peel is a good source of dietary fiber, it has been

used for the development of cellulose-based prebiotic fiber through enzymatic hydrolysis (Phirom-on & Apiraksakorn, 2021). Salini and Usha., 2015 studied the fructan distribution in seven banana cultivars and among them, Nendran had the highest fructan content (1433.3 mg/100 g). They also found a significant increase in the yield of fructans from 1.4% to 6.5% by pectinase pre-treatment (Shalini & Antony, 2015). Further, they evaluated the prebiotic potential of isolated Nendran fructans and the study demonstrated a high prebiotic activity score by promoting the growth of *Lactobacillus plantarum*, and the activity was even higher than commercial FOS and inulin (Shalini et al., 2017). A recent research reported FOS content of 1.34 ± 0.01 mg/100g dw and an exceptionally high level of inulin content of 37.442 ± 5.72 g/100g dw in Gros Michel banana (*Musa sapientum*) (Pongmalai & Devahastin, 2020).

1.2.11. Current research in banana

Currently, there are many national and international organizations and research institutions working on various aspects of bananas. In order to promote collaborative research on bananas, the Banana Asia and Pacific Network (BAPNET) was first founded in 1991 as Asia and Pacific Network (ASPNET) and changed its name to BAPNET in 2001. This committee convenes biennially to evaluate progress, pinpoint research requirements, and identify areas for collaboration and synergy among countries. The network is managed by Alliance Bioversity- International Center for Tropical Agriculture (CIAT) ("BAPNET," n.d.). The International Network for the Improvement of Banana and Plantain (INIBAP) was established in 1984, in Washington DC (USA), by a group of donor countries and organizations. The initiative aims to enhance banana and plantain production, particularly benefiting developing countries, by supporting and coordinating research. It strengthens regional and national programs focused on developing improved and disease-free genetic material and facilitates the exchange of such material through regional and global trials of new cultivars. Additionally, the initiative coordinates the collection and dissemination of relevant information and supports training programs for technicians and scientists in developing countries (*INIBAP*, n.d.).

The Centre de Coopération Internationale en Recherche Agronomique pour le Développement (CIRAD, France) works to develop hybrid disease-resistant varieties of bananas (CIRAD, n.d.). The International Institute of Tropical Agriculture (IITA) in Nigeria focuses on banana breeding and crop improvement (IITA, n.d.). The Taiwan Banana Research Institute (TBRI, Taiwan**)** is a pioneer institute in the field of research on banana breeding, crop improvement, pest management, and maintenance and conservation of banana germplasm.

TBRI has a germplasm collection of 229 accessions of bananas (*Taiwan Banana Research Institute - TBRI | Improving the Understanding of Banana*, n.d.).

In India, many research institutions work in various fields of banana research. The Indian Council of Agricultural Research-National Research Centre for Banana (ICAR-NRCB) located in Tamil Nadu focuses entirely on banana research. Various fields, such as crop improvement, postharvest value addition, physicochemical characterization, and germplasm conservation of bananas are the key research areas in NRCB. The research institutes such as Banana Research Station (BRS, Kerala), Tamil Nadu Agricultural University (TNAU, Tamil Nadu), Central Institute for Subtropical Horticulture (CISH, Lucknow), Indian Institute of Horticultural Research (IIHR, Karnataka) also focus on studies on crop improvement, post-harvest handling, value addition, germplasm maintenance, integrated pest management of bananas in India. Studies regarding the taxonomy, systematics, and plant physiology of Musa genera and bananas were an important research area at Calicut University, Kerala (Sreejith & Sabu, 2017). They also maintain a huge germplasm of many endangered and rare bananas.

1.3. Rationale of the present study

Currently, the global incidence of inflammatory bowel disease (IBD) and gut-related diseases is increasing steeply (Banerjee et al., 2023). IBD encompasses a range of gastrointestinal tract conditions marked by persistent inflammation, including Crohn's disease (CD) and ulcerative colitis (UC) (Chapman-Kiddell et al., 2010). The growing trend of urbanization, accompanied by higher consumption of ultra-processed foods, poor dietary habits, and lack of sleep is causing an increase in IBD cases among young adults and even adolescents in India. IBD requires lifelong therapy and constant monitoring causing a significant healthcare burden to the population (Banerjee et al., 2023). Through modulation of diet and gut microbiota, issues of IBD can be addressed to an extent. Studies have demonstrated the importance of the gut microbiome in regulating the risk of a variety of chronic diseases, such as obesity, type 2 diabetes, cardiovascular disease, inflammatory bowel disease, and general well-being (R. K. Singh et al., 2017). Therefore, there is a growing importance in prebiotic research and the development of functional foods to meet these requirements. The demand for convenience foods i.e., ready-to-eat (RTE) and ready-to-cook (RTC) products which require minimal time and effort to cook is growing quickly due to socio-economic changes, hectic lifestyles, and increased urbanization. Currently, due to the increased health awareness, RTC products with specific health benefits are experiencing high market demand.

Although unripe bananas are recognized for their prebiotic potential, there have been limited efforts to utilize this potential and develop convenient food products from this commodity. This highlights a significant research opportunity in this area to develop convenient foods from unripe bananas through technological interventions to meet public health.

Red banana, Cavendish, Grand Nain, Robusta, and Monthan are popular banana varieties globally, known for their high prebiotic content, including bioactive carbohydrates like RS, fructan, and fiber (Afzal et al., 2022; Pereira & Maraschin, 2015). *Musa* (AAB) cv. Nendran is a popular cultivated variety of banana in South Indian states, especially in Kerala. Nendran is consumed in both raw and ripe form. Nendran attains bunch maturity after 5-6 months from flowering, the long and thick fruits with good keeping quality make unripe Nendran the best option for the preparation of the world-famous Kerala banana chips and as the first weaning food of babies (Chitra, 2015). The ripe Nendran, a popular fruit of Kerala, is widely used to prepare various value-added products and unripe Nendran is still an underutilized commodity. Even though unripe Nendran-derived weaning powders are popular in the market, there have been no value-added products with novel utility developed from this commodity. Despite its prevalence, there are no previous reports on the complete nutritional profile and bioactive carbohydrate content (RS, fructan, & fiber) of Nendran, nor have there been efforts to develop value-added products from its unripe pulp to harness its prebiotic benefits.

Given Nendran's indigenous nature in Kerala, our study aims to explore the complete nutritional profile, bioactive carbohydrates (RS, fiber, fructan), phytochemicals, and value addition scope of Nendran pulp in novel forms. Similarly, unripe Nendran peel is also an underutilized and underexplored commodity. Nendran peel accounts for nearly 35% of the total weight of bananas and is typically discarded as waste. Each year, about 40 million tonnes of peel are generated and the majority of these peels are often dumped away in landfills. A substantial portion of this priceless raw material is wasted due to inefficient agricultural waste management techniques and a lack of awareness. Transforming banana by-products into useful commodities would enhance agricultural development, and market viability of banana pulp-based products and also contribute to a circular economy (Alzate Acevedo et al., 2021; Zou et al., 2022). Even though Nendran peel is consumed traditionally in Nendran prevalence areas and is known for its anti-diabetic potential, but lacks scientific validation. The UN 2030 agenda for sustainable development aims to eliminate food waste and maximize food resources (*Transforming Our World: The 2030 Agenda for Sustainable Development*, n.d.) and our study aligns with this mission.

The present study focused on the extensive phytochemical, nutritional, and prebiotic characterization (bioactive carbohydrates - RS, fructan, fiber) of Nendran peel. Understanding the potential and current scenario of underutilization, through this work, we aim to explain the untapped health potentials of both pulp and peel of unripe Nendran bananas, investigation on its phytochemical profile, and utilization of it in novel forms. These interventions on value addition of a previously underutilized agricultural crop can help in improving the income of farmers and provide nutritious food to consumers as well. Building upon this background, the following objectives have been formulated.

1.4. Objectives

- Value addition of raw Nendran pulp and studies on its nutrient content, bioactive carbohydrates & shelf stability analysis.
- Phytochemical exploration studies of unripe Nendran pulp and product.
- Evaluation of process-induced changes in the RS content of raw pulp, and its relation to GI-GL.
- Phytochemical exploration studies in unripe Nendran peel and evaluation of its anti-inflammatory and α-glucosidase inhibition potential.
- Exploration of bioactive components in banana peel and scope for value addition.

The thesis is organized into 7 chapters and each objective is discussed in detail in the five working chapters.

Chapter **1** gives a general introduction and literature review on bananas, covering their origin, production statistics, post-harvest uses, phytochemicals, and health benefits.

Chapter **2** includes studies on the assessment of the value addition potential of unripe Nendran pulp and the development of a novel product banana grit (BG) from the pulp of unripe Nendran. The novel utilities of grit offer a way to position bananas in a new form rather than conventional weaning food. The chapter also discusses the proximate analysis, bioactive carbohydrate content, mineral composition, and shelf life analysis of the product.

Chapter **3** discusses extensive phytochemical characterization studies conducted in the unripe Nendran pulp as well as BG. The study revealed the presence of carotenoids, β-sitosterol, glycolipids viz. monogalactosyldiacylglycerol (MGDG), digalactosyldiacylglycerol (DGDG), acyl steryl glycosides (ASG) viz. sitoindoside-II, sitoindoside-I, sterylglycoside (β-Sitosterol β-D-glucopyranoside), and glucocerebroside (GC) in BG as well as in pulp. The

present work serves as the first report on the isolation of GC from *Musa* species and also the first report on phytochemical isolation studies from the Nendran cultivar. Literature shows that these compounds have a myriad of health benefits, which emphasize the potential health benefits of BG consumption.

Chapter **4** discusses exclusively studies on the RS content of unripe Nendran pulp and processed-induced changes in it and its relation with GI. This chapter describes the *in vitro* starch hydrolysis and prediction of GI of BG. Further, the GI-GL values of two preparations of BG i.e., BG upma and porridge were assessed at the clinical level in collaboration with Madras Diabetes Research Foundation (MDRF), Chennai and the data showed a high correlation with *in vitro* predicted GI. The data on the RS content of BG was compared with preparations like rice, oats, and chapati, and found that BG preparations contained more RS compared to these items, indicating the nutritional superiority of BG in terms of RS content over these products.

After completing our studies on the pulp, we have focused on the peel, since peel is the major by-product generated during the BG production. Considering its potential application in the functional food industry we have conducted extensive phytochemical and nutrient evaluation of peel which is described in detail in Chapters 5 & 6. Building upon our discovery of GCs from the pulp of Nendran bananas for the first time, we were curious to explore the presence of GCs in banana peel and evaluate their anti-inflammatory properties. The phytochemical exploration studies were conducted in unripe Nendran peel for the isolation of GC (Chapter **5)**. The studies revealed the presence of eighteen molecular species of glucocerebroside containing α- and ω-hydroxy fatty acids from the peel. The GC consortium exhibited remarkable *in vitro* anti-inflammation and α-glucosidase inhibition potential.

Chapter **6** discusses proximate composition and bioactive carbohydrate content in peel. Through this work, we have identified lyophilized raw banana peel as a potent source of bioactive carbohydrates. Lyophilized raw Nendran peel contains RS (18.11 ± 0.06%), dietary fiber (26.87 ± 0.92%), and fructan (1.34 ± 0.31%). The chapter also discusses the *in vitro* immunomodulation properties and α-glucosidase potential of methanol extract of peel. These studies indicate the scope for value addition potential of unripe peel for the development of prebiotic supplements as well as functional food ingredients.

Chapter **7** summarizes the entire work carried out in the thesis.

1.5. References

1. Afzal, M. F., Khalid, W., Akram, S., Khalid, M. A., Zubair, M., Kauser, S., Abdelsamea Mohamedahmed, K., Aziz, A., & Anusha Siddiqui, S. (2022). Bioactive profile and functional food applications of banana in food sectors and health: A review. *International Journal of Food Properties*, *25*(1), 2286–2300. https://doi.org/10.1080/10942912.2022.2130940

2. Agama-Acevedo, E., Islas-Hernandez, J. J., Osorio-Díaz, P., Rendón-Villalobos, R., Utrilla-Coello, R. G., Angulo, O., & Bello-Pérez, L. A. (2009). Pasta with Unripe Banana Flour: Physical, Texture, and Preference Study. *Journal of Food Science*, *74*(6). https://doi.org/10.1111/j.1750-3841.2009.01215.x

3. Agama-Acevedo, E., Islas-Hernández, J. J., Pacheco-Vargas, G., Osorio-Díaz, P., & Bello-Pérez, L. A. (2012). Starch digestibility and glycemic index of cookies partially substituted with unripe banana flour. *LWT-Food Science and Technology*, *46*(1), 177–182. https://www.sciencedirect.com/science/article/pii/S0023643811003367

4. Ahmed, J., Thomas, L., & Khashawi, R. (2020). Influence of hot-air drying and freeze-drying on functional, rheological, structural and dielectric properties of green banana flour and dispersions. *Food Hydrocolloids*, *99*, 105331. https://doi.org/10.1016/j.foodhyd.2019.105331

5. Alzate Acevedo, S., Díaz Carrillo, Á. J., Flórez-López, E., & Grande-Tovar, C. D. (2021). Recovery of banana waste-loss from production and processing: A contribution to a circular economy. *Molecules*, *26*(17), 5282. https://doi.org/10.3390%2Fmolecules26175282

6. Andriani, I., Faridah, D. N., Talitha, Z. A., & Budi, F. S. (2021). Physicochemical characterization of resistant starch type V (RSV) from manggu cassava starch (Manihot esculenta). *Food Research (Malaysia)*. https://agris.fao.org/search/en/providers/122640/records/6511acda401e7bb65a2b5cf5

7. Anyasi, T. A., Jideani, A. I. O., & Mchau, G. R. A. (2013). Functional Properties and Postharvest Utilization of Commercial and Noncommercial Banana Cultivars. *Comprehensive Reviews in Food Science and Food Safety*, *12*(5), 509–522. https://doi.org/10.1111/1541-4337.12025

8. Aparicio-Saguilán, A., Sáyago-Ayerdi, S. G., Vargas-Torres, A., Tovar, J., Ascencio-Otero, T. E., & Bello-Pérez, L. A. (2007). Slowly digestible cookies prepared from resistant starch-rich lintnerized banana starch. *Journal of Food Composition and Analysis*, *20*(3–4), 175–181. https://www.sciencedirect.com/science/article/pii/S0889157506001438

9. *APEDA*. (n.d.). Retrieved July 6, 2024, from https://agriexchange.apeda.gov.in/India%20Production/India_Productions.aspx?cat=fruit&hscode=1042

10. Augustin, L. S., Kendall, C. W., Jenkins, D. J., Willett, W. C., Astrup, A., Barclay, A. W., Björck, I., Brand-Miller, J. C., Brighenti, F., & Buyken, A. E. (2015). Glycemic index, glycemic load and glycemic response: An International Scientific Consensus Summit from the International Carbohydrate Quality Consortium (ICQC). *Nutrition, Metabolism and Cardiovascular Diseases*, *25*(9), 795–815. https://doi.org/10.1016/j.numecd.2015.05.005

11. *Banana Market Review*. (n.d.). https://www.fao.org/markets-and-trade/publications/en/?category=104691

12. Banerjee, R., Pal, P., Patel, R., Godbole, S., Komawar, A., Mudigonda, S., Akki, Y., Gaddam, A., Pasula, N. P., & Joseph, S. (2023). Inflammatory bowel disease (IBD) in rural and urban India: Results from community colonoscopic evaluation of more than 30,000 symptomatic patients. *The Lancet Regional Health-Southeast Asia*, *19*. https://www.thelancet.com/journals/lansea/article/PIIS2772-3682(23)00119-1/fulltext

13. BAPNET. (n.d.). *Musanet.Org*. Retrieved August 7, 2024, from https://musanet.org/regional-networks/bapnet/

14. Barclay, A. W., Augustin, L. S., Brighenti, F., Delport, E., Henry, C. J., Sievenpiper, J. L., Usic, K., Yuexin, Y., Zurbau, A., & Wolever, T. M. (2021). Dietary glycaemic index labelling: A global perspective. *Nutrients*, *13*(9), 3244. https://www.mdpi.com/2072-6643/13/9/3244

15. Bashmil, Y. M., Ali, A., Bk, A., Dunshea, F. R., & Suleria, H. A. (2021). Screening and characterization of phenolic compounds from australian grown bananas and their antioxidant capacity. *Antioxidants*, *10*(10), 1521. https://www.mdpi.com/2076-3921/10/10/1521

16. Batista, A., Silva, R., Cappato, L., Ferreira, M., Nascimento, K., Schmiele, M., Esmerino, E., Balthazar, C., Silva, H., & Moraes, J. (2017). Developing a synbiotic fermented milk using probiotic bacteria and organic green banana flour. *Journal of Functional Foods*, *38*, 242–250. https://doi.org/10.1016/j.jff.2017.09.037

17. Bennett, R. N., Shiga, T. M., Hassimotto, N. M. A., Rosa, E. A. S., Lajolo, F. M., & Cordenunsi, B. R. (2010). Phenolics and Antioxidant Properties of Fruit Pulp and Cell Wall Fractions of Postharvest Banana (Musa acuminata Juss.) Cultivars. *Journal of Agricultural and Food Chemistry*, *58*(13), 7991–8003. https://doi.org/10.1021/jf1008692

18. Berry, C. S. (1986). Resistant starch: Formation and measurement of starch that survives exhaustive digestion with amylolytic enzymes during the determination of dietary fibre. *Journal of Cereal Science*, *4*(4), 301–314. https://www.sciencedirect.com/science/article/pii/S0733521086800340

19. Best, R., Lewis, D. A., & Nasser, N. (1984). The anti-ulcerogenic activity of the unripe plantain banana (Musa species). *British Journal of Pharmacology*, *82*(1), 107. https://www.ncbi.nlm.nih.gov/pmc/articles/PMC1987262/

20. Bezerra, C. V., Rodrigues, A. M. da C., Amante, E. R., & Silva, L. H. M. da. (2013). Nutritional potential of green banana flour obtained by drying in spouted bed. *Revista Brasileira de Fruticultura*, *35*, 1140–1146. https://doi.org/10.1590/S0100-29452013000400025

21. Bhavani, M., Morya, S., Saxena, D., & Awuchi, C. G. (2023). Bioactive, antioxidant, industrial, and nutraceutical applications of banana peel. *International Journal of Food Properties*, *26*(1), 1277–1289. https://doi.org/10.1080/10942912.2023.2209701

22. Bi, Y., Zhang, Y., Jiang, H., Hong, Y., Gu, Z., Cheng, L., Li, Z., & Li, C. (2017). Molecular structure and digestibility of banana flour and starch. *Food Hydrocolloids*, *72*, 219–227. https://www.sciencedirect.com/science/article/pii/S0268005X17303600

23. Biernacka, B., Dziki, D., Różyło, R., & Gawlik-Dziki, U. (2020). Banana powder as an additive to common wheat pasta. *Foods*, *9*(1), 53. https://www.mdpi.com/2304-8158/9/1/53

24. Biliaderis, C. G. (1991). The structure and interactions of starch with food constituents. *Canadian Journal of Physiology and Pharmacology*, *69*(1), 60–78. https://doi.org/10.1139/y91-011. https://doi.org/10.1139/y91-011

25. Bojarczuk, A., Skąpska, S., Khaneghah, A. M., & Marszałek, K. (2022). Health benefits of resistant starch: A review of the literature. *Journal of Functional Foods*, *93*, 105094. https://www.sciencedirect.com/science/article/pii/S1756464622001645

26. Bonavita, G. (EST). (n.d.). *FAOSTAT*. https://www.fao.org/faostat/en/#home

27. Brodkorb, A., Egger, L., Alminger, M., Alvito, P., Assunção, R., Ballance, S., Bohn, T., Bourlieu-Lacanal, C., Boutrou, R., & Carrière, F. (2019). INFOGEST static in vitro simulation of gastrointestinal food digestion. *Nature Protocols*, *14*(4), 991–1014. https://www.nature.com/articles/s41596-018-0119-1

28. Brouns, F., Kettlitz, B., & Arrigoni, E. (2002). Resistant starch and "the butyrate revolution." *Trends in Food Science & Technology*, *13*(8), 251–261. https://www.sciencedirect.com/science/article/pii/S0924224402001310

29. Canfora, E. E., Jocken, J. W., & Blaak, E. E. (2015). Short-chain fatty acids in control of body weight and insulin sensitivity. *Nature Reviews Endocrinology*, *11*(10), 577–591. https://www.nature.com/articles/nrendo.2015.128

30. Carneiro, L., & Leloup, C. (2020). Mens sana in corpore sano: Does the Glycemic Index Have a Role to Play? *Nutrients*, *12*(10), 2989. https://www.mdpi.com/2072-6643/12/10/2989

31. Chang, R., Liu, J., Ji, F., Fu, L., Xu, K., Yang, Y., & Ma, A. (2024). Hypoglycemic effect of recrystallized resistant starch on high-fat diet-and streptozotocin-induced type 2 diabetic mice via gut microbiota modulation. *International Journal of Biological Macromolecules*, *261*, 129812. https://www.sciencedirect.com/science/article/pii/S0141813024006159

32. Chapman-Kiddell, C. A., Davies, P. S., Gillen, L., & Radford-Smith, G. L. (2010). Role of diet in the development of inflammatory bowel disease. *Inflammatory Bowel Diseases*, *16*(1), 137–151. https://academic.oup.com/ibdjournal/article-abstract/16/1/137/4628285

33. Chen, Z., Liang, N., Zhang, H., Li, H., Guo, J., Zhang, Y., Chen, Y., Wang, Y., & Shi, N. (2024). Resistant starch and the gut microbiome: Exploring beneficial interactions and dietary impacts. *Food Chemistry: X*, *21*, 101118. https://www.sciencedirect.com/science/article/pii/S2590157524000051

34. Chitra, P. (2015). Development of banana-based weaning food mixes for infants and its nutritional quality evaluation. *Reviews on Environmental Health*, *30*(2), 125–130. https://doi.org/10.1515/reveh-2015-0002

35. CIRAD. (n.d.). *Working together for tomorrow's agriculture*. CIRAD. Retrieved August 7, 2024, from https://www.cirad.fr/en

36. Costa, R. S., Oliveira, R. F., Henry, F. C., Mello, W. A., & Gaspar, C. R. (2023). Development of prebiotic yogurt with addition of green-banana biomass (Musa spp.). *Anais Da Academia Brasileira de Ciências*, *95*(suppl 1), e20220532. https://doi.org/10.1590/0001-3765202320220532

37. Cummings, J. H., Antoine, J.-M., Azpiroz, F., Bourdet-Sicard, R., Brandtzaeg, P., Calder, P. C., Gibson, G. R., Guarner, F., Isolauri, E., Pannemans, D., Shortt, C., Tuijtelaars, S., & Watzl, B. (2004). Gut health and immunity. *European Journal of Nutrition*, *43*(S2), ii118–ii173. https://doi.org/10.1007/s00394-004-1205-4

38. da Mota, R. V., Lajolo, F. M., Cordenunsi, B. R., & Ciacco, C. (2000). Composition and functional properties of banana flour from different varieties. *Starch-Stärke*, *52*(2-3), 63–68. https://doi.org/10.1002/(SICI)1521-379X(200004)52:2/3%3C63::AID-STAR63%3E3.0.CO;2-V

39. Das, M., Rajan, N., Biswas, P., & Banerjee, R. (2022). A novel approach for resistant starch production from green banana flour using amylopullulanase. *LWT*, *153*, 112391. http://dx.doi.org/10.1016/j.lwt.2021.112391

40. De Bruyne, T., Pieters, L., Deelstra, H., & Vlietinck, A. (1999). Condensed vegetable tannins: Biodiversity in structure and biological activities. *Biochemical Systematics and Ecology*, *27*(4), 445–459. https://www.sciencedirect.com/science/article/pii/S030519789800101X

41. Denham, T. P., Haberle, S. G., Lentfer, C., Fullagar, R., Field, J., Therin, M., Porch, N., & Winsborough, B. (2003). Origins of agriculture at Kuk Swamp in the highlands of New Guinea. *Science*, *301*(5630), 189–193. https://doi.org/10.1126/science.1085255

42. DES,Government of Kerala, D., Government of Kerala. (n.d.). *Agriculture Statistics 2005-2020*. Retrieved July 7, 2024, from https://ecostat.kerala.gov.in/

43. Dibakoane, S. R., Du Plessis, B., Da Silva, L. S., Anyasi, T. A., Emmambux, M. N., Mlambo, V., & Wokadala, O. C. (2023). Nutraceutical Properties of Unripe Banana Flour Resistant Starch: A Review. *Starch - Stärke*, *75*(9–10), 2200041. https://doi.org/10.1002/star.202200041

44. *Digestible and Resistant Starch Assay Kit*. (n.d.). Megazyme. Retrieved February 14, 2024, from https://www.megazyme.com/digestible-and-resistant-starch-assay-kit

45. Dome, K., Podgorbunskikh, E., Bychkov, A., & Lomovsky, O. (2020). Changes in the crystallinity degree of starch having different types of crystal structure after mechanical pretreatment. *Polymers*, *12*(3), 641. https://www.mdpi.com/2073-4360/12/3/641

46. Durrani, C. M., & Donald, A. M. (1995). Physical characterisation of amylopectin gels. *Polymer Gels and Networks*, *3*(1), 1–27. https://www.sciencedirect.com/science/article/pii/096678229400005R

47. Englyst, H. N., & Cummings, J. H. (1985). Digestion of the polysaccharides of some cereal foods in the human small intestine. *The American Journal of Clinical Nutrition*, *42*(5), 778–787. https://www.sciencedirect.com/science/article/pii/S0002916523350184

48. Englyst, H. N., Kingman, S., & Cummings, J. (1992). Classification and measurement of nutritionally important starch fractions. *European Journal of Clinical Nutrition*, *46*, S33-50.

49. Englyst, H., Wiggins, H. S., & Cummings, J. H. (1982). Determination of the non-starch polysaccharides in plant foods by gas-liquid chromatography of constituent sugars as alditol acetates. *Analyst*, *107*(1272), 307–318. https://pubs.rsc.org/en/content/articlehtml/2021/qr/an9820700307

50. Faisant, N., Buléon, A., Colonna, P., Molis, C., Lartigue, S., Galmiche, J. P., & Champ, M. (1995). Digestion of raw banana starch in the small intestine of healthy humans:

Structural features of resistant starch. *British Journal of Nutrition*, *73*(1), 111–123. https://doi.org/10.1079/BJN19950013

51. *FAO-Banana facts*. (n.d.). Retrieved July 6, 2024, from https://www.fao.org/economic/est/est-commodities/oilcrops/bananas/bananafacts/en/

52. *FAOSTAT*. (n.d.). Retrieved January 20, 2024, from https://www.fao.org/faostat/en/#data/QCL/visualize

53. Fida, R., Pramafisi, G., & Cahyana, Y. (2020). Application of banana starch and banana flour in various food product: A review. *IOP Conference Series: Earth and Environmental Science*, *443*(1), 012057. https://doi.org/10.1088/1755-1315/443/1/012057

54. Forster, M., Rodríguez Rodríguez, E., Darias Martín, J., & Díaz Romero, C. (2003). Distribution of nutrients in edible banana pulp. *Food Technology and Biotechnology*, *41*(2), 167–171. https://hrcak.srce.hr/clanak/170260

55. Foster-Powell, K., Holt, S. H., & Brand-Miller, J. C. (2002). International table of glycemic index and glycemic load values: 2002. *The American Journal of Clinical Nutrition*, *76*(1), 5–56. https://hrcak.srce.hr/clanak/170260

56. *FSSAI, 2019*. (n.d.). Retrieved August 19, 2024, from https://www.fssai.gov.in/upload/advisories/2019/06/5d164a5daa382Direction_Advertising_Claims_28_06_2019.pdf

57. Ghosal, S. (1985). Steryl glycosides and acyl steryl glycosides from Musa paradisiaca. *Phytochemistry*, *24*(8), 1807–1810. https://www.sciencedirect.com/science/article/pii/S003194220082556X

58. *GI Foundation*. (n.d.). Retrieved August 19, 2024, from https://www.gisymbol.com/our-mission/

59. *GIFSA*. (n.d.). Welcome to the GI Foundation. Retrieved August 19, 2024, from https://www.gifoundation.com/

60. Giraldo-Gómez, G. I., Rodríguez-Barona, S., & Sanabria-González, N. R. (2019). Preparation of instant green banana flour powders by an extrusion process. *Powder Technology*, *353*, 437–443. http://dx.doi.org/10.1016/j.powtec.2019.05.050

61. Gomes, S., Vieira, B., Barbosa, C., & Pinheiro, R. (2022). Evaluation of mature banana peel flour on physical, chemical, and texture properties of a gluten-free Rissol. *Journal of Food Processing and Preservation*, *46*(8), e14441. https://doi.org/10.1111/jfpp.14441

62. Goñi, I., Garcia-Alonso, A., & Saura-Calixto, F. (1997). A starch hydrolysis procedure to estimate glycemic index. *Nutrition Research*, *17*(3), 427–437. https://doi.org/10.1016/S0271-5317(97)00010-9

63. Granfeldt, Y., Björck, I., Drews, A., & Tovar, J. (1994). An in vitro procedure based on chewing to predict metabolic response to starch in cereal and legume products. *The American Journal of Clinical Nutrition*, *59*(3), 777S-777S. https://www.researchgate.net/profile/Juscelino-Tovar/publication/322285339_

64. Gray, A., & Threlkeld, R. J. (2015). *Nutritional recommendations for individuals with diabetes*. https://europepmc.org/books/nbk279012

65. Guo, J., Tan, L., & Kong, L. (2022). Multiple levels of health benefits from resistant starch. *Journal of Agriculture and Food Research*, *10*, 100380. https://www.sciencedirect.com/science/article/pii/S2666154322001132

66. Haslam, E. (1996). Natural Polyphenols (Vegetable Tannins) as Drugs: Possible Modes of Action. *Journal of Natural Products*, *59*(2), 205–215. https://doi.org/10.1021/np960040+

67. *Healthier Choice Symbol*. (n.d.). Health Promotion Board. Retrieved August 19, 2024, from https://hpb.gov.sg/food-beverage/healthier-choice-symbol

68. Hermansen, K., Rasmussen, O., Gregersen, S., & Larsen, S. (1992). Influence of Ripeness of Banana on the Blood Glucose and Insulin Response in Type 2 Diabetic Subjects. *Diabetic Medicine*, *9*(8), 739–743. https://doi.org/10.1111/j.1464-5491.1992.tb01883.x

69. Hettiaratchi, U. P. K., Ekanayake, S., & Welihinda, J. (2011). Chemical compositions and glycemic responses to banana varieties. *International Journal of Food Sciences and Nutrition*, *62*(4), 307–309. https://doi.org/10.3109/09637486.2010.537254

70. Hoffmann Sardá, F. A., De Lima, F. N. R., Lopes, N. T. T., Santos, A. D. O., Tobaruela, E. D. C., Kato, E. T. M., & Menezes, E. W. (2016). Identification of carbohydrate

parameters in commercial unripe banana flour. *Food Research International*, *81*, 203–209. https://doi.org/10.1016/j.foodres.2015.11.016

71. *Horticulture: Fruits: Banana*. (n.d.). Retrieved July 7, 2024, from https://agritech.tnau.ac.in/horticulture/horti_fruits_banana.html

72. IITA. (n.d.). Banana and plantain crop improvement. *IITA*. Retrieved August 7, 2024, from http://www.iita.org/research/our-research-themes/improving-crops/banana-plantain-crop-improvement/

73. *INIBAP*. (n.d.). Improving the Understanding of Banana. Retrieved August 7, 2024, from http://www.promusa.org/INIBAP

74. Jenkins, D. J., Wolever, T. M., Taylor, R. H., Barker, H., Fielden, H., Baldwin, J. M., Bowling, A. C., Newman, H. C., Jenkins, A. L., & Goff, D. V. (1981). Glycemic index of foods: A physiological basis for carbohydrate exchange. *The American Journal of Clinical Nutrition*, *34*(3), 362–366. https://www.sciencedirect.com/science/article/pii/S000291652342816X

75. Jenkins, P. J., Cameron, R. E., & Donald, A. M. (1993). A Universal Feature in the Structure of Starch Granules from Different Botanical Sources. *Starch - Stärke*, *45*(12), 417–420. https://doi.org/10.1002/star.19930451202

76. Joint, F. (1998). *Carbohydrates in human nutrition*. Report of a Joint FAO/WHO Expert Consultation. (1998). *FAO Food and Nutrition Paper*, *66*, 1–140.

77. Kaur, L., Dhull, S. B., Kumar, P., & Singh, A. (2020). Banana starch: Properties, description, and modified variations - A review. *International Journal of Biological Macromolecules*, *165*, 2096–2102. https://doi.org/10.1016/j.ijbiomac.2020.10.058

78. Khawas, P., & Deka, S. C. (2017). Effect of modified resistant starch of culinary banana on physicochemical, functional, morphological, diffraction, and thermal properties. *International Journal of Food Properties*, *20*(1), 133–150. https://doi.org/10.1080/10942912.2016.1147459

79. Khoza, M., Kayitesi, E., & Dlamini, B. C. (2021). Physicochemical characteristics, microstructure and health promoting properties of green banana flour. *Foods*, *10*(12), 2894. https://doi.org/10.3390/foods10122894

80. Kim, D. (2020). Glycemic index. In *Obesity* (pp. 183–189). Elsevier. https://doi.org/10.1016/B978-0-12-818839-2.00014-4

81. Krishnan, K., & Vijayalakshmi, N. R. (2005). Alterations in lipids & lipid peroxidation in rats fed with flavonoid rich fraction of banana (Musa paradisiaca) from high background radiation area. *Indian Journal of Medical Research*, *122*(6), 540. https://citeseerx.ist.psu.edu/document?repid=rep1&type=pdf&doi=cb084fae5dbba7776e381bfe7c39318893bf630c

82. Kumar, P. S., Saravanan, A., Sheeba, N., & Uma, S. (2019). Structural, functional characterization and physicochemical properties of green banana flour from dessert and plantain bananas (Musa spp.). *LWT*, *116*, 108524. http://dx.doi.org/10.1016/j.lwt.2019.108524

83. Lairon, D., & Amiot, M. J. (1999). Flavonoids in food and natural antioxidants in wine. *Current Opinion in Lipidology*, *10*(1), 23–28. https://journals.lww.com/co-lipidology/abstract/1999/02000/Flavonoids_in_food_and_natural_antioxidants_in.5.aspx

84. LeBlanc, J. G., Chain, F., Martín, R., Bermúdez-Humarán, L. G., Courau, S., & Langella, P. (2017). Beneficial effects on host energy metabolism of short-chain fatty acids and vitamins produced by commensal and probiotic bacteria. *Microbial Cell Factories*, *16*(1), 79. https://doi.org/10.1186/s12934-017-0691-z

85. Lehmann, U., & Robin, F. (2007). Slowly digestible starch–its structure and health implications: A review. *Trends in Food Science & Technology*, *18*(7), 346–355. https://www.sciencedirect.com/science/article/pii/S0924224407000817

86. Lejju, B. J., Robertshaw, P., & Taylor, D. (2006). Africa's earliest bananas? *Journal of Archaeological Science*, *33*(1), 102–113. https://www.sciencedirect.com/science/article/pii/S030544030500155X

87. Lewis, D. A., Fields, W. N., & Shaw, G. P. (1999). A natural flavonoid present in unripe plantain banana pulp (Musa sapientum L. var. Paradisiaca) protects the gastric mucosa from aspirin-induced erosions. *Journal of Ethnopharmacology*, *65*(3), 283–288. https://www.sciencedirect.com/science/article/pii/S0378874199000057

88. Li, C., Hu, Y., Li, S., Yi, X., Shao, S., Yu, W., & Li, E. (2023). Biological factors controlling starch digestibility in human digestive system. *Food Science and Human Wellness*, *12*(2), 351–358. https://www.sciencedirect.com/science/article/pii/S2213453022001495

89. Lim, Y. Y., Lim, T. T., & Tee, J. J. (2007). Antioxidant properties of several tropical fruits: A comparative study. *Food Chemistry*, *103*(3), 1003–1008. https://www.sciencedirect.com/science/article/pii/S0308814606007825

90. Lockyer, S., & Nugent, A. (2017). Health effects of resistant starch. *Nutrition Bulletin*, *42*(1), 10–41. https://doi.org/10.1111/nbu.12244

91. Lopes, S., Borges, C. V., de Sousa Cardoso, S. M., de Almeida Pereira da Rocha, M. F., & Maraschin, M. (2020). Banana (Musa spp.) as a source of bioactive compounds for health promotion. *Handbook of Banana Production, Postharvest Science, Processing Technology, and Nutrition*, 227–244. http://dx.doi.org/10.1002/9781119528265.ch12

92. Marichelvam, M. K., Jawaid, M., & Asim, M. (2019). Corn and rice starch-based bio-plastics as alternative packaging materials. *Fibers*, *7*(4), 32. https://www.mdpi.com/2079-6439/7/4/32. https://www.mdpi.com/2079-6439/7/4/32

93. Marta, H., Cahyana, Y., Djali, M., Arcot, J., & Tensiska, T. (2019). A comparative study on the physicochemical and pasting properties of starch and flour from different banana *(Musa spp.)* cultivars grown in Indonesia. *International Journal of Food Properties*, *22*(1), 1562–1575. https://doi.org/10.1080/10942912.2019.1657447

94. Mattila, P., Hellström, J., & Törrönen, R. (2006). Phenolic Acids in Berries, Fruits, and Beverages. *Journal of Agricultural and Food Chemistry*, *54*(19), 7193–7199. https://doi.org/10.1021/jf0615247

95. McCleary, B. V., McLoughlin, C., Charmier, L. M. J., & McGeough, P. (2020). Measurement of available carbohydrates, digestible, and resistant starch in food ingredients and products. *Cereal Chemistry*, *97*(1), 114–137. https://doi.org/10.1002/cche.10208

96. Morais, M. B., Feste, A., Miller, R. G., & Lifschitz, C. H. (1996). Effect of resistant and digestible starch on intestinal absorption of calcium, iron, and zinc in infant pigs. *Pediatric Research*, *39*(5), 872–876. https://www.nature.com/articles/pr19962541

97. Nadeeshani, H., Samarasinghe, G., Silva, R., Hunter, D., & Madhujith, T. (2021). Proximate composition, fatty acid profile, vitamin and mineral content of selected banana varieties grown in Sri Lanka. *Journal of Food Composition and Analysis*, *100*, 103887. https://www.sciencedirect.com/science/article/pii/S0889157521000879

98. *NHB-BANANA*. (n.d.). Retrieved July 7, 2024, from https://nhb.gov.in/report_files/banana/BANANA.htm

99. Nida, S., Moses, J. A., & Anandharamakrishnan, C. (2023). Converting fruit waste to 3D printed food package casings: The case of banana peel. *Circular Economy*, *2*(1), 100023. https://doi.org/10.1016/j.cec.2022.100023

100. Nimsung, P., Thongngam, M., & Naivikul, O. (2007). Compositions, morphological and thermal properties of green banana flour and starch. *Agriculture and Natural Resources*, *41*(5), 324–330. https://www.thaiscience.info/journals/Article/TKJN/10471511.pdf

101. Nugent, A. P. (2005). Health properties of resistant starch. *Nutrition Bulletin*, *30*(1), 27–54. https://doi.org/10.1111/j.1467-3010.2005.00481.x

102. Oladele, E.-O., & Williamson, G. (2016). Impact of resistant starch in three plantain (Musa AAB) products on glycaemic response of healthy volunteers. *European Journal of Nutrition*, *55*, 75–81. https://doi.org/10.1007/s00394-014-0825-6

103. Oliveira, L., Freire, C., Silvestre, A., Cordeiro, N., Torres, I., & Evtuguin, D. (2006). Lipophilic extractives from different morphological parts of banana plant "Dwarf Cavendish." *Industrial Crops and Products*, *23*(2), 201–211. https://doi.org/10.1016/j.indcrop.2005.06.003

104. Osuji, J. O., Okoli, B. E., Vuylsteke, D., & Ortiz, R. (1997). Multivariate pattern of quantitative trait variation in triploid banana and plantain cultivars. *Scientia Horticulturae*, *71*(3–4), 197–202. https://www.sciencedirect.com/science/article/pii/S0304423897001015

105. Oupathumpanont, O., & Wisansakkul, S. (2021). Glutenfree Pasta Products with Improved Nutritional Profile by Using Banana Flour. *Journal of Food and Nutrition Research*, *9*(6), 313–320. http://dx.doi.org/10.12691/jfnr-9-6-7

106. Ovando-Martinez, M., Sáyago-Ayerdi, S., Agama-Acevedo, E., Goñi, I., & Bello-Pérez, L. A. (2009). Unripe banana flour as an ingredient to increase the undigestible carbohydrates of pasta. *Food Chemistry*, *113*(1), 121–126. https://doi.org/10.1016/j.foodchem.2008.07.035

107. Pannangpetch, P., Vuttivirojana, A., Kularbkaew, C., Tesana, S., Kongyingyoes, B., & Kukongviriyapan, V. (2001). The antiulcerative effect of Thai *Musa* species in rats. *Phytotherapy Research*, *15*(5), 407–410. https://doi.org/10.1002/ptr.766

108. Pelissari, F. M., Andrade-Mahecha, M. M., Sobral, P. J. do A., & Menegalli, F. C. (2012). Isolation and characterization of the flour and starch of plantain bananas (Musa paradisiaca). *Starch-Stärke*, *64*(5), 382–391. https://doi.org/10.1002/star.201100133

109. Pereira, A., & Maraschin, M. (2015). Banana (Musa spp) from peel to pulp: Ethnopharmacology, source of bioactive compounds and its relevance for human health. *Journal of Ethnopharmacology*, *160*, 149–163. https://doi.org/10.1016/j.jep.2014.11.008

110. Perin, D., & Murano, E. (2017). Starch Polysaccharides in the Human Diet: Effect of the Different Source and Processing on its Absorption. *Natural Product Communications*, *12*(6), 1934578X1701200. https://doi.org/10.1177/1934578X1701200606

111. Phirom-on, K., & Apiraksakorn, J. (2021). Development of cellulose-based prebiotic fiber from banana peel by enzymatic hydrolysis. *Food Bioscience*, *41*, 101083. https://www.sciencedirect.com/science/article/pii/S221242922100208X

112. Pongmalai, P., & Devahastin, S. (2020). Profiles of prebiotic fructooligosaccharides, inulin and sugars as well as physicochemical properties of banana and its snacks as affected by ripening stage and applied drying methods. *Drying Technology*, *38*(5–6), 724–734. https://doi.org/10.1080/07373937.2019.1700517

113. Prabha, P., Karpagam, T., Varalakshmi, B., & Packiavathy, A. S. C. (2011). Indigenous anti-ulcer activity of Musa sapientum on peptic ulcer. *Pharmacognosy Research*, *3*(4), 232. https://www.ncbi.nlm.nih.gov/pmc/articles/PMC3249781/

114. Raben, A., Tagliabue, A., Christensen, N. J., Madsen, J., Holst, J. J., & Astrup, A. (1994). Resistant starch: The effect on postprandial glycemia, hormonal response, and satiety. *The American Journal of Clinical Nutrition*, *60*(4), 544–551. https://www.sciencedirect.com/science/article/pii/S0002916523184760

115. Regina, A., Kosar-Hashemi, B., Ling, S., Li, Z., Rahman, S., & Morell, M. (2010). Control of starch branching in barley defined through differential RNAi suppression of starch branching enzyme IIa and IIb. *Journal of Experimental Botany*, *61*(5), 1469–1482. https://academic.oup.com/jxb/article-abstract/61/5/1469/443185

116. Ren, X., Chen, J., Molla, M. M., Wang, C., Diao, X., & Shen, Q. (2016). In vitro starch digestibility and in vivo glycemic response of foxtail millet and its products. *Food & Function*, *7*(1), 372–379. https://doi.org/10.1039/c5fo01074h

117. Ritthiruangdej, P., Parnbankled, S., Donchedee, S., & Wongsagonsup, R. (2011). Physical, chemical, textural and sensory properties of dried wheat noodles supplemented with unripe banana flour. *Agriculture and Natural Resources*, *45*(3), 500–509. https://www.academia.edu/download/73858517/Physical_Chemical_Textural_and_Sensory_P20211030-18373-1dqr8e.pdf

118. Rosado, C. P., Rosa, V. H. C., Martins, B. C., Soares, A. C., Almo, A., Monteiro, E. B., Mulder, A. da R. P., Moura-Nunes, N., & Daleprane, J. B. (2021). Green banana flour supplementation improves obesity-associated systemic inflammation and regulates gut microbiota profile in mice fed high-fat diets. *Applied Physiology, Nutrition, and Metabolism*, *46*(12), 1469–1475. https://doi.org/10.1139/apnm-2021-0288

119. Saifullah, R., Abbas, F., Yeoh, S., & Azhar, M. (2009). Utilization of green banana flour as a functional ingredient in yellow noodle. *International Food Research Journal*, *16*(3), 373–379. http://www.ifrj.upm.edu.my/16%20%283%29%202009/10%5B1%5D%20Saifullah.pdf

120. Segain, J. P., De La Blétiere, D. R., Bourreille, A., Leray, V., Gervois, N., Rosales, C., Ferrier, L., Bonnet, C., Blottiere, H. M., & Galmiche, J. P. (2000). Butyrate

inhibits inflammatory responses through NFκB inhibition: Implications for Crohn's disease. *Gut*, *47*(3), 397–403. https://gut.bmj.com/content/47/3/397.abstract

121. Segura-Badilla, O., Kammar-García, A., Mosso-Vázquez, J., Ávila-Sosa Sánchez, R., Ochoa-Velasco, C., Hernández-Carranza, P., & Navarro-Cruz, A. R. (2022). Potential use of banana peel (Musa cavendish) as ingredient for pasta and bakery products. *Heliyon*, *8*(10), e11044. https://doi.org/10.1016/j.heliyon.2022.e11044

122. Seung, D. (2020). Amylose in starch: Towards an understanding of biosynthesis, structure and function. *New Phytologist*, *228*(5), 1490–1504. https://doi.org/10.1111/nph.16858

123. Shalini, R., Abinaya, G., Saranya, P., & Antony, U. (2017). Growth of selected probiotic bacterial strains with fructans from Nendran banana and garlic. *LWT-Food Science and Technology*, *83*, 68–78. https://www.sciencedirect.com/science/article/pii/S0023643817302141

124. Shalini, R., & Antony, U. (2015). Fructan distribution in banana cultivars and effect of ripening and processing on Nendran banana. *Journal of Food Science and Technology*, *52*, 8244–8251. ttps://doi.org/10.1007%2Fs13197-015-1927-8

125. Siji, S., & Nandini, P. V. (2017). Chemical and nutrient composition of selected banana varieties of Kerala. *International Journal of Advanced Engineering, Management and Science*, *3*(4), 239829. https://www.neliti.com/publications/239829/chemical-and-nutrient-composition-of-selected-banana-varieties-of-kerala

126. Singh, B., Singh, J. P., Kaur, A., & Singh, N. (2016). Bioactive compounds in banana and their associated health benefits–A review. *Food Chemistry*, *206*, 1–11. https://doi.org/10.1016/j.foodchem.2016.03.033

127. Singh, J., Dartois, A., & Kaur, L. (2010). Starch digestibility in food matrix: A review. *Trends in Food Science & Technology*, *21*(4), 168–180. https://www.sciencedirect.com/science/article/pii/S0924224409003008

128. Singh, R. K., Chang, H.-W., Yan, D., Lee, K. M., Ucmak, D., Wong, K., Abrouk, M., Farahnik, B., Nakamura, M., Zhu, T. H., Bhutani, T., & Liao, W. (2017). Influence

of diet on the gut microbiome and implications for human health. *Journal of Translational Medicine*, *15*(1), 73. https://doi.org/10.1186/s12967-017-1175-y

129. Singh, R., Kaushik, R., & Gosewade, S. (2018). Bananas as underutilized fruit having huge potential as raw materials for food and non-food processing industries: A brief review. *The Pharma Innovation Journal*, *7*(6), 574–580.

130. Smith, P. M., Howitt, M. R., Panikov, N., Michaud, M., Gallini, C. A., Bohlooly-Y, M., Glickman, J. N., & Garrett, W. S. (2013). The Microbial Metabolites, Short-Chain Fatty Acids, Regulate Colonic Treg Cell Homeostasis. *Science*, *341*(6145), 569–573. https://doi.org/10.1126/science.1241165

131. Sothornvit, R., & Pitak, N. (2007). Oxygen permeability and mechanical properties of banana films. *Food Research International*, *40*(3), 365–370. http://dx.doi.org/10.1016/j.foodres.2006.10.010

132. Southgate, D. A. T. (1969a). Determination of carbohydrates in foods. I.—Available carbohydrate. *Journal of the Science of Food and Agriculture*, *20*(6), 326–330. https://doi.org/10.1002/jsfa.2740200602

133. Southgate, D. A. T. (1969b). Determination of carbohydrates in foods II.—Unavailable carbohydrates. *Journal of the Science of Food and Agriculture*, *20*(6), 331–335. https://doi.org/10.1002/jsfa.2740200603

134. Sreejith, P., & Sabu, M. (2017). *Edible Bananas of South India: Taxonomy & Phytochemistry*. Indian Association for Angiosperm Taxonomy.

135. Sulaiman, S. F., Yusoff, N. A. M., Eldeen, I. M., Seow, E. M., Sajak, A. A. B., & Ooi, K. L. (2011). Correlation between total phenolic and mineral contents with antioxidant activity of eight Malaysian bananas (Musa sp.). *Journal of Food Composition and Analysis*, *24*(1), 1–10. http://dx.doi.org/10.1016%2Fj.jfca.2010.04.005

136. Suntharalingam, S., & Ravindran, G. (1993). Physical and biochemical properties of green banana flour. *Plant Foods for Human Nutrition*, *43*, 19–27. https://doi.org/10.1007/BF01088092

137. *Taiwan Banana Research Institute—TBRI | Improving the understanding of banana*. (n.d.). Retrieved August 7, 2024, from https://promusa.org/Taiwan+Banana+Research+Institute+-+TBRI

138. Tako, M., Tamaki, Y., Teruya, T., & Takeda, Y. (2014). The principles of starch gelatinization and retrogradation. *Food and Nutrition Sciences*, *2014*. https://www.scirp.org/html/6-2701086_42262.htm

139. Talengera, D. (n.d.). *The biology of bananas*. Retrieved February 12, 2024, from https://docplayer.net/20913279-The-biology-of-bananas-and-plantains.html

140. Tester, R. F., Karkalas, J., & Qi, X. (2004). Starch—Composition, fine structure and architecture. *Journal of Cereal Science*, *39*(2), 151–165. https://www.sciencedirect.com/science/article/pii/S0733521003001139

141. Thanyapanich, N., Jimtaisong, A., & Rawdkuen, S. (2021). Functional Properties of Banana Starch (Musa spp.) and Its Utilization in Cosmetics. *Molecules*, *26*(12), Article 12. https://doi.org/10.3390/molecules26123637

142. Tharanathan, R. N. (2002). Food-Derived Carbohydrates—Structural Complexity and Functional Diversity. *Critical Reviews in Biotechnology*, *22*(1), 65–84. https://doi.org/10.1080/07388550290789469

143. Tolhurst, G., Heffron, H., Lam, Y. S., Parker, H. E., Habib, A. M., Diakogiannaki, E., Cameron, J., Grosse, J., Reimann, F., & Gribble, F. M. (2012). Short-chain fatty acids stimulate glucagon-like peptide-1 secretion via the G-protein–coupled receptor FFAR2. *Diabetes*, *61*(2), 364–371. https://diabetesjournals.org/diabetes/article-abstract/61/2/364/14608

144. Topping, D. L., Fukushima, M., & Bird, A. R. (2003). Resistant starch as a prebiotic and synbiotic: State of the art. *Proceedings of the Nutrition Society*, *62*(1), 171–176. https://doi.org/10.1079/pns2002224

145. *Transforming our world: The 2030 Agenda for Sustainable Development*. (n.d.). Retrieved July 29, 2024, from https://sdgs.un.org/2030agenda

146. Tribess, T. B., Hernández-Uribe, J. P., Méndez-Montealvo, M. G. C., Menezes, E. W., Bello-Perez, L. A., & Tadini, C. C. (2009). Thermal properties and resistant starch content of green banana flour (Musa cavendishii) produced at different drying

conditions. *LWT - Food Science and Technology*, *42*(5), 1022–1025. https://doi.org/10.1016/j.lwt.2008.12.017

147. Trinidad, T. P., Wolever, T. M., & Thompson, L. U. (1996). Effect of acetate and propionate on calcium absorption from the rectum and distal colon of humans. *The American Journal of Clinical Nutrition*, *63*(4), 574–578. https://www.sciencedirect.com/science/article/pii/S0002916523192549

148. Tudorică, C. M., Kuri, V., & Brennan, C. S. (2002). Nutritional and Physicochemical Characteristics of Dietary Fiber Enriched Pasta. *Journal of Agricultural and Food Chemistry*, *50*(2), 347–356. https://doi.org/10.1021/jf0106953

149. Udenfriend, S., Lovenberg, W., & Sjoerdsma, A. (1959). Physiologically active amines in common fruits and vegetables. *Archives of Biochemistry and Biophysics*, *85*(2), 487–490. https://www.sciencedirect.com/science/article/pii/0003986159905168

150. Urooj, A., & Puttraj, Sh. (1999). Digestibility index and factors affecting rate of starch digestion in vitro in conventional food preparation. *Nahrung / Food*, *43*(1), 42–47. https://doi.org/10.1002/(SICI)1521-3803(19990101)43:1<42::AID-FOOD42>3.0.CO;2-Q

151. Vijayakumar, S., Presannakumar, G., & Vijayalakshmi, N. R. (2009). Investigations on the Effect of Flavonoids from Banana, *Musa Paradisiaca* L. on Lipid Metabolism in Rats. *Journal of Dietary Supplements*, *6*(2), 111–123. https://doi.org/10.1080/19390210902861825

152. Villaverde, J. J., Oliveira, L., Vilela, C., Domingues, R. M., Freitas, N., Cordeiro, N., Freire, C. S., & Silvestre, A. J. (2013). High valuable compounds from the unripe peel of several Musa species cultivated in Madeira Island (Portugal). *Industrial Crops and Products*, *42*, 507–512. https://www.sciencedirect.com/science/article/pii/S0926669012003597

153. Wall, M. M. (2006). Ascorbic acid, vitamin A, and mineral composition of banana (Musa sp.) and papaya (Carica papaya) cultivars grown in Hawaii. *Journal of Food Composition and Analysis*, *19*(5), 434–445. https://www.sciencedirect.com/science/article/pii/S088915750600007X

154. Wang, S., Li, C., Copeland, L., Niu, Q., & Wang, S. (2015). Starch Retrogradation: A Comprehensive Review. *Comprehensive Reviews in Food Science and Food Safety*, *14*(5), 568–585. https://doi.org/10.1111/1541-4337.12143

155. Wu, R., Tang, X., Kang, X., Luo, Y., Wang, L., Li, J., Wu, X., & Liu, D. (2019). Effect of a Chinese medical nutrition therapy diet on gut microbiota and short chain fatty acids in the simulator of the human intestinal microbial ecosystem (SHIME). *Journal of Functional Foods*, *62*, 103555. https://www.sciencedirect.com/science/article/pii/S1756464619304797

156. Yi, D., Maike, W., Yi, S., Xiaoli, S., Dianxing, W., & Wenjian, S. (2021). Physiochemical Properties of Resistant Starch and Its Enhancement Approaches in Rice. *Rice Science*, *28*(1), 31–42. https://doi.org/10.1016/j.rsci.2020.11.005

157. Younes, H., Levrat, M., Demigné, C., & Rémésy, C. (1995). Resistant starch is more effective than cholestyramine as a lipid-lowering agent in the rat. *Lipids*, *30*(9), 847–853. https://doi.org/10.1007/BF02533961

158. Zaini, H. B. M., Sintang, M. D. B., & Pindi, W. (2020). The roles of banana peel powders to alter technological functionality, sensory and nutritional quality of chicken sausage. *Food Science & Nutrition*, *8*(10), 5497–5507. https://doi.org/10.1002%2Ffsn3.1847

159. Zandonadi, R. P., Botelho, R. B. A., Gandolfi, L., Ginani, J. S., Montenegro, F. M., & Pratesi, R. (2012). Green banana pasta: An alternative for gluten-free diets. *Journal of the Academy of Nutrition and Dietetics*, *112*(7), 1068–1072. https://www.sciencedirect.com/science/article/pii/S221226721200473X

160. Zheng, Z., Stanley, R., Gidley, M. J., & Dhital, S. (2016). Structural properties and digestion of green banana flour as a functional ingredient in pasta. *Food & Function*, *7*(2), 771–780. https://doi.org/10.1039/C5FO01156F

161. Zou, F., Tan, C., Zhang, B., Wu, W., & Shang, N. (2022). The valorization of banana by-products: Nutritional composition, bioactivities, applications, and future development. *Foods*, *11*(20), 3170. https://doi.org/10.3390%2Ffoods11203170

Chapter 2

Value addition of raw Nendran pulp and studies on its nutrient content, bioactive carbohydrates & shelf stability analysis

2.1. Introduction

2.1.1. *Musa* (AAB) cv. Nendran

Raw banana *Musa* (AAB) cv. Nendran (Fig. 2.1.) is a popular cultivated variety of *banana* in South Indian states (Tamil Nadu, Kerala, Karnataka), and elsewhere in the world. 'Nendran' has different names in various parts of the world, such as 'Rejeli' in North Indian states, 'French plantain/Horn plantain' in England, 'Hooru plantain' in Denmark, 'Banana cent livers' in France, 'Pisang feige/Hornfeermige' in Germany, 'Pisang candi' in Indonesia, 'Pisang lang/Pisang Nangka/Pisang ton dok' in Malaysia, 'Bhangoaisan' in the Philippines, and 'Kluai nga chang' in Thailand (Sreejith & Sabu, 2017).

Fig. 2.1. Nendran habit with mature infructescence

A mature unripe Nendran infructescence weighs approximately 12-15 kg with 4-6 hands, around 9 kg of pulp, and 4.5 kg of peel. Nendran attains bunch maturity after 5-6 months from flowering, the long and thick fruits with good keeping quality make unripe Nendran the best option for the preparation of the world-famous Kerala banana chips (Chitra, 2015). The

Nendran fruits are large, and thick (20-27 cm long and 14-18 cm circumference) with a thick-leathery peel having three prominent ridges and a distinct nipple. The interior colour of the fruit will remain creamy, and yellowish when it is raw and eventually turns yellowish orange during ripening, simultaneously the peel colour also turns yellow. When the peel is green, the flavour of the pulp is bland and its texture is starchy, as the peel changes to yellow, brown to black, the sweetness increases, and the texture becomes soft (Sreejith & Sabu, 2017).

2.1.2. Cultivation practices of Nendran banana

Banana is mainly cultivated in tropical humid lowlands and is grown from the sea level to 1000 m above mean sea level. Soil with good fertility and an assured supply of moisture is best suited for banana cultivation. Nendran is cultivated as both a rainfed and irrigated crop. The recommended spacing for Nendran bananas is 2.0 × 2.0 meters, with a planting density of 2500 suckers per hectare. Organic manures like vermicompost (2 kg/pit), groundnut cake/neem cake (1 kg/pit), farm yard manure (FYM-10 kg/plant), nitrogen-phosphorous-potassium (NPK) biofertilizer-Plant Growth Promoting Rhizobacteria (PGPR-mixture, 50-100 g/pit) are usually applied at the time of planting. The additional nutrient requirement for Nendran during the growing period includes FYM/Compost: 20 kg, rock phosphate: 200, and ash: 1 kg. These nutrients were applied in two equal split doses in the 2^{nd} and 4^{th} months after planting. Nendran bananas planted in October under deep water table conditions need specific irrigation practices. They require nearly 40 L of irrigation per plant once every two days during the summer season for higher bunch yield. Nendran bananas are vulnerable to pests like the banana pseudostem weevil and diseases like Sigatoka leaf spot. Management practices include field sanitation, swabbing mud slurry around the pseudostem, and using entomopathogens for pest control. For diseases, burning affected leaves and employing bioagents are usually practiced (*Organic_production_of_banana.Pdf*, n.d.; *VFPCK* -, n.d.).

2.1.3. Nendran clones and traditional uses of Nendran

Nendran has many cultivated varieties (clones) including Manjeri Nendran (early maturing), Kaliyethan (common variety in Thiruvananthapuram district), Quintal Nendran (high-yielding), Attu Nendran (tall variety, long fruits), Chengazhikkodan (fruits are tasty and golden yellow in colour), Nedunendran (fruits are bigger, high-yielding), Mindoli (late maturing, fruits are bigger), Mettuppalayam (tall variety, high yielding, long duration), Zanzibar (very big fruits, with two or three hands in a bunch), Attunendran (suitable for rain-fed crop). Among them, Chengalikodan is a very popular variety of Thrissur, that has conferred the geographical indication tag and is known for its unique shape, red spots on the peel, colour, and taste (Fig.

2.2.). This particular variety of Nendran was given as an offering to lord Krishna in Guruvayoor Temple during the festival of Onam, hence of great religious significance(Sreejith & Sabu, 2017; *VFPCK* -, n.d.).

Fig. 2.2. Ripe Chengalikodan banana

(Source: https://english.mathrubhumi.com/features/agriculture/soil-quality-increased-value-of-chengalikodan-bananas-1.5257602)

Ripe Nendran bananas were used for the preparation of halwa, payasam, and various snacks showcasing their versatility and culinary appeal. However, the unripe Nendran has yet to garner recognition in the public domain and remains as an underutilized commodity. Traditionally, it is used for making banana chips, as a weaning food for babies, and in selected culinary dishes (Fig. 2.3.). Apart from its use as a weaning food, no other value-added products derived from unripe Nendran pulp with novel applications are available in the market. So far, no efforts have been made to harness the prebiotic benefit of Nendran and its utilization in novel forms.

Fig. 2.3. Traditional preparations of unripe Nendran banana

(Sources:https://keralahypermarketonline.com/product/banana-chips-500-gms/, http://www.lincyscookart.com/2015/08/vazhakka-thoran-raw-banana-thoran.html, https://www.myforkinglife.com/green-banana-porridge/)

2.2. Objectives

Given the Indigenous nature of Nendran in Kerala and understanding the current scenario of underutilization, our study aims to explore the nutritional profile, bioactive carbohydrates content, value addition scope of Nendran pulp, and the development of novel products from the commodity and its characterization studies. From this background, the following objectives were formulated.

- Evaluation of proximate composition and bioactive carbohydrate content (dietary fiber content and fructan) of unripe pulp.
- Development of novel products from unripe Nendran pulp.
- Product optimization and diversification studies.
- Analysis of proximate composition and bioactive carbohydrate content of the product.
- Estimation of total carotenoid content, mineral composition, and shelf life analysis of product.

2.3. Materials and methods

2.3.1. Chemicals and standards

The HPLC grade solvents were purchased from Merck Life Science Pvt Ltd (Mumbai, India). The carotenoid HPLC standard (β-carotene - catalogue no. C4582-10MG) was procured from Sigma-Aldrich, India. Potato dextrose agar (GM096-500G), nutrient agar (M0871-500G), agar powder (GRM026-500G), and peptone (RM-001) were procured from Hi-media. The Total Dietary Fiber Assay Kit (K-TDFR) and Fructan Assay Kit (K-FRU) were procured from Megazyme Ltd., Ireland. Other reagents used were of standard analytical grade.

2.3.2. Voucher specimen deposition

The voucher specimen of Nendran (*Musa* (AAB) cv. Nendran) was collected on 15th May 2019 from local organic farmers in Vellayani, Ookode (8°25'54.3"N 77°00'14.8"E) Thiruvananthapuram District, Kerala, India. The specimen was identified and deposited at the Herbarium of Jawaharlal Nehru Tropical Botanic Garden & Research Institute Thiruvananthapuram, Kerala, India (TBGT voucher number: TBGT 94628, Fig. 2.4.).

Fig. 2.4. Voucher specimen of Nendran

2.3.3. Raw material collection

The mature unripe Nendran banana (16.32 kg) of 150 days of maturity from flowering, was purchased from 'Nostalgia-organic farm' in Vellayani, Ookode, Thiruvananthapuram, Kerala. The collected raw material was used for the studies discussed in chapters 2 & 3. The images of Nendran banana habit, infructescence, and different stages of maturity are shown in Fig. 2.5.

2.3.4. Proximate analysis of unripe pulp

The moisture, fat, protein, ash, and carbohydrate content of BG was determined according to AOAC Method, 1990 (*AOAC: Official Methods of Analysis (Volume 1)*, n.d.).

2.3.4.1. Moisture content

The moisture content was determined by the oven-drying method. The sample (5 g) was kept in the oven at 105 ˚C for 3 hours until a constant weight was obtained.

2.3.4.2. Fat content

Fat content in samples was determined by using the Soxhlet extraction method. The sample (5 g) was packed in a paper thimble and extracted with 300 mL of hexane at 40 °C for 6 hours.

2.3.4.3. Protein content

The total protein content was determined using the Kjeldhal method and total protein content was calculated using the conversion factor (6.25).

2.3.4.4. Ash content

The sample (5 g) was placed on a Bunsen burner for charring, the charred sample was then incinerated in a muffle furnace at 550 °C for 24 hours.

2.3.4.5. Carbohydrate content

The carbohydrate content of the sample was calculated by the difference of mean values of moisture, protein, fat, and ash from hundred.

Total carbohydrates (%) = 100 - (Moisture + Protein + Fat + Ash)

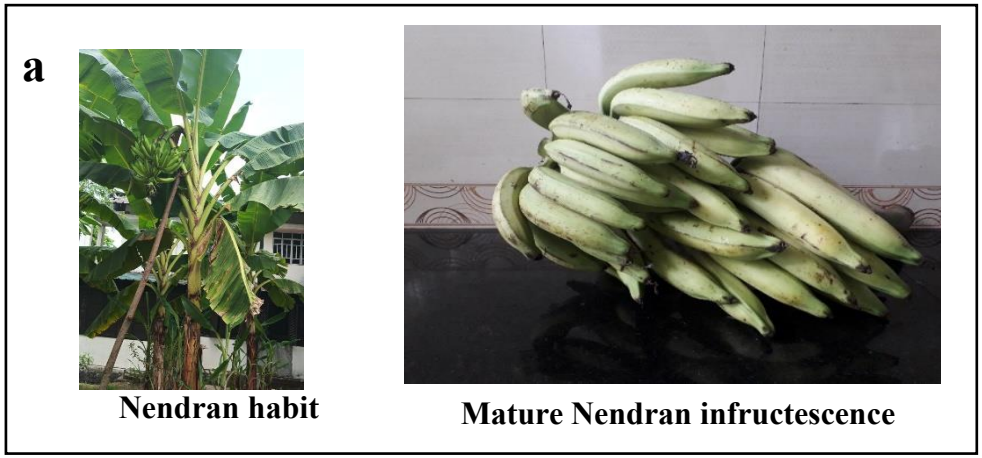

Fig. 2.5. a-e. Nendran habit, mature Nendran infructescence & different stages of maturity of Nendran banana

2.3.5. Estimation of total dietary fiber (TDF) content of unripe pulp

Unripe pulp's TDF content was estimated using the Megazyme Total Dietary Fiber Assay Kit (K-TDFR). The method is based on AACC method 32-05.01 and AOAC Method 985.29. The assay was conducted according to the manufacturer's instructions. The TDF content was determined by treating the sample (1 g, in 40 mL of 2-(N-morpholino) ethanesulfonic acid-tris(hydroxymethyl)aminomethane (MES-TRIS) buffer solution, pH 8.2) with heat stable α-amylase (50 µL, 3000 U/mL) at 100 °C to gelatinize, hydrolyze and depolymerize the starch. Further, the sample was incubated at 60 °C with protease (100 µL, 50 mg/mL; ~ 350 tyrosine U/mL) to solubilize and depolymerize proteins. Then following the addition of amyloglucosidase (200 µL, 3300 U/mL) to hydrolyze starch fragments into glucose; four volumes of ethanol were then added to precipitate soluble fiber and eliminate depolymerized protein and glucose. The solution was passed through a Gooch crucible containing celite. The residue was washed with acetone, 95% ethanol, and 78% ethanol. It was then dried and weighed. Further, one sample was used to assess the protein content and the other one was used for measuring the ash content (*Total Dietary Fiber Assay Kit*, n.d.). The TDF is calculated by the weight of the dried residue less the weight of the protein and ash (Scheme 2.1.).

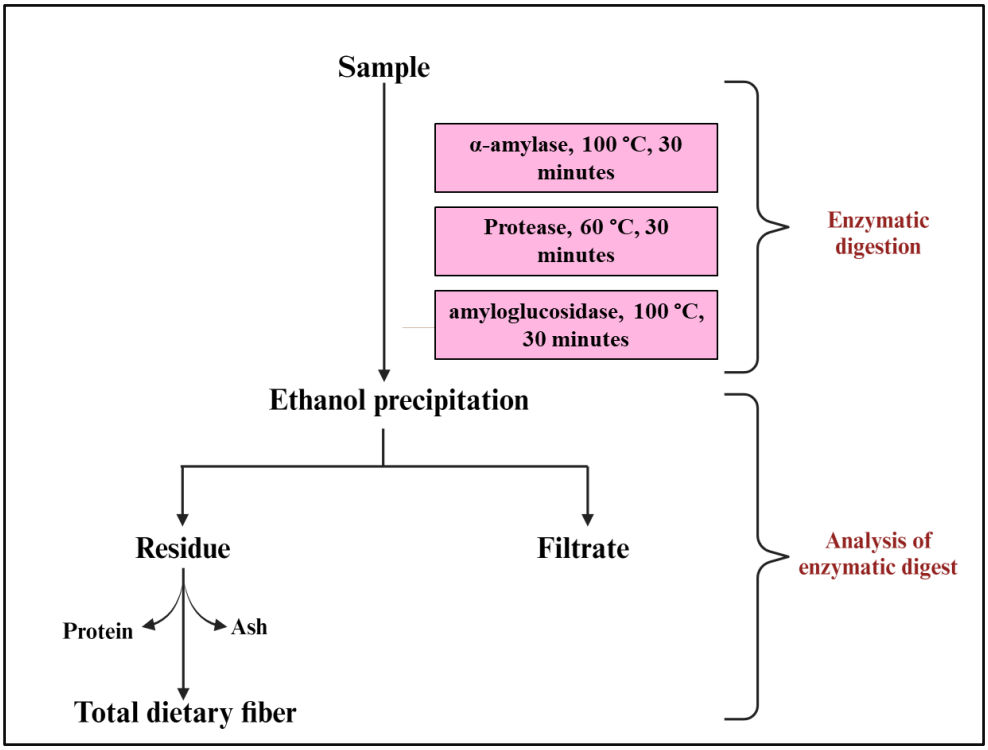

Scheme 2.1. TDF content analysis (Source: Megazyme Total Dietary Fiber Assay Kit method, scheme created with BioRender.com)

2.3.6. Estimation of fructan content of unripe pulp

The fructan content in the sample was assessed using the Megazyme Fructan Assay Kit (K-FRUC). This kit is designed for precise measurement of fructan in food products containing starch, sucrose, and other sugars as well as plant extracts and animal feed. It is included in three approved techniques for determining fructans: AOAC method 2016.14 (for adult nutritional products and infant formula), AOAC method 999.03 (for foods), and AOAC method 2018.07 (for animal feed). The assay was performed following the manufacturer's guidelines. The initial phase of the assay involves the removal of interfering substances i.e., sucrose and starch using sucrase, pullulanase, maltase, and β-amylase to monomeric glucose and fructose. The glucose and fructose were removed from the solution by treating with sodium borohydride to sorbitol and mannitol. In the second phase, fructan was cleaved to glucose and fructose by treatment with exo-inulinase, endo-inulinase, and endo-levanase. The glucose and fructose derived from fructan were quantified using the P-hydroxybenzoic acid hydrazide (PAHBAH) reducing sugar assay (*Fructan Assay Kit*, n.d.). The schematic representation of the assay protocol is given in Scheme 2.2.

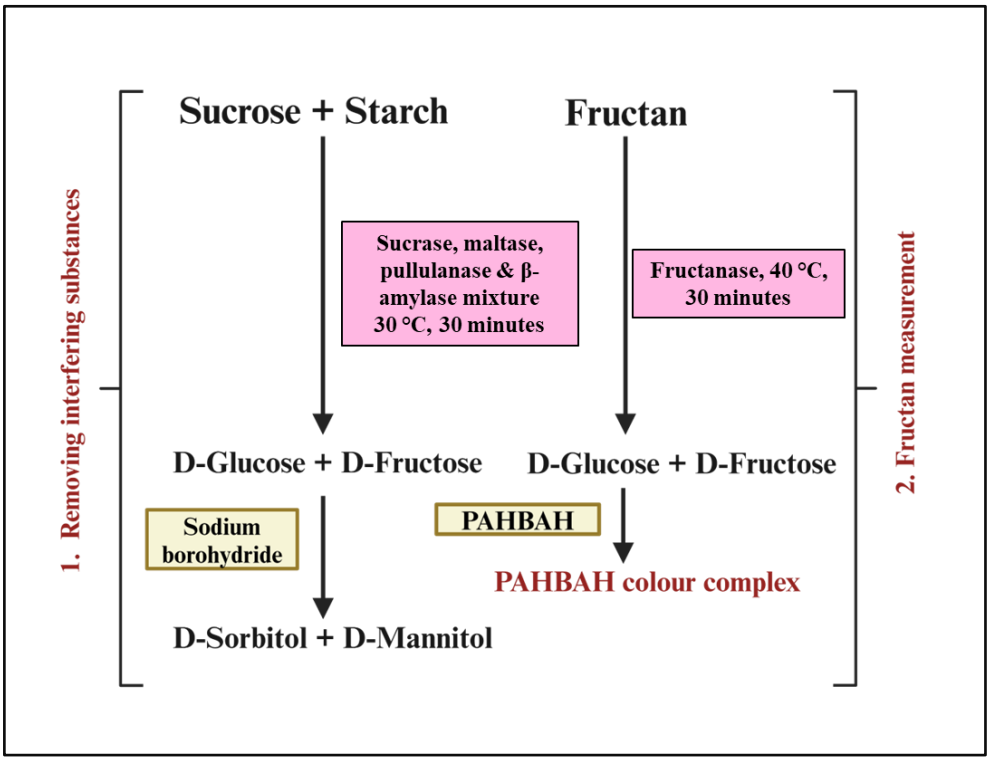

Scheme 2.2. Fructan content estimation (Source: Megazyme Fructan Assay Kit method, scheme created with BioRender.com)

2.3.7. Value addition of unripe Nendran pulp-development of novel banana grit (BG)

The pulp of Nendran was converted to a novel RTC product 'BG' by preliminary treatments and drying techniques. Fully matured Nendran banana, i.e., before ripening, was used to prepare BG. BG was prepared from the unripe pulp of Nendran by pre-treatments and drying. As the processing details of BG are part of technology transfer (discussed under section 2.4.13.) those details are not mentioned in the thesis.

2.3.8. Assessment of raw material from different locations

The suitability of raw materials from different locations for preparing BG was evaluated. Mature unripe Nendran was purchased from the Wayanad district of Kerala and compared with Nendran collected from Thiruvananthapuram. Proximate analysis of both pulp was carried out according to the AOAC method (*AOAC: Official Methods of Analysis (Volume 1)*, n.d.) and BG was prepared from both raw materials.

2.3.9. Proximate analysis of BG

The proximate composition of BG was analyzed according to methods mentioned in section 2.3.4. (*AOAC: Official Methods of Analysis (Volume 1)*, n.d.).

2.3.10. Determination of soluble, insoluble, and TDF content of BG

The soluble, insoluble, and TDF content of BG was determined using the Megazyme Total Dietary Fiber Assay Kit (K-TDFR). The assay was conducted according to the manufacturer's instructions (*Total Dietary Fiber Assay Kit*, n.d.) and the schematic representation of the procedure is given in Scheme 2.3.

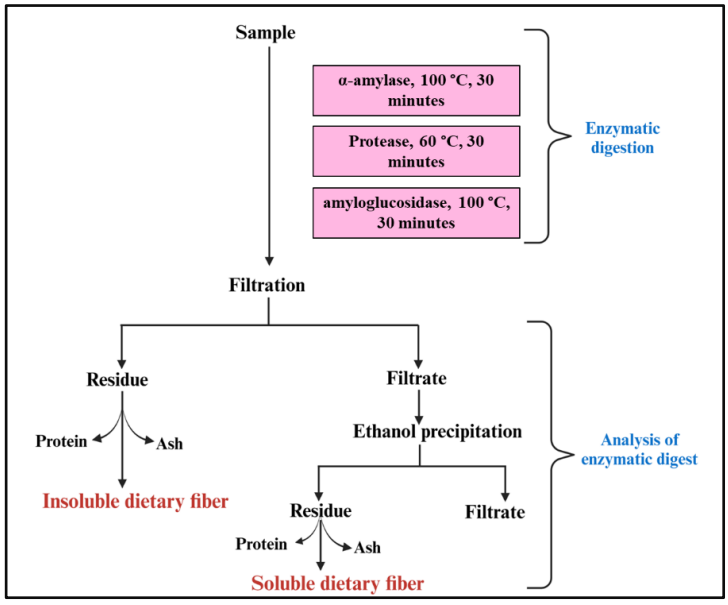

Scheme 2.3. Soluble and insoluble dietary fiber content analysis (Source: Megazyme Total Dietary Fiber Assay Kit method, scheme created with BioRender.com)

2.3.11. Determination of fructan content of BG

The fructan content of BG was determined according to the procedure mentioned in section 2.3.6.

2.3.12. Mineral composition of BG

The mineral composition of BG was estimated using inductively coupled plasma mass spectrometry (ICP-MS, Thermo scientific iCAP RQ ICPMS) analysis.

2.3.13. Evaluation of pesticide content of BG

The pesticide residue analysis of BG was conducted at the pesticide residue research and analytical laboratory, college of Agriculture, Vellayani, Thiruvananthapuram based on the AOAC approved (AOAC 20th Edition 2016:2007.01) quick, easy, cheap, effective, rugged, and safe (QuEChERS) method for analysis of pesticide residue in fruits and vegetables (Lehotay, 2007). The presence of 98 pesticides was screened in BG.

2.3.14. Evaluation of total carotenoid content (TCC) of BG

The TCC of BG was estimated as per the literature report with slight modification (Rodriguez-Amaya & Kimura, 2004). The TCC of BG was evaluated by preparing two extracts, i.e., hexane and acetone. In brief, BG (100 g) was powdered and passed through 20 mesh and extracted with hexane at 70 °C for 6 hours in a Soxhlet apparatus, which yielded 413.5 mg of hexane extract, and from that 2.5 mg of sample was taken for total carotenoid content measurement. For acetone extraction, BG (6 g) was powdered and passed through 20 mesh, from that a portion of the sample (3 g) was extracted with 50 mL chilled acetone for 30 minutes and the process was repeated until the sample was colourless. The extract was then transferred to petroleum ether (25 mL) and the absorbance was read at 450 nm in an ultraviolet-visible (UV-VIS) spectrophotometer (UV-2600, Shimadzu, Japan) and quantified using the absorption coefficient of 2500 (recommended for the estimation of carotenoid mixtures).

$$\text{Total carotenoid content } (\mu g/g) = \frac{A \times V\,(mL) \times 10^4}{A_{1cm}^{1\%} \times \text{sample weight (g)}}$$

Where A is the absorbance at a specified wavelength, V is the total volume of extract (25 mL), $A_{1cm}^{1\%}$ is the absorption coefficient (2500). The total carotenoid content of BG hexane extract was measured by dissolving 2.5 mg of the extract in 10 mL of petroleum ether and the total carotenoid content was measured as described above. Further to this, the variation in the carotenoid content of BG with location (Wayanad and Thiruvananthapuram) and variation in TCC with ripening of Nendran was also evaluated by preparing the acetone extract.

2.3.15. Qualitative HPLC-diode array detector (DAD) profiling of carotenoids in the BG hexane extract

The carotenoid fingerprinting of the BG was performed by using the hexane extract of BG and analyzed with the analytical Nexera X2 HPLC system (Shimadzu, Japan) equipped with a reverse phase, shim-pack GISS 5µm C18 column (250 × 4.6 mm, Shimadzu) connected to a Photo Diode Array (PDA) detector (SPD-M20A) and an autosampler (SIL-30AC). The mobile phase comprised of acetonitrile:methanol:tetrahydrofuran (ACN:MeOH:THF 40:56:4) with a flow rate of 1 mL/minutes, and isocratic elution for 30 minutes. The weighed β-carotene standard (5 mg) was dissolved in THF (10 mL) and 20 µL of the sample was injected. The hexane extract (50 mg) of BG (extraction procedure mentioned under section 2.3.14.) was dissolved in 2 mL of THF and filtered through a 0.2 µm nylon filter (Micro-Por Minigen Syringe Filter, Genetix Biotech Asia, New Delhi) prior to analysis, and 20 µL of the sample was injected. The column temperature was maintained at 25 ºC and eluting peaks were monitored at 450 nm (Bushway, 1986).

2.3.16. Shelf life evaluation of BG

For the shelf life evaluation, BG was packed in polyethylene-polypropylene blend packaging material, sealed under vacuum, and stored at room temperature (27-33 °C) and evaluated the change in three critical parameters such as moisture content, microbial load, and colour characteristics periodically for one year.

2.3.16.1. Change in moisture content

Change in the moisture content of the sample was analyzed following the AOAC method mentioned in section 2.3.4.1.

2.3.16.2. Enumeration of microorganism in BG-yeast & mold count and total plate count

The yeast and mold count was determined using potato dextrose agar medium and, the bacterial count (total plate count/aerobic plate count) was evaluated using nutrient agar medium following the methods of the bacteriological analytical manual (1992), Compendium of Methods for the Microbiological Examination of Foods (1992) & FSSAI Manual of Methods of Analysis-Microbiological Examination of Food and Water (ELLIOT et al., n.d.; *Manual-Microbiology-Methods.Pdf*, n.d.; Salfinger & Tortorello, 2015).

For yeast and mold determination, potato dextrose agar medium was prepared by dissolving 7.8 g of potato dextrose agar and 2 g of agar powder in 200 mL of distilled water and the nutrient agar medium for total plate count enumeration was prepared by dissolving 5.8 g of nutrient agar and 2 g of agar powder in 200 mL of distilled water followed by autoclaving for 20 minutes. Weighed 1 g of BG was mixed with 10 mL of peptone (0.1%) water and vortexed.

From this 10 mL tube, 1 mL was taken and added to a 9 mL tube. Likewise, it was serially diluted up to 10^{-4} dilutions. The appropriate dilution of the sample (1 mL) was inoculated in petri plates under aseptic conditions in a laminar airflow cabinet and the molten media at about 45 °C was poured into each plate aseptically. The petri plates were incubated at 35 °C for 24 hours to enumerate the bacterial count and for 48 hours for yeast and mold count. The average count of two plates was recorded and expressed as the number of colony-forming units per g (CFU/g).

$$\text{CFU/g} = \frac{\text{No.of colonies}}{\text{Dilution factor} \times \text{Volume of sample pipetted}}$$

2.3.16.3. Change in colour characteristics

Change in colour values of BG was determined by using Hunter Lab Colorimeter. The changes in L*, a*, and b* values were measured during one year of storage time. the yellowness index of BG was calculated using the measured L, a* and b* values (Hirschler, 2012).

$$\text{Yellowness index} = 142.86 \times (b^*/L)$$

2.3.17. Product improvement

One important observation made during the shelf life study was the gradual decline in the bright yellow colour of BG. Hence new interventions were taken to improve the colour characteristics and to retain the yellow colour. The BG was pretreated to improve the colour and the change in colour characteristics of the improved samples was analyzed periodically for one year.

2.3.18. Various preparations using BG

An array of delicacies ranging from wholesome breakfast, BG upma, BG-green gram mix upma, BG Italian delight, BG-hot and sour, BG-cream cheese, to flavoured health drinks & porridge, payasam, etc. were prepared from BG with 6-8 minutes of cooking. Preparations like BG gruel, and BG-milk porridge can be formulated from BG even without cooking attributing BG a RTC as well as ready-to-reconstitute (RTR) status.

2.3.19. Statistical analysis

All the experiments, except the estimation of soluble and insoluble fiber (n=1) and estimation of mineral content, were conducted in triplicates (n=3), with data presented as the mean ± standard deviation (SD). Statistical analysis was performed using IBM SPSS Statistics 26 (SPSS Inc., Chicago, USA). An independent samples t-test was used to compare the means of two samples, with a significance level set at $P \leq 0.05$.

2.4. Result and discussion

Before directly entering to the value addition trials, initially, the value addition potential of Nendran pulp was evaluated by assessing its proximate content, total dietary fiber content, and fructan content. Further a novel product 'BG' was developed from unripe Nendran pulp and evaluated its proximate composition, bioactive carbohydrate content, shelf life, and total carotenoid content.

2.4.1. Proximate composition of unripe pulp

The mature unripe Nendran, nearly 150 days old after flowering, 20-27 cm long, and 16 cm around, apex lengthily pointed with floral relicts (Fig. 2.6a.). The mature unripe fruit pulp is greyish-white (Fig. 2.6b.). Pulp has a moisture content of 59.67 ± 0.13%, and the protein, fat, and ash content were 0.23 ± 0.01%, 0.31 ± 0.04%, and 1.21 ± 0.08% respectively. Carbohydrates content by difference is 38.58% ± 0.18% (Table 2.1). Drying 100 g of unripe Nendran pulp yields nearly 40 g of dried pulp, which was a comparatively good yield and indicates the value addition potential of unripe Nendran pulp.

Fig. 2.6a. Mature unripe Nendran

Fig. 2.6b. Mature unripe Nendran pulp

Table 2.1. Proximate composition of unripe Nendran pulp

Parameters	Amount (%)
Moisture	59.67± 0.13
Protein	0.23 ± 0.01
Fat	0.31 ± 0.04
Ash	1.21 ± 0.08
Carbohydrate (by difference)	38.58 ± 0.18

Mean±SD (n=3)

2.4.2. Estimation of TDF content of pulp

In 1953, Prof. Hipsley introduced the term dietary fiber to describe the indigestible components of the plant cell wall. Since then, the definition has undergone numerous updates. Dietary fiber was described in 2000 by the American Association of Cereal Chemists (AACC) as the edible portions of plants that are either fully or partially fermented in the large intestine of humans and resist digestion and absorption in the small intestine (He et al., 2022). As per the widely recognized definition from Codex Alimentarius Alinorm in 2009, dietary fiber is defined as an edible carbohydrate polymer composed of three or more monomeric units that resist digestion by endogenous enzymes and, consequently, are neither broken down nor absorbed in the small intestine. Dietary fibers are categorized based on their structures into non-starch polysaccharides, RS, and resistant oligosaccharides (Guan et al., 2021). Based on its solubility and fermentable nature, dietary fiber is divided into soluble dietary fiber and insoluble fiber. Soluble fiber is viscous and gets fermented in the large intestine by gut microbiota to SCFAs. Examples of soluble dietary fiber include inulin, gum, pectin, glucomannan, FOS, galacto-oligosaccharides (GOS), and β-glucan. The insoluble dietary fiber is insoluble, non-viscous, non/least fermentable fiber e.g., cellulose, hemicellulose, lignin, cutin, suberin, etc. (Dhingra et al., 2012).

The total dietary fiber content of unripe pulp was found to be 7.24% on dw and 2.89% on wet basis (wb, n=1). Consumption of dietary fiber imparts numerous health benefits. The insoluble dietary fiber adds bulk to the diet, accelerates colonic transit, and provides improved bowel health (*IDA-Position-Paper-Fibre-24.12.18.Pdf*, n.d.). Soluble dietary fiber get converted primarily to SCFAs (acetate, propionate, and butyrate) by probiotics in the gut (Dhingra et al., 2012; He et al., 2022). SCFA provides energy to the colonocytes, promotes the secretion of mucosa, and thereby aids in colon health. The SCFAs not only lower the risk of gastrointestinal diseases but also play crucial roles as activators for GPCRs engaged in immune system modulation (Segain et al., 2000; Smith et al., 2013). Activated GPCR coupled free fatty acid receptors 2 and 3 (FFAR2, FFAR3) enhance the secretion of GLP-1 and PYY from intestinal L cells and improve insulin secretion and sensitivity thereby exerting beneficial effects in subjects with diabetes and obesity (Tolhurst et al., 2012).

Semaglutide, a GLP-1 receptor agonist available under the brand names Wegovy, Ozempic, and Rybelsus, is used as an anti-obesity drug for long-term weight management as well as an antidiabetic drug for type 2 diabetes. Unlike GLP-1, semaglutide boasts an extended half-life of about 7 days in the blood (165-184 hours), making it preferable for patients seeking effective weight loss. However, recent reports have highlighted the associated side effects of the drug

(FDA, 2024). In contrast, fermentable fiber demonstrates the ability to control appetite and provide satiety for extended periods with fewer associated side effects. This makes it a promising avenue for managing diabetes and obesity, leading to an increased focus on researching fermentable fibers that function as prebiotics. Fiber consumption also regulates the secretion of 'CCK', another satiety hormone that regulates the secretion of pancreatic enzymes (Waddell & Orfila, 2023). CCK regulates gastric emptying, rate of digestion, and absorption. Compared to non-diabetic persons, diabetes patients exhibit lower plasma levels of CCK and faster stomach emptying rates. Fiber supplementation was found to enhance postprandial CCK concentration and reduce plasma insulin and glucose responses (Bourdon et al., 2001).

Other benefits associated with bioactive carbohydrates include decreased blood cholesterol level (Dhingra et al., 2012), reduced risk of hypertension, coronary heart disease, stroke, and various gastrointestinal disorders (Anderson et al., 2009). increased absorption of calcium and magnesium, hypoglycemic effect (Guo et al., 2022), and increased satiety thus aiding in weight management in obesity and diabetes (Hughes et al., 2022). Health benefits associated with dietary fiber consumption are outlined in Fig. 2.7. The dietary fiber content of unripe pulp indicates the value-addition potential of unripe Nendran pulp.

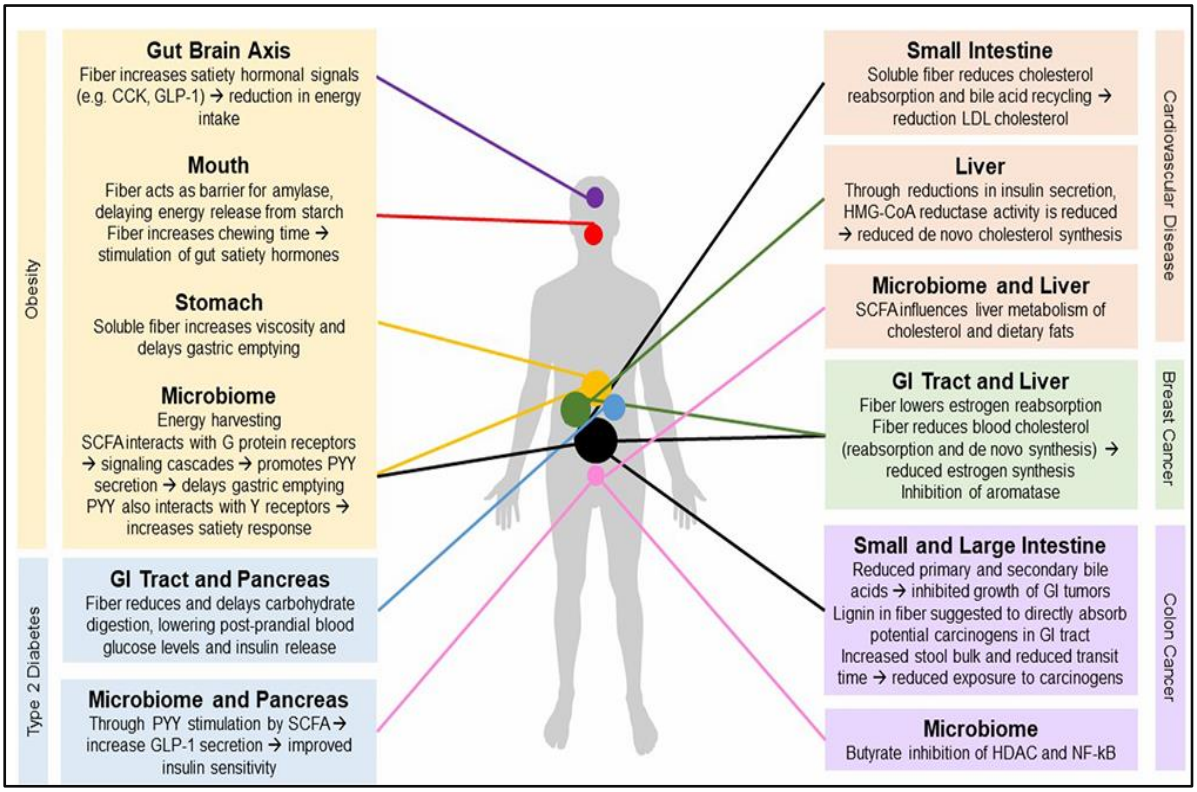

Fig. 2.7. Health benefits associated with dietary fiber consumption
(Source: Waddell & Orfila, 2023, http://dx.doi.org/10.1080/10408398.2022.2061909)

2.4.3. Estimation of fructan content of pulp

Fructans, the oligo- and polysaccharides, consist of short chains of fructose units that terminate with a single D-glucose unit at the reducing end. Based on their linkage patterns, fructans are categorized into three primary types: the inulin group, which primarily or exclusively features (2→1) fructosyl-fructose linkages; the levan group, which comprises (2→6) fructosyl-fructose links either solely or mostly; and the branching group, which has notable amounts of both (2→1) and (2→6) fructosyl-fructose connections (Pérez-López & Simpson, 2020).

The analysis of fructan content in unripe pulp revealed that it contains 0.04% and 0.12% of fructan on wb and db respectively (n=1). A study by Shalini and Usha,2015 reported a remarkably high amount of fructan content of 1.4% in the Nendran banana and they found that the pectinase enzyme pretreatment significantly increased total fructans from an initial 1.4 to 6.5% (Shalini & Antony, 2015). The differences in the fructan content observed in the same matrix (unripe Nendran pulp) can be attributed to differences in several factors such as differences in soil conditions, cultivar used, etc. (Shalini & Antony, 2015). Also, the method they employed for fructan quantification is the Megazyme fructan HK kit (K-FRUHK), which is designed for measuring all FOS and fructan polysaccharides. However, the fructan assay kit (K-FRUC) that we have used is designed for the precise measurement of fructan in food products containing starch, sucrose, and other sugars (*Fructan Assay Kit*, n.d.; *Fructan HK Assay Kit*, n.d.). These factors may have contributed to the reported higher values of fructan in the study by Shalini and Usha, 2015.

Clinical trials have demonstrated that fructan supplementation exerts favourable effects on health, encompassing improved glycemic control, enhanced prebiotic activity by promoting the abundance of *Bifidobacterium*, *Lactobacillus*, improved laxation, reduced risk of colon cancer, increased insulin sensitivity, and immunomodulation properties (de Carvalho Correa et al., 2023). The presence of fructan further reinforces the health benefits of unripe pulp consumption for better gut health.

2.4.4. Preparation of BG

A novel, preservative, and additive-free product coined ‘BG’ was developed for the first time from the pulp of unripe Nendran banana. BG was prepared using the pulp of matured unripe Nendran banana (150 days old after flowering; 20-27 cm long and 16 cm around) by pre-treatment and drying (Scheme 2.4.). Different stages in the BG production are shown in Fig. 2.8.

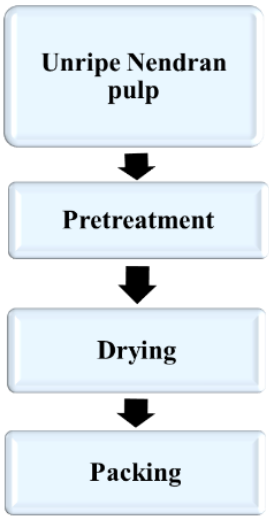

Scheme 2.4. BG production

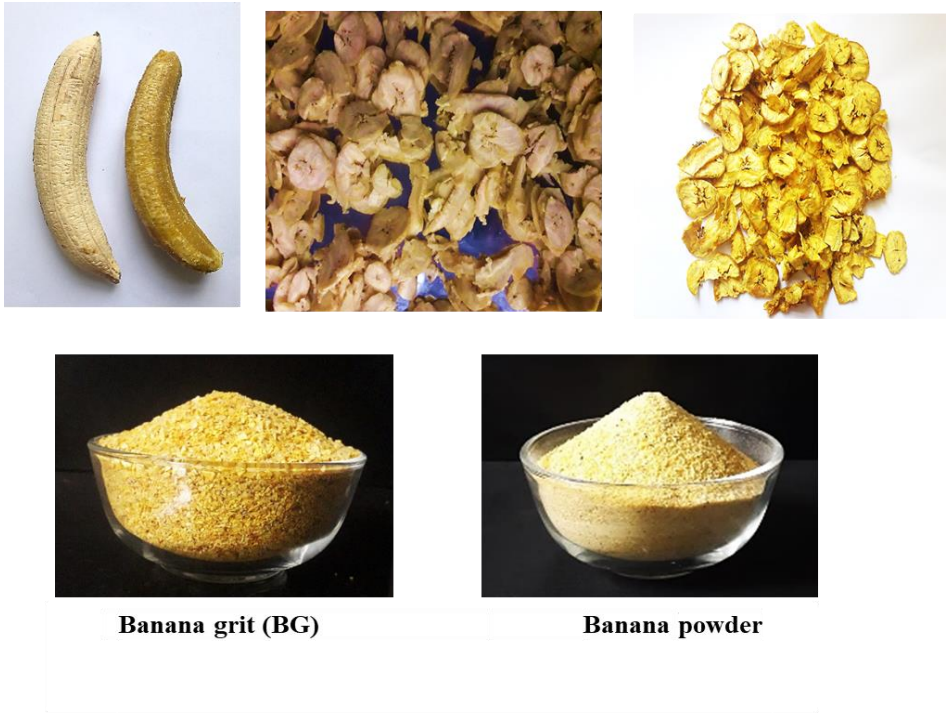

Fig. 2.8. Different stages in the BG processing

To the best of our knowledge, there has been no previous attempt to develop raw Nendran as grits, which can have wider applications as porridge, flavoured health drinks, gruel, and BG-vegetable mix (BG-veg mix) that can be consumed as a main course food (Fig. 2.9.). Along with BG, the banana powder is obtained as a byproduct during the processing of BG. From 3.3 kg of unripe banana, 2 kg pulp is obtained and the yield of dried product from this pulp was 800 g (40%), and from this, the final yield of BG and banana powder was 520 g (65%) and 280 g (25%) respectively (Scheme 2.5.).

Fig. 2.9. Unripe Nendran, novel BG, and products formulated from BG

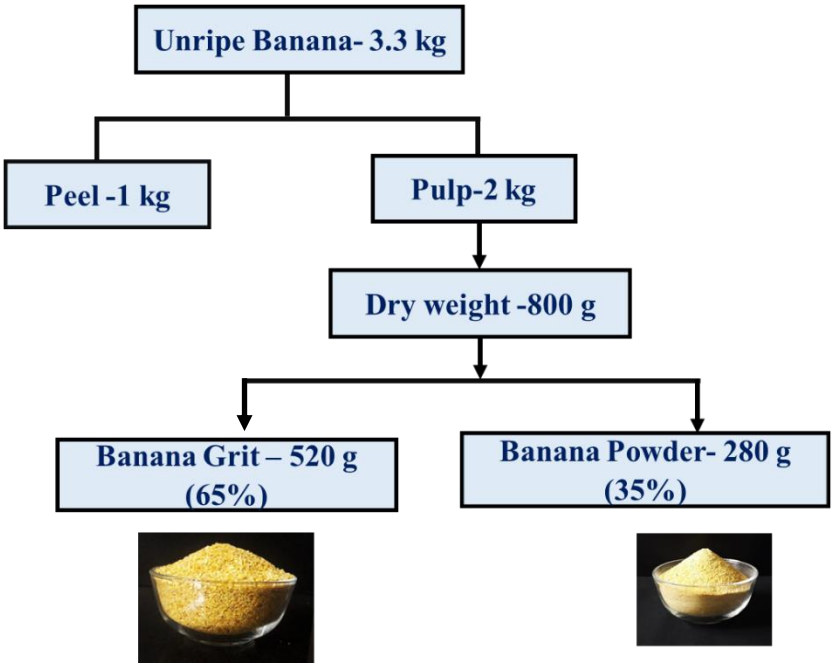

Scheme 2.5. BG yield pattern

BG in RTC and RTR form offers a way to position banana in new forms rather than conventional weaning food. This Scientific & Technical Know-how developed by us focuses on the potential of utilizing an indigenous vegetable crop (raw banana) as a source of healthy carbohydrates alternative to cereal-based diet. These interventions on value addition can help in improving the income of farmers and at the same time provide nutritious food to consumers.

2.4.5. Assessment of raw material from different locations

The suitability of raw materials collected from different locations was assessed for BG preparation. Mature unripe Nendran was purchased from the Wayanad district of Kerala and compared with Nendran collected from Thiruvananthapuram (Fig. 2.10.).

The proximate analysis of each pulp was carried out (Table 2.2.) and BG was successfully developed from raw materials from Wayanad and Thiruvananthapuram. The moisture content of Wayanad Nendran pulp was lower than that of Thiruvananthapuram Nendran, resulting in a slightly higher yield of BG when using Nendran sourced from Wayanad. Additionally, the raw material cost is also lower in Wayanad, which is a critical factor from an industrial perspective. However, the colour of BG produced from Wayanad Nendran is less compared to that produced from Thiruvananthapuram Nendran (Fig. 2.10.).

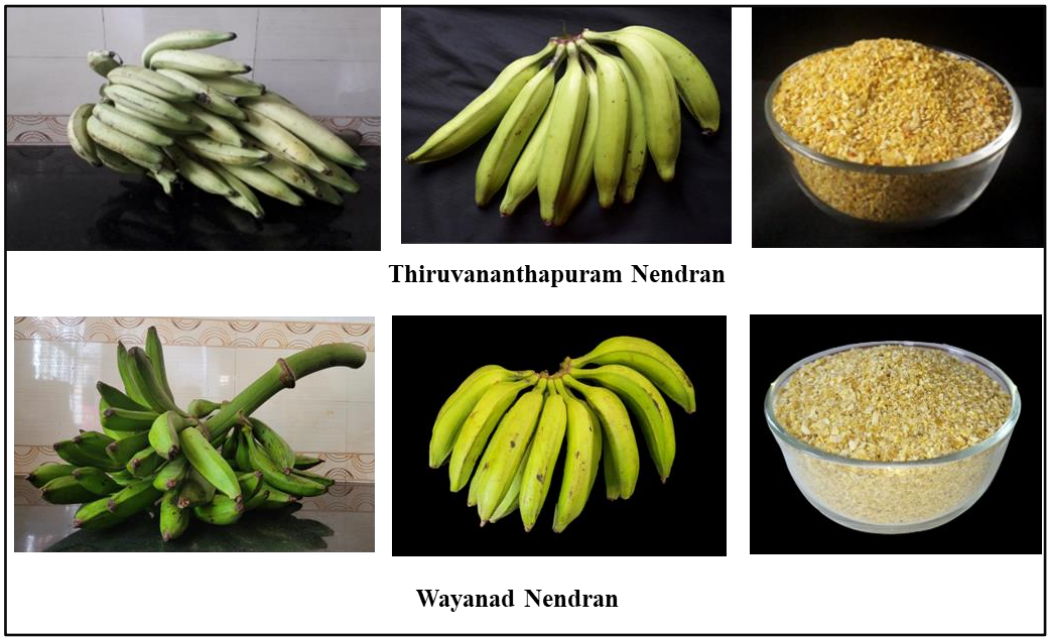

Fig. 2.10. Images of Nendran and BG from different locations

Table 2.2. Proximate composition of Nendran from Wayanad and Thiruvananthapuram

Parameters	Wayanad Nendran Pulp	Thiruvananthapuram Nendran Pulp
Moisture (%)	56.47 ± 0.42^{a}	59.67 ± 0.13^{b}
Protein (%)	0.19 ± 0.01^{a}	0.23 ± 0.01^{b}
Fat (%)	0.17 ± 0.06^{a}	0.31 ± 0.04^{b}
Ash (%)	1.18 ± 0.06^{a}	1.21 ± 0.08^{b}
Carbohydrate (%)	41.99 ± 0.13^{a}	38.58 ± 0.18^{b}
Pulp-to-peel ratio	1.51 ± 0.89^{a}	1.84 ± 1.21^{b}

Data expressed as mean±SD (n=3) and values with different superscripts in the same raw are significantly different ($p \leq 0.05$)

2.4.6. Proximate composition and bioactive carbohydrates content of BG

The proximate analysis showed that BG has a low moisture content (2.83 ± 0.05 %), 1.46 ± 0.03% ash content, 0.41 ± 0.13% fat, 3.97 ± 0.22% protein content, and high carbohydrate content (91.31 ± 0.17 %, Table 2.3.). The low moisture and fat content of the BG indicates the high shelf stability of the product. Screening of bioactive carbohydrates in BG revealed a total dietary fiber content of 7.38±0.03%. This fiber is distributed as 5.66% insoluble fiber and 1.69% soluble fiber and the fructan content was found to be 0.07 ± 0.01% (Table 2.4.). Dietary fiber and fructan are molecules known for their beneficial effects in maintaining a healthy gut (detailed in sections 2.4.2. & 2.4.3. of this chapter) and recognizing their significance, the World Health Organization (WHO) recommends a daily fiber intake of 25 g to support optimal health (*WHO Updates Guidelines on Fats and Carbohydrates*, n.d.).

Table 2.3. Proximate composition of BG

Parameters	**Amount (%)***
Moisture	2.83±0.05
Fat	0.41±0.13
Ash	1.46±0.03
Protein	3.97±0.22
Carbohydrate (by difference)	91.31 ±0.18

* wet basis, Mean±SD (n=3)

Table 2.4. Total dietary fiber and fructan content of BG

Parameter	**Amount (%)***
Total dietary fiber	7.38±0.03
Insoluble fiber[#]	5.66
Soluble fiber[#]	1.69
Fructan	0.07±0.01

*wet basis, Mean±SD (n=3, [#]n=1)

2.4.7. Mineral composition of BG

The mineral composition analysis of BG showed that BG is a good source of potassium, and magnesium (Table 2.5.). Potassium and magnesium play pivotal roles in human metabolism. Research indicates that elevated intake of these minerals is associated with improved blood pressure levels and a decreased risk of coronary heart disease and stroke(Houston & Harper, 2008). According to the literature, potassium deficiency has been linked to disturbances in glucose metabolism. Experimental studies have shown that induced hypokalemia, a condition characterized by low serum potassium levels, can lead to reduced insulin sensitivity and impaired glucose tolerance (Chatterjee et al., 2011). In hyperglycemic glucose clamp studies (intravenous infusions of glucose), where hypokalemia was induced either through thiazide diuretics or low-potassium diets, researchers observed declines in insulin release in response to hyperglycemia (Gorden, 1973; Helderman et al., 1983). This decrease in pancreatic β-cell sensitivity to hyperglycemia and reduced insulin release suggest a direct impact of potassium levels on glucose metabolism(Helderman et al., 1983). Furthermore, studies have demonstrated that correcting potassium deficiency through supplementation can reverse the defects in insulin release caused by hypokalemia, highlighting the vital relationship between low potassium levels and glucose abnormalities. These findings underscore the importance of maintaining adequate potassium levels for optimal glucose metabolism and insulin sensitivity (Chatterjee et al., 2011; D'Elia, 2024; Gorden, 1973; Helderman et al., 1983). Magnesium is also a critical molecule with great physiological significance as it is a main co-factor in numerous enzymatic reactions (Barbagallo et al., 2021). Magnesium plays a critical role in insulin signalling by involving in the phosphorylation of insulin receptor kinase and in insulin-mediated cellular glucose uptake. Research demonstrates that a reduced dietary magnesium intake is associated with a higher risk of type 2 diabetes and glucose intolerance (Barbagallo, 2015). The substantial quantities of these two elements in BG serve as strong indicators of its suitability for individuals with diabetes, accentuating its potential health advantages for this population.

Table 2.5. Mineral composition of BG

Minerals	Content (mg/100 g)
Aluminum (Al)	0.66
Arsenic (As)	BDL*
Cadmium (Cd)	BDL
Calcium (Ca)	1.07
Chromium (Cr)	0.006
Cobalt (Co)	0.001
Copper (Cu)	0.12
Iron (Fe)	0.22
Magnesium (Mg)	39.58
Manganese (Mn)	0.25
Nickel (Ni)	0.012
Potassium (K)	445.05
Selenium (Se)	0.0004
Lead (Pb)	0.004
Lithium (Li)	BDL
Zinc (Zn)	0.149
Boron (B)	0.22
Vanadium (V)	0.017
Gallium (Ga)	BDL
Rubidium (Rb)	0.690
Strontium (Sr)	0.040
Indium (In)	BDL
Cesium (Cs)	0.002
Barium (Ba)	0.074
Titanium (Ti)	BDL
Bismuth (Bi)	0.01

n=1, *BDL- Below Detectable Limit

2.4.8. Pesticide content of BG

One important concern with bananas is the presence of pesticide content in them. Hence the pesticide residue of BG was analyzed. BG was tested for 98 pesticides belonging to various classes including organochlorine compounds, organophosphorus compounds, synthetic pyrethroids, herbicides, and carbamates. All the analyzed pesticides were below the detectable limit in BG.

2.4.9. Evaluation of TCC of BG

One of the characteristic attributes of BG is its bright yellow colour which in turn is linked with the carotenoid content in the BG, hence attempts were made to quantify the total carotenoid content in BG. According to the National Institute of Nutrition data (2017) (Longvah et al., 2017), the carotenoid content of raw banana *(Musa × paradisiaca*) was 224 µg/100 g. Whereas, an exceptionally high level of carotenoid content i.e. 3466 ± 11.78 µg/100 g of BG and 3819 ± 15.82 µg/100 g of BG (Fig. 2.11.) was obtained through the acetone and

hexane extraction routes respectively. The hot extraction method followed in the case of hexane may have resulted in the higher TCC value of hexane extract. The high amount of carotenoids in BG indicates the suitability of BG for alleviating vitamin A deficiency.

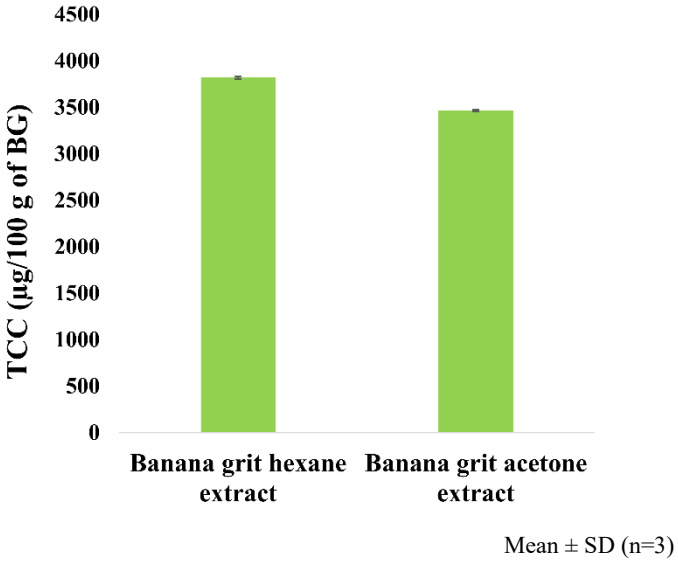

Fig. 2.11. TCC of BG (hexane and acetone extract route)

Further, the TCC of unripe Nendran pulp and ripe Nendran pulp sourced from Thiruvananthapuram was evaluated and the values were 3704 ± 21.18 µg/100 g and 4002 ± 28.99 µg/100 g on db (Fig. 2.12.). Literature data shows that the carotenoid content of the ripe bananas of cultivars like Monthan, Poovan, Red, and Robusta was very low and it ranges from 252 to 314 µg/100 g (Longvah et al., 2017).

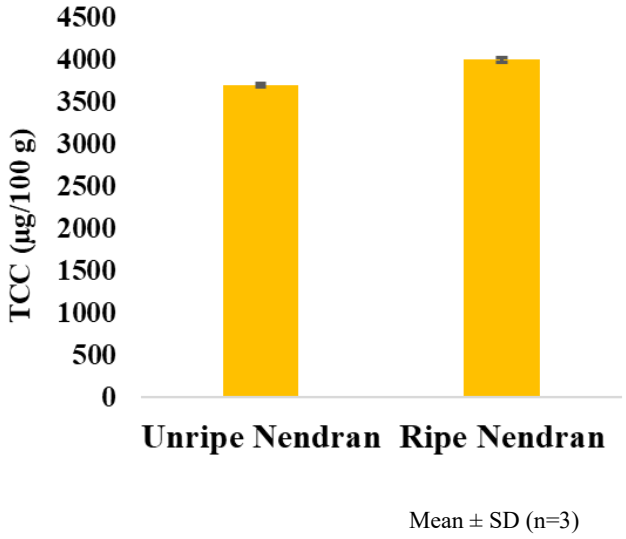

Fig. 2.12. TCC of unripe and ripe Nendran pulp (db)

Further to this, the variation in the carotenoid content of BG prepared from Wayanad and Thiruvananthapuram was evaluated. Interestingly, the TCC of grit developed from Wayand Nendran was 1466 ± 10.43 µg/100 g (Fig. 2.13.). The study indicates the variation in the TCC of BG when raw material was sourced from different locations.

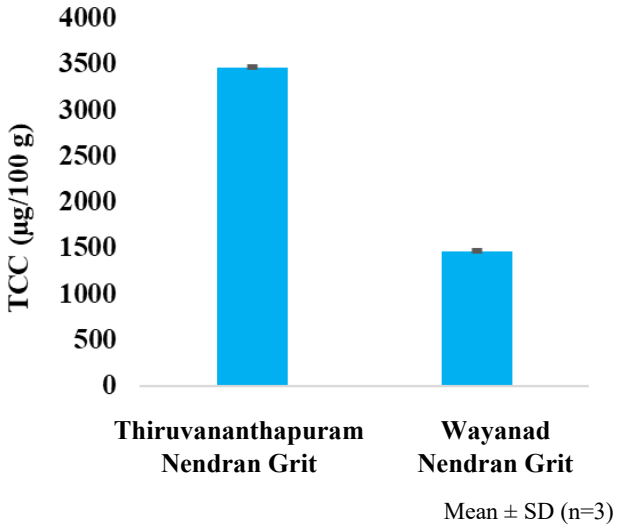

Fig. 2.13. TCC of Thiruvananthapuram Nendran grit and Wayanad Nendran grit

2.4.10. Qualitative HPLC-DAD profiling of carotenoids in the BG hexane extract

The HPLC profiling of the hexane extract was carried out for the identification of carotenoids in BG. The standard β-carotene peak was identified at a retention time of 21.30 minutes (Fig. 2.14a.). In the extract, the peak at a retention time of 21.40 minutes corresponds to β-carotene along with other unidentified peaks (Fig. 2.14b.). The presence of β-carotene was further confirmed by spiking with standard β-carotene (Fig. 2.14c.). Among the carotenoids, α-carotene and β-carotene have a high level of provitamin A activity (Englberger et al., 2006). Even though the micronutrient requirements in our body is very minimal, their impact on our body's health is crucial and deficiency of any of them can lead to mild to severe even life-threatening conditions. According to WHO, iron, vitamin A, and iodine deficiencies are the most widespread nutritional issues worldwide, particularly affecting children and pregnant women. Annually, 250,000 to 500,000 children with vitamin A deficiency go blind, and half of these children die within a year of becoming blind (*Vitamin A Deficiency*, n.d.). Since BG is a good source of provitamin A carotenoids, it can also help in alleviation of Vitamin A deficiency.

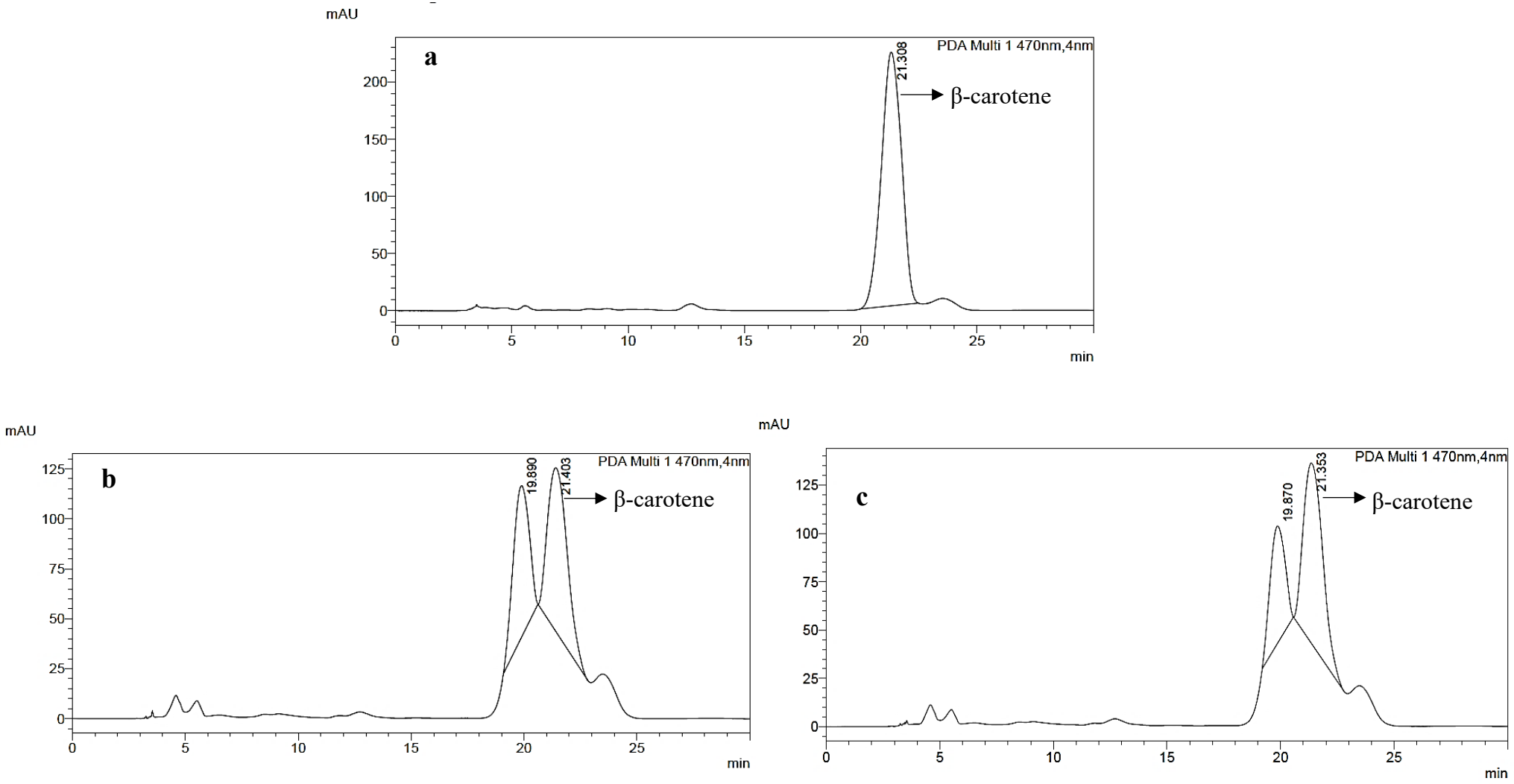

Fig. 2.14a. HPLC chromatogram of β-carotene standard, **Fig. 2.14b.** HPLC chromatogram of BG hexane extract, **Fig. 2.14c.** BG hexane extract spiked with standard β-carotene

2.4.11. Shelf life evaluation of BG

The shelf life of a food product is the duration from its production until it becomes unsuitable for consumption under specified environmental conditions (Awulachew, 2021). The moisture content and microbial load are two critical parameters that change significantly during the storage of a dry, low-fat product. Therefore, these parameters in BG were periodically evaluated over one year of storage. Additionally, since the product's colour is an important factor in attracting customers, changes in colour were also assessed throughout the study period.

2.4.11.1. Change in moisture content

The moisture content of processed products indicates their shelf life. The high moisture content in food can lead to microbial spoilage and a shorter shelf life (Chitrakar et al., 2019). Critical evaluation of the changes in the moisture content of BG over one year of storage revealed that the moisture content of the product remained below 10% for the first nine months, indicating the high shelf life of BG. However, after nine months, the moisture content was monitored monthly and showed a rapid increase. By the 12th month, the moisture content had risen from 3.58% to 12.55% (Fig. 2.15.).

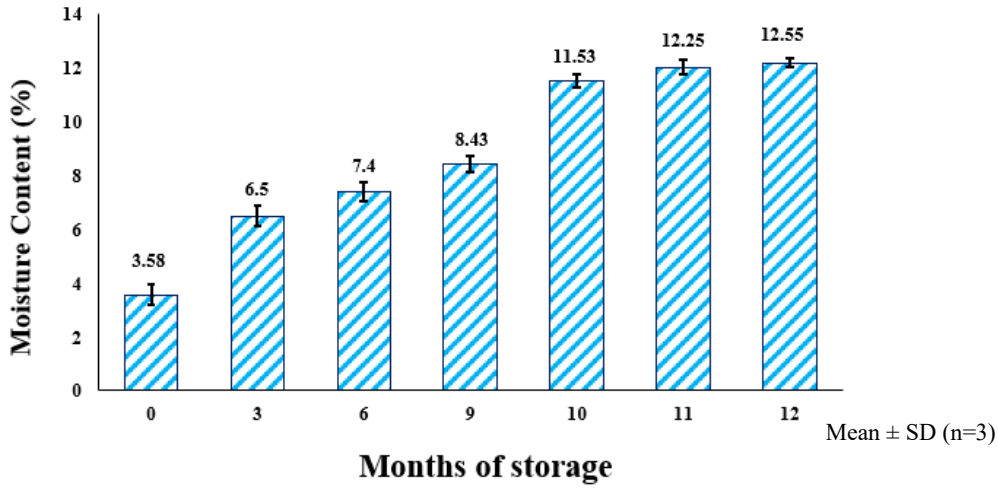

Fig. 2.15. Change in moisture content of BG during one year of storage

2.4.11.2. Enumeration of microorganism in BG-yeast & mold count and total plate count

Mold and bacterial growth are significant threats to the shelf life of food products. Hence, the microorganisms in the product was regularly assessed during storage. Periodic evaluations of the aerobic plate count and yeast & mold count of BG showed no microbial contamination during the first six months of storage. However, as the moisture content increased, the microbial count also increased. By the ninth month, the moisture content had risen to 8.43%, marking the

onset of microbial contamination. In the twelfth month of storage, the total plate count and yeast & mold count of BG were 2×10^4 CFU/g and 2×10^4 CFU/g respectively (Table 2.6.). According to the revised microbiological standards by the Food Safety and Standards Authority of India (FSSAI) for fruits, vegetables, and their products (2018), the maximum allowable limits for aerobic plate count and yeast & mold count for dried or dehydrated vegetables are 1×10^5 CFU/g and 1×10^4 CFU/g respectively (*Gazette_Notification_Fruits_Vegetables_04_04_2018.Pdf*, n.d.). Up to 11 months, these values of BG are within the FSSAI-prescribed limits, indicating that the product remains shelf-stable for up to 11 months.

Table 2.6. Change in microbial load of the BG during one year of storage

Month of storage	Aerobic Plate Count (CFU/g)	Yeast & Mold Count (CFU/g)
0	Nil	Nil
3	Nil	Nil
6	Nil	Nil
9	08×10^2	01×10^2
10	1.4×10^3	02×10^2
11	1.7×10^3	03×10^2
12	02×10^4	02×10^4

Mean±SD (n=3)

2.4.11.3. Change in colour characteristics

Product colour is a crucial factor from the customer's perspective, and products with bright colours are generally preferred in the market. BG's bright yellow colour is associated with its carotenoid content. Therefore, we evaluated BG's colour value and yellowness index during the storage study (Table 2.7.).

Table 2.7. Change in colour value and yellowness index of BG during one year of storage

Month of storage	Colour value	Yellowness Index
0	L*= 65.87±0.20	87.22
	a*= 07.12±0.04	
	b*= 40.22±0.09	
3	L*= 69.67±0.13	53.06
	a*= 03.74±0.03	
	b*= 25.88±0.06	
6	L*=72.28 ±0.28	48.91
	a*= 03.22± 0.04	
	b*= 24.75±0.10	
9	L*= 72.75±0.31	39.68
	a*= 03.23± 0.01	
	b*= 20.21±0.12	
12	L*= 73.89±0.26	34.80
	a*= 03.15±0.02	
	b*= 18.00±0.26	

Mean±SD (n=3)

In the initial month of storage, the yellowness index of BG was 87.22 and the TCC value was 2347 ± 34.5 µg/100 g and the product had a bright yellow colour (Fig. 2.16a.). A gradual decrease in the intensity of the bright yellow colour of grit was visible after 3 months of storage which was evident from the yellowness index also (Table 2.7.). The colour depletion became more visible by the end of 6 months of storage. From 6 months onwards the colour becomes light yellow and by the end of a year of storage, the products attain a cream colour (Fig. 2.16b.) with a TCC content of 111 ± 8.28 µg/100 g and yellowness index of 34.80.

Fig. 2.16a. BG-0 month of storage

Fig. 2.16b. BG-12th month of storage

The reason behind the colour depletion of BG is the light and oxygen-induced degradation of carotenoids present in the matrix. There are multiple ways of carotene degradation namely, auto-oxidation, thermal degradation, photodegradation, and photo-isomerization. Due to the conjugated double bonds and electron-rich nature of the chromophore carotenoids are highly light-sensitive (Verduin et al., 2020). When exposed to heat and light, carotenoids tend to undergo isomerization from the all-trans configuration to various cis-configurations. During photo-isomerization, all-trans β-carotene transforms into different cis-configurations, while in the photodegradation process, β-carotene experiences hydrogen abstraction, leading to the formation of β-carotene radicals (Verduin et al., 2020). Thus, resulting in carotenoid depletion and fading of the products.

This light-induced carotenoid degradation can be addressed in different ways. Literature suggests the use of modified atmosphere packaging (MAP) as nitrogen flushing in packaging material such as the low density polyethylene (LDPE)/aluminum (Al)/polyester (PET); biaxially oriented polypropylene(BOPP)/metalized BOPP and BOPP/metalized BOPP with an oxygen scavenger helps in the better retention of β-carotene in the sweet potato chips (Júnior et al., 2018), which in turn will help the retention of the yellow colour of the product. Another way is the usage of a primary packing with vacuum-sealed polypropylene pouches followed by an outer carton packaging which will prevent the direct interaction of light and oxygen with the product and hence reduce the photo-oxidative degradation of carotenoids.

2.4.12. Product improvement

As colour depletion of the product was observed during the storage study, we have explored a cost-effective method to naturally retain the colour of BG. A pretreatment step has been introduced in the grit-making procedure (since this is part of technology transfer the process details are not mentioned in the thesis) to retain the colour and the yellowness index of the product was evaluated periodically (Table 2.8.). During the initial month, the yellowness index of BG was 100.05 with a TCC of 2735 ± 10.2 µg/100 g, and the product had a bright yellow colour (Fig. 2.17a.). By the end of one year of storage, the product retained the yellow colour with a yellowness index of 65.93 and TCC of 1013 ± 8.80 µg/100 g, making BG yellow and attractive for consumers even after one year of manufacturing (Fig. 2.17b.).

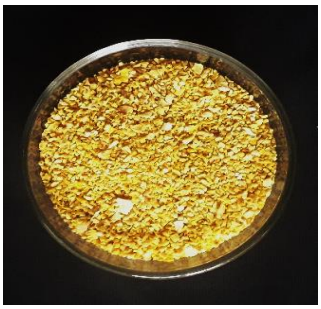

Fig. 2.17a. BG -0 month of storage

Fig. 2.17b. BG -12th month of storage

Table 2.8. Change in colour value and yellowness index of pretreated BG during one year of storage

Month of storage	Colour value	Yellowness Index
0	L*= 65.92±0.21 a*= 06.38±0.13 b*= 46.16±0.76	100.05
3	L*= 63.79±0.03 a*= 06.13±0.01 b*= 43.10±0.04	96.51
6	L*= 64.10±0.13 a*= 06.08± 0.01 b*= 41.44±0.36	92.364
9	L*= 65.52±0.15 a*= 05.24± 0.04 b*= 36.53±0.05	79.64
12	L*= 71.51±1.07 a*= 04.09±0.01 b*= 30.80±0.01	65.93

Mean±SD (n=3)

2.4.13. Significant outcome-technology transfer of BG

A significant outcome of this work was the technology transfer of BG, and BG-green gram combo (an improved version of the basic product) to the Kochi-based company Ms. MOZA ORGANIC Pvt. Ltd. on 1st January 2021 (Fig. 2.18.). The demonstration of BG and green gram production to the industry (Fig. 2.19.) was done on 9th January 2021 using 20 kg raw banana and 5 kg green gram as raw material. Another notable highlight we had during the journey was the official launch of products by the Hon. Director General (DG) of Council of Scientific and

Industrial Research (CSIR) at the World Food India 2023 event on 3rd November 2023, at the CSIR stall, New Delhi (Fig. 2.20.).

Fig. 2.18. Technology transfer event of BG

Fig. 2.19. Product development demonstration to the industry delegates

Fig. 2.20. The official launch of products by the Hon. Director-General (DG) of CSIR at the World Food India 2023 event on 3rd November 2023, at the CSIR stall, New Delhi

Since BG was a new product in the market, product popularization through media was critical for the consumer acceptance of the product. Hence CSIR-National Institute of Interdisciplinary Science and Technology (CSIR-NIIST) has taken the initiative to publish newspaper reports about BG in 'Mathrubhumi' and 'The Hindu' newspapers (Fig. 2.21. & Fig. 2.22). Following these reports, numerous online platforms also covered the news about BG and its technology transfer event (https://acumenias.in/current-affairs-detail/bananagrit, https://www.drishtiias.com/daily-updates/daily-news-analysis/banana grit, https://journalsofindia.com/banana-grit/, https://youtu.be/qL5dz8rV6C8).

02 നാട്ടുവർത്തമാനം

ഏത്തയ്ക്കായിൽനിന്നു പോഷകമൂല്യമുള്ള പുതിയ ഉത്പന്നങ്ങൾ

ഗവേഷണ നേട്ടവുമായി നിസ്റ്റ്

നേട്ടങ്ങളുടെ നാലു പതിറ്റാണ്ടുകൾ പിന്നിട്ട്

Fig. 2.21. Newspaper report about BG in 'Mathrubhumi' newspaper (Published on 17-01-2021, Mathrubhumi Thiruvananthapuram Edition)

Banana grit for that good gut feeling

Developed by NIIST scientists, the product can be used to make wide range of dishes

SPECIAL CORRESPONDENT
THIRUVANANTHAPURAM

Here is some good news for the health-conscious public and banana farmers plagued by falling prices.

Scientists at the CSIR-National Institute for Interdisciplinary Science and Technology (NIIST) at Pappanamcode here in Kerala have come up with a new product, banana grit or granules, developed from raw Nendran bananas.

Billed as an ideal ingredient for a healthy diet, banana grit can be used for making a wide range of dishes, according to the NIIST. The product resembles to 'rava' and broken wheat.

"The concept was introduced to utilise the presence of resistant starch in bananas, which is reported to improve gut health. Hence, the dishes prepared with banana grit and its byproduct, banana powder, incline to the new focus on gut health, which the scientific community is widely discussing now to maintain health and well-being," the NIIST said.

The Institute added that years of research on the Nendran variety helped it open up a new application for the starch-rich banana.

Generally consumed ripe, Nendran banana also finds use in typical Kerala dishes such as *avial* and *thoran*. The granules can be used for making *upma*, or it can be mixed with banana powder for porridge, with milk or coconut milk for use as a health drink. Banana powder can be used for making cakes and breads, along with refined wheat flour.

Developing new uses for Nendran also comes as a boon to farmers who have often been struggling against falling prices, according to the scientists.

The technology had been transferred to Kochi-based Moza Organic and the product is expected to be in the market soon.

New on the menu: Banana grit is set to hit the market soon.

Fig. 2.22. Newspaper report about BG in 'The Hindu' newspaper (Published on 04-01-2021, The Hindu Thiruvananthapuram Edition)

2.4.14. Various preparations using BG

The novel utilities of BG, rather than for the conventional use for the preparation of weaning food (porridge) make it stand out from the conventional unripe banana powders available in the market. As previously discussed, an array of delicacies ranging from wholesome breakfasts like BG upma and BG-green gram mix upma to innovative dishes such as BG Italian delight, BG-hot and sour, and BG-cream cheese were prepared from BG. These dishes typically require only 6-8 minutes of cooking. BG combined with vegetables makes for a nutritious breakfast, while the BG and milk combination serves as a delicious porridge. BG along with green gram is an improved version of the basic product BG and it's a perfect blend of protein and carbohydrate. The banana powder formed as a by-product during BG production also can be used for porridge preparation (Fig. 2.23.). Through product optimization trials, recipes were standardized for various products using BG (Table 2.9.).

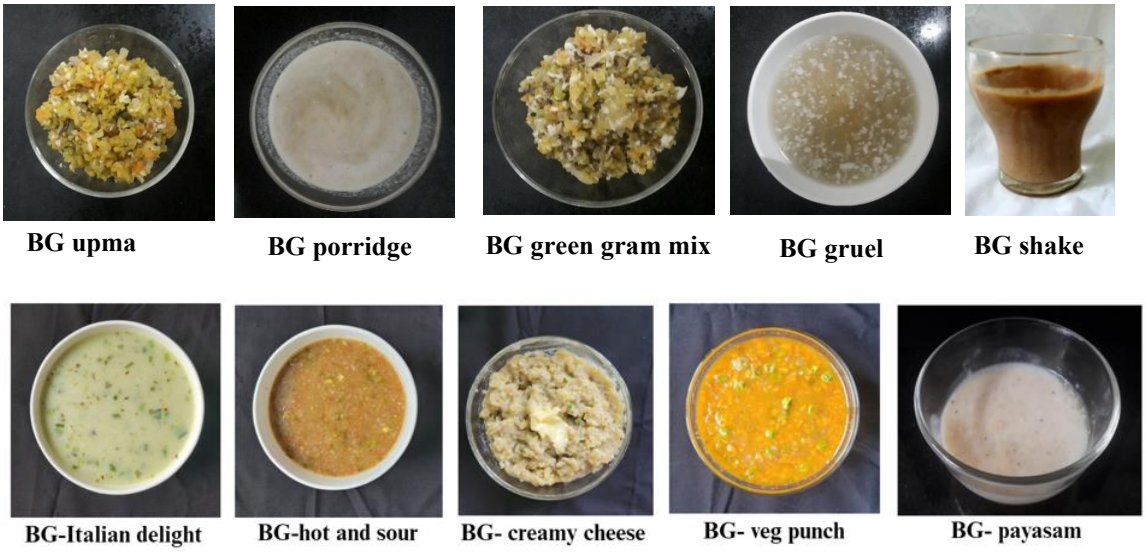

Fig. 2.23. Various preparations using BG

Table 2.9. Recipes for product development using BG

Product	Ingredients to be added*	Cooking instruction
BG upma	BG-50 g Green chilli-2 g Carrot-20 g Onion-15 g Grated coconut-5 g Curry leaves-2 g Ginger-2 g Mustard-1g Oil-5 mL Water- 200 mL	In a hot pan, season the oil with mustard, then add BG, sliced onion, carrot, ginger, and curry leaves, and sort them. Add water, and salt, and allow it to boil. Cook for 3-4 minutes. Add grated coconut mix well and serve hot.
BG-green gram upma	BG-green gram mix-50 g Green chilli-2 g Carrot-20 g Onion-15 g Grated coconut-5 g Curry leaves-2 g Ginger-2 g Mustard-1 g Oil-5 mL Water- 200 mL Salt- as per taste	In a hot pan, season the oil with mustard, then add BG-green gram, sliced onion, carrot, ginger, and curry leaves., sort them. Add water, and salt and allow it to boil. Cook for 3-4 minutes. Add grated coconut mix well and serve hot.

BG porridge	BG- 10 g Milk - 100 mL Sugar-preference	To BG, add boiling milk. Close it using a lid and allow it to stand for 10 minutes. Add sugar as per requirement. Remark: If thick porridge is preferred, the porridge can be cooked for 4 minutes. Garnish with fruits like ripe banana, apple, raisins, and dates as per choice.
BG gruel	BG - 10 g Water - 50 mL Grated coconut- as per taste Salt – as per taste	To BG, add a sufficient quantity of boiling water to soak the grit. Close it using a lid and allow it to stand for 4 minutes. Then add water sufficient to make a gruel, garnish with coconut grating, and add salt to taste and drink it hot. Remark: If thick gruel is preferred, it can be cooked for 4 minutes.
BG payasam	BG-10 g Water – ¼ glass (50 mL) Milk – ¼ glass (50 mL) Milkmaid – 1 tablespoon or as per taste Sugar - as per requirement Raisins and nuts Ghee - sufficient to sort raisins and nuts Cardamom powder- a pinch	Boil BG with ¼ glass of water, then add milk and continue boiling, after 5 minutes add milkmaid and mix well, if required sugar can be added. Then season with raisins sorted in ghee, and garnish with cardamom.
BG shake	BG - 10 g Milk - 50 mL Cocoa powder – if cocoa flavor is appreciated or it can be omitted Sugar-preference	To BG, add a sufficient quantity of boiling water to soak the grit. Close it using a lid and allow it to stand for 4 minutes. Then add milk, cocoa, and sugar and beat in a juicer bowl of mixer to make a shake.

BG-oats mix	BG-oats formulation mix: BG- 10 g Rolled oats flake- 10 g Raisins- 1 g Almonds- 1 g Cashew nut- 1 g Milk- 250 mL	To the BG-oats formulation mix, add milk, and mix well. Cook the product for 6 minutes on medium flame with occasional stirring. Add sugar /honey to taste (optional).
BG hot and sour mix	BG- 25 g Onion powder- 3 g Shallot powder- 3 g Garlic powder- 1 g Ginger powder- 0.3 g Tomato powder- 5 g Coriander leaf powder- 0.5 g Sugar- 0.1 g Green peas- 2 g Carrot- 1 g Spring onion dried- 0.2 g Salt- 2 g **Seasoning oil** Garlic oleoresin- 50 mg Black pepper oleoresin- 25 mg Capsicum oleoresin- 30 mg Cumin oleoresin- 25 mg Oil- 5 g Water 350 mL	Boil 350 mL of water and add seasoning mix, seasoning oil, and BG to it and keep for 10 minutes and serve hot. If thick consistency soup is required, cook the mix for 6 minutes on medium flame.
BG veg punch	BG- 25 g Onion powder- 5 g Shallot powder- 3 g Garlic powder- 1 g Tomato powder- 3 g Coriander leaf powder-0.2 g Sugar- 3 g Corn flour- 1 g Spring onion powder- 0.5g Salt- 2 g Oregano- 0.2 g **Seasoning oil** Garlic oleoresin- 50 mg Black pepper oleoresin- 25 mg Capsicum oleoresin- 30 mg Cumin oleoresin- 25 mg Oil- 5 g Water- 350 mL	Boil 350 mL of water and add seasoning mix, seasoning oil, and BG to it and keep for 10 minutes and serve hot. If thick consistency soup is required, cook the mix for 6 minutes on medium flame.

BG Italian delight	BG- 25 g Onion powder- 2.5 g Shallot powder- 2.5 g Garlic powder- 1 g Milk powder- 8 g Rosemary- 50 mg Corn flour- 1 g Spring onion powder- 0.5 g Spring onion dried- 200 mg Salt- 2 g Oregano- 100 mg Black pepper powder- 100 mg Salt- 2 g **Seasoning oil** Garlic oleoresin- 50 mg Black pepper oleoresin- 25 mg Oil- 5 g Water- 350 mL	Boil 350 mL of water and add seasoning mix, seasoning oil, and BG to it and keep for 10 minutes and serve hot. If a thick consistency is preferred, cook the mixture for 6 minutes and add 20 g of Mozzarella cheese and have as 'BG creamy cheese'
BG for garnishing		Use BG for garnishing at the end of cooking any recipes, and also for soups.

*Serving Suggestion for 1 person

2.5. Conclusion

Unripe banana 'Nendran' (*Musa* (AAB) cv. Nendran), an indigenous banana of Kerala, is an underutilized commodity. The current chapter discusses the proximate composition, total dietary fiber content, and fructan content of unripe Nendran pulp thereby indicating the value addition potential of unripe pulp. Further, a novel product, BG was developed from the pulp of the unripe Nendran banana by pre-treatment and drying. BG is a novel preservative-free and additive-free product, which is in RTC as well as RTR form. BG in RTC and RTR form offers a way to position banana in a new form rather than the conventional weaning food. This Scientific & Technical Know-how developed by us focuses on the potential of utilizing an indigenous vegetable crop (raw banana) as a source of healthy carbohydrates alternative to cereal-based diet. These interventions on value addition can help in improving the income of farmers and at the same time provide nutritious food to consumers. Shelf-life studies showed

that the product was shelf-stable for 11 months. Even though a gradual decrease in the bright yellow colour of BG was observed during storage, further product improvement trials helped to retain the colour for up to one year. BG was screened for the presence of 98 pesticides according to the AOAC method and they were below the detectable limit in BG. BG demonstrated nutrient superiority, by containing bioactive carbohydrates- fructan & dietary fiber, minerals- potassium, and magnesium, and TCC of 3466 ± 11.78 µg/100 g which helps in positioning it as a promising alternative to cereals. The presence of a considerable amount of dietary fiber BG indicates its suitability for promoting gut health and thereby providing overall wellness. Furthermore, being gluten-free makes the product suitable for individuals with gluten allergy. The significant outcome of this work is the technology transfer of BG to Ms. MOZA ORGANIC Pvt. Ltd. Kochi, India.

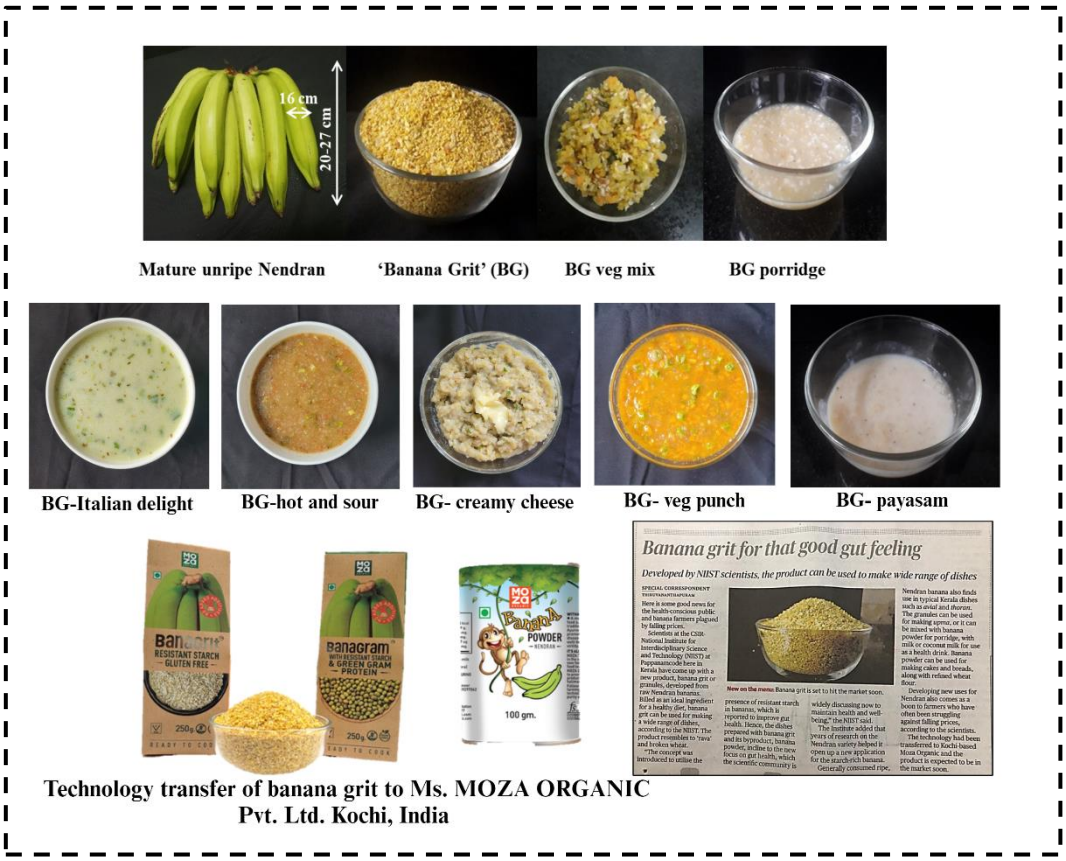

Fig. 2.24. Chapter 2 graphical abstract (Created with BioRender.com)

2.6. References

1. Anderson, J. W., Baird, P., Davis Jr, R. H., Ferreri, S., Knudtson, M., Koraym, A., Waters, V., & Williams, C. L. (2009). Health benefits of dietary fiber. *Nutrition Reviews*, *67*(4), 188–205. https://doi.org/10.1111/j.1753-4887.2009.00189.x
2. *AOAC: Official Methods of Analysis (Volume 1)*. (n.d.). Official Methods of Analysis of the Association of Analytical Chemists International (2005). *Official Methods: Gaithersburg, MD, USA*.
3. Awulachew, M. T. (2021). Understanding to the shelf-life and product stability of foods. *Journal of Food Technology and Preservation, 5 (8),* 1-5.
4. Barbagallo, M. (2015). Magnesium and type 2 diabetes. *World Journal of Diabetes*, *6*(10), 1152. https://doi.org/10.4239/wjd.v6.i10.1152
5. Barbagallo, M., Veronese, N., & Dominguez, L. J. (2021). Magnesium in aging, health and diseases. *Nutrients*, *13*(2), 463. https://doi.org/10.3390/nu13020463
6. Bourdon, I., Olson, B., Richter, B. D., Davis, P. A., Schneeman, B. O., & Backus, R. (2001). Beans, as a source of dietary fiber, increase cholecystokinin and apolipoprotein B48 response to test meals in men. *The Journal of Nutrition*, *131*(5), 1485–1490. https://www.sciencedirect.com/science/article/pii/S0022316622138253
7. Bushway, R. J. (1986). Determination of. Alpha.-and. Beta.-carotene in some raw fruits and vegetables by high-performance liquid chromatography. *Journal of Agricultural and Food Chemistry*, *34*(3), 409–412. https://doi.org/10.1016/S0315-5463%2882%2972531-3
8. Chatterjee, R., Yeh, H.-C., Edelman, D., & Brancati, F. (2011). Potassium and risk of Type 2 diabetes. *Expert Review of Endocrinology & Metabolism*, *6*(5), 665–672. https://doi.org/10.1586/eem.11.60
9. Chitra, P. (2015). Development of banana-based weaning food mixes for infants and its nutritional quality evaluation. *Reviews on Environmental Health*, *30*(2), 125–130. https://doi.org/10.1515/reveh-2015-0002
10. Chitrakar, B., Zhang, M., & Adhikari, B. (2019). Dehydrated foods: Are they microbiologically safe? *Critical Reviews in Food Science and Nutrition*, *59*(17), 2734–2745. https://doi.org/10.1080/10408398.2018.1466265
11. de Carvalho Correa, A., Lopes, M. S., Perna, R. F., & Silva, E. K. (2023). Fructan-type prebiotic dietary fibers: Clinical studies reporting health impacts and recent advances

in their technological application in bakery, dairy, meat products and beverages. *Carbohydrate Polymers*, 121396. https://doi.org/10.1016/j.carbpol.2023.121396

12. D'Elia, L. (2024). Potassium intake and human health. In *Nutrients* (Vol. 16, Issue 6, p. 833). MDPI. https://www.mdpi.com/2072-6643/16/6/833
13. Dhingra, D., Michael, M., Rajput, H., & Patil, R. (2012). Dietary fibre in foods: A review. *Journal of Food Science and Technology*, *49*, 255–266. https://doi.org/10.1007%2Fs13197-011-0365-5
14. Elliot, E. L., Kaysner, C. A., & Tamplin, M. L. (n.d.). *F]). Bacteriological Analytical Manual 7th edition, 1992*.
15. Englberger, L., Wills, R. B. H., Blades, B., Dufficy, L., Daniells, J. W., & Coyne, T. (2006). Carotenoid Content and Flesh Color of Selected Banana Cultivars Growing in Australia. *Food and Nutrition Bulletin*, *27*(4), 281–291. https://doi.org/10.1177/156482650602700401
16. FDA, C. for D. E. and. (2024). Medications Containing Semaglutide Marketed for Type 2 Diabetes or Weight Loss. *FDA*. https://www.fda.gov/drugs/postmarket-drug-safety-information-patients-and-providers/medications-containing-semaglutide-marketed-type-2-diabetes-or-weight-loss
17. *Fructan Assay Kit*. (n.d.). Megazyme. Retrieved January 25, 2024, from https://www.megazyme.com/fructan-assay-kit
18. *Fructan HK Assay Kit*. (n.d.). Megazyme. Retrieved January 25, 2024, from https://www.megazyme.com/fructan-hk-assay-kit
19. *Gazette_Notification_Fruits_Vegetables_04_04_2018.pdf*. (n.d.). Retrieved June 26, 2024, from https://fssai.gov.in/upload/uploadfiles/files/Gazette_Notification_Fruits_Vegetables_04_04_2018.pdf
20. Gorden, P. (1973). Glucose Intolerance with Hypokalemia: Failure of Short-term Potassium Depletion in Normal Subjects to Reproduce the Glucose and Insulin Abnormalities of Clinical Hypokalemia. *Diabetes*, *22*(7), 544–551. https://doi.org/10.2337/diab.22.7.544
21. Guan, Z.-W., Yu, E.-Z., & Feng, Q. (2021). Soluble dietary fiber, one of the most important nutrients for the gut microbiota. *Molecules*, *26*(22), 6802. https://doi.org/10.3390/molecules26226802

22. Guo, J., Tan, L., & Kong, L. (2022). Multiple levels of health benefits from resistant starch. *Journal of Agriculture and Food Research*, *10*, 100380. https://www.sciencedirect.com/science/article/pii/S2666154322001132
23. He, Y., Wang, B., Wen, L., Wang, F., Yu, H., Chen, D., Su, X., & Zhang, C. (2022). Effects of dietary fiber on human health. *Food Science and Human Wellness*, *11*(1), 1–10. https://doi.org/10.1016/j.fshw.2021.07.001
24. Helderman, J. H., Elahi, D., Andersen, D. K., Raizes, G. S., Tobin, J. D., Shocken, D., & Andres, R. (1983). *Prevention of the Glucose Intolerance of Thiazide Diuretics by Maintenance of Body Potassium*. *32*. https://doi.org/10.2337/diab.32.2.106
25. Hirschler, R. (2012). Whiteness, yellowness, and browning in food colorimetry. *Color in Food: Technological and Psychophysical Aspects. Editorial JL Caivano & Buera MP EE. UU*, 93–104. https://api.taylorfrancis.com/content/chapters/edit/download?identifierName=doi&identifierValue=10.1201/b11878-13&type=chapterpdf
26. Houston, M. C., & Harper, K. J. (2008). Potassium, magnesium, and calcium: Their role in both the cause and treatment of hypertension. *The Journal of Clinical Hypertension*, *10*(7), 3–11. https://doi.org/10.1111%2Fj.1751-7176.2008.08575.x
27. https://english.mathrubhumi.com/features/agriculture/soil-quality-increased-value-of-chengalikodan-bananas-1.5257602
28. https://keralahypermarketonline.com/product/banana-chips-500-gms/,
29. http://www.lincyscookart.com/2015/08/vazhakka-thoran-raw-banana-thoran.html,
30. https://www.myforkinglife.com/green-banana-porridge/
31. Hughes, R. L., Alvarado, D. A., Swanson, K. S., & Holscher, H. D. (2022). The prebiotic potential of inulin-type fructans: A systematic review. *Advances in Nutrition*, *13*(2), 492–529. https://doi.org/10.1093%2Fadvances%2Fnmab119
32. *IDA-position-paper-fibre-24.12.18.pdf*. (n.d.). Retrieved July 10, 2024, from https://idaindia.com/wp-content/uploads/2018/12/IDA-position-paper-fibre-24.12.18.pdf
33. Júnior, L. M., Ito, D., Ribeiro, S. M. L., da Silva, M. G., & Alves, R. M. V. (2018). Stability of β-carotene rich sweet potato chips packed in different packaging systems. *LWT*, *92*, 442–450. https://www.sciencedirect.com/science/article/pii/S0023643818302056
34. Lehotay, S. (2007). AOAC official method 2007.01 pesticide residues in foods by acetonitrile extraction and partitioning with Magnesium Sulfate. *Journal of AOAC*

International, *90*(2), 485–520. https://nucleus.iaea.org/sites/fcris/Shared%20Documents/SOP/AOAC_2007_01.pdf

35. Longvah, T., Anantan, I., Bhaskarachary, K., Venkaiah, K., & Longvah, T. (2017). *Indian food composition tables*. National Institute of Nutrition, Indian Council of Medical Research Hyderabad. https://www.academia.edu/download/51599403/IFCT.pdf
36. *Manual-Microbiology-Methods.pdf*. (n.d.). FSSAI Manual of Methods of AnalysisMicrobiological Examination of Food and Water. https://www.fssai.gov.in/upload/uploadfiles/files/Manual-Microbiology-Methods.pdf
37. *Organic_production_of_banana.pdf*. (n.d.). Retrieved May 6, 2024, from https://kau.in/sites/default/files/documents/organic_production_of_banana.pdf
38. Pérez-López, A. V., & Simpson, J. (2020). The sweet taste of adapting to the desert: Fructan metabolism in Agave species. *Frontiers in Plant Science*, *11*, 520148. https://www.frontiersin.org/journals/plantscience/articles/10.3389/fpls.2020.00324/full
39. Rodriguez-Amaya, D. B., & Kimura, M. (2004). *HarvestPlus handbook for carotenoid analysis* (Vol. 2). International Food Policy Research Institute (IFPRI) Washington.
40. Salfinger, Y., & Tortorello, M. L. (2015). *Compendium of methods for the microbiological examination of foods*. American Public Health Association.
41. Segain, J. P., De La Blétiere, D. R., Bourreille, A., Leray, V., Gervois, N., Rosales, C., Ferrier, L., Bonnet, C., Blottiere, H. M., & Galmiche, J. P. (2000). Butyrate inhibits inflammatory responses through NFκB inhibition: Implications for Crohn's disease. *Gut*, *47*(3), 397–403. https://gut.bmj.com/content/47/3/397.abstract
42. Shalini, R., & Antony, U. (2015). Fructan distribution in banana cultivars and effect of ripening and processing on Nendran banana. *Journal of Food Science and Technology*, *52*, 8244–8251. https://doi.org/10.1007%2Fs13197-015-1927-8
43. Smith, P. M., Howitt, M. R., Panikov, N., Michaud, M., Gallini, C. A., Bohlooly-Y, M., Glickman, J. N., & Garrett, W. S. (2013). The Microbial Metabolites, Short-Chain Fatty Acids, Regulate Colonic T_{reg} Cell Homeostasis. *Science*, *341*(6145), 569–573. https://doi.org/10.1126/science.1241165
44. Sreejith, P., & Sabu, M. (2017). *Edible Bananas of South India: Taxonomy & Phytochemistry*. Indian Association for Angiosperm Taxonomy.
45. Tolhurst, G., Heffron, H., Lam, Y. S., Parker, H. E., Habib, A. M., Diakogiannaki, E., Cameron, J., Grosse, J., Reimann, F., & Gribble, F. M. (2012). Short-chain fatty acids

stimulate glucagon-like peptide-1 secretion via the G-protein–coupled receptor FFAR2. *Diabetes*, *61*(2), 364–371. https://diabetesjournals.org/diabetes/article-abstract/61/2/364/14608

46. *Total Dietary Fiber Assay Kit*. (n.d.). Megazyme. Retrieved February 14, 2024, from https://www.megazyme.com/total-dietary-fiber-assay-kit
47. Verduin, J., Den Uijl, M. J., Peters, R. J. B., & Van Bommel, M. R. (2020). Photodegradation products and their analysis in food. *J. Food Sci. Nutr*, *6*(67.10), 24966. http://dx.doi.org/10.24966/FSN-1076/100067
48. *VFPCK* -. (n.d.). Retrieved May 5, 2024, from https://www.vfpck.org/package_of_practices.asp?ID=4
49. *Vitamin A deficiency*. (n.d.). Retrieved July 2, 2024, from https://www.who.int/data/nutrition/nlis/info/vitamin-a-deficiency
50. Waddell, I. S., & Orfila, C. (2023). Dietary fiber in the prevention of obesity and obesity-related chronic diseases: From epidemiological evidence to potential molecular mechanisms. *Critical Reviews in Food Science and Nutrition*, *63*(27), 8752–8767. https://doi.org/10.1080/10408398.2022.2061909
51. *WHO updates guidelines on fats and carbohydrates*. (n.d.). Retrieved July 9, 2024, from https://www.who.int/news/item/17-07-2023-who-updates-guidelines-on-fats-and-carbohydrates

Chapter 3

Phytochemical exploration of raw Nendran pulp and product

3.1. Introduction

3.1.1. Phytochemicals and their characterization

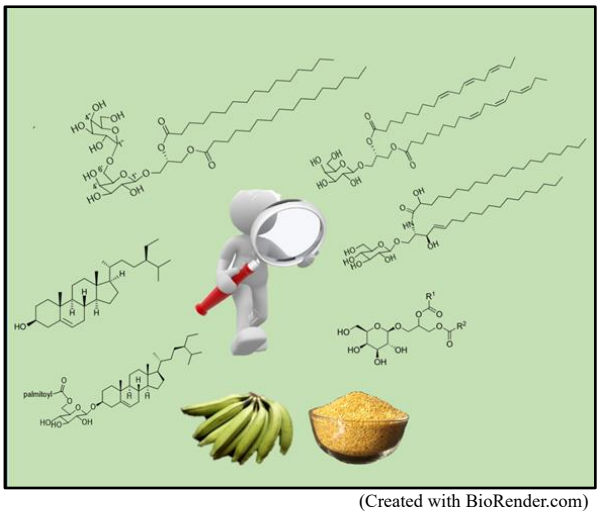

(Created with BioRender.com)

Plants are a reservoir of bioactive constituents, known as secondary metabolites, which play a crucial role in defending against invading microbes, predators, herbivores, and environmental stress. Research indicates that over 2,00,000 chemical compounds have been identified within the plant kingdom from the 391,000 described plant species (D'Amelio Sr, 1998; Divekar et al., 2022). Phytochemicals fall into various classes such as lipids, phenols, tannins, flavonoids, alkaloids, saponins, glycosides, volatile oils, resins, biogenic amines, terpenoids, organic acids, sterols and carotenoids (D'Amelio Sr, 1998; Divekar et al., 2022). With the diverse chemical structures and biological properties, phytochemicals offer a range of health advantages to humans, beyond their benefits to plants, through exhibiting diverse pharmacological effects including anti-cancer, anti-microbial, anti-inflammatory, and antioxidant properties (Saxena, 2023). Flavonoids, phenolics, phytoalexins, anthocyanins, triterpenes, steryl glycosides, carotenoids, phytoalexins, biogenic amines, and sterols were the phytochemicals reported from various parts of bananas. These compounds were attributed with a broad range of pharmacological benefits such as anti-diabetic, antioxidant, anti-inflammatory, anti-microbial, and anti-helminthic properties (Oguntibeju, 2019).

Characterization of plant bioactive compounds gained wide recognition due to their potential application in various fields including pharmaceuticals, nutraceuticals, and natural product research. The phytochemical exploration studies involve three basic steps, i.e., extraction, isolation, and characterization (De Silva et al., 2017). The extraction method plays a crucial role in obtaining the phytochemicals from the matrix. Traditionally, percolation, maceration, solvent extraction, and Soxhlet extraction techniques have been used for extracting the bioactive compounds from the matrix. Recently, more sophisticated and efficient

techniques such as ultrasound extraction, microwave-assisted extraction, supercritical fluid extraction, and enzyme-assisted extraction have been employed for extraction purposes (De Silva et al., 2017; Saxena, 2023). Following extraction, the analysis and characterization of the extracts are performed through non-chromatographic (spectrophotometric) or chromatographic techniques. Conventional chromatographic techniques include column chromatography and planar chromatography, such as thin-layer chromatography (TLC) and paper chromatography. Separation and purification of various phytochemicals are performed using open-column chromatography or its automated version, flash chromatography (Tsao Rong & Li HongYan, 2013). Gas chromatography and HPLC are two popular chromatographic techniques used to separate, identify, and quantify the bioactive compounds in the extracts. Spectroscopic techniques such as nuclear magnetic resonance (NMR), and mass spectrometry (MS) were extensively used for the structural elucidation of compounds (Saxena, 2023).

The proton (^{1}H), phosphorous (^{31}P), and carbon (^{13}C) NMR spectra offer essential information for structural elucidation. The distortionless enhancement by polarization transfer (DEPT) experiment is used to determine the multiplicity of carbon atoms. Comprehensive two-dimensional NMR (2D NMR) experiments are typically performed to gather detailed structural insights. These 2D NMR techniques include correlation spectroscopy (COSY), which reveals information about directly coupled protons, ^{13}C-^{1}H shift correlation experiments such as heteronuclear single quantum coherence (HSQC), which facilitates the understanding of carbon-to-proton assignment transfer and heteronuclear multiple bond correlation (HMBC) helps to integrate fragments derived from other correlation sequences, aiding in molecular identification and structural elucidation (Emwas et al., 2019). The MS detectors are highly useful for the identification of bioactives which are present in very low concentrations. When tandem spectrometry (MS-MS) is used in conjunction with HPLC, better fragmentation patterns of the precursor and daughter ions are produced, giving more structural information needed for compound identification (McLafferty, 1981).

3.1.2. Literature review on the phytochemicals in Nendran banana

In 2015, Sreejith and his team conducted extensive studies on edible bananas in South India. They collected the edible bananas cultivated in south India and unripe fruit pulp of 13 cultivars with different ploidy levels (AA, AB, AAB & ABB) was extracted with methanol and subjected to gas chromatography-MS (GC-MS) analysis to characterize the phytochemical composition and Nendran was one among the selected bananas (Sreejith & Sabu, 2017). In the Nendran banana, 23 compounds were identified through GC-MS analysis, out of which 17 compounds

were found to be predominant. Seven compounds were found to be specific to the Nendran cultivar only. It comprises erythritol; 2-isopropyl-2-methyl-butanedioic acid; phthalic acid; di(2-propylpentyl) ester; 9,12-octadecadienoic acid(Z)-methyl ester; caprolactam; 1,3-dipalmitic trimethylsilyl ether and delta. 1, and alpha-cyclohexaneacetic acid (Sreejith & Sabu, 2017). In the year 2017, Shivasankara and co-workers conducted a detailed investigation to study the influence of seasons on the volatile compounds of two banana cultivars (Grand Naine and Nendran) under Kerala conditions. The fresh fruit pulp of each cultivar was subjected to Solid-Phase Microextraction (SPME) of volatiles and subsequent GC-MS analysis. The study indicated that total volatile compounds were higher in Grand Naine compared to cv. Nendran and with increased temperature, volatile aroma compounds decreased in Grand Naine and Nendran. More than 50 major volatile compounds were identified from both cultivars irrespective of season. The major classes of compounds identified were esters, alcohols, aldehydes, ketones, acids, phenols, and hydrocarbons (KS Shivashankara et al., 2017).

3.2. Objectives

Even though Nendran is one of the favourite banana cultivars of Kerala, no attempts have been made so far to characterize the complete phytochemical composition of Nendran. Few studies were carried out by researchers to characterize the volatile compounds present in Nendran. Apart from these investigations, comprehensive literature on phytochemicals in unripe Nendran bananas remains scarce. Hence, we have decided to undertake studies to further explore the phytochemicals in unripe pulp and the product prepared out of it. While abundant literature exists on the phytochemicals in raw materials, data on their presence in processed products is notably scarce. Yet, it is these processed forms that ultimately enter our bodies, making it crucial to study the phytochemicals in processed foods to fully understand their impact on our health and well-being.

The objectives of this chapter are as follows:

- Phytochemical profiling of unripe Nendran pulp.
- Phytochemical profiling of product made from the unripe pulp (BG).

3.3. Materials and methods

The phytochemical composition of unripe Nendran pulp and BG was explored using the traditional route of solvent extraction of bioactive compounds from the matrix followed by the isolation of individual compounds through column chromatography and preparative TLC and preparative HPLC routes. The structure elucidation was done with the aid of NMR, and High-Resolution Electrospray Ionization Mass Spectrometry (HR-ESI-MS) analysis.

3.3.1. General procedures

Structure elucidation of the isolated phytochemicals by chromatography was carried out by 1D (^{1}H, ^{13}C NMR, and DEPT-135) and 2D NMR (COSY, HSQC, and HMBC) analysis. The isolated compounds were dissolved in deuterated chloroform ($CDCl_3$), and deuterated methanol (CD_3OD), ^{1}H, and ^{13}C NMR were recorded on a Bruker Ascend^{TM} 500 megahertz (MHz) spectrometer at 500 and 125 MHz, respectively. The chemical shifts (δ) were given in parts per million (ppm), coupling constants in hertz (Hz), and multiplicities are reported as s for singlet, d for doublet, dd for double doublet, m for multiplet, etc. HR-ESI-MS analysis was conducted on a Thermo Scientific Exactive mass spectrometer with an Orbitrap analyzer, and the ions are given in m/z. The specific optical rotation of compounds was measured with a JASCO P-2000 polarimeter (JASCO, USA).

3.3.2. Chemicals and standards

All the solvents used for isolation and purification were of standard analytical grade. The TLC aluminium sheets (Silica gel 60 F_{254}) and silica gel (230-400 mesh & 100-200 mesh) were obtained from Merck (Mumbai, India). The NMR solvents were purchased from Merck Life Science Pvt Ltd (Mumbai, India).

3.3.3. Raw material collection for BG preparation and phytochemical analysis

Details about the raw material (unripe Nendran) used for the study are reported in chapter 2 of this thesis. For the phytochemical studies, the peel (5.09 kg) and pulp (10.35 kg) of mature unripe Nendran banana (16.32 kg) was separated, and the pulp (3.98 kg) was sliced, lyophilized. For lyophilization, the initial freezing was done at -40 ºC for 3 hours at ambient pressure. For the drying step, the initial shelf temperature was set at -40 ºC for 1 hour at 500 millitorr (mTorr). The temperature was further reduced to -10 ºC at a rate of -10 ºC reduction in each 2 hours. Meanwhile, the pressure was also reduced to 300 mTorr. Then a holding was given for 2 hours at -5 ºC at 300 mTorr. Then the temperature was increased to 5 ºC and maintained for 2 hours at 250 mTorr pressure and further, the temperature increased to 10 ºC and maintained for 1 hour 30 minutes at 200 mTorr pressure. The temperature was finally raised to 25 ºC at a rate of increase of 5 ºC in every 4 hours and the final applied vacuum was 100 mTorr. The lyophilized pulp (1.63 kg), and stored at -20 °C for further analysis. The remaining pulp (6.17 kg) was pre-treated and dried to produce BG (2.40 kg) (Scheme 3.1.).

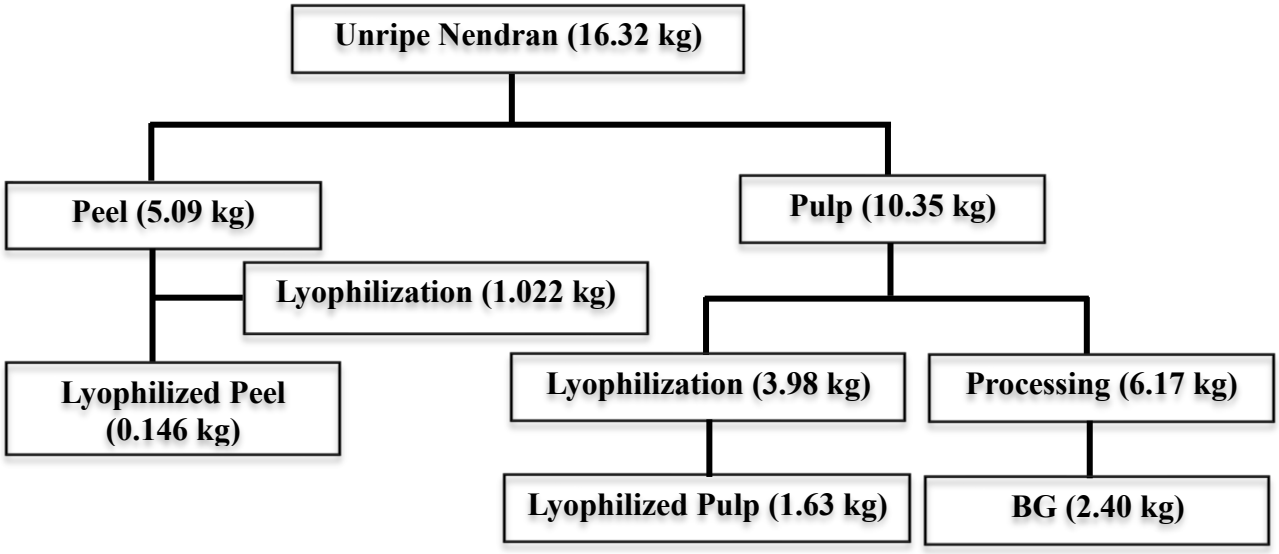

Scheme 3.1. Banana processing for phytochemical exploration studies

3.3.4. Phytochemical exploration of BG through column chromatography

3.3.4.1. Extraction protocol for isolation of phytochemicals

BG (1 kg) was ground and passed through 20 mesh before extraction and sequentially extracted with chloroform ($CHCl_3$, 3.5 L), ethanol (4 L), and hydro-alcohol (1:1 v/v, ethanol:water 4 L) at 800 rpm using an overhead stirrer (Hei-TORQUE 100, Heidolph, Germany). After extraction, each extract was kept for settling and filtered through Whatman no. 1 filter paper, fitted with Buchner funnel to remove starch, then extracts were concentrated under vacuum (Hei-vap, Heidolph, Germany), which afforded 3.18 g, 4.39 g and 14.16 g of $CHCl_3$, ethanol and hydro-alcohol extracts, respectively (Scheme 3.2.).

The phytochemical distribution pattern of the $CHCl_3$ extract was monitored on TLC, with different mobile phase systems comprising 1:1 hexane:ethyl acetate (EtOAc), $CHCl_3$:MeOH (2:1, 8:1), and $CHCl_3$:EtOAc (7:3, 10:1), by charring with 15% sulphuric acid (H_2SO_4) in ethanol. The TLC chamber was oven-dried and allowed to attain room temperature for each elution with the aforementioned mobile phase systems prior to the use. The $CHCl_3$:MeOH (8:1) system showed the best separation pattern of compounds, hence, this ratio was adopted for checking the TLC of the isolates in further studies (Fig. 3.1).

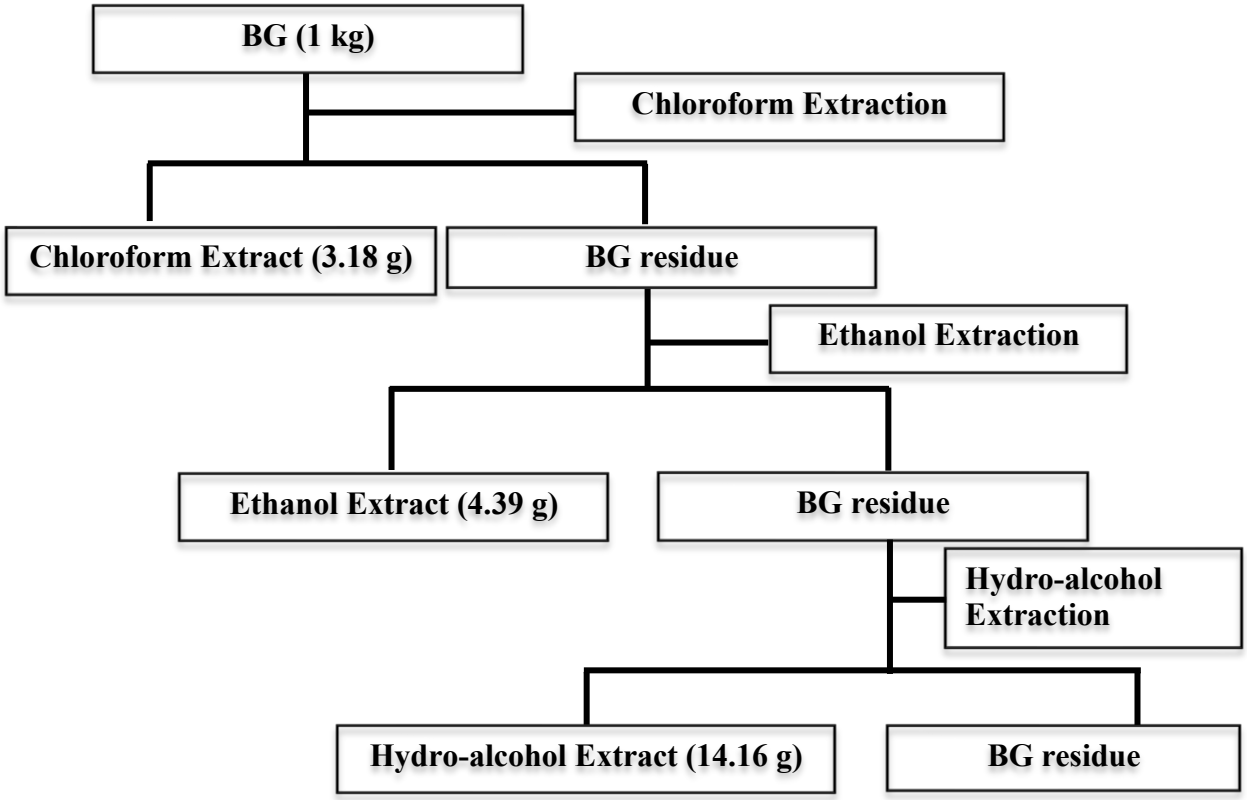

Scheme 3.2. Sequential extraction of BG

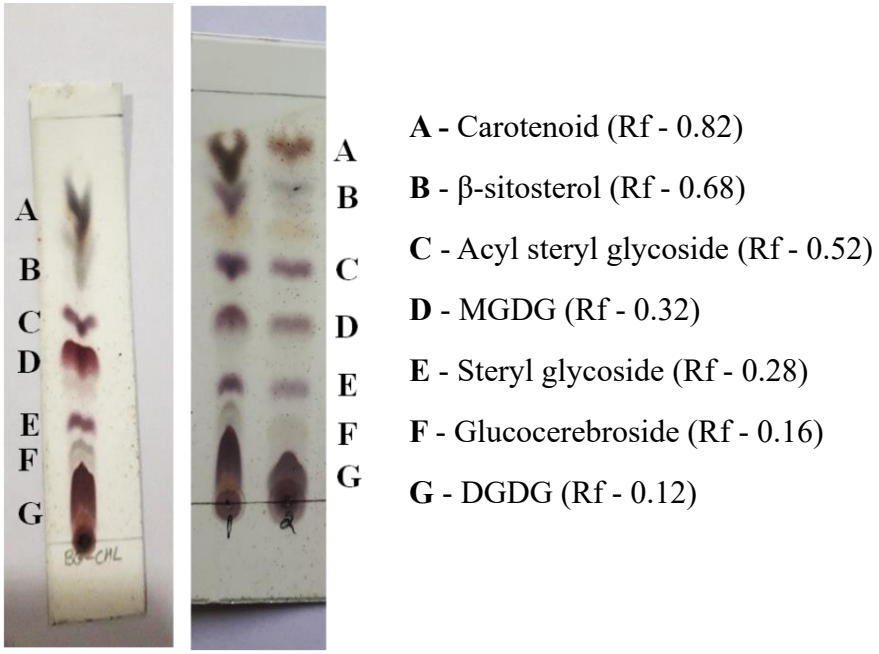

Fig. 3.1. TLC charring pattern of BG $CHCl_3$ extract (TLC code: BG-CHL), unripe pulp $CHCl_3$ extract (TLC code: 1) and unripe pulp acetone extract (TLC code: 2) developed in $CHCl_3$:MeOH (8:1) system

3.3.4.2. Purification of $CHCl_3$ extract by column chromatography

The $CHCl_3$ extract (2.8 g) was adsorbed and loaded on a silica (230-400 mesh) column (60 × 3 cm) and sequentially eluted with 800 mL of 100% $CHCl_3$ which yielded 15 fractions. Further, 200 mL each of 1-10%, 15%, 20%, and 50% MeOH in $CHCl_3$ combination was added and each percentage solution was collected as separate fractions, which afforded 13 fractions. Finally, the column was eluted with 100 mL of 100% MeOH. The TLC pattern of all 29 fractions was monitored with $CHCl_3$:MeOH (8:1) system and visualized by charring with 15% H_2SO_4 in ethanol. The fractions which showed similar TLC patterns were pooled, which resulted in a total of nine ($C_{2\text{-}6}$, C_8, C_{10}, C_{11}, and C_{13}; Fig. 3.2.) 100% $CHCl_3$ fractions and twelve $CHCl_3$-MeOH fractions ($CM_{1\text{-}10}$, CM_{15} and CM_{20}). Only the fractions that showed prominent TLC patterns were further explored for compound isolation.

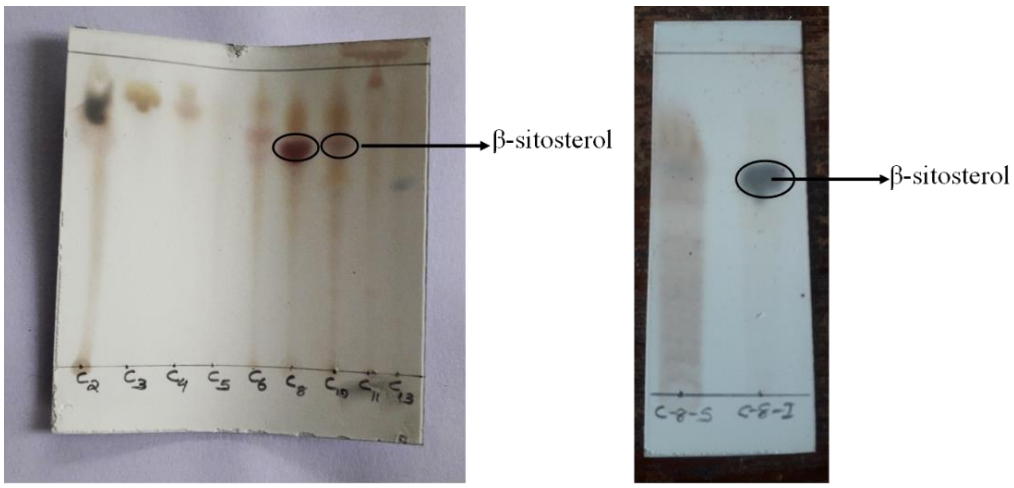

Fig. 3.2. TLC charring pattern of nine $CHCl_3$ fractions (C2-6, C8, C10, C11 and C13) and the AMT soluble portion (C-8-S) and AMT insoluble portion (C-8-I) of fraction C8 developed in $CHCl_3$:MeOH (8:1) system

3.3.4.3. Repurification of fractions and pure compound isolation

Two fractions (C_8 and C_{10}) among the nine 100% $CHCl_3$ fractions, were having a purple-pink prominent charring spot (retention factor (Rf) 0.68) in TLC when developed in $CHCl_3$:MeOH (8:1) system. The combination of ACN:MeOH:THF (AMT) in the ratio 40:56:4, when added to these fractions, compound **1** precipitated (216.2 mg from C_8 and 2.3 mg from C_{10}, TLC pattern provided in Fig. 3.2.), the compound was then dissolved in $CDCl_3$ and ^1H and ^{13}C NMR spectra were recorded. Next, we attempted the purification of seven fractions from $CHCl_3$ and $CM_{1\text{-}3}$ but could not succeed in isolating compounds in pure form. Further, we tried purification of CM_4 (108.9 mg) on a silica gel column (230-400 mesh) and it afforded 6 sub-

fractions, one sub-fraction (52.5 mg) was further purified on a silica gel column of 100-200 mesh, packed with hexane-EtOAc (1:1, v/v) and eluted with the same solvent system and it afforded 7.2 mg of compound **3** (Rf 0.52). The ^{1}H and ^{13}C NMR spectrum of compound **3** was recorded in $CDCl_3$. Other fractions ($CM_{5\text{-}6,\ 20}$), did not yield any compounds in pure form. When 100 % MeOH was added to the CM_7 fraction, a white precipitate (compound **4**, 33.9 mg) was observed and the ^{1}H NMR spectrum was taken in $CDCl_3$, and since the NMR spectrum showed a poor splitting pattern, the compound was peracetylated. In brief, the compound (12.8 mg) was dissolved in pyridine (2 mL) and acetic anhydride (1.5 mL) under a nitrogen atmosphere at room temperature. After overnight stirring, the mixture was transferred to a saturated sodium bicarbonate ($NaHCO_3$) solution (20 mL) and extracted with EtOAc (3 x 30 mL). The combined organic layers were further washed with distilled water (2 x 30 mL), dried over anhydrous sodium sulfate (Na_2SO_4), and concentrated. The residue was subjected to purification over a silica gel column (100-200 mesh) with 100 % hexane and EtOAc in hexane combination (5%-50%) to afford the acetylated product (8.1 mg), the ^{1}H and ^{13}C NMR spectrum of this acetylated compound were recorded in $CDCl_3$.

On addition of MeOH individually to $CM_{8\text{-}10}$, as in the case of CM_7, a MeOH insoluble and MeOH soluble portions were generated. The MeOH insoluble portion of CM_8 and CM_9 (27.4 mg and 7 mg, respectively) showed the exact TLC pattern as that of compound **4** when developed in the $CHCl_3$:MeOH 8:1 system. The MeOH soluble portions of $CM_{7\text{-}10}$ were pooled (90 mg) and separated on a silica gel column (230-400 mesh), which yielded two compounds. The first compound (13.8 mg) showed the same Rf (0.28) and charring pattern as that of compound **4**. The TLC comparison of all the compounds (one from the column and two from the insoluble fraction of $CM_{8,9}$) showing similarity with compound **4** is shown in Fig. 3.3.

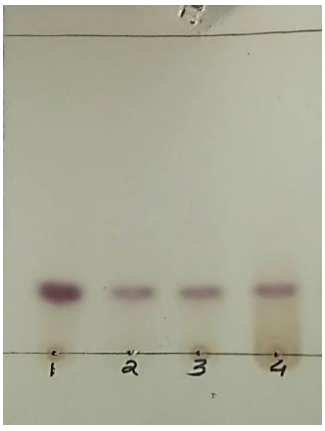

Fig. 3.3. TLC pattern of compounds showing similar Rf and charring (TLC code 2-4) pattern as that of compound **4** (TLC code 1). TLC developed in $CHCl_3$:MeOH (8:1) system

The second compound, i.e. compound **7** (32 mg) showed a more polar nature (Rf 0.16) than that of compound **4**, when developed in $CHCl_3$:MeOH 8:1 system and its ^1H NMR spectrum was recorded in $CDCl_3$. In addition, compound **7** was peracetylated as detailed for compound **4**. The ^1H and ^{13}C NMR spectrum of the peracetylated compound **7** was recorded in $CDCl_3$. The fraction eluted with 15% MeOH in $CHCl_3$ combination (CM_{15}, 250 mg) showed a deep purple-coloured charring spot (compound **6**) with Rf 0.12 when developed in $CHCl_3$:MeOH 8:1 system. The ^1H NMR spectrum of compound **6** was recorded in $CDCl_3$, however, due to the poor splitting pattern in ^1H NMR, compound **6** (68 mg) was acetylated and subsequent column purification afforded the peracetylated form of compound **6** (51.6 mg). The ^1H and ^{13}C NMR spectra and 2D NMR experiments of peracetylated compound **6** were recorded in $CDCl_3$. HR-ESI-MS analysis with direct injection was carried out on compound **6** in the underivatized and derivatized form (peracetylated form).

3.3.4.4. Purification of ethanol extract by column chromatography

The ethanol extract (4.39 g) was dissolved in MeOH and separated into MeOH-soluble and insoluble portions. The MeOH soluble portion was concentrated under vacuum (2.80 g) and taken for further studies. The extract (2.80 g) was adsorbed on silica (100-200 mesh) and then loaded on a silica column (230-400 mesh). The column length was 60 cm with a bed length of 40 cm and an internal diameter of 3 cm. The extract was fractionated using eluents 100% hexane, 100% $CHCl_3$, 100% EtOAc, 100% MeOH, and MeOH-water (7:3 v/v), each 300 mL. The TLC charring pattern of the fractions was monitored by developing TLC in a $CHCl_3$:MeOH (8:1) system and charring with 15% H_2SO_4 in ethanol. The charring spots in the hexane (60.90 mg), $CHCl_3$ (84.60 mg), and EtOAc (180.48 mg) fractions showed charring spots similar to the compounds identified earlier from the $CHCl_3$ extract of BG and hence these fractions were not explored further. The MeOH (1.02 g) and MeOH-water (1.47 g) fractions showed some interesting polar spots was further explored.

The fractions were pooled (2.49 g) and passed through a C18 sep-pack cartridge (Waters, USA) to remove the silica from the extract and then the extract (900 mg) was loaded on a silica column (230-400 mesh) with a bed length of 35 cm and an internal diameter of 3 cm. The extract was fractionated with eluents 100% $CHCl_3$, 5:95, 7:93, 8:92,10:90,15:85, 20:80, 25:75, 30:70, 35:65 $CHCl_3$:MeOH (v/v) and 100% MeOH. The TLC pattern of each test tube was checked and tubes with the promising pattern were pooled. This has resulted in 10 fractions (fraction 1 to fraction 10) and the NMR spectra (^1H & ^{31}P) of all these fractions were taken in $CDCl_3$. Further different approaches were taken to identify compounds in each fraction, which

led to the isolation of compound **4** (17.40 mg), compound **5** (12.91 mg), and compound **6** (80.93 mg).

3.3.4.5. Purification of hydro-alcohol extract by column chromatography

Different approaches such as column chromatography and preparative HPLC were adopted to characterize the phytochemicals present in the hydro-alcohol extract of BG. Since the yield of compounds was very low and as fraction was enriched with sucrose, no palpable result was obtained through any of these approaches.

3.3.5. Phytochemical exploration studies of BG through preparative TLC method

After the completion of phytochemical exploration studies through the column chromatography method, we have continued our exploration to find more phytoconstituents of BG through the preparative TLC method. Accordingly, BG (500 g) was sequentially extracted with hexane, acetone, ethanol, and hydro-alcohol (1:1, ethanol:water v/v) at 1000 rpm for 6 hours in a magnetic stirrer (IKA, RCT BS022). Each extract was concentrated under vacuum, which afforded hexane extract (560 mg), acetone extract (120 mg), ethanol (705 mg), and hydro-alcohol extract (7 g) of BG (Scheme 3.3.)

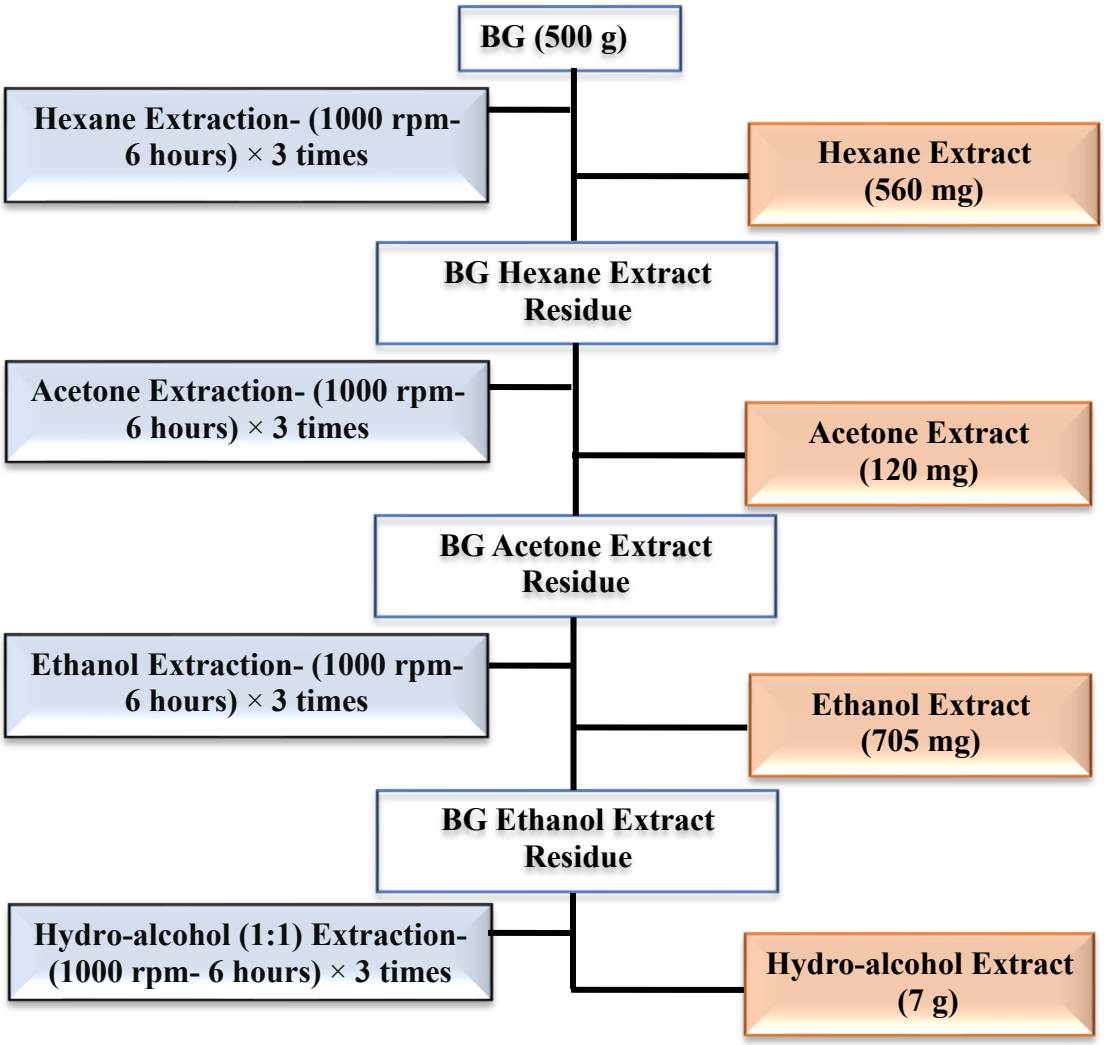

Scheme 3.3. Sequential extraction of BG for isolation of compounds by preparative TLC

The hexane and acetone extracts were further explored via the preparative TLC method. The hexane extract (70 mg) was spotted on a TLC plate and developed in the $CHCl_3$:MeOH 8:1 system. A portion of the TLC was cut, charred, and used as a reference for scrapping out the compounds. A prominent charring spot corresponding to Rf 0.68 was scrapped out and the compound was eluted from silica with EtOAc, ^1H NMR spectra were recorded in $CDCl_3$ and identified as compound **1** (19.5 mg). Similarly, the acetone extract (100 mg) of BG was also spotted on a TLC plate and developed in $CHCl_3$:MeOH 8:1 system, and charring spot corresponding to 0.68, 0.32, and 0.12 were scrapped out and eluted with EtOAc, and the solvent was removed under vacuum, which led to isolation of compound **1** (1.1 mg), compound **5** (5 mg), and compound **6** (2 mg), respectively. Compound **5** obtained through the preparative TLC method was dissolved in $CDCl_3$ and recorded the ^1H, ^{13}C, 2D NMR spectra, and further confirmed by HR-ESI-MS analysis.

3.3.6. Phytochemical exploration studies of unripe pulp

3.3.6.1. Phytochemical exploration studies through preparative TLC method

The lyophilized unripe Nendran pulp (100 g) was sequentially extracted with hexane, acetone, ethanol, and hydro-alcohol (1:1, ethanol:water v/v) which yielded 218 mg, 58.8 mg, 145.3 mg, and 2.8 g extracts, respectively (Scheme 3.4.). The hexane (60 mg) and acetone extracts (50 mg) were subjected to preparative TLC analysis as mentioned under section 3.3.5. The preparative TLC exploration of hexane extract afforded 3.8 mg of compound **1** (Rf 0.68), 1.5 mg of compound **2** (Rf 0.48), and 1.8 mg of compound **5** (Rf 0.32). The ^1H and ^{13}C NMR spectrum of compound **2** was recorded in $CDCl_3$. The preparative TLC exploration of acetone extract yielded 3 mg of compound **2** (Rf 0.48), 4.2 mg of compound **5** (Rf 0.32), and 4.7 mg of compound **6** (Rf 0.12).

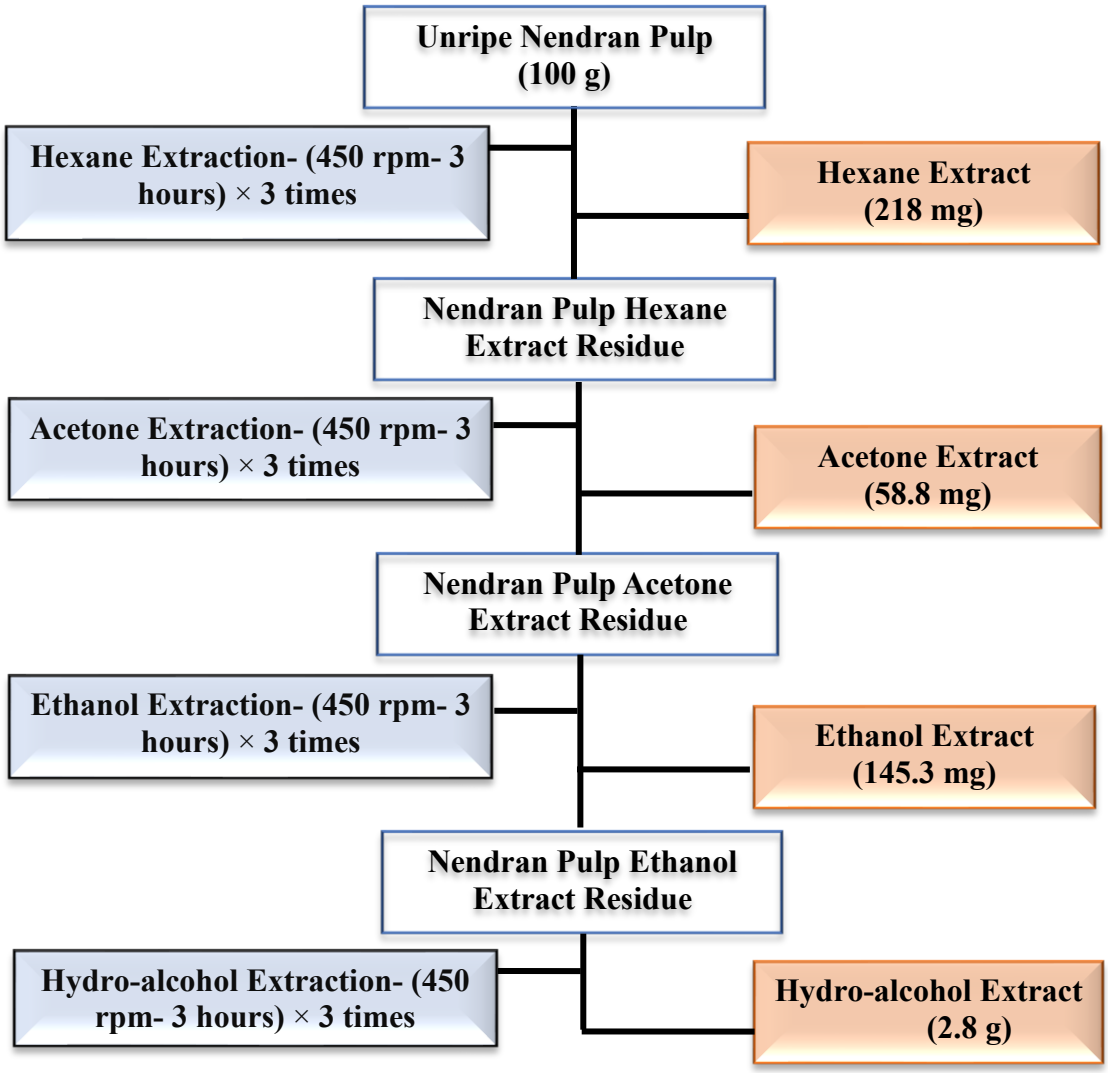

Scheme 3.4. Sequential extraction of unripe Nendran for isolation of compounds by preparative TLC

3.3.6.2. Phytochemical exploration studies of unripe Nendran pulp through column chromatography and preparative HPLC method

Among the molecules isolated from BG, compound 7 exhibited characteristic glycolipid signals and amide (NH) protons in NMR. The presence of compound 7 was explored in the unripe pulp to confirm that compound 7 is not an artefact formed during the BG preparation process.

In brief, 500 g of lyophilized unripe pulp was sequentially extracted with $CHCl_3$ and acetone, which yielded 2.09 g and 325 mg $CHCl_3$ and acetone extracts, respectively. Each extract was separately chromatographed on a silica gel column (230-400 mesh) and eluted with 100 % $CHCl_3$ followed by 5-50% MeOH in $CHCl_3$ which yielded 35.3 mg and 15.1 mg of compound **7** from the $CHCl_3$ and acetone extracts, respectively. The compound **7** (40 mg) so obtained was dissolved in MeOH (1.2 mL) and filtered through a 0.2 µm nylon syringe filter

(Micro-Por Minigen Syringe Filter, Genetix Biotech Asia, New Delhi), and the clear solution was injected into the preparative HPLC system connected to a reverse phase Luna 5 μm C18 (2) column 25 cm × 21.2 mm (Phenomenex, USA) for further purification. The mobile phase system consisted of 100% MeOH with a flow rate of 5 mL per minute. The sample injection volume was 1 mL and the fractions were collected by monitoring the eluting peaks at 205 nm. The collected fractions were evaporated under vacuum in a rotatory evaporator. ^{1}H and ^{13}C NMR, 2D NMR spectra of compound **7** was taken in $CDCl_3$:CD_3OD (2:1 v/v), and further analysed by HR-ESI-MS.

3.3.7. Confirmation of molecules by specific optical rotation

The specific optical rotation of compound **1** and peracetylated compound **4** was analyzed by preparing 0.61% and 0.92% solutions of compounds in $CHCl_3$, and the values were recorded with JASCO P 200 polarimeter.

3.4. Result and discussion

3.4.1. Phytochemical exploration studies of BG and unripe Nendran pulp

The phytochemical composition of BG and unripe pulp were explored by column chromatography, preparative TLC, and preparative HPLC, and the structural characterization of pure compounds were carried out with the aid of NMR, HR-ESI-MS & specific optical rotation data. The crude $CHCl_3$ extract of BG showed 7 prominent charring spots with Rf ranging from 0.1 to 0.8 (Fig. 3.1.) in $CHCl_3$:MeOH (8:1) system, and we were able to identify the compounds corresponding to all these charring spots. The compound corresponding to Rf 0.82 appeared as a carotenoid based on its bright orange colour in TLC. Compounds corresponding to the other six prominent charring spots (compounds **1**, **3-7**) were identified (Fig. 3.1.) and discussed in detail here.

Phytochemicals were isolated from unripe pulp by preparative TLC and column chromatography routes. It was observed that the TLC profile of the $CHCl_3$ and acetone extracts of the unripe Nendran pulp displayed perfect resemblance to that of the $CHCl_3$ extract of BG (Fig. 3.1.). Preparative TLC isolation of hexane and acetone extracts of unripe pulp afforded compounds **1**, **2**, and **5** and compounds **2**, **5**, and **6**, respectively. On the other hand, the $CHCl_3$ and acetone extracts were subjected to column chromatography for the isolation of compound **7**. The NMR spectral data of compounds 1-7 are given in the section 3.4.2. The structures of compounds identified are given in Fig. 3.4. and structural characterization was explained in detail in the section 3.4.3.

3.4.2. NMR spectral data of compounds 1-7

Compound (1): ^{1}H-NMR ($CDCl_3$) 0.61 m, 0.70-0.79 m, 0.85 m, 0.94 m, 0.98-1.11 m, 1.18 m, 1.37-1.47 m, 1.78 m, 1.95 m, 2.13-2.23 (2H, m), 3.45 (1H, m), 5.28 (1H, d, J=3.25 Hz); ^{13}C-NMR ($CDCl_3$) 11.8, 11.9, 18.7, 19.0, 19.4, 19.8, 21.0, 23.0, 24.3, 26.0, 28.2, 29.1, 29.7, 31.6, 31.9, 33.9, 36.1, 36.5, 37.2, 39.7, 42.2, 42.3, 45.8, 50.1, 56.0, 56.7, 71.8, 121.7, 140.7.

Compound (2): ^{1}H-NMR ($CDCl_3$) 0.61 m, 0.74-85 m, 0.94 s, 0.96-1.13 m, 1.16-1.29 m, 1.35-1.44 m, 1.72-2.00 m, 2.29 m, 3.31 (2H, m), 3.38 (1H, m), 3.50 (2H, m), 4.18 (1H, d, J=12.36 Hz), 4.32 (1H, d, J=7.60 Hz), 4.45 (1H, m), 5.29 (3H, m); ^{13}C-NMR ($CDCl_3$) 11.8, 11.9, 14.1, 18.7, 19.0, 19.3, 19.8, 21.0, 22.6, 23.0, 24.3, 24.9, 26.1, 27.2, 28.2, 29.2-29.8, 31.9, 33.9, 34.2, 36.1, 36.7, 37.2, 38.9, 39.7, 42.3, 45.8, 50.1, 56.1, 56.7, 63.1, 70.0, 73.6, 73.9, 75.9, 79.5, 101.2, 122.1, 130.0, 140.3, 174.7.

Compound (3): ^{1}H-NMR ($CDCl_3$) 0.61 m, 0.74-0.86 m, 0.93 s, 0.98-1.12 m, 1.15-1.27 m, 1.35-1.65 m, 1.78 m, 1.84-1.97 m, 2.28 m, 3.30 (2H, m), 3.39 (1H, m), 3.49 (2H, m), 4.19 (1H, dd, J=1.6, 12.0 Hz), 4.31 (1H, d, J=7.70 Hz), 4.41 (1H, dd, J=4.83, 12.08 Hz), 5.29 (1H, m); ^{13}C-NMR ($CDCl_3$) 11.8, 11.9, 14.1, 18.7, 19.0, 19.3, 19.8, 21.0, 22.7, 23.0, 24.3, 24.9, 26.0, 28.2, 29.1-29.7, 31.6, 31.8, 31.9, 33.9, 34.2, 36.1, 36.7, 37.2, 38.9, 39.7, 42.3, 45.8, 50.1, 56.0, 56.7, 63.1, 70.0, 73.5, 73.9, 75.9, 79.5, 101.2, 122.1, 140.2, 174.7.

Compound (4): ^{1}H-NMR ($CDCl_3$) 0.60 (3H, s), 0.71-0.80 (8H, m), 0.85 (4H, m), 0.92 (3H, s), 0.94-1.12 (7H, m), 1.13-1.31 (7H, m), 1.32-1.64 (11H, m), 1.73-1.86 (3H, m), 1.93 (3H, s), 1.95 (3H, s), 1.97 (3H, s), 2.00 (3H, s), 2.09-2.21 (2H, m), 3.42 (1H, m), 3.61 (1H, ddd, J=2.41, 4.68, 9.89 Hz), 4.04 (1H, dd, J=2.18, 12.18 Hz), 4.19 (1H, dd, J=4.83, 12.23 Hz), 4.52 (1H, d, J=8.00 Hz), 4.89 (1H, t, J=8.80 Hz), 5.01 (1H, t, J=9.70 Hz), 5.13 (1H, t, J=9.53 Hz), 5.29 (1H, d, J=4.90 Hz); ^{13}C-NMR ($CDCl_3$) 11.8, 11.9, 18.7, 19.0, 19.3, 19.8, 20.62, 20.65, 20.7, 20.8, 21.0, 23.0, 24.3, 26.0, 28.2, 29.1, 29.4, 31.8, 31.9, 33.9, 36.1, 36.7, 37.2, 38.9, 39.7, 42.3, 45.8, 50.1, 56.0, 56.7, 62.1, 68.5, 71.5, 71.6, 72.9, 80.0, 99.6, 122.1, 140.3, 169.3, 169.4, 170.3, 170.7.

Compound (5): ^{1}H-NMR ($CDCl_3$) 0.72-0.85 m, 1.21-1.32 m, 1.91-2.03 m, 2.25 (q, J=7.91 Hz), 2.63 bs, 2.67-2.76 m, 2.83 bs, 2.91 bs, 3.49 (1H, t, J=4.85 Hz), 3.53 (1H, m), 3.58 (1H, m), 3.68 (1H, dd, J=6.33, 11.23 Hz), 3.79-3.86 (2H, m), 3.91 (1H, d, J=5.35 Hz), 3.95 (1H, m), 4.14 (1H, dd, J=6.48, 11.98 Hz), 4.22 (1H, d, J=7.44 Hz), 4.32 (1H, dd, J=3.04, 12.75 Hz), 5.22-5.34 m; ^{13}C-NMR ($CDCl_3$) 14.1, 14.2, 20.5, 22.5, 24.8, 25.5, 25.6, 27.2, 29.0-29.7, 31.5, 34.1, 34.2, 62.7, 62.8, 68.3, 69.4, 70.2, 71.6, 73.4, 74.5, 103.9, 127.1-128.3, 130.0, 130.2, 131.9, 173.5, 173.7.

Compound (6): ^{1}H-NMR ($CDCl_3$) 0.85-0.90 m, 1.23-1.33 m, 1.60 m, 1.97 s, 2.05-2.08 m, 2.13 s, 2.29 m, 3.44 (1H, app t, J=8.65 Hz), 3.65 (1H, dd, J=5.50, 9.5 Hz), 3.78 (1H, dd, J=5.15, 9.90 Hz), 3.85 (1H, t, J=5.58 Hz), 3.98 (1H, dd, J=4.40, 10.50 Hz), 4.08-4.15 (3H, m), 4.21 (1H, m), 4.31 (1H, d, J=10.75 Hz), 4.48 (1H, d, J=7.85 Hz), 4.95 (1H, d, J=2.80 Hz), 5.00 (1H, dd, J=2.30, 10.30 Hz), 5.11 (1H, dd, J=3.35, 10.91 Hz), 5.18 (2H, m), 5.29 (1H, m), 5.42 (1H, d, J=1.70 Hz), 5.45 (1H, d, J=1.85 Hz); ^{13}C-NMR ($CDCl_3$) 14.11, 20.56-20.68, 22.67, 24.69, 24.85, 27.20, 29.12-29.67, 31.90, 34.05, 61.56, 62.26, 65.52, 66.57, 67.13, 67.37, 67.50, 67.64, 67.89, 68.62, 69.64, 70.90, 71.52, 96.75, 101.66, 169.42, 169.97, 170.08, 170.17, 170.43, 170.67, 172.79, 173.35.

Compound (7): ^{1}H-NMR ($CDCl_3$:CD_3OD) 0.80 (t, J=6.62 Hz), 1.18 m, 1.26-1.72 m, 1.93 m, 2.01 m, 3.15 (t, J=7.88 Hz), 3.20 m, 3.26 m, 3.31 m, 3.61-3.67 m, 3.78 m, 3.85 m, 3.90-3.99 m, 4.04 (app t, J=6.90 Hz), 4.18 (d, J=7.70 Hz), 5.28 m, 5.40 (dd, J=7.23, 15.28 Hz), 5.65 (dt, J=6.00, 15.25 Hz); ^{13}C-NMR ($CDCl_3$:CD_3OD) 13.8, 22.5, 25.1-34.4, 53.1, 61.3, 68.2, 69.9, 71.7, 71.9, 72.0, 73.3, 76.2, 76.3, 103.0, 128.4, 129.2, 130.4, 133.6, 175.8.

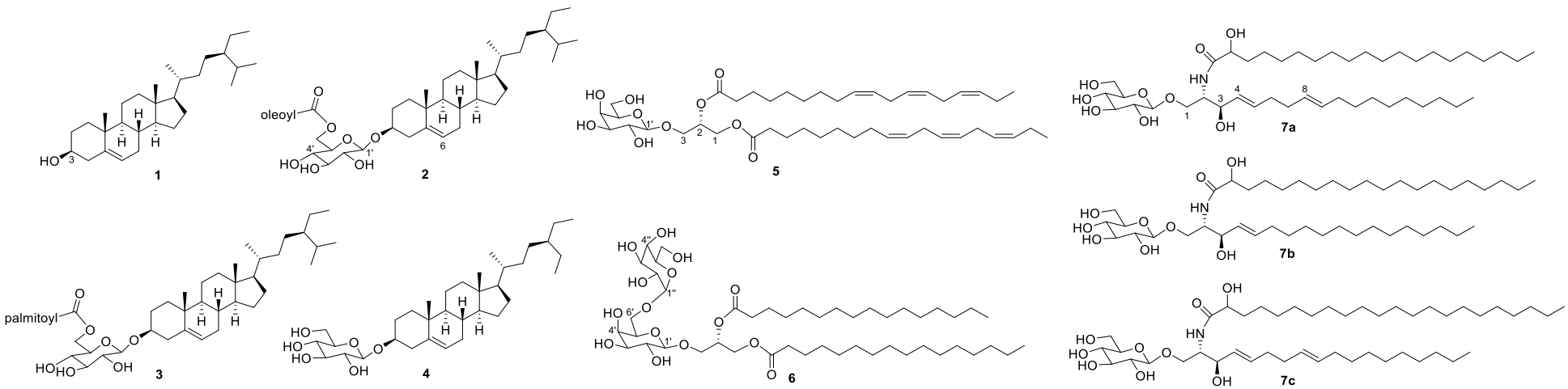

Fig. 3.4. Structures of compounds **1-7**. Compound **1** - β-Sitosterol, Compound **2** - Sitoindoside-II, Compound **3** - Sitoindoside-I, Compound **4** - β-Sitosterol-β-D-glucopyranoside, Compound **5** - Monogalactosyldiacylglycerol (MGDG), Compound **6** - Digalactosyldiacylglycerol (DGDG), Compound **7** – Glucocerebroside (GC)

3.4.3. Structural characterization of compounds 1-7

Compound **1** exhibited characteristic chemical shifts of aliphatic phytosterol in ^{1}H and ^{13}C NMR, with the presence of C3-OH and olefinic proton signals (Fig. 3.5.), its non-polar nature was evident from TLC. Vilela *et al.* reported sterols such as β-sitosterol, campesterol, and stigmasterol from the ripe pulp of ten *Musa* species (Vilela et al., 2014). Hence, compound **1** was readily identified as **β-sitosterol** (Fig. 3.4.), further confirmed by NMR spectral comparison in Biological Magnetic Resonance Data Bank. The specific optical rotation of compound **1** was found to be -30.25°, which was in agreement with the reported value of -30° (Johnson, 1958). Efficient precipitation of β-sitosterol from the hexane extract upon the addition of AMT (40:56:4) was an accidental observation we had during the sample preparation for HPLC analysis of carotenoids.

Compound **2** exhibited characteristic carbohydrate chemical shifts between 3-5 ppm, with δ_H 4.32 ppm (J = 7.6 Hz) indicating anomeric proton H-1' with β-configuration. The presence of downfield chemical shifts for H-6' (δ_H 4.45, 4.18 ppm) in ^{1}H NMR suggests the presence of an ester functionality on C6'-OH, with an aliphatic chain (Fig. 3.6.). The presence of a steryl group was evident from NMR, which along with the conventional glycosidic linkage ($\delta_{C\text{-}1'}$ 101.2 ppm) suggests compound **2** as an acyl steryl glycoside (ASG). By consideration of COSY correlations (Fig. 3.7.) and diaxial coupling constants of 9 Hz for $\delta_{H\text{-}4'}$ 3.31 ppm and $\delta_{H\text{-}2'}$ 3.29 ppm, the carbohydrate moiety was confirmed as D-glucose. A three integration in ^{1}H NMR in the olefinic region suggests the presence of one unsaturation in the aliphatic chain and with characteristic H-6 of the steryl moiety, which along with chemical shift considerations of ^{1}H and ^{13}C NMR resemble β-sitosterol. Ghosal *et al.* reported extensively on the isolation and characterization of steryl glycosides and sitoindosides from the peel of *M. paradisiaca* and their anti-ulcerogenic activity (Ghosal, 1985). The presence of olefinic carbons at δ_C 130 ppm indicates oleoyl moiety of the acyl group, which based on the published report by Ghosal *et al.* suggest compound **2** as **sitoindoside-II** (Fig. 3). Accordingly, compound **3** (Fig. 3.8.) was elucidated as **sitoindoside-I** (Fig. 3.4.) with a palmitoyl chain evident by the presence of only one olefin proton ($\delta_{H\text{-}6}$ 5.3 ppm) from the β-sitosteryl moiety, which was further evident from the ^{13}C NMR. Compound **4** exhibited characteristic carbohydrate signals in the ^{1}H NMR that along with steroidal region resemble a sterylglycoside. However, due to poor splitting pattern in ^{1}H NMR in $CDCl_3$, compound **4** was peracetylated (Fig. 3.9.) and confirmed as a **β-sitosterol β-D-glucopyranoside** (Fig. 3.4.) by NMR, which was in agreement with literature (Faizi et al., 2001). The specific optical rotation of the peracetylated form of compound **4** was found to be -22.9°, which was in agreement with the reported value of -23.9° (Coutts et al., 1957).

Compound **5** (Fig. 3.10.) exhibited characteristic carbohydrate signals in the ^{1}H NMR along with aliphatic chain, thus, resembling a glycolipid. Presence of COSY correlations for H-2 with H-3, H-1; H-1' with H-2'; H-6' with H-5', and HMBC correlation for H-2' with C1', C3'; H-4' with C2', which along with coupling constants confirmed the presence of D-galactose appended to a glycerol backbone as a β-glycoside. The downfield chemical shifts of H-2, H-1, and HMBC correlation of H-1' with C3 indicate the presence of ester groups in *sn*-1,2 positions and *sn*-3 with glycosidic linkage (Fig. 3.11.), thus, compound **5** is a **monogalactosyldiacylglycerol (MGDG)**. The presence of olefinic protons between 5-5.5 ppm suggests the presence of unsaturated fatty acids. HR-ESI-MS analysis (Fig. 3.12.) with direct injection was carried out to identify prominent molecular species, and two ions were observed. Ion at m/z 775.5367 $[M+H]^+$, which against the calculated 775.5360 $[M+H]^+$, confirms the molecular formula $C_{45}H_{74}O_{10}$ that corresponds to MGDG 36:6. Ion at m/z 799.5354 $[M+Na]^+$, which against the calculated 799.5336 $[M+Na]^+$, confirms the molecular formula $C_{45}H_{76}O_{10}$ that corresponds to MGDG 36:5. Blackbourn et al. reported the presence of high proportion of mono- and di-galactosyl diacylglycerols (MGDGs and DGDGs) in banana peel, with polyunsaturated fatty acids (PUFAs) such as α-linolenic acid (18:3ω3), PUFAs in MGDGs account for 94% of the fatty acid content (Blackbourn et al., 1990). Hence, one of the molecular species, MGDG 36:6 was identified as compound **5** (Fig. 3.4.). The second molecular species, MGDG 36:5 has two possibilities, MGDG (18:3ω3/18:2ω6) or MGDG (18:2ω6/18:3ω3).

Compound **6** exhibited characteristic disaccharide signals in the ^{1}H NMR, which along with aliphatic region resemble **digalactosyldiacylglycerol (DGDG).** However, due to poor splitting pattern in ^{1}H NMR, compound **6** was peracetylated and characterized (Fig. 3.13.). Presence of key COSY correlations of H-2' with H-1', H-3'; H-4' with H-5', H-3'; H-2'' with H-1'', H-3''; H-4'' with H-5'', H-3'' aided in identification of the anomeric protons H-1' and H-1'' with β and α configurations, respectively. Coupling constants of 1.9 and 1.7 Hz for H-4'' and H-4', respectively, confirm the presence of digalactosyl moiety. Presence of COSY correlation of H-2 with H-3, H-1 helped in identification of the protons of the glycerol backbone in ^{1}H NMR. Presence of key HMBC correlations of H-3 with C1' and H-6' with C1'' confirm the glycosidic linkages of DGDG (Fig. 3.14.). HR-ESI-MS analysis with direct injection was carried out to identify the molecular species (Fig. 3.15.). DGDG account for higher proportion of saturated fatty acid such as palmitic acid (Blackbourn et al., 1990). HR-ESI-MS analysis of the underivatized compound **6** exhibited an ion at m/z 915.6029 $[M+Na]^+$, which against the calculated 915.6021 $[M+Na]^+$ with palmitic esters, confirms the molecular formula $C_{47}H_{88}O_{15}$ that corresponds to compound **6** (Fig. 3.4.). A prominent ion at m/z 847.4677 $[M+Na]^+$, which

against the calculated 847.4667 $[M+Na]^+$, suggest the molecular formula $C_{40}H_{72}O_{17}$ that corresponds to a DGDG containing a nonadioic acid in *sn*-1 or *sn*-2 along with palmitic acid. Nonadioic acid was one of the dioic acids reported in the lipophilic extracts of ripe pulp from banana cultivars (Vilela et al., 2014). HR-ESI-MS analysis of the derivatized peracetylated compound **6** showed corresponding ions with an increase in mass by 294 due to acetylation of 7 x OH groups of digalactosyl moiety (Fig. 3.16.). Signals in mass spectra depend on the ionizing capability of the compounds, hence, DGDG with an extra carboxylic acid functionality in nonadioc acid is intense compared to compound **6** with palmitic acid (Fig. 3.15.).

Compound **7** exhibited characteristic glycolipid signals in NMR, which was initially analyzed by peracetylation NMR (Fig. 3.17.). Based on diaxial coupling constants and characteristic 8 Hz coupling constant of the anomeric proton, the monosaccharide of the acetylated derivative was determined as D-glucose with β-glycosidic linkage. Presence of a characteristic amide NH proton and HMBC correlations, indicate the presence of a ceramide backbone with sugar appendage at the C1 position. However, the presence of a C3-C4 double bond was unusual in the derivative, perhaps, an elimination reaction followed during peracetylation as shown in the scheme (Scheme 3.5.), thus, confirming compound **7** as **glucocerebroside (GC)**.

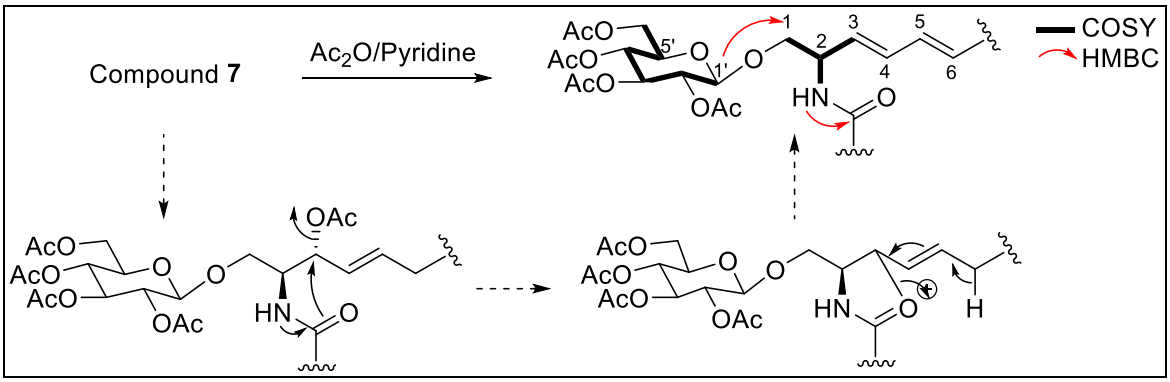

Scheme 3.5. Plausible mechanistic pathway during peracetylation of compound **7**, with key COSY & HMBC correlations

Based on the NMR, compound **7** in its original state NMR (Fig. 3.18.) or in its peracetylated form NMR (Fig. 3.17.) constitute a mixture of molecular species. We resorted to HR-ESI-MS analysis for generic information of the sphingosine backbone as well as aliphatic chains of the amide. HR-ESI-MS through LC afforded one of the parent ion measured as 770.6146 $[M+H]^+$, which against the calculated 770.6146 correspond to molecular formula $C_{44}H_{83}NO_9$, thus,

revealing one of the molecular species **7a** (Fig. 3.4. and Fig. 3.19a.). Presence of $[M+Na]^+$, $[2M+Na]^+$ peaks, and fragment peaks 752.6045 and 590.5514 corresponding to $[M-OH]^+$ calculated for 752.6035 and $[M\text{-glucose}]^+$ calculated for 590.5507, respectively confirm a sphingadienine backbone with 2-hydroxyeicosanoic acid as the aliphatic chain for molecular species **7a**. A second parent ion measured as 794.6127 $[M+Na]^+$, which against the calculated 794.6122 correspond to molecular formula $C_{44}H_{85}NO_9$, thus, revealing the second molecular species **7b** (Fig. 3.4. and Fig. 3.19b.). Presence of $[2M+Na]^+$ peak, and fragment peaks 610.5782 and 592.5675 corresponding to $[M\text{-glucose}+H]^+$ calculated for 610.5774 and $[M\text{-glucose-OH}]^+$ calculated for 592.5663, respectively confirm a sphingosine backbone with 2-hydroxyeicosanoic acid as the aliphatic chain for molecular species **7b**. A third parent ion measured as 820.6282 $[M+Na]^+$, which against the calculated 820.6279 correspond to molecular formula $C_{46}H_{87}NO_9$, thus, revealing the third molecular species **7c** (Fig. 3.4. and Fig. 3.19c.). The presence of $[2M+Na]^+$ peak, and fragment peaks 780.6361 and 618.5830 corresponding to $[M-OH]^+$ calculated for 780.6348 and $[M\text{-glucose-OH}]^+$ calculated for 618.5820, respectively confirm sphingadienine backbone with 2-hydroxydocosanoic acid as the aliphatic chain for molecular species **7c**. Both 2-hydroxyeicosanoic and 2-hydroxydocosanoic acids were reported as fatty acids components in banana cultivar Dwarf Cavendish (Oliveira et al., 2006).

To determine the position of double bond in sphingadienine and sphingosine backbone, we resorted to 2D NMR of compound **7**. Presence of key COSY correlations of H-3 with H-4, H-2; H-5 with H-4, H-6; and the presence of key HMBC correlations of H-3 with C2, C1, C4, C5; and H-1 with C1' (anomeric carbon) confirm the position of the double bond at C4 of sphingadienine and sphingosine backbone NMR (Fig. 3.20.). The characteristic '*E*' geometry of C4-C5 was determined from trans coupling constant of 15 Hz in ^1H NMR, but due to merging of signals between 5.2 to 5.3 ppm corresponding to the second double bond and due to the presence of molecular species, it was difficult to determine the double bond geometry and position. However, based on the consensus structure of sphingoids from plants, we report C8-C9 double bond with '*E*' geometry (Shirakura et al., 2012). The stereochemistry of C2 and C3 is highly conserved in sphingoids, however, the configuration of the hydroxy position of the aliphatic acid was left unassigned. To the best of our knowledge, the present work is the first report on the isolation and characterization of GCs from *Musa* species.

3.4.4. Review of literature on health benefits of identified compounds

3.4.4.1. Steroids and steroid derivatives

Phytosterols are molecules, found in plants, animals, and fungi, and have a structural similarity to cholesterol. β-sitosterol, a well-recognized phytosterol, showcases a diverse array of pharmacological activities that make it a promising compound in the field of medicine. Its anticancer properties, including the induction of apoptosis and inhibition of cell growth in cancer cell lines, MCF-7 and MDA-MB-231, highlight its potential in cancer treatment (Saeidnia et al., 2014). Additionally, β-sitosterol's antioxidant effects contribute to improving antioxidant status and preventing lipid peroxidation, which can be beneficial in combating oxidative stress-related conditions. Studies show that the administration of β-sitosterol reduces the levels of glucose and glycated hemoglobin (HbA1c) in streptozotocin-induced diabetic rats (Saeidnia et al., 2014). The hypocholesterolemic effects further underscore its therapeutic potential in managing cholesterol levels. It lowers the risk of atherosclerosis, heart attacks, and coronary artery disease by lowering the level of low-density lipoprotein (LDL) cholesterol (Gupta, 2020). The effect of β-sitosterol on the serum lipids was well studied. Administration of 25 g of β-sitosterol for a prolonged period results in the lowering of serum total cholesterol, and total lipid level (Best et al., 1955).

Steryl glycosides are sterols glycosylated at their 3β-hydroxy group. Glycosylation of sterols makes them an important component of the cell membrane and provides resistance against stress to the cells. Besides this, there are many benefits associated with steryl glycoside administration (Shimamura, 2020). β-Sitosterol-β-D-glucoside is a molecule with numerous biological potentials. β-Sitosterol β-D-glucoside isolated from sweet potato exhibited anti-breast cancer activity in MCF-7 and MDA-MB-231 breast cancer cell lines (Xu et al., 2018). β-Sitosterol β-D-glucopyranoside isolated from the fruits of *Cupressus sempervirens was* found to mimic estrogenic properties and thus stimulate glucose utilization in skeletal muscle cells (Pandey et al., 2021). Similar to steryl glycosides, ASG also possess cholesterol-lowering effects. Supplementation of ASG purified from soybean oil, 6.1 mg for two weeks, was found to exert cholesterol-lowering effects in C57BL/6J mice (Lin et al., 2011).

3.4.4.2. Glycolipids

Glycolipids, which are glycoconjugates of lipids, are typically located on the outer surface of eukaryotic cell membranes. They play a crucial role in maintaining membrane stability and facilitating cell-to-cell communication. Two classes of glycolipids include gangliosides and cerebrosides, both of which are glycosphingolipids, consisting of a carbohydrate and a

sphingolipid (*Glycolipids - Latest Research and News | Nature*, n.d.). MGDG, DGDG, and GC were the glycolipids we isolated in our study. MGDGs and DGDGs are predominantly found in the thylakoid membrane of plant chloroplasts, which are overlooked in nutrition applications as they are dispersed in biomass (Sahaka et al., 2020). The literature provides numerous evidence supporting the health benefits associated with all these identified compounds. MGDG is a molecule with great physiological significance. Due to its amphiphilic nature, MGDG is an attractive ingredient in the pharmaceutical field and exhibits therapeutic anti-cancer, anti-viral, and anti-inflammatory activities (Abedin & Barua, 2021). Similar to MGDG, DGDG also offers numerous health benefits. In a placebo-controlled clinical study, the role of oral supplementation of wheat polar lipids (oil and powder) containing glucosylceramides (1.7 mg) and DGDG (11.5 mg) was evaluated for its effects on skin hydration and other age-related symptoms. The results of the study demonstrated a positive impact of oral supplementation of polar lipids on subjects, showing significantly increased skin hydration, elasticity, and smoothness, along with decreased transepidermal water loss, roughness, and wrinkledness in the treated groups compared to the placebo (Bizot et al., 2017). These findings underscore the potential of DGDG and other polar lipids in promoting skin health and addressing age-related skin concerns. Apart from the pivotal role in the cosmetic industry MGDG and DGDG exert anti-inflammatory and anti-cancer properties (Bruno et al., 2005; Maeda et al., 2008; Ulivi et al., 2011).

MGDG isolated from *Rosa canina* was reported with anti-inflammatory properties (Larsen et al., 2003), and in a separate study, this property is explained by antagonism of toll-like receptor 4 (TLR4) receptor that was demonstrated by a MGDG probe (Liu et al., 2016). A combination of simvastatin, a lipid-lowering drug, and MGDG was studied in a murine model of sepsis and the results showed that this combination possesses the potential in sepsis therapy and prevention (Apaya et al., 2015). MGDG isolated from the methanolic extract of *Euphorbia helioscopia* L. was reported for free-radical scavenging activity (EC_{50} = 5.2 µg/mL) (Cateni et al., 2014). MGDG was reported as the active principle in traditional *Ophioglossum vulgatum* L. ointment for wound healing activity (Clericuzio et al., 2014). MGDG isolated from *Actinidia chrysantha* was reported as a ligand for peroxisome proliferator-activated receptor gamma (PPARγ), implicated in numerous diseases, with an IC_{50} value of 1.64 µM (Martin et al., 2013). The chloroform extract of leaves of *Cassia fistula* L. exhibited *in vitro* antiplasmodial activity where MGDG was the active principle (Grace et al., 2012). The active principle in the ethanolic extract from leaves of *Allium ursinum* L. for antiaggregatory effect was attributed to MGDG (Sabha et al., 2012). MGDG was reported as a superoxide generation

inhibitor, isolated from *Perilla frutescens*, with an IC_{50} value of 21 μM, comparable to rosmarinic acid and caffeic acid (Takahashi et al., 2011). A substantial presence of MGDG in most green vegetables of over 200 mg/kg fresh weight is considered to play a major role in the human diet, hence, glycolipids can be designated as a nutraceutical (Larsen et al., 2003). A MGDG enriched extract of *Crassocephalum rabens* showed significant suppression of B16 melanoma growth in C57BL/6J mice, comparable to chemotherapeutic drug cisplatin (Hou et al., 2007). MGDG isolated from *Armoracia rusticana*, *Wasabia japonica*, and *Amaranthus tricolor* inhibited proliferation of a range of cancer cells and cyclooxygenase enzymes, implicated in inflammation (Jayaprakasam et al., 2004; Weil et al., 2005). α-Linolenic acid (ALA) is well-known for its anticancer activity (Kim et al., 2014), interestingly, compound **5** isolated from *Citrus hystrix* exhibited anticancer activity at a dose ten times lesser than ALA in mouse skin (Murakami et al., 1995).

Another interesting glycolipid that we came across in the study was GC. They were known for immunomodulatory and anti-inflammatory properties. GC exerts immunomodulatory and anti-inflammatory functions by promoting T lymphocytes & Natural killer T (NKT) cells (Margalit et al., 2005, 2006). These findings suggest that GC-induced immune modulation may be beneficial in treating non-alcoholic steatohepatitis and other immune-mediated conditions (Margalit et al., 2006). Similarly, GC treatment ameliorates concanavalin A-induced hepatitis by inhibition of NKT lymphocytes (Margalit et al., 2005). In addition, being a source of ceramide, GC have shown application in cosmetics by playing an important role in the skin barrier function in retaining moisture and also has shown relevance as a dietary supplement (Jiang et al., 2021). The health benefits and significance of GCs and ceramides, and their application in the cosmetic field were discussed in detail in Chapter 5.

Consumption of BG helps to introduce these bioactive compounds to our body thus providing health benefits. Our findings not only contribute to expanding the understanding of the nutritional composition of BG but also hold promise for enhancing its value as a functional food ingredient. Consuming BG facilitates the intake of bioactive compounds known for their health benefits, thereby promoting overall well-being. Our study not only expands the BG's nutritional profile but also underscores its potential as a valuable functional food ingredient.

Fig. 3.5. ^{1}H and ^{13}C NMR of compound **1**

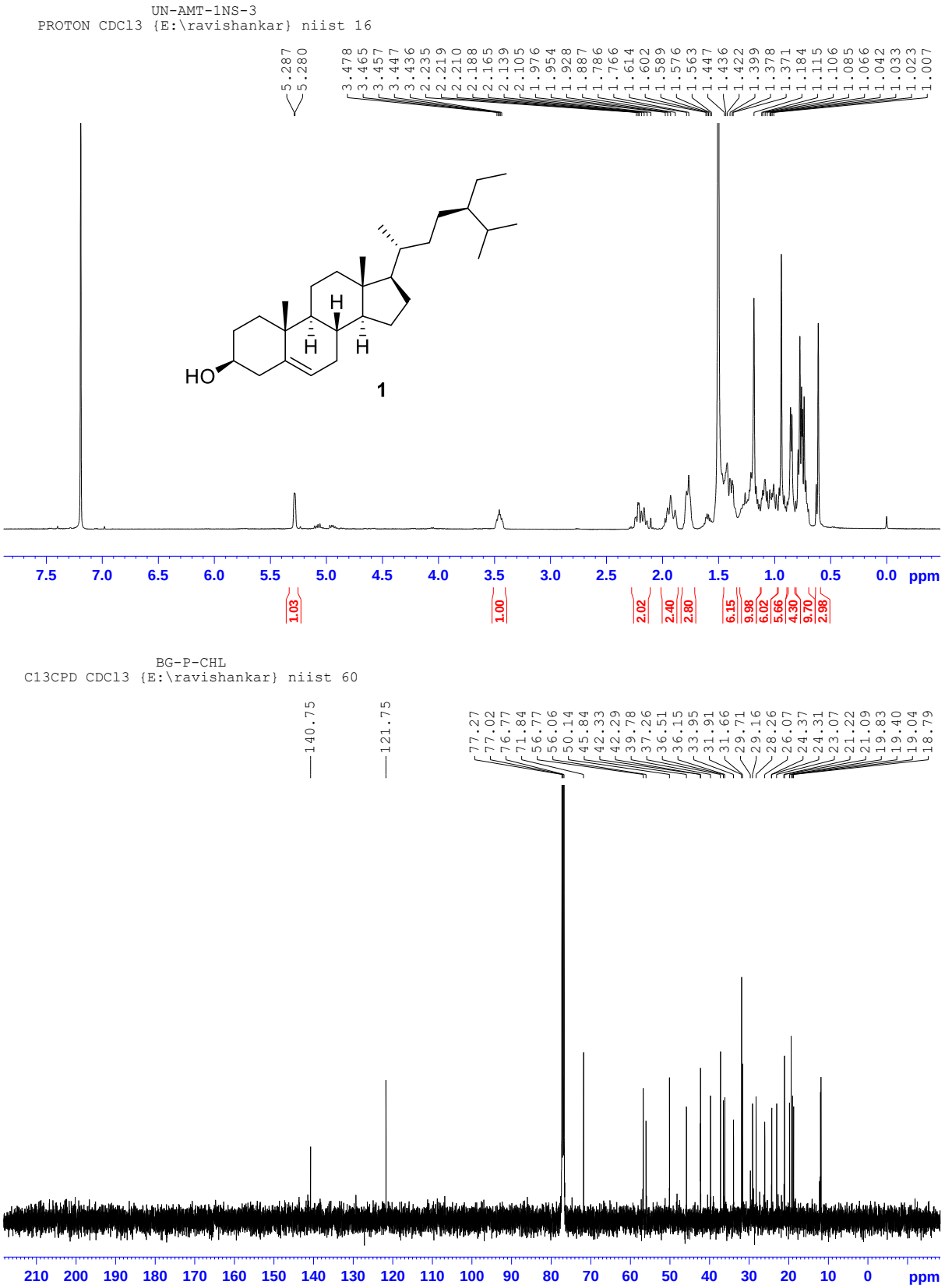

Fig. 3.6. ^{1}H and ^{13}C NMR of compound **2**

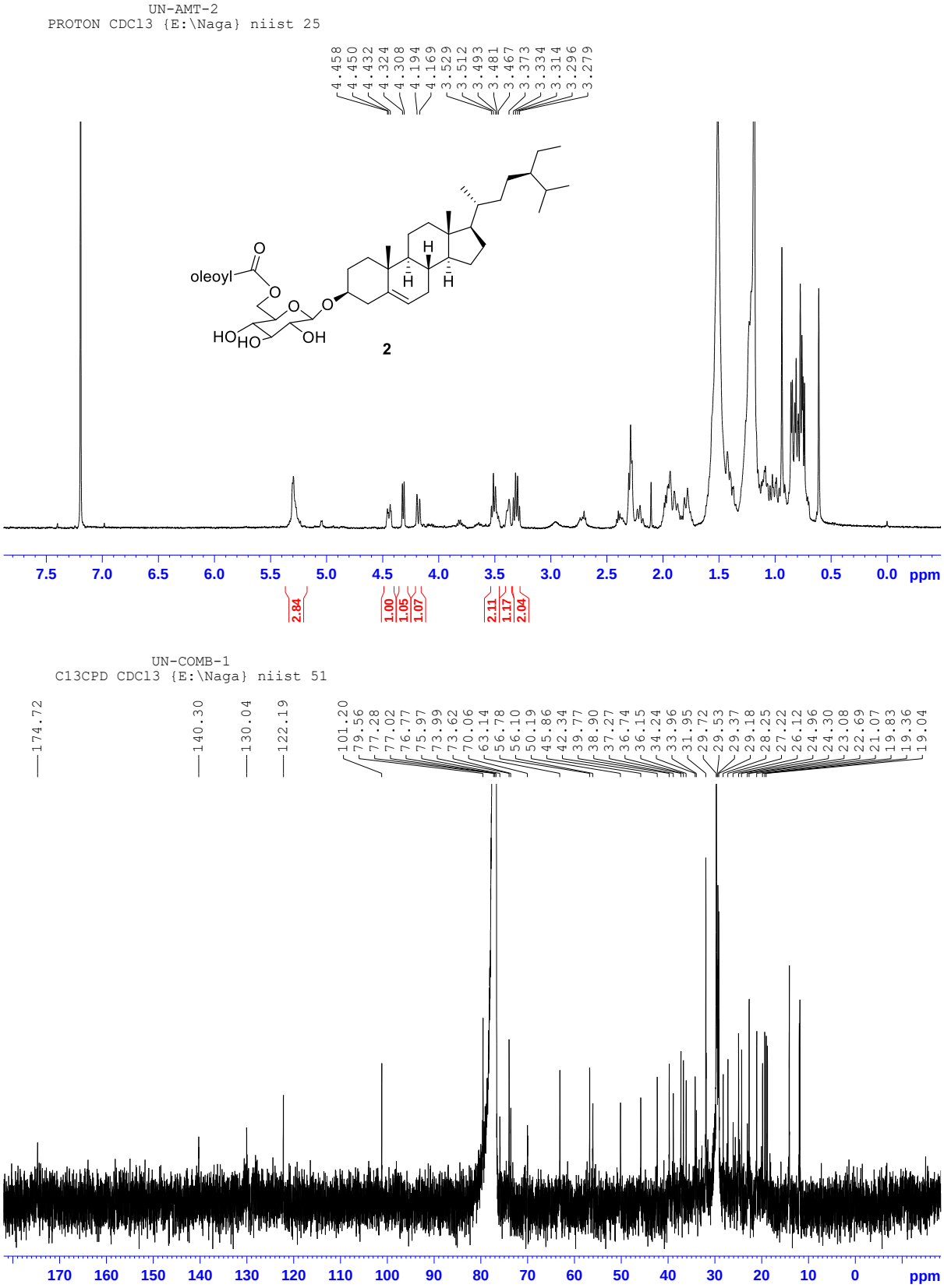

Fig. 3.7. COSY NMR of compound **2**

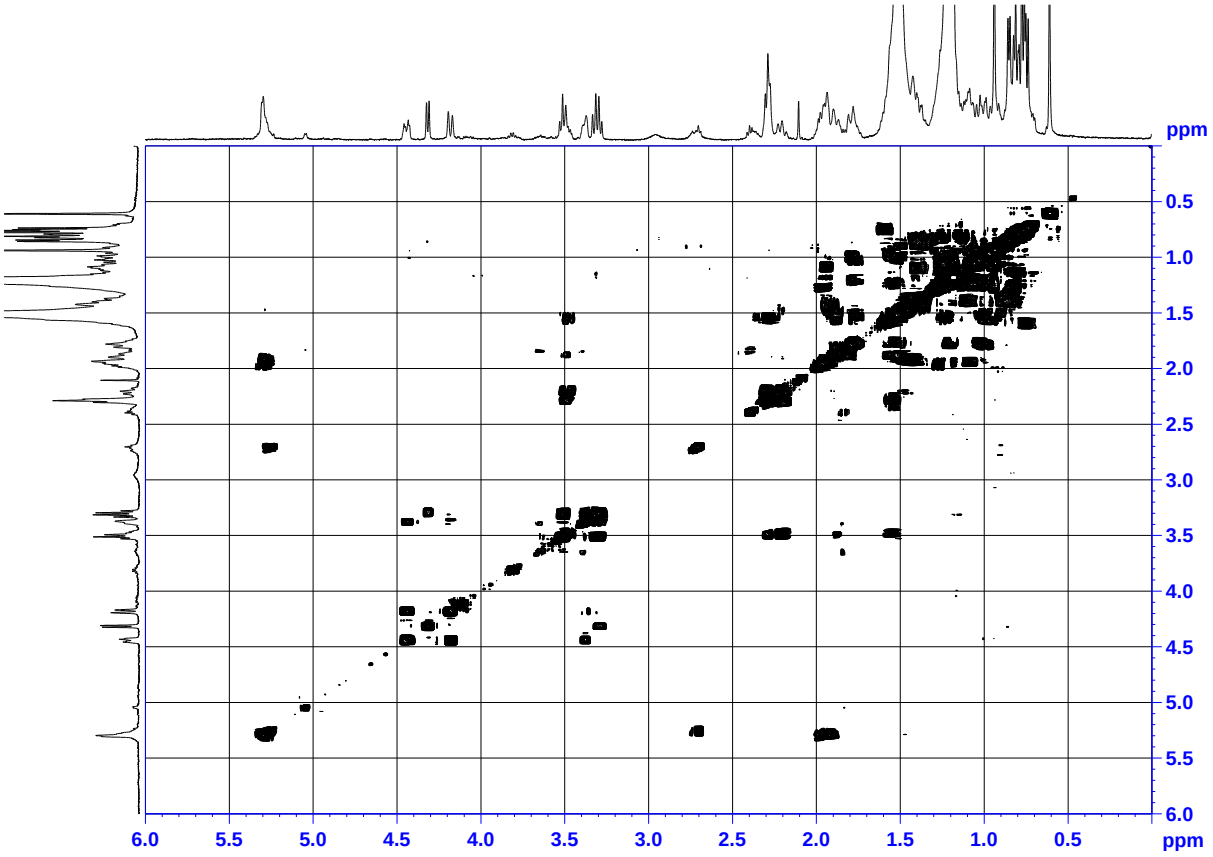

Fig. 3.8. ^{1}H and ^{13}C NMR of compound **3**

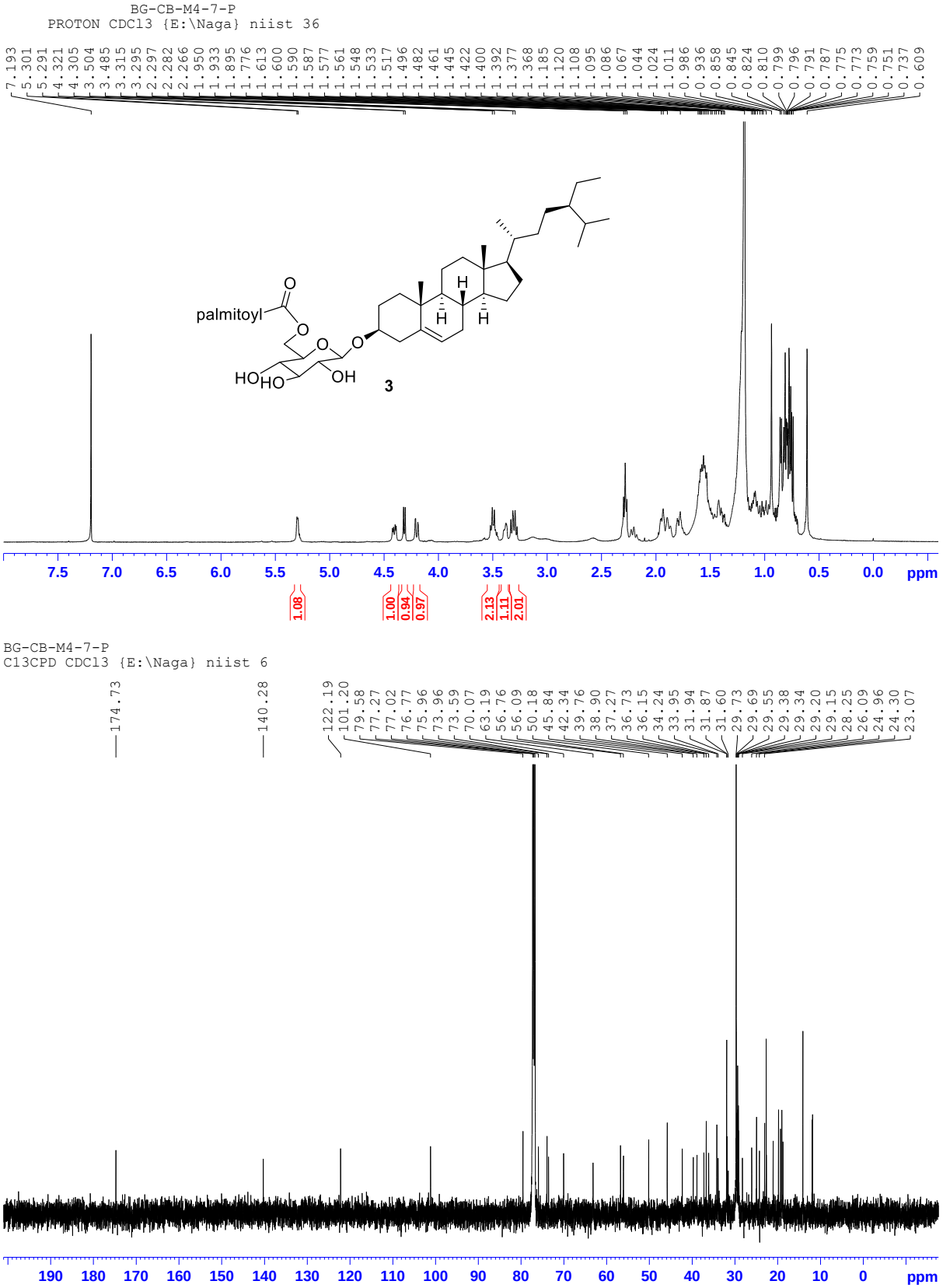

Fig. 3.9. ^{1}H and ^{13}C NMR of peracetylated compound **4**

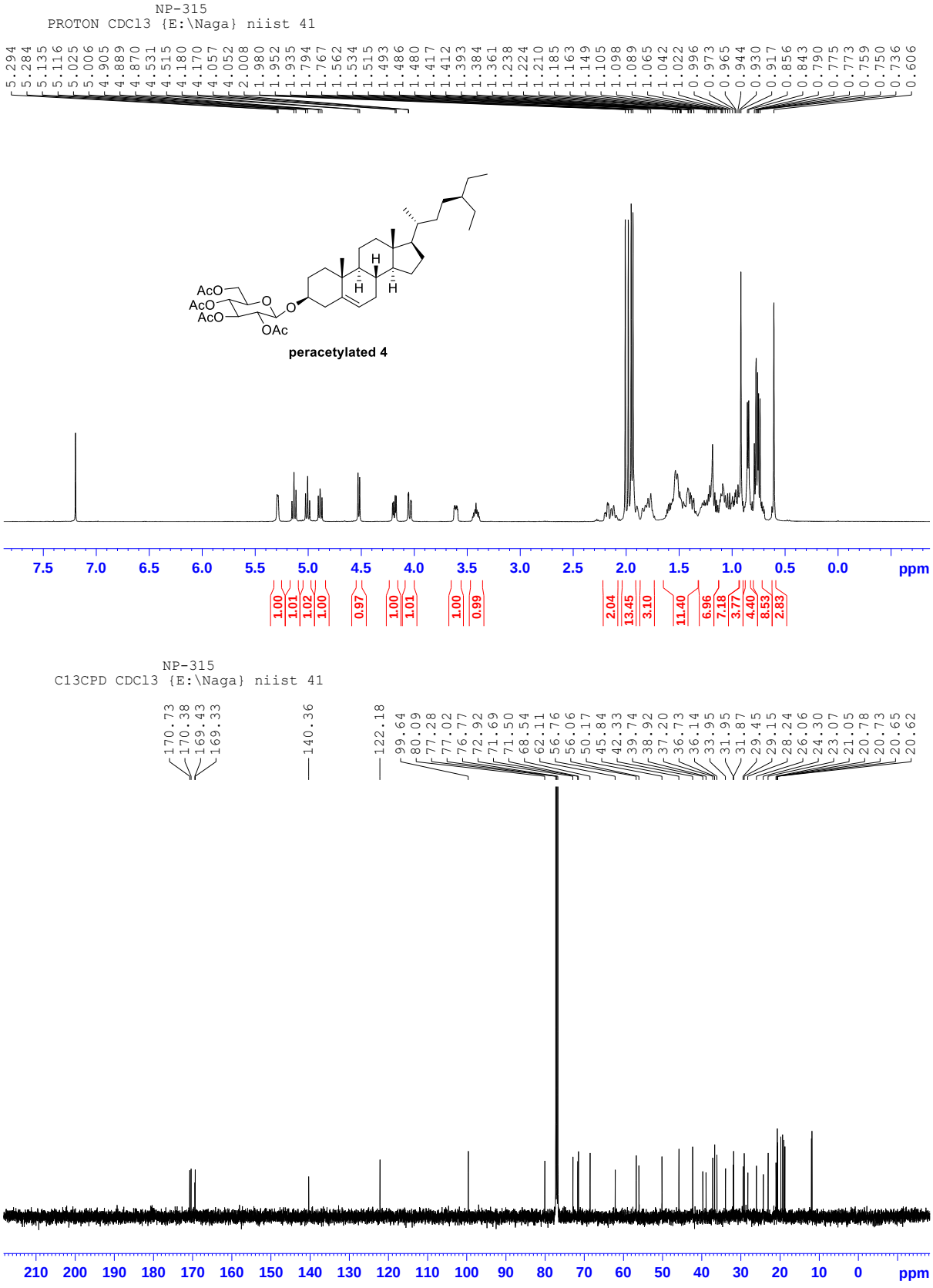

Fig. 3.10. ^{1}H and ^{13}C NMR of compound **5**

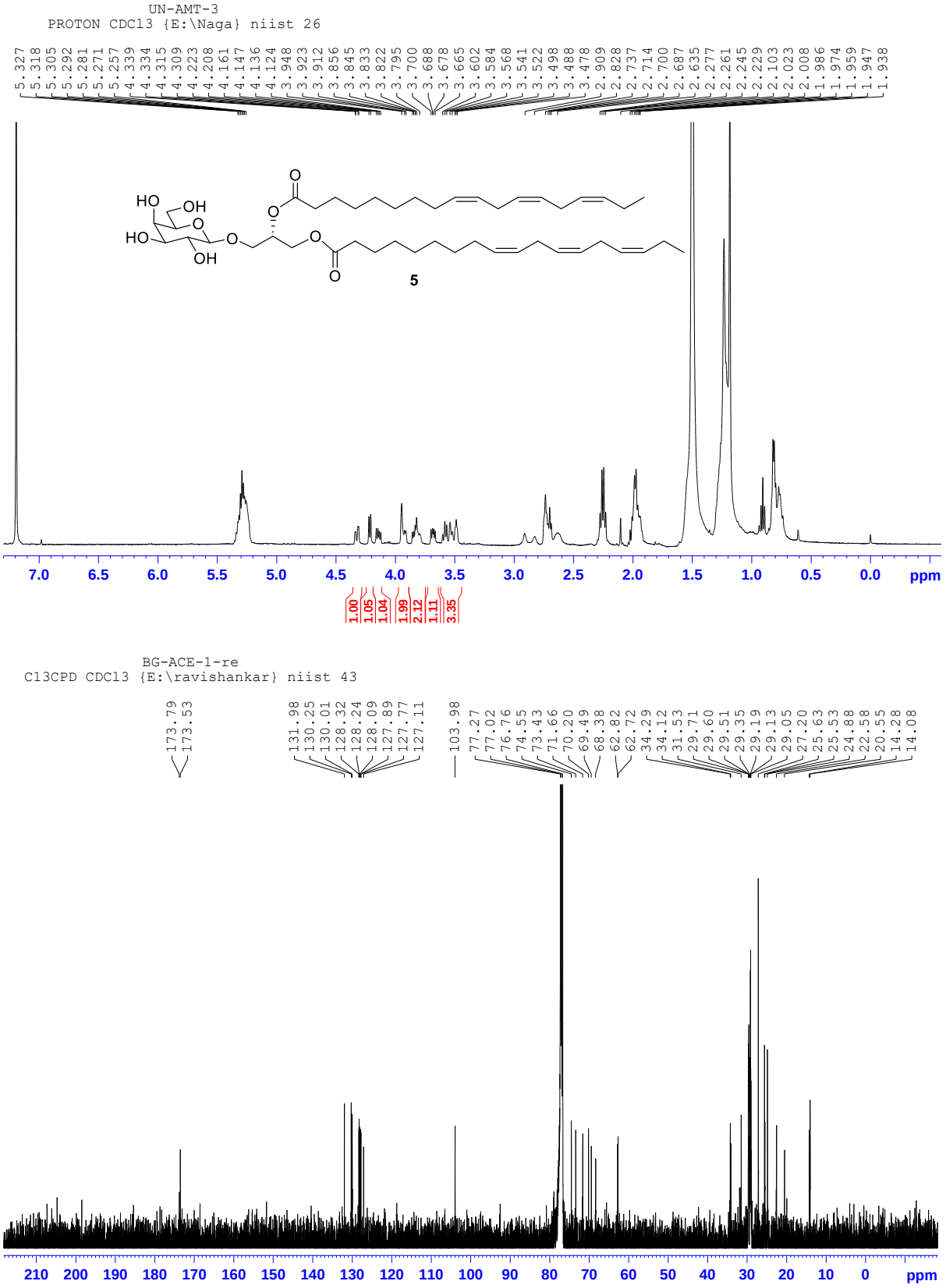

Fig. 3.11. COSY and HMBC NMRs of compound **5**

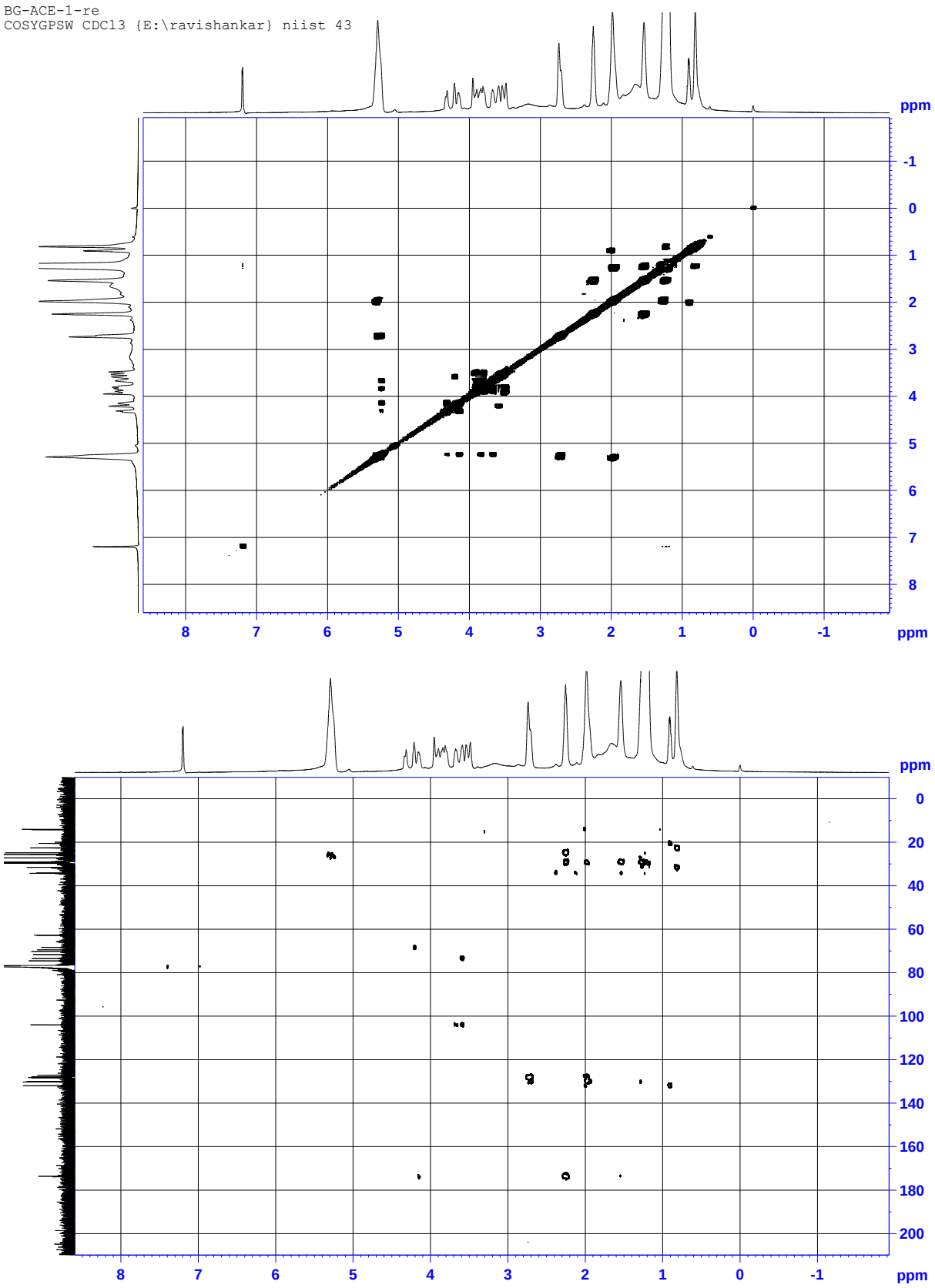

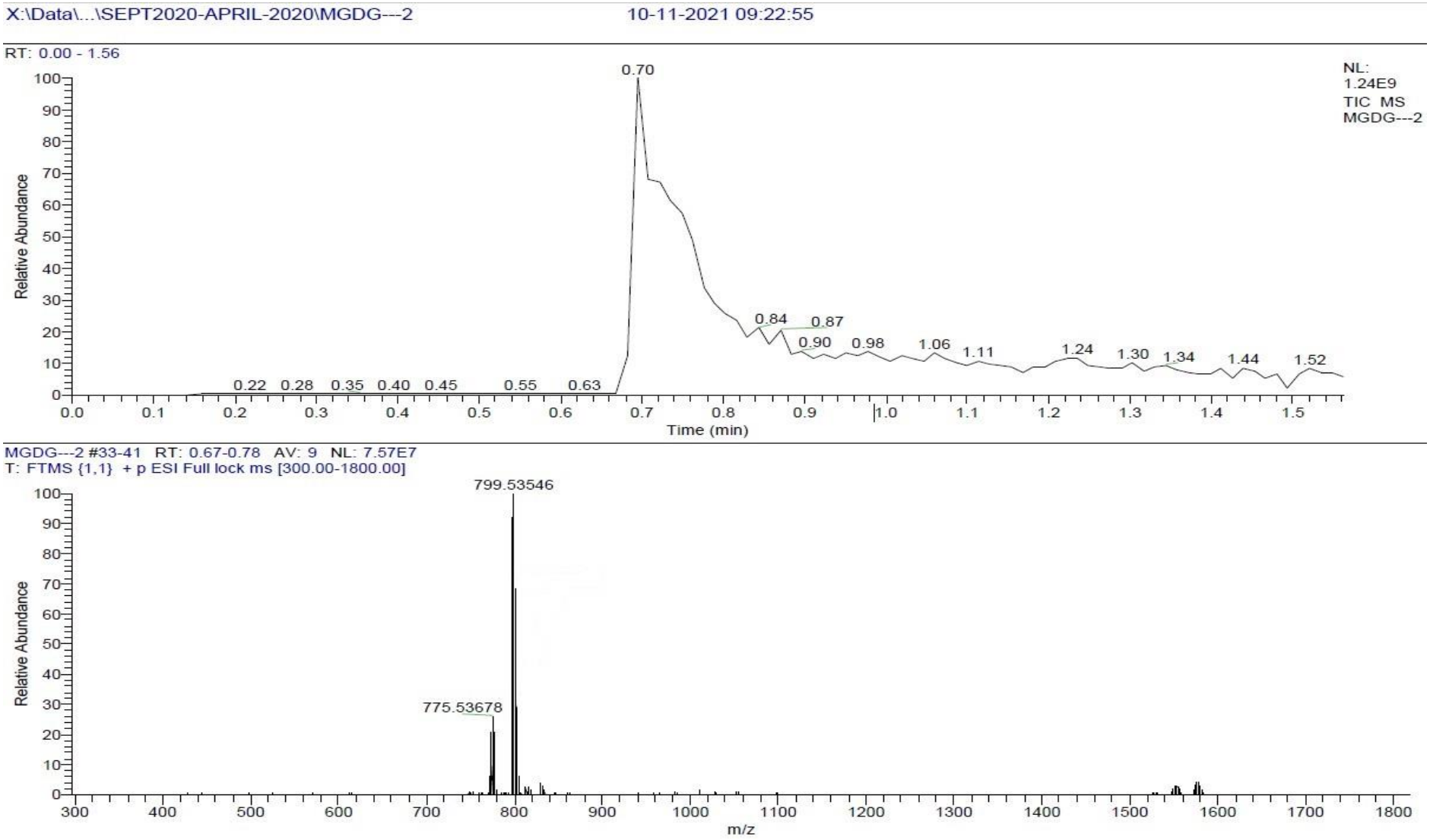

Fig. 3.12. HR-ESI-MS of compound **5**

Fig. 3.13. ^{1}H and ^{13}C NMR of peracetylated compound **6**

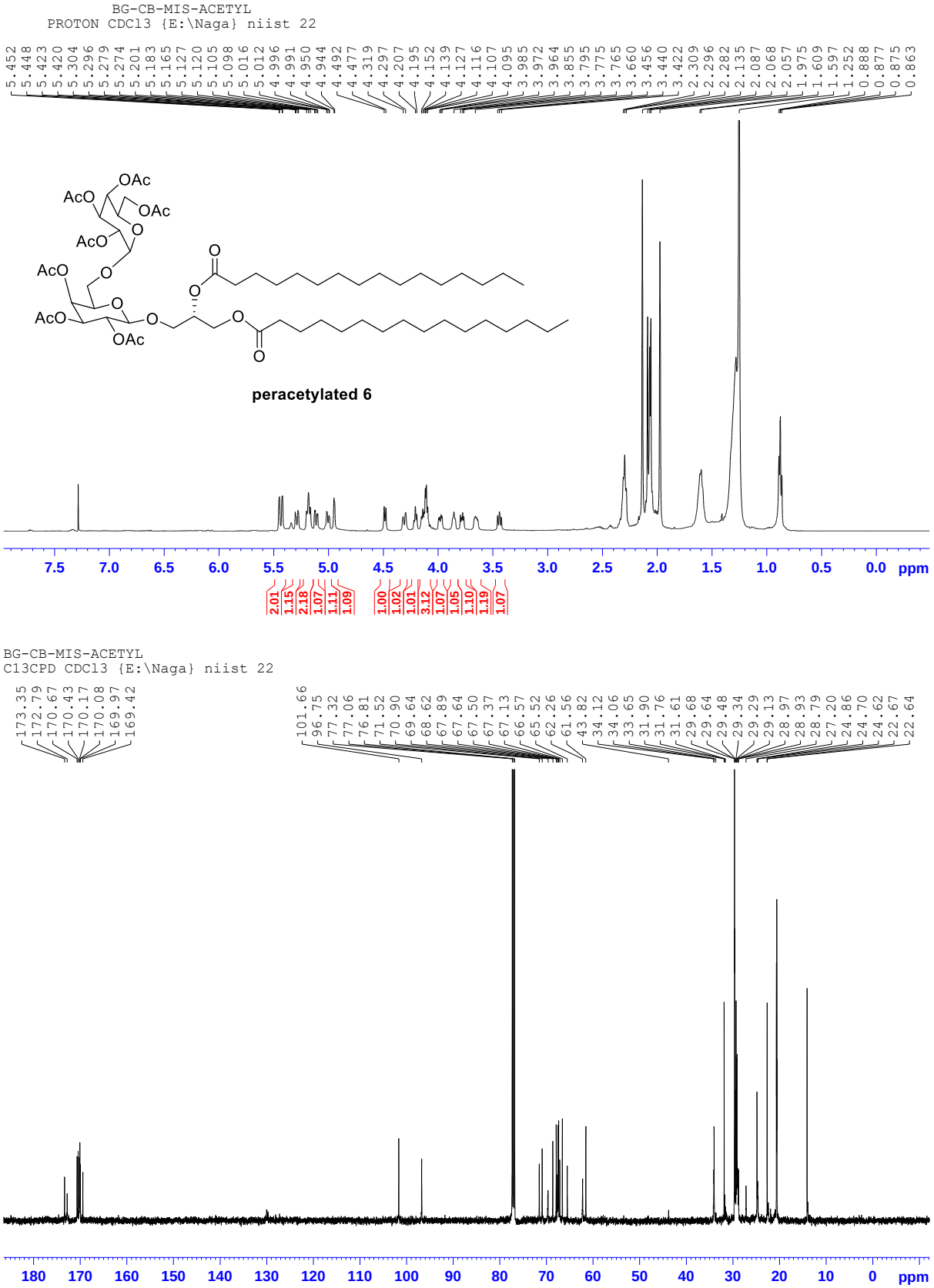

Fig. 3.14. COSY and HMBC NMRs of peracetylated compound **6**

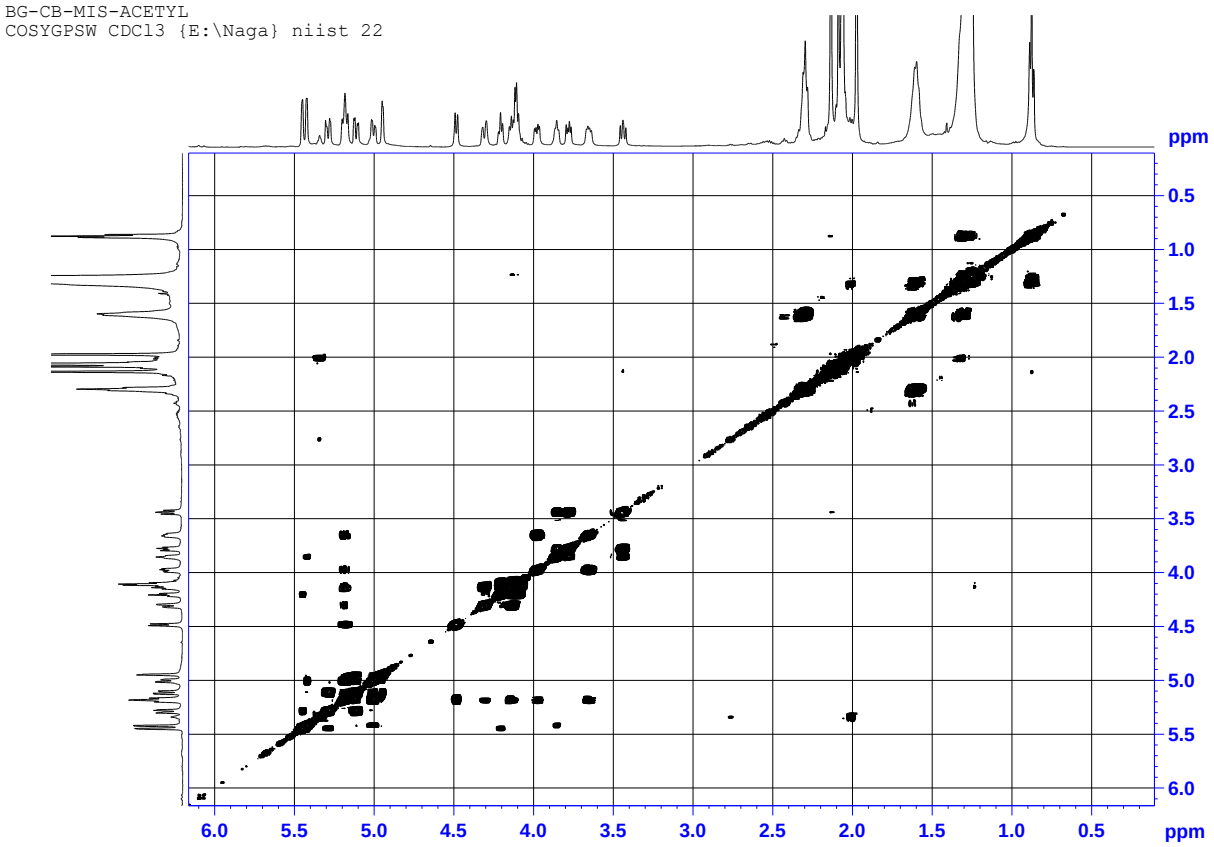

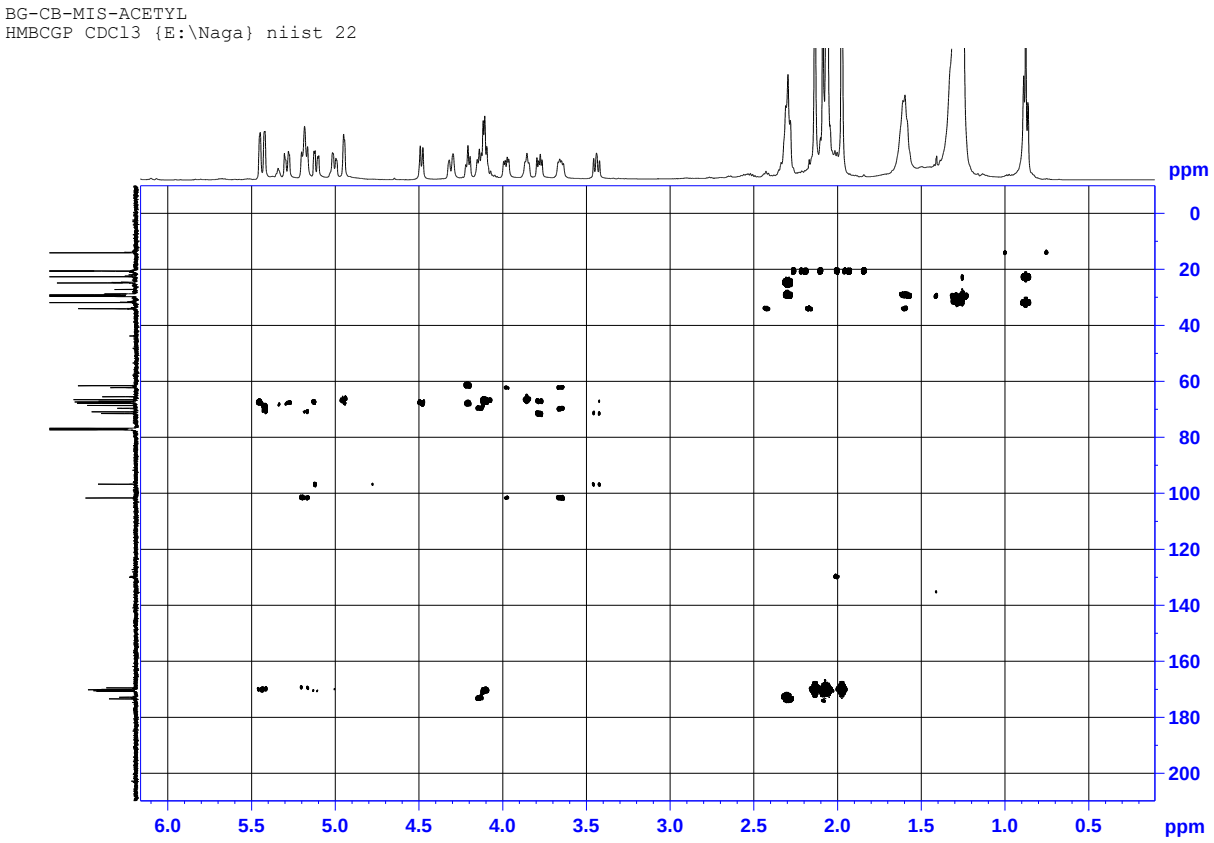

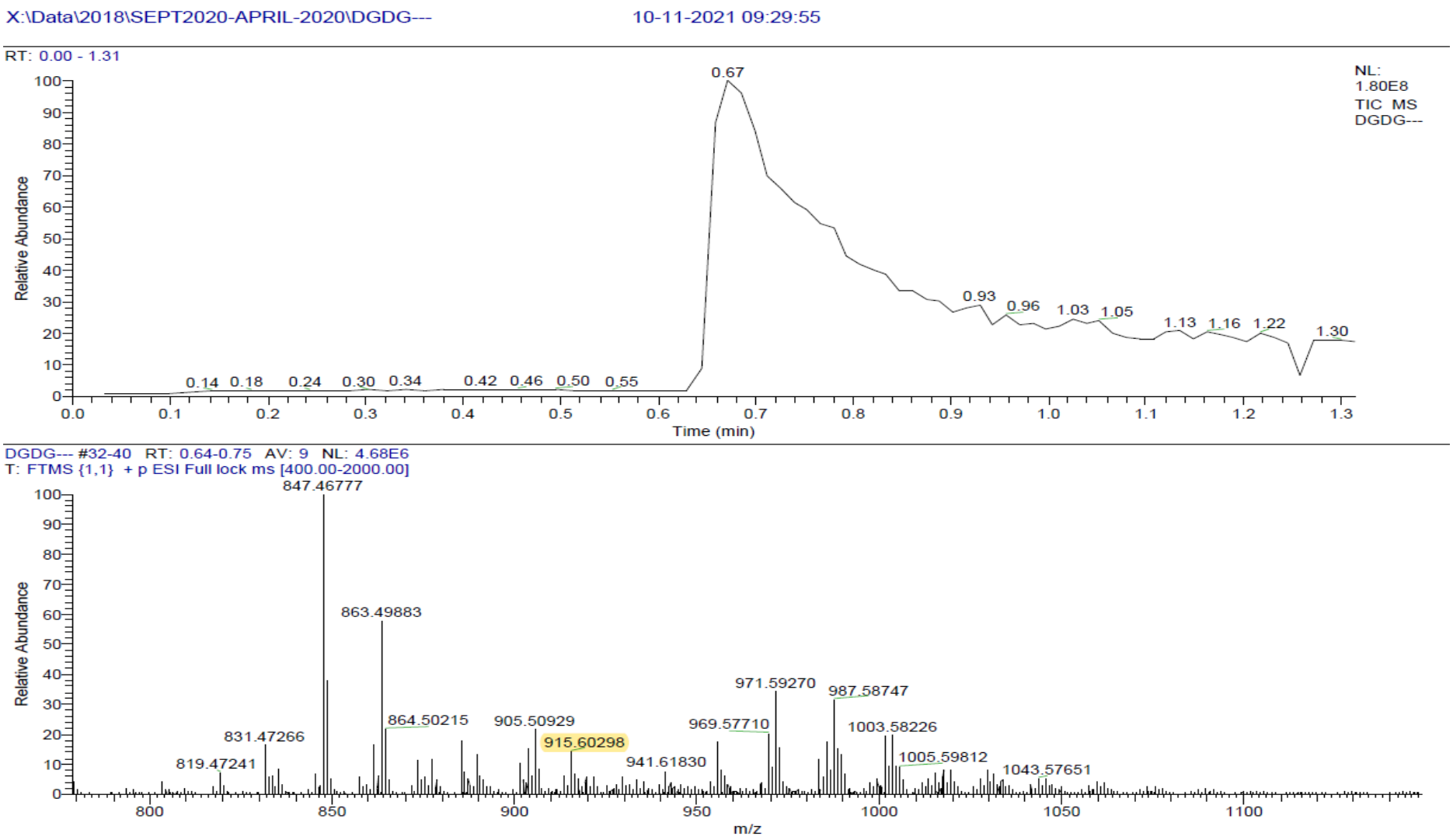

Fig. 3.15. HR-ESI-MS of compound **6**

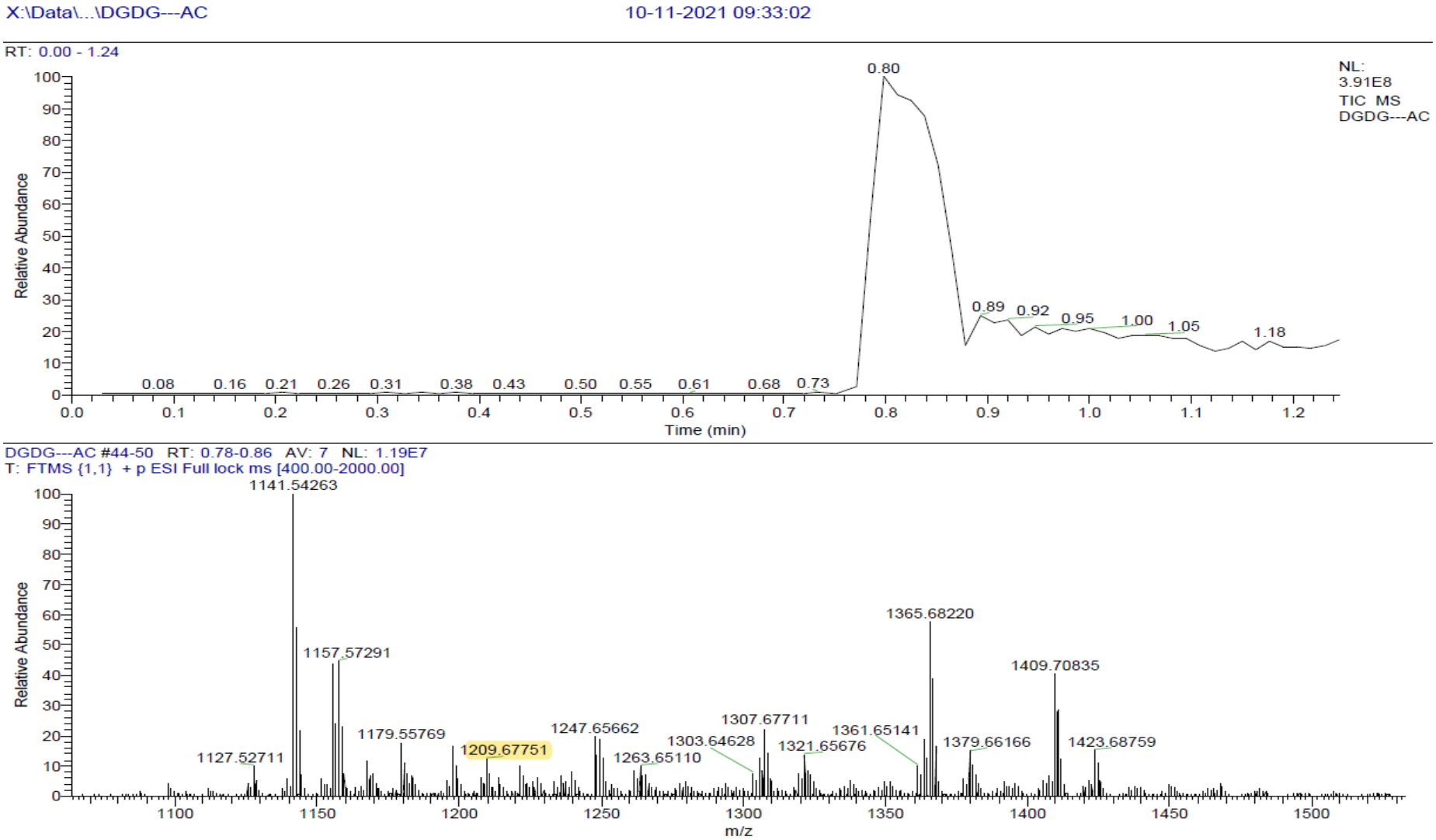

Fig. 3.16. HR-ESI-MS of peracetylated compound **6**

Fig. 3.17. ^{1}H and ^{13}C NMR of peracetylated compound **7**

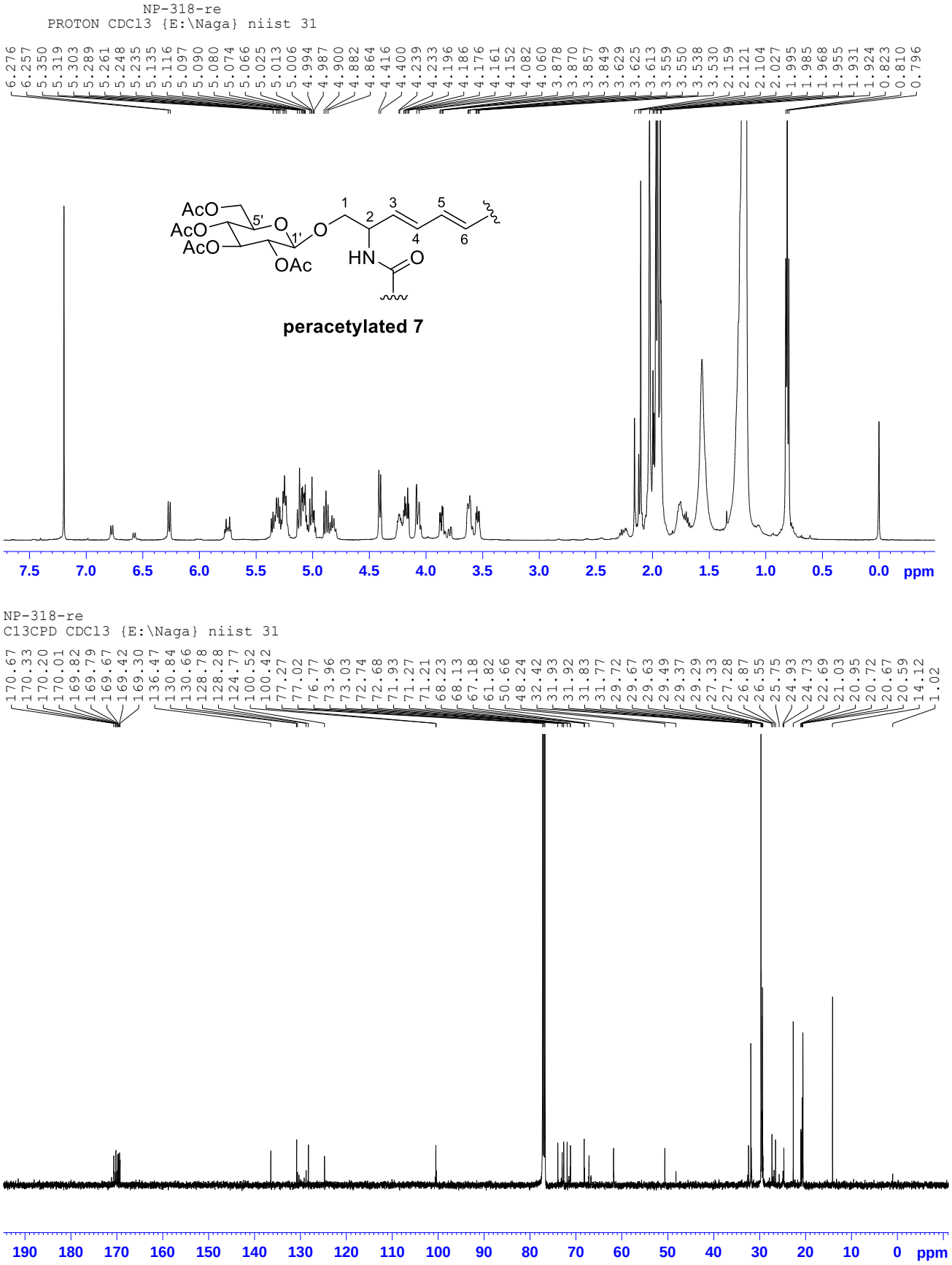

Fig. 3.18. ^{1}H and ^{13}C NMR of compound **7**

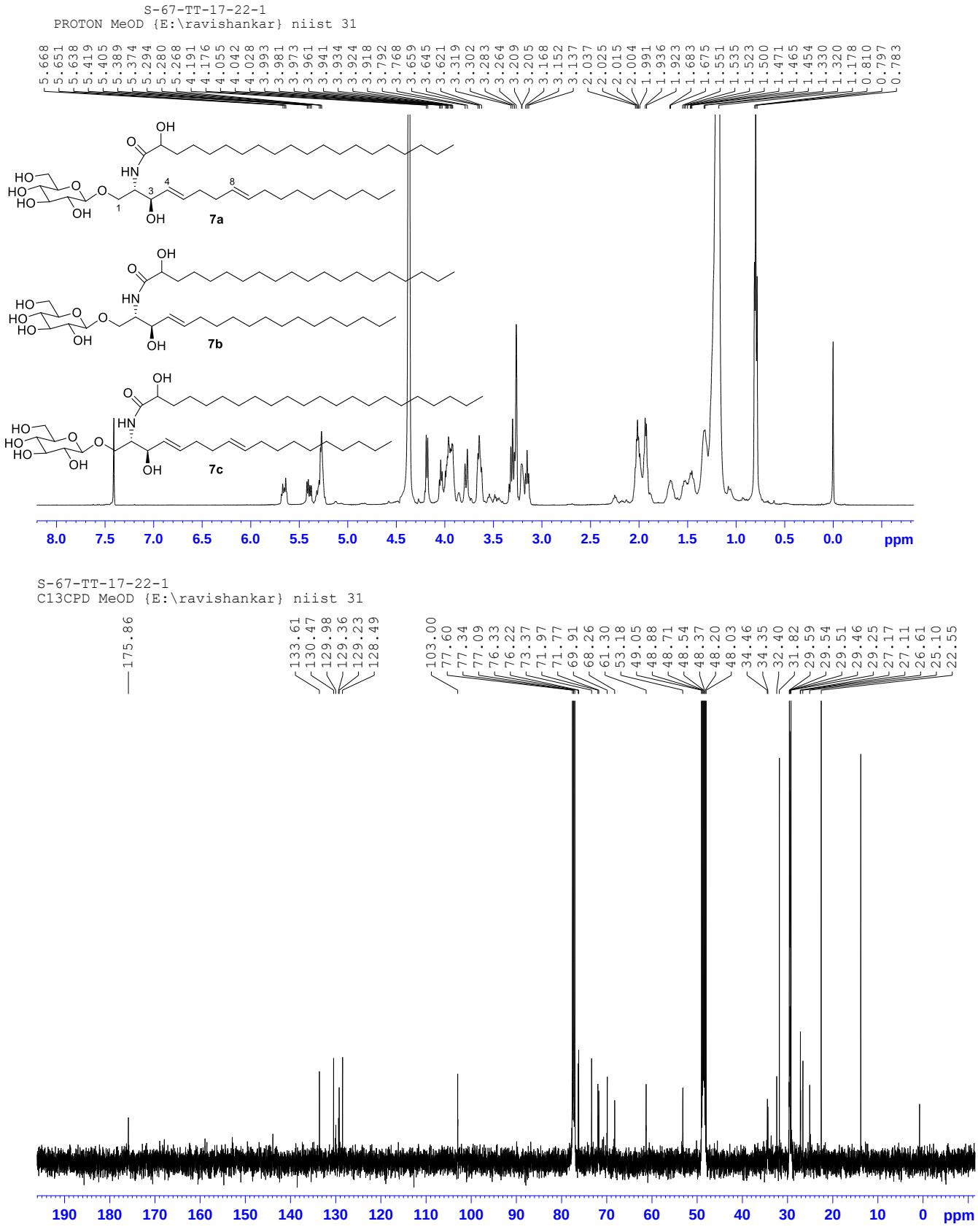

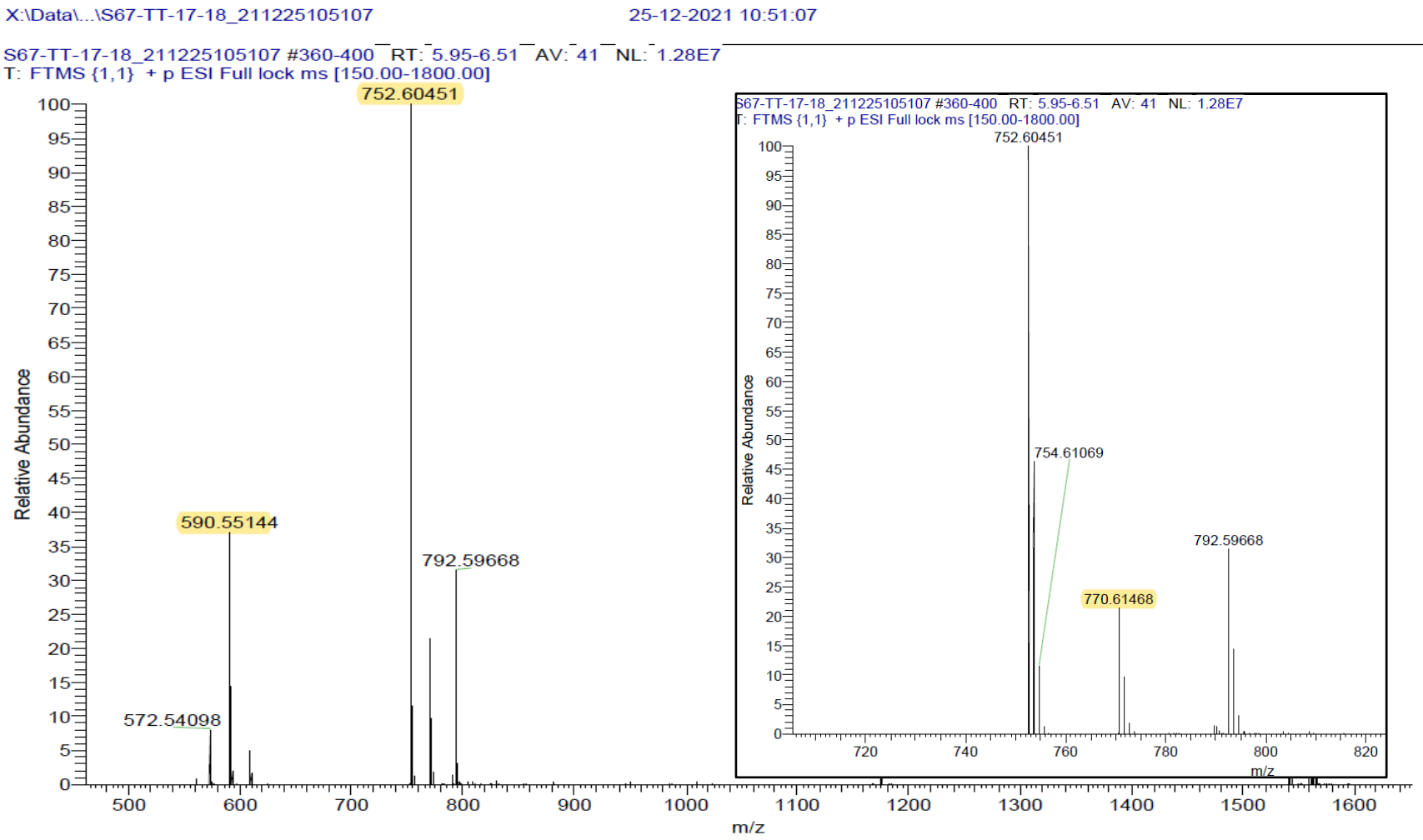

Fig. 3.19a. HR-ESI-MS of compound **7a**

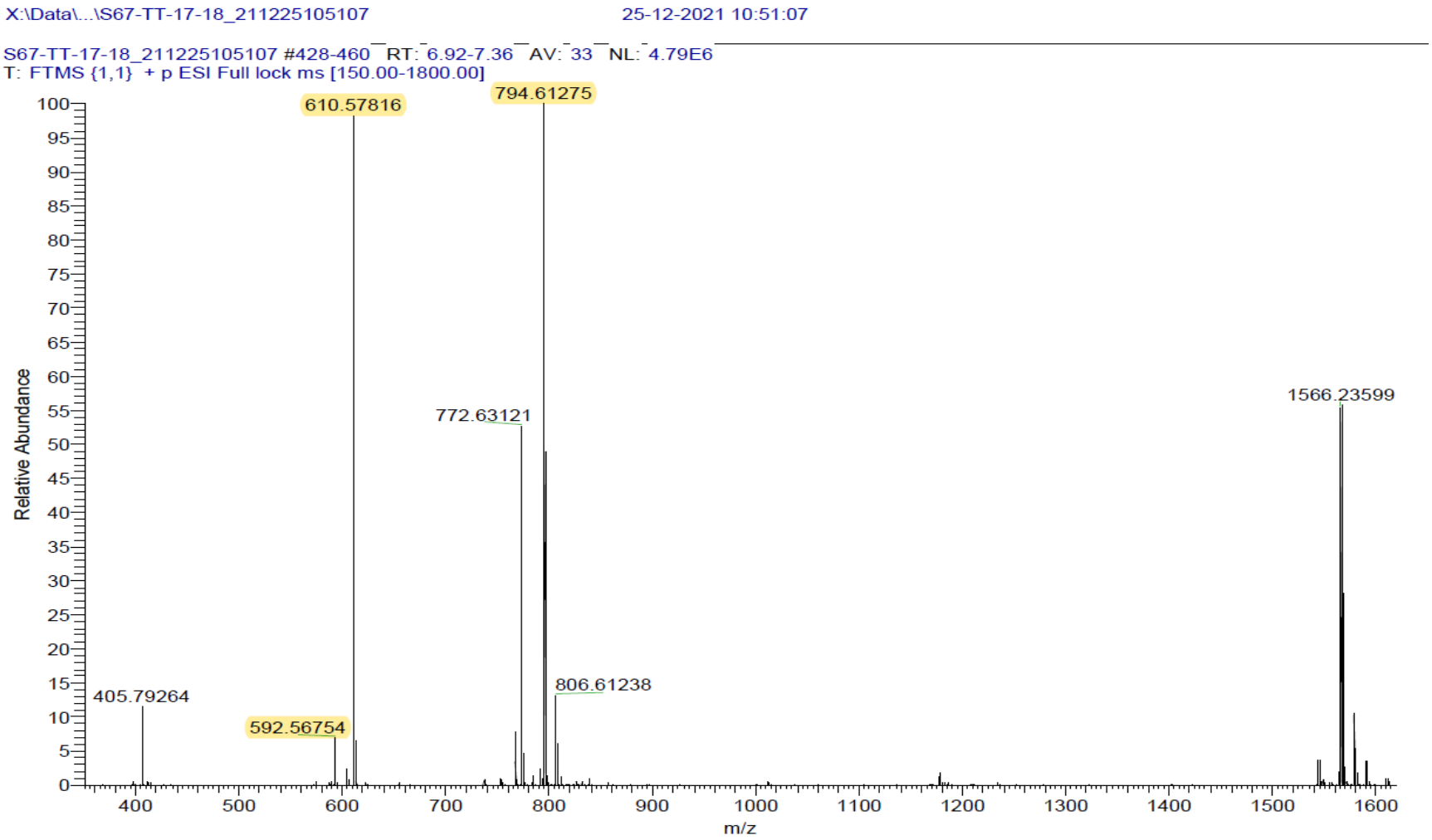

Fig. 3.19b. HR-ESI-MS of compound **7b**

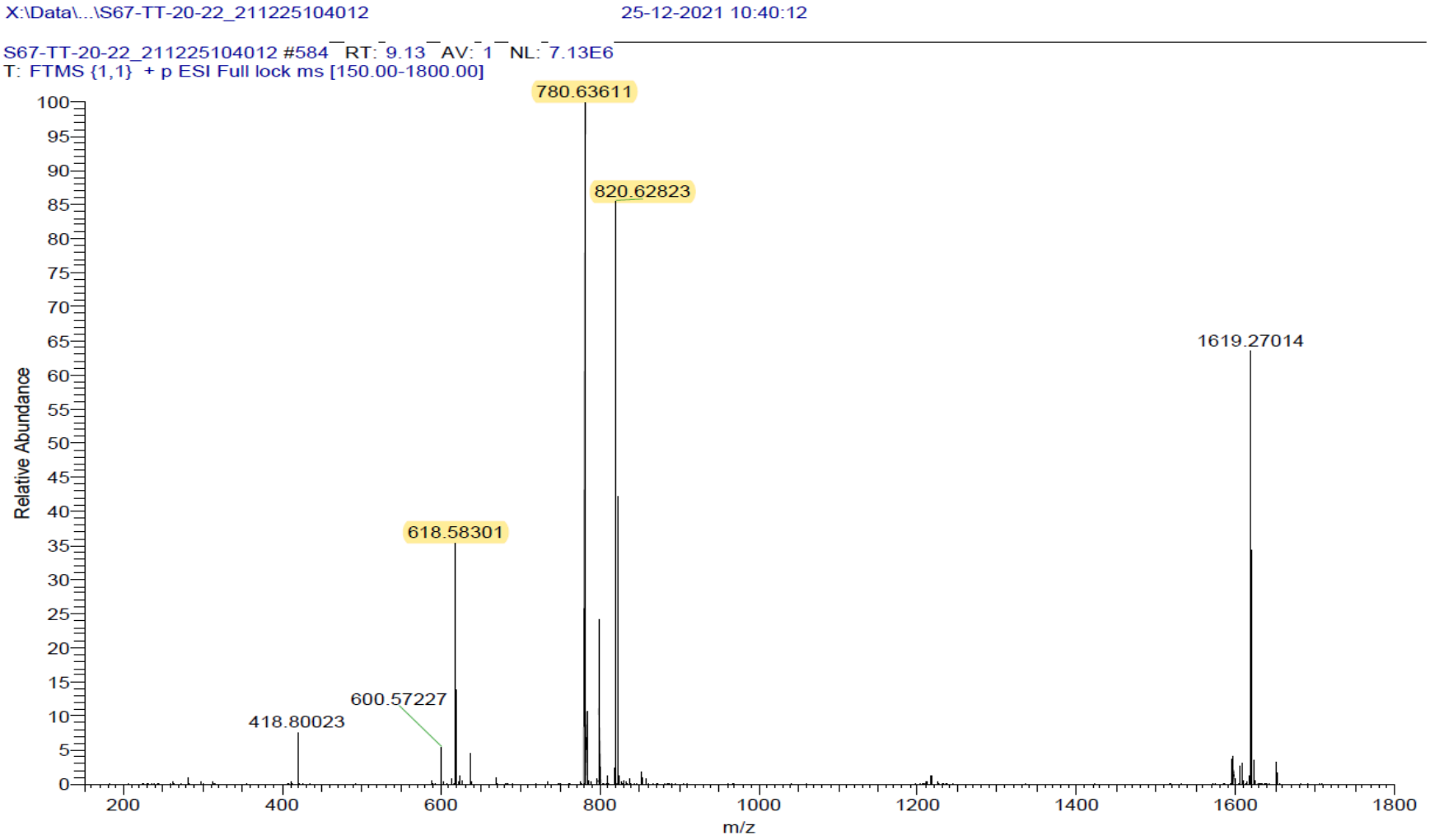

Fig. 3.19c. HR-ESI-MS of compound **7c**

Fig. 3.20. COSY and HMBC NMRs of compound **7**

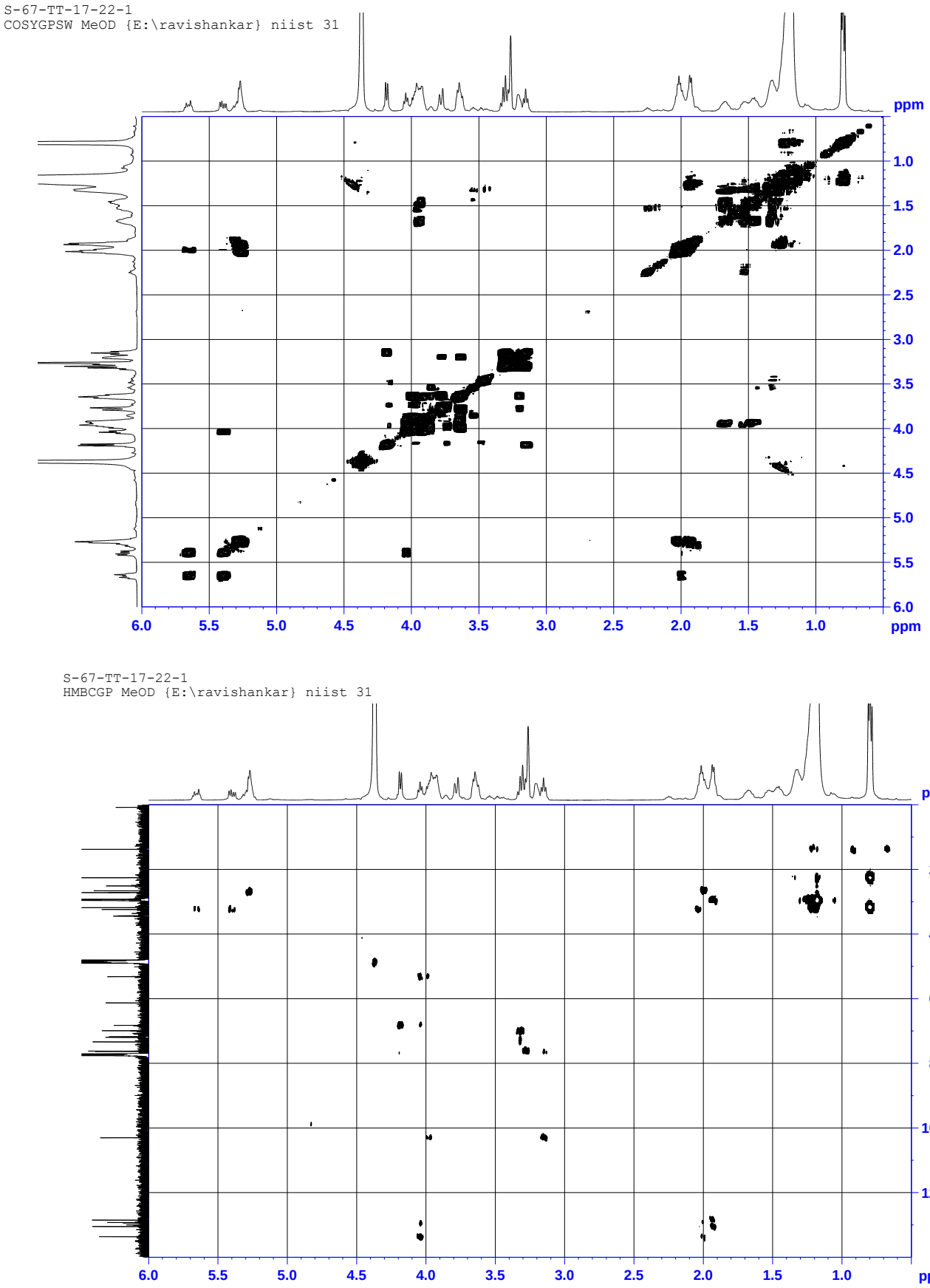

3.5. Conclusion

The current chapter exclusively discusses the phytochemical exploration studies of BG and unripe Nendran pulp. A detailed phytochemical analysis from the organic extracts of BG and as well as unripe pulp revealed the presence of β-sitosterol, glycolipids viz. MGDG, DGDG, ASG viz. sitoindoside-II, sitoindoside-I, sterylglycoside (β-Sitosterol β-D-glucopyranoside), GC and carotenoids. An exhaustive NMR and HR-ESI-MS analysis aided in providing structural details of the isolated phytochemicals. The present work serves as the first report on the isolation of GCs from *Musa* species and also the first report on phytochemical isolation studies from the Nendran cultivar. Literature shows that the phytochemicals isolated from unripe Nendran and BG have a myriad of health benefits. Our study indicates that these compounds withstand processing treatment and emphasizes that convenient products derived from indigenous crops add variety to the diet and provide bioactive molecules with immense health benefits. Consumption of BG introduces a spectrum of bioactive compounds to the body, augmenting basic nutrition with potential health benefits. These compounds, as those of essential vitamins, are required in low doses for optimal functioning of the body. Incorporating BG into the diet can contribute to overall health and well-being, highlighting the significance of diversifying dietary choices for optimal nutrition.

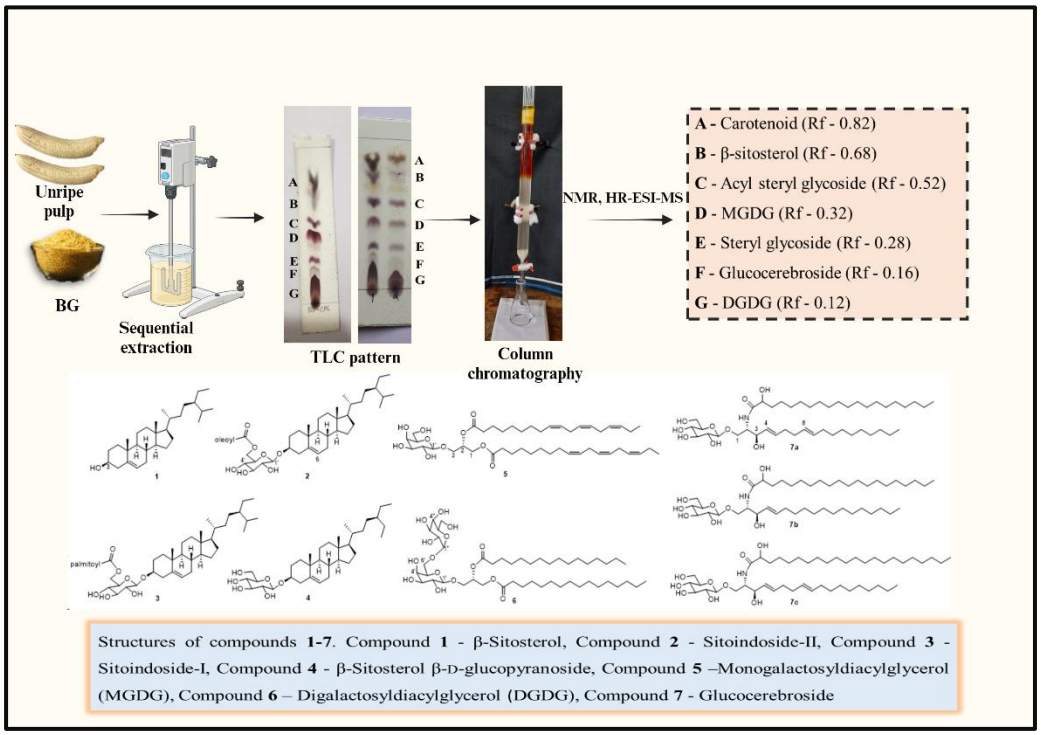

Fig. 3.21. Chapter 3 graphical abstract (Created with BioRender.com)

3.6. References

1. Abedin, M. R., & Barua, S. (2021). Isolation and purification of glycoglycerolipids to induce apoptosis in breast cancer cells. *Scientific Reports*, *11*(1), 1298. https://doi.org/10.1038/s41598-020-80484-x
2. Apaya, M. K., Lin, C.-Y., Chiou, C.-Y., Yang, C.-C., Ting, C.-Y., & Shyur, L.-F. (2015). Simvastatin and a Plant Galactolipid Protect Animals from Septic Shock by Regulating Oxylipin Mediator Dynamics through the MAPK-cPLA2 Signaling Pathway. *Molecular Medicine*, *21*(1), 988–1001. https://doi.org/10.2119/molmed.2015.00082
3. Best, M. M., Duncan, C. H., Van Loon, E. J., & Wathen, J. D. (1955). The effects of sitosterol on serum lipids. *The American Journal of Medicine*, *19*(1), 61–70. https://www.amjmed.com/article/0002-9343(55)90274-6/pdf
4. Bizot, V., Cestone, E., Michelotti, A., & Nobile, V. (2017). Improving skin hydration and age-related symptoms by oral administration of wheat glucosylceramides and digalactosyl diglycerides: A human clinical study. *Cosmetics*, *4*(4), 37. https://doi.org/10.3390/cosmetics4040037
5. Blackbourn, H. D., Jeger, M. J., John, P., Telfer, A., & Barber, J. (1990). Inhibition of degreening in the peel of bananas ripened at tropical temperatures.: IV. Photosynthetic capacity of ripening bananas and plantains in relation to changes in the lipid composition of ripening banana peel. *Annals of Applied Biology*, *117*(1), 163–174. https://doi.org/10.1111/j.1744-7348.1990.tb04204.x
6. Bruno, A., Rossi, C., Marcolongo, G., Di Lena, A., Venzo, A., Berrie, C. P., & Corda, D. (2005). Selective in vivo anti-inflammatory action of the galactolipid monogalactosyldiacylglycerol. *European Journal of Pharmacology*, *524*(1–3), 159–168. https://doi.org/10.1016/j.ejphar.2005.09.023
7. Cateni, F., Zilic, J., Altieri, T., Zacchigna, M., Procida, G., Gaggeri, R., Rossi, D., & Collina, S. (2014). Lipid metabolites with free-radical scavenging activity from Euphorbia helioscopia L. *Chemistry and Physics of Lipids*, *181*, 90–98. https://www.sciencedirect.com/science/article/pii/S0009308414000310
8. Clericuzio, M., Burlando, B., Gandini, G., Tinello, S., Ranzato, E., Martinotti, S., & Cornara, L. (2014). Keratinocyte wound healing activity of galactoglycerolipids from the fern Ophioglossum vulgatum L. *Journal of Natural Medicines*, *68*(1), 31–37. https://doi.org/10.1007/s11418-013-0759-y
9. Coutts, R. T., Stenlake, J. B., & Williams, W. D. (1957). The chemistry of the Aristolochia species. Part III. Aristolochic acids and related substances from

Aristolochia reticulata and A. indica. *Journal of the Chemical Society (Resumed)*, *814*, 4120–4124. https://pubs.rsc.org/en/content/articlepdf/1957/jr/jr9570004120

10. D'Amelio Sr, F. S. (1998). *Botanicals: A phytocosmetic desk reference*. CRC Press. https://books.google.com/books?hl=en&lr=&id=dLRCxs7Iyo8C&oi=fnd&pg=PA1&dq=D%E2%80%99Amelio,+1998&ots=a1y6mNnTIQ&sig=rGWvgHGpg7CTujIDq4vZ0ih9lW8
11. De Silva, G. O., Abeysundara, A. T., & Aponso, M. M. W. (2017). Extraction methods, qualitative and quantitative techniques for screening of phytochemicals from plants. *American Journal of Essential Oils and Natural Products*, *5*(2), 29–32. https://www.essencejournal.com/pdf/2017/vol5issue2/PartA/5-1-31-491.pdf
12. Divekar, P. A., Narayana, S., Divekar, B. A., Kumar, R., Gadratagi, B. G., Ray, A., Singh, A. K., Rani, V., Singh, V., Singh, A. K., Kumar, A., Singh, R. P., Meena, R. S., & Behera, T. K. (2022). Plant Secondary Metabolites as Defense Tools against Herbivores for Sustainable Crop Protection. *International Journal of Molecular Sciences*, *23*(5), 2690. https://doi.org/10.3390/ijms23052690
13. Emwas, A.-H., Roy, R., McKay, R. T., Tenori, L., Saccenti, E., Gowda, G. N., Raftery, D., Alahmari, F., Jaremko, L., & Jaremko, M. (2019). NMR spectroscopy for metabolomics research. *Metabolites*, *9*(7), 123. https://www.mdpi.com/2218-1989/9/7/123
14. Faizi, S., Ali, M., Saleem, R., Irfanullah, & Bibi, S. (2001). Complete ^{1}H and ^{13}C NMR assignments of stigma-5-en-3-*O*-β-glucoside and its acetyl derivative. *Magnetic Resonance in Chemistry*, *39*(7), 399–405. https://doi.org/10.1002/mrc.855
15. Ghosal, S. (1985). Steryl glycosides and acyl steryl glycosides from *Musa paradisiaca. Phytochemistry*, *24*(8), 1807–1810. https://www.sciencedirect.com/science/article/pii/S003194220082556X
16. *Glycolipids—Latest research and news | Nature*. (n.d.). Retrieved July 4, 2024, from https://www.nature.com/subjects/glycolipids
17. Grace, M. H., Lategan, C., Graziose, R., Smith, P. J., Raskin, I., & Lila, M. A. (2012). Antiplasmodial Activity of the Ethnobotanical Plant *Cassia fistula*. *Natural Product Communications*, *7*(10), 1934578X1200701. https://doi.org/10.1177/1934578X1200701002
18. Gupta, E. (2020). β-Sitosterol: Predominant Phytosterol of Therapeutic Potential. In P. Mishra, R. R. Mishra, & C. O. Adetunji (Eds.), *Innovations in Food Technology* (pp. 465–477). Springer Singapore. https://doi.org/10.1007/978-981-15-6121-4_32

19. Hou, C.-C., Chen, Y.-P., Wu, J.-H., Huang, C.-C., Wang, S.-Y., Yang, N.-S., & Shyur, L.-F. (2007). A galactolipid possesses novel cancer chemopreventive effects by suppressing inflammatory mediators and mouse B16 melanoma. *Cancer Research*, *67*(14), 6907–6915. https://aacrjournals.org/cancerres/article-abstract/67/14/6907/533218
20. Jayaprakasam, B., Zhang, Y., & Nair, M. G. (2004). Tumor Cell Proliferation and Cyclooxygenase Enzyme Inhibitory Compounds in *Amaranthus tricolor*. *Journal of Agricultural and Food Chemistry*, *52*(23), 6939–6943. https://doi.org/10.1021/jf048836z
21. Jiang, C., Ge, J., He, B., & Zeng, B. (2021). Glycosphingolipids in filamentous fungi: Biological roles and potential applications in cosmetics and health foods. *Frontiers in Microbiology*, *12*, 690211. https://doi.org/10.3389%2Ffmicb.2021.690211
22. Johnson, A. (1958). Notes—Isolation of βSitosterol from Cassia Absus, Linn. *The Journal of Organic Chemistry*, *23*(11), 1814–1815. https://doi.org/10.1021/jo01105a628
23. Kim, K.-B., Nam, Y. A., Kim, H. S., Hayes, A. W., & Lee, B.-M. (2014). α-Linolenic acid: Nutraceutical, pharmacological and toxicological evaluation. *Food and Chemical Toxicology*, *70*, 163–178. https://www.sciencedirect.com/science/article/pii/S0278691514002439
24. KS, Shivashankara., KC, Pavithra., GA, Geetha., TK, Roy., Patil, Prakash., & Menon, Rema. (2017). Seasonal influence on volatile aroma constituents of two banana cultivars (Grand Naine and Nendran) under Kerala conditions. *Journal of Horticultural Sciences.*, *12*(2). https://agris.fao.org/search/en/providers/123941/records/6511ac88401e7bb65a2b58e8
25. Larsen, E., Kharazmi, A., Christensen, L. P., & Christensen, S. B. (2003). An Antiinflammatory Galactolipid from Rose Hip (*Rosa c anina*) that Inhibits Chemotaxis of Human Peripheral Blood Neutrophils in Vitro. *Journal of Natural Products*, *66*(7), 994–995. https://doi.org/10.1021/np0300636
26. Lin, X., Ma, L., Moreau, R. A., & Ostlund, R. E. (2011). Glycosidic Bond Cleavage is Not Required for Phytosteryl Glycoside-Induced Reduction of Cholesterol Absorption in Mice. *Lipids*, *46*(8), 701–708. https://doi.org/10.1007/s11745-011-3560-2
27. Liu, X., Dong, T., Zhou, Y., Huang, N., & Lei, X. (2016). Exploring the Binding Proteins of Glycolipids with Bifunctional Chemical Probes. *Angewandte Chemie International Edition*, *55*(46), 14330–14334. https://doi.org/10.1002/anie.201608827

28. Maeda, N., Kokai, Y., Ohtani, S., Sahara, H., Kumamoto-Yonezawa, Y., Kuriyama, I., Hada, T., Sato, N., Yoshida, H., & Mizushina, Y. (2008). Anti-tumor effect of orally administered spinach glycolipid fraction on implanted cancer cells, colon-26, in mice. *Lipids*, *43*, 741–748. https://doi.org/10.1186%2Fs13014-016-0729-0
29. Margalit, M., Ghazala, S. A., Alper, R., Elinav, E., Klein, A., Doviner, V., Sherman, Y., Thalenfeld, B., Engelhardt, D., Rabbani, E., & Ilan, Y. (2005). Glucocerebroside treatment ameliorates ConA hepatitis by inhibition of NKT lymphocytes. *American Journal of Physiology-Gastrointestinal and Liver Physiology*, *289*(5), G917–G925. https://doi.org/10.1152/ajpgi.00105.2005
30. Margalit, M., Shalev, Z., Pappo, O., Sklair-Levy, M., Alper, R., Gomori, M., Engelhardt, D., Rabbani, E., & Ilan, Y. (2006). Glucocerebroside ameliorates the metabolic syndrome in OB/OB mice. *Journal of Pharmacology and Experimental Therapeutics*, *319*(1), 105–110. https://jpet.aspetjournals.org/content/319/1/105.short
31. Martin, H., McGHIE, T. K., & Lunken, R. C. (2013). A PPARγ ligand present in Actinidia fruit (Actinidia chrysantha) is identified as dilinolenoyl galactosyl glycerol. *Bioscience Reports*, *33*(3), e00036. https://portlandpress.com/bioscirep/article-abstract/33/3/e00036/56022
32. McLafferty, F. W. (1981). Tandem Mass Spectrometry. *Science*, *214*(4518), 280–287. https://doi.org/10.1126/science.7280693
33. Murakami, A., Nakamura, Y., Koshimizu, K., & Ohigashi, H. (1995). Glyceroglycolipids from Citrus hystrix, a Traditional Herb in Thailand, Potently Inhibit the Tumor-Promoting Activity of 12-O-Tetradecanoylphorbol 13-Acetate in Mouse Skin. *Journal of Agricultural and Food Chemistry*, *43*(10), 2779–2783. https://doi.org/10.1021/jf00058a043
34. Oguntibeju, O. O. (2019). Antidiabetic, anti-inflammatory, antibacterial, anti-helminthic, antioxidant and nutritional potential of *Musa paradisiaca*. *Asian Journal of Pharmceutical and Clinical Research*, *12*(10), 9–13. https://www.academia.edu/download/74937056/20932.pdf
35. Oliveira, L., Freire, C. S. R., Silvestre, A. J. D., Cordeiro, N., Torres, I. C., & Evtuguin, D. (2006). Lipophilic extractives from different morphological parts of banana plant "Dwarf Cavendish." *Industrial Crops and Products*, *23*(2), 201–211. https://www.sciencedirect.com/science/article/pii/S0926669005000725
36. Pandey, J., Dev, K., Chattopadhyay, S., Kadan, S., Sharma, T., Maurya, R., Sanyal, S., Siddiqi, M. I., Zaid, H., & Tamrakar, A. K. (2021). β-Sitosterol-D-glucopyranoside

mimics estrogenic properties and stimulates glucose utilization in skeletal muscle cells. *Molecules*, *26*(11), 3129. https://doi.org/10.3390/molecules26113129

37. Sabha, D., Hiyasat, B., Grötzinger, K., Hennig, L., Schlegel, F., Mohr, F.-W., Rauwald, H. W., & Dhein, S. (2012). Allium ursinum L.: Bioassay-guided isolation and identification of a galactolipid and a phytosterol exerting antiaggregatory effects. *Pharmacology*, *89*(5–6), 260–269. https://karger.com/pha/article/89/5-6/260/272082
38. Saeidnia, S., Manayi, A., Gohari, A. R., & Abdollahi, M. (2014). *The story of beta-sitosterol-a review. European Journal of Medicinal Plants, 4*(5), 590-609. https://www.researchgate.net/profile/SoodabehSaeidnia/publication/260126253_The_Story_of_Beta-sitosterol-_A_Review/links/0a85e5306d3065f2e0000000/The-Story-of-Beta-sitosterol-A-Review.pdf?uid=563b4f0a2a
39. Sahaka, M., Amara, S., Wattanakul, J., Gedi, M. A., Aldai, N., Parsiegla, G., Lecomte, J., Christeller, J. T., Gray, D., & Gontero, B. (2020). The digestion of galactolipids and its ubiquitous function in Nature for the uptake of the essential α-linolenic acid. *Food & Function*, *11*(8), 6710–6744. https://pubs.rsc.org/en/content/articlehtml/2020/fo/d0fo01040e
40. Saxena, R. (2023). Exploring approaches for investigating phytochemistry: methods and techniques. *Medical Research, Nursing, Health and Midwife Participation*, *4*(2), 65–73. http://medalionjournal.com/index.php/go/article/view/76
41. Shimamura, M. (2020). Structure, metabolism and biological functions of steryl glycosides in mammals. *Biochemical Journal*, *477*(21), 4243–4261. https://portlandpress.com/biochemj/article-abstract/477/21/4243/226958
42. Shirakura, Y., Kikuchi, K., Matsumura, K., Mukai, K., Mitsutake, S., & Igarashi, Y. (2012). 4,8-Sphingadienine and 4-hydroxy-8-sphingenine activate ceramide production in the skin. *Lipids in Health and Disease*, *11*(1), 108. https://doi.org/10.1186/1476-511X-11-108
43. Sreejith, P., & Sabu, M. (2017). *Edible Bananas of South India: Taxonomy & Phytochemistry*. Indian Association for Angiosperm Taxonomy.
44. Takahashi, M., Sugiyama, Y., Kawabata, K., Takahashi, Y., Irie, K., Murakami, A., Kubo, Y., Kobayashi, K., & Ohigashi, H. (2011). 1,2-Di- *O* -α-linolenoyl-3- *O* -β-galactosyl- *sn* -glycerol as a Superoxide Generation Inhibitor from *Perilla frutescens* var. *Crispa*. *Bioscience, Biotechnology, and Biochemistry*, *75*(11), 2240–2242. https://doi.org/10.1271/bbb.110414

45. Tsao Rong, T. R., & Li HongYan, L. H. (2013). *Analytical techniques for phytochemicals.* Handbook of Plant Food Phytochemicals; sources, stability, and extraction, Jhon Wiley & Sons, Ltd. https://www.cabidigitallibrary.org/doi/full/10.5555/20133403422
46. Ulivi, V., Lenti, M., Gentili, C., Marcolongo, G., Cancedda, R., & Descalzi Cancedda, F. (2011). Anti-inflammatory activity of monogalactosyldiacylglycerol in human articular cartilage in vitro: Activation of an anti-inflammatory cyclooxygenase-2 (COX-2) pathway. *Arthritis Research & Therapy*, *13*(3), 1–12. https://doi.org/10.1186/ar3367
47. Vilela, C., Santos, S. A., Villaverde, J. J., Oliveira, L., Nunes, A., Cordeiro, N., Freire, C. S., & Silvestre, A. J. (2014). Lipophilic phytochemicals from banana fruits of several Musa species. *Food Chemistry*, *162*, 247–252. https://www.sciencedirect.com/science/article/pii/S0308814614006074
48. Weil, M. J., Zhang, Y., & Nair, M. G. (2005). Tumor Cell Proliferation and Cyclooxygenase Inhibitory Constituents in Horseradish (*Armoracia rusticana*) and Wasabi (*Wasabia japonica*). *Journal of Agricultural and Food Chemistry*, *53*(5), 1440–1444. https://doi.org/10.1021/jf048264i
49. Xu, H., Li, Y., Han, B., Li, Z., Wang, B., Jiang, P., Zhang, J., Ma, W., Zhou, D., & Li, X. (2018). Anti-breast-cancer activity exerted by β-sitosterol-D-glucoside from sweet potato via upregulation of microRNA-10a and via the PI3K–Akt signaling pathway. *Journal of Agricultural and Food Chemistry*, *66*(37), 9704–9718. https://doi.org/10.1021/acs.jafc.8b03305

Chapter 4

Process-induced changes in the resistant starch (RS) content of raw pulp, and its relation to the glycemic index and glycemic load (GI-GL)

4.1. Introduction

In general, unripe bananas are reported to have a high amount of RS, which belongs to the RS2 category, which is resistant to digestion due to its crystalline structure (Faisant et al., 1995). Processing and cooking steps have been found to greatly affect the RS2 content (detailed in the review of literature section 1.2.8.1. of Chapter 1). To the best of our knowledge, there is no literature data on the RS content of unripe Nendran and processed induced changes in it. Hence we have evaluated the RS content of BG and its relation to GI, process-induced changes in RS content of unripe pulp, and the variation in RS content when measured by different methods. Further, we evaluated the starch fractions (RDS, SDS, & RS) of some of the commonly consumed food items (rice, oats, and chapathi) and compared the RS content of the above items with BG.

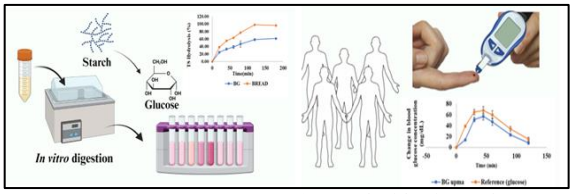

(Created with BioRender.com)

4.2. Objectives

- *In vitro* GI prediction of BG.
- Evaluation of GI-GL of BG through clinical studies.
- Estimation of the RS content of BG through different methods.
- Evaluation of RS content in the unripe Nendran pulp and its processed products.
- Estimation of starch fractions in commonly consumed food items.

4.3. Materials and methods

4.3.1. Chemicals and enzymes

The enzymes invertase (catalogue no. I4504), pancreatin (catalogue no. P7545), amyloglucosidase (catalogue no. 10113), and pepsin (catalogue no. P7000) were purchased from Sigma-Aldrich, Germany for the *in vitro* starch digestion and GI prediction assay. The glucose oxidase-peroxidase (GOD-POD) kit was acquired from Biosystem Pvt. Ltd. India. The Digestible and RS Assay Kit (K-DSTRS**)** was procured from Megazyme Ltd., Ireland.

4.3.2. BG preparation

The infructescence (73.96 kg) of mature unripe banana *Musa* (AAB) cv. Nendran was purchased from local organic farmers in Vellayani, Thiruvananthapuram District, Kerala, India.

The pulp (43.62 kg) and peel (16.06 kg) were separated and the pulp was pre-treated and dried to develop a novel product 'BG' (11.35 kg, the product discussed in Chapter 2) and was used for further studies.

4.3.3. *In vitro* GI prediction

The *in vitro* prediction of GI of BG was performed according to Goni et al., 1997 and Ren et al., 2016 with some modifications (Goñi et al., 1997; Ren et al., 2016). Before analysis, BG (10 g) was cooked with 50 mL of water for 6 minutes on medium flame, and from that 3.20 g of cooked BG (according to procedure minimum 0.50 g starch was required for analysis) was used for the analysis. The sample portion i.e., 3.20 g has 0.60 g starch. The white bread (0.80 g) was used as the reference food.

The samples were mixed with 10 mL of freshly made pepsin solution (pepsin 5 g/L, guar gum 5 g/L in 0.05 mol/L hydrochloric acid (HCl), and 5 glass balls). Subsequently, the samples were incubated for half an hour at 37 °C in a water bath. Next, 0.1 M acetate buffer (10 mL, pH 5.5, 37 °C) was added and then the starch digestion was initiated by adding 5 mL of the enzyme mixture. For preparing the enzyme mixture 3 g of pancreatin was mixed with 20 mL of water for 10 minutes over a magnetic stirrer. Subsequently, the mixture was centrifuged for 10 minutes at 1500 rpm, yielding 15 mL of pancreatin supernatant. To the supernatant, 0.75 mL of amyloglucosidase (1200 U/mL) and 1 mL of invertase (3000 U/mL) were added. The samples were kept in a horizontal shaking water bath (37 °C, 160 rpm). An aliquot of 0.2 mL was withdrawn at various time points (20, 40, 60, 80, 100, 120, and 180 minutes) during starch hydrolysis and its glucose content was measured using GOD-POD kit. The optical density (OD) values were measured by Shimadzu UV 2600 spectrophotometer (Shimadzu, Japan). A glucose standard curve with concentrations ranging from 0.6 ppm to 10 ppm ($y = 0.0135x + 0.0097$, $R^2 = 0.997$) was used for calculating the glucose content.

Based on glucose measurements taken at various time points (20, 40, 60, 80, 100, 120, and 180 minutes), the kinetics of *in vitro* starch digestibility and the estimated glycemic index (eGI) of BG were calculated. The glucose content was converted to starch by multiplying with 0.9 and then the total starch hydrolysis percentage at each time point was calculated. These values were further used for the prediction of GI. Goni found that the starch hydrolysis follows a first-order equation i.e., $C = C_\infty(1 - e^{-kt})$ where C, C_∞ , and k represent the percentage of starch hydrolyzed at time t (minutes), the maximum hydrolysis extent, and the kinetic constant, respectively (Goñi et al., 1997). Each food has its characteristic C_∞ and k value. By giving the total starch hydrolysis percentage at each time point (20, 40, 60, 80, 100, 120, and 180 minutes)

as input, the C_∞ and k values of samples were calculated using the SYSTAT- SigmaPlot V15 software.

Goni through his extensive studies found that the *in vivo* glycemic response is best correlated with the percentage of starch hydrolysis at 90 minutes (H_{90}). The H_{90} value can be obtained by a single point measurement of glucose at 90 minutes during the experiment or this value can be derived from the C_∞ and k values ($H_{90} = C_\infty(1 - e^{-kt})$, where t=90). He introduced the equation $eGI = 39.21 + 0.803H_{90}$ to predict the GI based on this single-point measurement of glucose in the *in vitro* study. Goni introduced another equation i.e., eGI = 39.71 + 0.549HI for the estimation of GI. Here the hydrolysis index (HI) was calculated based on the relationship between the area under the hydrolysis curve (AUC) for the test food and the AUC for a reference food (white bread). The AUC was calculated as the integral of the kinetic equation, so here the glucose measurement at each point of starch digestion is considered for predicting the GI (Goñi et al., 1997). We have adopted both equations i.e., $eGI = 39.21 + 0.803H_{90}$ and eGI = 39.71 + 0.549HI for predicting the GI of BG to find their correlation with clinical GI values.

4.3.4. Available carbohydrate content analysis and clinical GI-GL studies

4.3.4.1. Estimation of available carbohydrate content

As the available carbohydrate content is crucial in determining the portion size to be served in the GI studies, the available carbohydrate content of BG upma and BG porridge was determined using the Megazyme Available Carbohydrates Assay Kit (K-ACHDF). The initial steps of the assay measure the hydrolysis of digestible starch to glucose and traces of maltose, followed by the specific hydrolysis of sucrose, maltose, lactose, and isomaltose to their respective monomers. Next, the enzymes hexokinase (HK) and adenosine-5'-triphosphate (ATP) phosphorylate the resultant D-glucose and D-fructose to form glucose-6-phosphate (G-6-P) and fructose-6-phosphate (F-6-P), respectively. The enzyme glucose-6-phosphate dehydrogenase (G6P-DH) subsequently oxidises the generated G-6-P to gluconate-6-phosphate, and nicotinamide-adenine dinucleotide phosphate ($NADP^+$) to gluconate-6-phosphate with the generation of reduced nicotinamide-adenine dinucleotide phosphate hydrogen (NADPH). The amount of D-glucose and NADPH produced in this reaction will be stoichiometric. The rise in absorbance at 340 nm is used to calculate the amount of generated NADPH. Similarly, phosphoglucose isomerase (PGI) changes F-6-P into G-6-P. The resulting G-6-P combines with NADP+ to generate gluconate-6-phosphate and NADPH, which causes a further increase in absorbance (at 340 nm) proportional to the quantity of D-fructose (*Available Carbohydrates Assay Kit*, n.d.).

4.3.4.2. Clinical GI-GL evaluation-study design

The clinical GI-GL study of BG was done in collaboration with the Madras Diabetes Research Foundation (MDRF), Chennai, India. Two preparations i.e., BG upma (a South Indian preparation) and BG porridge were developed from BG which can be easily prepared by consumers, and the GI value of these preparations was evaluated at the clinical level. The GI of test foods - BG upma, and BG porridge was determined in 15 healthy participants. This study was conducted using internationally recognized GI protocol by FAO/WHO, 1998 ("Carbohydrates in Human Nutrition. Report of a Joint FAO/WHO Expert Consultation," 1998) and further recommended guidelines by the International Dietary Carbohydrate Task Force for GI methodology (Wolever et al., 2006) and ISO (International Organization for Standardization, 2010) which have been validated and published elsewhere for GI (Henry et al., 2008; Wolever et al., 2019). The procedures in this study adhered to international ethical standards for human research and received approval from the institutional ethics committee at MDRF, Chennai, India. All participants provided informed consent. The study is registered with the Clinical Trials Registry India (CTRI) under the number CTRI/2024/04/065286. The participants were recruited from the participant roster of MDRF.

4.3.4.2.1. Preparation of test food

The test food was standardized and prepared at the MDRF's test kitchen. The standardized recipe used for the preparation of BG upma and BG porridge is given below.

4.3.4.2.1.1. Standardized recipe used for the preparation of BG upma

Ingredients	Quantity
BG	315 g
Onion	105 g
Groundnut Oil	40 g
Salt	12.5 g
Black gram whole	10.5 g
Green Chilly	10.5 g
Mustard	5 g
Curry Leaves	5 g
Ginger	2 g
Water	800 mL

For the preparation of BG upma, 315 g of BG was cooked with 800 mL water, and onion, green chilies, ginger, and curry leaves were added in the preparation to enhance the taste. The

cooking time of BG upma was 16 minutes and the final cooked weight of the upma was 1052 g. The method of preparation involves roasting, sautéing, boiling, and simmering.

4.3.4.2.1.2. Standardized recipe used for the preparation of BG porridge

Ingredients	Quantity
BG	200 g
Salt	10 g
Water	2000 mL

The second preparation, BG porridge was prepared by mixing 200 g of BG with 2000 mL of water and cooked for 15 minutes at high flame with occasional stirring to avoid scorching of grits. The final cooked weight of BG porridge was 1915 g.

4.3.4.2.2. Inclusion and exclusion criteria

The study included healthy men and women aged 18 to 45, with a body mass index (BMI) ≥18.5 to ≤ 22.9 kg/m², who were willing to consume the test and reference food, had no known food allergies or intolerances, and were not taking any medications that could affect glucose tolerance. The study excluded individuals with specific dietary restrictions, pregnant or breastfeeding women, those with a history of diabetes mellitus, anyone with a disease or taking medication that could impact nutrient digestion and absorption, and those who had undergone major medical or surgical events in the last 3 months (Fig. 4.1.)

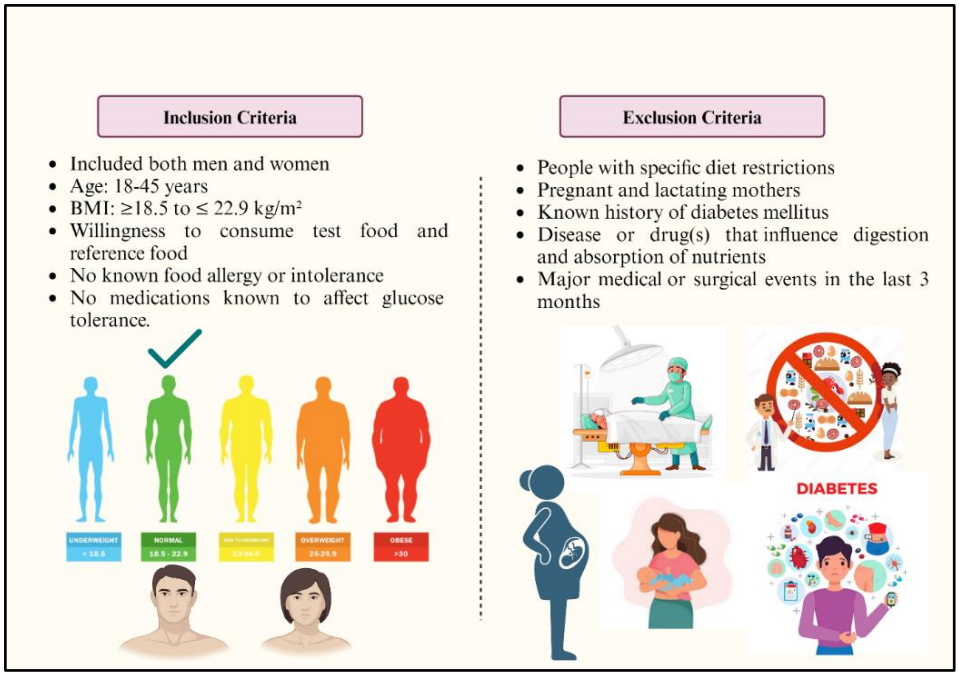

Fig. 4.1. Inclusion and exclusion criteria for the clinical GI-GL evaluation studies (Created with BioRender.com)

4.3.4.2.3. Estimation of GI-GL

Participants who were not accustomed to finger-prick blood sampling (capillary blood sampling) practiced the procedure beforehand to control the anxiety-related effects on blood glucose response. The study involved each participant undergoing 3 days of reference food testing and 1 day of test food in a random sequence, with a 2-day washout period between measurements to prevent carry-over effects. On each test day, participants arrived at the GI testing center in the morning after a 10-12 hour overnight fast. A brief questionnaire on the previous day's diet (24-hour recall) including the last previous physical activity, meal, smoking, and alcohol and caffeine-containing drinks was obtained to ensure that the participants maintained a similar diet and physical activity on pretest dates and refrained from smoking and alcohol during the study period.

The test food containing 50 g available carbohydrate i.e., 269 g of BG upma, along with 250 mL of water was given to all the study participants. A 55 g of monohydrate glucose dissolved in 250 mL of water was given as the reference test food for GI studies. Since the portion size of BG porridge was so unreal for consumption a portion containing 25 g of available carbohydrate (309 g of BG porridge) was given to all the study participants. Monohydrate glucose (27.5 g) dissolved in 125 mL of water was given as the reference food for GI studies.

Fasting blood samples were collected at -5 minutes and 0 minutes via finger-prick using an automatic lancet device before food consumption, with the baseline value being the average of these two measurements. Participants then consumed a 50 g portion of available carbohydrate from the test foods, BG upma and BG porridge, on different occasions. The first bite or sip marked time 0, and the initial blood sample was taken exactly 15 minutes afterward, with additional samples collected at 30, 45, 60, 90, and 120 minutes' post-meal. During the subsequent 2 hours of GI testing, participants drank 250 mL of water. The incremental area under the curve (IAUC) for blood glucose levels, in response to both the reference and test foods, was calculated using the trapezoid rule, excluding the area below the fasting baseline (Augustin et al., 2015; Brouns et al., 2005; "Carbohydrates in Human Nutrition. Report of a Joint FAO/WHO Expert Consultation," 1998; EFSA Panel on Dietetic Products, 2012; International Organization for Standardization, 2010; Wolever et al., 2019). The average and standard error of the mean (SEM) of the IAUC were computed for both the reference food and the test food. The GI of the test food was determined by expressing each participant's IAUC

following the test food as a percentage of their average reference IAUC. The GI of the test food was then represented by the mean of these values (Brouns et al., 2005; Joint, 1998).

$$\mathrm{GI} = \frac{\text{Blood glucose IAUC for test food}}{\text{IAUC value of the reference food}} \times 100$$

4.3.5. Evaluation of starch fractions (RDS. SDS, and RS) of BG

The starch fractions in BG were evaluated through two methods- the modified Englyst method and the Megazyme kit method to assess the variation in results obtained through two methods.

4.3.5.1. *In vitro* starch digestion and evaluation of starch fractions of BG through modified Englyst method

BG was analyzed for its starch fractions based on Englyst *et al.*, 1992 and Ren *et al.,* 2016, with some modifications (Englyst et al., 1992; Ren et al., 2016). The digestion time in the procedure is 2 hours. In a 50 mL centrifuge tube, the sample was mixed with acetate buffer (25 mL, 0.1 M, pH 5.2) and 2 glass balls. The tube was incubated in a boiling water bath for 30 minutes. After cooling the tube to 37 °C, 0.3 mL invertase (3000 U/mL) was added, and further incubated at 37 °C for 30 minutes. Further, 0.2 mL of aliquot was added to absolute ethanol (4 mL) to get the free glucose (FG) portion. As above, the samples were mixed with 10 mL of freshly made pepsin solution (pepsin 5 g/L, guar gum 5 g/L in 0.05 mol/L HCl, and 5 glass balls). Subsequently, the samples were incubated for half an hour at 37 °C in a water bath. Next, 0.1 M acetate buffer (10 mL, pH 5.5, 37 °C) was added and then the starch digestion was initiated by adding 5 mL of the enzyme mixture. For preparing the enzyme mixture, 3 g of pancreatin was mixed with 20 mL of water for 10 minutes over a magnetic stirrer. Subsequently, the mixture was centrifuged for 10 minutes at 1500 rpm, yielding 15 mL of pancreatin supernatant. To the supernatant, 0.75 mL of amyloglucosidase (1200 U/mL) and 1 mL of invertase (3000 U/mL) were added. The samples were kept in a horizontal shaking water bath (37 °C, 160 rpm), and after 20 and 120 minutes 0.2 mL of aliquots were withdrawn and added into ethanol (4 mL) to obtain the glucose portion for 20 minutes (G_{20}) and 120 minutes (G_{120}). After G_{120} samples had been collected, the tubes were incubated in a boiling-water bath (30 minutes), further, cooled to 0 °C, and mixed with 7 M potassium hydroxide (10 mL). The tubes were incubated in ice for 30 minutes and from this 0.2 mL of sample was added to 1 mL of acetic acid (1 mol/L) containing amyloglucosidase (40 µL, 100 U/mL). Further, the tube was incubated at 70 °C for 30 minutes and a boiling-water bath for 10 minutes. The tube was then cooled to 30 °C and added 20 mL of water to obtain the total glucose portion (TG). The samples

(FG, G_{20}, G_{120}, and TG) were centrifuged for five minutes at 1500 rpm. A GOD-POD diagnostic kit was used to determine the amount of glucose present in the supernatant. The absorbance was measured using a Shimadzu UV 2600 spectrophotometer (Shimadzu, Japan). A glucose standard curve with concentrations ranging from 0.6 ppm to 10 ppm ($y = 0.0342x - 0.0081$, $R^2 = 0.998$) was used for estimating the glucose content in the samples. From the values of glucose measured during each time, the following equations were used to calculate the amount of total starch (TS), rapidly digestible starch (RDS), slowly digestible starch (SDS), and RS.

$$RDS = (G_{20} - FG) \times 0.9$$
$$SDS = (G_{120} - G_{20}) \times 0.9$$
$$TS = (TG - FG) \times 0.9$$
$$RS = (TG - G_{120}) \times 0.9$$

4.3.5.2. *In vitro* starch digestion and evaluation of starch fractions of BG through Megazyme kit method

The Megazyme digestible and RS assay kit (K-DSTRS) was used to analyze the starch fractions and the assay was done according to the manufacturer's instructions. The samples are incubated in maleate buffer (pH 6.0) containing pancreatic α-amylase and amyloglucosidase (PAA/AMG) for up to 4 hours at 37 °C with constant stirring. Aliquots of the reaction solution are taken at specific time intervals: 20 minutes (for RDS measurement), 120 minutes (for SDS measurement, calculated as SDS = starch value at 120 minutes - starch value at 20 minutes), and 240 minutes (for measuring TDS and RS). The aliquots (1 mL) collected for measuring the RDS, SDS, and TDS were transferred to acetic acid (50 mM, 20 mL) to stop the reaction. From these solutions, 0.1 mL aliquots are incubated with 0.1 mL of amyloglucosidase (AMG, 100 U/mL) to hydrolyze any leftover maltose into glucose, which is subsequently measured using the GOD-POD reagent. For RS content measurement, a 4 mL aliquot is taken from the stirring solution after 240 minutes, mixed with an equal volume of ethanol, and thoroughly combined. Following the centrifugation process, the pellet was washed with 50% ethanol before being resuspended in sodium hydroxide solution to dissolve RS. The solution was then neutralized and AMG was used to hydrolyze the starch into glucose. The GOD-POD reagent is used to quantify the resultant glucose and the TS is calculated by summing TDS and RS (*Digestible and Resistant Starch Assay Kit*, n.d.; McCleary et al., 2020). Further, the changes in the starch fractions in BG after cooking were also evaluated using the above method.

4.3.6. Analysis of process-induced changes in the RS content of unripe pulp

As there is no literature data available on the RS content of unripe pulp and its process-induced changes, it was studied in detail. The RS content of unripe pulp and processed products (P1 and P2) was evaluated. Since the process treatments are part of future technology transfer, the processing details are not mentioned here. We have procured commercial raw banana powders C1 and C2 and evaluated their RS content also. After evaluating their RS content in the uncooked form, the cooking-induced changes in the RS content were also evaluated.

Before analysis, all the samples were powdered and passed through mesh 50 to ensure the uniform particle size of the samples. For evaluating the cooking-induced changes in the RS content, 10 g of both processed samples, P1 & P2, were cooked with 100 mL water for 5 minutes under a medium flame, which was the banana powder to water ratio normally used for the preparation of banana porridge. Samples C1 and C2 were cooked according to the manufacturer's instructions, 10 g of product with 250 mL of water, and cooked for 5 minutes over medium flame. This cooking method was used to replicate the RS content that a consumer would likely obtain by following the exact cooking instructions given by the manufacturer. The BG powder was cooked for 5 minutes in both water ratios i.e., 1:10 and 1:25 to evaluate the retention of RS in BG after cooking under different water ratios. The Megazyme kit (*Digestible and Resistant Starch Assay Kit*, n.d.; McCleary et al., 2020) was used for evaluating the RS content of the samples.

4.3.7. Evaluation of starch fractions in commonly consumed food items

The SDS, RDS, TDS, RS, and TS content of some of the commonly consumed food items including oats, rice, and chapathi was evaluated using the Megazyme kit (*Digestible and Resistant Starch Assay Kit*, n.d.; McCleary et al., 2020). Rolled oats were prepared by mixing 30 g of oats with 100 mL of water and cooking over medium flame for 5 minutes, stirring occasionally. Matta rice (100 g) was pressure-cooked with 250 mL of water over medium flame for 2 whistles, and the excess water was drained after cooking. Chapathi was prepared by kneading 100 g of wheat flour with 70 mL of water into a smooth dough, which was divided into small balls, rolled into flat discs, and cooked on a preheated tawa over medium flame for 2 minutes, flipping as needed. The RS content of the samples was compared with BG, to evaluate the nutritional superiority of BG over these products.

4.3.8. Statistical analysis

All the *in vitro* experiments were carried out in triplicates (n=3), statistically analyzed by IBM SPSS Statistics version-26, and data presented as the mean ± SD. One-way ANOVA was

used followed by Tukey's test and a P value equal to or less than 0.05 was considered to indicate significance. The clinical GI data was presented as the mean ± SEM. The SYSTAT-SigmaPlot V15 software was used for finding the parameters C_∞ & k values. The OriginPro 16 software was used for the calculation of the AUC of samples for the GI prediction studies.

4.4. Result and discussion

4.4.1. *In vitro* starch digestion and prediction of GI

Goni introduced a simple *in vitro* procedure, in which the rate of hydrolysis of starchy foods could be measured and which could be further used to estimate the metabolic glycemic response of a food. He found that starch hydrolysis follows a first-order equation [$C=C_\infty(1 - e^{-kt})$] and introduced two equations for the prediction of GI of food ($GI= 39.21 + 0.803H_{90}$ and $GI = 39.71 + 0.549HI$). We have adopted both these equations for the prediction of GI of BG. The *in vitro* starch digestion pattern of BG and the reference food (white bread) was analyzed, a curve was plotted between time and total starch hydrolysis percentage at specific time points (Fig. 4.2.). From the calculated percentage of starch hydrolysis at different time points (20, 40, 60, 80, 100, 120, and 180 minutes) we have calculated the C_∞ and k values using the SYSTAT-SigmaPlot V15 software. The C_∞ value of BG was found to be 64.98 ± 1.28% with a k value of 0.014 min^{-1} where the C_∞ and k values of bread were 83.78 ± 1.65% and 0.026 min^{-1} respectively.

As Goni et al. (1997) observed a robust correlation between *in vivo* glycemic responses and the H_{90} value during *in vitro* digestion, Goni proposed an equation, $GI = 39.21 + 0.803H_{90}$, as a means to predict the GI of food based on the H_{90} value. The H_{90} value of BG was computed using the obtained C_∞ and k values [$H_{90}= C_\infty(1-e^{-kt})$, where $C_\infty= 64.98 \pm 1.28\%$, k= 0.014 and t=90] and the calculated H_{90} value was 46.47 ± 0.56%. The H_{90} value measured during the experiment was 44.21 ± 1.60%. Both experimental value and value derived through the equation showed similar H_{90} values. The H_{90} values were used for predicting the GI of BG by resolving the equation $GI = 39.21 + 0.803H_{90,}$ and the GI value was found to be 76.52 ± 0.45. Similarly, the calculated and measured H_{90} value of bread was 75.82 ± 0.34% and 75.94 ± 0.18% respectively, and the estimated GI value of bread was 100.09 ± 0.27.

The alternative equation $eGI = 39.71 + 0.549HI$ was also adopted to predict the GI of BG. Here, the HI serves as a critical parameter, representing the ratio between the AUC of BG and the AUC of white bread, expressed as a percentage. The AUC value was calculated using the OriginPro 2016 software and the obtained HI value was 63.26±0.14% which was then applied to the equation $eGI = 39.71 + 0.549HI$. The eGI of BG through this equation was 74.44 ± 0.07.

Notably, both predictive equations, GI = 39.21 + 0.803H_{90} and eGI = 39.71 + 0.549HI, yielded remarkably similar results for the estimated GI of BG. Based on this result, we feel that the use of H_{90} would simplify GI prediction by avoiding the calculation of C_{∞}, k, and AUC and also help to reduce the experimental time, as this value is just a one-point measurement of glucose at 90 minutes of the hydrolytic process. While this protocol offers a valuable screening tool for categorizing foods into low, medium, and high GI groups, facilitating a rapid evaluation without the complexities and ethical concerns of clinical GI studies, it is important to note that its simulation of the digestion process does not equate to a comprehensive clinical GI assessment.

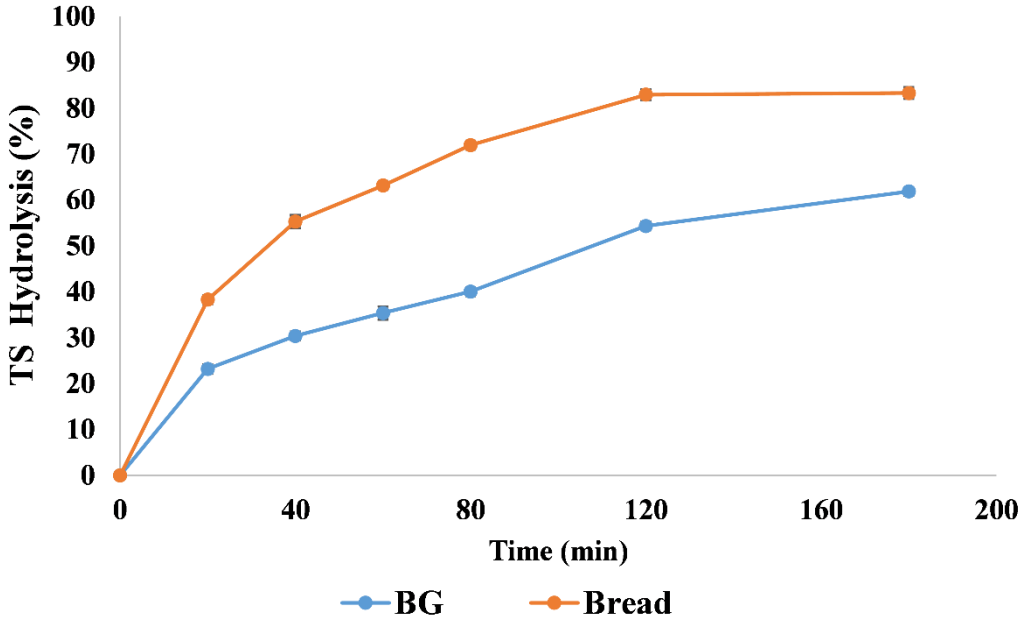

TS Hydrolysis (%)- total starch hydrolysis percentage

Fig. 4.2. *In vitro* starch hydrolysis pattern of BG and reference food (white bread)

4.4.2. Available carbohydrate content analysis and clinical GI-GL studies

After the *in vitro* prediction, the GI of two BG preparations (upma and porridge) was evaluated at the clinical level also in collaboration with MDRF. The test food was standardized and prepared at the MDRF's test kitchen. The standardized recipe used for the preparation of BG upma and BG porridge was given in section 4.3.4.2.1. The determination of available carbohydrate content in the matrix is critical for determining the portion size of the meal to be served in the clinical GI-GL studies. Available carbohydrates in BG encompass mainly the digestible starch and free sugars like glucose, fructose, sucrose, maltose, and some

oligosaccharides. The Megazyme available carbohydrates assay kit (K-ACHDF) was utilized for determining the available carbohydrate content of BG upma and BG porridge.

The BG upma was found to have an available carbohydrate content of 18.60%. For clinical GI testing, portions of the reference and test foods must have an equivalent amount of available carbohydrate (usually 50 g) (Foster-Powell et al., 2002). Hence 269 g of BG upma containing 50 g of available carbohydrate was given to each participant in the clinical GI-GL studies. Monohydrate glucose (55 g) dissolved in 250 mL of water was given as the reference test food for GI studies of BG upma. The available carbohydrate content in BG porridge was 8.10%. In the case of foods with low to moderate available carbohydrate content, it is justified to lower the carbohydrate load to 25 g to avoid an unrealistically large meal size and to adjust to 25 g carbohydrate in the referent food portion (Brouns et al., 2005). Hence, 309 g of BG porridge containing 25 g of available carbohydrate was given to the participants in the clinical GI studies, and monohydrate glucose (27.5 g) dissolved in 125 mL of water was given as the reference food. The moisture content of BG upma was found to be 69.70%, whereas BG porridge had a high moisture content of 89.30%. Differences in the final moisture content of the cooked product have resulted in the difference in the available carbohydrate content of upma and porridge even though both were prepared from the same raw material BG.

The clinical GI-GL evaluation of BG upma included fifteen participants with normal BMI. Out of which 1 participant with > 30% coefficient of variation (CV) was removed as an outlier. Another 2 participants found it difficult and hence did not consume test food and 2 participants dropped out from the study due to personal reasons. Hence, the GI was declared based on 10 participants. The GI study of BG porridge included fifteen participants with normal BMI. Out of which 1 participant with >30% CV was removed as an outlier per ISO GI protocol. Thus, the GI was declared based on 14 participants. The GI values were calculated according to the methods mentioned in section 4.3.4. The individual Gl value and the SEM obtained for the BG upma, and BG porridge are shown in Table 4.1. and Table 4.2. respectively.

Table 4.1. Individual mean IAUC of reference & BG upma

Sl. No.	Age in years	BMI (Kg/m^2)	Mean IAUC-reference food (mg/dL×minutes)	Mean IAUC-BG upma (mg/dL×minutes)	GI of BG upma
1	26	22.8	3008	1999	66
2	28	22.9	5270	4046	77
3	24	21.4	4358	2025	46
4	23	22.3	6814	3784	56
5	20	19.0	6816	2390	35
6	24	20.5	#	#	#
7	18	21.6	4699	4530	96
8	20	19.7	#	#	#
9	24	19.9	5053	5374	106
10	23	23.1	3982	3180	80
11	22	22.7	7321	3679	50
12	20	18.6	6201	6083	98
13	22	27.5	**	**	**
14	18	21.8	##	##	##
15	19	20.1	##	##	##
Mean	22	22.0	5352	3709	71
SEM*	01	01.0	444	434	08

SEM*- Standard Error of Mean, **>30% CV, #did not consume test food, ##dropout

Table 4.2. Individual mean IAUC of reference & BG porridge

Sl. No.	Age in years	BMI (Kg/m^2)	Mean IAUC-reference food (mg/dL×minutes)	Mean IAUC-BG porridge (mg/dL×minutes)	GI of BG porridge
1	41	22.7	3194	3103	97
2	31	19.8	5580	3136	56
3	26	22.8	1165	1265	109
4	28	22.8	2922	3266	112
5	26	19.1	4156	1328	32
6	24	21.2	3349	3439	103
7	23	22.3	**	**	**
8	28	22.8	4046	1832	45
9	24	20.0	3112	2498	80
10	27	19.4	3496	1410	40
11	19	20.0	3099	2478	80
12	18	21.9	2935	990	34
13	27	22.5	5232	4636	89
14	22	22.5	5154	2933	57
15	32	21.1	3474	2258	65
Mean	26	21.0	3637	2469	71
SEM*	1	0.4	306	276	7

SEM*- Standard Error of Mean, **>30% CV

The study outcomes, as illustrated in Fig. 4.3a. (comparison of IAUC of BG upma and glucose) and Fig. 4.3b. (comparison of IAUC of BG porridge and glucose) revealed respective GI values of 71 ± 8 and 71 ± 7 (Table 4.3.). It is worth noting that the results of the GI prediction studies were consistent with the clinical GI-GL studies. Literature findings suggest that unit operations like heating affect the GI of the food. In the presence of water starch granules swell as water is absorbed, amylose molecules leach out and lead to disintegration of the granules. Thus, heat treatment improves the availability of starch for enzyme action resulting in increased GI compared to raw products (Zhang et al., 2021). Despite their historical caution, high GI foods play a pivotal role in specific nutritional contexts. Over the past millennia, cereals, dairy, and meat have been primary energy sources. As we approach 2050, diversifying our energy sources is imperative.

The product of the food's GI value and the amount of available carbohydrates in grams per serving is the food's GL (Kim, 2020). GL is calculated by multiplying the food's carbohydrate content in a specified serving size by its GI value, and then dividing the result by 100 (Foster-Powell et al., 2002). A GL value of 10 or below is categorized as low, 11-19 as medium, and 20 or above as high. Foods with a higher GL are anticipated to elicit a more significant increase in serum glucose and insulin responses per serving compared to those with a lower GL (Kim, 2020). As GL is a measure of the glycemic impact of a serving of food, it gives a more realistic idea about the glycemic response of a food. The portion size used for the GL calculation of BG upma and BG porridge i.e., 100 g and 150 g respectively, were chosen based on the portion size that can be consumed ideally by a consumer. Our study revealed that a 100 g serving of BG upma had a GL value of 13.19, categorizing it as a medium GL food, while a 150 g serving of BG porridge had a GL of 8.61, placing it in the low GL category (Table 4.3.). Despite having high GI values, foods with low or moderate GL values are considered ideal for individuals with diabetes. For instance, watermelon, despite its GI of 76, has a very low GL of 6 due to its high water content, making it suitable for consumption by diabetic individuals (Atkinson et al., 2008; *WATERMELON – Glycemic Index*, n.d.). Similarly, a restricted portion of BG porridge can be consumed even by diabetic individuals.

Even though the GI data of BG in upma and porridge forms are the same, there are some striking observations when we look into individual forms. BG, when given in the form of a porridge showed a 29 mg/dL glucose shoot comparable to that of reference food (28 mg/dL). Whereas with respect to BG in upma form, it can be noticed that the shoot of blood glucose is 17 mg/dL when compared to that of reference food (39 mg/dL). Similar way when we compare

the presence of glucose in the blood at 90th minutes with respect to BG porridge it was almost 5 mg/dL incomparable to glucose (9 mg/dL). Whereas in the case of BG upma at the 90th minute, 22 mg/dL glucose remained, however, the reference food gave a different trend (34 mg/dL) unlike the trend observed in the case of BG porridge. Here probably it can be inferred that the starch matrix hydrolysis and blood glucose shoot and its sustenance in the blood depends on the forms in which we consume it. This difference may be attributed to the variation in starch gelatinization due to the differences in the amount of water used during the cooking process. With respect to BG upma the BG to water ratio was 1: 2.5 and with respect to BG porridge the ratio was 1: 10. Diabetic persons who wish to have the benefits of BG can consume it in dry form like upma rather than porridge.

4.3a.

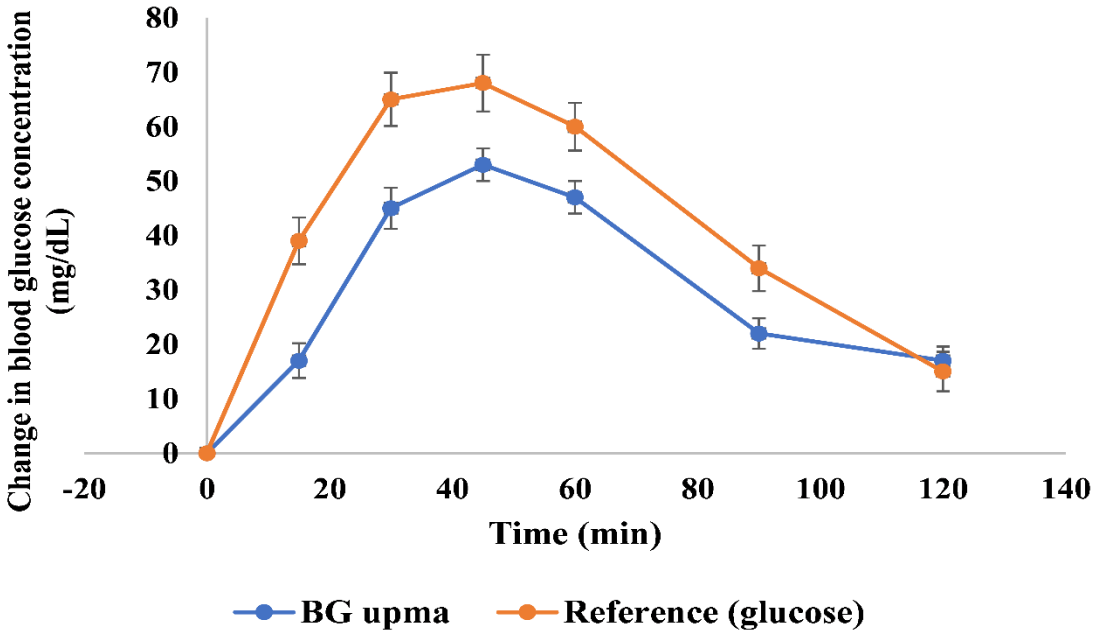

Fig. 4.3a. Graph showing the change in blood glucose level between reference food and test food (BG upma) over a period of 2 hours

4.3b.

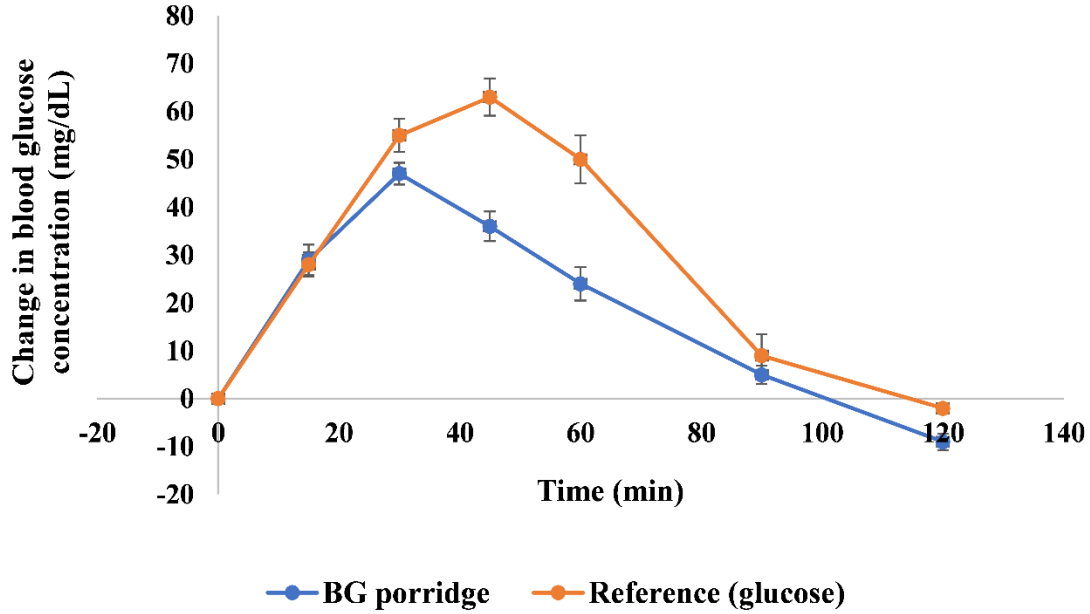

Fig. 4.3b. Graph showing the change in blood glucose level between reference food and test food (BG porridge) over a period of 2 hours

Table 4.3. Clinical GI-GL values of BG upma and BG porridge

Food for GI testing	Weight of BG before cooking (g)	Weight after cooking (g)	Portion served per person in clinical study (g)	Amount of available carbohydrate in served portion size for clinical studies(g)	Amount of reference (monohydrate glucose) used (g)	Portion size taken for calculating GL (g)	Amount of available carbohydrate in portion size taken for GL calculation (g)*	GI	GL
BG upma	315	1052	269	50	55	100	18.58	71±8	13.19
BG porridge	200	1915	309	25	27.50	150	12.13	71±7	8.61

*Portion size used for the GL calculation of BG upma and BG porridge i.e., 100 g and 150 g respectively, were chosen based on the portion size that can be consumed ideally by a consumer.

4.4.3. Starch fractions in BG

Our initial investigations into the estimation of starch fractions in BG by employing a 2-hour digestion procedure involving invertase, pepsin, pancreatin, and amyloglucosidase enzymes (Englyst et al., 1992; Ren et al., 2016) revealed 80.49 ± 2.68% TS, 21.44 ± 2.34% SDS, 16.95 ± 0.79% RDS and 42.08 ± 2.85% RS content. Further investigation using a 4-hour digestion protocol, which is the average time of residence of food in the human small intestine, with a saturated level of PAA/AMG enzymes using the Megazyme kit (K-DSTRS) revealed that BG contained only 4.44 ± 0.08% of RS. The values of RDS, SDS, TDS, and TS were 71.91 ± 0.76%, 1.33 ± 0.34%, 77.69 ± 0.35%, and 81.64 ± 0.78%. (Table 4.4.). The reduced RS content may have contributed to the high GI of BG. When processing RS2 category of starch at high moisture levels, and normal cooking temperatures it disrupts the starch granule structure, potentially causing gelatinization and therefore enhancing its digestibility (Magallanes-Cruz et al., 2020), this may be the reason behind the observed reduced RS content of BG.

The retention of RS in BG after cooking was analyzed by preparing two dishes with different moisture contents to check the effect of gelatinization on RS retention. BG, 30 g was cooked with 120 mL of water for 6 minutes under a medium flame, resulting in a final cooked weight of approximately 100 g. This preparation with a 1:4 BG to water ratio mimics the preparation of BG upma. A preparation similar to BG porridge was prepared by mixing 30 g of BG with 300 mL of water (BG: water 1:10) and cooked for 6 minutes under medium flame, yielding a final cooked weight of nearly 220 g (fluid-like consistency). The cooked products were screened using K-DSTRS kit to assess RS retention and changes in other fractions. The moisture content of all the samples was measured according to the AOAC method (AOAC, 2005). The result reveals that BG even after cooking in both forms retains the 4% RS content (Table 4.4.). The BG upma exhibited a moisture content of approximately 77%, with the remaining 23% dry matter consisting mainly of starch, fiber, ash, protein, and negligible amounts of fat. Similarly, the BG porridge had a moisture content of 93%, leaving 7% of dry matter. Analysis of starch fractions in the cooked products revealed that consuming 100 g of BG cooked in the form of upma would provide an individual with approximately 18.73% TS and 0.99% RS. On the other hand, consuming 100 g of BG porridge provides approximately 5.76% TS and 0.30% RS. Consumption of RS exerts numerous health benefits (detailed in the review of literature section 1.2.8.2. of Chapter 1). RS upon the colonic fermentation by prebiotics produces SCFA, especially butyrate, which plays a crucial role in maintaining colon

health by serving as a primary energy source for colonocytes, reducing the risk of colon cancer, modulating the gut pH, and thereby increasing the growth of beneficial bacteria and suppressing the proliferation of pathogenic strains (Chen et al., 2024). Butyrate exhibits anti-inflammatory properties by inhibiting the production of pro-inflammatory cytokines, such as TNF-α, increasing the GLP-1 secretion, and modulating the GALT, an integral part of the human immune system (Chen et al., 2024; Cummings et al., 2004; Lockyer & Nugent, 2017; Segain et al., 2000).

The study revealed that the unripe Nendran pulp contains 81.56 ± 1.42% TS and a significant amount of RS i.e., 41.58 ± 0.60% and 39.97 ± 0.81% of TDS on a db. The data was in accordance with literature data on unripe bananas. The unripe Nendran pulp has nearly 57% moisture content and hence consumed raw, it delivers a notable nutritional profile, offering approximately 35.10% TS and 17.89% RS. Due to processing steps employed in BG preparation, a nearly 10% reduction in the RS content was observed (BG RS content-4.44%). Apparently, the TDS content of BG was found to be 75.13 ± 0.42%, nearly double the amount of TDS present in the unripe pulp (Table 4.4.).

Table 4.4. Amount of TS and starch fractions (RDS, SDS, TDS, & RS) distribution pattern in the samples

Sample	Starch fraction[#]	Starch "as is" (g/100 g)	Moisture Content (%)	Starch "db" (g/100 g)
Unripe Nendran pulp	RDS (0-20 min)	3.04±0.31[a]	57±2	7.05±0.40[a]
	SDS (20-120 min)	5.96±0.39[c]		13.85±0.28[b]
	TDS (0-240 min)	17.21±1.15[b]		39.97±0.81[b]
	RS (not digested within 240 min)	17.89±1.09[c]		41.58±0.60[b]
	TS (TDS+RS)	35.10±2.24[c]		81.56±1.42[a]
BG	RDS (0-20 min)	69.53±0.81[d]	3.3±0.1	71.91±0.76[b]
	SDS (20-120 min)	1.29±0.33[b]		1.33±0.34[a]
	TDS (0-240 min)	75.13±0.42[c]		77.69±0.35[a]
	RS (not digested within 240 min)	4.30±0.07[b]		4.44±0.08[a]
	TS (TDS+RS)	79.43±0.35[d]		81.64±0.78[a]
BG cooked as upma*	RDS (0-20 min)	16.83±0.93[c]	77±1	73.13±0.87[b]
	SDS (20-120 min)	0.50±0.06[a]		2.18±0.15[a]
	TDS (0-240 min)	17.74±0.73[b]		77.14±0.20[a]
	RS (not digested within 240 min)	0.99±0.06[a]		4.29±0.06[a]
	TS (TDS+RS)	18.73±0.78[b]		81.44±0.14[a]
BG cooked as porridge**	RDS (0-20 min)	5.07±0.02[b]	93	72.41±0.25[b]
	SDS (20-120 min)	0.09[a]		1.33±0.05[a]
	TDS (0-240 min)	5.46±0.03[a]		78.04±0.46[a]
	RS (not digested within 240 min)	0.30[a]		4.26±0.02[a]
	TS (TDS+RS)	5.76±0.03[a]		82.30±0.48[a]

Mean±SD (n=3)

#RDS (0-20 min)- rapidly digestible starch, SDS (20-120 min)- slowly digestible starch, TDS (0-240 min)- total digestible starch, RS (starch not digested within 240 min)- resistant starch., TS (TDS+RS)-total starch). *BG cooked with BG:water ratio 1:4 which is equivalent to the water requirement for the preparation of BG upma. **BG cooked with BG:water ratio 1:10 which is equivalent to the water requirement for the preparation of BG porridge. db- dry basis
Values with different superscript in each starch fraction category in the same column are significantly different ($p \leq 0.05$).

4.4.4. RS content in the unripe Nendran pulp and the process-induced changes in RS content

Further evaluation of the RS content of processed unripe Nendran samples (P1 & P2) and commercial samples (C1 & C2) revealed more than 35% RS content except BG (4%) (Fig. 4.4.). But a significant reduction was observed in the RS content of products after cooking. The porridges of P1 and P2 were prepared in 1:10 sample-to-water ratio. The porridges prepared from samples P1 and P2 retained 10.33 ± 0.03% and 9.15 ± 0.03% RS on dw respectively. Whereas, a drastic decrease in RS content was observed in the commercial samples when it is cooked according to manufacturers' instructions (sample: water ratio is 1:25). The cooked samples C1 and C2 retained only 0.81 ± 0.14% and 0.54 ± 0.04% RS on dw respectively. In the case of samples C1 and C2, a 1:25 sample-to-water ratio was used to replicate the RS content that a consumer would likely obtain by following the exact cooking instructions provided by the manufacturer. One important observation we had during the study was the retention of the RS content of BG even when it is cooked as thick porridge (RS- 4.26 ± 0.01%) or loose porridge (RS- 3.80 ± 0.21 %) (Fig. 4.5.).

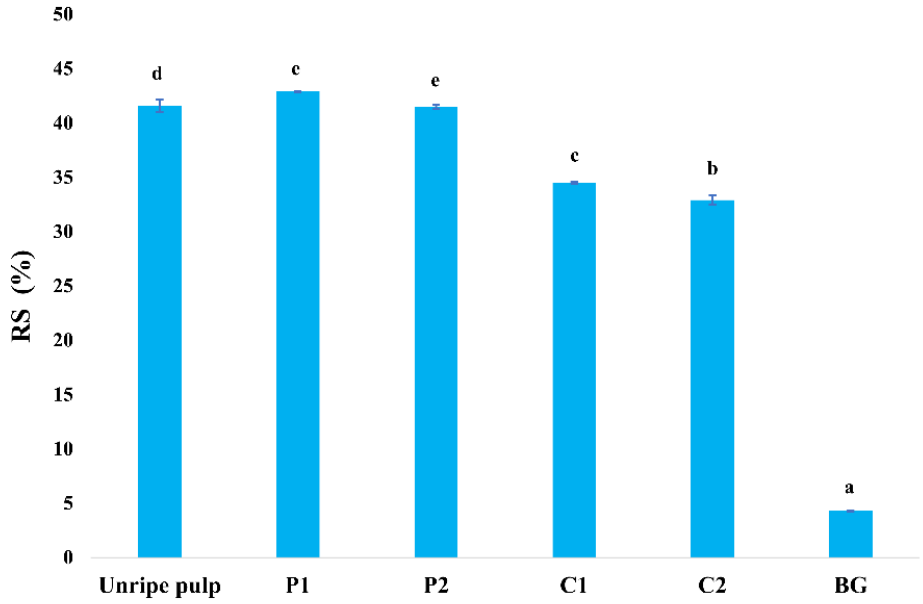

Mean±SD (n=3) values with different superscripts are significantly different (p≤0.05)

Fig. 4.4. RS content in processed and commercial banana samples (db)

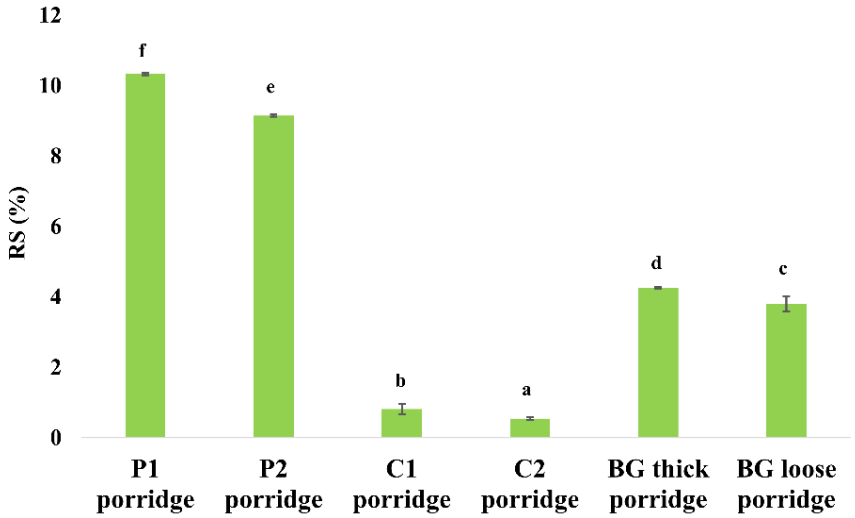

Mean±SD (n=3) values with different superscripts are significantly different ($p \leq 0.05$)

Fig. 4.5. RS content in processed and commercial banana samples after cooking (db)

4.4.5. Evaluation of starch fractions in commonly consumed food items

The starch fractions distribution pattern was evaluated in some of the commonly consumed food items such as cooked Matta rice, chapathi, and oats, and data was compared with BG cooked as upma (Fig. 4.6.). The study revealed some interesting facts. To get a clear understanding of how much starch each food item will contribute upon consumption, all the data were analyzed wet basis.

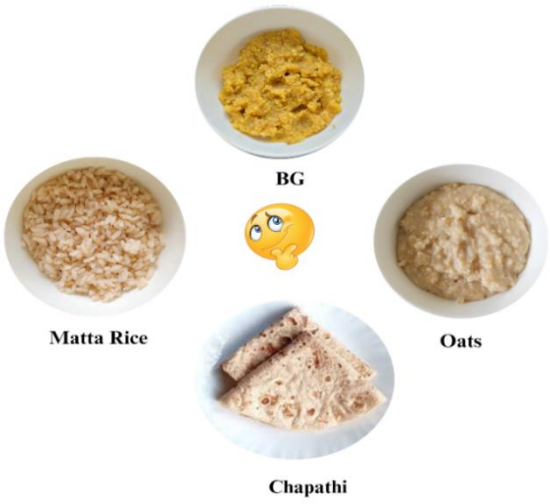

Fig. 4.6. Samples selected for comparison of starch fractions (Created with BioRender.com)

From the study, it was found that 100 g oats porridge has a moisture content of 87% and the remaining 13% is the solid matter distributed between fat, carbohydrate, minerals, and protein. Out of the 13%, the TS content of oats was 7.45 ± 0.03% and the starch fractions were distributed as 6.38% RDS, 0.41% SDS, 7.25 ± 0.03% TDS, and 0.21% RS. Similarly, 100 g cooked chapathi has a moisture content of 21% and the remaining 79% is the solid matter, out of which 56.32 ± 0.10% is TS. The starch fractions were distributed as 52.85 ± 0.13% RDS, 7.39 ± 0.10% SDS, 56.26 ± 0.10% TDS, and 0.06% RS. Cooked matta rice has a moisture content of 79% and the remaining 21% is the solid matter distributed between fat, carbohydrate, minerals, and protein. Out of the 21%, the TS content of matta rice was 16.99 ± 0.01% and the starch fractions were distributed as 16.61 ± 0.05% RDS, 1.30 ± 0.05% SDS, 16.57 ± 0.01% TDS, and 0.42% RS. BG cooked as upma has a moisture content of 77%, TS content of 18.73 ± 0.78%, 16.83 ± 0.93% RDS, 0.50 ± 0.05% SDS, 17.74 ± 0.72% TDS, and 1.15 ± 0.10% RS.

The TS was found to be highest in chapathi compared to other products since the moisture content of chapathi was the least (21%), compared to the moisture content of BG upma (77%), oats (89%), and rice (79%). Eating 100 g of chapathi will provide nearly 56% starch, whereas cooked rice, oats and BG will provide less than 20% starch as they contain more moisture content. A 100 g of chapathi delivers nearly 56% starch, of which 52.85 ± 0.13% is RDS, hence it may result in a rapid shoot in the blood glucose level. Among the foods compared, chapathi showed the least RS content (0.05%) (Fig. 4.8.). On the other hand, 100 g Matta rice has only 16.61 ± 0.05% RDS and 0.41% RS (Fig. 4.7. & Fig. 4.8.), the data indicates that reduced portion size of Matta rice combined with adequate amount of fiber-rich vegetables can be consumed even by diabetic individuals.

Despite the significant variation in starch fraction distribution pattern between cooked rice and chapathi, both foods were found to have nearly the same GI at the clinical level (GI of chapathi: 65.66 ± 4.22; GI of rice: 78.23 ± 4.24), placing them both in the high-GI category (Devindra et al., 2017). For clinical GI-GL studies, portion sizes are standardized to ensure that each food provides 50 g of available carbohydrates. This standardized portion size for chapathi and rice may probably the reason behind the similar GI values observed for both foods.

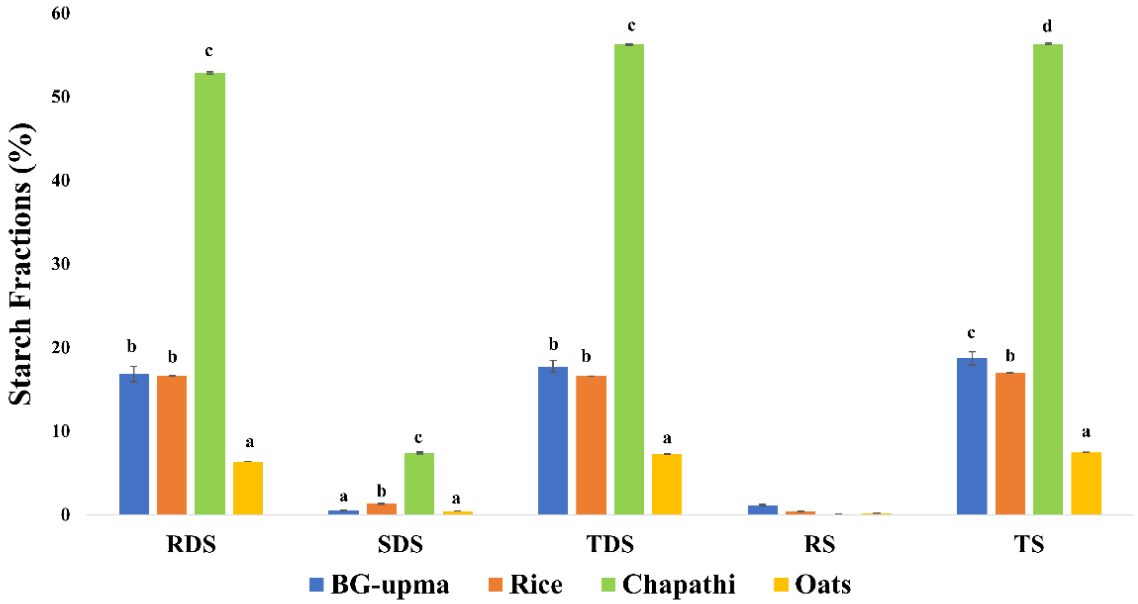

Mean±SD (n=3) values with different superscripts are significantly different (p≤0.05)

Fig. 4.7. Distribution pattern of starch fractions in the samples (wb)

The study also figures out the nutrient superiority of BG in terms of RS content (1.15 ± 0.10%) compared to oats (0.21%), chapathi (0.06%), and rice (0.42%) (Fig. 4.8.).

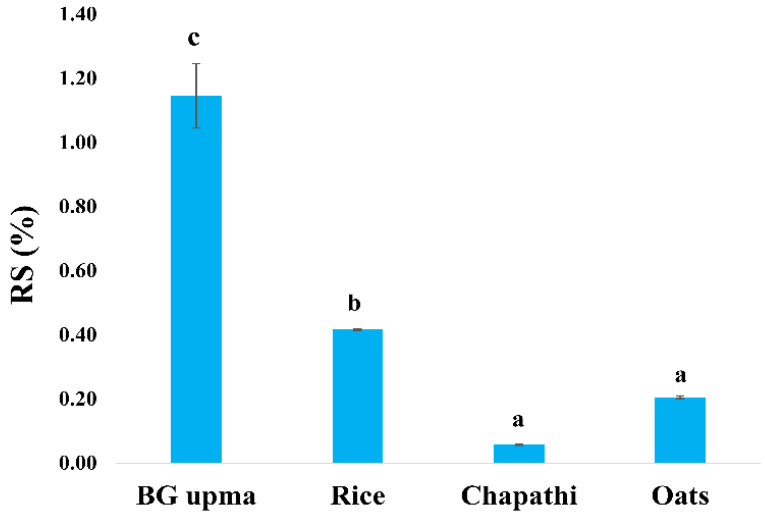

Mean±SD (n=3) values with different superscripts are significantly different (p≤0.05)

Fig. 4.8. Distribution pattern of RS in the samples (wb)

4.5. Conclusion

Two preparations, BG upma and BG porridge were screened for GI at clinical level. BG cooked in both forms exhibited a high GI and medium GL in clinical studies. In this study, by comparing banana grit in porridge and upma forms, we have narrated the differences in blood glucose surge and sustenance with variations in cooking procedures. Even though high in GI, BG has a medium GL value makes it suitable for consumption by diabetic people also. We have also conducted an *in vitro* GI prediction study, which showed a high correlation with the clinical GI values. Upon screening for RS content, we found that BG has only 4.44% RS. According to the literature, raw bananas are considered as a rich source of RS. Our study demonstrated that raw Nendran has 41% RS, but the unit operations we employed resulted in a 10% reduction of RS and we also noticed the variation in the RS content of pulp, when it is subjected to different processing steps. Our study emphasizes the importance of selecting appropriate unit operations when designing products (functional foods) with a low GI. The evaluation of starch fractions distribution pattern in commonly consumed food items such as oats, rice, and chapathi indicated the nutritional superiority of BG in terms of RS content compared to these items. Further studies are ongoing to refine our processing techniques to preserve the inherent RS content of unripe bananas for catering to the needs of people with diabetes and related conditions.

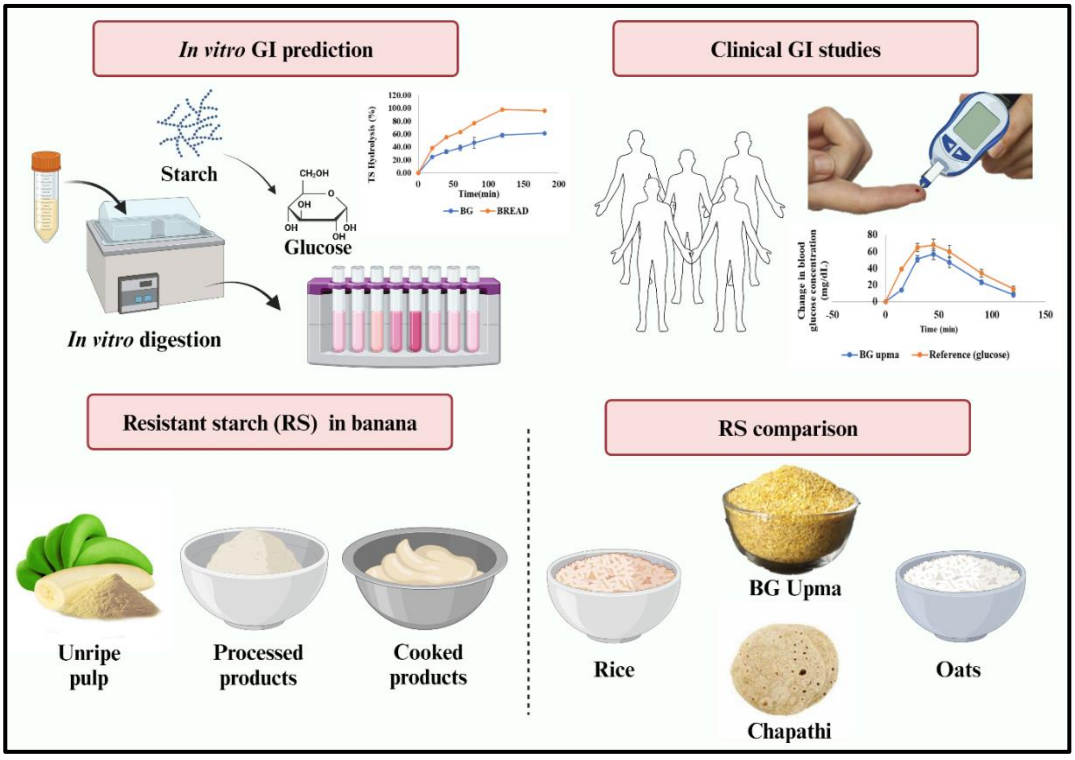

Fig. 4.9. Chapter 4 graphical abstract (Created with BioRender.com)

4.6. References

1. AOAC, C. (2005). Official methods of analysis of the Association of Analytical Chemists International. *Official Methods: Gaithersburg, MD, USA*.
2. Atkinson, F. S., Foster-Powell, K., & Brand-Miller, J. C. (2008). International tables of glycemic index and glycemic load values: 2008. *Diabetes Care*, *31*(12), 2281–2283. https://doi.org/10.2337/dc08-1239
3. Augustin, L. S., Kendall, C. W., Jenkins, D. J., Willett, W. C., Astrup, A., Barclay, A. W., Björck, I., Brand-Miller, J. C., Brighenti, F., & Buyken, A. E. (2015). Glycemic index, glycemic load and glycemic response: An International Scientific Consensus Summit from the International Carbohydrate Quality Consortium (ICQC). *Nutrition, Metabolism and Cardiovascular Diseases*, *25*(9), 795–815. https://doi.org/10.1016/j.numecd.2015.05.005
4. *Available Carbohydrates Assay Kit*. (n.d.). Megazyme. Retrieved February 14, 2024, from https://www.megazyme.com/available-carbohydrates-assay-kit
5. Brouns, F., Bjorck, I., Frayn, K., Gibbs, A., Lang, V., Slama, G., & Wolever, T. (2005). Glycaemic index methodology. *Nutrition Research Reviews*, *18*(1), 145–171. http://dx.doi.org/10.1079/NRR2005100
6. Carbohydrates in human nutrition. Report of a Joint FAO/WHO Expert Consultation. (1998). *FAO Food and Nutrition Paper*, *66*, 1–140.
7. Chen, Z., Liang, N., Zhang, H., Li, H., Guo, J., Zhang, Y., Chen, Y., Wang, Y., & Shi, N. (2024). Resistant starch and the gut microbiome: Exploring beneficial interactions and dietary impacts. *Food Chemistry: X*, *21*, 101118. https://www.sciencedirect.com/science/article/pii/S2590157524000051
8. Cummings, J. H., Antoine, J.-M., Azpiroz, F., Bourdet-Sicard, R., Brandtzaeg, P., Calder, P. C., Gibson, G. R., Guarner, F., Isolauri, E., Pannemans, D., Shortt, C., Tuijtelaars, S., & Watzl, B. (2004). PASSCLAIM1?Gut health and immunity. *European Journal of Nutrition*, *43*(S2), ii118–ii173. https://doi.org/10.1007/s00394-004-1205-4
9. Devindra, S., Chouhan, S., Katare, C., Talari, A., & Prasad, G. B. K. S. (2017). Estimation of glycemic carbohydrate and glycemic index/load of commonly consumed cereals, legumes and mixture of cereals and legumes. *International Journal of Diabetes in Developing Countries*, *37*(4), 426–431. https://doi.org/10.1007/s13410-016-0526-1
10. *Digestible and Resistant Starch Assay Kit*. (n.d.). Megazyme. Retrieved February 14, 2024, from https://www.megazyme.com/digestible-and-resistant-starch-assay-kit

11. EFSA Panel on Dietetic Products, N. and A. (NDA). (2012). Guidance on the scientific requirements for health claims related to appetite ratings, weight management, and blood glucose concentrations. *EFSA Journal*, *10*(3), 2604. https://doi.org/10.2903/j.efsa.2012.2604
12. Englyst, H. N., Kingman, S., & Cummings, J. (1992). Classification and measurement of nutritionally important starch fractions. *European Journal of Clinical Nutrition*, *46*, S33-50.
13. Faisant, N., Buléon, A., Colonna, P., Molis, C., Lartigue, S., Galmiche, J. P., & Champ, M. (1995). Digestion of raw banana starch in the small intestine of healthy humans: Structural features of resistant starch. *British Journal of Nutrition*, *73*(1), 111–123. https://doi.org/10.1079/BJN19950013
14. Foster-Powell, K., Holt, S. H., & Brand-Miller, J. C. (2002). International table of glycemic index and glycemic load values: 2002. *The American Journal of Clinical Nutrition*, *76*(1), 5–56. https://doi.org/10.1093/ajcn/76.1.5
15. Goñi, I., Garcia-Alonso, A., & Saura-Calixto, F. (1997). A starch hydrolysis procedure to estimate glycemic index. *Nutrition Research*, *17*(3), 427–437. https://doi.org/10.1016/S0271-5317(97)00010-9
16. Henry, C., Lightowler, H., Newens, K., Sudha, V., Radhika, G., Sathya, R., & Mohan, V. (2008). Glycaemic index of common foods tested in the UK and India. *British Journal of Nutrition*, *99*(4), 840–845. https://doi.org/10.1017/s0007114507831801
17. International Organization for Standardization. (2010). *Food products—Determination of the glycaemic index (GI) and recommendation for food classification*. ISO.
18. Joint, F. (1998). *Carbohydrates in human nutrition*.
19. Kim, D. (2020). Glycemic index. In *Obesity* (pp. 183–189). Elsevier. https://doi.org/10.1016/B978-0-12-818839-2.00014-4
20. Lockyer, S., & Nugent, A. (2017). Health effects of resistant starch. *Nutrition Bulletin*, *42*(1), 10–41. https://doi.org/10.1111/nbu.12244
21. Magallanes-Cruz, P. A., Bello-Pérez, L. A., Agama-Acevedo, E., Tovar, J., & Carmona-Garcia, R. (2020). Effect of the addition of thermostable and non-thermostable type 2 resistant starch (RS2) in cake batters. *Lwt*, *118*, 108834. https://www.sciencedirect.com/science/article/pii/S0023643819311764
22. McCleary, B. V., McLoughlin, C., Charmier, L. M. J., & McGeough, P. (2020). Measurement of available carbohydrates, digestible, and resistant starch in food

ingredients and products. *Cereal Chemistry*, *97*(1), 114–137. https://doi.org/10.1002/cche.10208

23. Ren, X., Chen, J., Molla, M. M., Wang, C., Diao, X., & Shen, Q. (2016). In vitro starch digestibility and in vivo glycemic response of foxtail millet and its products. *Food & Function*, *7*(1), 372–379. https://doi.org/10.1039/c5fo01074h
24. Segain, J. P., De La Blétiere, D. R., Bourreille, A., Leray, V., Gervois, N., Rosales, C., Ferrier, L., Bonnet, C., Blottiere, H. M., & Galmiche, J. P. (2000). Butyrate inhibits inflammatory responses through NFκB inhibition: Implications for Crohn's disease. *Gut*, *47*(3), 397–403. https://gut.bmj.com/content/47/3/397.abstract
25. *WATERMELON – Glycemic Index*. (n.d.). Retrieved February 17, 2024, from https://glycemicindex.com/2021/11/watermelon/
26. Wolever, T. M., Meynier, A., Jenkins, A. L., Brand-Miller, J. C., Atkinson, F. S., Gendre, D., Leuillet, S., Cazaubiel, M., Housez, B., & Vinoy, S. (2019). Glycemic index and insulinemic index of foods: An interlaboratory study using the ISO 2010 method. *Nutrients*, *11*(9), 2218. https://doi.org/10.3390%2Fnu11092218
27. Wolever, T. M., Yang, M., Zeng, X. Y., Atkinson, F., & Brand-Miller, J. C. (2006). Food glycemic index, as given in glycemic index tables, is a significant determinant of glycemic responses elicited by composite breakfast meals. *The American Journal of Clinical Nutrition*, *83*(6), 1306–1312. https://doi.org/10.1093/ajcn/83.6.1306
28. Zhang, K., Dong, R., Hu, X., Ren, C., & Li, Y. (2021). Oat-Based Foods: Chemical Constituents, Glycemic Index, and the Effect of Processing. *Foods*, *10*(6), 1304. https://doi.org/10.3390/foods10061304

Chapter 5

Glucocerebrosides (GCs) in unripe Nendran peel and evaluation of its anti-inflammatory and α-glucosidase inhibition potential

5.1. Introduction

5.1.1. Glycosphingolipids

Glycosphingolipids are the primary component of the outer leaflet of the eukaryotic cell membranes. They are amphipathic molecules with an outer glycan portion and an inner lipid tail consisting of a ceramide unit. A ceramide consists of sphingosine and a long-chain fatty acid, connected by an amide linkage (Demir, 2021). The unique structure enables them to function as structural membrane components and signalling molecules (Desplanque et al., 2020). In higher animal cells, the glycan part is usually glucose or galactose thus forming glucosylceramide or galactosylceramide (Fig. 5.1.). These basic units are further extended by the addition of monosaccharides. The number of extensions of galactosylceramide is limited. But the glucosylceramides serve as a precursor of lactosylceramides and gangliosides (Varki et al., 1999).

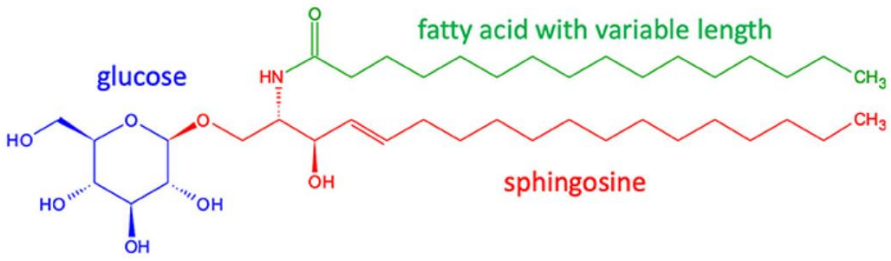

Fig. 5.1. General structure of glucocerebroside

(Source: Desplanque et al., 2020, https://doi.org/10.3389/fphys.2020.558090)

The ceramide moiety also exhibits substantial structural diversity. The sphingosine base can differ in the number of double bonds and acyl chain length (C16-20), while the fatty acid attached to the sphingosine can range from C16 to C34, and vary in saturation and hydroxylation (Fig. 5.2.). These variations are specific to cell types and developmental stages, indicating a functional purpose. For example, brain gangliosides often contain the C20 ceramide homolog in glycosphingolipids (Uchida & Park, 2021; Varki et al., 1999).

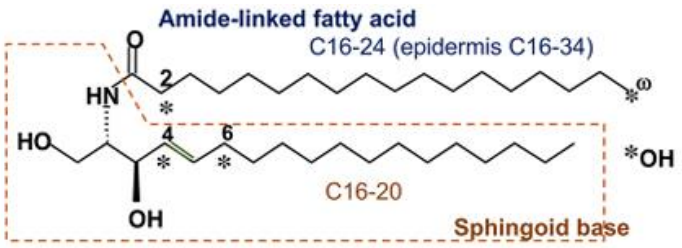

Fig. 5.2. General structure of ceramide

(Source: Uchida & Park, 2021, https://doi.org/10.1007/s40257-021-00619-2)

The synthesis of glucosylceramides or glucocerebrosides (GC) occurs in the Golgi apparatus by the enzyme glucocerebroside synthase also called glucosylceramide synthase. The degradation of GC to ceramide and glucose occurs in lysosomes by the action of the glucocerebrosidase enzyme (Fig. 5.3.). The glucocerebrosidase enzyme is encoded by the beta-glucocerebrosidase (GBA) genes and mutations in them result in enzyme deficiency which leads to the accumulation of GCs in organs such as liver, and central nervous system. This lysosomal storage disease is termed 'Gaucher disease', characterized by an enlarged spleen and liver, anaemia, and skeletal deformations (Desplanque et al., 2020). Apart from Gaucher disease, a strong correlation was observed between Parkinson's disease and GBA mutation (Avenali et al., 2020).

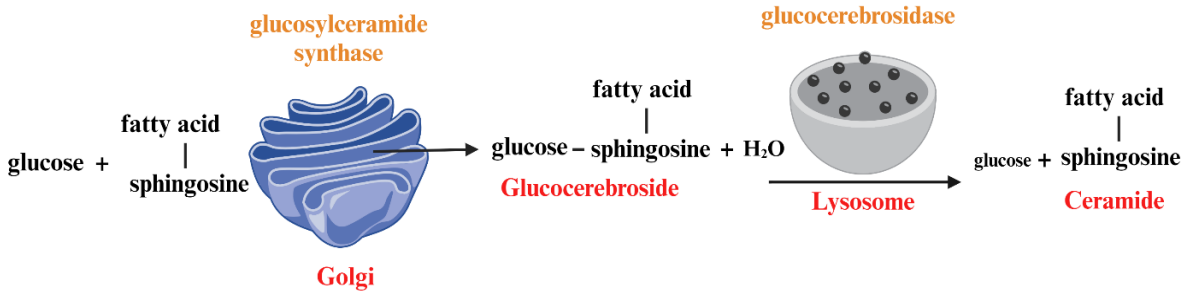

Fig. 5.3. Glucocerebroside synthesis and metabolism (Source: Desplanque et al., 2020, https://doi.org/10.3389/fphys.2020.558090, image created with BioRender.com)

5.1.2. Therapeutic potentials of GC

GC exerts immunomodulatory and anti-inflammatory functions by promoting the regulatory T lymphocytes & NKT cells (Margalit et al., 2005, 2006). GC treatment ameliorates concanavalin A-induced hepatitis by inhibition of NKT lymphocytes (Margalit et al., 2005). In another study, leptin-deficient OB/OB mice, which received a daily GC injection (1.5 µg intraperitoneally) for 8 weeks exhibited significant improvement in the metabolic abnormalities typical of leptin deficiency compared to the control group. Notable reductions in liver size and hepatic fat content, reduction in serum triglyceride levels, normalization of

glucose tolerance, and a 1.6-fold increase in the peripheral/intrahepatic NKT lymphocyte ratio were observed in the GC-treated mice. GC-treated mice also showed a 33% reduction in serum interferon-gama (IFN-γ) levels and a 2.6-fold increase in serum interleukin 10 (IL-10) levels. These findings suggest that GC-induced immune modulation may be beneficial in treating non-alcoholic steatohepatitis and other immune-mediated conditions (Margalit et al., 2006). GC isolated from *Cordyceps militaris*, an edible fungus demonstrated anti-inflammation potential by lowering the expression of cyclooxygenase-2 (COX-2) protein in lipopolysaccharide (LPS)-stimulated RAW 264.7 macrophages and reducing the generation of inducible nitric oxide synthase (iNOS) protein (Chiu et al., 2016). The sphingolipids isolated from wheat showed anti-cancer properties in HCT-116 and HT-29 human colon cancer cells (Zhu et al., 2013).

5.1.3. Application of ceramide in cosmetics

The skin's barrier function is based on the stratum corneum layer located in the uppermost skin. Ceramides along with cholesterol and fatty acids form the major component of stratum corneum. Thus, ceramides play a critical role in the skin barrier function and regulating transepidermal water loss, also involved in epidermal self-renewal and immune regulation (Bhatia et al., 2022; Li et al., 2020; Uchida & Park, 2021). Mainly 18 classes of ceramides were identified in the stratum corneum which varies with their heterogeneity in the fatty acids (non-hydroxy, α-hydroxy, and ω-hydroxy, esterified ω-hydroxy) and sphingoid base (dihydrosphingosine, sphingosine, phytosphingosine, 6-hydroxy-sphingosine, and dihydroxy-sphinganine). Each of these ceramide classes contains 300-1000 species based on their combination of fatty acid and sphingoid base (Li et al., 2020). Mainly, α-hydroxy, nonhydroxy, and ω-hydroxy fatty acid substitution are seen in the skin ceramides (Coderch et al., 2003). An altered ceramide profile in the skin results in skin diseases such as psoriasis, xerosis, and atopic dermatitis (Uchida & Park, 2021). Hence the role of the topical application and oral intake of ceramides was researched widely and ceramide-incorporated skin-care products are now popular in the market. Various body creams, lotions, and moisturizers supplemented with ceramides (Re'equil ceramide moisturizer, Dr. Sheth's Ceramide & Vitamin C Body Lotion, Eucerin Eczema Relief Body Creme, CeraVe Suncare Sunscreen Face, Eucerin Smoothing Repair Dry Skin Lotion, CeraVe Moisturizing Lotion, SPF 30 etc.) are available in the market (Kahraman et al., 2019).

Kimata et al., 2006, investigated the effects of oral intake of konjac ceramide (1.8 mg/day) on atopic dermatitis in 25 children for two weeks. The 'ceramide group' had significant reductions in Scoring Atopic Dermatitis (SCORAD) index scores, allergic skin responses, and

immunoglobulin E (IgE) production. The study also proved the reason for reduced allergic responses occurs through Type 1 helper (Th1) cytokine response (Kimata, 2006). In another clinical study, oral supplementation of *Oryza* GC and ceramides decreased transepidermal water loss, and enhanced skin barrier function with their efficacy depending on fatty acid length. GCs and ceramides with C18 to C26 fatty acids strongly promoted barrier function by increasing the production of ceramides (Hiroshi et al., 2023). Topical application of ceramide cream increases skin hydration, reduces trans-epidermal water loss and barrier function, making it suitable for dry skin (Spada et al., 2018). Another study investigated the effect of daily application of ceramide-containing sunscreen for 4 weeks in sixty volunteers. Results showed a reduction in skin redness, erythema index, trans-epidermal water loss, and increase in skin hydration, indicating that daily use of ceramide-containing sunscreen enhances skin hydration and barrier function (Cao et al., 2024). Glucosylsphingolipids extracted from rice aid in moisturizing the skin and enhancing its barrier function (Bhatia et al., 2022; Leo et al., 2022). Currently plant ceramides are increasingly used as skin-health-promoting ingredients in cosmetics.

5.2. Objective

The primary byproduct generated during the BG production process is the banana peel waste. The banana processing industries, worldwide, generate tonnes of this waste material every day. Valorization of waste is instrumental in reducing the environmental and economic burden of waste material and transitioning to a circular economy by developing value-added products (Zou et al., 2022). Repurposing banana by-products into valuable commodities could significantly boost agricultural development (Zou et al., 2022).

Building upon our discovery of GCs from the pulp of Nendran bananas for the first time (chapter 3), we were interested in exploring the presence of GCs in the banana peel and evaluating its immunomodulatory potential. The usage of α-glucosidase inhibitors is proven to be the most efficient approach for controlling postprandial hyperglycemia and associated adverse physiological complications, in type 2 diabetes (Hossain et al., 2020). Apart from that they are broad-spectrum anti-viral agents (de Melo et al., 2006). The traditional knowledge regarding the usage of banana peel for the management of diabetes led us to examine the α-glucosidase inhibition potential of GCs isolated from Nendran peel. Considering the versatile benefits of GC, we have conducted phytochemical exploration studies in the peel with the following objectives.

- Isolation and characterization of GC from unripe Nendran peel.
- Evaluation of the *in vitro* anti-inflammatory and immunomodulatory potential of isolated GC in RAW 264.7 cell line.
- Assessment of α-glucosidase inhibition potential of GC.

5.3. Materials and methods

5.3.1. General procedures

NMR spectra of isolated compounds were analyzed in CD_3OD, ^{1}H and ^{13}C NMR were recorded on a Bruker Ascend™ 500 MHz spectrometer at 500 and 125 MHz, respectively. The HR-ESI-MS analysis of GC fractions was carried out on a Thermo Scientific Exactive mass spectrometer with an Orbitrap mass analyzer, and an Accela 600 pump system and the ions are given in m/z.

5.3.2. Chemicals and standards

All the solvents used for isolation and purification studies were of standard analytical grade. The TLC aluminium sheets (silica gel 60 $F_{254,}$ catalogue no. 1.05554.0007) and the silica gel (230-400 mesh, catalogue no. 6.18609) & 100-200 mesh (catalogue no. 6.18608), NMR solvent (CD_3OD, catalogue no.151947-50-SB) and gradient grade MeOH (catalogue no. 1.06007) were purchased from Merck Life Science Pvt Ltd, Mumbai, India. The murine macrophage cell line, RAW 264.7 was procured from the National Centre for Cell Science (NCCS), Pune, India. Chemicals and reagents for cell culture studies including Dulbecco's Modified Eagle Medium (DMEM) high glucose medium (catalogue no. AT007-1L), fetal bovine serum (FBS, catalogue no. RM10432-500ML), antibiotics-100X (with 10,000 U Penicillin, 10 mg streptomycin and 25 µg amphotericin B per ml in 0.9% normal saline, catalogue no. A002A-5X50ML), 3-(4,5-dimethylthiazol-2-yl)-2,5-diphenyl tetrazolium bromide (MTT, catalogue no. TC191-1G), dimethyl sulfoxide (DMSO, catalogue no. TC349-100ML), bovine serum albumin (BSA, catalogue no. TC548-5G) were procured from HiMedia, India.

The 3,3′,5,5′-Tetramethylbenzidine (TMB catalogue no. 555214) substrate was procured from BD Biosciences, San Diego. Pierce™ bicinchoninic acid (BCA) protein assay kit (catalogue no. 23227) and Halt™ protease inhibitor cocktail-100X (PIC, catalogue no. 87786), were purchased from Thermo Scientific, USA. The primary antibodies; TNF-α (catalogue no. ITT07014), interleukin-6 (IL-6, catalogue no. ITT06087), IL-10 (catalogue no. ITT06894), interleukin-13 (IL-13, catalogue no. ITT06813), COX-2 (catalogue no. ITT07003), interleukin-1alpha (IL-1α, catalogue no. ITT06893), INF-γ (catalogue no. ITT06045), & monocyte chemoattractant protein-1 (MCP-1, catalogue no. ITT07577), and secondary antibody (goat

anti-Rabbit IgG/HRP, catalogue no. ITSAH134) were procured from ImmunoTag, USA. LPS from *Escherichia coli (E. coli)* (catalogue no. L6529-1MG), radioimmunoprecipitation assay (RIPA) buffer-10X (catalogue no. 20-188), α-glucosidase from *Saccharomyces cerevisiae* (Type 1, lyophilized powder ≥10 units/mg protein, catalogue no. G5003-1KU), *p*-nitrophenyl-α-D-glucopyranoside (pNPG, catalogue no. 487506-5GM), Griess reagent (catalogue no. G4410-1G), acarbose (catalogue no. A8980-1G), and dexamethasone (catalogue no. D4902-100MG) were obtained from Sigma-Aldrich (Darmstadt, Germany), and all the other chemicals were of standard analytical grade.

5.3.3. Raw material collection for phytochemical analysis

To conduct the phytochemical exploration studies, mature Nendran infructescence (40.34 kg) was purchased from local organic farmers in Vellayani, Thiruvananthapuram District, Kerala, India. The peel (13.91 kg) and pulp (25.65 kg) were separated. The peel (13.91 kg) was lyophilized using VirTis Genesis-25 EL lyophilizer and the lyophilization protocol was the same as mentioned in material and method section 3.3.3. of Chapter 3. The lyophilized peel (1.50 kg) was collected, sealed and stored at -20°C until further analysis.

5.3.4. Phytochemical exploration studies of banana peel for the isolation of GC

5.3.4.1. Extraction protocol for isolation of GC

For the isolation of GC, the lyophilized banana peel was subjected to extraction with EtOAc, $CHCl_3$, and MeOH separately. Three solvents with varying polarities, namely $CHCl_3$ (non-polar), EtOAc (mid-polar), and MeOH (polar), were selected to assess the extractability of GCs across different polarity ranges.

The lyophilized banana peel was powdered and passed through mesh 10 before extraction and the powdered banana peel (250 g) was extracted with EtOAc (1.5 L) for 6 hours at 700 rpm using an overhead stirrer (Hei-TORQUE 100, Heidolph, Germany). After 6 hours, the extract was collected, kept for settling and filtered through Whatman no. 1 filter paper, fitted with a Buchner funnel, then extracts were concentrated under vacuum in a rotary evaporator (Hei-vap, Heidolph, Germany). This process was repeated twice, and the extracts pooled. The same process was followed in the case of $CHCl_3$ and MeOH extraction of banana peel. The yields of extracts were 11.1 g, 14.09 g, and 12.32 g of EtOAc, MeOH, and $CHCl_3$ extracts, respectively (Fig. 5.4.).

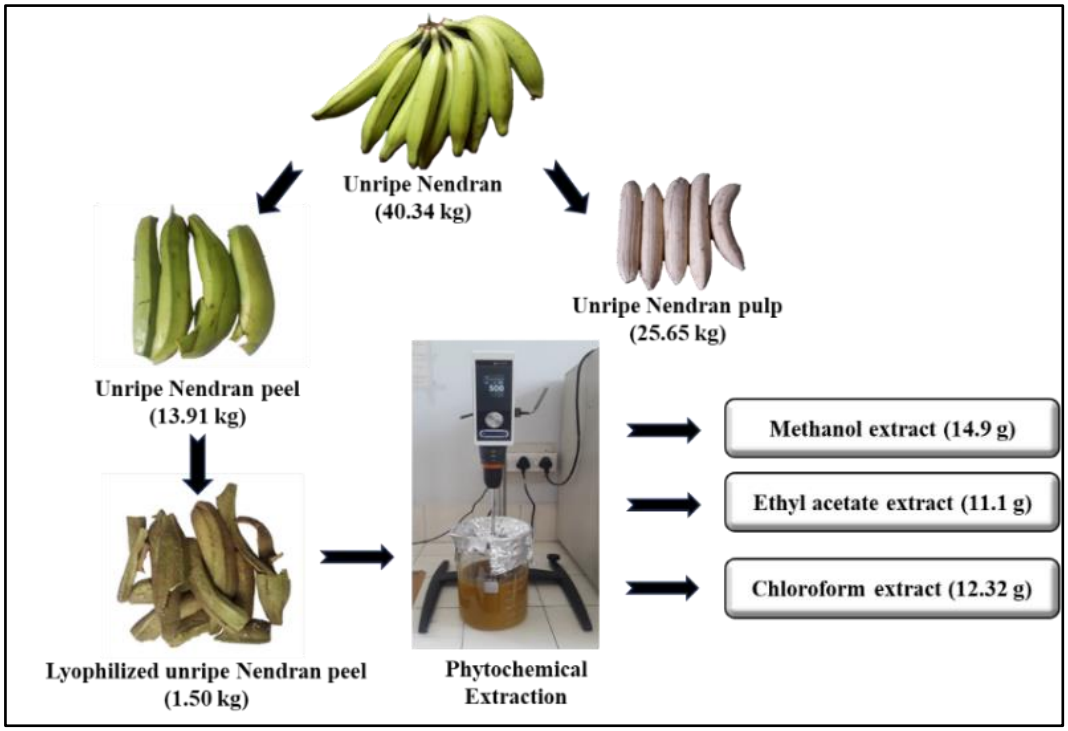

Fig. 5.4. Processing of unripe Nendran peel for phytochemical exploration studies (Created with BioRender.com)

5.3.4.2. Purification of extracts by column chromatography

Before proceeding to the isolation protocols, the TLC pattern of EtOAc, $CHCl_3$, and MeOH extracts was compared with the GC isolated from the banana pulp and the presence of the GC was confirmed in all three extracts (Fig. 5.5a - Fig. 5.5c.).

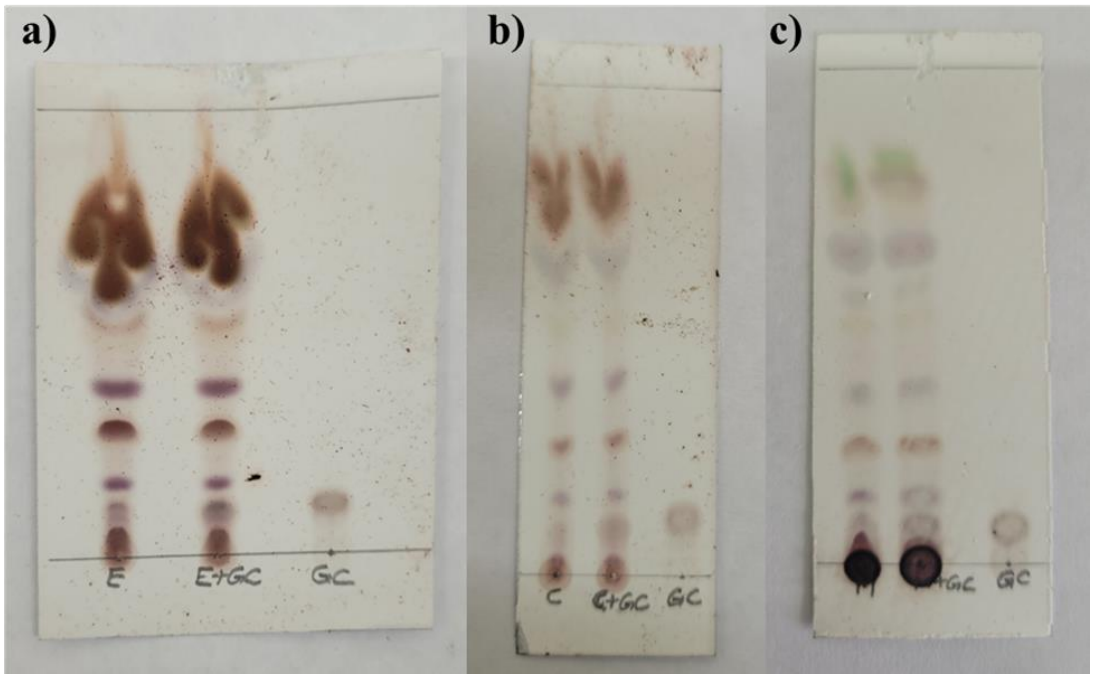

Fig. 5.5a. TLC charring pattern of banana peel extract (E- EtOAc extract, E+GC- co-spot of EtOAc extract, and GC standard) compared with GC standard developed in $CHCl_3$:MeOH (8:1) system. **Fig. 5.5b.** TLC charring pattern of banana peel extract (C- $CHCl_3$ extract, C+GC- co-spot of $CHCl_3$ extract and GC standard) compared with GC standard developed in $CHCl_3$:MeOH (8:1) system. **Fig. 5.5c.** TLC charring pattern of banana peel extract (M- MeOH extract, M+GC- co-spot of MeOH extract and GC standard) compared with GC standard developed in $CHCl_3$:MeOH (8:1) system.

All three extracts were explored for the isolation of GC individually, and the isolation protocol is described below.

5.3.4.2.1. Exploration of EtOAc extract

The EtOAc extract (10 g) was loaded on a silica column (230-400 mesh), the column length was 60 cm, and the bed length was 50 cm with an internal diameter of 3.5 cm. The extract was fractionated using the eluents $CHCl_3$ and MeOH-$CHCl_3$ in the following ratios 5:95, 10:90, 20:80 & 50:50, respectively, and obtained five fractions. The TLC pattern of these fractions was checked and found that the 20:80 MeOH-$CHCl_3$ fraction (1.13 g) contains GCs along with other compounds and was subjected to the second level of purification. The 20:80 MeOH-$CHCl_3$ fraction was loaded on a silica column (230-400 mesh), the column length was 30 cm and the bed length was 25 cm with an internal diameter of 1 cm, and eluted with 100% $CHCl_3$,

5:95, 10:90, 20:80, 30:70 and 50:50 MeOH-$CHCl_3$ ratios, respectively, which yielded six fractions. The 10:90 MeOH-$CHCl_3$ fraction (109.8 mg) was found to contain GCs with few other categories of compounds; hence, the fraction was further purified using a narrow glass column (0.5 × 20 cm). Three fractions obtained from purification [BP-GC-TT-15-18 (23.7 mg), BP-GC-TT-19-23 (21.7 mg) & BP-GC-TT-24-26 (8.2 mg)] were separately submitted for NMR and HR-ESI-MS analysis as they showed a slight difference in Rf and charring pattern. After the completion of exploration studies in the EtOAc extract, the $CHCl_3$ and MeOH extracts were also explored for the presence of GCs (Scheme 5.1.).

5.3.4.2.2. Exploration of MeOH extract

The purification protocol adopted in the EtOAc extract was followed here, which resulted in two fractions: GCs [BP-MeOH-GC-1 (81.30 mg) and BP-MeOH-GC-2 (20.61 mg)]. These two fractions were subjected to HR-ESI-MS analysis for identification of GCs (Scheme 5.1.).

5.3.4.2.3. Exploration of $CHCl_3$ extract

The $CHCl_3$ extract was initially fractioned using the eluents $CHCl_3$, and MeOH- $CHCl_3$ in the ratios 5:95, 10:90, 20:80, and 50:50, and obtained five fractions.

In contrast to the EtOAc and MeOH extracts, the 10:90 MeOH-$CHCl_3$ fraction was found to contain GCs along with other compounds. This fraction was further purified and obtained two fractions of GCs [BP-CHL-GC-1 (45.13 mg) and BP-CHL-GC-2 (169 mg)] and both fractions were subjected to HR-ESI-MS analysis (Scheme 5.1.).

Scheme 5.1. Phytochemical exploration studies carried out in unripe Nendran peel

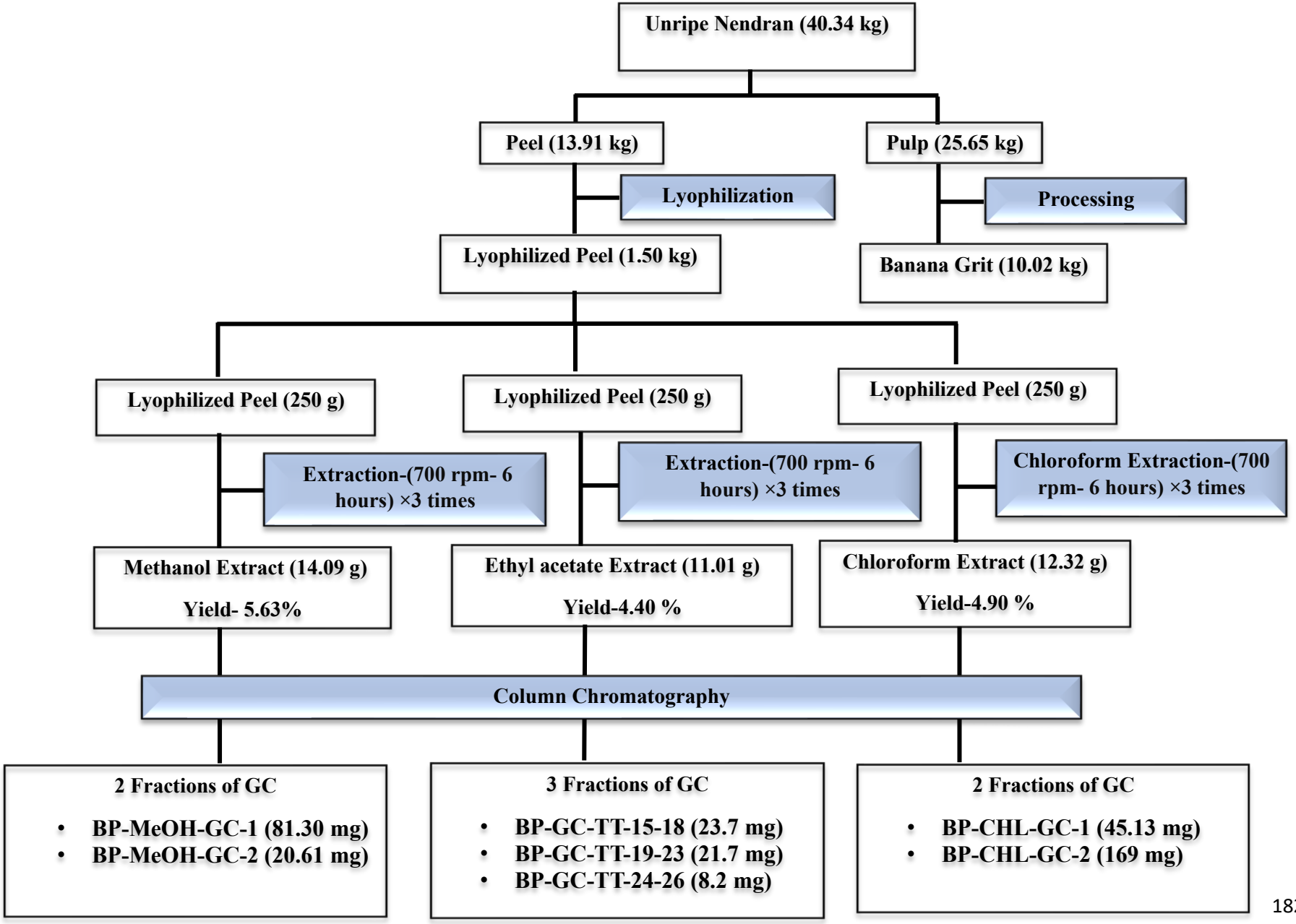

5.3.4.3. HR-ESI-MS analysis of GC fractions

The mobile phase consists of 0.1% formic acid in water (A) and MeOH (B), with an isocratic elution [A(3%)/B(97%)] with a flow rate of 150 µL/minute for a total runtime of 15 minutes. Samples were dissolved in gradient grade MeOH with a few drops of $CHCl_3$, and the injection volume was 2 µL. The mass range was 100-1500 m/z, analyzed in a positive ionization mode. From the extensive HR-ESI-MS analysis, it was found that the fractions BP-CHL-GC-1 and BP-CHL-GC-2 contain more molecular species of GCs, hence, these fractions were pooled and purified again through a narrow glass column (0.5 × 20 cm), and the resultant GC consortium (103.27 mg) was used for further evaluating *in vitro* anti-inflammatory, and α-glucosidase inhibition potential.

5.3.4.4. Evaluation of immunomodulatory effects of GCs

The immunomodulatory effects of GCs were evaluated *in vitro* in the murine macrophage cell line, RAW 264.7. In a culture flask (25 cm^2), murine macrophage RAW 264.7 cells were cultured in DMEM high glucose media with 10% FBS and 1% antibiotics at 37 °C and 5% CO_2. The morphology of the cells was observed under a microscope to monitor any changes (Kwon et al., 2018). The sample was dissolved in DMSO (10 mg/60 µL), and diluted with cell culture medium to obtain the desired concentrations for treatment.

5.3.4.5. Determination of cell viability by MTT assay

The effect of GCs on the viability of cells was evaluated by assessing the number of metabolically active cells through the reduction of MTT to formazan through a colorimetric assay (Mosmann, 1983). In brief, RAW 264.7 cells (5 × 10^3 cells/well) were cultured and treated with 5, 10, 25, 50, 100, and 200 µg/mL of GCs, and incubated for 24 hours. After the incubation period, MTT solution was added, and cells were incubated for 3 hours at 37 °C with 5% CO_2. Then, the supernatants were withdrawn, DMSO was used for solubilizing the formazan crystals, and absorbance was measured at 570 nm using a multimode reader (Tecan infinite® 200). The cell viability was assessed by following the equation

$$\text{Cell viability (\%)} = \frac{\text{OD of experimental group x 100}}{\text{OD of control group}}$$

5.3.4.6. Evaluation of nitric oxide (NO) production by Griess reaction

The amount of NO produced in the cells was determined by measuring the amount of nitrite accumulated in the culture supernatants using the Griess reagent (Green et al., 1982). The RAW 264.7 cells (5 × 10^3 cells/well) were plated, treated with GC consortium of the following concentrations 5, 10, 25, and 50 µg/mL, and incubated for 4 hours. After the incubation period,

1 µg/mL LPS was added to each well and kept for 24 hours incubation at 37 °C with 5% CO_2. Following that, culture supernatants (50 µL) were diluted with equal volumes of the Griess reagent, and incubated for 20 minutes at room temperature (28 °C) in the dark. The absorbance at 540 nm was measured in a multimode reader (Tecan infinite® 200 PRO). The culture medium was used as blank and NO concentration in the supernatants was determined from a standard curve generated with sodium nitrite ($NaNO_2$).

5.3.4.7. Evaluation of pro and anti-inflammatory cytokines production

5.3.4.7.1. Cell lysate preparation-RIPA method

RAW 264.7 cells at a density of 3×10^5 cells/well were seeded in six-well plates, then treated with GCs of the concentrations 25 and 50 µg/mL, and incubated for 4 hours. After incubation, 1 µg/mL LPS was added to each well and kept for 24 hours incubation at 37 °C in a 5% CO_2 atmosphere. After 24 hours, media from each well was collected, and the plates were kept on ice. The collected media was centrifuged at 5000 rpm for 10 minutes at 4 °C, and the supernatant was stored at -80 °C. Adhered cells were washed with 200 µL of phosphate buffered saline (PBS), then 200 µL of RIPA lysis buffer (Sigma-Aldrich, catalogue no. 20-188) containing PIC Inhibitors (Thermo Scientific, catalogue no. 87786), and incubated for 5 minutes on ice. Cells were scraped, the lysate was transferred to a vial and constant agitation was given at 4 °C for 30 minutes. The lysate was then sonicated three times at 30 kHz for 1 minute each with at least 1 minute repose on ice in between. After that, the cell lysate was centrifuged at 12000 rpm, 4 °C for 20 minutes. The supernatant was collected and stored at -80 °C (Lakshmi et al., 2021).

5.3.4.7.2. Determination of protein content

Cellular protein content was determined by BCA protein assay (Smith et al., 1985). The cell lysate (10 µL) was mixed thoroughly with 200 µL of freshly prepared BCA working reagent (Reagent A: B, 50:1). The reaction was incubated for 30 minutes at 37 °C and cooled to room temperature (28 °C). The absorbance was determined at 562 nm using a microplate reader (Tecan infinite® 200 PRO). The cellular protein content was calculated in comparison with the BSA standard curve, and the results were expressed as mg/mL.

5.3.4.7.3. Enzyme-linked immunosorbent assay (ELISA)

The immuno plate was coated with 100 µL/well of the collected media and incubated at 4 °C for 12 hours. Then the media was discarded and wells were gently rinsed with PBS containing 0.05% Tween 20. The antigen coated on the plate was blocked by adding 100 µL/well of blocking buffer (5% BSA+ 0.5% Tween 20 in PBS) for 1 hour at 37 °C. After incubation, the blocking buffer was aspirated and gently rinsed with PBS containing 0.05%

Tween 20. After that, 100 µL of the primary antibody solution (TNF-α, IL-1α, INF-γ, IL-6, IL-10, IL-13, MCP-1, COX-2) was added to each well and incubated for 2 hours at 4 °C with gentle continuous shaking. The primary antibody was collected after incubation, and the plates were gently rinsed with PBS containing 0.05% Tween 20. Then 100 µL of horseradish peroxidase-conjugated IgG secondary antibody was added into each well, and incubated for 2 hours at 4 °C with gentle shaking. The secondary antibody was recollected and plates were rinsed with PBS containing 0.05% Tween 20. Then 100 µL/well freshly prepared TMB substrate was added and incubated in the dark for 30 minutes at room temperature. To that 50% H_2SO_4 (50 µL/well) was added to terminate the reaction. The absorbance was monitored at 490 nm using a microplate reader (Tecan infinite® 200 PRO) and results were expressed as OD/mg of cell protein (Engvall & Perlmann, 1971; Saranya et al., 2017).

5.3.4.8. Evaluation of α-glucosidase inhibition potential of GC

α-glucosidase assay followed in this study is based on the procedure of Pistia-Brueggeman and Hollingsworth (2011) with slight modifications. Briefly, 20 µL α-glucosidase (1.25 U/mL of 0.05 M potassium phosphate buffer, pH 6.8), 200 µL GC consortium (six different concentrations, 0.88-44 µg/mL) was added to vials, and incubated at room temperature for 5 minutes. Then the hydrolysis process was initiated with the addition of 200 µL pNPG solution (1mM) as the substrate. After 20 minutes, the reaction was terminated by adding 500 µL of 1 M sodium carbonate (Na_2CO_3) and then diluted with 580 µL of distilled water. The absorbance of the solution was recorded at 405 nm (Pistia-Brueggeman & Hollingsworth, 2001) using Biorad multimode microplate reader (BioTek Instruments Inc., Winooski, VT). Acarbose was used as the positive control.

The inhibition rate of the GC was calculated by

$$\% \text{ Inhibition} = \frac{\text{Absorbance of control-Absorbance of sample}}{\text{Absorbance of control}} \times 100$$

The IC_{50} value was the concentration of α-glucosidase inhibitor needed to inhibit 50% of α-glucosidase activity under the assay condition. The same protocol was followed to determine the IC_{50} value of acarbose. The IC_{50} value was obtained by plotting a graph with the concentration of test samples in µg/mL along the X-axis against percentage inhibition in the Y-axis.

5.3.4.9. Statistical analysis

All the experiments were carried out in triplicates (n=3) and the data were recorded as the mean ± SEM. All the data were statistically analyzed by IBM Statistical Package for Social

Science 26 (SPSS Inc., Chicago, USA). One-way analysis of variance (ANOVA) followed by Tukey's post hoc tests was used for multiple comparisons analysis, and $P \leq 0.05$ is considered significant. To compare the means of two samples (IC_{50} value of acarbose and GCs), an independent sample t-test was employed.

5.4. Results and discussion

5.4.1. Phytochemical exploration studies of banana peel for the isolation of GC

For the study, a total of 40.34 kg of infructescence was procured, from which 13.91 kg of peel was obtained. This substantial peel yield, representing 34% of the infructescence weight, demonstrates significant potential for peel valorization. When the peel was lyophilized, it resulted in 1.50 kg of peel, indicating that the peel contains around 90% moisture and around 10% dry matter. The lyophilized peel was utilized for the exploration of GCs.

5.4.1.1. Exploration of EtOAc extract

As discussed in section 5.3.4.2.1. the column chromatography separation of EtOAc extract yielded three fractions of GC [BP-GC-TT-15-18 (23.7 mg), BP-GC-TT-19-23 (21.7 mg) & BP-GC-TT-24-26 (8.2 mg)]. The ^{1}H, and ^{13}C NMR spectra of these fractions were recorded in CD_3OD (Fig. 5.6 - Fig. 5.11.). The NMR spectra unambiguously revealed the presence of GCs in the isolated fractions which is in line with our previous studies in the unripe banana pulp. Further, the molecular species of GC in each fraction were identified using HR-ESI-MS analysis. The fatty acid composition of the dichloromethane extracts of different parts of the banana plant reported by Oliveira et al. includes saturated, unsaturated, diacid, α- and ω-hydroxy fatty acids (Oliveira et al., 2006). The α-hydroxy fatty acids reported were 2-Hydroxyeicosanoicacid, 2-Hydroxydocosanoicacid, 2-Hydroxytetracosanoicacid and 2-Hydroxyhexacosanoicacid. The ω-hydroxy fatty acids reported were 18-Hydroxyoctadecanoicacid, 20-Hydroxyeicosanoicacid, 22-Hydroxydocosanoicacid, 24-Hydroxytetracosanoicacid, 25-Hydroxypentacosanoicacid, 26-Hydroxyhexacosanoicacid, 27-Hydroxyheptacosanoicacid, and 28-Hydroxyoctacosanoicacid (Oliveira et al., 2006).

GCs are distinguished by variation in aliphatic acids conjugated as amide. Based on the report from Oliveira et al. (2006), the GC fractions in the present study clearly showed the presence of α- and ω-hydroxy fatty acids from exact mass calculations and HR-ESI-MS analysis. These observations have facilitated an unambiguous identification of eighteen molecular species of GC in the present work (Fig. 5.12.). The identified molecular species of GC conjugated with α-hydroxy fatty acids in the fraction BP-GC-TT-15-18 were **2** and **3**, and

those conjugated with ω-hydroxy fatty acids were **7**, **8**, **9**, **10**, **12**, and **16**. The fraction BP-GC-TT-19-23 contained molecular species of GC conjugated only with ω-hydroxy fatty acids, which include **7**, **8**, **9**, **10**, and **18**. Similarly, the fraction BP-GC-TT-24-26 also contained molecular species of GC conjugated only with ω-hydroxy fatty acids viz. **7**, **15**, and **17** (Fig. S14-S29).

5.4.1.2. Exploration of MeOH extract

The HR-ESI-MS analysis of the GC fraction BP-MeOH-GC-1 revealed the presence of only one α-hydroxy fatty acid conjugated GC (**4**), and six ω-hydroxy fatty acid conjugated GCs (**7**, **9**, **10**, **12**, **16**, and **17**). The fraction BP-MeOH-GC-2 was found to contain GC conjugated only with ω-hydroxy fatty acids (**7**, **9**, **10**, **12**, and **16**) (Fig. 5.29. - Fig. 5.40.).

5.4.1.3. Exploration of $CHCl_3$ extract

The HR-ESI-MS analysis of the GC fraction BP-CHL-GC-1 showed that it contains GC conjugated with ω-hydroxy fatty acids only (**10**, **12**, **14**, and **16**). Fraction BP-CHL-GC-2 was found to contain three α-hydroxy fatty acid conjugated GCs (**1**, **5**, and **6**), and ten ω-hydroxy fatty acids conjugated GCs (**7**, **8**, **9**, **10**, **11**, **12**, **13**, **15**, **17**, and **18**). Molecular species **1**, **5**, and **6** were exclusively present in BP-CHL-GC-2 only ((Fig. 5.41. – Fig. 5.57.). As the HR-ESI-MS analysis depicted that the $CHCl_3$ fractions were most abundant with molecular species of GCs, these two fractions were pooled and purified again through a narrow glass column (0.5 × 20 cm). The resultant GC consortium (103.27 mg) was used for evaluating the *in vitro* anti-inflammatory, and α-glucosidase inhibition potential of GCs.

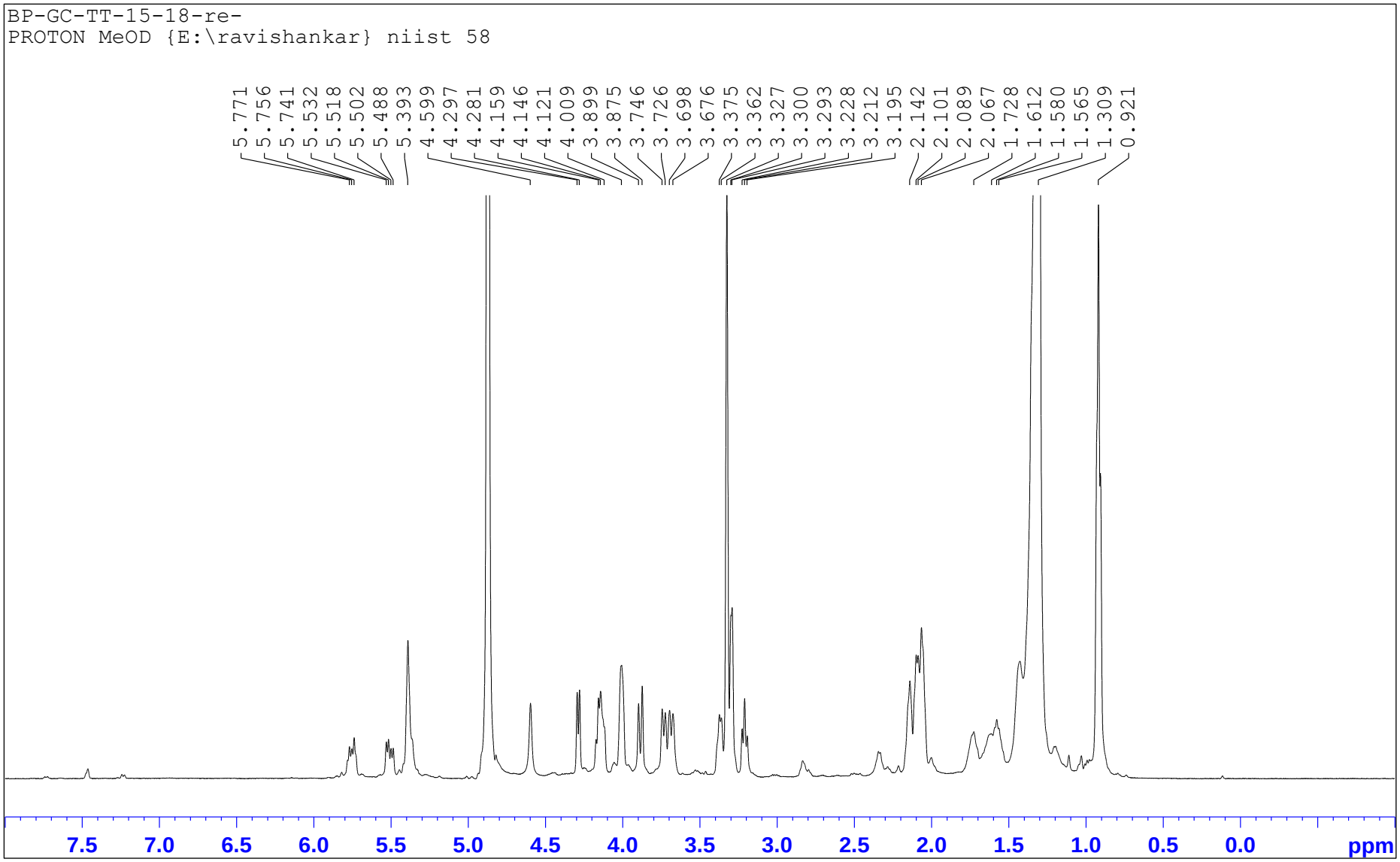

Fig. 5.6. ^{1}H NMR of GC fraction BP-GC-TT-15-18

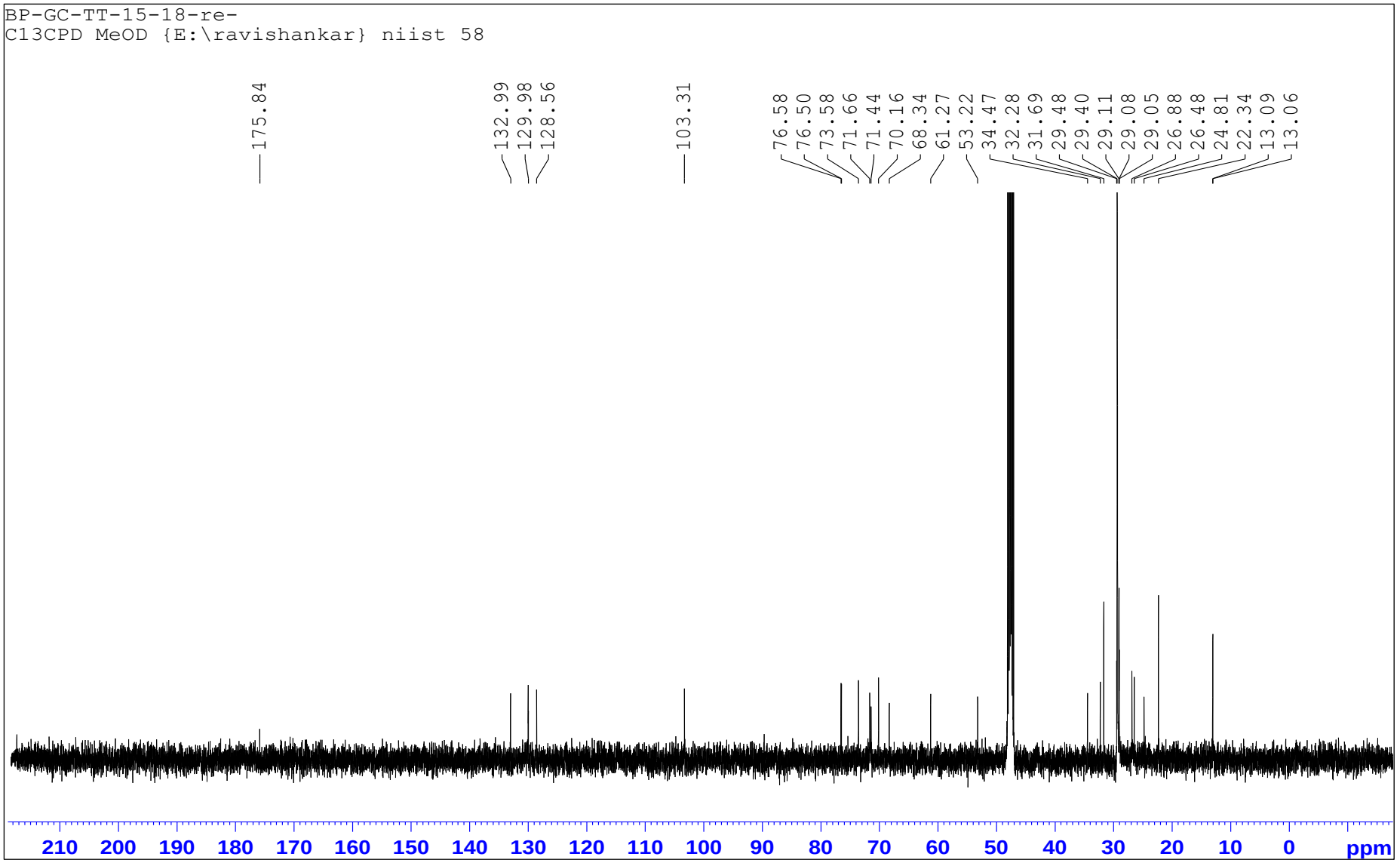

Fig. 5.7. ^{13}C NMR of GC fraction BP-GC-TT-15-18

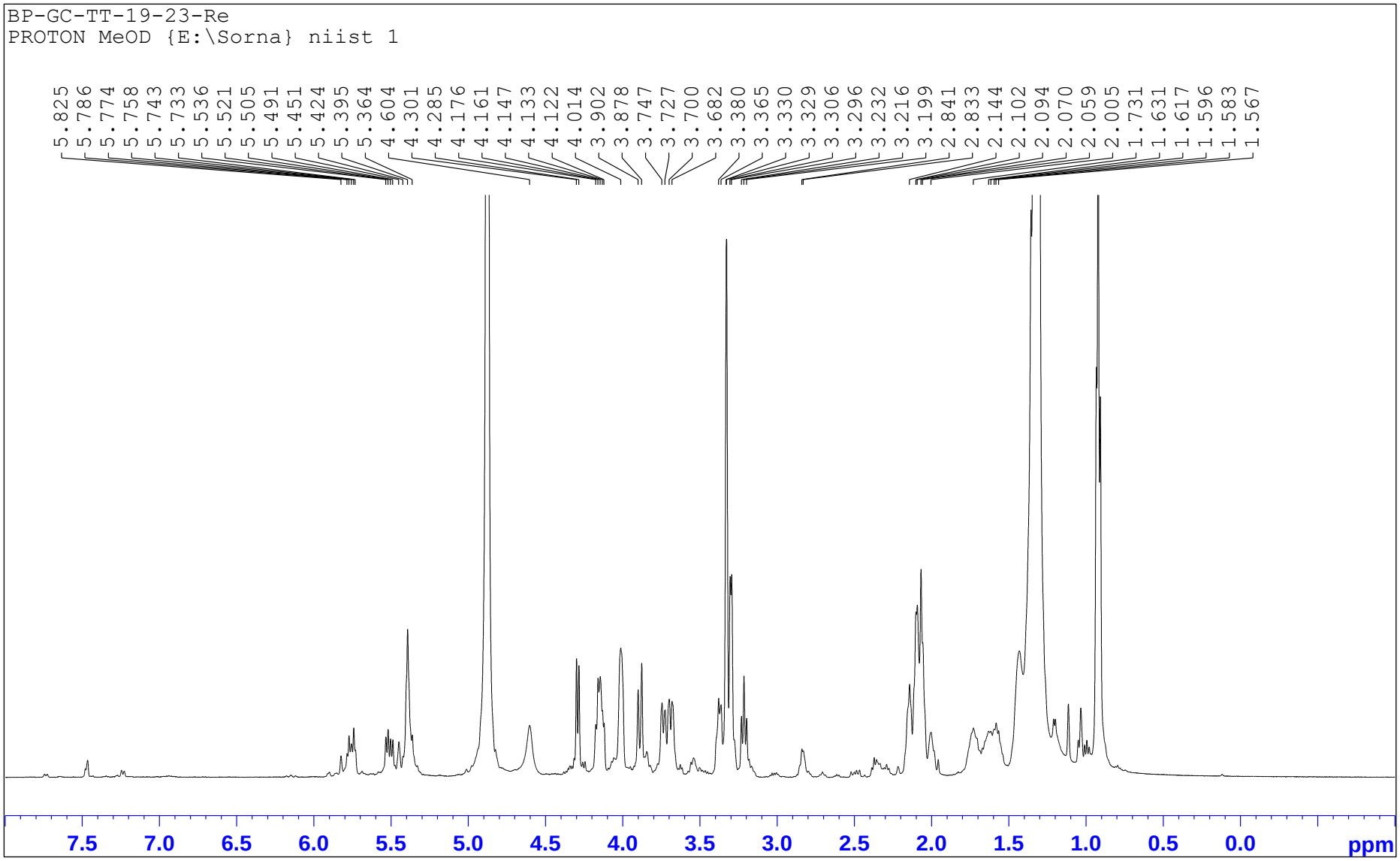

Fig. 5.8. ^{1}H NMR of GC fraction BP-GC-TT-19-23

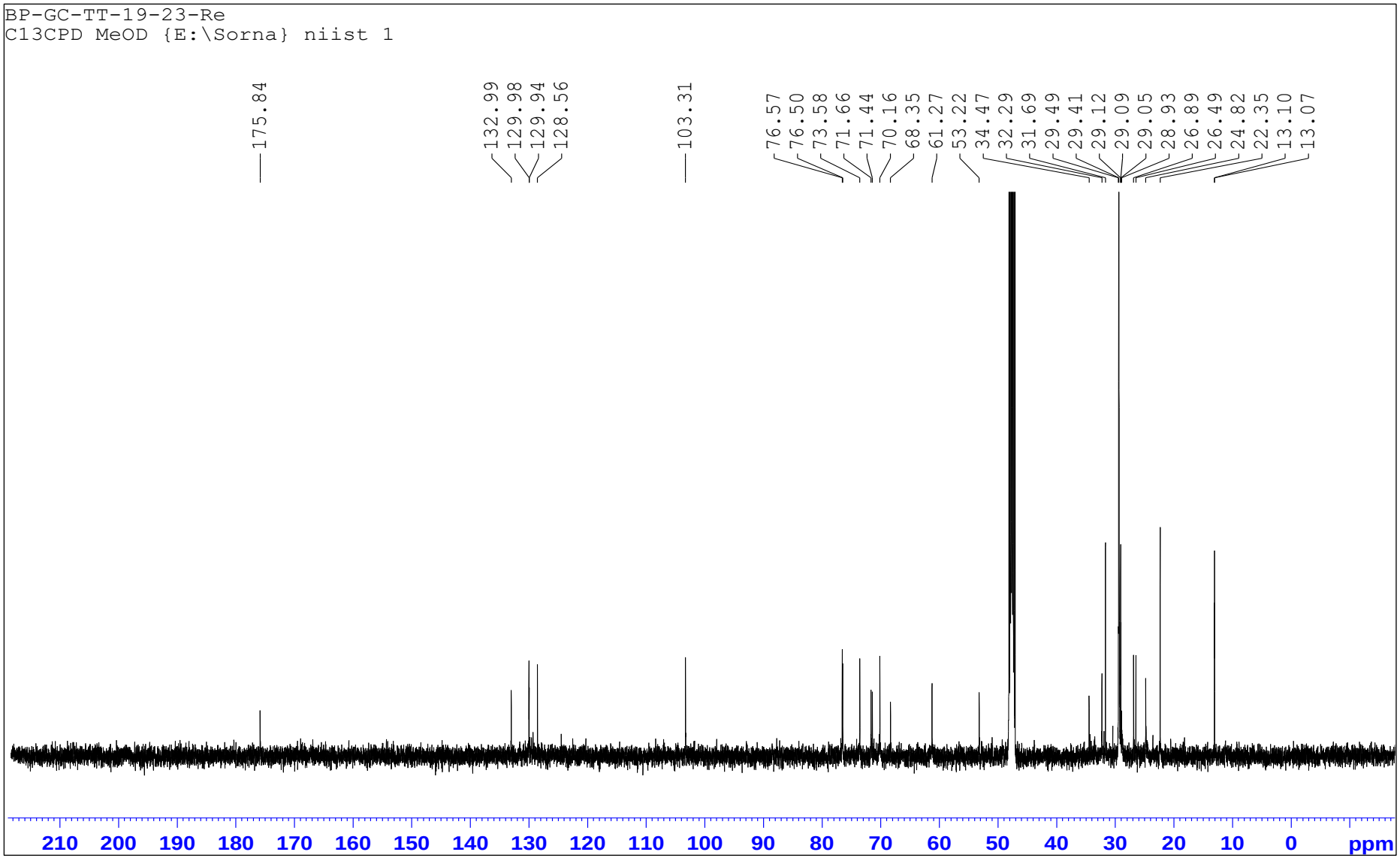

Fig. 5.9. ^{13}C NMR of GC fraction BP-GC-TT-19-23

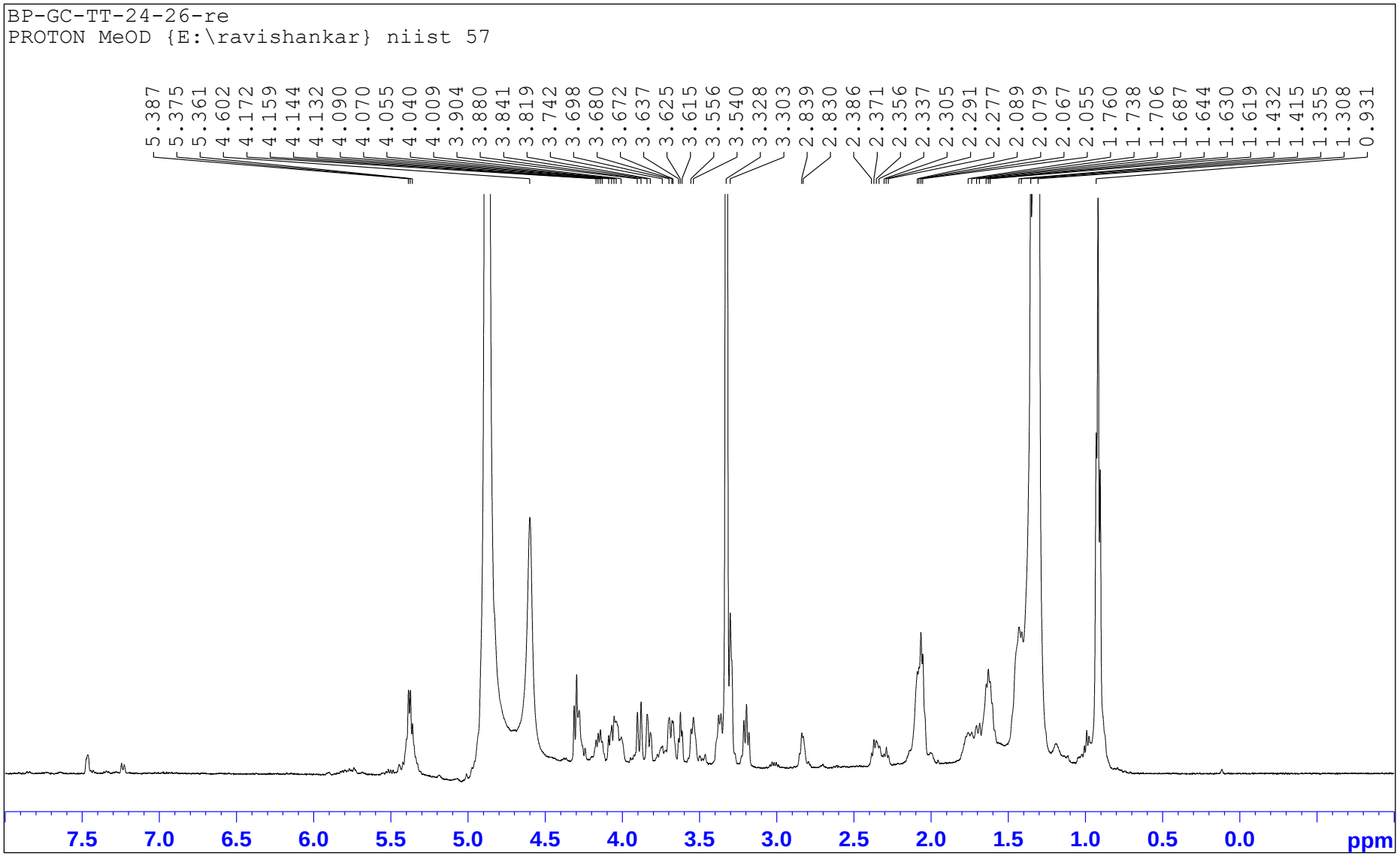

Fig. 5.10. ^{1}H NMR of GC fraction BP-GC-TT-24-26

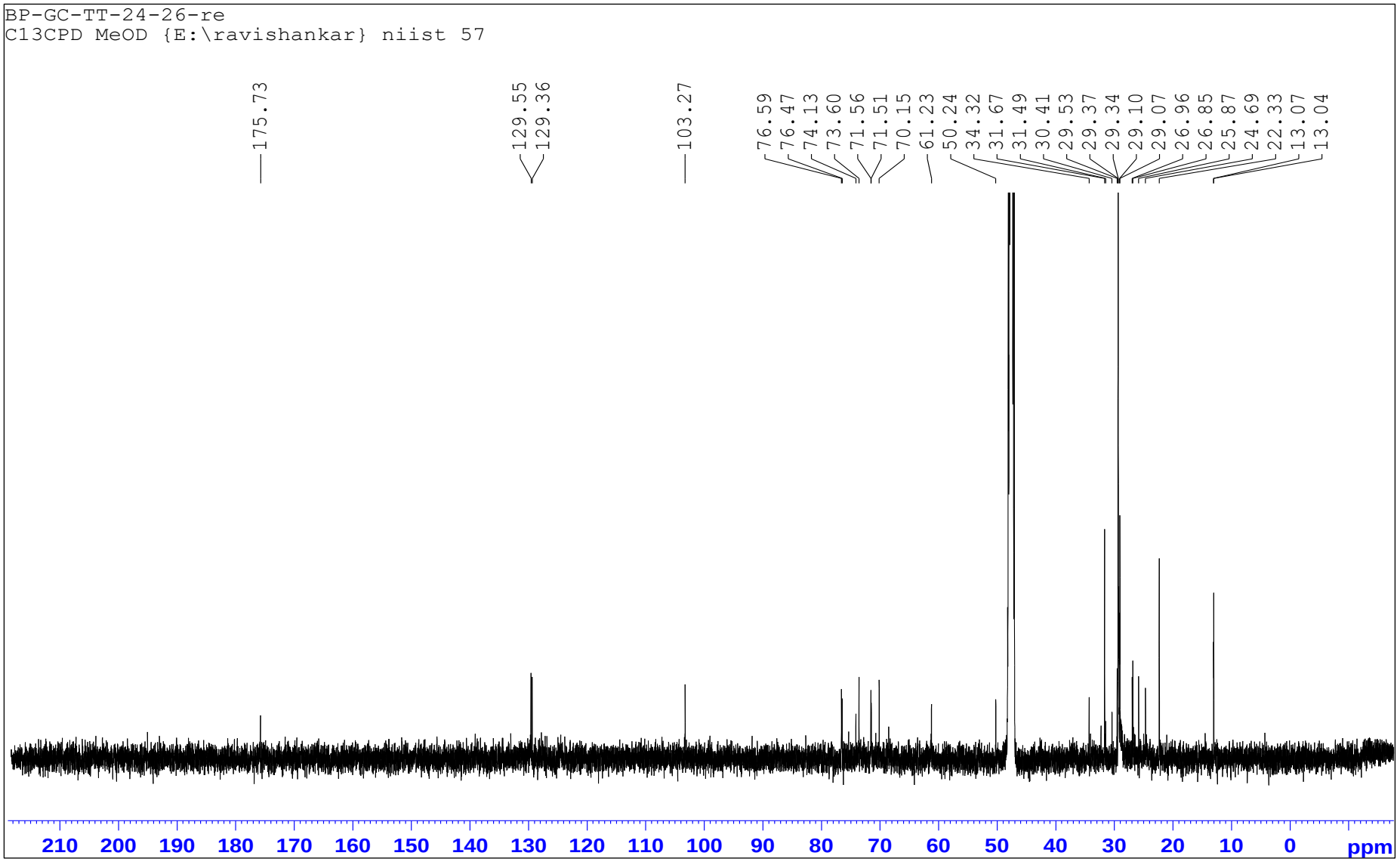

Fig. 5.11. ^{13}C NMR of GC fraction BP-GC-TT-24-26

Fig. 5.12. Structures of molecular species of GCs identified from the unripe Nendran banana peel

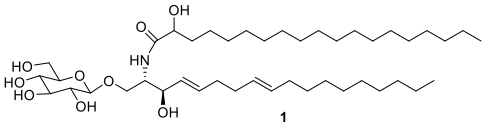

Exact mass 778.58

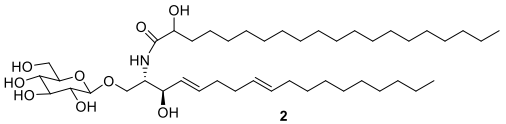

Exact mass 792.60

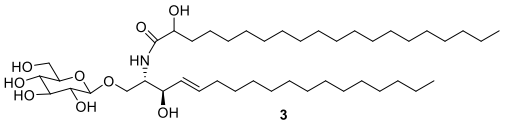

Exact mass 794.61

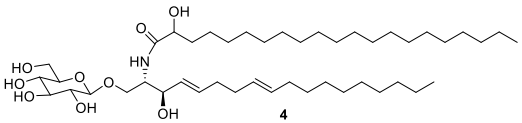

Exact mass 806.61

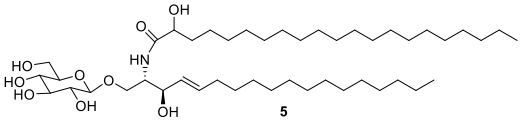

Exact mass 824.66

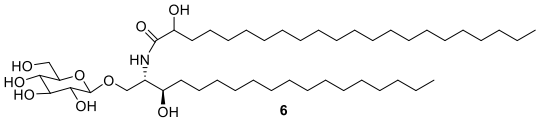

Exact mass 806.61

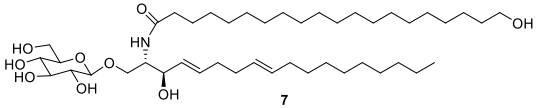

Exact mass 792.60

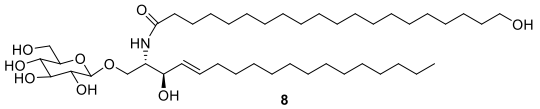

Exact mass 794.61

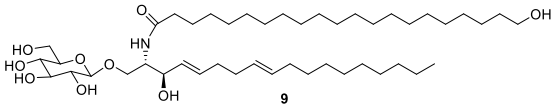

Exact mass 806.61

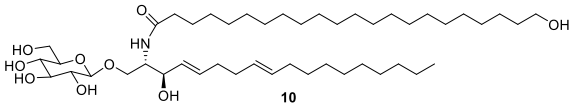

Exact mass 820.63

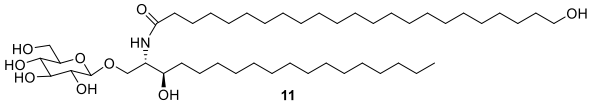

Exact mass 838.67

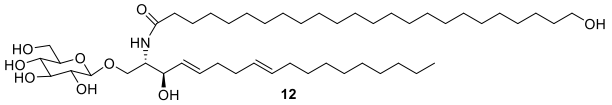

Exact mass 848.66

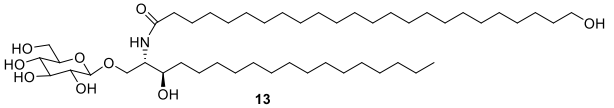

Exact mass 852.69

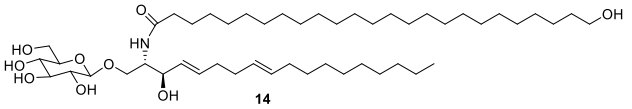

Exact mass 862.67

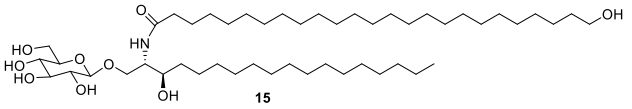

Exact mass 866.71

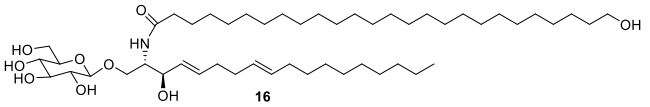

Exact mass 876.69

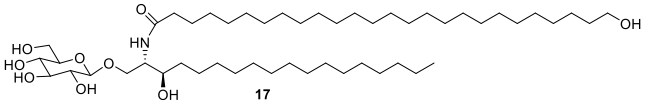

Exact mass 880.72

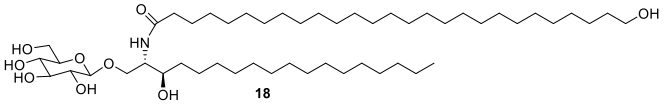

Exact mass 894.74

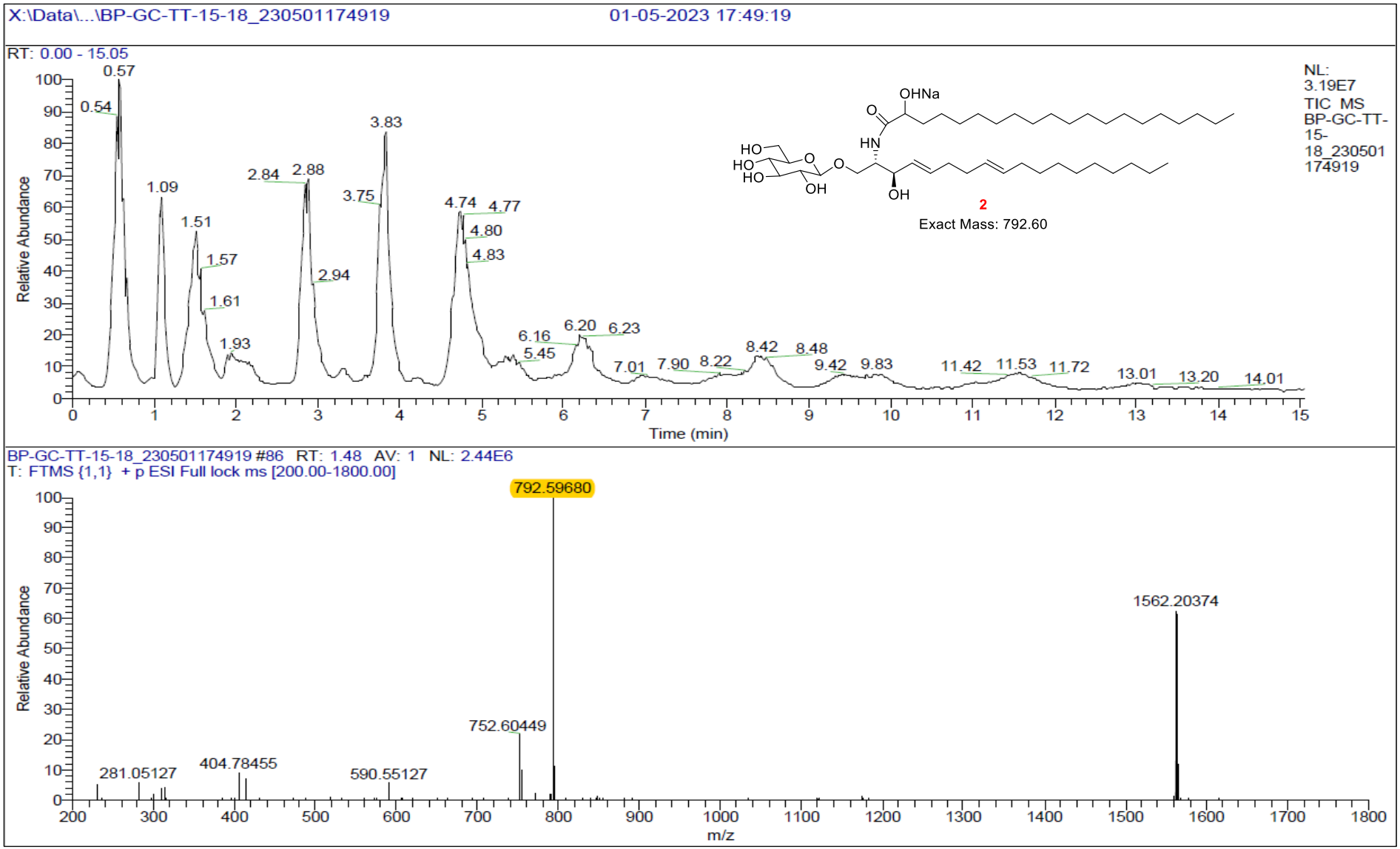

Fig. 5.13. HR-ESI-MS of BP-GC-TT-15-18-RT-1.48

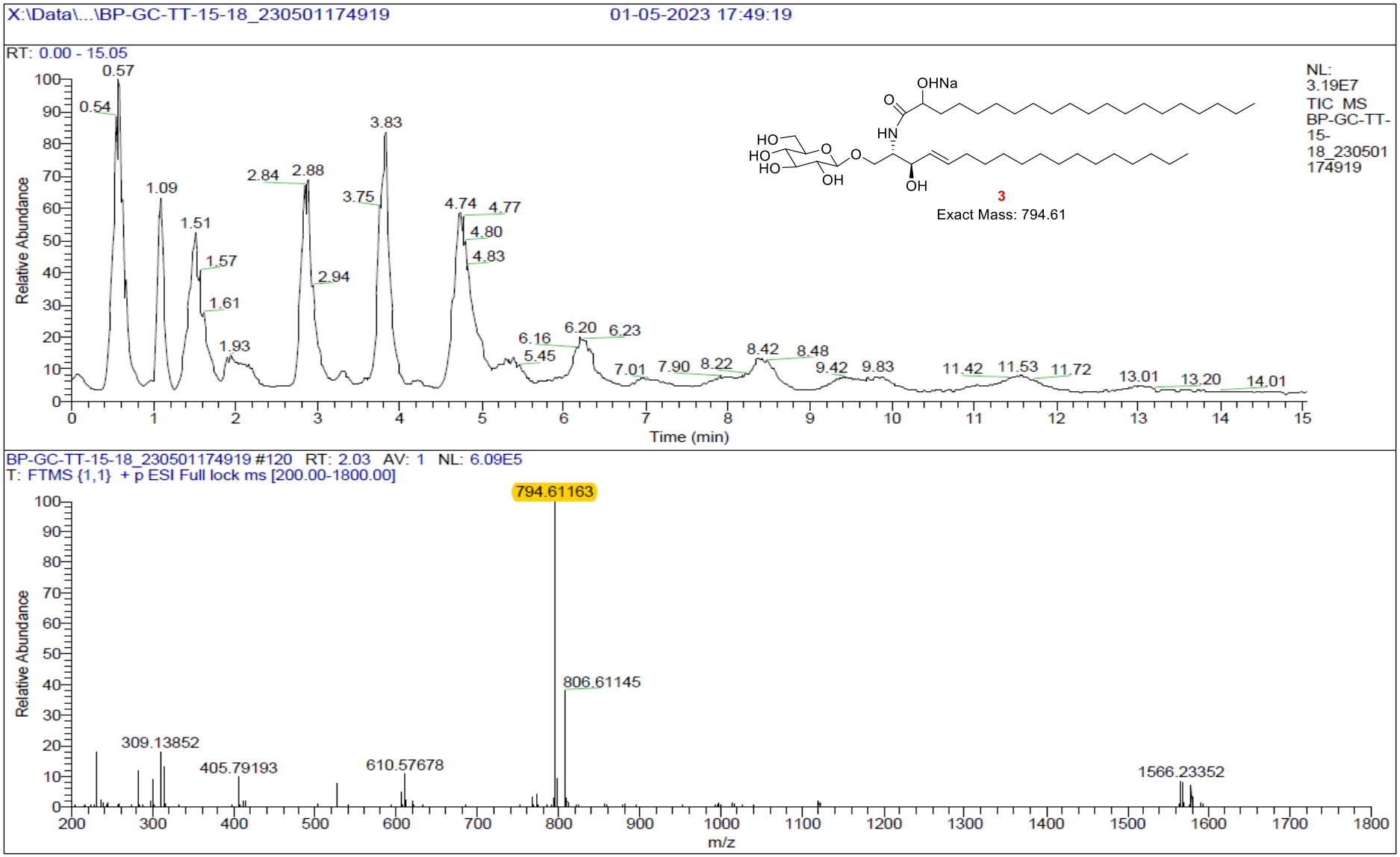

Fig. 5.14. HR-ESI-MS of BP-GC-TT-15-18-RT-2.03

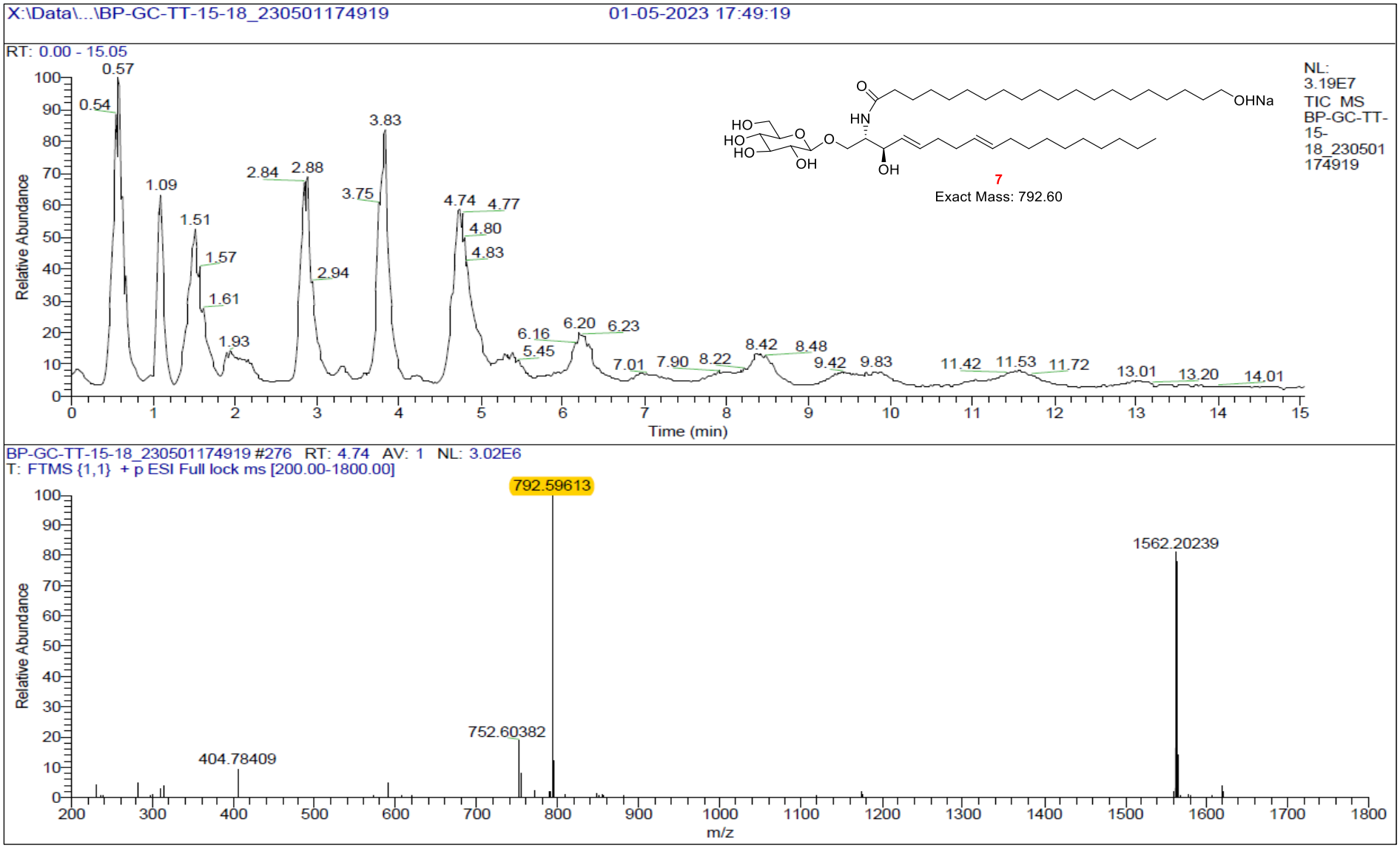

Fig. 5.15. HR-ESI-MS of BP-GC-TT-15-18-RT-4.74

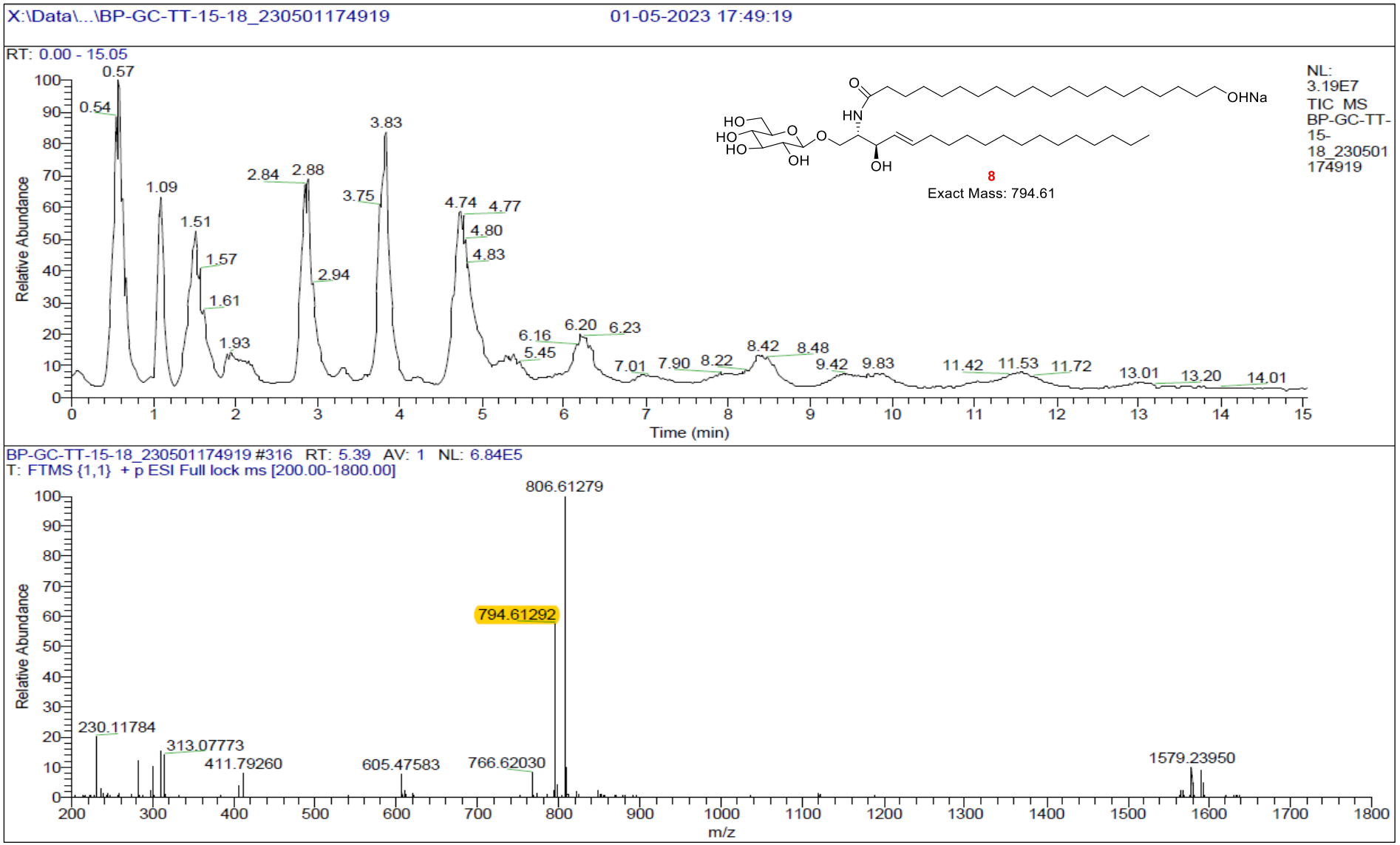

Fig. 5.16. HR-ESI-MS of BP-GC-TT-15-18-RT-5.39

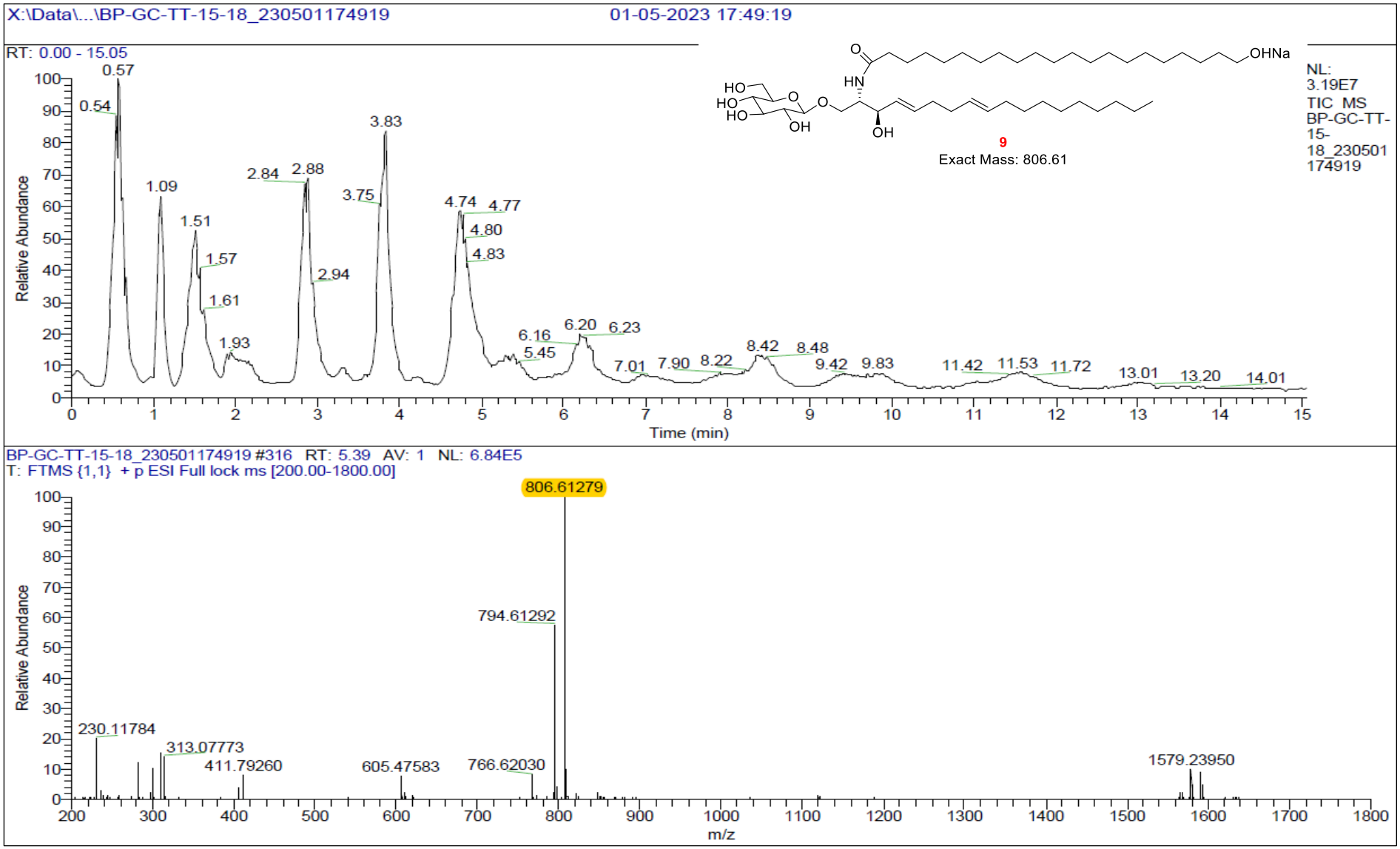

Fig. 5.17. HR-ESI-MS of BP-GC-TT-15-18-RT-5.39′

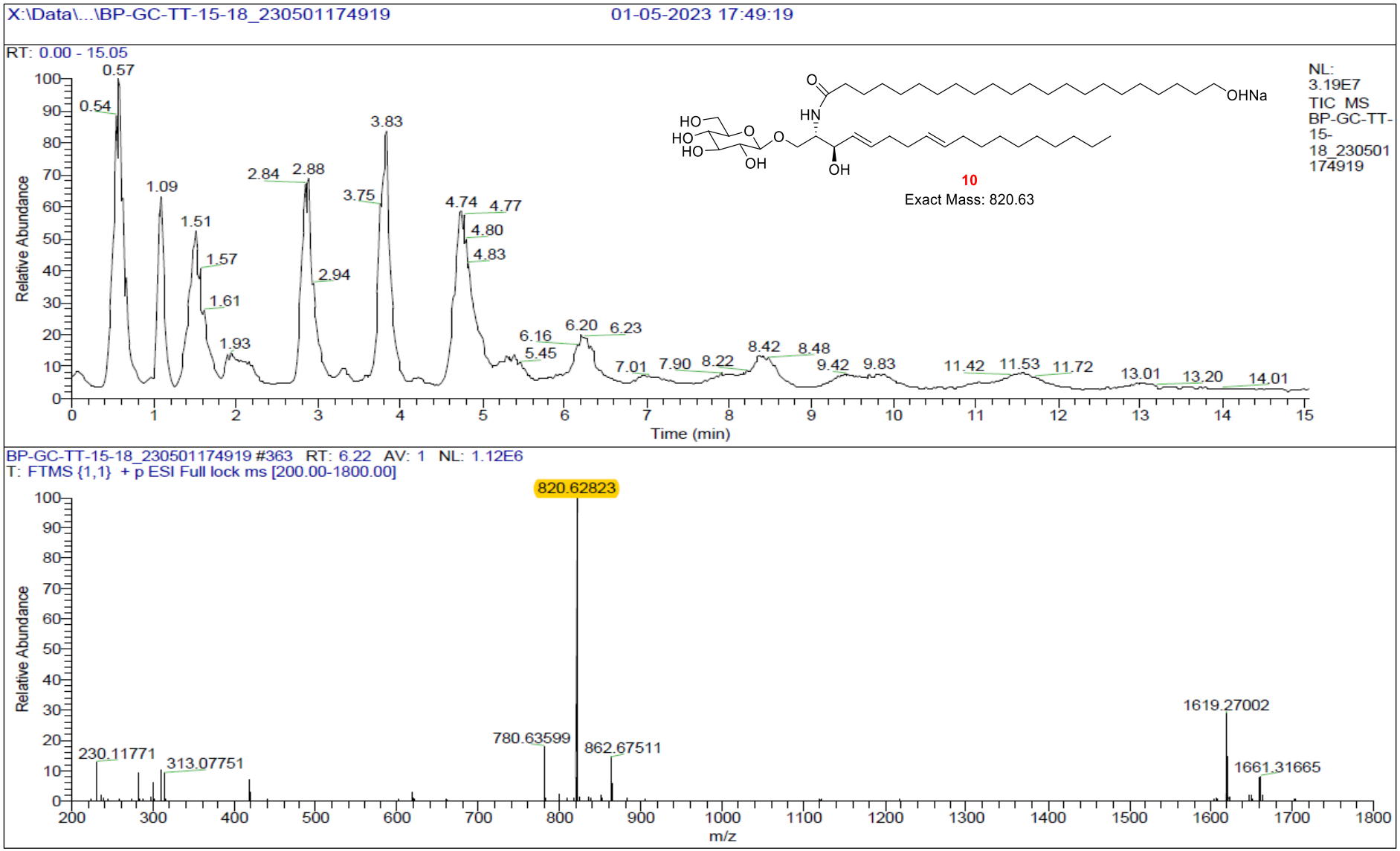

Fig. 5.18. HR-ESI-MS of BP-GC-TT-15-18-RT-6.22

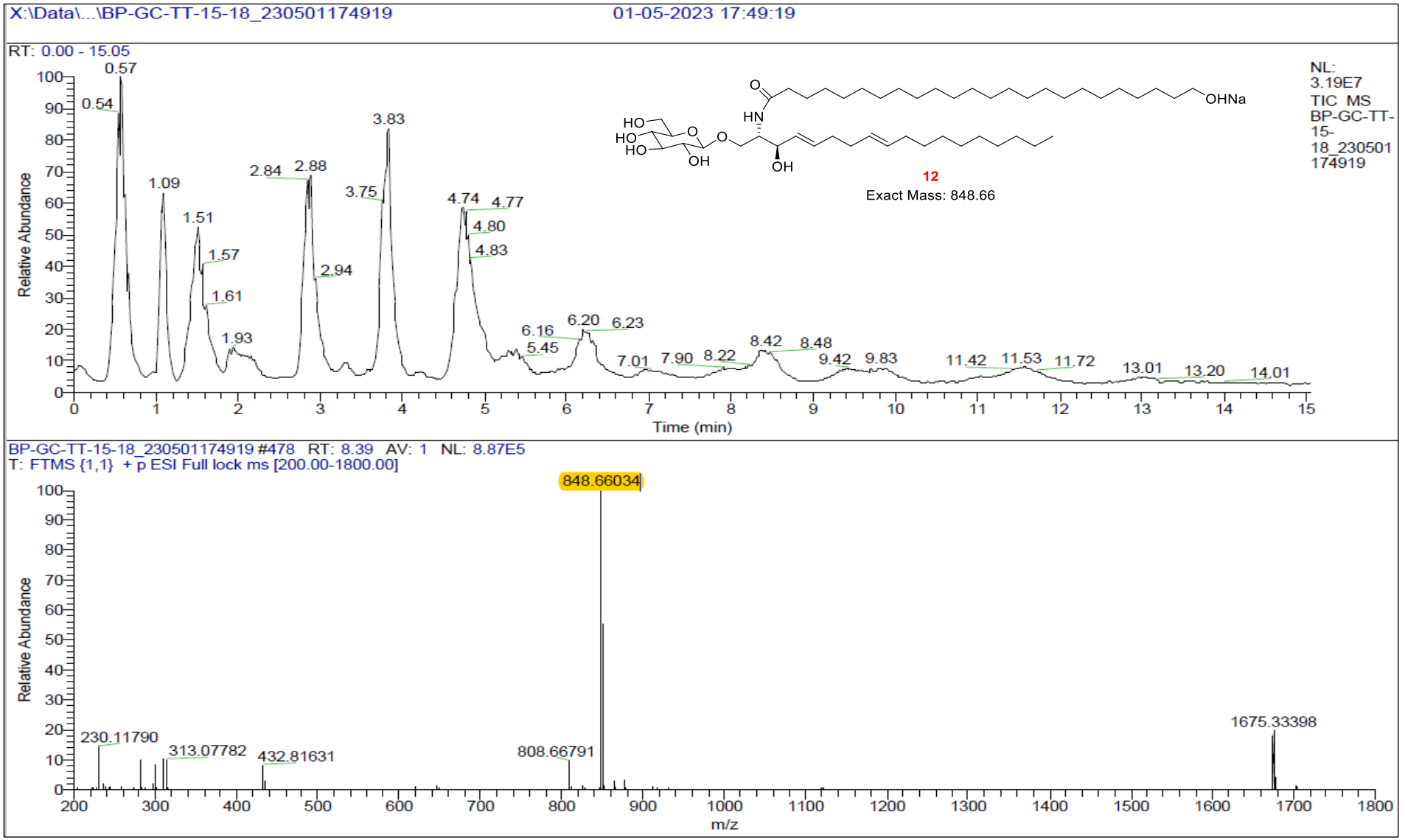

Fig. 5.19. HR-ESI-MS of BP-GC-TT-15-18-RT-8.39

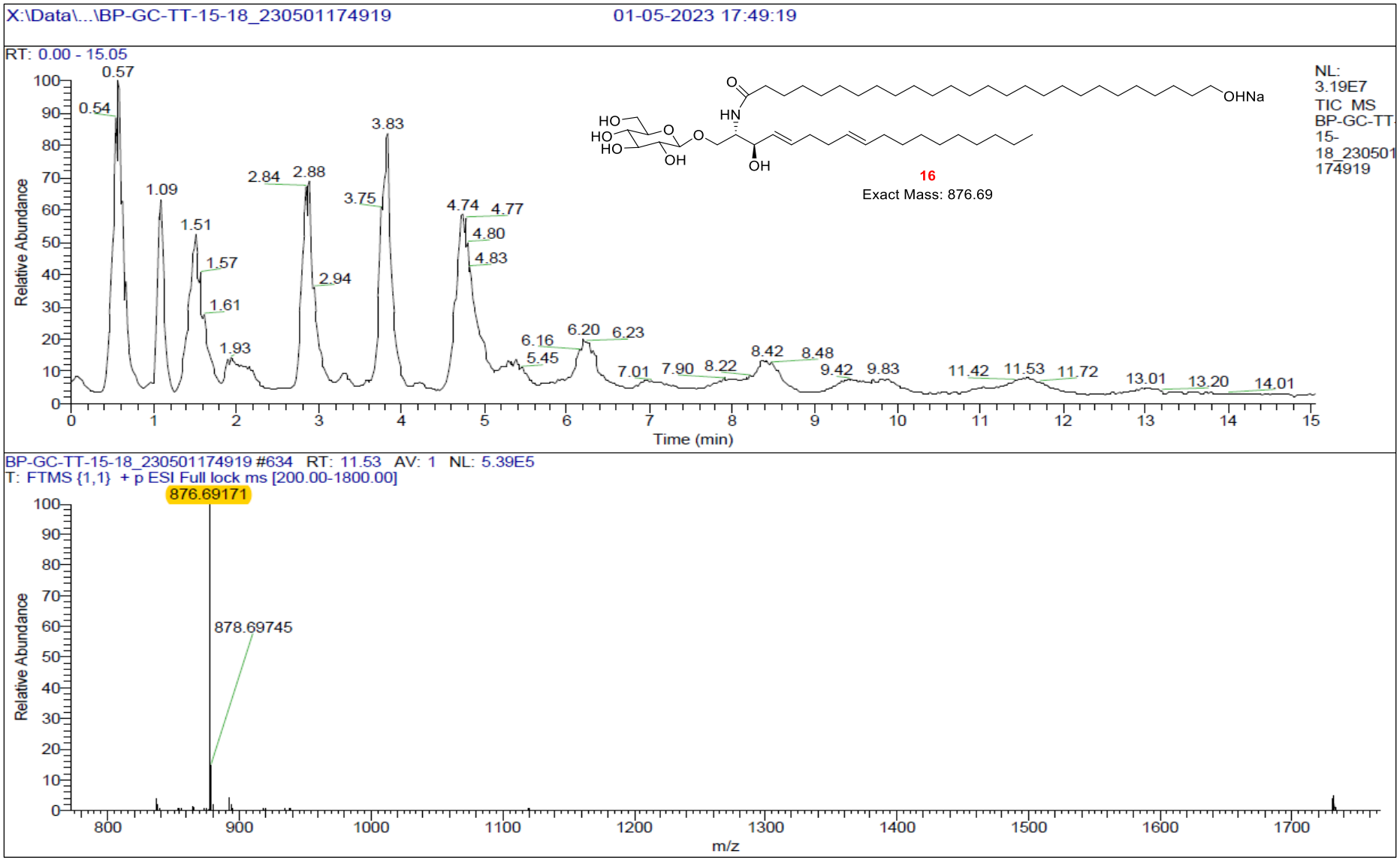

Fig. 5.20. HR-ESI-MS of BP-GC-TT-15-18-RT-11.53

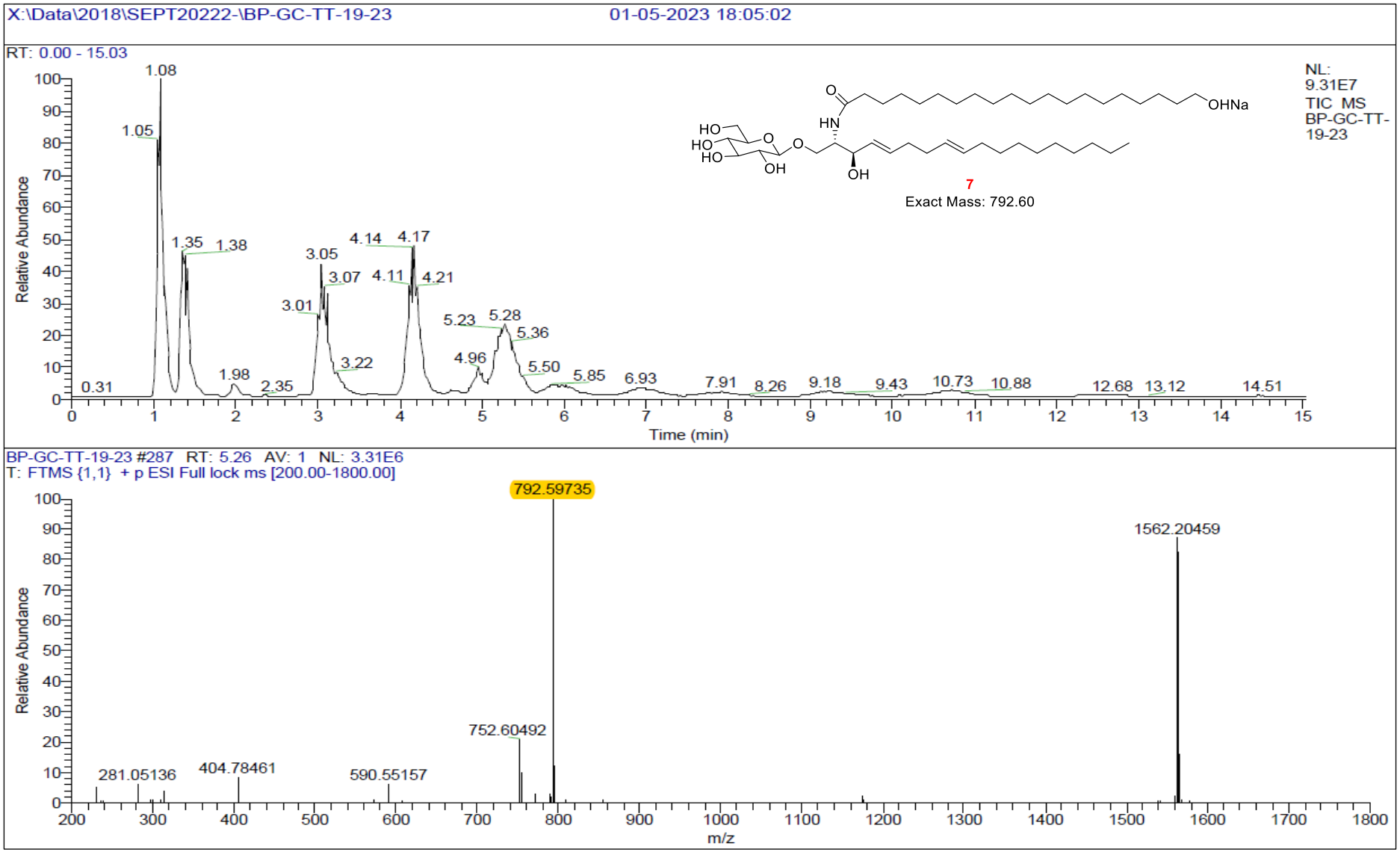

Fig. 5.21. HR-ESI-MS of BP-GC-TT-19-23-RT-5.26

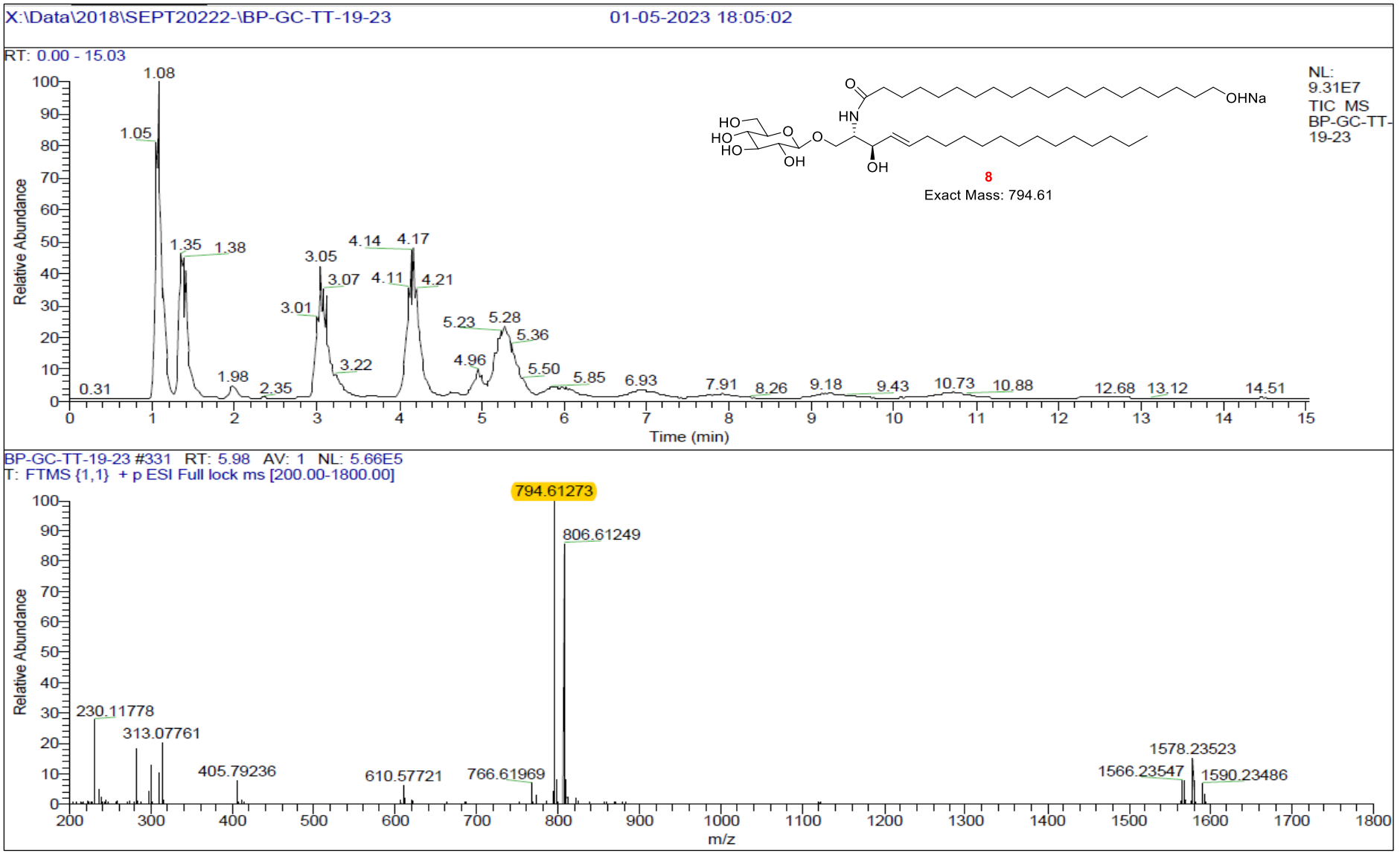

Fig. 5.22. HR-ESI-MS of BP-GC-TT-19-23-RT-5.98

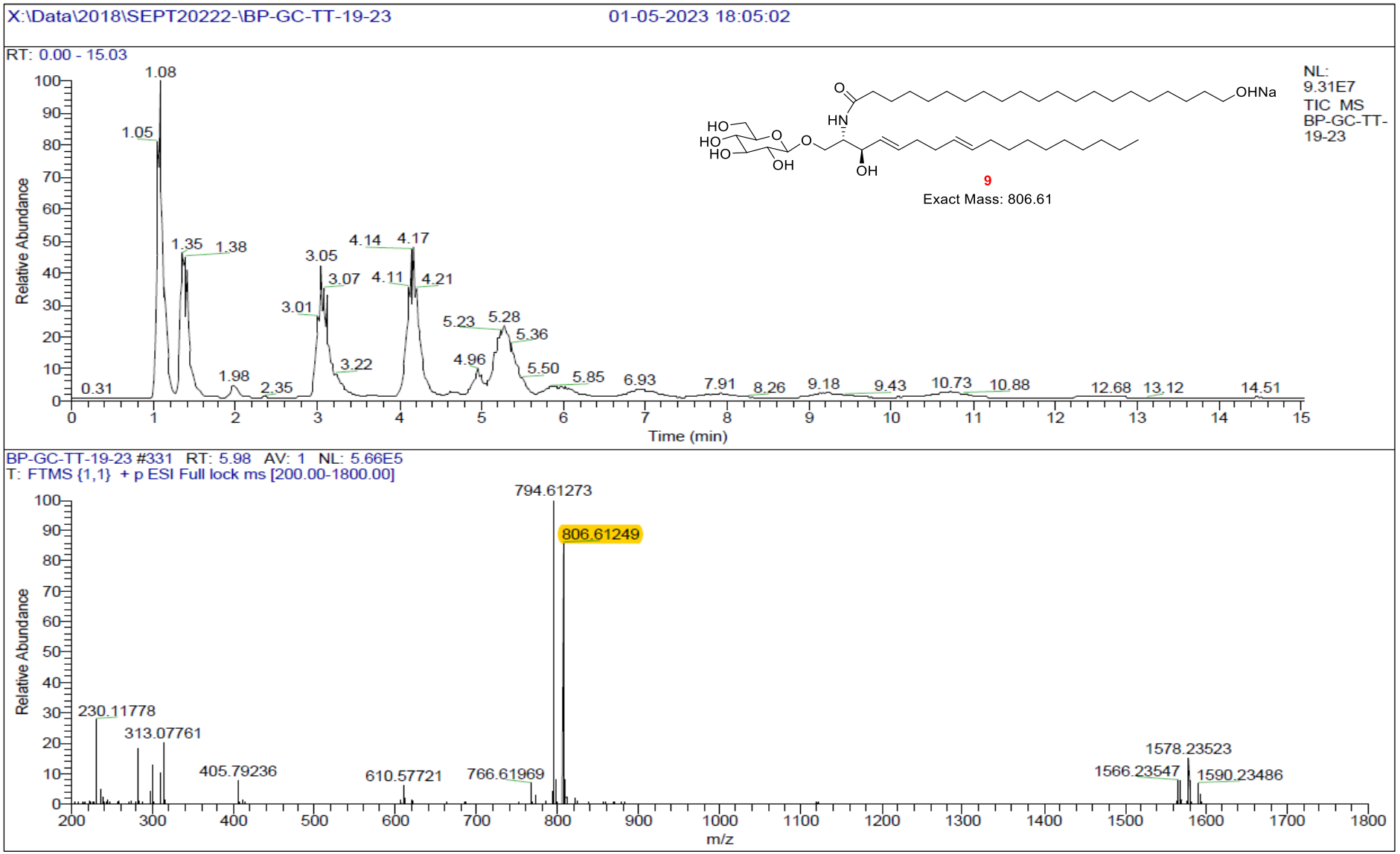

Fig. 5.23. HR-ESI-MS of BP-GC-TT-19-23-RT-5.98′

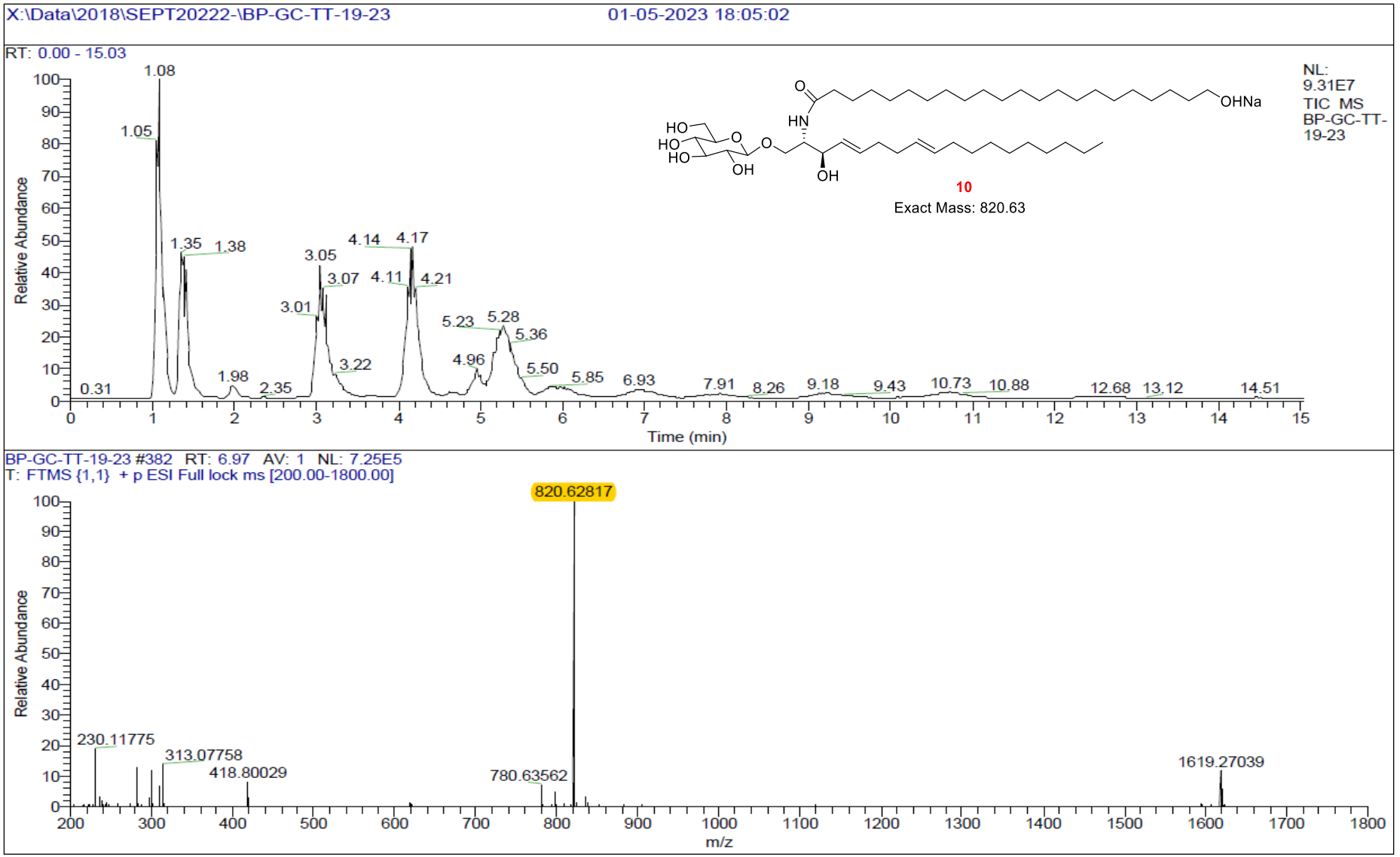

Fig. 5.24. HR-ESI-MS of BP-GC-TT-19-23-RT-6.97

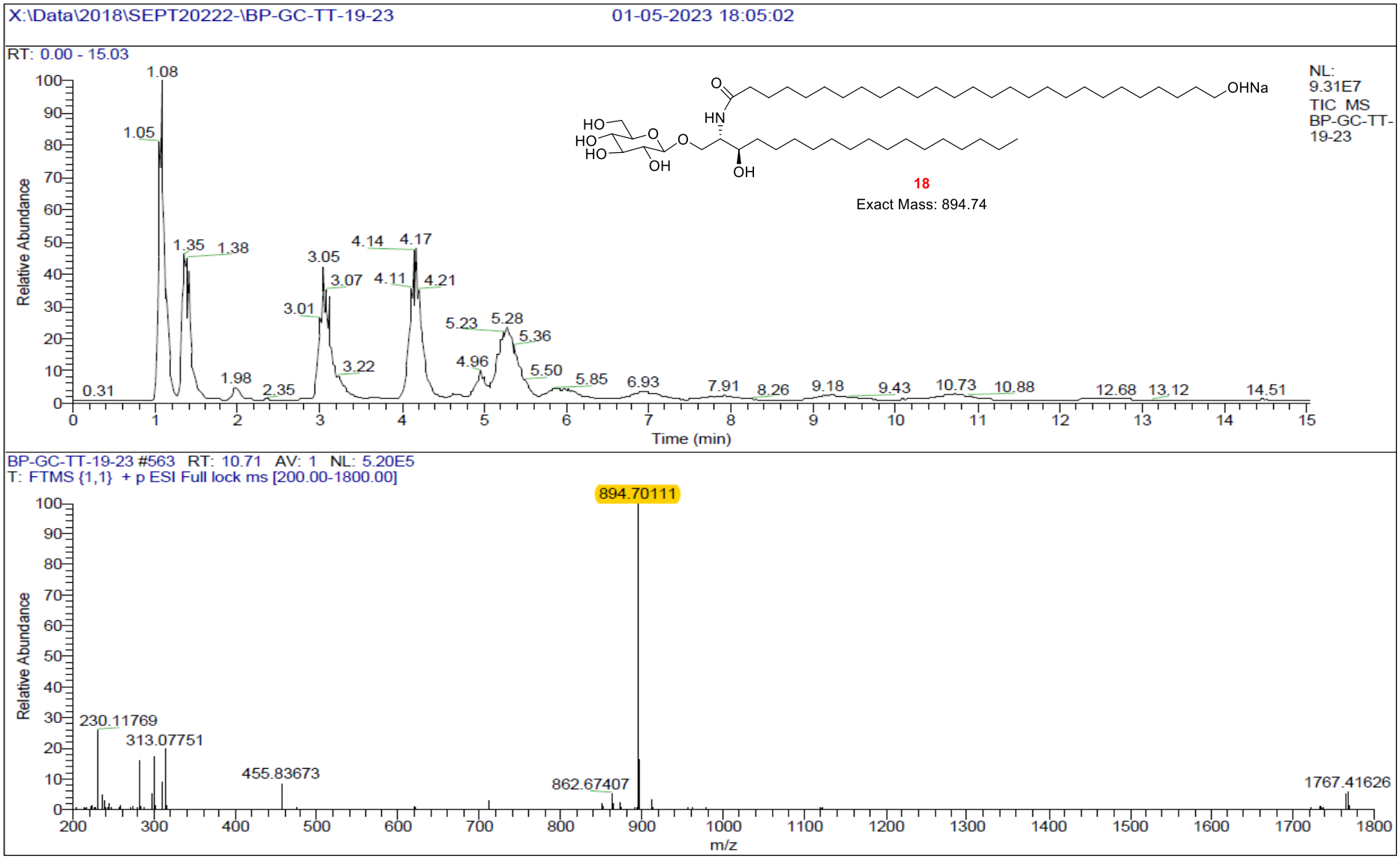

Fig. 5.25. HR-ESI-MS of BP-GC-TT-19-23-RT-10.71

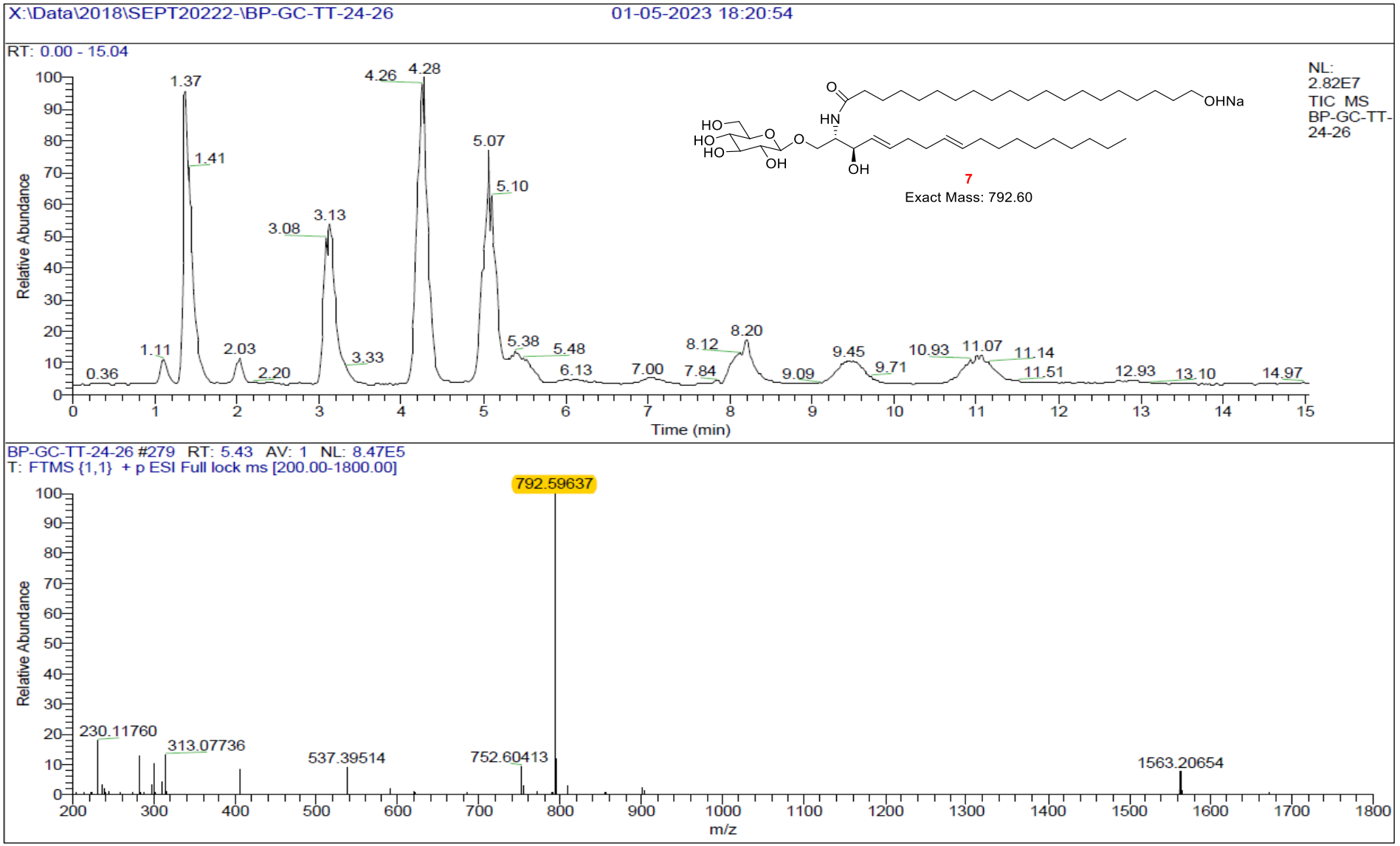

Fig. 5.26. HR-ESI-MS of BP-GC-TT-24-26-RT-5.43

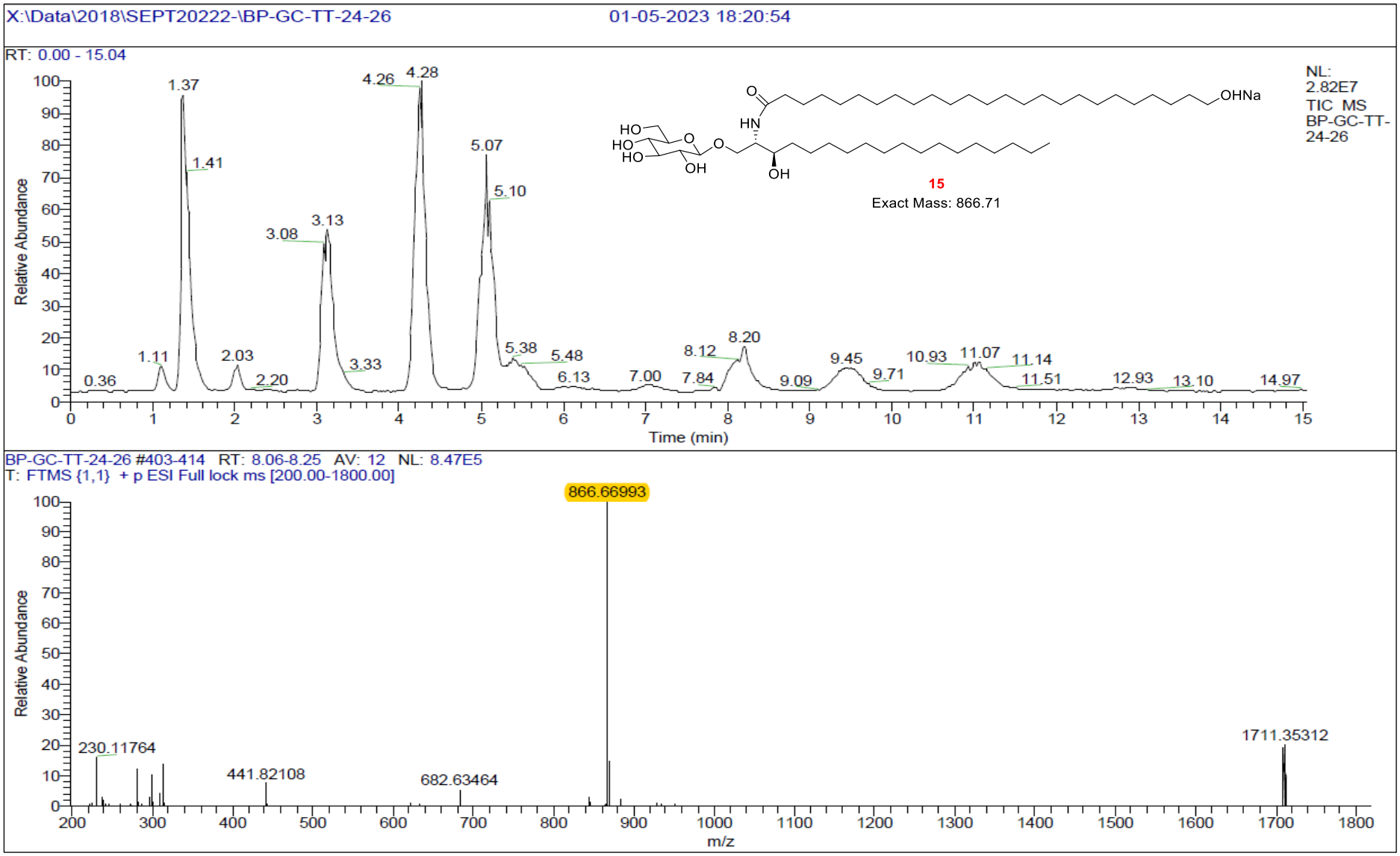

Fig. 5.27. HR-ESI-MS of BP-GC-TT-24-26-RT-8.06-8.25

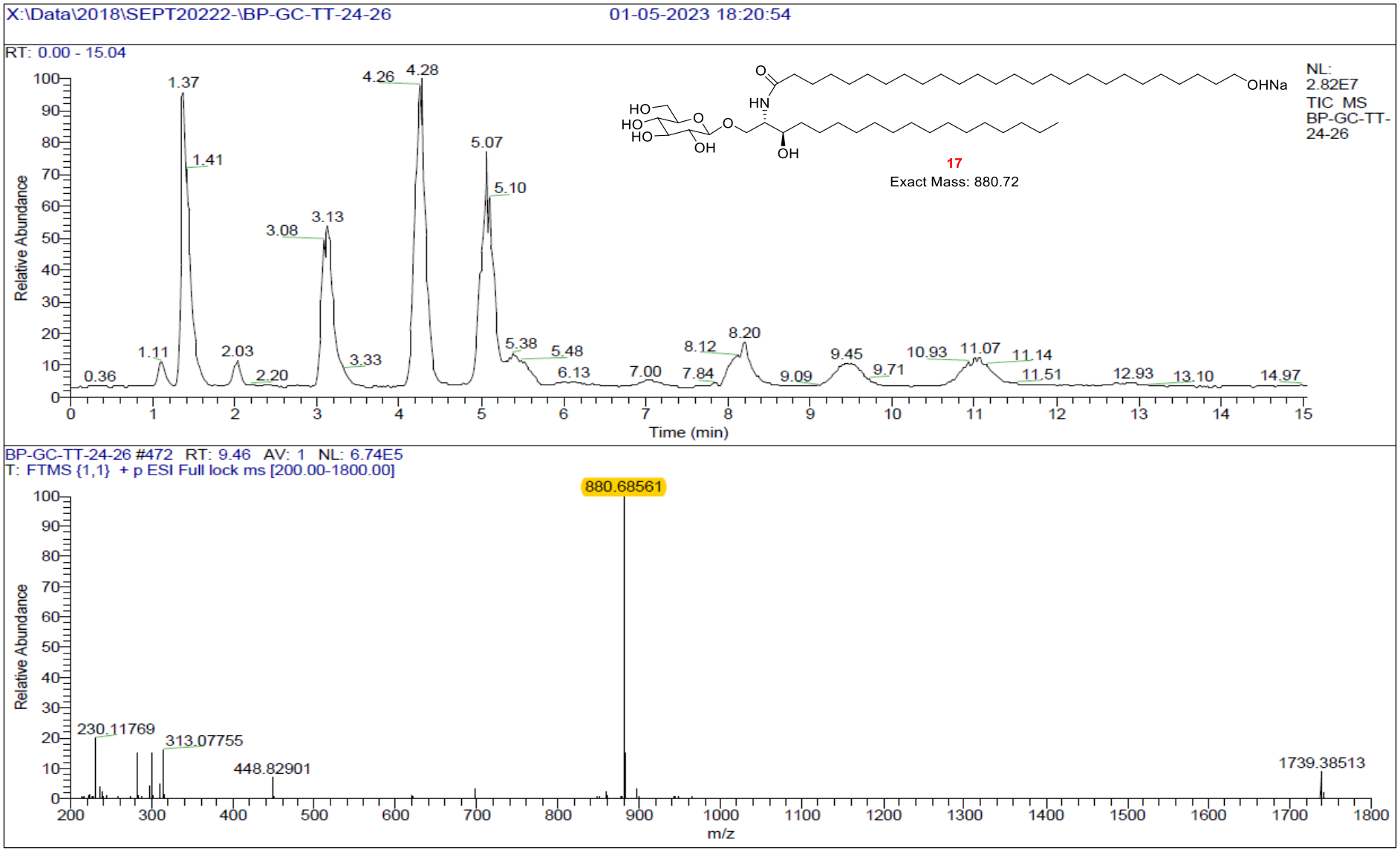

Fig. 5.28. HR-ESI-MS of BP-GC-TT-24-26-RT-9.46

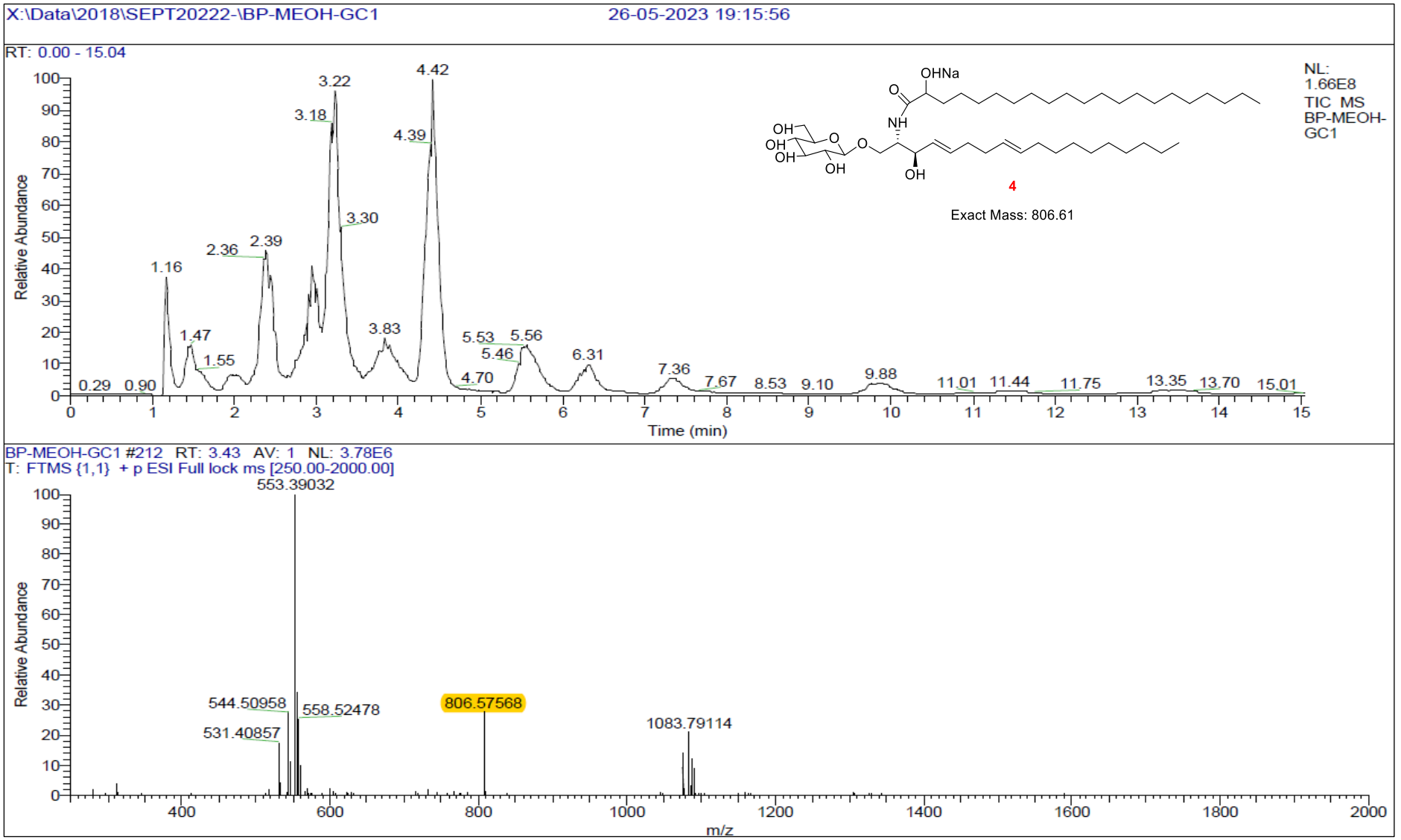

Fig. 5.29. HR-ESI-MS of BP-MEOH-GC-1-RT-3.43

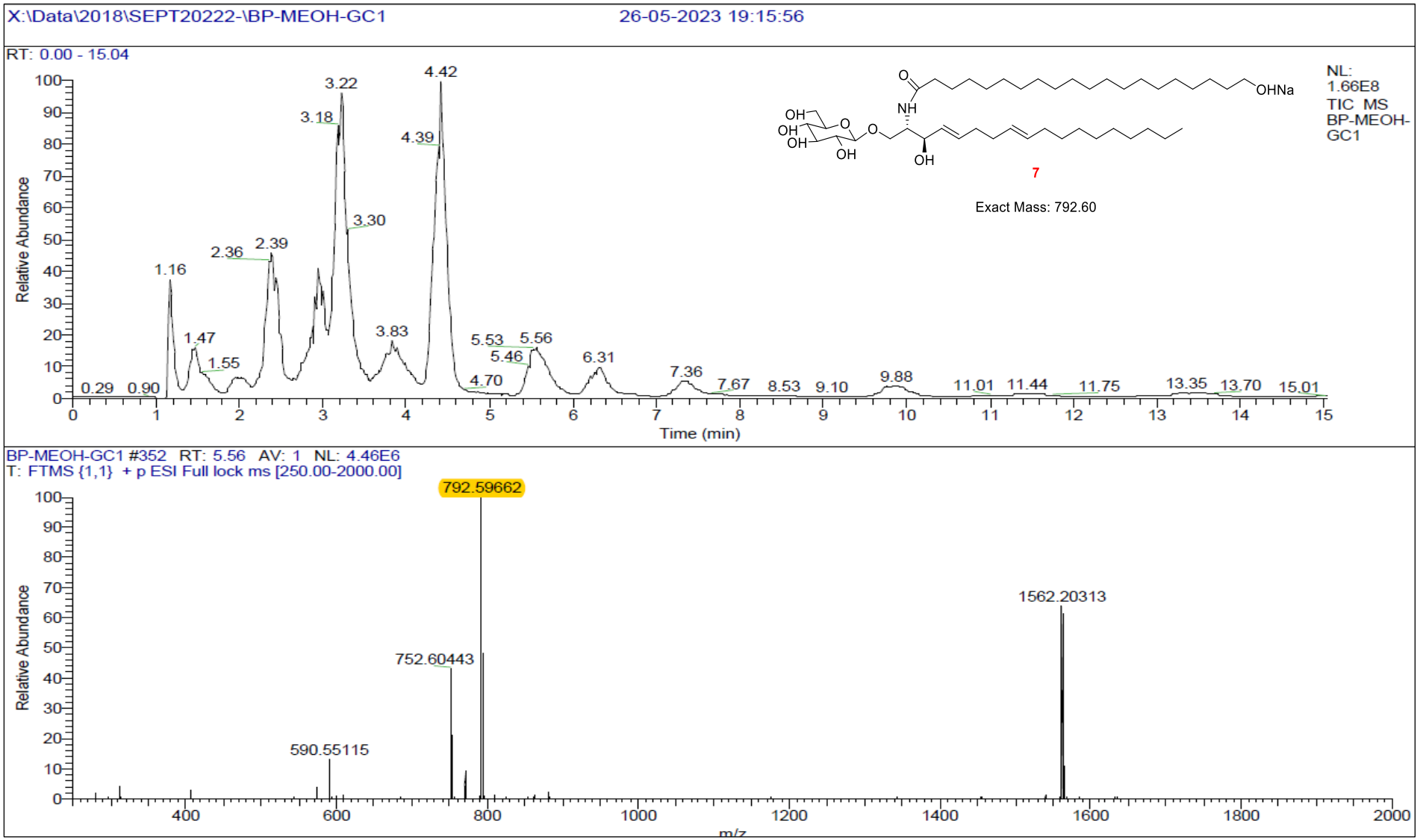

Fig. 5.30. HR-ESI-MS of BP-MEOH-GC-1-RT-5.56

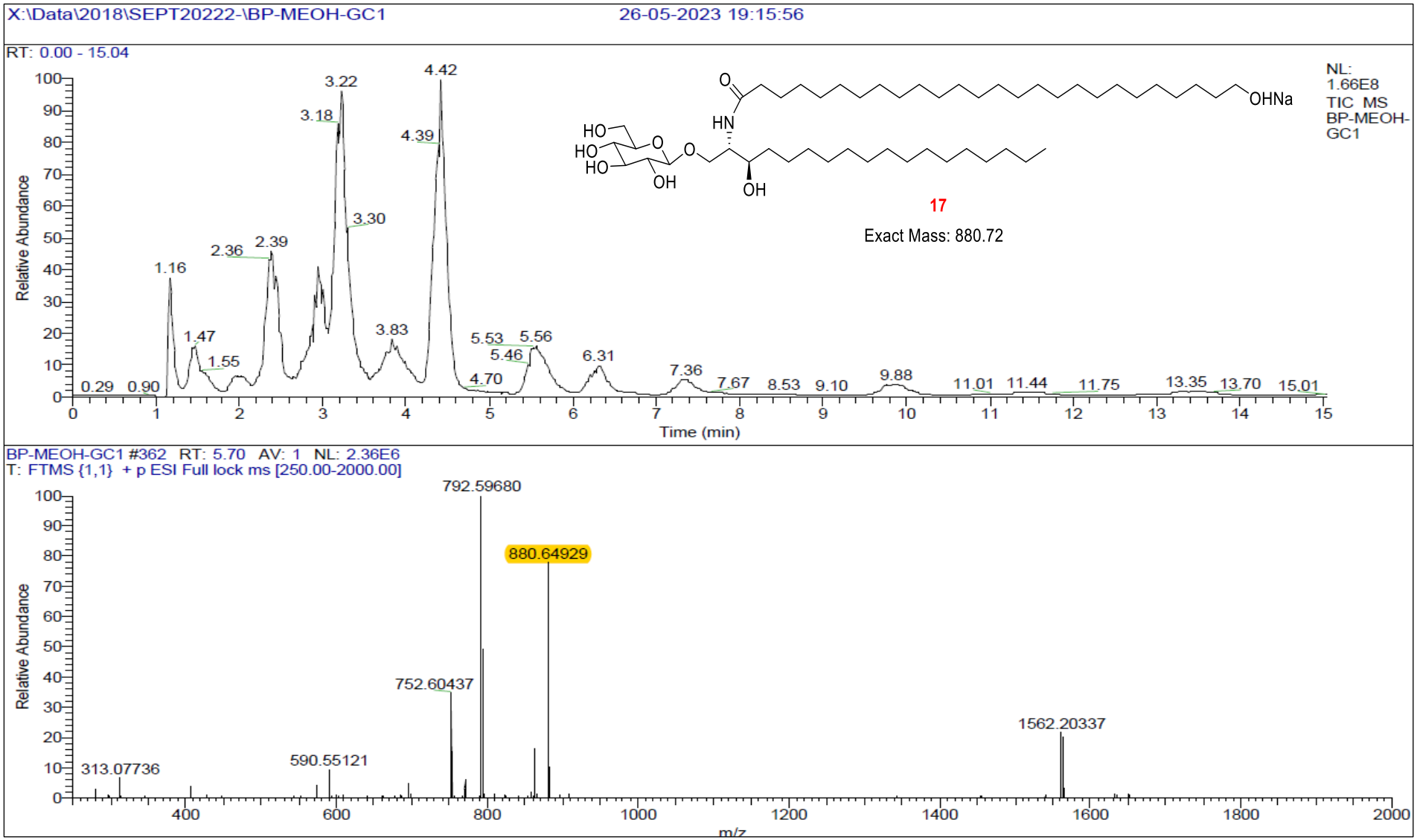

Fig. 5.31. HR-ESI-MS of BP-MEOH-GC-1-RT-5.70

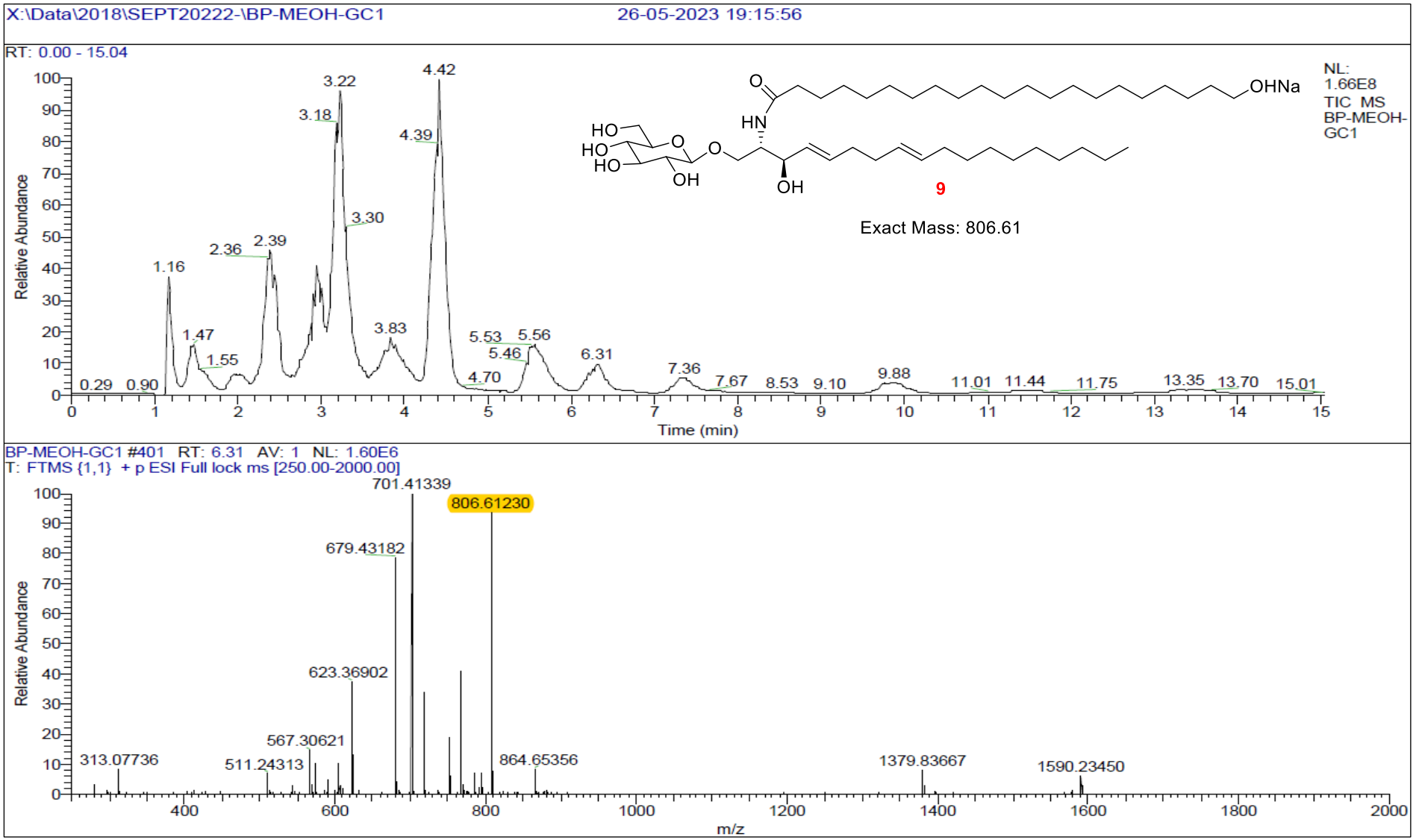

Fig. 5.32. HR-ESI-MS of BP-MEOH-GC-1-RT-6.31

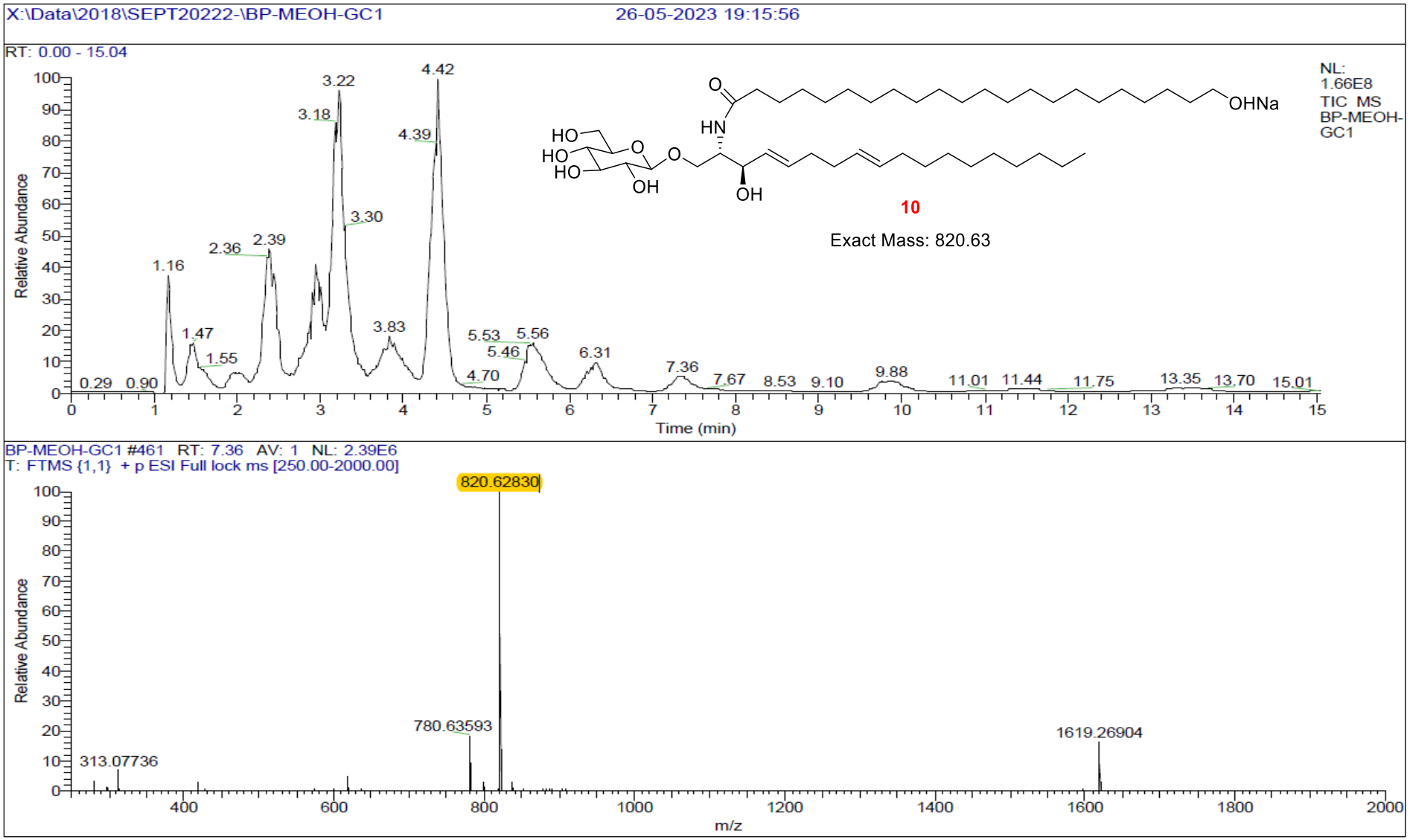

Fig. 5.33. HR-ESI-MS of BP-MEOH-GC-1-RT-7.36

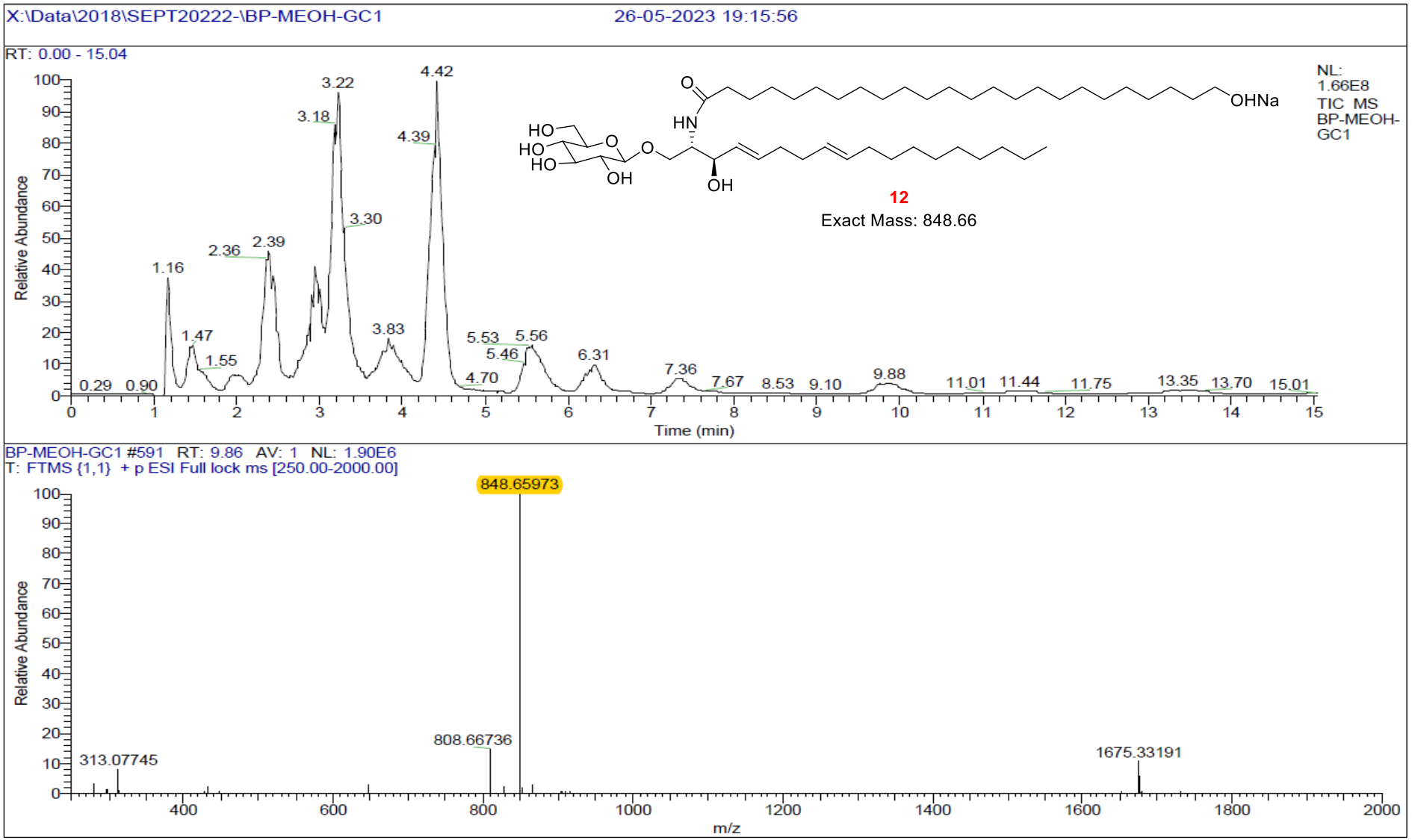

Fig. 5.34. HR-ESI-MS of BP-MEOH-GC-1-RT-9.86

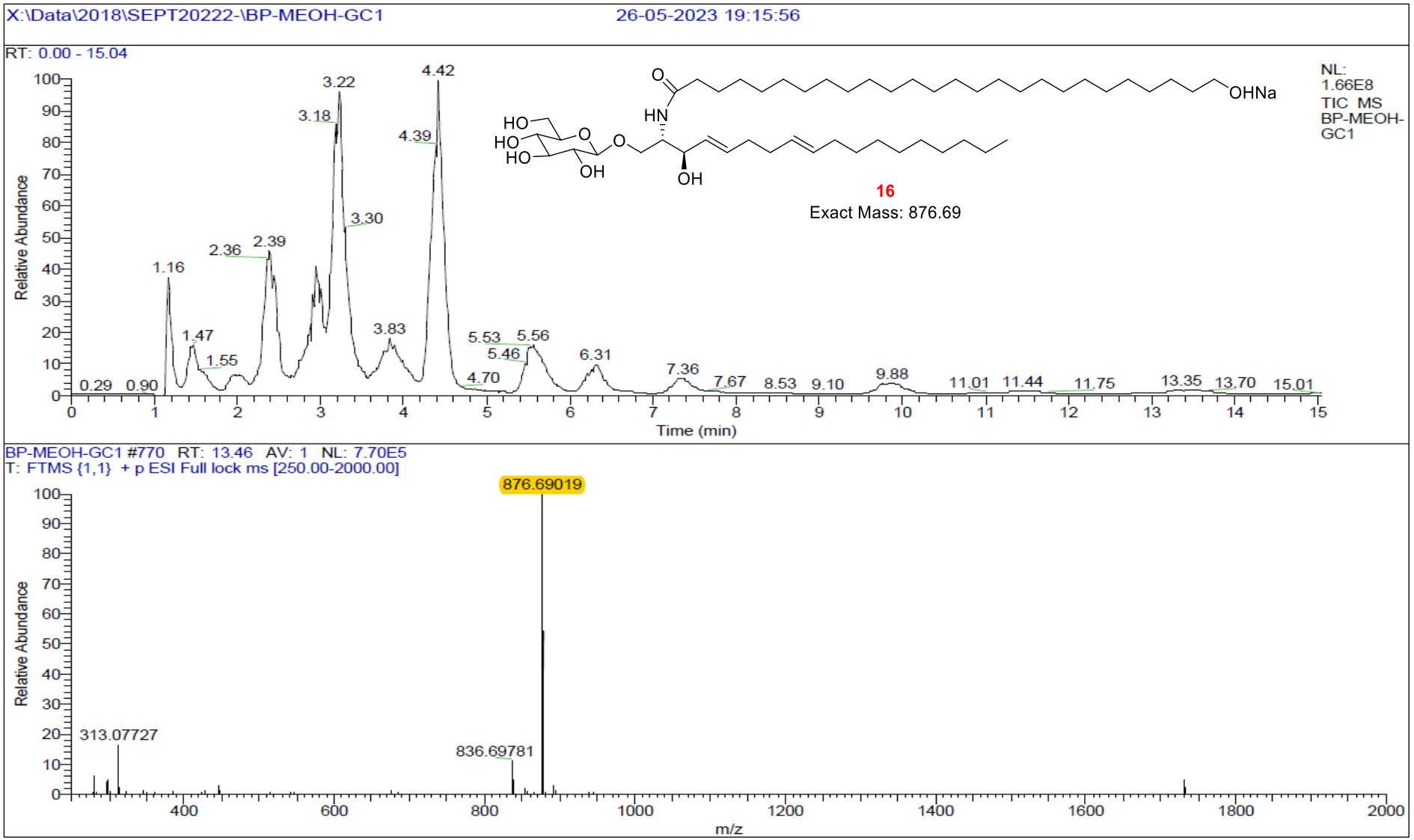

Fig. 5.35. HR-ESI-MS of BP-MEOH-GC-1-RT-13.46

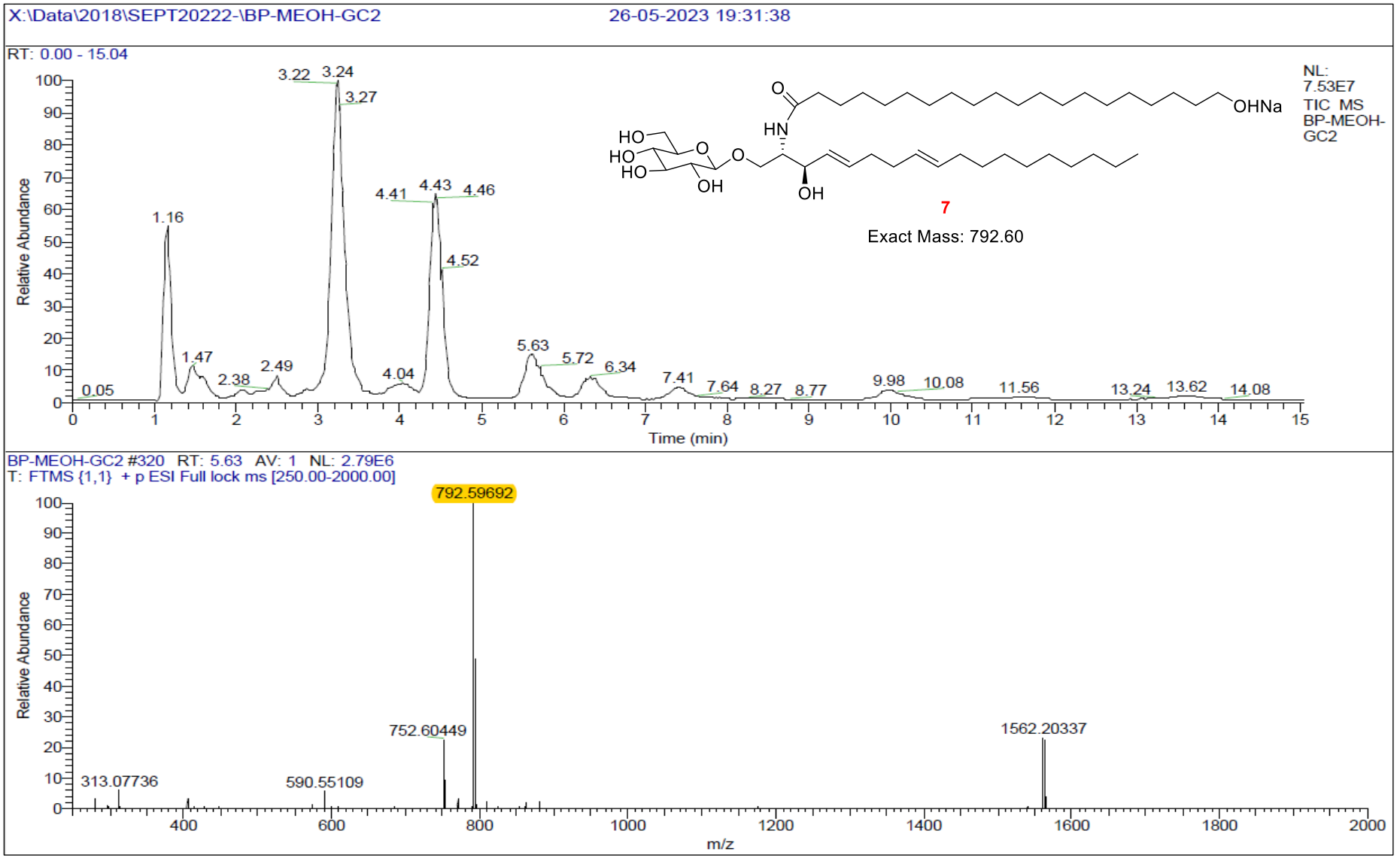

Fig. 5.36. HR-ESI-MS of BP-MEOH-GC-2-RT-5.63

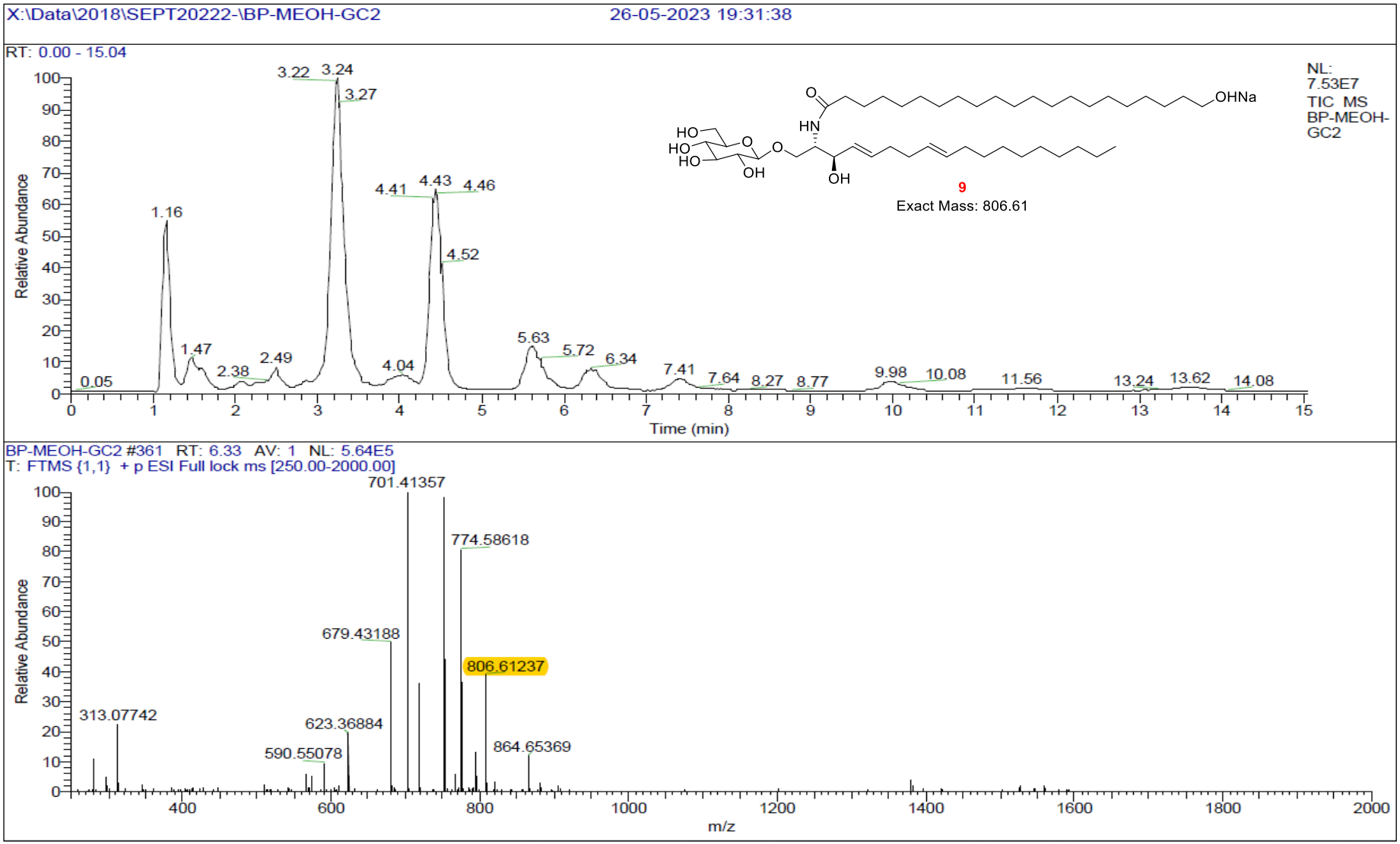

Fig. 5.37. HR-ESI-MS of BP-MEOH-GC-2-RT-6.33

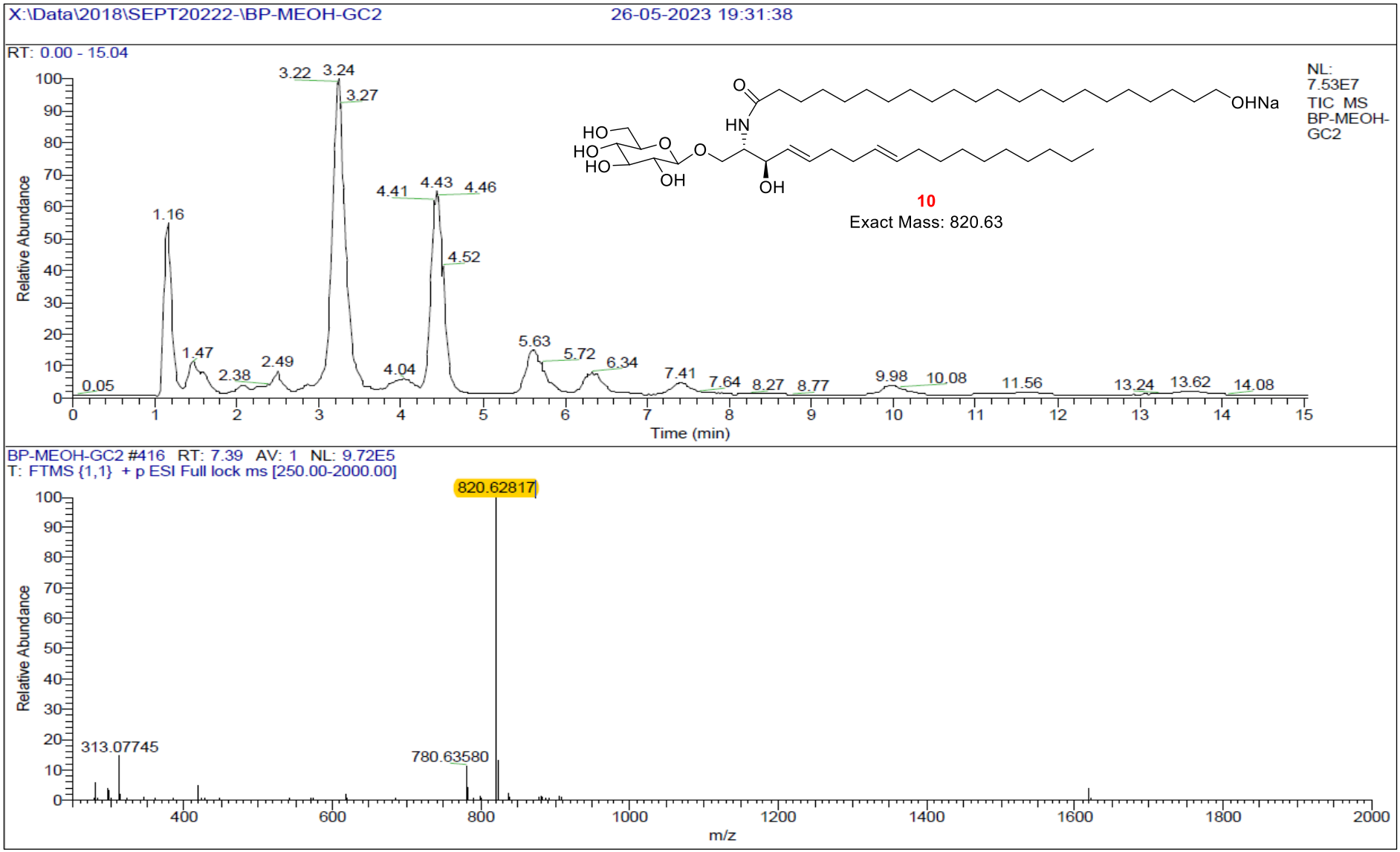

Fig. 5.38. HR-ESI-MS of BP-MEOH-GC-2-RT-7.39

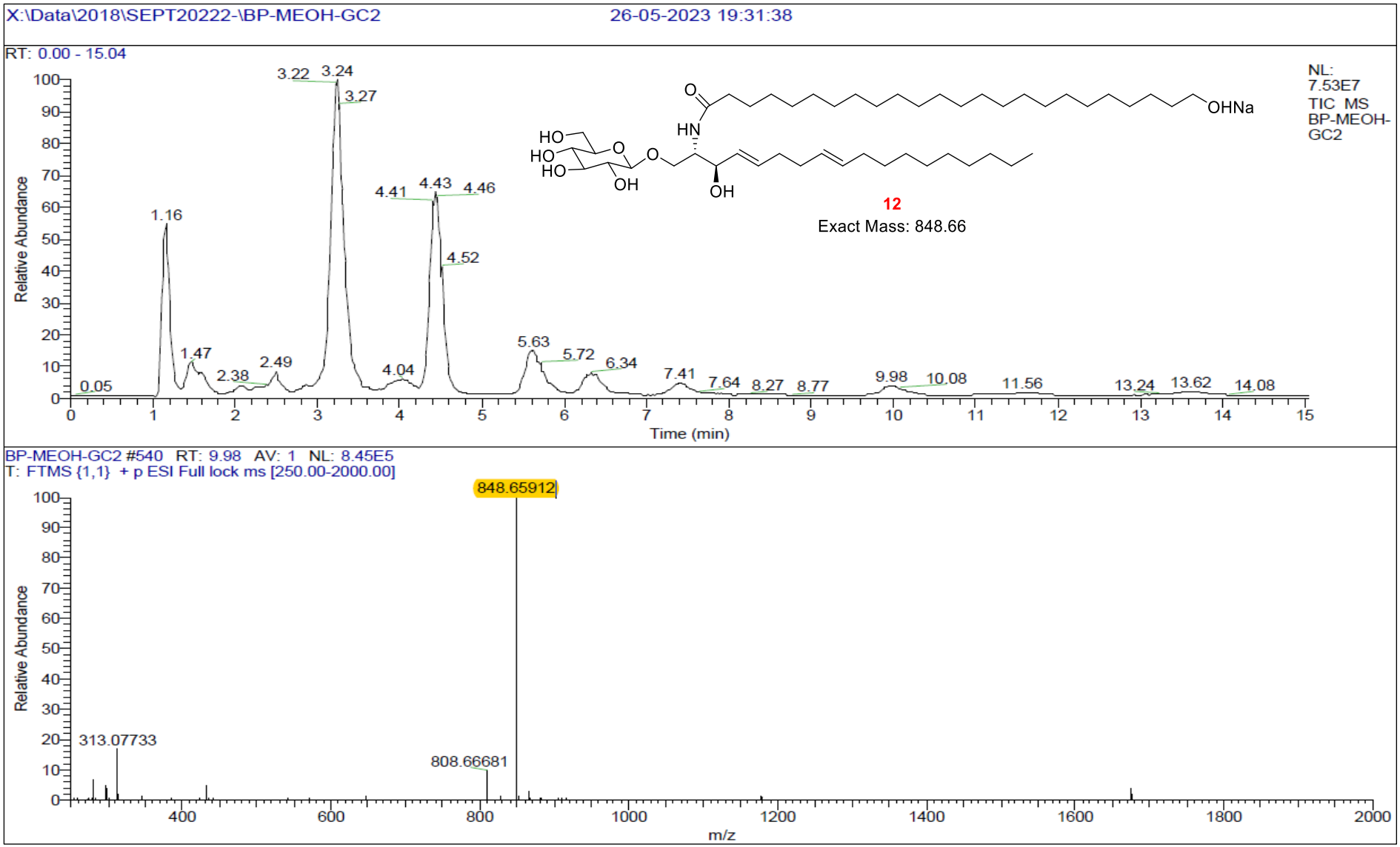

Fig. 5.39. HR-ESI-MS of BP-MEOH-GC-2-RT-9.98

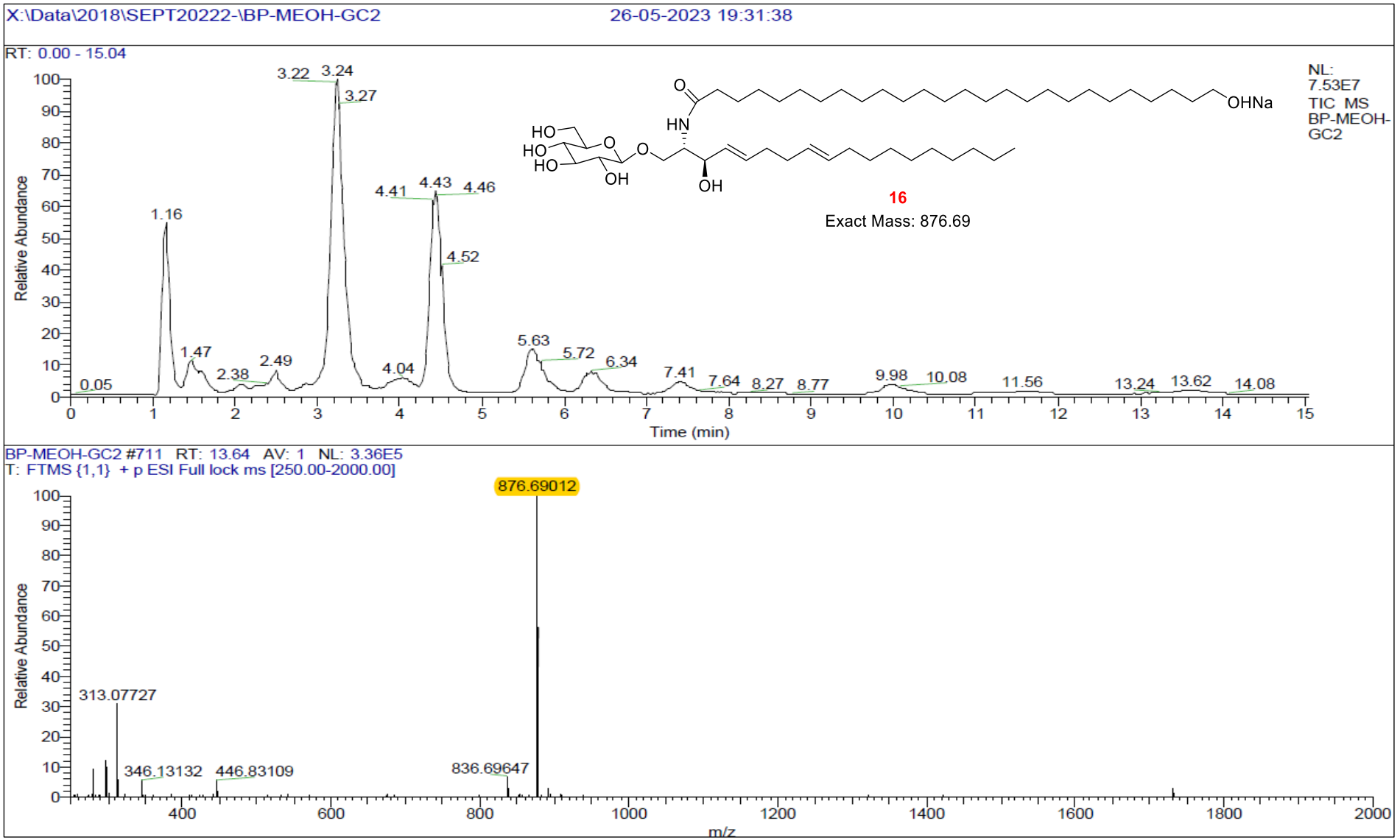

Fig. 5.40. HR-ESI-MS of BP-MEOH-GC-2-RT-13.64

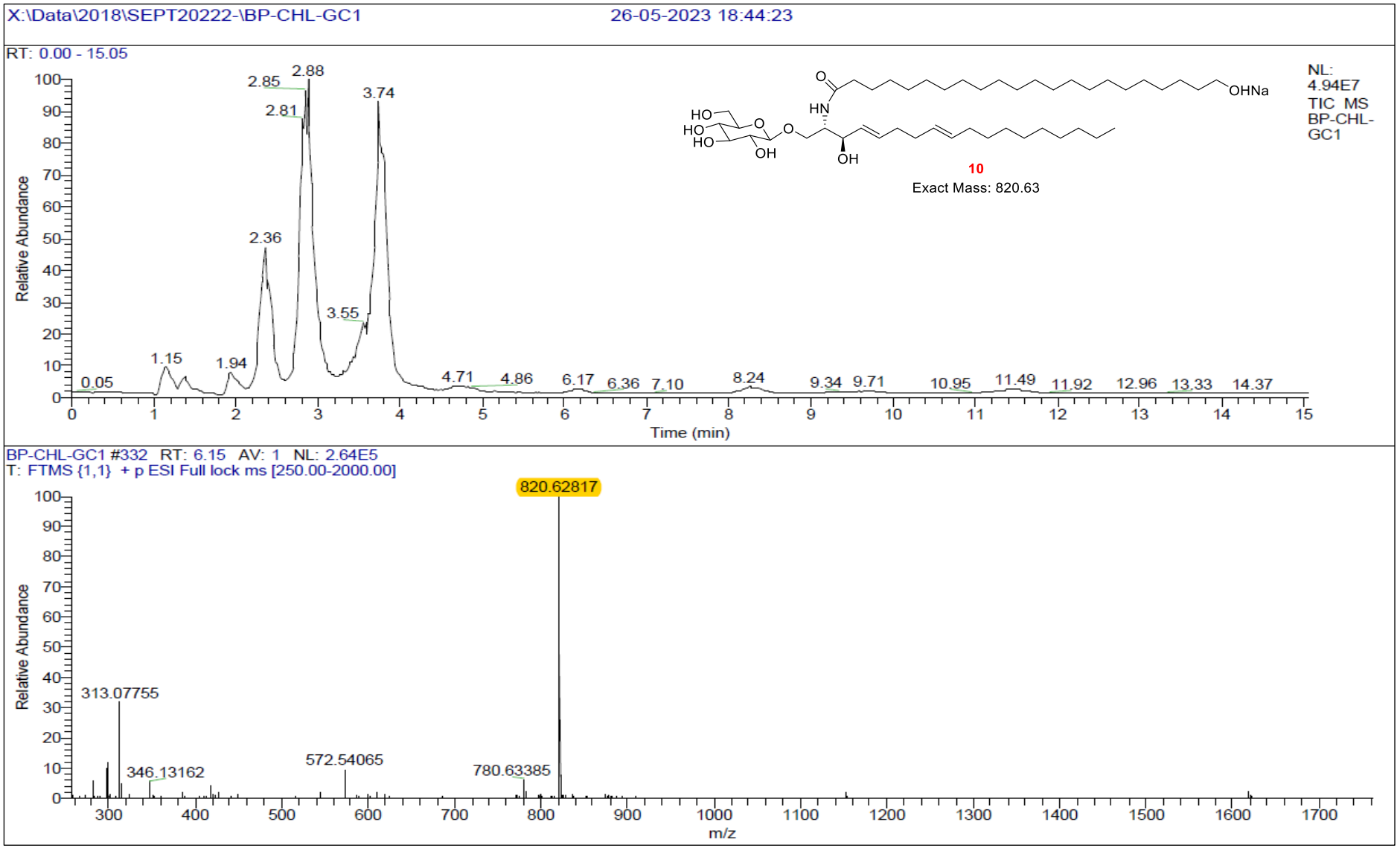

Fig. 5.41. HR-ESI-MS of BP-CHL-GC-1-RT-6.15

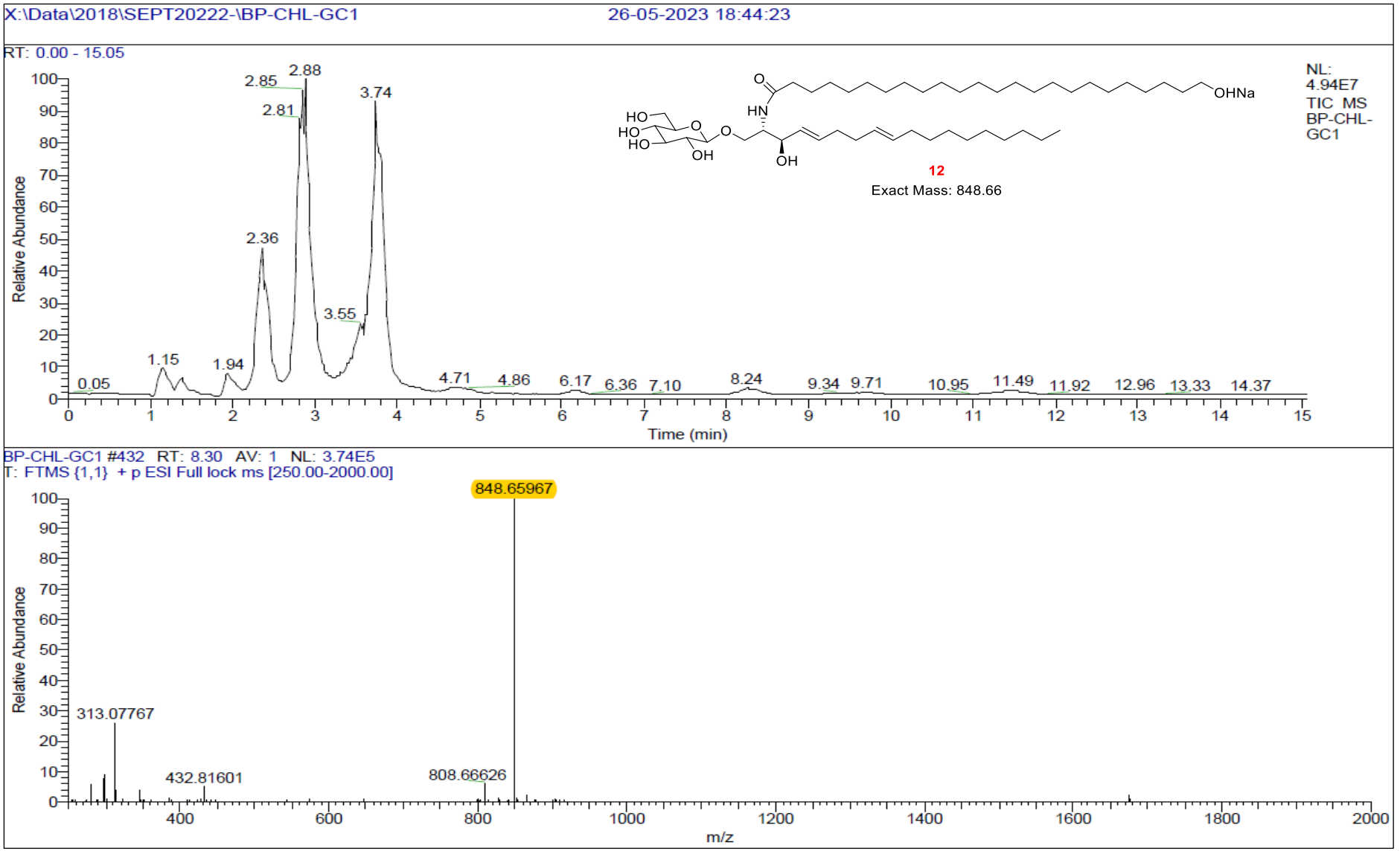

Fig. 5.42. HR-ESI-MS of BP-CHL-GC-1-RT-8.30

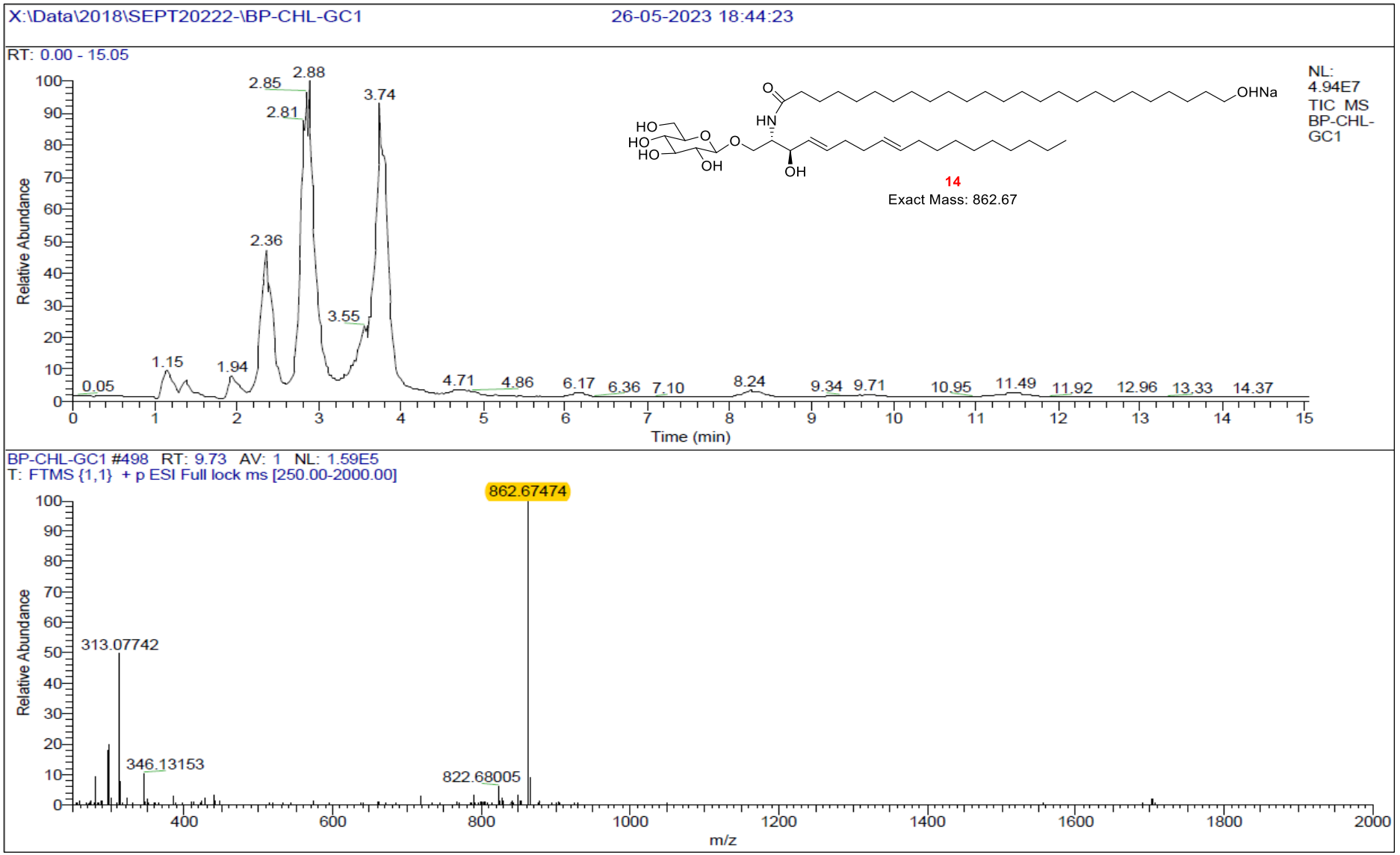

Fig. 5.43. HR-ESI-MS of BP-CHL-GC-1-RT-9.73

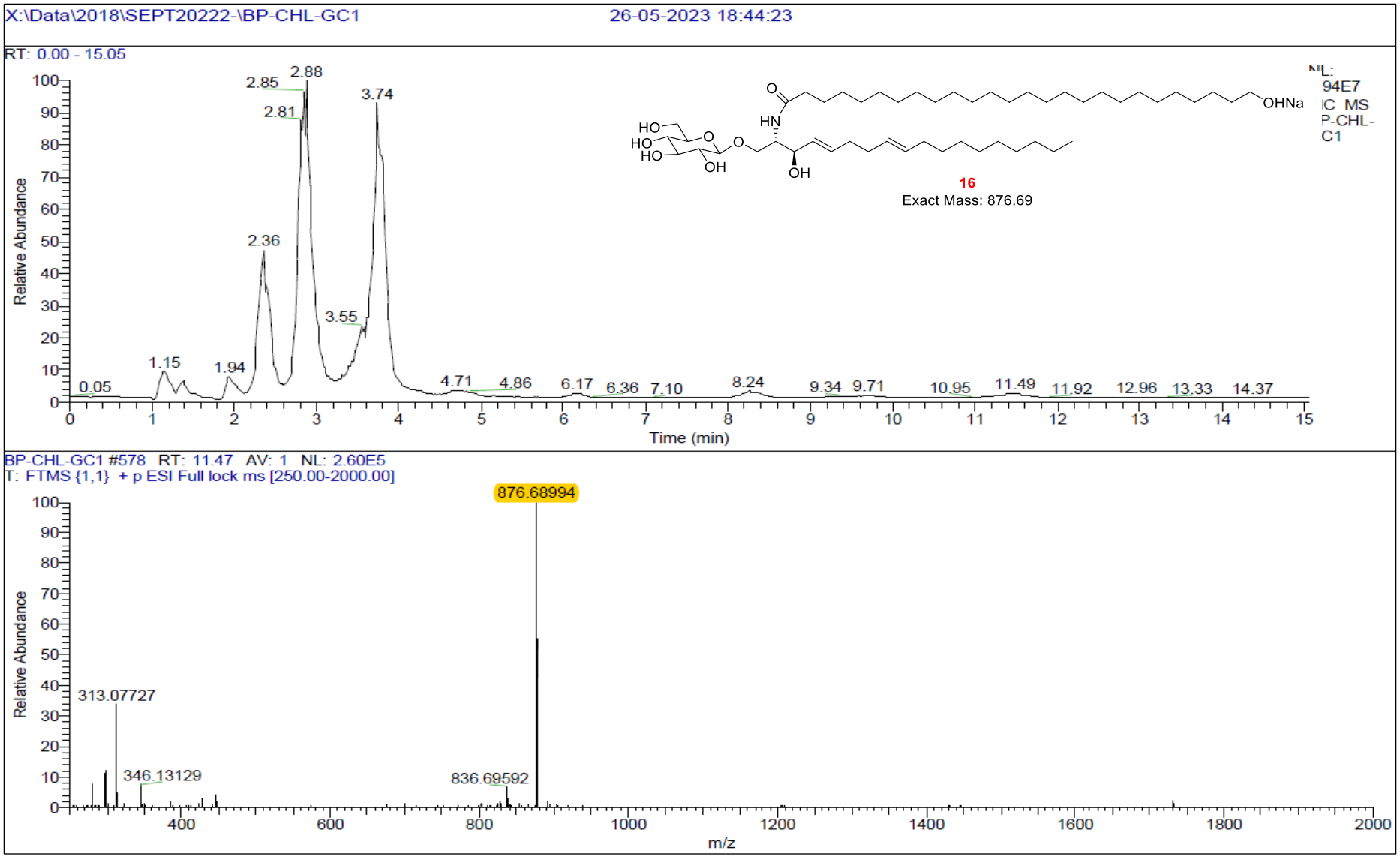

Fig. 5.44. HR-ESI-MS of BP-CHL-GC-1-RT-11.47

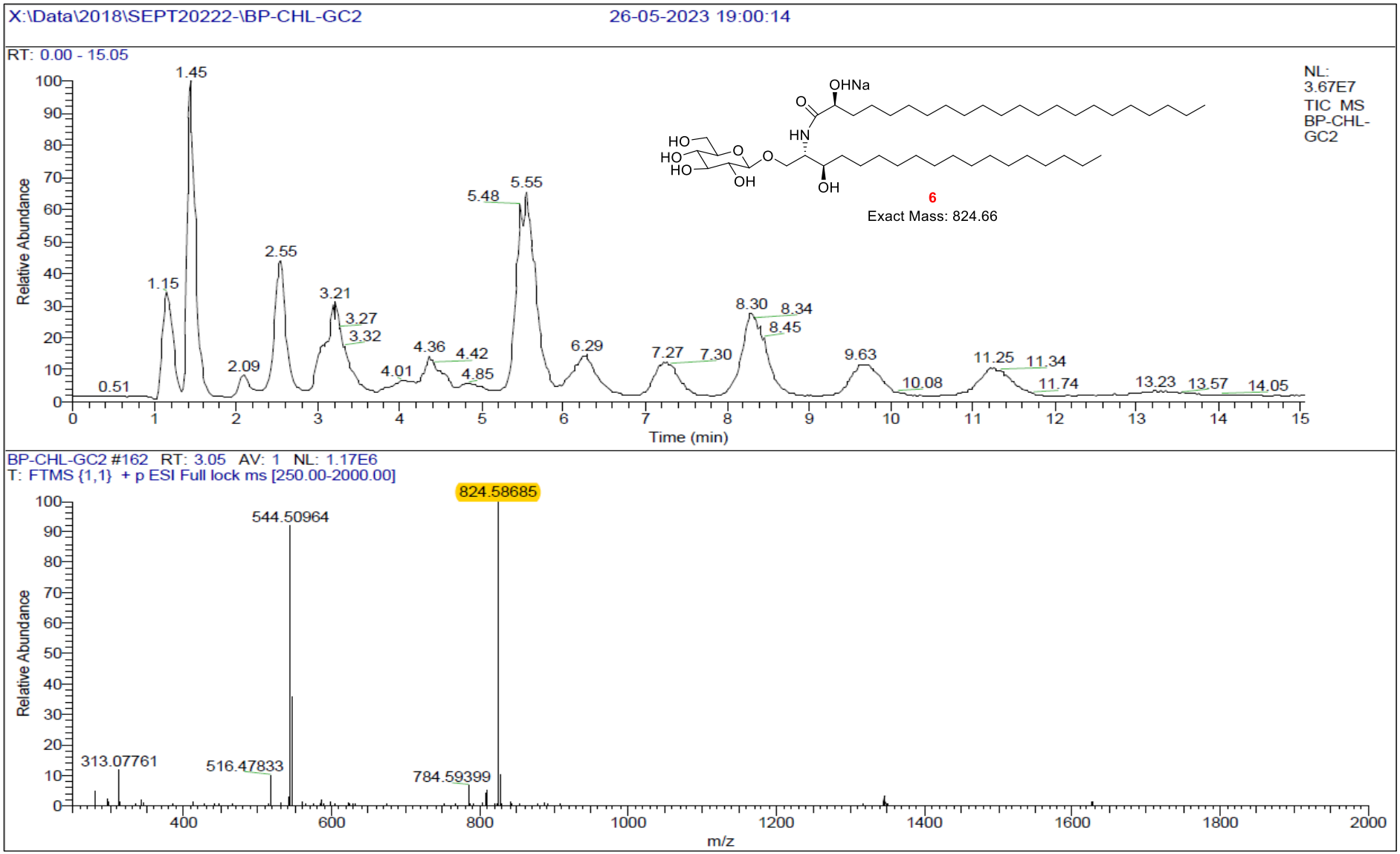

Fig. 5.45. HR-ESI-MS of BP-CHL-GC-2-RT-3.05

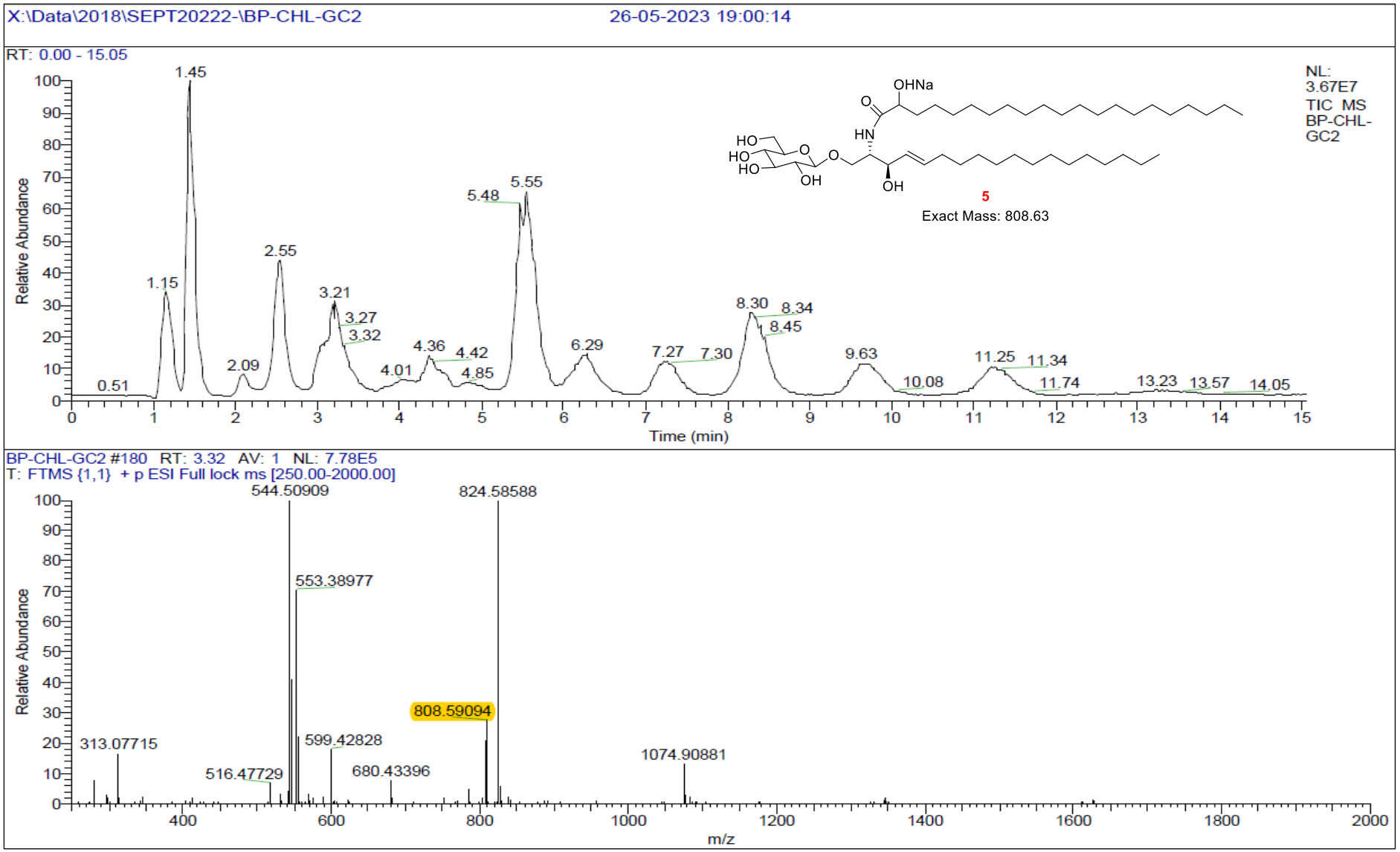

Fig. 5.46. HR-ESI-MS of BP-CHL-GC-2-RT-3.32

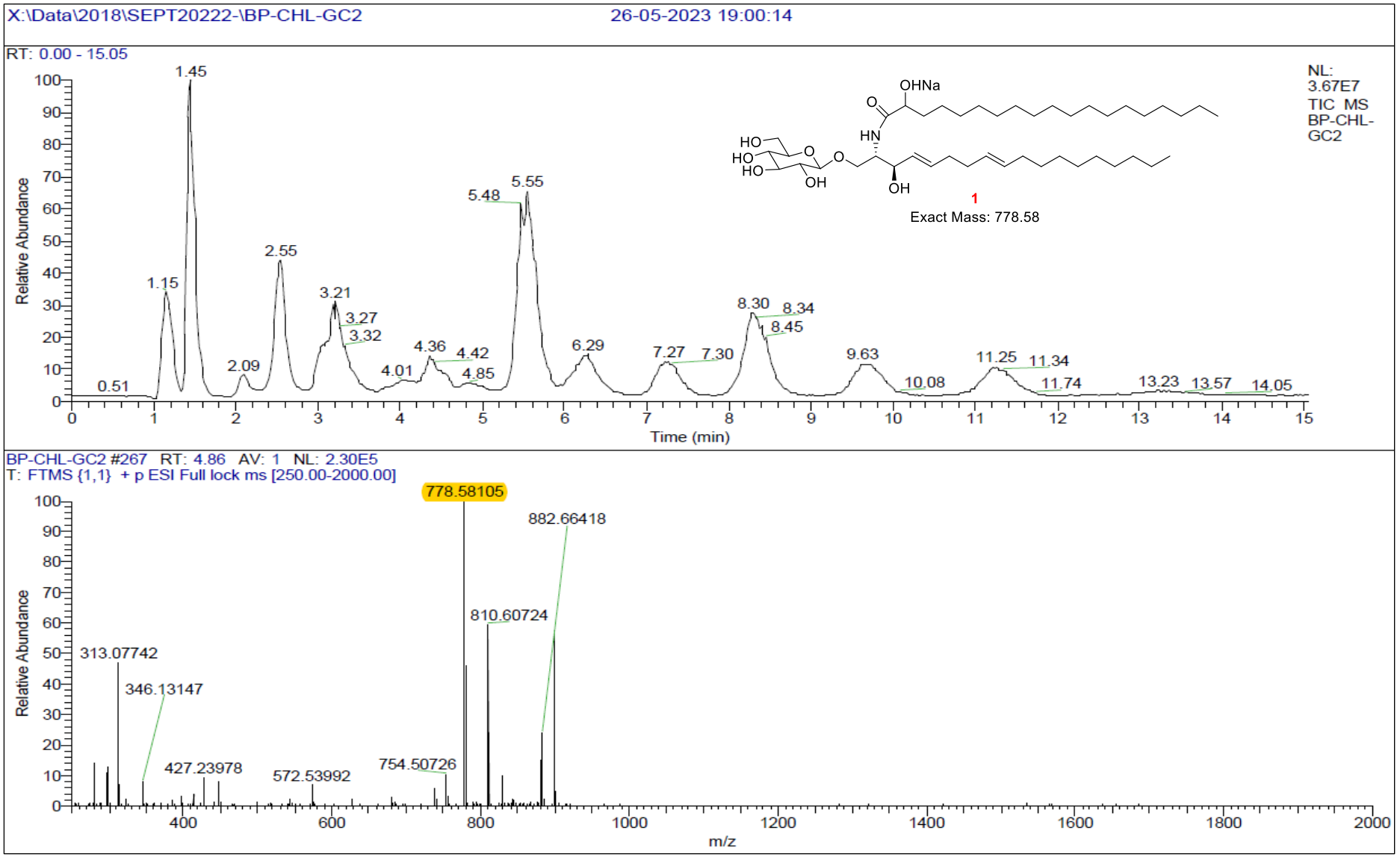

Fig. 5.47. HR-ESI-MS of BP-CHL-GC-2-RT-4.86

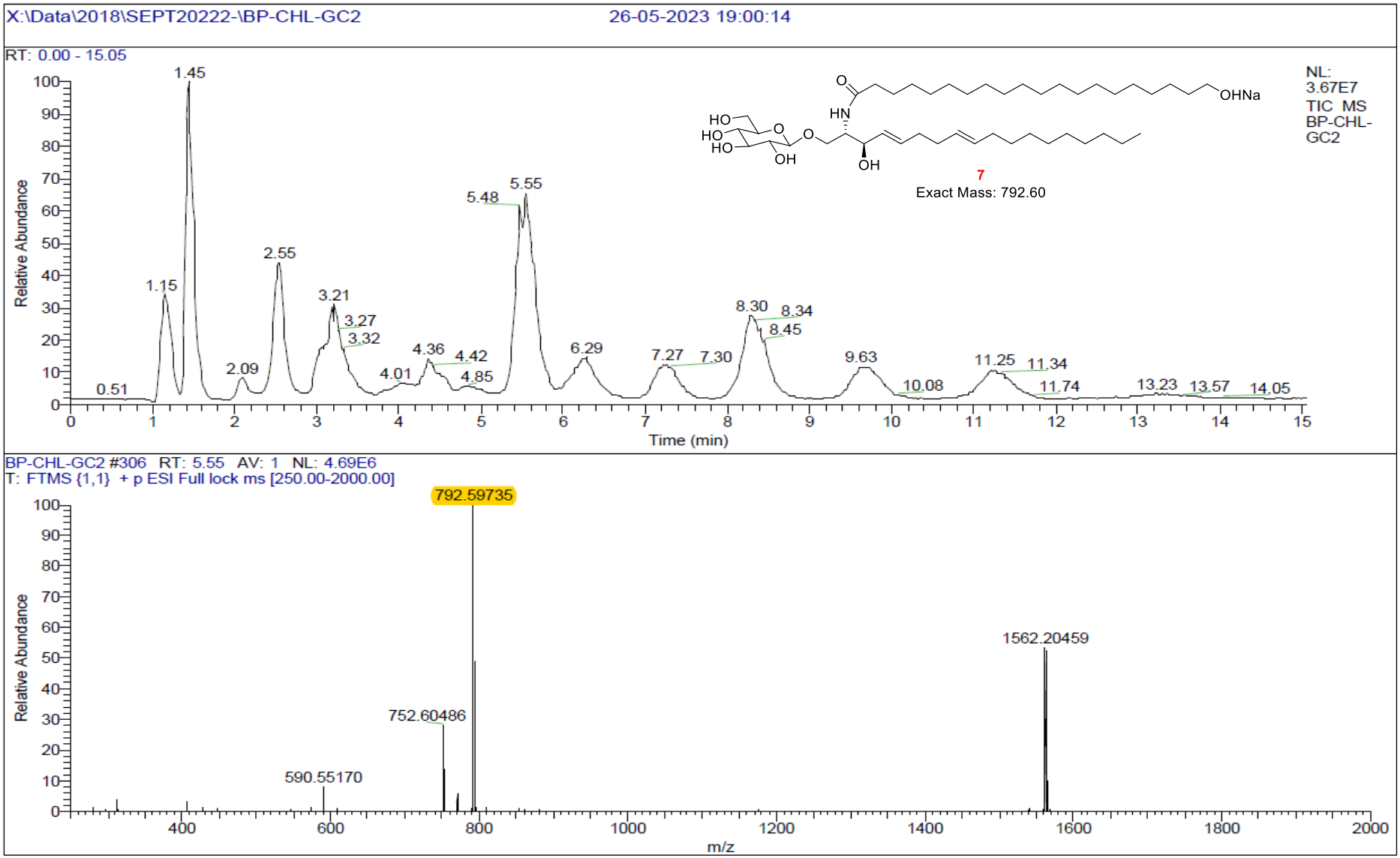

Fig. 5.48. HR-ESI-MS of BP-CHL-GC-2-RT-5.55

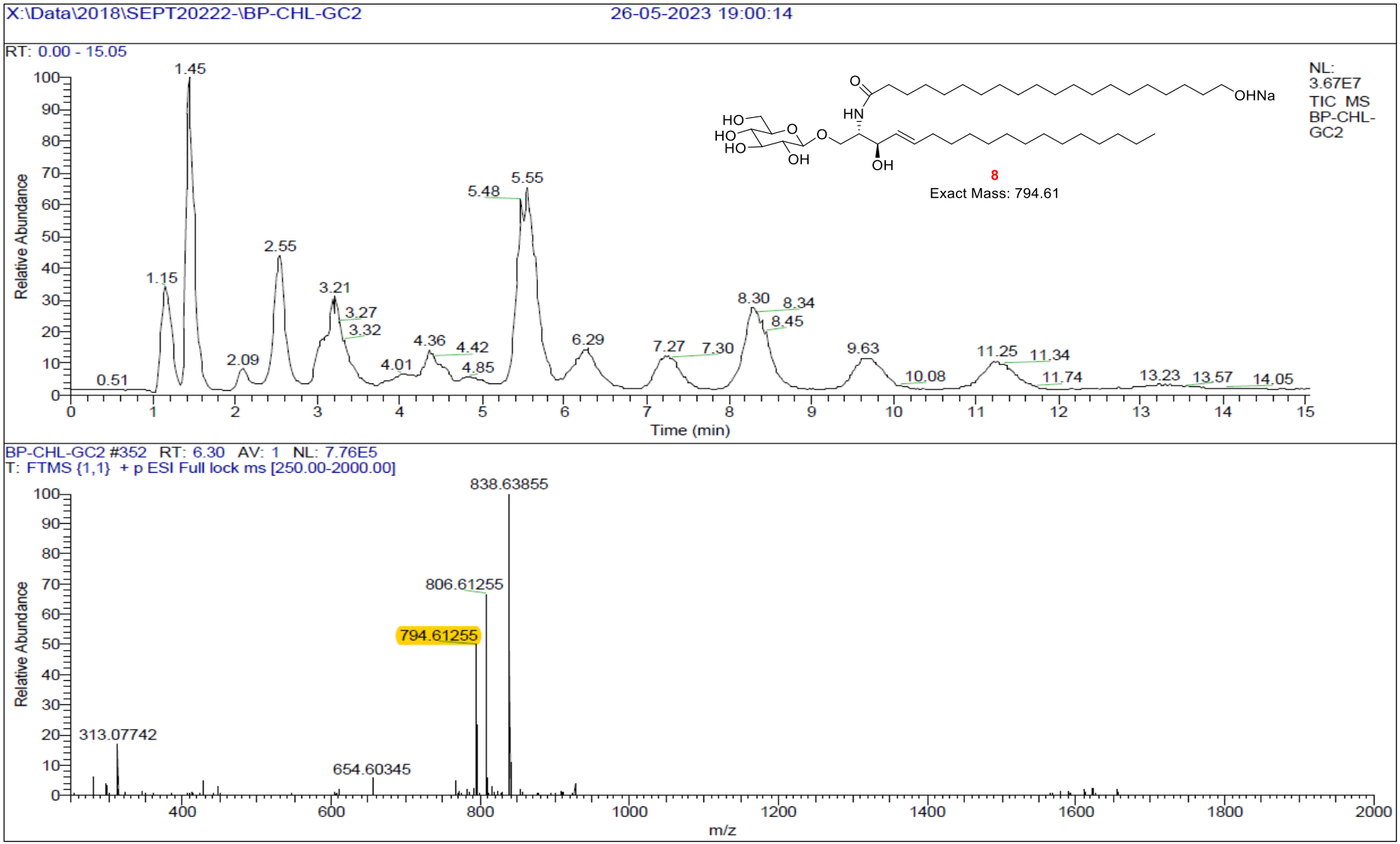

Fig. 5.49. HR-ESI-MS of BP-CHL-GC-2-RT-6.30

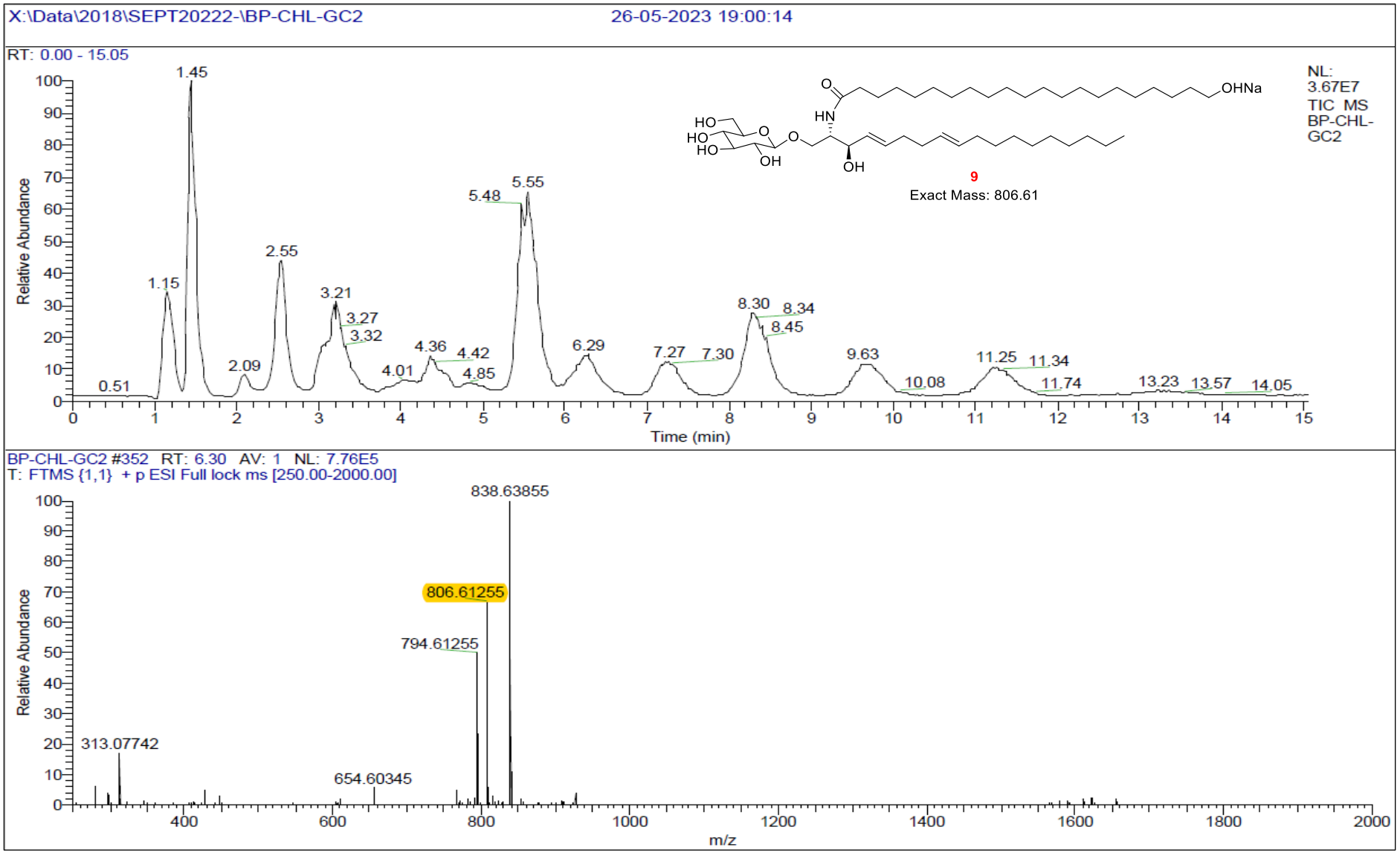

Fig. 5.50. HR-ESI-MS of BP-CHL-GC-2-RT-6.30′

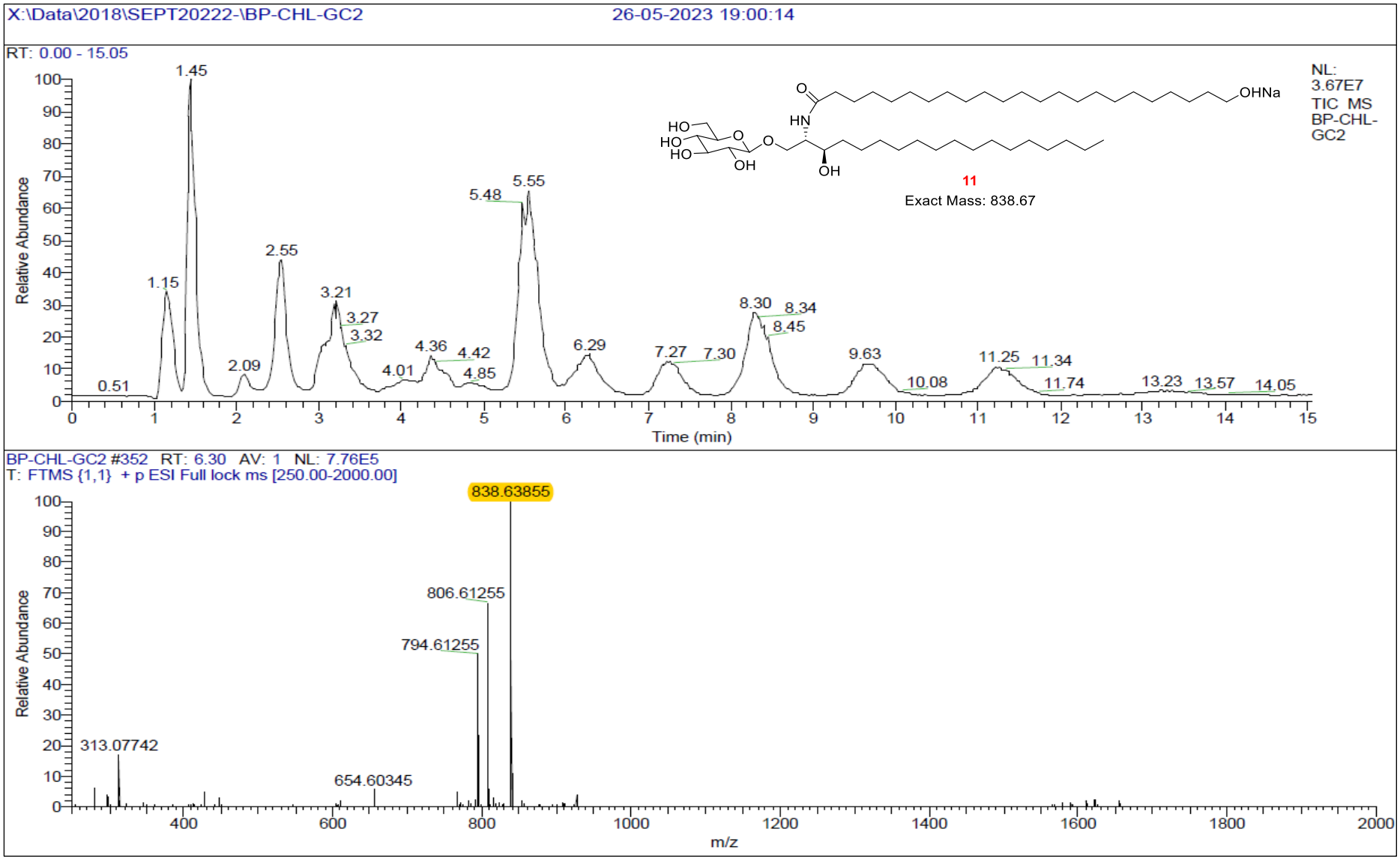

Fig. 5.51. HR-ESI-MS of BP-CHL-GC-2-RT-6.30″

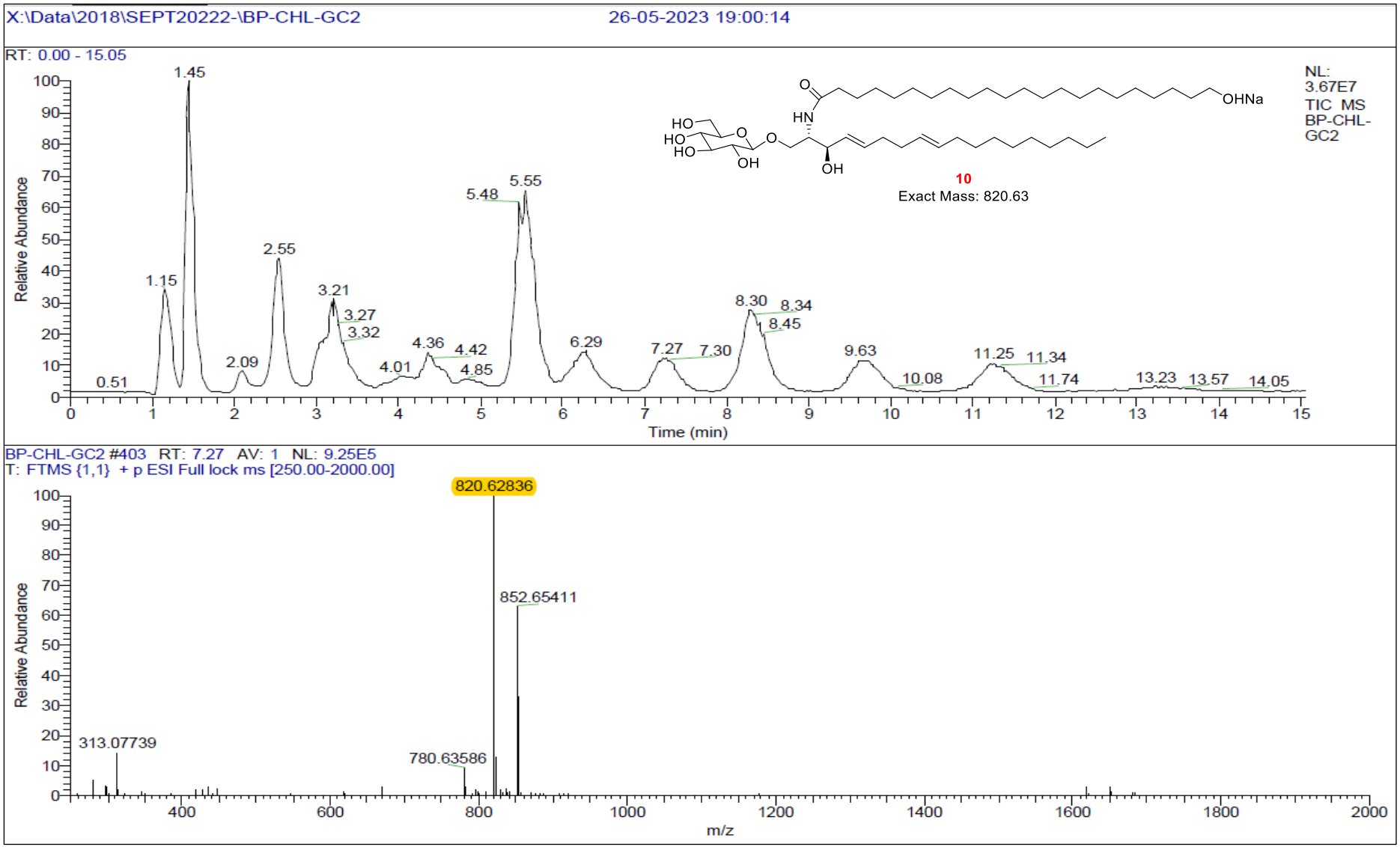

Fig. 5.52. HR-ESI-MS of BP-CHL-GC-2-RT-7.27

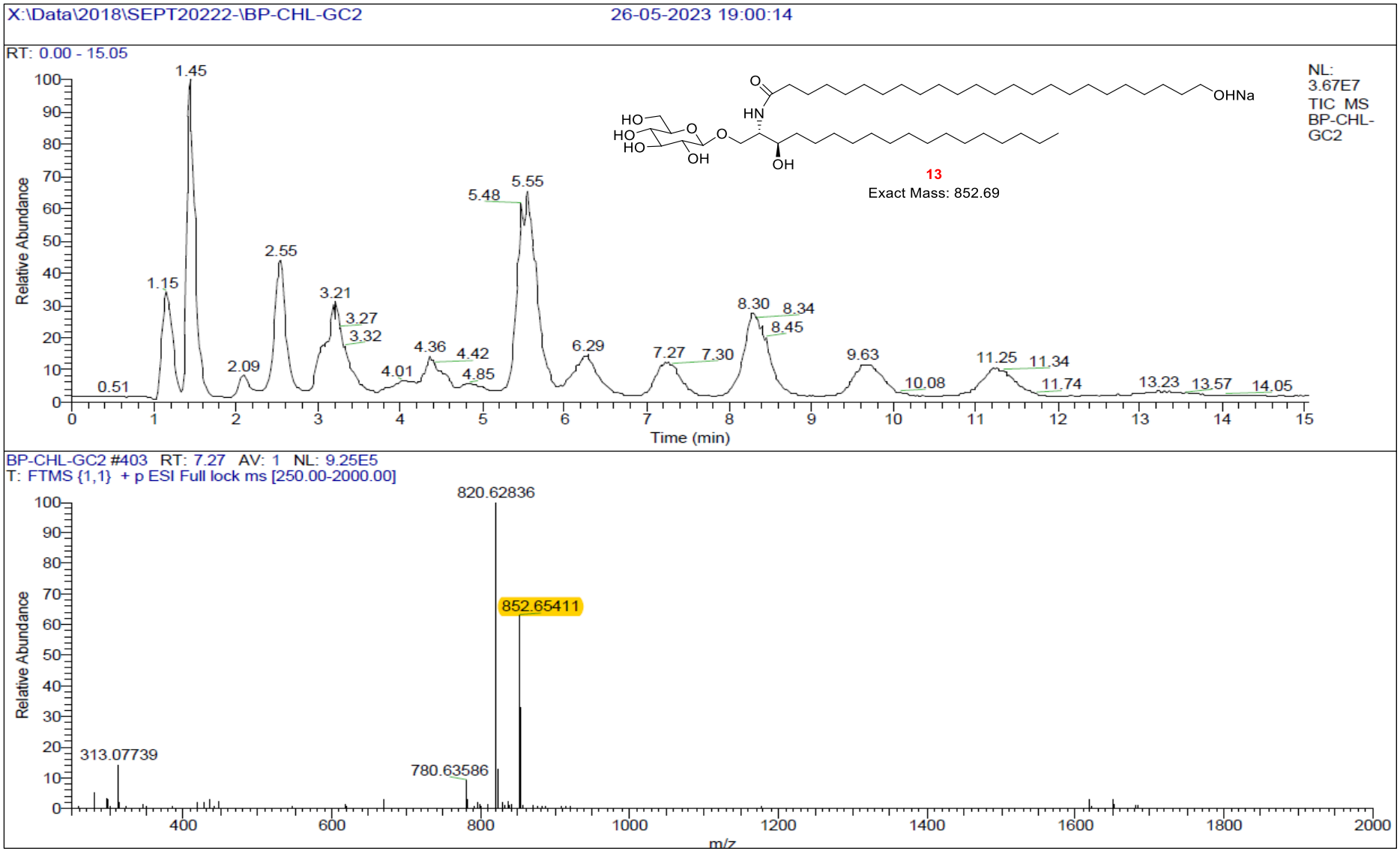

Fig. 5.53. HR-ESI-MS of BP-CHL-GC-2-RT-7.27′

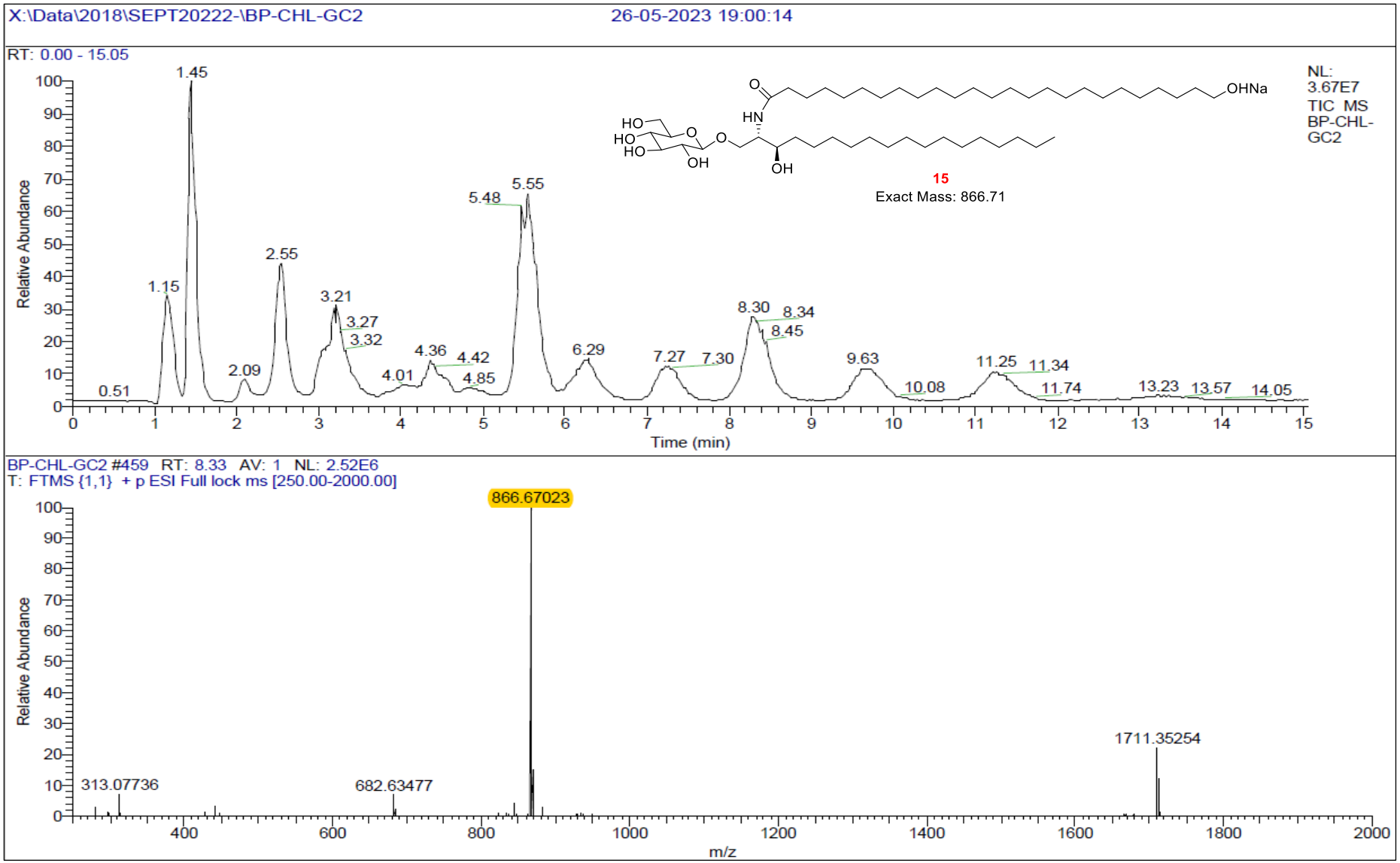

Fig. 5.54. HR-ESI-MS of BP-CHL-GC-2-RT-8.33

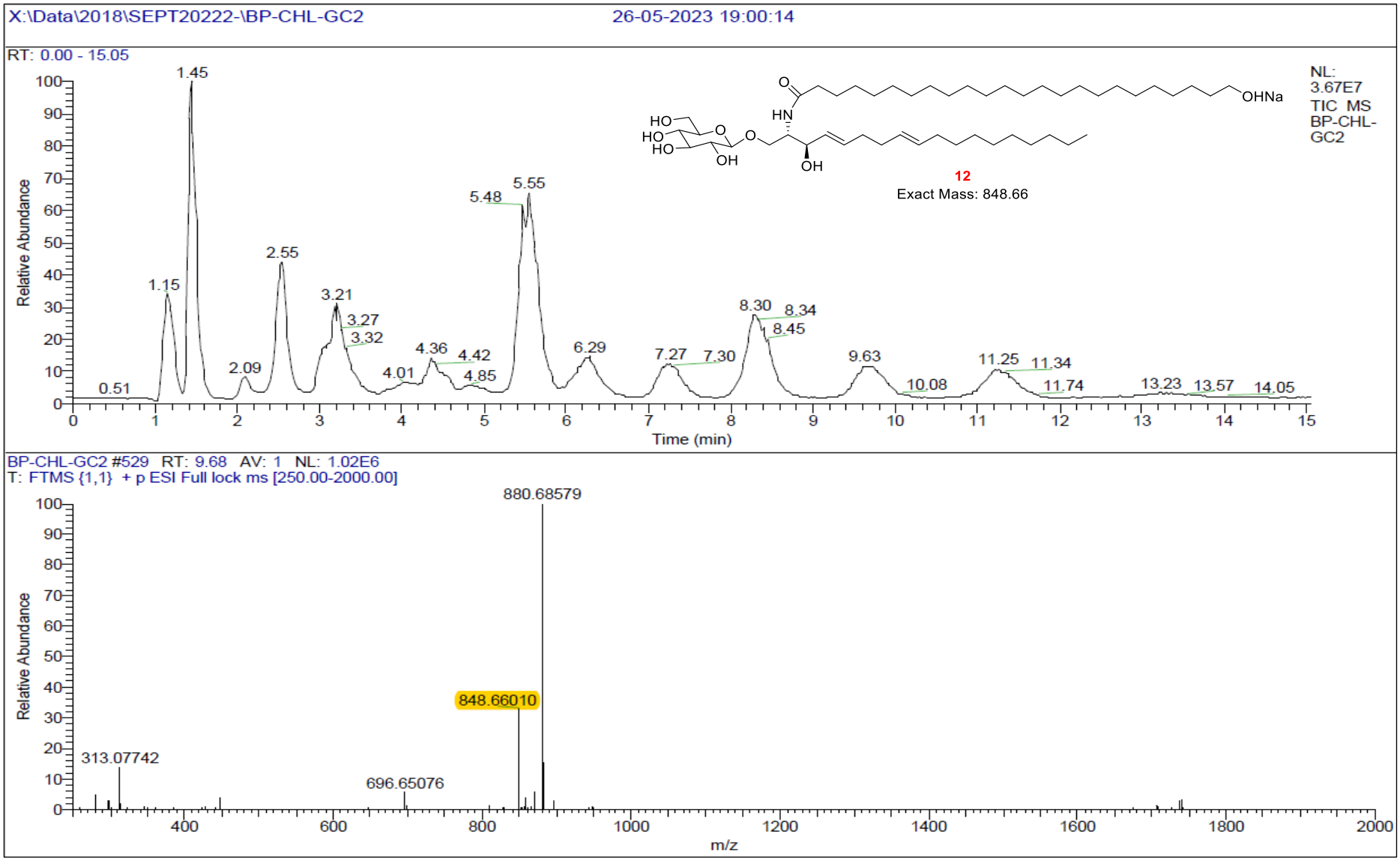

Fig. 5.55. HR-ESI-MS of BP-CHL-GC-2-RT-9.68

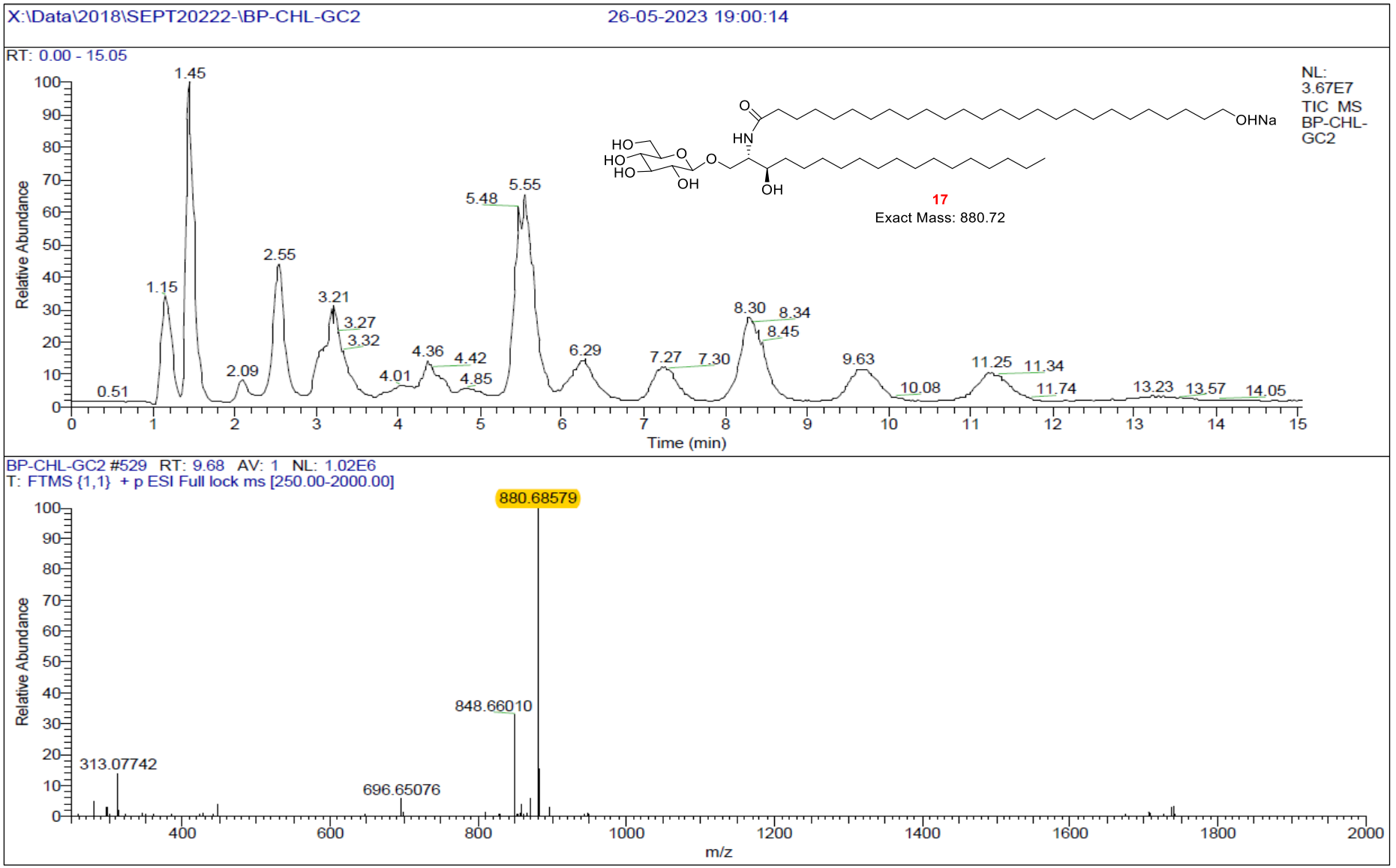

Fig. 5.56. HR-ESI-MS of BP-CHL-GC-2-RT-9.68′

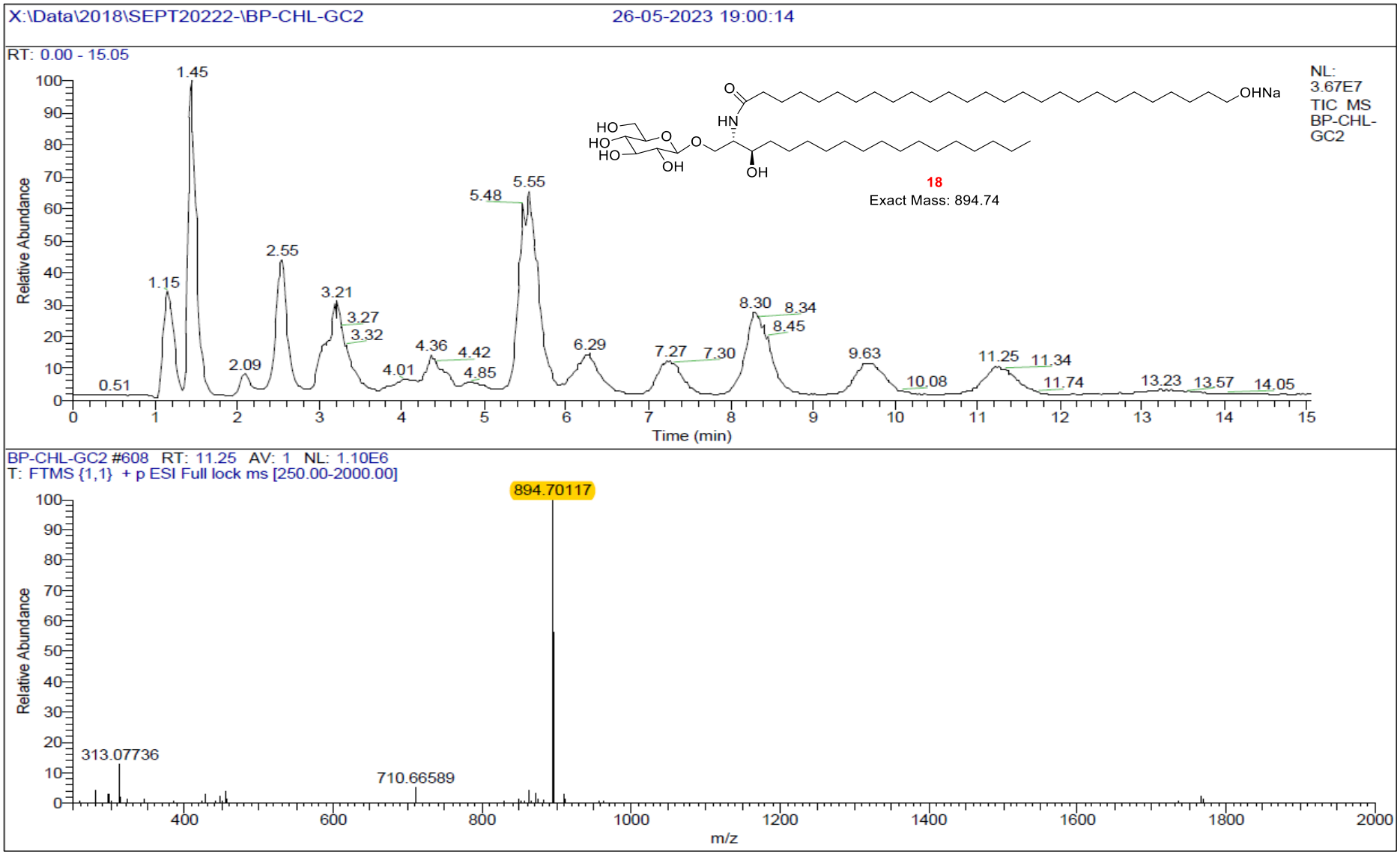

Fig. 5.57. HR-ESI-MS of BP-CHL-GC-2-RT-11.25

5.4.2. Evaluation of immunomodulatory effects of GCs

Inflammation refers to a complex immunological response that is connected to the gradual release of pro-inflammatory cytokines. Macrophages play a key role in the inflammatory process by providing an immediate defence against foreign agents. When induced by an inflammation stimulus such as LPS, they initiate the production of a variety of pro-inflammatory mediators including TNF-α, IL-6, COX-2, NO, etc. (Geller & Billiar, 1998; Huang et al., 2014). Suppression of these pro-inflammatory cytokines is critical for treating inflammatory diseases. Hence the potential of GCs for the suppression of NO production and its role in the release of pro and anti-inflammatory cytokines were evaluated.

5.4.2.1. Determination of cell viability by MTT assay

The cytotoxicity of the GC consortium was assessed using MTT assay by assessing the viability of RAW 264.7 macrophages. Samples of the concentrations 5, 10, 25, 50, 100 & 200 µg/mL were used for assessing the cytotoxicity of the sample, and the results are shown in Fig. 3. As depicted in the figure (Fig. 5.58.), the GCs of concentrations ranging from 5 µg/mL to 50 µg/mL had negligible effects on cell viability, with no significant difference between the control group and the sample-treated group. However, with an increase in concentration to 100 and 200 µg/mL, the viability of RAW 264.7 macrophages significantly decreased to 85.05 ± 0.94% and 71.44 ± 0.82%, respectively. Based on this observation, GC consortium of concentrations ranging from 5 to 50 µg/mL were selected for the evaluation of NO production by Griess reaction.

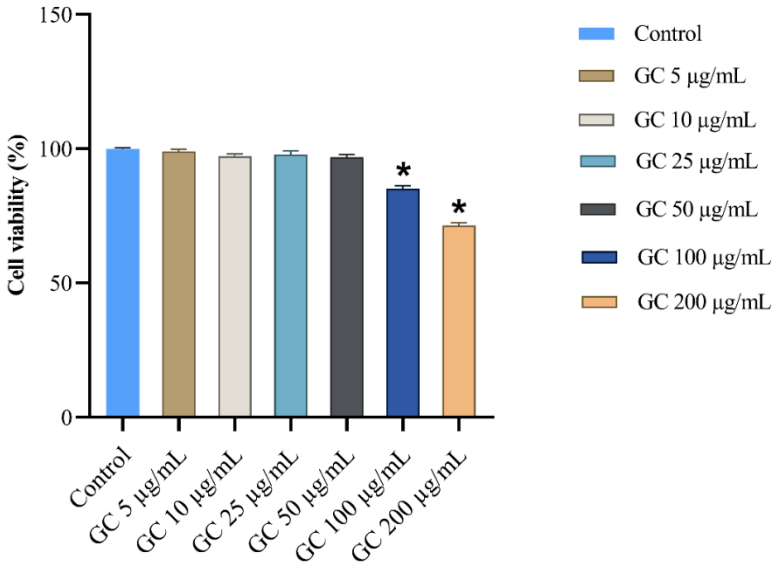

Fig. 5.58. Effect of GCs on the viability of RAW 264.7 cells. The cells were treated with GC consortium of concentrations ranging from 5 to 200 µg/mL and viability (%) was assessed after 24 hours of exposure and significance was determined through ANOVA, *$p \leq 0.05$ (vs. control)

5.4.2.2. Evaluation of NO production by Griess reaction

Stimulation of macrophages by LPS triggers an overproduction of NO through the breakdown of L-arginine. In the mammalian immune response to inflammatory signals, the generation of NO is controlled by iNOS in macrophage cells (Baek et al., 2020). The progression of inflammation is the main cause of many disease conditions, including, Alzheimer's disease and Parkinson's disease. In a comprehensive review by Facchin and team., 2022 on inflammatory biomarkers on an LPS-induced RAW 264.7 cell model points out that measurement of NO levels may be sufficient to screen for possible anti-inflammatory action of a compound in these cells (Facchin et al., 2022). Hence the anti-inflammation potential of the GC consortium was first evaluated by monitoring its role in the suppression of NO production in LPS-induced RAW 264.7 cells.

To assess the influence of GCs in the NO production in macrophages, RAW264.7 cells were stimulated with LPS, and nitrite production was analyzed using the Griess reaction. GCs at concentrations 5, 10, 25 & 50 µg/mL were evaluated for their inhibitory effect on the NO production in LPS-activated RAW264.7 macrophages. The addition of LPS significantly increased the NO production of cells, and the treatment suppressed the NO production in a dose-dependent manner (Fig. 5.59). Upon treatment with LPS, the NO production increased to 37.70 ± 1.46 µM from the basal level of 6.76 ± 0.40 µM (control) and the positive control dexamethasone significantly reduced the NO production to 10.72 ± 0.47 µM compared to the LPS treated groups. The cells treated with GC consortium of the concentrations 10 & 25 µg/mL showed a significant reduction in the NO production to 25.22 ± 0.40 µM and 17.33 ± 0.70 µM respectively. Whereas GC consortium at a dose of 50 µg/mL showed a reduction in NO production to 10.75 ± 0.58 µM, which is on par with dexamethasone (10.72 ± 0.47 µM) (Fig. 5.59.). Based on assay results, GC of concentrations 25 & 50 µg/mL were selected for further studies.

There are only a few reports discussing the anti-inflammation properties of GC. Literature data demonstrated the anti-inflammatory potential of GC isolated from *Cordyceps militaris*, an edible fungus. GC was able to prevent the accumulation of the pro-inflammatory iNOS protein and thereby reducing the NO production. It also reduced the expression of cyclooxygenase-2 protein in LPS-stimulated macrophages (Chiu et al., 2016). Similarly, the observed reduction in the NO production upon GC treatment may be due to its potential to prevent the accumulation of iNOS.

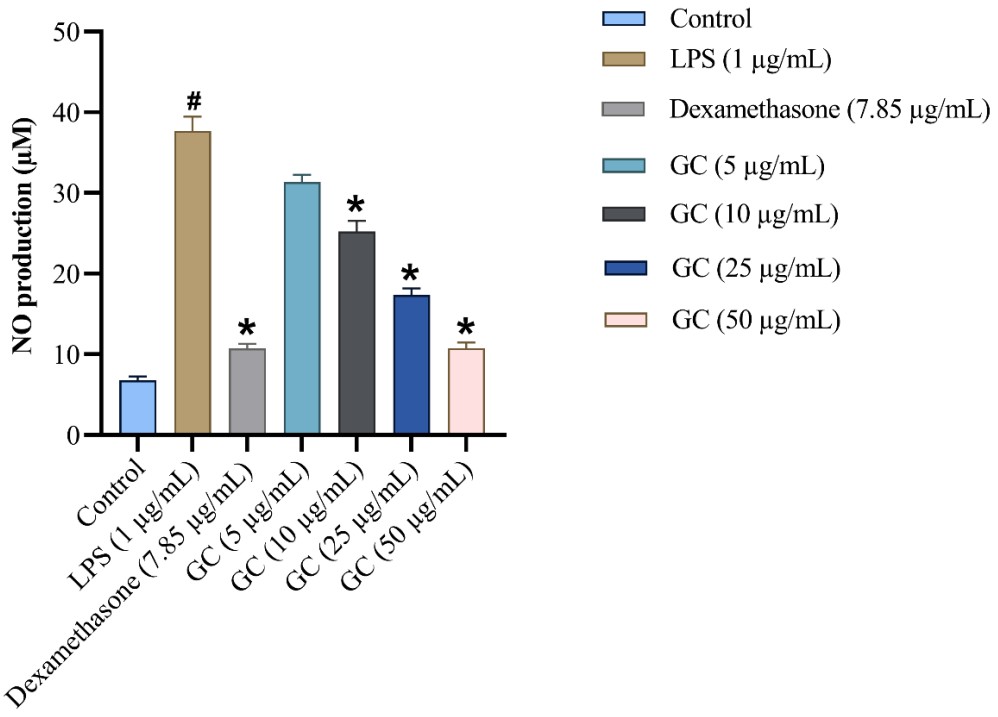

Fig. 5.59. Effect of GCs on the NO production of RAW 264.7 cells induced by LPS. The cells were treated with GC consortium of concentrations ranging from 5 to 50 µg/mL and NO production (µM) was assessed after 24 hours of exposure and significance was determined through ANOVA, $^{\#}p \leq 0.05$ (vs. control), $*p \leq 0.05$ (vs. LPS)

5.4.2.3. Effect of GCs on pro and anti-inflammatory cytokines secretion

To study the effects of GCs on cytokine production in inflamed cells, the ELISA technique was employed. Cytokines play a crucial role in regulating inflammation in the body. Among the doses tested (25 & 50 µg/mL), 50 µg/mL of GC consortium significantly suppressed the production of pro-inflammatory cytokines, including IL-1α, IFN-γ, TNF-α, MCP-1, COX-2, and IL-6, while stimulated the production of anti-inflammatory cytokines IL-10 and IL-13 to a degree that matches to that of dexamethasone (7.85 µg/mL) (Fig. 5.60a & Fig. 5.60b.). It is noteworthy that at the dose of 50 µg/mL, GCs even outperformed dexamethasone by reducing the production of pro-inflammatory cytokines, IL-1α, TNF-α, COX-2, & IL-6, and increasing the production of the anti-inflammatory cytokine IL-10.

Upon LPS stimulation, the activated macrophages primarily produce pro-inflammatory cytokines, which play a crucial role in triggering inflammatory responses. Pro-inflammatory cytokines like interleukin-1 beta (IL-1β), interleukin-6 (IL-6), and TNF-α have been implicated in the development of pathological pain, supported by ample evidence. The anti-inflammatory

cytokines are a series of immunoregulatory molecules that control the pro-inflammatory cytokine response. Among them, IL-10 stands out for its potent anti-inflammatory properties, by suppressing the expression of inflammatory cytokines such as TNF-α, IL-6, and IL-1α by activated macrophages. Moreover, IL-10 has the ability to up-regulate endogenous anti-cytokines and down-regulate pro-inflammatory cytokine receptors. Thus, it can counter-regulate the production and function of pro-inflammatory cytokines at multiple levels (Iyer & Cheng, 2012; Martinez-Espinosa et al., 2021; Zhang & An, 2007). As evident from the ELISA analysis, the increased level of IL-10 upon GC treatment may be the mechanism behind the anti-inflammation potential of GC.

The impact of GCs on immune-mediated disorders has been extensively researched using various animal models. The findings indicate that it possesses remarkable anti-inflammatory, immunomodulatory, and anti-malignant properties. This is primarily achieved by promoting dendritic cells, natural killer T cells, and regulatory T cells. It is noteworthy that the breakdown of GCs to ceramide may significantly contribute to these positive outcomes. (Ilan et al., 2009). Our study is the first to report the anti-inflammatory benefits of GC extracted from unripe Nendran peel. Our findings suggest that GC can reduce LPS-induced inflammation by decreasing the secretion of pro-inflammatory cytokines and increasing the production of anti-inflammatory agents. Although *in vitro* studies provide quick results, they are inherently limited in their ability to replicate the intricate complexities of organ systems and the internal environment of the human body. Therefore, these studies warrant additional validation through pre-clinical and clinical studies.

Fig. 5.60a.

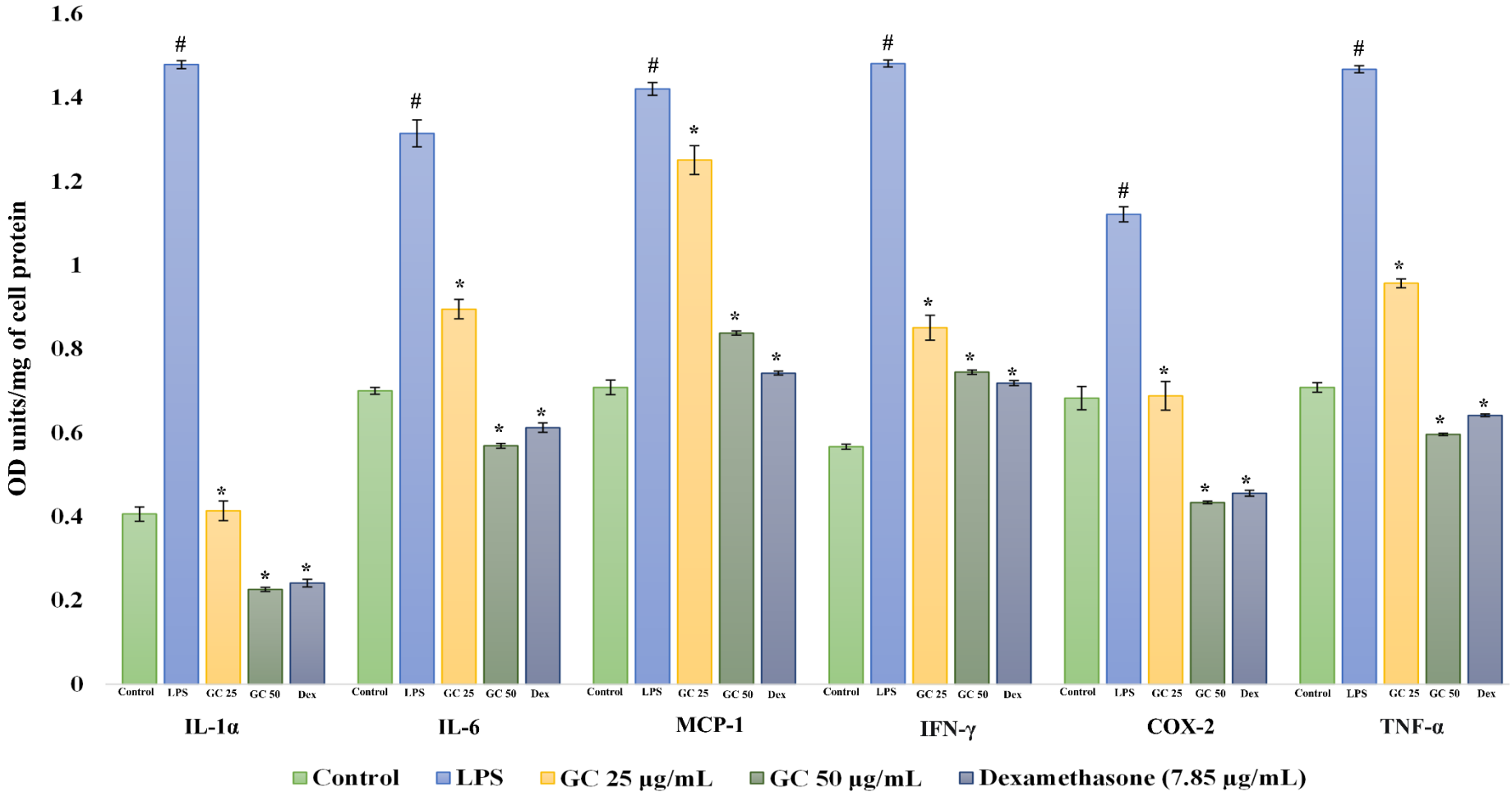

Fig. 5. 60a. Effect of GCs on the secretion of pro-inflammatory cytokines in the RAW 264.7 macrophage cells induced by LPS. $^{\#}p \leq 0.05$ (vs. control), $^{*}p \leq 0.05$ (vs. LPS)

Fig. 5.60b.

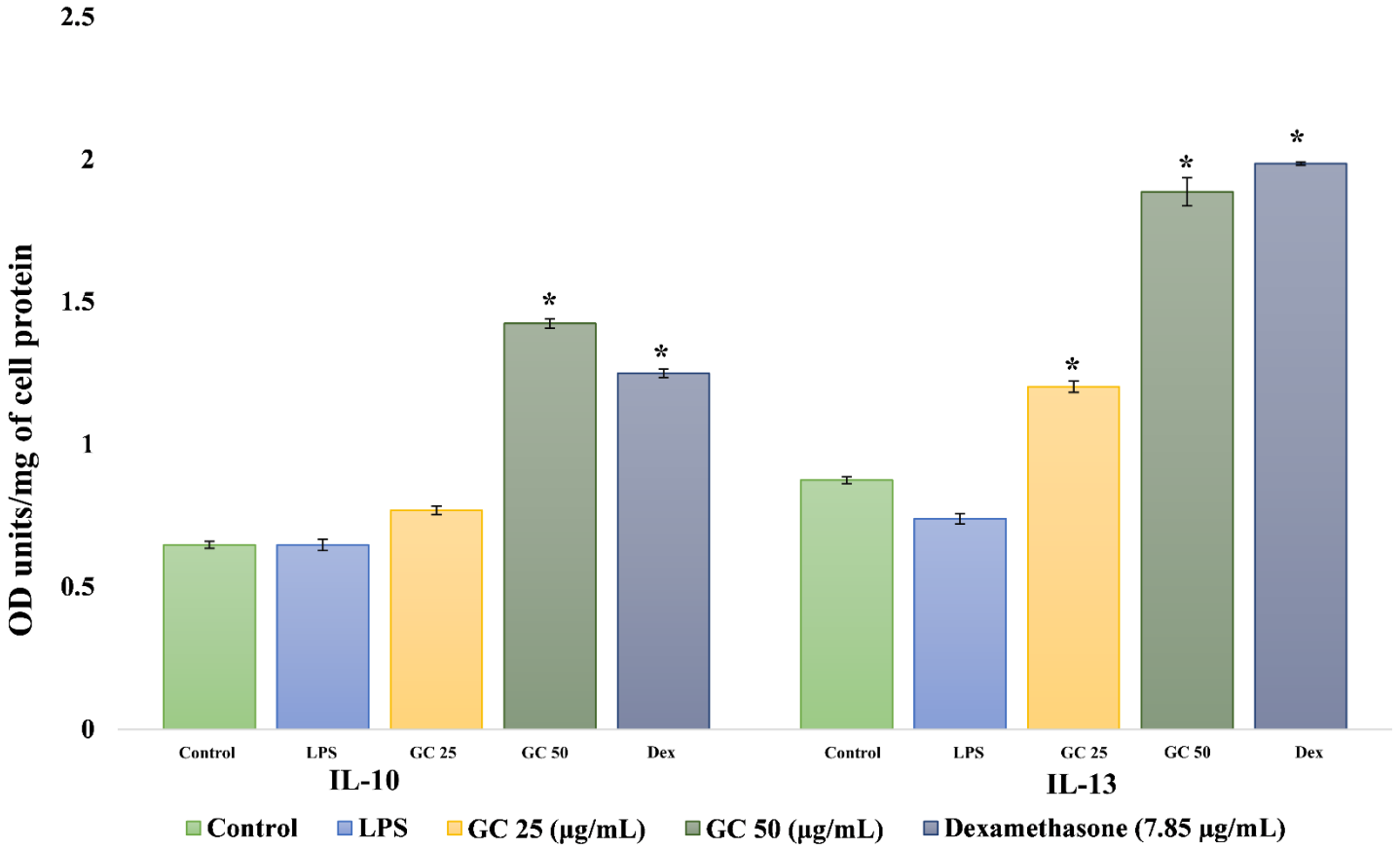

Fig. 5.60b. Effect of GCs on the secretion of anti-inflammatory cytokines in the RAW 264.7 macrophage cells induced by LPS. *p ≤ 0.05 (vs. LPS)

5.4.3. Evaluation of α-glucosidase inhibition potential of GCs

Due to the incredible therapeutic potential in the treatment of conditions like diabetes, metastatic cancer, HIV infection, and lysosomal storage diseases, glucosidase inhibitors are currently an important area of research (de Melo et al., 2006). Our study extensively evaluated the α-glucosidase inhibition potential of GCs and compared it with the standard drug acarbose (Fig. 5.61a & 5.61b). Acarbose and GC consortium demonstrated a dose-dependent α-glucosidase inhibition. However, with GCs, a dose-dependent inhibition pattern is observed within the concentration range of 0.88 μg/mL to 18 μg/mL. At 18 μg/mL concentration, GCs demonstrated nearly 100% α-glucosidase inhibition. Beyond this range, i.e., from 20 to 44 μg/mL, a plateau is evident in the inhibition curve, as maximum inhibition is achieved at the 18 μg/mL concentration itself. The study demonstrated that 87.32 ± 1.99 μg/mL of acarbose was required to inhibit 50% of α-glucosidase activity where as a remarkably lower amount i.e., 5.12 ± 0.51 μg/mL of GC consortium was only required to exhibit the same effect (Fig. 5.61c). Acarbose functions by reversibly inhibiting α-glucosidases, which leads to a decrease in the rapid increase of blood glucose levels after a meal, thereby reducing post-prandial hyperglycemia (Martin & Montgomery, 1996). A similar mechanism may be responsible for the α-glucosidase inhibition potential of GC.

It is surprising that there has been no previous literature discussing the α-glucosidase inhibition potential of GC. Even comprehensive reviews discussing the α-glucosidase inhibition potential of various bioactive compounds such as flavonoids, phenolic compounds, polysaccharides, betulinic acid, tannins, steroids, anthocyanins, galangin, procyanidins, hydroxyl-α-sanshool, hydroxyl-β-sanshool, erythritol, ganomycin, saponins, avicularin, oleanolic acids, ursolic acid, etc., also did not include GC in that category (Hossain et al., 2020; Yin et al., 2014). Our preliminary study findings indicate that GC may have the potential to be a potent α-glucosidase inhibitor, which necessitates further evaluation and confirmation.

Fig. 5.61a.

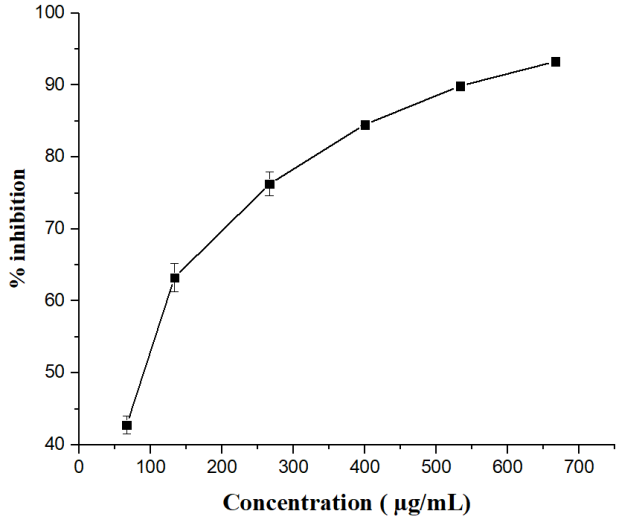

Fig. 5.61b.

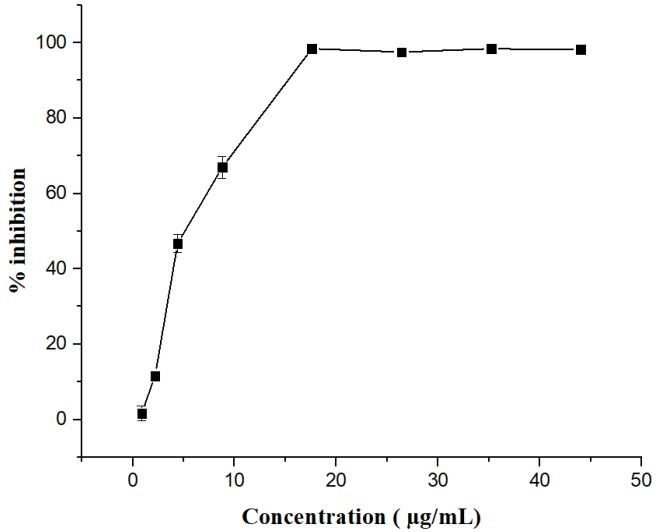

Fig. 5.61c.

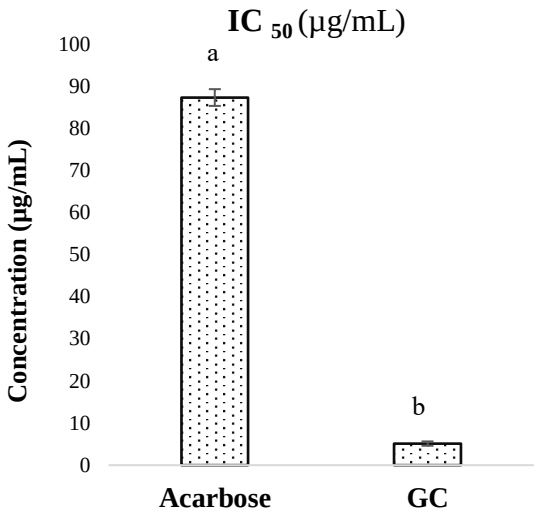

Fig. 5.61a. α-glucosidase inhibition potential of acarbose, **Fig. 5.61b.** α-glucosidase inhibition potential of GCs, **Fig. 5.61c.** IC_{50} value of acarbose and GC consortium. Standard acarbose is compared with GC consortium and means with different superscript letters in the graph show significant difference at $p \leq 0.05$

5.5. Conclusion

Unripe banana comprises more than one-fourth of its weight as peel. Our study sheds light on the scope for valorization of the unripe banana peel (*Musa* AAB) cv. Nendran. The present study demonstrates the isolation and characterization of GC molecular species. GCs are distinguished by variation in aliphatic acids conjugated as amide containing α- and ω-hydroxy fatty acids. The study further proves the anti-inflammatory potential of the isolated GCs in LPS-induced murine macrophage RAW 264.7 cells by suppressing the NO production and decreasing the secretion of pro-inflammatory cytokines. GC consortium has also shown remarkable α-glucosidase inhibition potential. The *in vitro* studies, being far away from the normal physiology of the human system, warrant further evaluation to confirm the affirmed results.

The identification of GCs in unripe banana peel, demonstrating dual anti-inflammatory and α-glucosidase inhibition properties, shows the significance of studying this matrix for wider applications. Moreover, considering the versatile benefits, including their potential use in cosmetics, GCs present a promising avenue for both functional foods and skincare formulations. The present study being the first report on GCs from the banana peel, warrants the development of a cost-effective and 'green process' for the isolation of GC from the banana peel and its effective utilization. Harnessing the therapeutic qualities of GCs may contribute to the creation of effective and multifaceted products for health and cosmetic applications.

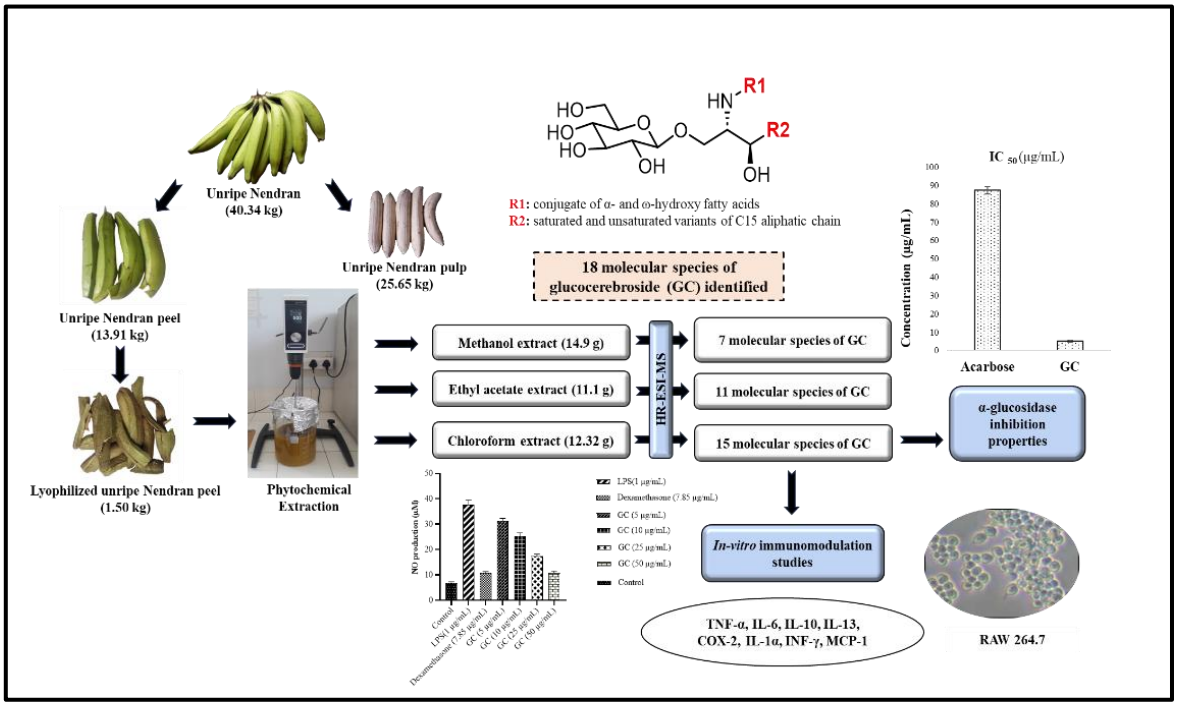

Fig. 5.62. Chapter 5 graphical abstract (Created with BioRender.com)

5.6. References

1. Avenali, M., Blandini, F., & Cerri, S. (2020). Glucocerebrosidase defects as a major risk factor for Parkinson's disease. *Frontiers in Aging Neuroscience*, *12*, 97. https://www.frontiersin.org/articles/10.3389/fnagi.2020.00097/full
2. Baek, S.-H., Park, T., Kang, M.-G., & Park, D. (2020). Anti-inflammatory activity and ROS regulation effect of sinapaldehyde in LPS-stimulated RAW 264.7 macrophages. *Molecules*, *25*(18), 4089. 10.3390/molecules25184089.
3. Bhatia, R., Tilak, P., Patil, S., Deshmukh, M., & Jain, D. (2022). Role of ceramides in skin disease and skin care formulations-A Review. *Rabindra Bharati Journal of Philosophy*, 14, 127-134. http://210.212.169.38/xmlui/handle/123456789/10785
4. Cao, Y., Zhang, X., He, X., Wang, W., Yi, Y., & Ai, Y. (2024). Efficacy of ceramide-containing sunscreen on skin barrier. *Journal of Cosmetic Dermatology*, *23*(2), 525–528. https://doi.org/10.1111/jocd.15977
5. Chiu, C.-P., Liu, S.-C., Tang, C.-H., Chan, Y., El-Shazly, M., Lee, C.-L., Du, Y.-C., Wu, T.-Y., Chang, F.-R., & Wu, Y.-C. (2016). Anti-inflammatory cerebrosides from cultivated Cordyceps militaris. *Journal of Agricultural and Food Chemistry*, *64*(7), 1540–1548. https://doi.org/10.1021/acs.jafc.5b05931
6. Coderch, L., Lopez, O., De La Maza, A., & Parra, J. L. (2003). Ceramides and Skin Function: *American Journal of Clinical Dermatology*, *4*(2), 107–129. https://doi.org/10.2165/00128071-200304020-00004
7. de Melo, E. B., da Silveira Gomes, A., & Carvalho, I. (2006). α-and β-Glucosidase inhibitors: Chemical structure and biological activity. *Tetrahedron*, *62*(44), 10277–10302. http://dx.doi.org/10.1016/j.tet.2006.08.055
8. DEMİR, K. (2021). Chapter Ten Gangliosides and Autoimmunity -Kenan Demir and Selim Görgün. *Human Autoimmunity and Associated Diseases*, 113.
9. Desplanque, M., Bonte, M.-A., Gressier, B., Devos, D., Chartier-Harlin, M.-C., & Belarbi, K. (2020). Trends in Glucocerebrosides Research: A Systematic Review. *Frontiers in Physiology*, *11*, 558090. https://www.frontiersin.org/articles/10.3389/fphys.2020.558090/full
10. Engvall, E., & Perlmann, P. (1971). Enzyme-linked immunosorbent assay (ELISA) quantitative assay of immunoglobulin G. *Immunochemistry*, *8*(9), 871–874. https://doi.org/10.1016/0019-2791(71)90454-X

11. Facchin, B. M., Dos Reis, G. O., Vieira, G. N., Mohr, E. T. B., da Rosa, J. S., Kretzer, I. F., Demarchi, I. G., & Dalmarco, E. M. (2022). Inflammatory biomarkers on an LPS-induced RAW 264.7 cell model: A systematic review and meta-analysis. *Inflammation Research*, *71*(7), 741–758. https://doi.org/10.1007/s00011-022-01584-0
12. Geller, D. A., & Billiar, T. R. (1998). Molecular biology of nitric oxide synthases. *Cancer and Metastasis Reviews*, *17*, 7–23. https://doi.org/10.1023/a:1005940202801
13. Green, L. C., Wagner, D. A., Glogowski, J., Skipper, P. L., Wishnok, J. S., & Tannenbaum, S. R. (1982). Analysis of nitrate, nitrite, and [15N] nitrate in biological fluids. *Analytical Biochemistry*, *126*(1), 131–138. https://doi.org/10.1016/0003-2697(82)90118-x
14. Hiroshi, S., Shogo, T., Kenchi, M., Akari, Y., Yoshiaki, M., & Toshio, M. (2023). Diverse effects of single molecules of rice-derived functional lipids, glucosylceramides, ceramides, and β-sitosterol glucoside, on epidermal and lung functions. *Glycative Stress Research*, *10*(3), 94–109. https://www.jstage.jst.go.jp/article/gsr/10/3/10_94/_article/-char/ja/
15. Hossain, U., Das, A. K., Ghosh, S., & Sil, P. C. (2020). An overview on the role of bioactive α-glucosidase inhibitors in ameliorating diabetic complications. *Food and Chemical Toxicology*, *145*, 111738. https://doi.org/10.1016/j.fct.2020.111738
16. Huang, H., Hu, G., Wang, C., Xu, H., Chen, X., & Qian, A. (2014). Cepharanthine, an alkaloid from Stephania cepharantha Hayata, inhibits the inflammatory response in the RAW264. 7 cell and mouse models. *Inflammation*, *37*, 235–246. https://doi.org/10.1007/s10753-013-9734-8
17. Ilan, Y., Elstein, D., & Zimran, A. (2009). Glucocerebroside: An evolutionary advantage for patients with Gaucher disease and a new immunomodulatory agent. *Immunology and Cell Biology*, *87*(7), 514–524. https://doi.org/10.1038/icb.2009.42
18. Iyer, S. S., & Cheng, G. (2012). Role of interleukin 10 transcriptional regulation in inflammation and autoimmune disease. *Critical Reviews in Immunology*, *32*(1), 23-63. https://doi.org/10.1615/critrevimmunol.v32.i1.30
19. Kahraman, E., Kaykın, M., Şahin Bektay, H., & Güngör, S. (2019). Recent advances on topical application of ceramides to restore barrier function of skin. *Cosmetics*, *6*(3), 52. https://doi.org/10.3390/cosmetics6030052
20. Kimata, H. (2006). Improvement of atopic dermatitis and reduction of skin allergic responses by oral intake of konjac ceramide. *Pediatric Dermatology*, *23*(4), 386–389. https://doi.org/10.1111/j.1525-1470.2006.00268.x

21. Kwon, H.-K., Jo, W.-R., & Park, H.-J. (2018). Immune-enhancing activity of C. militaris fermented with Pediococcus pentosaceus (GRC-ON89A) in CY-induced immunosuppressed model. *BMC Complementary and Alternative Medicine*, *18*, 1–14. https://doi.org/10.1186/s12906-018-2133-9
22. Lakshmi, S., Renjitha, J., B Sasidhar, S., & Priya, S. (2021). Epoxyazadiradione induced apoptosis/anoikis in triple-negative breast cancer cells, MDA-MB-231, by modulating diverse cellular effects. *Journal of Biochemical and Molecular Toxicology*, *35*(6), 1–17. https://doi.org/10.1002/jbt.22756
23. Leo, T. K., Tan, E. S. S., Amini, F., Rehman, N., Ng, E. S. C., & Tan, C. K. (2022). Effect of rice (Oryza sativa L.) ceramides supplementation on improving skin barrier functions and depigmentation: An open-label prospective study. *Nutrients*, *14*(13), 2737. https://www.mdpi.com/2072-6643/14/13/2737
24. Li, Q., Fang, H., Dang, E., & Wang, G. (2020). The role of ceramides in skin homeostasis and inflammatory skin diseases. *Journal of Dermatological Science*, *97*(1), 2–8. https://www.sciencedirect.com/science/article/pii/S0923181119303706
25. Margalit, M., Ghazala, S. A., Alper, R., Elinav, E., Klein, A., Doviner, V., Sherman, Y., Thalenfeld, B., Engelhardt, D., Rabbani, E., & Ilan, Y. (2005). Glucocerebroside treatment ameliorates ConA hepatitis by inhibition of NKT lymphocytes. *American Journal of Physiology-Gastrointestinal and Liver Physiology*, *289*(5), G917–G925. https://doi.org/10.1152/ajpgi.00105.2005
26. Margalit, M., Shalev, Z., Pappo, O., Sklair-Levy, M., Alper, R., Gomori, M., Engelhardt, D., Rabbani, E., & Ilan, Y. (2006). Glucocerebroside ameliorates the metabolic syndrome in OB/OB mice. *Journal of Pharmacology and Experimental Therapeutics*, *319*(1), 105–110. https://jpet.aspetjournals.org/content/319/1/105.short
27. Martin, A. E., & Montgomery, P. A. (1996). Acarbose: An α-glucosidase inhibitor. *American Journal of Health-System Pharmacy*, *53*(19), 2277–2290.
28. Martinez-Espinosa, I., Serrato, J. A., & Ortiz-Quintero, B. (2021). Role of IL-10-producing natural killer cells in the regulatory mechanisms of inflammation during systemic infection. *Biomolecules*, *12*(1), 4. https://doi.org/10.3390%2Fbiom12010004
29. Mosmann, T. (1983). Rapid colorimetric assay for cellular growth and survival: Application to proliferation and cytotoxicity assays. *Journal of Immunological Methods*, *65*(1–2), 55–63. https://doi.org/10.1016/0022-1759(83)90303-4
30. Oliveira, L., Freire, C., Silvestre, A., Cordeiro, N., Torres, I., & Evtuguin, D. (2006). Lipophilic extractives from different morphological parts of banana plant “Dwarf

Cavendish." *Industrial Crops and Products*, *23*(2), 201–211. http://dx.doi.org/10.1016/j.indcrop.2005.06.003

31. Pistia-Brueggeman, G., & Hollingsworth, R. I. (2001). A preparation and screening strategy for glycosidase inhibitors. *Tetrahedron*, *57*(42), 8773–8778. http://dx.doi.org/10.1016/S0040-4020(01)00877-8
32. Saranya, J., Shilpa, G., Raghu, K. G., & Priya, S. (2017). Morus alba leaf lectin (MLL) sensitizes MCF-7 cells to anoikis by inhibiting fibronectin mediated integrin-FAK signaling through ras and activation of P38 MAPK. *Frontiers in Pharmacology*, *8*, 220849. https://doi.org/10.3389/fphar.2017.00034
33. Smith, P. etal, Krohn, R. I., Hermanson, G., Mallia, A., Gartner, F., Provenzano, Md., Fujimoto, E., Goeke, N., Olson, B., & Klenk, D. (1985). Measurement of protein using bicinchoninic acid. *Analytical Biochemistry*, *150*(1), 76–85. https://doi.org/10.1016/0003-2697(85)90442-7
34. Spada, F., Barnes, T. M., & Greive, K. A. (2018). Skin hydration is significantly increased by a cream formulated to mimic the skin’s own natural moisturizing systems. *Clinical, Cosmetic and Investigational Dermatology*, *Volume 11*, 491–497. https://doi.org/10.2147/CCID.S177697
35. Uchida, Y., & Park, K. (2021). Ceramides in Skin Health and Disease: An Update. *American Journal of Clinical Dermatology*, *22*(6), 853–866. https://doi.org/10.1007/s40257-021-00619-2
36. Varki, A., Cummings, R., Esko, J., Freeze, H., Hart, G., & Marth, J. (1999). Glycosphingolipids. In *Essentials of Glycobiology*. Cold Spring Harbor Laboratory Press. https://www.ncbi.nlm.nih.gov/books/NBK20699/
37. Yin, Z., Zhang, W., Feng, F., Zhang, Y., & Kang, W. (2014). α-Glucosidase inhibitors isolated from medicinal plants. *Food Science and Human Wellness*, *3*(3–4), 136–174. https://doi.org/10.1016/j.fshw.2014.11.003
38. Zhang, J.-M., & An, J. (2007). Cytokines, inflammation, and pain. *International Anesthesiology Clinics*, *45*(2), 27–37. https://doi.org/10.1097%2FAIA.0b013e318034194e
39. Zhu, Y., Soroka, D. N., & Sang, S. (2013). Structure Elucidation and Chemical Profile of Sphingolipids in Wheat Bran and Their Cytotoxic Effects against Human Colon Cancer Cells. *Journal of Agricultural and Food Chemistry*, *61*(4), 866–874. https://doi.org/10.1021/jf3047863

40. Zou, F., Tan, C., Zhang, B., Wu, W., & Shang, N. (2022). The valorization of banana by-products: Nutritional composition, bioactivities, applications, and future development. *Foods*, *11*(20), 3170. https://doi.org/10.3389/fnagi.2020.00097

Chapter 6

Bioactive components in banana peel and scope for value addition

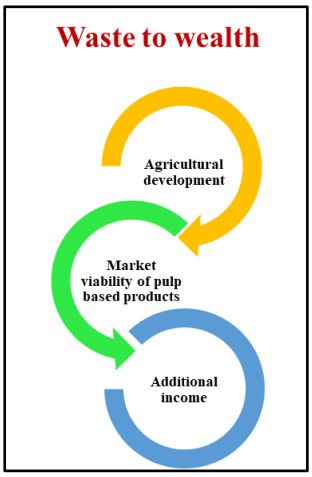

(Created with Microsoft Power Point)

6.1. Introduction

6.1.1. From waste to wealth: food waste and byproduct upcycling to functional ingredients

The UN 2030 agenda for sustainable development is a plan of action for people, the planet, and prosperity with 17 interconnected goals to achieve a better and more sustainable future for all (*Transforming Our World: The 2030 Agenda for Sustainable Development* n.d.). With a primary focus on 'no poverty, zero hunger, good health, and well-being' this plan calls for actions focused on eliminating waste and maximizing the food resources. Bioactive components including bioactive carbohydrates, specific minerals, fatty acids, proteins, antioxidants, prebiotics, vitamins, etc., imparts great health benefits. Hence the upcycling of food waste or byproducts such as peel or seed to functional foods is of paramount significance (Samtiya et al., 2021).

In addition to continuing efforts to decrease food waste, there is still an urgent need for the adoption of new methods and technologies to reach a zero-waste food system. In addition to the consumer-generated waste, the vegetable, fruit, meat, and grain processing industries generate millions of tonnes of food waste annually. This is a huge reservoir of beneficial non-nutrients like pigments, dietary fiber, prebiotics, and bioactive phytochemicals, as well as recyclable macromolecules and micronutrients like proteins, vitamins, and minerals (Udenigwe, 2023). Considerable scientific work has been dedicated to repurposing food waste and byproducts to create products with added value. This strategy has also been proposed as a means of addressing malnutrition and advancing a sustainable food system in rural regions, especially in low- and middle-income countries (LMICs), by creating niche markets and small businesses (Udenigwe, 2023).

6.1.2. Significance of banana peel as a source of bioactive components

In a society, where eating habits and lifestyle choices are rapidly changing, the critical role of a healthy digestive system in overall well-being is becoming increasingly evident. This

recognition has led to the development of foods aimed at digestive health, thereby indirectly improving general wellness. The primary factors that sustain a healthy gut are the prebiotic components like bioactive carbohydrates, probiotic gut flora, and the nutrients that they metabolize (Brouns et al., 2002). Bioactive carbohydrates, including dietary fiber, RS, and oligosaccharides, are vital for gut health, immune function, and metabolic regulation (Cummings et al., 2004; Raigond et al., 2015). Several epidemiological studies suggest that the population with high dietary fiber intake has a 25-35% reduced risk of developing colorectal cancer (Brouns et al., 2002). Fermentation of RS in the large intestine produces SCFA, especially butyrate, the primary nutrient for the colonocytes, and thereby plays a crucial role in colon health (Chen et al., 2024; Lockyer & Nugent, 2017). Oligosaccharides, such as FOS, GOS, and inulin exert prebiotic benefits mainly by promoting the growth of bifidobacteria species (Cummings et al., 2004; Hughes et al., 2022). Hence when consumed in adequate amounts these components support digestive health and thereby reduce the risk of several chronic lifestyle diseases, such as obesity, cancer, type II diabetes (*IDA-Position-Paper-Fibre-24.12.18.Pdf*, n.d.).

WHO recommends a daily fiber intake of 25 g (*WHO Updates Guidelines on Fats and Carbohydrates*, n.d.), yet many people fall short of this target. This motivated us to look into the bioactive carbohydrate content of raw banana peel, a major waste material of banana processing industries, for functional food development. Banana (*Musa* sp.) an important member of the Musaceae family, is a widely cultivated and consumed fruit crop around the tropical and subtropical regions (H. M. Zaini et al., 2022). Banana peels, comprising approximately 35% of the weight of bananas, are a significant by-product often discarded. With around 40 million tonnes generated annually, most of these peels are often dumped in landfills. This valuable resource is frequently wasted due to ineffective agricultural waste management practices and lack of awareness.

Banana peel harbours a diverse array of nutrients and bioactive compounds, such as tannins, flavones, steroids, polyphenols, flavanols, sterols, carotenoids, flavanones, triterpenoids, anthocyanins, etc. (Hikal et al., 2022). This rich composition underscores its significant therapeutic potential, including anti-microbial, antioxidant, anti-diabetic, anti-cancer, and anti-inflammatory properties (Hashim et al., 2023; Kumari et al., 2023; H. M. Zaini et al., 2022). Raw banana peel is a popular ingredient in Indian, Southeast Asian, and Caribbean cuisine. Banana peel is used as animal feed, it has applications in bioremediation and food packaging (Zou et al., 2022). The unripe peel of the ‘Saba’ variety was used to develop sausage with high

dietary fiber (H. B. M. Zaini et al., 2020). Peel is also used for the preparation of jelly, yellow noodles, biscuits, banana peel flakes, instant soup mix, ready-to-cook curry mix, sauce, and edible food wrappers (Bhavani et al., 2023; H. M. Zaini et al., 2022).

In Southern states of India, especially in Kerala, unripe Nendran pulp is used for making banana chips, and Nendran peel is the primary waste material generated during the processing. Similarly, in BG preparation also the industry will face issues with raw Nendran peel waste. The effective utilization of the peel will enhance the market viability of banana pulp-based products. Even though Nendran peel is included in many culinary preparations in Nendran prevalent areas, and is recognized for its anti-diabetic potential traditionally, there is no literature data on the bioactive carbohydrate content of Nendran peel and its value addition potential. Therefore, in this chapter, we have evaluated the bioactive carbohydrate content and the scope for of value addition of raw Nendran peel.

6.2. Objectives

Recognizing the potential of banana peel as a source of bioactive carbohydrates and its significance in the functional food industry, the following objectives have been formulated to evaluate the bioactive carbohydrate content and value addition scope of Nendran peel.

- Analysis of proximate composition and bioactive carbohydrate content (total dietary fiber content, fructan, and RS) of unripe peel.
- Estimation of total phenol content (TPC) and total flavonoid content (TFC).
- Assessment of *in vitro* immunomodulatory potential of methanolic extract of peel.
- Evaluation of α-glucosidase inhibition potential of methanolic extract of peel.

6.3. Materials and methods

6.3.1. Chemicals and reagents

Details of chemicals and reagents used for *in vitro* immunomodulatory and α-glucosidase inhibition assay are mentioned under the materials and methods section 5.3.1. of Chapter 5. The digestible and RS assay kit (K-DSTRS), fructan assay kit (K-FRUC), and total dietary fiber assay kit (K-TDFR) were procured from Megazyme Ltd, Ireland.

6.3.2. Raw material collection

For the studies, mature Nendran infructescence (21.14 kg) was purchased from local organic farmers in Vellayani, Thiruvananthapuram District, Kerala, India. The peel (6.21 kg) and pulp (11.61 kg) were separated. The pulp was utilized for the production of the novel product ‘BG and the peel was used for the studies outlined in this chapter. A portion of peel (100 g) was

utilized for the proximate composition analysis and the remaining portion (6.11 kg) was subjected to lyophilization. The lyophilized peel (0.63 kg) was used for the measurement of fructan content, fiber content, and for the preparation of the MeOH extract of the peel.

6.3.3. Proximate composition and bioactive carbohydrate content of the banana peel

The proximate analysis of the unripe Nendran peel was done according to the AOAC method (AOAC, 2005). The starch content of the peel i.e., RDS, SDS, TDS, and RS was measured using the digestible and RS assay kit (K-DSTRS). The fructan assay kit (K-FRUC) was employed for the measurement of fructan content in the peel. This kit offers validated methods for fructan determination, as outlined by AOAC standards, including AOAC method 999.03 for foods, AOAC method 2018.07 for animal feed, and AOAC method 2016.14 for infant formula and adult nutritionals (*Fructan Assay Kit*, n.d.). The K-TDFR assay kit was used to analyze total, soluble, and insoluble dietary fiber content. This method has been officially recognized by both AOAC and AACC (AOAC 991.43, AOAC 985.29, AACC 32-07.01, and AACC 32-05.01) (*Total Dietary Fiber Assay Kit*, n.d.).

6.3.4. MeOH extraction of banana peel

Lyophilized banana peel (200 g) was powdered and passed through mesh 10 before being extracted with MeOH (2 L) for 6 hours at 500 rpm using an overhead stirrer (Hei-TORQUE 100, Heidolph, Germany). After 6 hours, the extract was collected and filtered using Whatman no. 1 filter paper with a Buchner funnel. The extracts were concentrated under vacuum with a rotary evaporator (Hei-vap, Heidolph, Germany). This procedure was repeated twice, and the resulting extracts were combined, yielding 9.07 g of MeOH extract. This MeOH extract of banana peel (BPM) was utilized to assess the TPC and TFC of unripe banana peel, α-glucosidase inhibition potential, and evaluation of immunomodulatory potential in LPS-stimulated murine macrophage RAW 264.7 cells.

6.3.5. Evaluation of TPC

The TPC of BPM was evaluated according to the method developed by Singleton and Rossi. The gallic acid was used as standard and the stock solution was prepared by dissolving 0.5 g of gallic acid in 10 mL ethanol and made up to 100 mL using distilled water. The calibration curve was plotted with concentrations ranging from 100 to 500 µg/mL. A 20 µL of solution containing different concentrations of standards and samples was separately added to test tubes and then mixed with 100 µL of Folin-Ciocalteu reagent followed by 2.38 mL of distilled water. Tubes were incubated at room temperature (28 ºC) for 8 minutes and added 600 µL of 20% sodium carbonate solution. After 2 hours of incubation, the absorbance was measured at 765

nm with a UV-VIS spectrophotometer 2600 (Shimadzu, Japan), and the results were expressed as mg gallic acid equivalents/g dw (mg GAE/g) (Singleton & Rossi, 1965).

6.3.6. Evaluation of TFC

The TFC of BPM was measured using the aluminium chloride colorimetric method. The standard quercetin (25 mg) was dissolved in 50 mL of 80% ethanol and the calibration curve was plotted with the concentration ranging from 5 to 50 µg/mL. In each test tube, 1 mL of the solution containing various concentrations of standards and samples was combined with 1.5 mL of 95% ethanol, 0.1 mL of 10% aluminum chloride, 0.1 mL of 1M potassium acetate, and 2.8 mL of distilled water. The absorbance of the resulting mixture was then measured at 415 nm after 30 minutes of incubation at room temperature (28 ºC). The results were expressed as mg quercetin equivalent/g dw (mg QE/g) (Chang et al., 2002).

6.3.7. Evaluation of immunomodulatory effects of BPM

The immunomodulatory effects of BPM were assessed in LPS-stimulated murine macrophage RAW 264.7 cells by examining BPM's impact on NO production, as well as in the secretion of both pro-inflammatory and anti-inflammatory cytokines. BPM (10 mg) was dissolved in 60 µL of DMSO and then diluted with cell culture medium to achieve the required concentrations for treatments.

6.3.7.1. Determination of cell viability by MTT assay

The assay protocol was detailed under the materials and method section 5.3.4.5. of Chapter 5. BPM of concentrations 25, 50, 100, and 200 µg/mL were used to assess the extract's cytotoxic effect.

6.3.7.2. Evaluation of the role of BPM on NO production

BPM at concentrations 25, 50, and 100 µg/mL were evaluated for their NO inhibition potential. The protocol is detailed under the materials and method section 5.3.4.6. of Chapter 5.

6.3.7.3. Evaluation of pro and anti-inflammatory cytokines production

The effect of BPM (100 µg/mL) on pro and anti-inflammatory cytokines production was evaluated through ELISA analysis as mentioned in the materials and method section 5.3.4.7. of Chapter 5.

6.3.8. Evaluation of α-glucosidase inhibition potential of BPM

BPM at six concentrations (2 to 100 µg/mL) was used for assessing the α-glucosidase inhibition potential according to the method described in the materials and method section 5.3.4.8. of Chapter 5.

6.3.9. Statistical analysis

All the experiments, except the determination of soluble and insoluble fiber content (n=1), were carried out in triplicates (n=3) and the data were expressed as the mean ± SD. The data was statistically analyzed by IBM-SPSS 26 (SPSS Inc., Chicago, USA). ANOVA followed by Tukey's post hoc tests was used for multiple comparisons analysis, and $P \leq 0.05$ is considered significant. To compare the IC_{50} value of acarbose and BPM an independent sample t-test was used.

6.4. Results and discussion

6.4.1. Proximate composition and bioactive carbohydrate content of unripe Nendran peel

Unripe Nendran peel has a moisture content of 90.17 ± 0.2%, fat, protein, ash, and carbohydrate content were 0.63 ± 0.02%, 2.03 ± 0.11%, 1.27 ± 0.08% and 5.90 ± 0.30% respectively (Table 6.1.).

Table 6.1. Proximate composition of unripe Nendran banana peel

Parameters	Amount (%)
Moisture	90.17 ± 0.20
Ash	1.27 ± 0.08
Fat	0.63 ± 0.02
Protein	2.03 ± 0.11
Carbohydrate (by difference)	5.90 ± 0.30

Mean±SD (n=3)

Since the fresh banana peel showed a protein content of 2.03%, 100 g of lyophilized peel is expected to contain 20% protein, indicating that lyophilized peel can be an excellent source of protein. Currently, vegetable protein receives an overwhelming interest and given the high amount of protein in the peel, protein quality has to be assessed for its efficient utilization in functional foods. Further, the lyophilized peel contains 31.95 ± 0.83% of total starch with a notable portion of RS (18.11 ± 0.06%), TDS content of 13.64±0.01%, RDS content of 2.30 ± 0.15%, and SDS content of 5.87 ± 0.19% (Table 2.). The total dietary fiber content of

lyophilized Nendran peel was 26.87±0.92%, comprising 21.98% and 3.97% of soluble and insoluble dietary fibers respectively. The fructan content, which is soluble dietary fiber, was found to be 1.34±0.31 % (Table 2.). The presence of a notable amount of protein, dietary fiber, and RS indicates the scope for utilization of it as a functional food. Consumption of dietary fiber imparts numerous health benefits. Individuals with higher dietary fiber intake appear to have a significantly lower risk of developing coronary heart disease, cancer, stroke, hypertension, diabetes, obesity, gastrointestinal diseases and provide general digestive health (Anderson et al., 2009). Health benefits associated with dietary fiber consumption are detailed in the result and discussion section 2.4.2. of Chapter 2. The presence of a significant amount of bioactive carbohydrates in the banana peel indicates the scope for the development of functional food and pre-biotic supplements from unripe Nendran peel.

Table 6.2. Bioactive carbohydrate content of unripe Nendran peel

Parameter	Amount (%)*
Total starch (TDS+RS)	31.95 ± 0.83
RDS (0-20 minutes)	2.30±0.15
SDS (20-120 minutes)	5.87±0.19
TDS (0-240 minutes)	13.64±0.01
RS (starch not digested within 240 minutes)	18.11±0.06
Total dietary fiber	26.87±0.92
Insoluble fiber#	21.98
Soluble fiber#	3.97
Fructan	1.34±0.31

RDS (0-20 minutes)- rapidly digestible starch, SDS (20-120 minutes)- slowly digestible starch, TDS (0-240 minutes)- total digestible starch, RS (starch not digested within 240 minutes)- resistant starch
*Dry weight basis mean±SD (n=3), #n=1.

6.4.2. Evaluation of TPC &TFC content

The TPC and TFC values of Nendran peel were 35.20 ± 1.10 mg GAE/100 g and 17.12 ± 0.90 mg QE/100 g db respectively. The reported high TPC and TFC content of Nendran peel indicates the antioxidant potential of peel. Literature data shows that different banana cultivars exhibit varying levels of TPC and TFC content. Aquino et al., 2016, compared the TPC content of unripe peel of 15 banana cultivars in Brazil and the TPC value showed a range from 29.02 to 61 mg GAE/100g wb (Aquino et al., 2016). The TPC and TFC values vary with the solvents and extraction methods adopted for the study (Chaudhry et al., 2022).

6.4.3. Evaluation of immunomodulatory effects of BPM

6.4.3.1. Determination of cell viability by MTT assay

Before assessing the *in vitro* immunomodulatory effects of banana peel MeOH extract, a preliminary assessment of its cytotoxicity was conducted to find a safe dosage for subsequent immunomodulation studies. The MTT assay was employed to assess the cytotoxicity of BPM. Samples at concentrations of 25, 50, 100, and 200 µg/mL were tested, and the results are presented in Fig. 6.1. BPM at a concentration of 25 µg/mL had negligible effects on cell viability, showing no significant difference compared to the control group. However, as the concentration increased from 50 to 200 µg/mL, a notable decrease in RAW 264.7 macrophage viability was observed. At the highest concentration tested (200 µg/mL), cell viability was 83.94 ± 0.56%. Thus, BPM concentrations ranging from 25 to 100 µg/mL were chosen for further investigation of their impact on NO production in the cells.

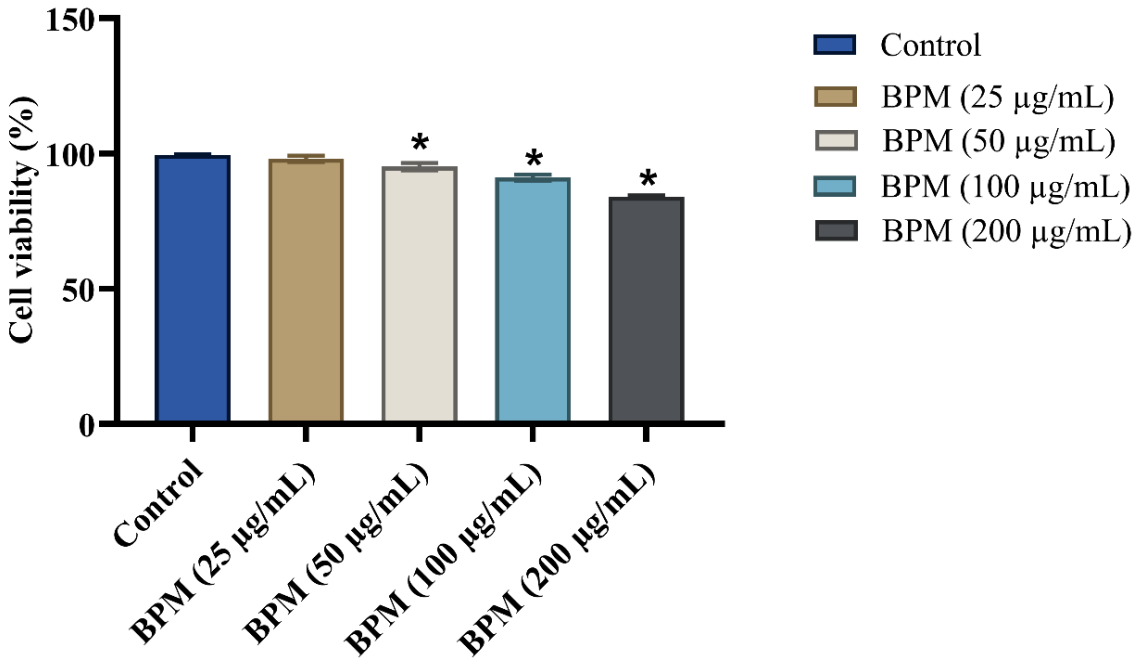

Fig. 6.1. Effect of BPM on the viability of RAW 264.7 cells. The cells were treated with BPM of concentrations ranging from 25 to 200 µg/mL and viability (%) was assessed after 24 hours of exposure and significance was determined through ANOVA, *$p \leq 0.05$ (vs. control)

6.4.3.2. Evaluation of NO production by Griess reaction

The RAW 264.7 murine macrophage cell line has been extensively employed in research to investigate the anti-inflammatory properties of various molecules and extracts. LPS, a key component of Gram-negative bacterial cell walls, triggers immediate inflammatory reactions by promoting the secretion of various inflammatory cytokines in diverse types of cells. Consequently, it is employed in experimental models to elicit inflammation (Skrzypczak-Wiercioch & Sałat, 2022). Following activation by LPS, macrophages initiate the inflammatory cascade by upregulating the production of NO, reactive oxygen species, and proinflammatory cytokines like TNF-α, COX-2, and IL-6 (Tian et al., 2021). The inhibition of these proinflammatory cytokines and mediators is a critical approach in treating inflammatory disorders. Consequently, the potential of BPM to suppress NO production and modulate the release of both pro and anti-inflammatory cytokines was investigated. To the best of our knowledge, there have been no reports discussing the *in vitro* anti-inflammatory potential of unripe Nendran peel.

LPS stimulation significantly elevated NO production in the RAW 264.7 cells, while treatment with BPM led to a dose-dependent suppression of NO production (Fig. 6.2.). Upon LPS treatment, NO production rose from the basal level of 8.31 ± 0.91 µM (control) to 44.85 ± 4.13 µM. Dexamethasone significantly reduced NO production to 27.27 ± 0.24 µM compared to LPS-treated groups. BPM at concentrations of 25 and 50 µg/mL exhibited significant reductions in NO production to 36.40 ± 3.36 µM and 30.89 ± 2.17 µM, respectively. Interestingly, BPM at a dose of 100 µg/mL demonstrated a reduction in NO production to 25.01 ± 2.09 µM, comparable to dexamethasone (27.27 ± 0.24 µM) (Fig. 6.2). Based on these assay results, BPM at a concentration of 100 µg/mL was chosen for ELISA analysis. The LPS-induced macrophages express transcriptionally inducible iNOS and thereby produce high amounts of NO (Francisco et al., 2011). The extract's ability to suppress iNOS activation may be the reason behind the observed dose-dependent reduction of NO production in the cells. Currently, dexamethasone is commonly used for treating inflammatory conditions, including rheumatoid arthritis, and pneumonia. However, it is associated with adverse effects such as weight gain, cardiovascular complications, cataracts, and osteoporosis. Hence, the quest for novel drugs with anti-inflammatory properties is of great importance (Tian et al., 2021). Our preliminary findings on the effect of BPM on NO production suggest the potential anti-inflammatory properties of unripe Nendran banana peel.

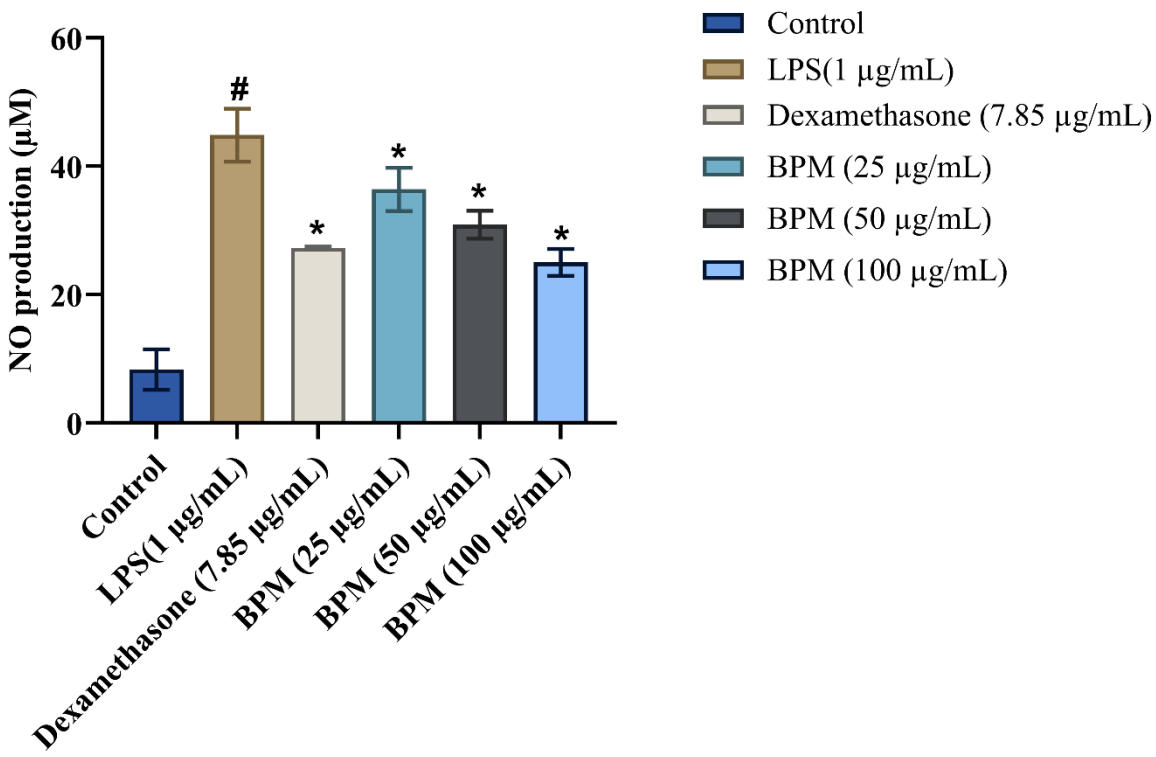

Fig. 6.2. Effect of BPM on the NO production of RAW 264.7 cells induced by LPS. The cells were treated with BPM of concentrations ranging from 25 to 100 µg/mL and NO production (µM) was assessed after 24 hours of exposure and significance was determined through ANOVA, $^{\#}p \leq 0.05$ (vs. control), $*p \leq 0.05$ (vs. LPS)

Despite extensive literature data on the antioxidant potential of banana peel, there is limited research focusing on its anti-inflammatory properties. Aqueous extract of fresh ripe peel of *Musa sapientum* Linn. showed highest NO inhibitory activity when compared with both fresh and dried unripe peel (MPharm, 2012). Similarly, 80% ethanol extract of *Musa sapientum* banana peel reduced inflammatory response by suppressing transcription factors such as NF-κB (Arlinda Silva Prameswari et al., 2017). The butanol fraction of Cavendish (AAA) banana peel generated from the peel's ethanol extract showed an anti-inflammatory response by inhibiting IL-6 and TNF-α secretion and down-regulating iNOS and COX-2 protein expression in LPS stimulated RAW264.7 macrophages (Hong et al., 2023). Our study is the first report on the anti-inflammation potential of unripe Nendran peel.

6.4.3.3. Effect of BPM on pro and anti-inflammatory cytokines secretion

The impact of BPM on modulating the secretion of inflammatory cytokines was evaluated at a concentration of 100 µg/mL. BPM significantly inhibited the release of pro-inflammatory

cytokines such as MCP-1, IFN-γ, IL-1α, TNF-α, COX-2, and IL-6 in comparison to cells treated solely with LPS (Fig. 6.3a.). Furthermore, BPM promoted the secretion of anti-inflammatory cytokines IL-10 and IL-13 (Fig. 6.3b.). Notably, BPM even outperformed dexamethasone in increasing the production of the anti-inflammatory cytokine IL-10. IL-10 functions predominantly as an anti-inflammatory agent, safeguarding the body against excessive immune reactions, particularly via the Jak1/Tyk2 and STAT3 signalling pathways. Moreover, it helps mitigate tissue damage and organ impairment following injury (Carlini et al., 2023).

The significant levels of TPC and TFC observed in BPM suggest the presence of polyphenols and flavonoids, which could contribute to their anti-inflammatory properties. Our studies in the unripe Nendran peel revealed the presence of eighteen molecular species of GC with potent anti-inflammation potential (detailed in Chapter 5). The presence of these compounds may be the reason behind the observed anti-inflammation potential of BPM. Recent studies demonstrate that natural bioactive compounds capable of enhancing IL-10 expression may serve as an effective strategy for preventing inflammation by elevating IL-10 levels (Carlini et al., 2023). The observed increase in IL-10 expression following BPM treatment underscores the potential of BPM as an immunomodulatory agent.

Fig. 6.3a.

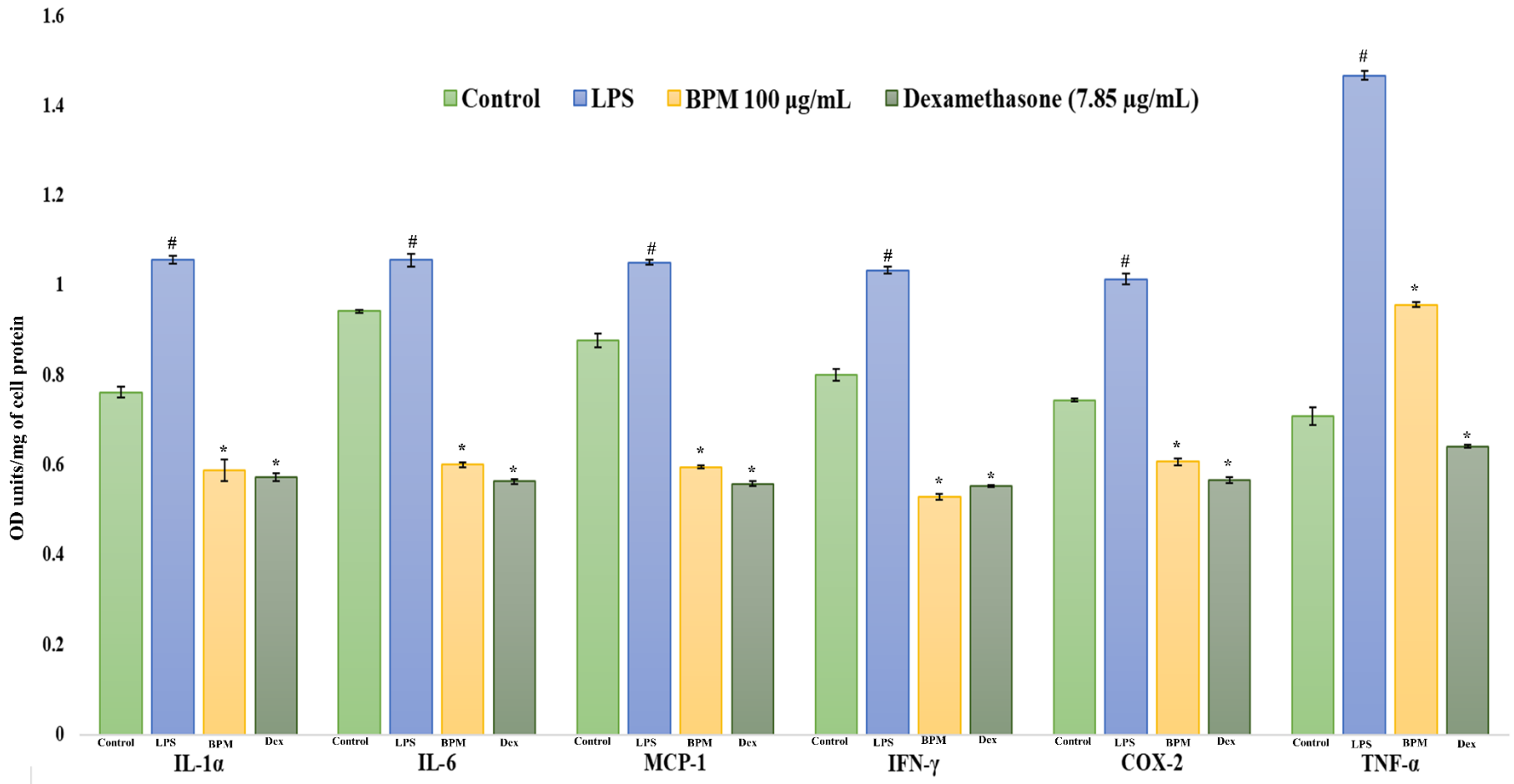

Fig. 6.3a. Effect of BPM on the secretion of pro-inflammatory cytokines in the RAW 264.7 macrophage cells induced by LPS. $^{\#}p \leq 0.05$ (vs. control), $^{*}p \leq 0.05$ (vs. LPS)

Fig. 6.3b.

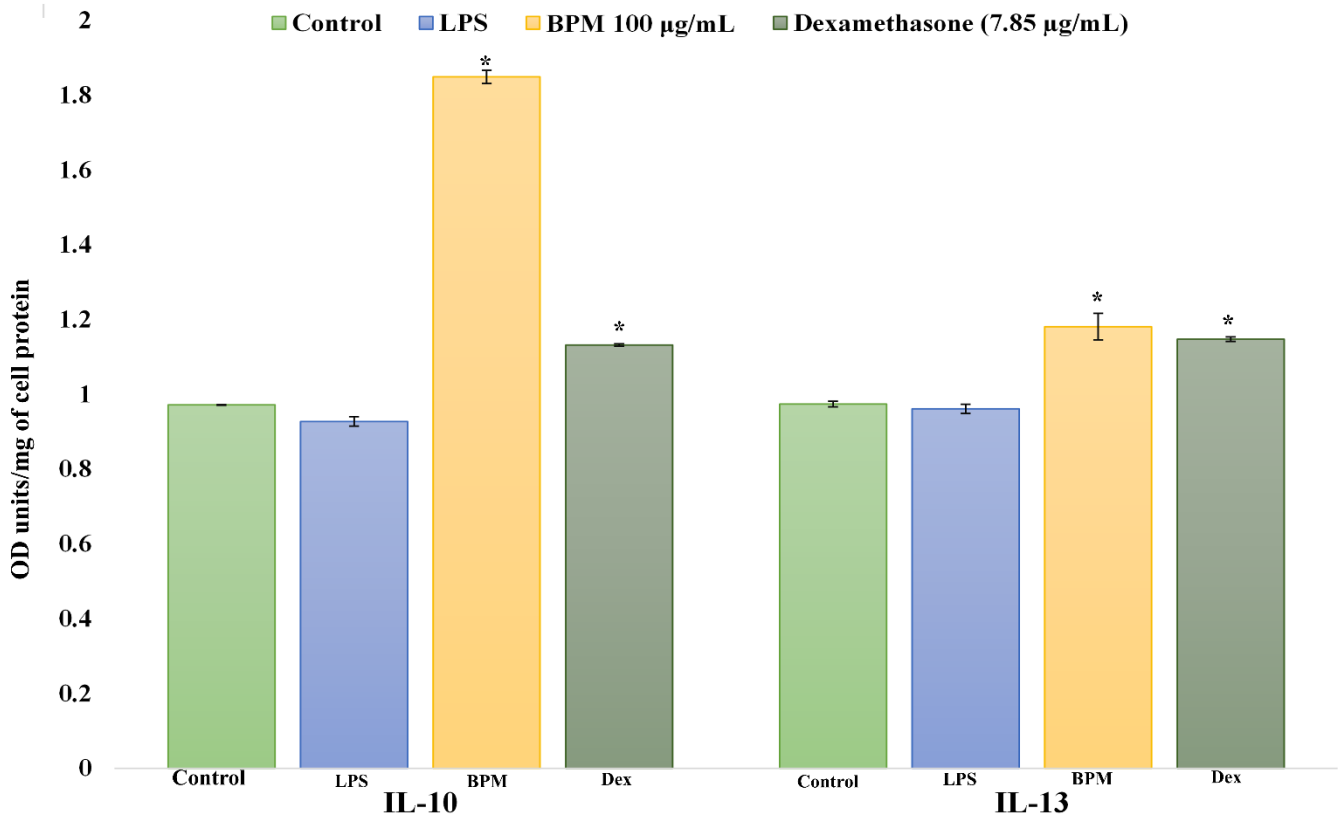

Fig. 6. 3b. Effect of BPM on the secretion of anti-inflammatory cytokines in the RAW 264.7 macrophage cells induced by LPS. *$p \leq 0.05$ (vs. LPS)

6.4.4. Evaluation of α-glucosidase inhibition potential of BPM

The α-glucosidase enzyme catalyzes carbohydrate digestion in the intestine and inhibition of this enzyme is one effective therapeutic strategy for controlling hyperglycemia associated with type-2 diabetes (Agrawal et al., 2022; Dirir et al., 2022; Hossain et al., 2020). Apart from its role in the regulation of postprandial hyperglycemia, α-glucosidase inhibitors are potent broad-spectrum anti-viral agents. The commercially available α-glucosidase inhibitors comprise acarbose, miglitol, voglibose, emiglitate, and castanospermine (Agrawal et al., 2022). Although these inhibitors are potential therapeutic agents, their usage is often associated with undesirable gastrointestinal side effects. Consequently, ongoing research endeavors aim to discover novel inhibitors characterized by enhanced efficacy and reduced side effects. Given the traditional use of banana peel in diabetes management, there exists promising potential for this matrix to serve as a valuable reservoir of therapeutic agents with α-glucosidase inhibition properties.

Our study revealed that BPM exhibits a significant level of α-glucosidase inhibition potential, which is comparable with that of the standard drug acarbose (Fig. 6.4a. &Fig. 6.4b.). Both acarbose and BPM exhibited dose-dependent α-glucosidase inhibition. The IC_{50} value of acarbose was found to be 85.95 ± 4.23 µg/mL whereas a relatively lower amount i.e., 58.42 ± 0.45 µg/mL of BPM was only required to impart the same effect (Fig. 6.4c.). The standard drug acarbose is a pseudo-tetrasaccharide that is composed of a nitrogen-bonded valienol moiety attached to isomaltotriose. It exhibits a higher binding affinity (10^4-10^5 times) than natural oligosaccharides for α-glucosidases and inhibits the enzyme competitively. Due to the formation of a hydrogen bond between ASP 568 in the enzyme's active site and the hydrogen atom of the amine group in acarbose, the binding affinity of acarbose to the enzyme is significantly higher than that of typical sugar substrates (Dirir et al., 2022). Comprehensive investigations are essential to elucidate the mechanism underlying the α-glucosidase inhibition potential of BPM. Further studies are warranted to isolate and identify the molecules responsible for the α-glucosidase inhibition capability to Nendran peel.

Fig. 6.4a.

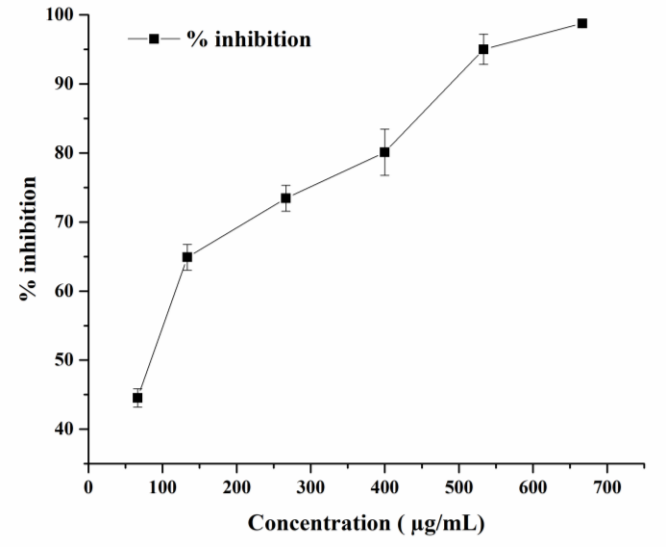

Fig. 6.4b.

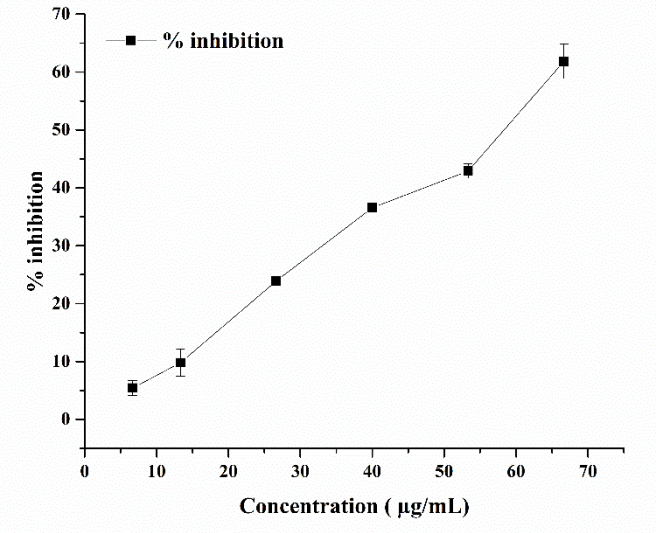

Fig. 6.4c.

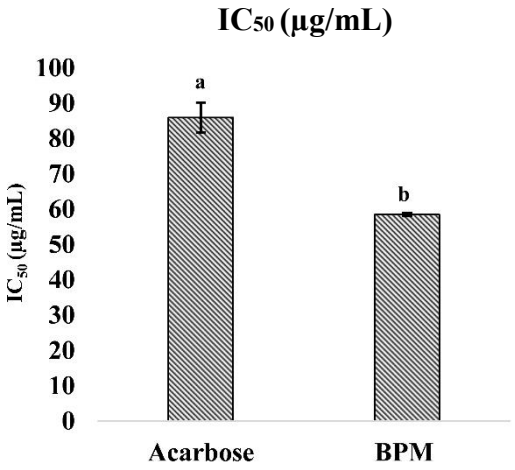

Fig. 6.4a. α-glucosidase inhibition potential of acarbose, **Fig. 6.4b.** α-glucosidase inhibition potential of BPM, **Fig. 6.4c.** IC_{50} value of acarbose and BPM. Standard acarbose is compared with BPM and means with different superscript letters in the graph show significant difference at $p \leq 0.05$

6.5. Conclusion

Bioactive carbohydrates, including dietary fiber, RS, and oligosaccharides, are pivotal in promoting gut health and enhancing immune function. Recognizing their significance, the WHO recommends a daily fiber intake of 25 g to support optimal health. Banana peel is a major waste from the raw banana processing industry. Considering its potential application in the functional food industry we have studied the bioactive carbohydrates in lyophilized raw Nendran banana peel. Through this work, we have identified lyophilized raw banana peel as a potent source of bioactive carbohydrates. Lyophilized raw Nendran peel contains RS (18.11 ± 0.06%), dietary fiber (26.87 ± 0.92%), and fructan (1.34 ± 0.31%). The methanolic extract of the peel exhibited high total phenolic and total flavonoid content. *In vitro* assays demonstrated the extract's potent anti-inflammatory properties by suppressing NO production in murine macrophages RAW 264.7 cells and enhancing IL-10 secretion. Additionally, our study revealed significant α-glucosidase inhibition potential of Nendran peel extract, comparable to the standard drug acarbose. The α-glucosidase inhibition potential of peel substantiates the traditional knowledge regarding banana peel dietary usage for diabetes. The findings from *in vitro* studies, although promising, necessitate further evaluation to elucidate the underlying mechanisms and identify specific bioactive compounds responsible for the affirmed results. The findings from our study suggest that unripe Nendran peel can be used directly or as an ingredient in functional foods for promoting gut health and general well-being.

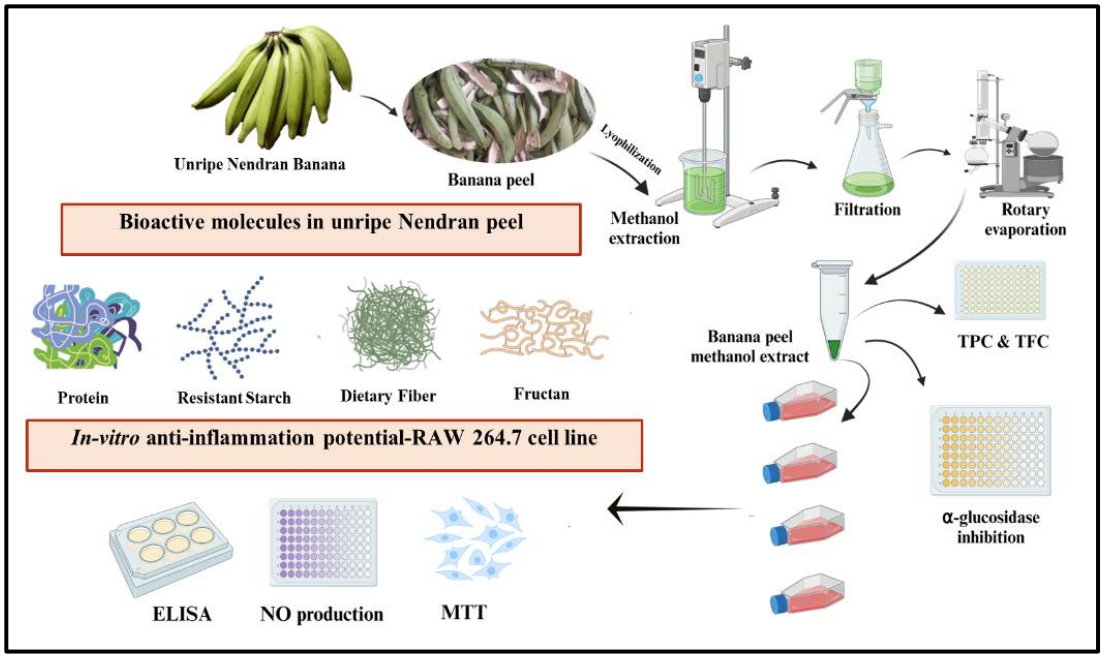

Fig. 6.5. Chapter 6 graphical abstract (Created with BioRender.com)

6.6. References

1. Agrawal, N., Sharma, M., Singh, S., & Goyal, A. (2022). Recent advances of α-glucosidase inhibitors: A comprehensive review. *Current Topics in Medicinal Chemistry*, *22*(25), 2069–2086. https://doi.org/10.2174/1568026622666220831092855
2. Anderson, J. W., Baird, P., Davis Jr, R. H., Ferreri, S., Knudtson, M., Koraym, A., Waters, V., & Williams, C. L. (2009). Health benefits of dietary fiber. *Nutrition Reviews*, *67*(4), 188–205. https://doi.org/10.1111/j.1753-4887.2009.00189.x
3. AOAC, C. (2005). Official methods of analysis of the Association of Analytical Chemists International. *Official Methods: Gaithersburg, MD, USA*.
4. Aquino, C. F., SALOmãO, L. C. C., RIBEIRO, S., SIQUEIRA, D. L. D., & Cecon, P. R. (2016). Carbohydrates, phenolic compounds and antioxidant activity in pulp and peel of 15 banana cultivars. *Revista Brasileira de Fruticultura*, *38*, e-090. http://dx.doi.org/10.1590/0100-29452016090
5. Arlinda Silva Prameswari, Kartika Puji Rahayu, Eria Nahrani Pranadita, Dyah Puspa, Ardani, & Wafiyah Hasana. (2017). The Effectiveness of Ambon Banana Peel Extract (Musa sapientum) as Atherosclerosis Prevention through Inhibition of NF-κβ and Increased eNOS Expression in Atherogenic Rat Model. *International Journal of Medical Research & Health Sciences*, *6*(9), 114–120.
6. Bhavani, M., Morya, S., Saxena, D., & Awuchi, C. G. (2023). Bioactive, antioxidant, industrial, and nutraceutical applications of banana peel. *International Journal of Food Properties*, *26*(1), 1277–1289. https://doi.org/10.1080/10942912.2023.2209701
7. Brouns, F., Kettlitz, B., & Arrigoni, E. (2002). Resistant starch and "the butyrate revolution." *Trends in Food Science & Technology*, *13*(8), 251–261. https://www.sciencedirect.com/science/article/pii/S0924224402001310
8. Carlini, V., Noonan, D. M., Abdalalem, E., Goletti, D., Sansone, C., Calabrone, L., & Albini, A. (2023). The multifaceted nature of IL-10: Regulation, role in immunological homeostasis and its relevance to cancer, COVID-19 and post-COVID conditions. *Frontiers in Immunology*, *14*, 1161067. https://doi.org/10.3389%2Ffimmu.2023.1161067
9. Chang, C.-C., Yang, M.-H., Wen, H.-M., & Chern, J.-C. (2002). Estimation of total flavonoid content in propolis by two complementary colorimetric methods. *Journal of Food and Drug Analysis*, *10*(3). https://doi.org/10.38212/2224-6614.2748

10. Chaudhry, F., Ahmad, M. L., Hayat, Z., Ranjha, M. M. A. N., Chaudhry, K., Elboughdiri, N., Asmari, M., & Uddin, J. (2022). Extraction and evaluation of the antimicrobial activity of polyphenols from banana peels employing different extraction techniques. *Separations*, *9*(7), 165. https://doi.org/10.3390/separations9070165
11. Chen, Z., Liang, N., Zhang, H., Li, H., Guo, J., Zhang, Y., Chen, Y., Wang, Y., & Shi, N. (2024). Resistant starch and the gut microbiome: Exploring beneficial interactions and dietary impacts. *Food Chemistry: X*, *21*, 101118. https://www.sciencedirect.com/science/article/pii/S2590157524000051
12. Cummings, J. H., Antoine, J.-M., Azpiroz, F., Bourdet-Sicard, R., Brandtzaeg, P., Calder, P. C., Gibson, G. R., Guarner, F., Isolauri, E., Pannemans, D., Shortt, C., Tuijtelaars, S., & Watzl, B. (2004). Gut health and immunity. *European Journal of Nutrition*, *43*(S2), ii118–ii173. https://doi.org/10.1007/s00394-004-1205-4
13. Dirir, A. M., Daou, M., Yousef, A. F., & Yousef, L. F. (2022). A review of alpha-glucosidase inhibitors from plants as potential candidates for the treatment of type-2 diabetes. *Phytochemistry Reviews*, *21*(4), 1049–1079. https://doi.org/10.1007/s11101-021-09773-1
14. Francisco, V., Figueirinha, A., Neves, B. M., García-Rodríguez, C., Lopes, M. C., Cruz, M. T., & Batista, M. T. (2011). Cymbopogon citratus as source of new and safe anti-inflammatory drugs: Bio-guided assay using lipopolysaccharide-stimulated macrophages. *Journal of Ethnopharmacology*, *133*(2), 818–827. https://doi.org/10.1016/j.jep.2010.11.018
15. *Fructan Assay Kit*. (n.d.). Megazyme. Retrieved January 25, 2024, from https://www.megazyme.com/fructan-assay-kit
16. Hashim, M., Hamid, Z., Gul, Z., & Akbar, A. (2023). Functional, nutritional and medicinal potential of banana peel. *Pure and Applied Biology (PAB)*, *12*(1), 470–490. http://dx.doi.org/10.19045/bspab.2023.120049
17. Hikal, W. M., Said-Al Ahl, H. A. H., Bratovcic, A., Tkachenko, K. G., Sharifi-Rad, J., Kačániová, M., Elhourri, M., & Atanassova, M. (2022). Banana Peels: A Waste Treasure for Human Being. *Evidence-Based Complementary and Alternative Medicine*, *2022*, 1–9. https://doi.org/10.1155/2022/7616452
18. Hong, Y.-H., Kao, C., Chang, C.-C., Chang, F.-K., Song, T.-Y., Houng, J.-Y., & Wu, C.-H. (2023). Anti-Inflammatory and T-Cell Immunomodulatory Effects of Banana Peel Extracts

and Selected Bioactive Components in LPS-Challenged In Vitro and In Vivo Models. *Agriculture*, *13*(2), 451. https://doi.org/10.3390/agriculture13020451

19. Hossain, U., Das, A. K., Ghosh, S., & Sil, P. C. (2020). An overview on the role of bioactive α-glucosidase inhibitors in ameliorating diabetic complications. *Food and Chemical Toxicology*, *145*, 111738. https://doi.org/10.1016/j.fct.2020.111738
20. Hughes, R. L., Alvarado, D. A., Swanson, K. S., & Holscher, H. D. (2022). The prebiotic potential of inulin-type fructans: A systematic review. *Advances in Nutrition*, *13*(2), 492–529. https://doi.org/10.1093%2Fadvances%2Fnmab119
21. *IDA-position-paper-fibre-24.12.18.pdf*. (n.d.). Retrieved July 10, 2024, from https://idaindia.com/wp-content/uploads/2018/12/IDA-position-paper-fibre-24.12.18.pdf
22. Kumari, P., Gaur, S. S., & Tiwari, R. K. (2023). Banana and its by-products: A comprehensive review on its nutritional composition and pharmacological benefits. *eFood*, *4*(5), e110. https://doi.org/10.1002/efd2.110
23. Lockyer, S., & Nugent, A. (2017). Health effects of resistant starch. *Nutrition Bulletin*, *42*(1), 10–41. https://doi.org/10.1111/nbu.12244
24. MPharm, S. R. (2012). Anti-inflammatory and antioxidant activities of extracts from Musa sapientum peel. *J Med Assoc Thai*, *95*(1), S142–S146. https://www.thaiscience.info/Article%20for%20ThaiScience/Article/62/10038948.pdf
25. Raigond, P., Ezekiel, R., & Raigond, B. (2015). Resistant starch in food: A review. *Journal of the Science of Food and Agriculture*, *95*(10), 1968–1978. https://doi.org/10.1002/jsfa.6966
26. Samtiya, M., Aluko, R. E., Dhewa, T., & Moreno-Rojas, J. M. (2021). Potential health benefits of plant food-derived bioactive components: An overview. *Foods*, *10*(4), 839. https://www.mdpi.com/2304-8158/10/4/839
27. Singleton, V. L., & Rossi, J. A. (1965). Colorimetry of total phenolics with phosphomolybdic-phosphotungstic acid reagents. *American Journal of Enology and Viticulture*, *16*(3), 144–158. https://doi.org/10.5344/ajev.1965.16.3.144
28. Skrzypczak-Wiercioch, A., & Sałat, K. (2022). Lipopolysaccharide-induced model of neuroinflammation: Mechanisms of action, research application and future directions for its use. *Molecules*, *27*(17), 5481. https://doi.org/10.3390/molecules27175481

29. Tian, Y., Zhou, S., Takeda, R., Okazaki, K., Sekita, M., & Sakamoto, K. (2021). Anti-inflammatory activities of amber extract in lipopolysaccharide-induced RAW 264.7 macrophages. *Biomedicine & Pharmacotherapy*, *141*, 111854. https://doi.org/10.1016/j.biopha.2021.111854
30. *Total Dietary Fiber Assay Kit*. (n.d.). Megazyme. Retrieved February 14, 2024, from https://www.megazyme.com/total-dietary-fiber-assay-kit
31. *Transforming our world: The 2030 Agenda for Sustainable Development | Department of Economic and Social Affairs*. (n.d.). Retrieved July 29, 2024, from https://sdgs.un.org/2030agenda
32. Udenigwe, C. C. (2023). From Waste to Wealth: Practical Considerations for Food Waste and Byproduct Upcycling to Biofunctional Components. *ACS Food Science & Technology*, *3*(1), 15–16. https://doi.org/10.1021/acsfoodscitech.2c00379
33. *WHO updates guidelines on fats and carbohydrates*. (n.d.). Retrieved July 9, 2024, from https://www.who.int/news/item/17-07-2023-who-updates-guidelines-on-fats-and-carbohydrates
34. Zaini, H. B. M., Sintang, M. D. B., & Pindi, W. (2020). The roles of banana peel powders to alter technological functionality, sensory and nutritional quality of chicken sausage. *Food Science & Nutrition*, *8*(10), 5497–5507. https://doi.org/10.1002%2Ffsn3.1847
35. Zaini, H. M., Roslan, J., Saallah, S., Munsu, E., Sulaiman, N. S., & Pindi, W. (2022). Banana peels as a bioactive ingredient and its potential application in the food industry. *Journal of Functional Foods*, *92*, 105054. http://dx.doi.org/10.1016/j.jff.2022.105054
36. Zou, F., Tan, C., Zhang, B., Wu, W., & Shang, N. (2022). The valorization of banana by-products: Nutritional composition, bioactivities, applications, and future development. *Foods*, *11*(20), 3170. https://doi.org/10.3390%2Ffoods11203170

Chapter 7

Summary, conclusion & future perspectives

Bananas belonging to the genus *Musa* of the Musaceae family, are a vital global crop, cultivated in over 130 countries, primarily in tropical and subtropical regions. In the green stage, bananas stand out for having high starch content predominantly RS, and boast a rich mineral profile by containing a good amount of potassium and magnesium. Further, the presence of a notable amount of bioactive carbohydrates makes bananas a good prebiotic source for gut health and general wellness. In addition to the nutritional benefits, banana has a plethora of bioactive compounds with numerous health benefits. Despite the nutritional richness, unripe banana is an underutilized matrix. Beyond traditional weaning foods, there are no novel products derived from unripe bananas with innovative applications in the market.

The 'Nendran' banana variety (*Musa* (AAB) cv. Nendran), widely cultivated in South India, holds popularity for its versatile uses. In its unripe state, 'Nendran' bananas are commonly utilized in culinary practices and for preparing banana chips. Despite its prevalence, there are no previous reports on the complete nutritional profile and bioactive carbohydrate content (RS, fructan, fiber) of Nendran, nor have there been efforts to develop value-added products from its unripe pulp to harness its prebiotic benefits. Given Nendran's indigenous nature in Kerala, understanding the potentials and current scenario of underutilization, the current investigation was conducted to explain the untapped health potentials of both pulp and peel of unripe Nendran bananas, investigation on its phytochemical profile, and utilization of it in novel forms. Through this research, we aim to contribute to the betterment of farmers' livelihoods and consumers' health alike.

Initially, the voucher specimen of Nendran was collected and deposited at the Herbarium of Jawaharlal Nehru Tropical Botanic Garden & Research Institute, Thiruvananthapuram, Kerala, India with TBGT voucher number TBGT 94628. Initial studies on unripe Nendran banana peel revealed the presence of a significant amount of bioactive carbohydrates, highlighting its value addition potential. Through comprehensive research, we have successfully developed a novel, preservative, and additive-free product 'BG' from the pulp of mature Nendran bananas, thereby adding significant value to this previously underutilized agricultural resource. Shelf-life studies

showed that the product was shelf-stable for 11 months. BG was screened for the presence of 98 pesticides according to the AOAC method and they were below the detectable limit in BG. BG demonstrated nutrient superiority, by containing bioactive carbohydrates- fructan & dietary fiber, minerals- potassium, and magnesium, and TCC of 3466 ± 11.78 µg/100 g which helps in positioning it as a promising alternative to cereals. The presence of a considerable amount of dietary fiber BG indicates its suitability for promoting gut health and thereby providing overall wellness. This RTC and RTR product offers versatility in consumption marking a breakthrough from the conventional use of unripe bananas as infant weaning food. A significant outcome of this work is the technology transfer of the developed product BG, facilitating its commercialization by M/s. MOZA ORGANIC Pvt. Ltd., Kochi, India. The novel product BG aims to unlock the nutritional potential of unripe Nendran bananas as a replacement for traditional cereal-based diet.

Further, a detailed phytochemical analysis of the organic extracts of BG and as well as unripe pulp revealed the presence of β-sitosterol, glycolipids viz. MGDG, DGDG, acyl steryl glycosides viz. sitoindoside-II, sitoindoside-I, sterylglycoside (β-Sitosterol β-D-glucopyranoside), GC and carotenoids. An exhaustive NMR and HR-ESI-MS analysis aided in providing structural details of the isolated phytochemicals. The present work serves as the first report on the isolation of GCs from *Musa* species and also the first report on phytochemical isolation studies from the Nendran cultivar. Literature shows that the phytochemicals isolated from unripe Nendran and BG have a myriad of health benefits. Thus, incorporating BG into the diet can contribute to overall health and well-being, highlighting the significance of diversifying dietary choices for optimal nutrition.

After completing the value addition trials and the phytochemical investigations, we have focused our studies on the process induced changes in the RS content of the pulp and its relation to GI. Two preparations, BG upma and BG porridge were then screened for GI. BG cooked in both forms exhibited a high GI and medium GL in clinical studies. Even though high in GI, it has a medium GL value makes it suitable for consumption by diabetic people also. We also conducted an *in vitro* GI prediction, which showed a high correlation with the clinical GI values. We have also studied the process induced changes in the RS content of pulp. RS content of BG assayed using a 2-hour digestion protocol revealed RS content of 42.08%. But further evaluation

with a 4-hour digestion protocol revealed that BG has only 4.44% RS and raw Nendran has 41% RS. The unit operations we employed resulted in a 10% reduction of RS, which may have resulted in the high GI of the product. Further studies revealed BG has a high RS content compared to oats, rice, and chapathi. The study helped us to understand the importance of selecting appropriate unit operations when designing products with a low GI.

Banana peel, the primary waste product generated during BG preparation, also holds untapped potential. The UN 2030 agenda for sustainable development calls for actions focused on eliminating waste and maximizing food resources. In line with this, we have explored the potent bioactive compounds and the bioactive components in the unripe Nendran peel to assess its value addition potential. The phytochemical investigation in the unripe peel has resulted in the isolation and characterization of eighteen molecular species of GC from the peel and the present investigation is the first report of GCs from banana peel. GCs are distinguished by variation in aliphatic acids conjugated as amide-containing α- and ω-hydroxy fatty acids. The study further proved the anti-inflammatory potential of the GC consortium in LPS-induced murine macrophage RAW 264.7 cells by suppressing the NO production and decreasing the secretion of pro-inflammatory cytokines. GC consortium at the dose of 50 µg/mL, even outperformed the standard drug dexamethasone (7.85 µg/mL) by reducing the production of pro-inflammatory cytokines, IL-1α, TNF-α, COX-2, & IL-6, and increasing the production of the anti-inflammatory cytokine IL-10. In addition to this, the GC consortium has also shown remarkable α-glucosidase inhibition potential with an IC_{50} value of 5.12 ± 0.51 µg/mL compared to the standard drug acarbose (IC_{50} = 87.32 ± 1.99 µg/mL), highlighting the scope for further studies on GC. The identification of GCs in unripe banana peel shows the significance of studying this matrix for application in functional foods and skincare formulations.

Further studies on peel revealed that raw banana peel is a potent source of bioactive carbohydrates. Lyophilized raw Nendran peel contains RS (18.11 ± 0.06%), dietary fiber (26.87 ± 0.92%), and fructan (1.34 ± 0.31%). The methanolic extract of the peel exhibited high total phenolic and total flavonoid content. *In vitro* assays demonstrated the extract's potent anti-inflammatory properties in murine macrophages RAW 264.7 cells. The MeOH extract of the peel at a dose of 100 µg/mL outperformed dexamethasone (7.85 µg/mL) in increasing the production of the anti-inflammatory cytokine IL-10. The extract also showed significant α-glucosidase inhibition potential by showing a lower IC_{50} value of 58.42 ± 0.45 µg/mL, compared to the standard

drug acarbose 85.95 ± 4.23 µg/mL. Our findings highlight the unripe Nendran banana peel's potential as a valuable source of bioactive compounds for functional food and pharmaceutical applications. Comparing the anti-inflammatory potential and α-glucosidase inhibition potential of the crude extract with that of isolated GCs reveals that the isolated GCs not only demonstrate superior activity but also surpass the performance of commercially available standard anti-inflammatory drug dexamethasone and α-glucosidase inhibitor acarbose. This highlights the significant therapeutic potential of GCs, underscoring the importance of further research to explore their use as novel pharmaceutical agents in the treatment of inflammatory conditions and diabetes management.

In conclusion, the present study has revealed the immense potential of the unripe Nendran banana, transforming it from an underutilized resource into a novel product BG, marking a breakthrough from the conventional use of unripe bananas as infant weaning food. By showcasing its high content of bioactive carbohydrates, essential minerals, and phytochemicals, the research positions BG as an alternative to traditional cereals, contributing to better gut health and overall wellness. Additionally, the pioneering work on the phytochemical profile of Nendran's pulp and peel, especially the discovery of GCs and bioactive carbohydrates in peel, not only expands scientific knowledge but also introduces sustainable solutions for banana peel waste utilization in the food and pharmaceutical industries. The technology transfer of BG underscores its impact, promising to enhance consumer health and farmer livelihoods while addressing global sustainability goals.

Future Perspectives

- Developing banana products with retained RS content for the management of diabetes, gut health, and lifestyle diseases.
- Validation of products -studies on gut health-promoting potential is warranted.
- The present study being the first report on GCs from banana peel, demands the development of a cost-effective and ‘green process’ for the isolation of GC from the banana peel and its effective utilization at the industrial level.
- Trials for peel value addition and evaluation of its prebiotic potential.

ABSTRACT

Name of student: Raveena Natakkakath Kaliyathan **Registration No. :** 10BB18A39036
Faculty of Study: Biological Science **Year of Submission:** 2024
AcSIR academic centre/CSIR Lab: CSIR-NIIST, Thiruvananthapuram
Name of the Supervisor: Dr. Reshma M V
Title of the thesis: Value Addition of Unripe 'Nendran' Banana (*Musa* (AAB) cv. Nendran) and Exploration of its Phytoconstituents

Bananas (genus *Musa*, family Musaceae) are a globally significant crop, primarily cultivated in tropical and subtropical regions. Despite their nutritional richness, particularly in the green stage with high resistant starch (RS) and a rich mineral profile (potassium, magnesium), unripe bananas remain underutilized beyond traditional applications. This study focuses on the 'Nendran' banana variety (*Musa* (AAB) cv. Nendran), widely grown in South India, aiming to harness its untapped potential and explore its phytoconstituents. We developed a novel, preservative & additive-free product Banana Grit (BG) from the mature, unripe Nendran banana pulp. BG contains bioactive carbohydrates (fructan, dietary fiber), essential minerals (potassium, magnesium), and a total carotenoid content (TCC) of 3466 ± 11.78 µg/100 g. BG's versatility in consumption, marking a breakthrough from the conventional use of unripe bananas as infant weaning food, positions it as a promising alternative to traditional cereals, with benefits for gut health and overall wellness. The technology transfer of BG to M/s. MOZA ORGANIC Pvt. Ltd., Kochi, India, is a significant outcome of this work. Clinical studies indicated that BG when prepared as upma or porridge, exhibited a high glycemic index (GI) but medium glycemic load (GL), making it suitable even for the diabetic population when consumed in restricted amounts. The *in vitro* GI prediction studies of BG showed a high correlation with clinical GI-GL studies. Further studies revealed the process induced changes in the RS content of unripe pulp. Additionally, the study identified significant phytochemicals in BG and unripe Nendran pulp, including β-sitosterol, glycolipids (MGDG, DGDG & GC), acyl steryl glycosides, and steryl glycosides, using NMR and HR-ESI-MS analysis. Notably, this is the first report of glucocerebroside (GC) from the *Musa* species and also the first report on phytochemical isolation studies from the Nendran cultivar. Further investigations into unripe Nendran banana peel, the primary waste generated during banana processing, revealed it as a potent source of bioactive compounds, including 18 molecular species of GCs, which exhibited remarkable anti-inflammatory and α-glucosidase inhibition potential than the standard drugs dexamethasone and acarbose respectively, indicating the scope for further research in this area. The peel also contained high RS (18.11 ± 0.06%), dietary fiber (26.87 ± 0.92%), and fructan (1.34 ± 0.31%), indicating the immense value addition potential of peel as a functional food and also for pharmaceutical applications. Our research not only sheds light on scientific knowledge about Nendran bananas but also contributes to global sustainability goals by developing value-added products from underutilized resources.

List of Publications Emanating from the Thesis Work

1. **Raveena, N. K**., Ingaladal, N., Reshma, M.V, & Lankalapalli, R. S. (2022). Phytochemical investigation of unripe banana (*Musa* AAB) cv. Nendran and its novel 'Banana Grits.' *Food Chemistry Advances*,*1*,100063. http://dx.doi.org/10.1016/j.focha.2022.100063
2. **Raveena, N. K**., Sornarani R., Priya S., Lankalapalli, R. S. & Reshma, M.V. (2024). First report on glucocerebrosides from unripe banana peel: its anti-inflammatory and α-glucosidase inhibition properties. Food Chemistry Advances, 4, 100700, https://doi.org/10.1016/j.focha.2024.100700
3. **Raveena, N. K,** Natarajan Kalpana, Karthikeyan Parkavi, Vasudevan Sudha, Raman Ganeshjeevan, Ranjit Mohan Anjana, Viswanathan Mohan, M. V. Reshma. Novel raw banana product: its resistant starch, fructan content, and glycemic index studies. (Manuscript to be communicated)
4. **Raveena, N. K**., & Reshma, M.V, Underutilized Food: Raw Nendran Banana Peel (Musa (AAB) cv. Nendran) - a Source of Bioactive Molecules. (Manuscript to be communicated)
5. **Raveena, N. K.**, & Reshma, M V. Starch-from structure to function-A Comprehensive Outlook on Physicochemical Properties, Glycemic Index, Resistant Starch, and Its Health Implications. (Review article to be communicated)

List of Publications Not Related to the Thesis

1. Somasekharan Nair Rajam, S., Neenthamadathil Mohandas, K., Vellolipadikkal, H., Viswanathan Leena, S., Kollery Suresh, V., **Natakkakath Kaliyathan, R**., Sreedharan Nair, R., Lankalapalli, R. S., & Mullan Velandy, R. (2020). Spice-infused palmyra palm syrup improved cell-mediated immunity in Wistar Albino rats. Journal of Food Biochemistry, 44(11), e13466. https://doi.org/10.1111/jfbc.13466
2. Athira, A. S., Kiruthika, R., Ingaladal, N., Krishnakumar, K. A., **Raveena, N. K**., Gopika, B., Reshma, M. V., & Lankalapalli, R. S. (2023). NMR-based Phytochemical Profiling of Palmyra Palm Syrup Infused with Dry Ginger, Black Pepper, and Long

Pepper. Current Nutraceuticals, 4(1). http://dx.doi.org/10.2174/2665978604666230112144757

3. Abhijith, B., **Raveena, N. K.**, Reshma, M.V., & Lankalapalli, R. S. (2023). Artifacts from the methanolic extract of *Solanum nigrum* Linn. Natural Product Research, 1–5. https://doi.org/10.1080/14786419.2023.2232931
4. A comparative study on resistant starch, fructan, fiber content, and prediction of glycemic index of commonly consumed foods in Kerala (Manuscript under preparation).
5. Development of trans fatty acid-free prebiotic cakes: physicochemical, microstructure, and textural studies (Manuscript under preparation).
6. Coconut Neera Sugar-Physicochemical Characterization and its Glycemic index & Glycemic load studies (Manuscript under preparation).
7. Physicochemical Characterization and its Glycemic index & Glycemic load studies of tender coconut water (Manuscript under preparation).
8. Anti-inflammatory potential of Priyala (*Buchanania lanzan* Spreng. Syn. *B.latifolia* Roxb.) seed (Manuscript under preparation).
9. Immunomodulation properties of Priyala formulation- *in vitro* and in vivo studies (Manuscript under preparation).
10. Fatty acid profile of virgin coconut oil revisited (Manuscript under preparation).

Technology Transfer

Technology transfer of ‘banana grit’ & ‘banagram’ (improved version of banana grit fortified with green gram) to MOZA ORGANIC Pvt. Ltd. Kochi, India on 1st January 2021.

List of Conference Presentations

1. 'Banana Grit from Unripe 'Nendran' Banana and Characterization of Its Starch Fractions'. **Raveena Natakkakath Kaliyathan**, Anjali Krishna T U, Reshma M V. FSN-P-34. pp 166. 51st annual national conference of Nutritional Society of India, on 7th-9th November 2019 at RGCB Thiruvananthapuram. (Poster presentation)
2. 'Novel Nendran banana grits and its phytochemical exploration studies'. **Raveena Natakkakath Kaliyathan**, Nagaraja Ingaladal, M.V. Reshma, & Ravi S. Lankalapalli. National seminar on recent trends in disease prevention and health management jointly organized by CSIR-National Institute for Interdisciplinary Science and Technology (NIIST) & Kerala Academy of Science (KAS) from 14-15 December, 2022 at CSIR-NIIST, Thiruvananthapuram. (**Best paper presentation award)**
3. 'Raw Nendran as "Grit"-Innovation for Sustainable Nutritional Security Using an Underutilized Crop'. NFA-022. **Raveena Natakkakath Kaliyathan**, Rafeena Rafi, and Reshma M V. 29th ICFoST organized by AFSTI (I)-HQ (Mysuru) Kollam & Cohin chapter during 5th-7th January 2023 at the AL SAJ conventional center, Thiruvananthapuram. (Poster presentation)
4. **'**From waste to wealth: unripe Nendran peel- a source of bioactive carbohydrates and glucocerebrosides'. **Raveena Natakkakath Kaliyathan**, Sornarani Rajan, S. Priya, M.V. Reshma, & Ravi S. Lankalapalli. SCIENTIA-2, Multidisciplinary international conference and research expo 2024 organized by Scholars connect, research forum of Christ College, Irinjalakuda, Kerala from 5-7, November 2024. (**Best paper presentation award)**
5. 'Phytochemical and bioactive carbohydrate profiling of Banana Grit: a novel functional food from unripe Nendran bananas. **Raveena Natakkakath Kaliyathan,** Nagaraja Ingaladal, M.V. Reshma, & Ravi S. Lankalapalli. International conference on advancements and innovations in phytochemistry, nutraceuticals and functional foods organized by Kerala Academy of Sciences, Thiruvananthapuram and Mar Athanasios College for Advanced Studies Tiruvalla (MACFAST) held at MACFAST, Tiruvalla, Kerala from 11-12, November 2024. (**Best paper presentation award)**

Abstracts for Conference Presentations

1. 51st annual national conference of Nutritional Society of India, on 7th-9th November 2019 at RGCB Thiruvananthapuram.

Banana grit from Unripe 'Nendran' Banana and Characterization of its Starch Fractions

Raveena Natakkakath Kaliyathan[1,2], Anjali Krishna T U[1], Reshma M V[1,2]

[1]Agro-Processing and Technology Division, CSIR-National Institute for Interdisciplinary Science and Technology (CSIR-NIIST), Thiruvananthapuram 695019, Kerala, India
[2]Academy of Scientific & Innovative Research (AcSIR), Ghaziabad 201002, India

Corresponding author: mvreshma@niist.res.in

Background: Banana is a popular tropical plant coming under the genus *Musa* of Musaceae family. Banana is a potential source of several bioactive compounds such as carotenoids, phenolics, biogenic amines and it is one of the resistant starch (RS) abundant commodity. RS is termed as bioactive carbohydrate due to its tremendous biological potentials. 'Nendran' is a popular cultivated variety of *Musa* × *paradisiaca* L. in Kerala. Though the unripe banana is rich in many minerals and functional nutrients, it is underutilized. Considering these facts there is a huge scope for developing value added products from unripe 'Nendran' for health benefits. The objective of the present study was to develop novel food product from unripe 'Nendran', with focus on its shelf life studies and estimation of starch fractions.

Materials and methods: Fresh unripe 'Nendran' was purchased from farmers and the pulp and peel were separated. The pulp was subjected to pretreatment, subsequent drying and final grinding to produce 'banana grits. The physicochemical properties of the product were determined and the shelf life stability of product was evaluated for seven months. An *in vitro* digestion protocol which mimics the human digestion was followed in order to determine the starch fractions in grit.

Result: A novel food product, banana grits was developed from unripe 'Nendran'. The proximate analysis showed that the banana grits have low moisture content (2.83±0.05%) and high carbohydrate content (91.31±0.18%). Shelf life studies showed that the product was shelf stable up to seven months. The *in vitro* digestion assay showed that the grit comprises of 84.74±6.74 % starch, out of which 50.63±7.60% was bioactive carbohydrate fraction.

Conclusion: A novel, highly shelf stable and preservative free banana grits was developed from 'Nendran' banana. Presence of high RS portion indicates immense biological potential of grit.

2. National seminar on recent trends in disease prevention and health management jointly organized by CSIR- NIIST & Kerala Academy of Science (KAS) from 14-15 Dec, 2022 at CSIR-NIIST

Novel Nendran banana grits and its phytochemical exploration studies

Natakkakath Kaliyathan Raveena,[1,3] Nagaraja Ingaladal,[2,3] M. V. Reshma,[1,3,*] and Ravi S. Lankalapalli[2,3]

[1]Agro-Processing and Technology Division, CSIR-National Institute for Interdisciplinary Science and Technology (CSIR-NIIST), Thiruvananthapuram 695019, Kerala, India
[2]Chemical Sciences and Technology Division, CSIR-National Institute for Interdisciplinary Science and Technology (CSIR-NIIST), Thiruvananthapuram 695019, Kerala, India
[3]Academy of Scientific & Innovative Research (AcSIR), Ghaziabad 201002, India

*Corresponding Author: mvreshma@niist.res.in

Abstract

Raw banana *Musa* (AAB) cv. Nendran is a popular cultivated variety of *Musa* in South Indian states (Tamil Nadu, Kerala, Karnataka), and elsewhere in the world. In the present investigation, we are showing a novel utility of unripe Nendran banana as 'Banana Grits' (BG) that can be consumed on daily basis like cereals and tubers. BG is a novel preservative and additive-free product, which is in ready-to-cook as well as ready-to-reconstitute form. The *in vitro* starch digestion pattern indicated that out of 80 % of total starch in BG, 21 % is slowly digestible starch (SDS) and 42 % is resistant starch (RS). The SDS and RS fractions of starch were known to have nutraceutical potential due to their low postprandial glycemic response and high indigestible carbohydrate content. The presence of SDS and RS in BG indicates that they may contribute to gut health and glycemic control. Estimation of the total carotenoid content of BG revealed a high level of carotenoid content i.e., greater than 3000 µg/100 g of BG. The high amount of carotenoids in BG indicates the suitability of BG for alleviating vitamin A deficiency. The technology of banana grit production was transferred to a Kochi-based company M/s. MOZA ORGANIC Pvt. Ltd. India on 1st January 2021 and we are expecting the launch of bana- grit, and bana-gra soon in national and international markets. A detailed phytochemical analysis of BG and as well as unripe Nendran pulp revealed the presence of β-sitosterol, sitoindoside-II, sitoindoside-I, sterylglycoside, monogalactosyldiacylglycerol (MGDG), digalactosyldiacylglycerol (DGDG), acyl steryl glycosides and glucocerebroside in them. Literature data shows that these phytochemicals were associated with a myriad of health benefits including anti-inflammatory, and anti-cancer properties. The present work serves as the first report on the isolation of glucocerebrosides from *Musa* species and also the first report on phytochemical isolation studies from the Nendran cultivar.

3. 29th ICFoST organized by AFSTI (I)-HQ (Mysuru) Kollam & Cohin chapter during 5th-7th January 2023 at the AL SAJ conventional center, Thiruvananthapuram.

Raw Nendran as "Grit"– Innovation for Sustainable Nutritional Security Using an Underutilized Crop

Raveena Natakkakath Kaliyathan,[1,2] Rafeena Rafi,[1] and Reshma M. V[1,2]
[1]Agro-Processing and Technology Division, CSIR-National Institute for Interdisciplinary Science and Technology (CSIR-NIIST), Thiruvananthapuram 695019, Kerala, India
[2]Academy of Scientific & Innovative Research (AcSIR), Ghaziabad 201002, India

Email: mvreshma@niist.res.in

Introduction: Raw banana *Musa* (AAB) cv. Nendran is an underutilized crop with untapped health potential and there is enormous scope for developing novel products from this commodity.

Objectives:

- Development of grits from raw 'Nendran', its physicochemical analysis, studies of starch fractions
- Shelf life evaluation and studies on starch fraction in raw banana and its ripening changes.

Materials and methods: A novel product 'Banana grit'(BG) was developed from unripe Nendran pulp and its physicochemical properties and shelf life was evaluated. The starch fractions in different maturity stages of Nendran and BG were estimated with an *in vitro* digestion protocol.

Result and conclusion: The starch content of Nendran drops from 23.12±2.22% to zero during the ripening process and the unripe pulp with high starch content was used for the preparation of novel BG. The novel BG is a preservative and additive-free 'ready-to-cook' product with a variety of cooking options. BG has a low moisture content (2.83±0.05%), high total carotenoid content (3000 µg/100 g of BG), high resistant starch content (42%), and shelf-stable up to nine months. The technology of banana grit production was transferred to a Kochi-based company M/s. MOZA ORGANIC Pvt. Ltd. India. The present work is an innovative step towards sustainable nutritional security from an underutilized indigenous crop which can improve the life of our farmers and the health of the consumers as well.

4. SCIENTIA-2, Multidisciplinary international conference and research expo 2024 organized by Scholars connect, research forum of Christ College, Irinjalakuda, Kerala from 5-7, November 2024.

From waste to wealth: unripe Nendran peel- a source of bioactive carbohydrates and glucocerebrosides

Raveena Natakkakath Kaliyathan [1,3], Sornarani Rajan[2,3], S Priya[1,3], Ravi S. Lankalapalli[2,3,*], Reshma M. V.[1,3,*]

[1]Agro-Processing and Technology Division, CSIR-National Institute for Interdisciplinary Science and Technology (CSIR-NIIST), Thiruvananthapuram 695019, Kerala, India
[2]Chemical Sciences and Technology Division, CSIR-National Institute for Interdisciplinary Science and Technology (CSIR-NIIST), Thiruvananthapuram 695019, Kerala, India
[3]Academy of Scientific & Innovative Research (AcSIR), Ghaziabad 201002, India

*Corresponding Authors: mvreshma@niist.res.in, ravishankar@niist.res.in

Abstract

Bananas (genus *Musa*, family Musaceae) are a globally significant crop, primarily cultivated in tropical and subtropical regions. The 'Nendran' banana variety (*Musa* (AAB) cv. Nendran), which is widely cultivated in South India, holds popularity for its versatile uses. In its unripe state, 'Nendran' bananas are commonly utilized in culinary practices and for preparing banana chips. The Unripe banana peel is the primary waste product generated by banana processing industries and is typically discarded as waste. Annually, about 40 million tonnes of peel are generated and the majority of these peels are often dumped away in landfills. In alignment with the UN 2030 Agenda for Sustainable Development, we have explored the potent bioactive components in the unripe Nendran peel to assess its value addition potential. Studies on peel revealed that raw Nendran peel is a potent source of bioactive carbohydrates including resistant starch (18.11 ± 0.06%), dietary fiber (26.87 ± 0.92%), and fructan (1.34 ± 0.31%). Bioactive carbohydrates are pivotal in promoting gut health and enhancing immune function. The phytochemical investigation in the unripe peel has resulted in the isolation and characterization of eighteen molecular species of glucocerebroside (GC), containing α- and ω-hydroxy fatty acids from the peel. Marking the first report of GCs from banana peel. GC is a molecule with immunomodulation potential and being a source of ceramides, it is highly valued in the cosmetic industry for its role in skin health. The *in vitro* anti-inflammation potential of the isolated GC consortium was assessed in RAW 264.7 murine macrophage cell line. The GC consortium at a dose of 50 µg/mL, showed a significant reduction in lipopolysaccharide (LPS)-induced nitric oxide (NO) production. The enzyme-linked immunosorbent assay (ELISA) analysis demonstrated GC's immunomodulation potential by showing a reduction in pro-inflammatory cytokines and an increase in anti-inflammatory cytokine production. Furthermore, GC exhibited potent α-glucosidase inhibition with an IC_{50} value of 5.12 ± 0.51 µg/mL, significantly lower than standard drug acarbose (IC_{50} = 87.32 ± 1.99 µg/mL). This research highlights the potential of GC as a promising candidate for therapeutic application due to its anti-inflammatory and α-glucosidase inhibition properties. These findings underscore the potential of unripe Nendran banana peel as a valuable source of bioactive compounds, paving the way for its use in functional foods and pharmaceutical applications.

5. International conference on advancements and innovations in phytochemistry, nutraceuticals and functional foods organized by Kerala Academy of Sciences (KAS), Thiruvananthapuram and Mar Athanasios College for Advanced Studies Tiruvalla (MACFAST) held at MACFAST, Tiruvalla, Kerala from 11-12, November 2024.

Phytochemical and Bioactive Carbohydrate Profiling of Banana Grit: A Novel Functional Food from Unripe Nendran Bananas

Natakkakath Kaliyathan Raveena,[1,3] Nagaraja Ingaladal,[2,3] M. V. Reshma,[1,3,*] and Ravi S. Lankalapalli[2,3]

[1]Agro-Processing and Technology Division, CSIR-National Institute for Interdisciplinary Science and Technology (CSIR-NIIST), Thiruvananthapuram 695019, Kerala, India
[2]Chemical Sciences and Technology Division, CSIR-National Institute for Interdisciplinary Science and Technology (CSIR-NIIST), Thiruvananthapuram 695019, Kerala, India
[3]Academy of Scientific & Innovative Research (AcSIR), Ghaziabad 201002, India
*Corresponding Authors: mvreshma@niist.res.in, ravishankar@niist.res.in

Abstract: Unripe banana 'Nendran' (*Musa* (AAB) cv. Nendran), an indigenous banana of Kerala, is an underutilized commodity. A novel product, BG was developed from the pulp of the unripe Nendran banana by pre-treatment and drying. BG is a novel preservative and additive-free product, which is in Ready to Cook (RTC) as well as Ready to Reconstitute (RTR) form. BG in RTC and RTR form offers a way to position banana in a new form rather than the conventional weaning food. Shelf-life studies showed that the product was shelf-stable for 11 months. BG was screened for the presence of 98 pesticides according to the AOAC method and they were below the detectable limit in BG. BG demonstrated nutrient superiority, by containing bioactive carbohydrates- resistant starch (4%), fructan (0.07 %), dietary fiber (7 %), minerals- potassium, and magnesium, and TCC of 3466 ± 11.78 µg/100 g which helps in positioning it as a promising alternative to cereals. The presence of a considerable amount of dietary fiber BG indicates its suitability for promoting gut health and thereby providing overall wellness. Furthermore, being gluten-free makes the product suitable for individuals with gluten allergy. The significant outcome of this work is the technology transfer of BG to Ms. MOZA ORGANIC Pvt. Ltd. Kochi, India. A detailed phytochemical analysis of BG revealed the presence of bioactive compounds including β-sitosterol, sitoindoside-II, sitoindoside-I, sterylglycoside, monogalactosyldiacylglycerol (MGDG), digalactosyldiacylglycerol (DGDG), acyl steryl glycosides and glucocerebroside. Literature data indicates that these compounds have numerous health benefits. The present work serves as the first report on the isolation of glucocerebrosides from *Musa* species and also the first report on phytochemical isolation studies from the Nendran cultivar. The study reveals that incorporating BG into the diet can contribute to overall health and well-being, highlighting the significance of diversifying dietary choices for optimal nutrition.

Food Chemistry Advances 1 (2022) 100063

Contents lists available at ScienceDirect

Food Chemistry Advances

journal homepage: www.elsevier.com/locate/focha

Phytochemical investigation of unripe banana (*Musa* AAB) cv. Nendran and its novel 'Banana Grits'

Natakkakath Kaliyathan Raveena[a,c], Nagaraja Ingaladal[b,c], M.V. Reshma[a,c,*], Ravi S. Lankalapalli[b,c,*]

[a] Agro-Processing and Technology Division, CSIR-National Institute for Interdisciplinary Science and Technology (CSIR-NIIST), Thiruvananthapuram 695019, Kerala, India
[b] Chemical Sciences and Technology Division, CSIR-National Institute for Interdisciplinary Science and Technology (CSIR-NIIST), Thiruvananthapuram 695019, Kerala, India
[c] Academy of Scientific & Innovative Research (AcSIR), Ghaziabad 201002, India

ARTICLE INFO

Keywords:
Banana
Nendran
Glycolipids
Glucocerebroside
Resistant starch
Carotenoids

ABSTRACT

Novel 'Banana Grits' (BG) was prepared from the pulp of unripe banana (*Musa* AAB) cv. Nendran, and their detailed phytochemical investigation is described. The present work serves as a first report of isolation and identification of glycolipids by exhaustive NMR and HR-ESI-MS analysis from Nendran that include glycolipids *viz.* monogalactosyldiacylglycerols, digalactosyldiacylglycerols, acyl steryl glycosides, glucocerebrosides, and steryl-glycoside. Proximate analysis, estimation of total carotenoid content, and the resistant starch content in BG are also reported. *In vitro* starch digestion pattern indicated that out of 80% of total starch in BG, 21% is slowly digestible starch (SDS) and 42% is resistant starch (RS). The presence of SDS and RS indicates that they may contribute to gut health and glycaemic control.

1. Introduction

Banana (*Musa* spp.) is one of the world's leading tropical fruit crop with immense economical value and occupy a pivotal role in human nutrition as a staple food (Aurore et al., 2009). India is the top banana-producing country in the world followed by China, Ecuador, Brazil, and Philippines (Nayar, 2010). In addition to the nutritional benefits, banana is a rich source of phytochemicals of therapeutic relevance (Pereira & Maraschin, 2015; Qamar & Shaikh, 2018; Singh et al., 2016). Phytochemical studies from various parts of *Musa* genera showed the presence of phenolics, flavonoids, anthocyanins, carotenoids, sterols and triterpenes, steryl glycosides, diarylheptanoids, phytoalexins, neurotransmitters, indoles, and amino acids. The phytochemicals associated with *M. paradisiaca* were attributed with a broad range of pharmacological benefits such as antidiabetic, antioxidant, anti-inflammatory, antimicrobial, and anti-helminthic (Oguntibeju, 2019).

Raw banana *Musa* (AAB) cv. Nendran is a popular cultivated variety of Musa in South Indian states (Tamil Nadu, Kerala, Karnataka), and elsewhere in the world. Nendran banana growing regions and its local name is given in the supplementary material under Table S1. It is consumed both in raw and ripe forms. Nendran attains bunch maturity after 5–6 months from flowering, the long and thick fruits with good keeping quality make unripe Nendran the best option for the preparation of the world-famous Kerala banana chips and as the first weaning food of babies in India (Chitra, 2015). The Nendran fruits are large, thick (20–27 cm long and 14–18 cm circumference) with a thick-leathery peel having three prominent ridges and a distinct nipple. The bunch of Nendran may weigh 12–15 kg with 4–6 hands, and each hand with 8–10 fingers (Sreejith & Sabu, 2017). The interior colour of the fruit will remain creamy, yellowish when it is raw and eventually turns yellowish orange during ripening, simultaneously the peel colour also turns yellow. When the peel is green, the flavour of the flesh is bland and its texture is starchy, as the peel changes to yellow, brown to black, the sweetness increases, and the texture becomes soft. 'Nendran' varieties include Nedunendran, Quintal Nendran, Chengalikodan, Manjeri Nendran, Wayanad local, Kaliyethan, Swarnamughi, Attu Nendran, etc. among them, Chengalikodan is a very popular variety that has conferred the geographical indication (GI) status and is known for its unique shape, red spots on the peel, colour, taste, etc. (Sreejith & Sabu, 2017). Nendran flower bracts were shown to possess anticancer activity, attributed to the presence of anthocyanins (Suman et al., 2018). A novel metalloprotease was reported from the peel of Nendran with collagenolytic and cytotoxic activities (Gurumallesh et al., 2019). Fructan from Nendran serves as a prebiotic, which stimulated the growth of lactic acid bacterial strains to varying degree (Shalini et al., 2017).

* Corresponding authors.
E-mail addresses: mvreshma@niist.res.in (M.V. Reshma), ravishankar@niist.res.in (R.S. Lankalapalli).

https://doi.org/10.1016/j.focha.2022.100063
Received 8 March 2022; Received in revised form 27 May 2022; Accepted 4 July 2022
Available online xxx

In the present study, the pulp of unripe banana (*Musa* AAB) cv. Nendran was converted to novel ready-to-cook 'Banana Grits' (BG) by preliminary treatments and drying techniques. Fully matured Nendran banana, *i.e.*, before ripening, was used to prepare BG. Maturity of Nendran can be defined as a fully grown stage that happens 150 days after flowering. Nendran banana, infructescence, and different stages of maturity are shown in the supplementary material under Figure S1. The peel colour of immature Nendran banana is dark green, and it becomes brownish-yellow with black marks at maturity. The immature fruit pulp is greyish white and later becomes creamy yellow and soft at maturity (Sreejith & Sabu, 2017). In the present study, we have used the maturity days (*i.e.*, around 150 days) as the selection criteria of Nendran banana for BG preparation, as this can be taken as the raw material selection criteria for commercial BG production. A detailed phytochemical investigation was conducted on the fruit pulp of the unripe Nendran pulp (UNP) and the converted BG. Moisture content of unripe Nendran pulp prior to BG preparation is also reported. We present the first report on isolation of glycolipids monogalactosyldiacylglycerols (MGDGs), digalactosyldiacylglycerols (DGDGs), acyl steryl glycosides, glucocerebrosides, and sterylglycoside from the organic extracts of UNP and BG. In addition, the proximate analysis, estimation of total carotenoid content, and the resistant starch content in BG is reported.

2. Materials and methods

2.1. General procedures

Structure elucidation of the isolated phytochemicals by chromatography was carried out by 1D (^{1}H, ^{13}C NMR, and DEPT-135) and 2D NMR (COSY, HSQC, and HMBC) analysis. The isolated compounds were dissolved in deuterated solvents ($CDCl_3$, CD_3OD), ^{1}H, and ^{13}C NMR were recorded on a Bruker Ascend^{TM} 500 MHz spectrometer at 500 and 125 MHz, respectively. The chemical shifts (δ) were given in parts per million (ppm), coupling constants in Hz, and multiplicities are reported as s for singlet, d for doublet, dd for double doublet, m for multiplet, etc. HR-ESI-MS (High-Resolution Electrospray Ionization Mass Spectrometry) analysis was conducted on a Thermo Scientific Exactive mass spectrometer with an Orbitrap analyzer, and the ions are given in *m/z*. The specific optical rotation of compounds was measured with a JASCO P-2000 polarimeter (JASCO, USA). The HPLC fingerprinting of carotenoids in the sample was performed on a Shimadzu HPLC (NexeraX2 HPLC system, Kyoto, Japan) connected to a PDA detector (SPD M20A). The total carotenoid content and glucose content were measured on a UV-2600, UV–VIS spectrophotometer (Shimadzu, Kyoto, Japan).

2.2. Chemicals and standards

All the solvents used for isolation and purification were of standard analytical grade. The TLC aluminium sheets (Silica gel 60 F_{254}) and silica gel (230–400 mesh & 100–200 mesh) were obtained from Merck (Mumbai, India). The NMR and HPLC grade solvents were purchased from Merck Life Science Pvt Ltd (Mumbai, India). The carotenoid HPLC standard (β-carotene - catalogue no. C4582–10MG), and the enzymes for *in vitro* starch digestion assay amyloglucosidase (catalogue no. 10,113), invertase (catalogue no. I4504), pancreatin (catalogue no. P7545), and pepsin (catalogue no. P7000) were procured from Sigma-Aldrich, India. The GOD-POD kit was purchased from Avecon Health Care Pvt. Ltd., India.

2.3. Raw material collection for BG preparation and phytochemical analysis

Nendran pulp (6.17 kg) from the indigenous Nendran banana cultivar from Kerala (India) was used for the preparation of novel BG, and the yield of BG was 2.4 kg (39%). The voucher specimen of Nendran (*Musa* (AAB) cv. Nendran) was collected on 15th May 2019 from local organic farmers in Vellayani, Ookode (8°25′54.3″N 77°00′14.8″E) Thiruvananthapuram District, Kerala, India, and the voucher specimen was deposited at Herbarium of JNTBGRI, Thiruvananthapuram, Kerala, India (Voucher number 94,628). BG was prepared from the unripe pulp of Nendran by pre-treatments and drying. For the phytochemical exploration studies, mature unripe Nendran banana (16.32 kg) was purchased from the exact location. The peel (5.09 kg) and pulp (10.35 kg) were separated, and the pulp (3.98 kg) was sliced, lyophilized (1.63 kg), and stored at −20 °C for further analysis. The remaining pulp (6.17 kg) was pre-treated and dried to produce BG (2.40 kg).

2.4. Proximate analysis of BG

The moisture, fat, protein, ash, and carbohydrate content of BG was determined according to AOAC Methods (AOAC, 1990). All the experiments were carried out in triplicates.

2.5. In vitro *starch digestibility of BG*

BG was analyzed for its starch fractions (slowly digestible starch, rapidly digestible starch & resistant starch) based on reported method (Englyst et al., 1992; Ren et al., 2016), with some modifications. The detailed methodology is given in the supplementary material (Method S1).

2.6. Phytochemical exploration of BG through column chromatography

2.6.1. Extraction protocol for isolation of phytochemicals

BG (1 kg) was ground and passed through 20 mesh before extraction and sequentially extracted with chloroform (3.5 L), ethanol (4 L), and hydro-alcohol (1:1 v/v, ethanol:water 4 L) at 800 rpm using an overhead stirrer (Hei-TORQUE 100, Heidolph, Germany). After extraction, each extract was kept for settling, and filtered through Whatman no. 1 filter paper, fitted with Buchner funnel to remove starch, then extracts were concentrated under vacuum (Hei-vap, Heidolph, Germany), which afforded 3.18 g, 4.39 g and 14.16 g of chloroform, ethanol and hydro-alcohol extracts, respectively. Schematic representation (Scheme S1) given under supplementary material shows the details of extraction protocol of BG. The phytochemical distribution pattern of the chloroform extract was monitored on TLC, with different mobile phase systems comprising 1:1 hexane:ethyl acetate (EtOAc), chloroform ($CHCl_3$):methanol (MeOH) (2:1, 8:1), and $CHCl_3$:EtOAc (7:3, 10:1), by charring with 15% H_2SO_4 in ethanol. The TLC chamber was oven dried and allowed to attain room temperature for each elution with the aforementioned mobile phase systems prior to the use. The $CHCl_3$:MeOH (8:1) system showed the best separation pattern of compounds, hence, this ratio was adopted for checking the TLC of the isolates in further studies (Fig. 3).

2.6.2. Purification of chloroform extract by column chromatography

The chloroform extract (2.8 g) was adsorbed and loaded on a silica (230–400 mesh) column (60 × 3 cm) and sequentially eluted with 800 mL of 100% chloroform which yielded 15 fractions. Further, 200 mL each of 1–10%, 15%, 20% and 50% methanol in chloroform combination was added and each percentage solution was collected as separate fractions, which afforded 13 fractions. Finally, the column was eluted with 100 mL of 100% methanol. The TLC pattern of all the 29 fractions was monitored with $CHCl_3$:MeOH (8:1) system and visualized by charring with 15% H_2SO_4 in ethanol. The fractions which showed similar TLC patterns were pooled, which resulted in a total of nine ($C_{2–6}$, C_8, C_{10}, C_{11}, and C_{13}; TLC pattern given in the supplementary material Figure S2) 100% chloroform fractions and twelve chloroform-methanol fractions ($CM_{1–10}$, CM_{15} and CM_{20}). Only the fractions that showed prominent TLC patterns were further explored for compound isolation.

2.6.3. Repurification of fractions and pure compound isolation

Two fractions (C_8 and C_{10}) among the nine 100% chloroform fractions, were having a purple-pink prominent charring spot (Rf 0.68) in TLC when developed in $CHCl_3$:MeOH (8:1) system. The combination of acetonitrile:methanol:tetrahydrofuran in the ratio 40:56:4, when added to these fractions, compound **1** precipitated (216.2 mg from C_8 and 2.3 mg from C_{10}, TLC pattern provided in supplementary material Figure S2), the compound was then dissolved in $CDCl_3$ and ^1H and ^{13}C NMR spectra were recorded. Next, we attempted purification of seven fractions from chloroform and CM_{1-3} but could not succeed in isolating compounds in pure form. Further, we tried purification of CM_4 (108.9 mg) on a silica gel column (230–400 mesh) and it afforded 6 sub-fractions, one sub-fraction (52.5 mg) was further purified on a silica gel column of 100–200 mesh, packed with hexane-ethyl acetate (1:1, v/v) and eluted with the same solvent system and it afforded 7.2 mg of compound **3** (Rf 0.52). The ^1H and ^{13}C NMR spectrum of compound **3** was recorded in $CDCl_3$. Other fractions ($CM_{5-6,\ 20}$), did not yield any compounds in pure form. When 100% methanol was added to the CM_7 fraction, a white precipitate (compound **4**, 33.9 mg) was observed and the ^1H NMR spectrum was taken in $CDCl_3$, and since the NMR spectrum showed poor splitting pattern, the compound was peracetylated. In brief, the compound (12.8 mg) was dissolved in pyridine (2 mL) and acetic anhydride (1.5 mL) under nitrogen atmosphere at room temperature. After overnight stirring, the mixture was transferred to saturated $NaHCO_3$ solution (20 mL) and extracted with EtOAc (3 × 30 mL). The combined organic layers were further washed with distilled water (2 × 30 mL), dried over anhydrous Na_2SO_4, and concentrated. The residue was subjected to purification over silica gel column (100–200 mesh) with 100% hexane and ethyl acetate in hexane combination (5%–50%) to afford the acetylated product (8.1 mg), the ^1H and ^{13}C NMR spectrum of this acetylated compound were recorded in $CDCl_3$.

On addition of methanol individually to CM_{8-10}, as in the case of CM_7, a methanol insoluble and methanol soluble portions were generated. The methanol insoluble portion of CM_8 and CM_9 (27.4 mg and 7 mg, respectively) showed the exact TLC pattern as that of compound **4** when developed in $CHCl_3$:MeOH 8:1 system. The methanol soluble portions of CM_{7-10} were pooled (90 mg) and separated on a silica gel column (230–400 mesh), which yielded two compounds. The first compound (13.8 mg) showed the same Rf (0.28) and charring pattern as that of compound **4**. The TLC comparison of all the compounds (one from the column and two from the insoluble fraction of $CM_{8,9}$) showing similarity with compound **4** is given in the supplementary material (Figure S3). The second compound, *i.e.* compound **7** (32 mg) showed more polar nature (Rf 0.16) than that of compound **4**, when developed in $CHCl_3$:MeOH 8:1 system and its ^1H NMR spectrum was recorded in $CDCl_3$. In addition, compound **7** was peracetylated as detailed for compound **4**. The ^1H and ^{13}C NMR spectrum of the peracetylated compound **7** was recorded in $CDCl_3$. The fraction eluted with 15% methanol in chloroform combination (CM_{15}, 250 mg) showed a deep purple coloured charring spot (compound **6**) with Rf 0.12, when developed in $CHCl_3$:MeOH 8:1 system. The ^1H NMR spectrum of compound **6** was recorded in $CDCl_3$, however, due to poor splitting pattern in ^1H NMR, compound **6** (68 mg) was acetylated and subsequent column purification afforded peracetylated form of compound **6** (51.6 mg). The ^1H and ^{13}C NMR spectra, and 2D NMR experiments of peracetylated compound **6** were recorded in $CDCl_3$. HR-ESI-MS analysis with direct injection was carried out on compound **6** in underivatized and derivatized form (peracetylated form). The yields of compounds obtained through column chromatography route are depicted in Table 1.

2.7. Phytochemical exploration studies of BG through preparative TLC method

After completion of phytochemical exploration studies through column chromatography method, we have continued our exploration to find more phytoconstituents of BG through the preparative TLC method. Accordingly, BG (500 g) was sequentially extracted with hexane, acetone, ethanol, hydro-alcohol (1:1, ethanol:water v/v) at 1000 rpm for 6 h in a magnetic stirrer (IKA, RCT BS022) and the schematic representation of extraction protocol is provided in the supplementary material (Scheme S2). Each extract was concentrated under vacuum, which afforded hexane extract (560 mg), acetone extract (120 mg), ethanol (705 mg), and hydro-alcohol extract (7 g) of BG. The hexane and acetone extracts were further explored via the preparative TLC method. The hexane extract (70 mg) was spotted on a TLC plate and developed in $CHCl_3$:MeOH 8:1 system. A portion of the TLC was cut and charred and used as a reference for scrapping out the compounds. A prominent charring spot corresponding to Rf 0.68 was scrapped out and the compound was eluted from silica with ethyl acetate, ^1H NMR spectra were recorded in $CDCl_3$ and identified as compound **1** (19.5 mg). Similarly, the acetone extract (100 mg) of BG was also spotted on a TLC plate and developed in $CHCl_3$:MeOH 8:1 system, and charring spot corresponding to 0.68, 0.32, and 0.12 were scrapped out and eluted with ethyl acetate, and the solvent was removed under vacuum, which led to isolation of compound **1** (1.1 mg), compound **5** (5 mg), and compound **6** (2 mg), respectively. Compound **5** obtained through preparative TLC method was dissolved in $CDCl_3$ and recorded the ^1H, ^{13}C, 2D NMR spectra, and further confirmed by HR-ESI-MS analysis. The yields of compounds obtained through the preparative TLC method is depicted in Table 1.

2.8. Phytochemical exploration studies of UNP

2.8.1. Phytochemical exploration studies through preparative TLC method

The lyophilized UNP (100 g) was sequentially extracted with hexane, acetone, ethanol, and hydro-alcohol (1:1, ethanol:water v/v) which yielded 218 mg, 58.8 mg, 145.3 mg, and 2.8 g extracts, respectively (supplementary material Scheme S3). The hexane (60 mg) and acetone extracts (50 mg) were subjected to preparative TLC analysis as mentioned under Section 2.7. The preparative TLC exploration of hexane extract afforded 3.8 mg of compound **1** (Rf 0.68), 1.5 mg of compound **2** (Rf 0.48), and 1.8 mg of compound **5** (Rf 0.32). The ^1H and ^{13}C NMR spectrum of compound **2** was recorded in $CDCl_3$. The preparative TLC exploration of acetone extract yielded 3 mg of compound **2** (Rf 0.48), 4.2 mg of compound **5** (Rf 0.32), and 4.7 mg of compound **6** (Rf 0.12). The yields of compounds obtained through the preparative TLC route is depicted in Table 1.

2.8.2. Phytochemical exploration studies of UNP through column chromatography and preparative HPLC method

In brief, 500 g of lyophilized UNP was sequentially extracted with chloroform and acetone, which yielded 2.09 g and 325 mg chloroform and acetone extracts, respectively. Each extract was separately chromatographed on a silica gel column (230–400 mesh) and eluted with 100% chloroform followed by 5–50% methanol in chloroform which yielded 35.3 mg and 15.1 mg of compound **7** from the chloroform and acetone extracts, respectively. The compound **7** (40 mg) so obtained was dissolved in methanol (1.2 mL) and filtered through a 0.2 μm nylon syringe filter (Micro-Por Minigen Syringe Filter, Genetix Biotech Asia, New Delhi), and the clear solution was injected into the preparative HPLC system connected to a reverse phase Luna 5 μ C18 (2) column 25 cm × 21.2 mm (Phenomenex, USA) for further purification. The mobile phase system consisted of 100% methanol with a flow rate of 5 mL per minute. The sample injection volume was 1 mL and the fractions were collected by monitoring the eluting peaks at 205 nm. The collected fractions were evaporated under vacuum in a rotatory evaporator. ^1H and ^{13}C NMR, 2D NMR spectra of compound **7** was taken in $CDCl_3$:CD_3OD (2:1 v/v), and further analysed by HR-ESI-MS. Yields of compound **7** obtained through the column chromatography route is depicted in Table 1.

Table 1
Yield (%) data of pure compounds obtained from BG and UNP through different isolation routes.

Compound Number	Compounds	Yield (%)						
		BG Column - Chloroform Extract	BG Preparative TLC		UNP Column		UNP Preparative TLC	
			Hexane Extract	Acetone Extract	Chloroform Extract	Acetone Extract	Hexane Extract	Acetone Extract
1	*β*-Sitosterol	0.024	0.031	0.0002	*	*	0.013	ND
2	Sitoindoside-II	ND	ND	ND	*	*	0.005	0.003
3	Sitoindoside-I	0.0008	ND	ND	*	*	ND	ND
4	*β*-Sitosterol *β*-D-glucopyranoside	0.009	ND	ND	*	*	ND	ND
5	MGDG	ND	ND	0.001	*	*	0.006	0.004
6	DGDG	0.028	ND	0.0004	*	*	ND	0.005
7	Glucocerebroside	0.003	ND	ND	0.007	0.003	ND	ND

ND - Not detected, * Not explored.

2.9. Confirmation of molecules by specific optical rotation

The specific optical rotation of compound **1** and peracetylated compound **4** was analyzed by preparing 0.61% and 0.92% solutions of compounds in $CHCl_3$, and the values were recorded with JASCO P 200 polarimeter.

2.10. Estimation of total carotenoid content of BG

The total carotenoid content in BG was estimated as per literature report with slight modification (Rodriguez-Amaya & Kimura, 2004). In brief, BG (100 g) was powdered and passed through 20 mesh and extracted with hexane at 70 °C for 6 h in a Soxhlet apparatus, which yielded 413.5 mg of hexane extract and from that 2.5 mg of sample was taken for total carotenoid content measurement.

For acetone extraction, BG (6 g) was powdered and passed through 20 mesh, from that a portion of the sample (3 g) was extracted with 50 mL chilled acetone for 30 min and the process was repeated until the sample was colourless. The extract was then transferred to petroleum ether (25 mL) and the absorbance was read at 450 nm in a UV–VIS spectrophotometer (UV-2600, Shimadzu, Japan) and quantified using the absorption coefficient of 2500 (recommended for estimation of carotenoid mixtures).

$$\text{Total carotenoid content}(\mu g/g) = \frac{A \times V(mL) \times 10^4}{A_{1cm}^{1\%} \times \text{sample weight}(g)}$$

Where A is the absorbance at a specified wavelength, V is the total volume of extract (25 mL), $A_{1cm}^{1\%}$ is the absorption coefficient (2500). The total carotenoid content of BG hexane extract was measured by dissolving 2.5 mg of the extract in 10 mL of petroleum ether and the total carotenoid content was measured as described above.

2.11. Qualitative HPLC-DAD profiling of carotenoids in the BG hexane extract

The carotenoid fingerprinting of the BG was performed by using the hexane extract of BG and analyzed with the analytical Nexera X2 HPLC system (Shimadzu, Japan) equipped with a reverse phase, shim-pack GISS 5 μm C18 column (250 × 4.6 mm, Shimadzu) connected to a PDA detector (SPD-M20A) and an autosampler (SIL-30AC). The mobile phase comprised of acetonitrile:methanol:tetrahydrofuran (40:56:4) with a flow rate of 1 mL/min, and isocratic elution for 30 min. The weighed *β*-carotene standard (5 mg) was dissolved in THF (10 mL) and 20 μL of the sample was injected. The hexane extract (50 mg) of BG (extraction procedure mentioned under Section 2.10) was dissolved in 2 mL of THF and filtered through a 0.2 μm nylon filter (Micro-Por Minigen Syringe Filter, Genetix Biotech Asia, New Delhi) prior to analysis, and 20 μL of the sample was injected. The column temperature was maintained at 25 ºC and eluting peaks were monitored at 450 nm (Bushway, 1986).

2.12. Statistical analysis

All the experiments (proximate analysis, *in vitro* starch digestibility, and total carotenoid content) were carried out in triplicates ($n = 3$) and the data were recorded as mean ± standard deviation (SD).

3. Results and discussion

3.1. Preparation of BG

Ripe Nendran banana is a popular fruit of Kerala, India, used in the preparation of sweet dishes, and the unripe Nendran is used in the preparation of raw banana fried chips and as weaning food. Hitherto attempts were not made to explore the phytochemicals and associated health benefits of unripe Nendran banana. The estimated moisture content of unripe Nendran pulp was 58.67 ± 0.13%. To the best of our knowledge, there has been no previous attempt to develop raw Nendran as grits, which can have wider applications as porridge, flavored health drinks, gruel, and BG-vegetable (veg) mix that can be consumed as a main course food (Fig. 1). BG is a novel preservative-free and additive-free product, which is in ready-to-cook as well as ready-to-reconstitute form. BG was prepared using the pulp of matured unripe Nendran banana (150 days old after flowering; 20–27 cm long and 16 cm around) by pre-treatment and drying.

3.2. Proximate analysis and in vitro starch digestibility of BG

The proximate analysis showed that BG has a low moisture content (2.83 ± 0.05%), 1.46 ± 0.03% ash content, 3.97 ± 0.22% protein content and high carbohydrate content (91.31 ± 0.17%). Since the main component of BG is starch, *in vitro* digestion studies have been carried out to quantify its rapidly digestible starch (RDS), slowly digestible starch (SDS), resistant starch (RS), and total starch (TS) content by measuring the glucose released during different phases of digestion (detailed data is given in the supplementary material, Table S2). *In vitro* starch digestion pattern indicated that 80.49 ± 2.68% is TS, 21.44 ± 2.34% is SDS, 16.95 ± 0.79% is RDS and 42.08 ± 2.85% is RS (Fig. 2a and b).

Starch from cereals and tubers is consumed worldwide as an energy source along with 'cooking bananas' which are in the tenth position in the list of staple foods. Unripe banana is considered as the RS-rich non-processed food, its RS content ranges between 47 and 57% (Fuentes-Zaragoza et al., 2010). The starch content of unripe fruit pulp of banana cultivars like Ney Poovan, Robusta, Rasthali, Poovan, Pachanadan, Nendran, Karpuravalli, Monthan, and Saba was recorded in the range of 80.35–86.76% on dry weight basis and the Nendran cultivar in particular found to have 84.75% starch content (Ravi & Mustaffa, 2013). To the best of our knowledge, RS content of raw Nendran banana is not reported so far. The SDS and RS fractions of starch were known to have nutraceutical potential due to their low postprandial glycaemic response and high indigestible carbohydrate content. Since the SDS fraction is slowly digested in the small intestine, it gives a low glycaemic value,

Fig. 1. Unripe Nendran, novel 'Banana Grit' (BG), and products formulated from BG.

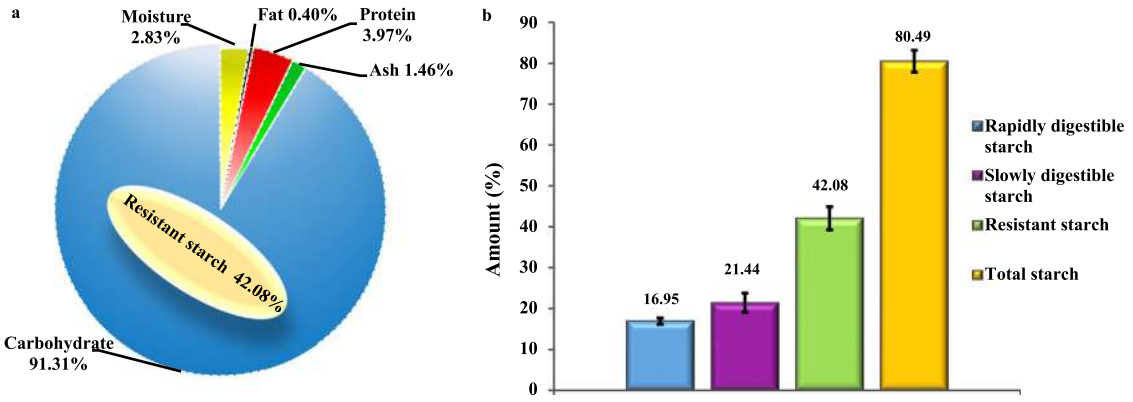

Fig. 2. **a:** Proximate composition of BG; **b:** Amount of starch fractions in BG measured through *in vitro* starch digestion of BG.

hence related to reduction in the risk of diabetes and other chronic diseases (Englyst et al., 1992; Jenkins et al., 2002). The RS portion escapes digestion in the small intestine and on reaching the large intestine it gets fermented by the gut microbiota. Hence, RS acts as a substrate for the growth of probiotic bacteria, accordingly, RS is considered as a prebiotic food (Lockyer & Nugent, 2017). RS was also found to have the hypocholesterolemic effect and also help in better absorption of minerals (Morais et al., 1996; Younes et al., 1995). Due to these facts, SDS and RS portions are considered as bioactive carbohydrates and hence BG can be considered as a gut-friendly food that can be of prebiotic nature.

3.3. Phytochemical exploration studies of BG and UNP

The phytochemical composition of BG and UNP were explored by column chromatography, preparative TLC, and preparative HPLC, and the structural characterization of pure compounds were carried out with the aid of NMR, HR-ESI-MS & specific optical rotation data. The sequential extraction of BG with different solvent systems afforded four extracts as mentioned in Section 2.6.1. Crude chloroform extract of BG showed 7 prominent charring spots with Rf ranging from 0.1 to 0.8 (Fig. 3) in $CHCl_3$:MeOH (8:1) system, hence, we focussed on phytochemicals isolated from the chloroform extract only. The compound corresponding to Rf 0.82 appeared as a carotenoid based on its bright orange colour in TLC. Compounds corresponding to the other six prominent charring spots (compound **1, 3–7**) were identified (Fig. 3) and discussed in detail here.

Phytochemicals were isolated from UNP by preparative TLC and column chromatography routes. It was observed that the TLC profile of the chloroform and acetone extracts of the UNP displayed perfect resemblance to that of the chloroform extract of BG (Fig. 3). Preparative TLC isolation of hexane and acetone extracts of UNP afforded compounds **1, 2**, and **5** and compounds **2, 5**, and **6**, respectively. On the other hand, the

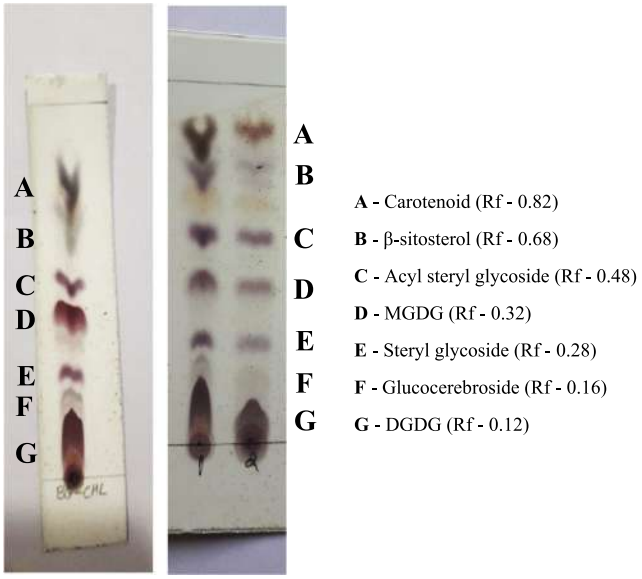

Fig. 3. TLC charring pattern of BG chloroform extract (TLC code: BG-CHL), UNP chloroform extract (TLC code: 1) and UNP acetone extract (TLC code: 2) developed in $CHCl_3$:MeOH (8:1) system.

chloroform and acetone extracts were subjected to column chromatography for isolation of compound **7**. NMR spectral data of compounds 1–7 are given in the supplementary material.

Compound **1** (supplementary material Figure S4) exhibited characteristic chemical shifts of aliphatic phytosterol in ^{1}H and ^{13}C NMR, with the presence of C3-OH and olefinic proton signals, its non-polar

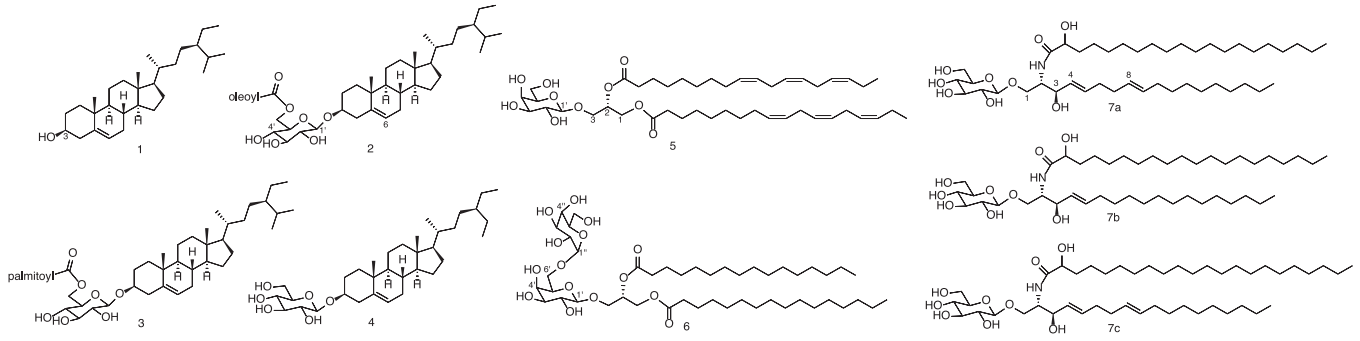

Fig. 4. Structures of compounds **1–7**. Compound **1** - *β*-Sitosterol, Compound **2** - Sitoindoside-II, Compound **3** - Sitoindoside-I, Compound **4** - *β*-Sitosterol *β*-D-glucopyranoside, Compound **5** - MGDG, Compound **6** - DGDG, Compound **7** - Glucocerebroside.

nature was evident from TLC. Vilela et al. reported sterols such as *β*-sitosterol, campesterol, and stigmasterol from the ripe pulp of ten *Musa* species (Vilela et al., 2014). Hence, compound **1** was readily identified as *β*-sitosterol (Fig. 4), further confirmed by NMR spectral comparison in Biological Magnetic Resonance Data Bank. The specific optical rotation of compound **1** was found to be −30.25°, which was in agreement with the reported value of −30° (Johnson, 1958). Efficient precipitation of *β*-sitosterol from the hexane extract upon addition of acetonitrile:methanol:tetrahydrofuran (40:56:4) was an accidental observation that happened during sample preparation for HPLC analysis for carotenoids.

Compound **2** (supplementary material Figure S5) exhibited characteristic carbohydrate chemical shifts between 3 and 5 ppm, with δ_H 4.32 ppm (J = 7.6 Hz) indicating anomeric proton H-1' with *β*-configuration. Presence of downfield chemical shifts for H-6' (δ_H 4.45, 4.18 ppm) in ^{1}H NMR suggest the presence of an ester functionality on C6'-OH, with an aliphatic chain. Presence of a steryl group was evident from NMR, which along with the conventional glycosidic linkage ($\delta_{C\text{-}1'}$ 101.2 ppm) suggest compound **2** as an acyl steryl glycoside (ASG). By consideration of COSY correlations (supplementary material Figure S6) and diaxial coupling constants of 9 Hz for $\delta_{H\text{-}4'}$ 3.31 ppm and $\delta_{H\text{-}2'}$ 3.29 ppm, the carbohydrate moiety was confirmed as D-glucose. A three integration in ^{1}H NMR in the olefinic region suggest the presence of one unsaturation in aliphatic chain and with characteristic H-6 of the steryl moiety, which along with chemical shift considerations of ^{1}H and ^{13}C NMR resemble *β*-sitosterol. Ghosal et al. reported extensively on isolation and characterization of steryl glycosides and sitoindosides (ASGs) from the peel of *M. paradisiaca* and their anti-ulcerogenic activity (Ghosal, 1985). Presence of olefinic carbons at δ_C 130 ppm indicate oleoyl moiety of the acyl group, which based on the published report by Ghosal et al. suggest compound **2** as sitoindoside-II (Fig. 4) (Ghosal, 1985). Accordingly, compound **3** (supplementary material Figure S7) was elucidated as sitoindoside-I (Fig. 4) with a palmitoyl chain evident by the presence of only one olefin proton ($\delta_{H\text{-}6}$ 5.3 ppm) from the *β*-sitosteryl moiety, which was further evident from the ^{13}C NMR. Compound **4** exhibited characteristic carbohydrate signals in the ^{1}H NMR that along with steroidal region resemble a sterylglycoside. However, due to poor splitting pattern in ^{1}H NMR in $CDCl_3$, compound **4** was peracetylated (supplementary material Figure S8) and confirmed as a *β*-sitosterol *β*-D-glucopyranoside (Fig. 4) by NMR, which was in agreement with literature (Faizi et al., 2001). The specific optical rotation of peracetylated form of compound **4** was found to be −22.9°, which was in agreement with the reported value of −23.9° (Coutts et al., 1957).

Compound **5** (supplementary material Figure S9) exhibited characteristic carbohydrate signals in the ^{1}H NMR along with aliphatic chain, thus, resembling a glycolipid. Presence of COSY correlations for H-2 with H-3, H-1; H-1' with H-2'; H-6' with H-5', and HMBC correlation for H-2' with C1', C3'; H-4' with C2', which along with coupling constants confirmed the presence of D-galactose appended to a glycerol backbone as a *β*-glycoside. The downfield chemical shifts of H-2, H-1, and HMBC correlation of H-1' with C3 indicate the presence of ester groups in *sn*-1,2 positions and *sn*-3 with glycosidic linkage (supplementary material Figure S10), thus, compound **5** is a MGDG. Presence of olefinic protons between 5 and 5.5 ppm suggest the presence of unsaturated fatty acids. HR-ESI-MS analysis (supplementary material Figure S11) with direct injection was carried out to identify prominent molecular species, and two ions were observed. Ion at *m/z* 775.5367 $[M+H]^+$, which against the calculated 775.5360 $[M+H]^+$, confirms the molecular formula $C_{45}H_{74}O_{10}$ that corresponds to MGDG 36:6. Ion at *m/z* 799.5354 $[M$+Na$]^+$, which against the calculated 799.5336 $[M$+Na$]^+$, confirms the molecular formula $C_{45}H_{76}O_{10}$ that corresponds to MGDG 36:5. Blackbourn et al. reported the presence of high proportion of mono- and di- galactosyl diacylglycerols (MGDGs and DGDGs) in banana peel, with polyunsaturated fattys acids (PUFAs) such as *α*-linolenic acid (18:3*ω*3), PUFAs in MGDGs account for 94% of the fatty acid content (Blackbourn et al., 1990). Hence, one of the molecular specie, MGDG 36:6 was identified as compound **5** (Fig. 4). The second molecular specie MGDG 36:5 has two possibilities, MGDG (18:3*ω*3/18:2*ω*6) or MGDG (18:2*ω*6/18:3*ω*3). MGDGs and DGDGs are predominantly found in the thylakoid membrane of plant chloroplasts, which are overlooked in nutrition applications as they are dispersed in biomass (Sahaka et al., 2020). In addition, compound **5** is a main constituent of a plant enriched extracts of many patents with a variety of product applications. Compound **5** is endowed with a wide-range of pharmacological benefits, extensively reported in literature and reviewed in the supplementary material.

Compound **6** exhibited characteristic disaccharide signals in the ^{1}H NMR, which along with aliphatic region resemble DGDG. However, due to poor splitting pattern in ^{1}H NMR, compound **6** was peracetylated and characterized (supplementary material Figure S12). Presence of key COSY correlations of H-2' with H-1', H-3'; H-4' with H-5', H-3'; H-2'' with H-1'', H-3''; H-4'' with H-5'', H-3'' aided in identification of the anomeric protons H-1' and H-1'' with *β* and *α* configurations, respectively. Coupling constants of 1.9 and 1.7 Hz for H-4'' and H-4', respectively, confirm the presence of digalactosyl moiety. Presence of COSY correlation of H-2 with H-3, H-1 helped in identification of the protons of the glycerol backbone in ^{1}H NMR. Presence of key HMBC correlations of H-3 with C1' and H-6' with C1'' confirm the glycosidic linkages of DGDG (supplementary material Figure S13). HR-ESI-MS analysis with direct injection was carried out to identify the molecular species (supplementary material Figure S14). DGDG account for higher proportion of saturated fatty acid such as palmitic acid (Blackbourn et al., 1990). HR-ESI-MS analysis of the underivatized compound **6** exhibited an ion at *m/z* 915.6029 $[M$+Na$]^+$, which against the calculated 915.6021 $[M$+Na$]^+$ with palmitic esters, confirms the molecular formula $C_{47}H_{88}O_{15}$ that corresponds to compound **6** (Fig. 4). A prominent ion at *m/z* 847.4677 $[M$+Na$]^+$, which against the calculated 847.4667 $[M$+Na$]^+$, suggest the molecular formula $C_{40}H_{72}O_{17}$ that corresponds to a DGDG containing a

nonadioic acid in *sn*-1 or *sn*-2 along with palmitic acid. Nonadioic acid was one of the dioic acids reported in the lipophilic extracts of ripe pulp from banana cultivars (Vilela et al., 2014). HR-ESI-MS analysis of the derivatized peracetylated compound **6** showed corresponding ions with increase in mass by 294 due to acetylation of 7 x OH groups of digalactosyl moiety (supplementary material Figure S15). Signals in mass spectra depend on the ionizing capability of the compounds, hence, DGDG with an extra carboxylic acid functionality in nonadioc acid is intense compare to compound **6** with palmitic acid (supplementary material Figure S14). A *n*-BuOH fraction of compound **6** from *Malva verticillata* was reported with anticancer activity in AGS cells (gastric cancer), with an with IC_{50} value 10.6 μM (Ko et al., 2018).

Compound **7** exhibited characteristic glycolipid signals in NMR, which was initially analyzed by peracetylation NMR (supplementary material Figure S16). Based on diaxial coupling constants and characteristic 8 Hz coupling constant of the anomeric proton, the monosaccharide of the acetylated derivative was determined as D-glucose with β-glycosidic linkage. Presence of a characteristic amide NH proton and HMBC correlations, indicate the presence of a ceramide backbone with sugar appendage at the C1 position. However, the presence of a C3-C4 double bond was unusual in the derivative, perhaps, an elimination reaction followed during peracetylation as shown in the supplementary material (Scheme S4), thus, confirming compound **7** as a glucocerebroside. Based on the NMR, compound **7** in its original state NMR (supplementary material Figure S17) or in its peracetylated form NMR (supplementary material Figure S16) constitute a mixture of molecular species. We resorted to HR-ESI-MS analysis for generic information of the sphingosine backbone as well as aliphatic chains of the amide. HR-ESI-MS through LC afforded one of the parent ion measured as 770.6146 $[M + H]^+$, which against the calculated 770.6146 correspond to molecular formula $C_{44}H_{83}NO_9$, thus, revealing one of the molecular species **7a** (Fig. 4 and 5a). Presence of $[M+Na]^+$, $[2M+Na]^+$ peaks, and fragment peaks 752.6045 and 590.5514 corresponding to $[M\text{-}OH]^+$ calculated for 752.6035 and $[M\text{-glucose}]^+$ calculated for 590.5507, respectively confirm a sphingadienine backbone with 2-hydroxyeicosanoic acid as the aliphatic chain for molecular specie **7a**. A second parent ion measured as 794.6127 $[M+Na]^+$, which against the calculated 794.6122 correspond to molecular formula $C_{44}H_{85}NO_9$, thus, revealing the second molecular specie **7b** (Fig. 4 and 5b). Presence of $[2M+Na]^+$ peak, and fragment peaks 610.5782 and 592.5675 corresponding to $[M\text{-glucose}+H]^+$ calculated for 610.5774 and $[M\text{-glucose-OH}]^+$ calculated for 592.5663, respectively confirm a sphingosine backbone with 2-hydroxyeicosanoic acid as the aliphatic chain for molecular specie **7b**. A third parent ion measured as 820.6282 $[M+Na]^+$, which against the calculated 820.6279 correspond to molecular formula $C_{46}H_{87}NO_9$, thus, revealing the third molecular specie **7c** (Fig. 4 and 5c). Presence of $[2M+Na]^+$ peak, and fragment peaks 780.6361 and 618.5830 corresponding to $[M\text{-}OH]^+$ calculated for 780.6348 and $[M\text{-glucose-OH}]^+$ calculated for 618.5820, respectively confirm sphingadienine backbone with 2-hydroxydocosanoic acid as the aliphatic chain for molecular specie **7c**. Both 2-hydroxyeicosanoic and 2-hydroxydocosanoic acids were reported as fatty acids components in banana cultivar "Dwarf Cavendish" (Oliveira et al., 2006). To determine the position of double bond in sphingadienine and sphingosine backbone, we resorted to 2D NMR of compound **7**. Presence of key COSY correlations of H-3 with H-4, H-2; H-5 with H-4, H-6; and the presence of key HMBC correlations of H-3 with C2, C1, C4, C5; and H-1 with C1' (anomeric carbon) confirm the position of double bond at C4 of sphingadienine and sphingosine backbone NMR (supplementary material Figure S18). The characteristic '*E*' geometry of C4-C5 was determined from trans coupling constant of 15 Hz in ^{1}H NMR, but due to merging of signals between 5.2 to 5.3 ppm corresponding to the second double bond and due to the presence of molecular species, it was difficult to determine the double bond geometry and position. However, based on the consensus structure of sphingoids from plants, we report C8-C9 double bond with '*E*' geometry (Shirakura et al., 2012). The stereochemistry of C2 and C3 is highly conserved in sphingoids, however, the configuration of the hydroxy position of the aliphatic acid was left unassigned. To the best of our knowledge, the present work is the first report on isolation and characterization of glucocerebrosides from *Musa* species. Glucocerebroside have an immunomodulatory effect and showed beneficial effect in clinical studies for type 2 diabetes or non-alcoholic steatohepatitis (Ilan et al., 2009). In addition, glucocerebrosides have shown application in cosmetics by playing an important role in the skin-barrier function in retaining moisture, and also has shown relevance as dietary supplement (Jiang et al., 2021).

3.4. Total carotenoid content of BG

One of the characteristic attributes of BG is its bright yellow colour which in turn is linked with the carotenoid content in the BG, hence attempts were made to quantify the total carotenoid content in BG by taking both the hot hexane extract and cold acetone extract of BG. According to the latest National Institute of Nutrition data (2017) (Longvah et al., 2017), the carotenoid content of raw banana (*Musa* × *paradisiaca*) was 224 μg/100 g. Whereas, an exceptionally high level of carotenoid content *i.e.* 3466 ± 11.78 μg/100 g of BG and 3819 ± 15.82 μg/100 g of BG was obtained through the acetone and hexane extraction routes, respectively (supplementary material Figure S19). Studies show that the carotenoid content of even the ripe bananas of cultivars like Monthan, Poovan, Red, and Robusta was very low and it ranges from 252 to 314 μg/100 g (Longvah et al., 2017). The high amount of carotenoids in BG indicates the suitability of BG for alleviating the vitamin A deficiency.

3.5. Qualitative HPLC-DAD profiling of carotenoids in the BG hexane extract

The HPLC profiling of the hexane extract was carried out for identification of carotenoids in BG. The standard β-carotene peak was identified at a retention time of 21.30 min (supplementary material Figure S20a). In the extract, peak at retention time 21.40 min correspond to β-carotene along with other unidentified peaks (supplementary material Figure S20b). Presence of β-carotene was further confirmed by spiking with standard β-carotene (supplementary material Figure S20c). among the carotenoids, α-carotene and β-carotene have a high level of provitamin A activity (Englberger et al., 2006). Even though the micronutrient requirements in our body is very minimal, their impact on our body's health is crucial and deficiency of any of them can lead to mild to severe even life-threatening conditions. According to WHO, deficiencies in iron, vitamin A and iodine were the most common around the world, particularly in children and pregnant women, and nearly 2,50,000–5,00,000 children who are vitamin A-deficient become blind every year, and half of them die within 12 months of losing their sight (https://www.who.int/data/nutrition/nlis/info/vitamin-a-deficiency). Since, BG is a good source of provitamin A carotenoids, it can also help in alleviation of Vitamin A deficiency.

4. Conclusion

In this study, we showed a novel utility of unripe Nendran banana as 'Banana Grits' that can be consumed on daily basis like cereals and tubers. *In vitro* starch digestion pattern indicated that out of 80% of total starch in BG, 21% is SDS and 42% is RS. The presence of SDS and RS indicates that they may contribute to gut health and glycaemic control. Estimation of total carotenoid content of BG revealed a high level of carotenoid content of greater than 3000 μg/100 g of BG in hexane or acetone extracts, thus, BG serves as a provitamin source to alleviate Vitamin A deficiency. A detailed phytochemical analysis from the organic extracts of BG and as well as UNP revealed the presence of glycolipids *viz.* MGDGs, DGDGs, ASGs, glucocerebrosides, and sterylglycoside. An exhaustive NMR and HR-ESI-MS analysis aided in providing structural

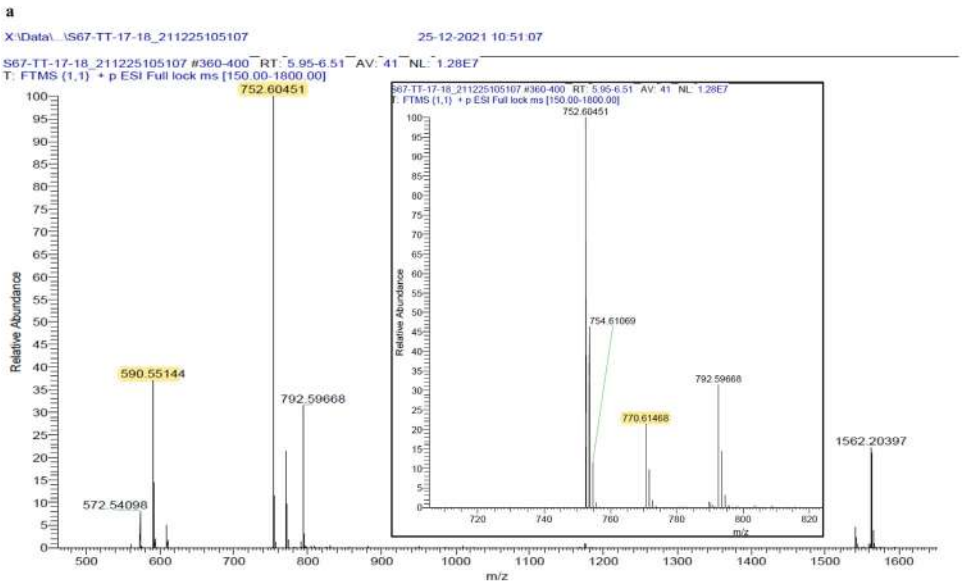

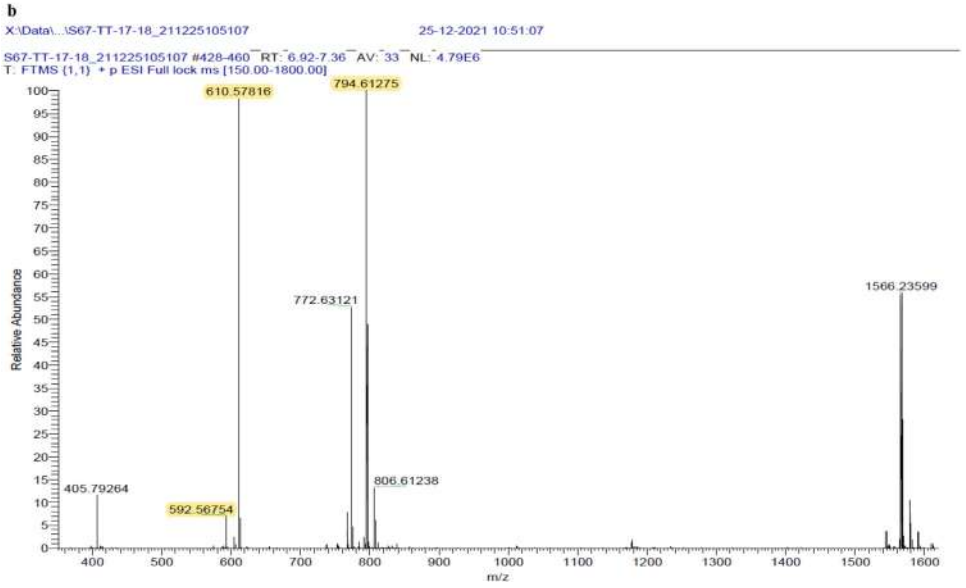

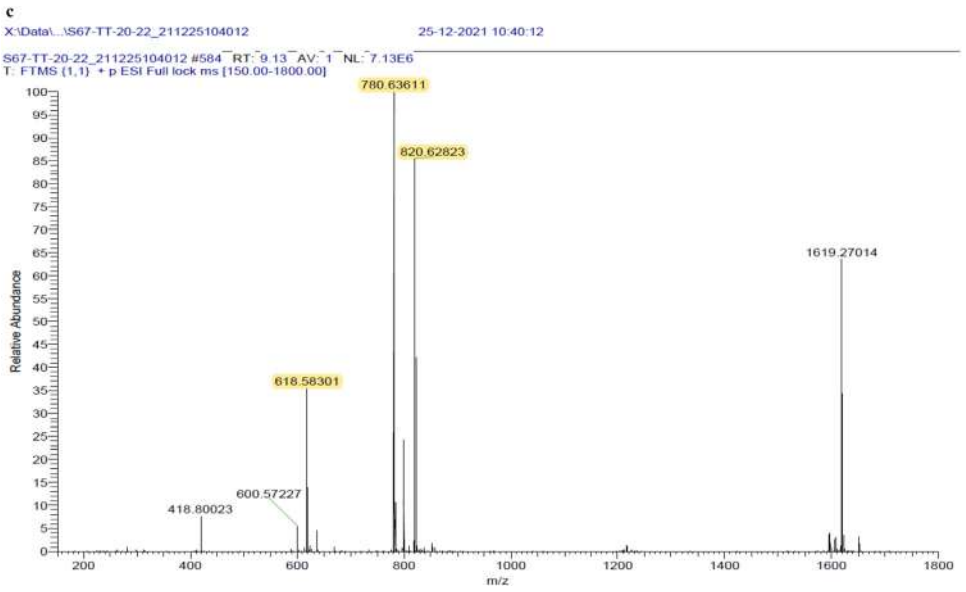

Fig. 5. **a:** HR-ESI-MS of compound **7a. b:** HR-ESI-MS of compound **7b. c:** HR-ESI-MS of compound **7c**.

Fig. 5. Continued

details of the isolated phytochemicals. The present work serves as the first report in isolation of glucocerebrosides from *Musa* species and also the first report on phytochemical isolation studies from the Nendran cultivar. Literature shows that the phytochemicals isolated from unripe Nendran and BG has myriad of health benefits. Thus, BG serves as a functional food, which is a ready-to-cook or ready-to-reconstitute form with no preservatives or additives. We have also blended BG with green gram in another product formulation (not discussed in this manuscript) to supplement the protein needs. The glycaemic load and glycaemic index studies of BG, gut health, and anti-inflammatory potential are planned for further validation of claims.

CRediT author statement

Natakkakath Kaliyathan Raveena: Data Curation, Visualization, **Nagaraja Ingaladal:** Data Curation, Visualization, **M. V. Reshma:** Conceptualization, Methodology, Writing- Reviewing and Editing., and **Ravi S. Lankalapalli:** Conceptualization, Methodology, Writing- Reviewing and Editing.

Declaration of Competing Interest

The authors declare that they have no known competing financial interests or personal relationships that could have appeared to influence the work reported in this paper.

Acknowledgements

NKR acknowledge CSIR for providing the CSIR-JRF fellowship support for Ph.D. Financial support from DST, Science and Engineering Research Board, India (Grant number: CRG/2020/002632) is gratefully acknowledged. We also acknowledge M/s. Moza Organic Pvt. Ltd. in Kochi, Kerala, India for the upcoming launch and promoting BG in the market.

Supplementary materials

Supplementary material associated with this article can be found, in the online version, at doi:10.1016/j.focha.2022.100063.

References

Aurore, G., Parfait, B., & Fahrasmane, L. (2009). Bananas, raw materials for making processed food products. *Trends in Food Science & Technology, 20*(2), 78–91. doi:10.1016/j.tifs.2008.10.003.

Blackbourn, H. D., Jeger, M. J., John, P., Telfer, A., & Barber, J. (1990). Inhibition of degreening in the peel of bananas ripened at tropical temperatures. *Annals of Applied Biology, 117*(1), 163–174. doi:10.1111/j.1744-7348.1990.tb04204.x.

Bushway, R. J. (1986). Determination of α- and β-carotene in some raw fruits and vegetables by high-performance liquid chromatography. *Journal of Agricultural and Food Chemistry, 34*(3), 409–412. doi:10.1021/jf00069a006.

Chitra, P. (2015). Development of banana-based weaning food mixes for infants and its nutritional quality evaluation. *Reviews on Environmental Health, 30*(2). doi:10.1515/reveh-2015-0002.

Coutts, R. T., Stenlake, J. B., & Williams, W. D. (1957). 814. The chemistry of the Aristolochia species. Part III. Aristolochic acids and related substances from Aristolochia reticulata and A. indica. *Journal of the Chemical Society (Resumed)*, 4120–4124. doi:10.1039/jr9570004120.

Determination of moisture. (1990). *Determination of moisture, ash, protein and fat official method of analysis of association of analytical chemist* (15th Edition). Washington DC: AOAC.

Englberger, L., Wills, R. B. H., Blades, B., Dufficy, L., Daniells, J. W., & Coyne, T. (2006). Carotenoid content and flesh color of selected banana cultivars growing in Australia. *Food and Nutrition Bulletin, 27*(4), 281–291. doi:10.1177/156482650602700401.

Englyst, H. N., Kingman, S. M., & Cummings, J. H. (1992). Classification and measurement of nutritionally important starch fractions. *European Journal of Clinical Nutrition, 46*(Suppl 2), S33–S50.

Faizi, S., Ali, M., Saleem, R., Irfanullah, & Bibi, S. (2001). Complete 1H and 13C NMR assignments of stigma-5-en-3-O-β-glucoside and its acetyl derivative. *Magnetic Resonance in Chemistry, 39*(7), 399–405. doi:10.1002/mrc.855.

Fuentes-Zaragoza, E., Riquelme-Navarrete, M. J., Sánchez-Zapata, E., & Pérez-Álvarez, J. A. (2010). Resistant starch as functional ingredient: A review. *Food Research International, 43*(4), 931–942. doi:10.1016/j.foodres.2010.02.004.

Ghosal, S. (1985). Steryl glycosides and acyl steryl glycosides from Musa paradisiaca. *Phytochemistry, 24*(8), 1807–1810. doi:10.1016/S0031-9422(00)82556-X.

Gurumallesh, P., Ramakrishnan, B., & Dhurai, B. (2019). A novel metalloprotease from banana peel and its biochemical characterization. *International Journal of Biological Macromolecules, 134*, 527–535. https://www.who.int/data/nutrition/nlis/info/vitamin-a-deficiency. doi:10.1016/j.ijbiomac.2019.05.051.

Ilan, Y., Elstein, D., & Zimran, A. (2009). Glucocerebroside: An evolutionary advantage for patients with Gaucher disease and a new immunomodulatory agent. *Immunology & Cell Biology, 87*(7), 514–524. doi:10.1038/icb.2009.42.

Jenkins, D. J. A., Kendall, C. W. C., Augustin, L. S. A., Franceschi, S., Hamidi, M., Marchie, A., et al., (2002). Glycemic index: Overview of implications in health and disease. *The American Journal of Clinical Nutrition, 76*(1), 266S–273S. doi:10.1093/ajcn/76/1.266S.

Jiang, C., Ge, J., He, B., & Zeng, B. (2021). Glycosphingolipids in filamentous fungi: Biological roles and potential applications in cosmetics and health foods. *Frontiers in Microbiology, 12*. doi:10.3389/fmicb.2021.690211.

Johnson, A. (1958). Isolation of β-Sitosterol from Cassia Absus, Linn. *The Journal of Organic Chemistry, 23*(11), 1814–1815. doi:10.1021/jo01105a628.

Ko, J.-. H., Cho, S. M., Joo, S.-. W., Kim, H.-. G., Lee, Y.-. G., Kang, S. C., et al., (2018). Glycosyl glycerides from the aerial parts of Malva verticillata and their chemopreventive effects. *Bioorganic Chemistry, 78*, 381–392. doi:10.1016/j.bioorg.2018.03.013.

Lockyer, S., & Nugent, A. P. (2017). Health effects of resistant starch. *Nutrition Bulletin, 42*(1), 10–41. doi:10.1111/nbu.12244.

Longvah, T., Ananthan, R., Bhaskar, K., & Venkaiah, K. (2017). *Indian food composition tables*. National Institute of Nutrition.

Morais, M. B., Feste, A., Miller, R. G., & Lifschitz, C. H. (1996). Effect of resistant and digestible starch on intestinal absorption of calcium, iron, and zinc in infant pigs. *Pediatric Research, 39*(5), 872–876. doi:10.1203/00006450-199605000-00022.

Nayar, N. M. (2010). The bananas: Botany, origin, dispersal. In *Horticultural reviews* (pp. 117–164). John Wiley & Sons, Inc. doi:10.1002/9780470527238.ch2.

Oguntibeju, O. O. (2019). Antidiabetic, anti-inflammatory, antibacterial, anti-helminthic, antioxidant and nutritional potential of Musa paradisiaca. *Asian Journal of Pharmaceutical and Clinical Research, 12*(10), 9–13. doi:10.22159/ajpcr.2019.v12i10.34239.

Oliveira, L., Freire, C. S. R., Silvestre, A. J. D., Cordeiro, N., Torres, I. C., & Evtuguin, D. (2006). Lipophilic extractives from different morphological parts of banana plant "Dwarf Cavendish. *Industrial Crops and Products, 23*(2), 201–211. doi:10.1016/j.indcrop.2005.06.003.

Pereira, A., & Maraschin, M. (2015). Banana (Musa spp) from peel to pulp: Ethnopharmacology, source of bioactive compounds and its relevance for human health. *Journal of Ethnopharmacology, 160*, 149–163. doi:10.1016/j.jep.2014.11.008.

Qamar, S., & Shaikh, A. (2018). Therapeutic potentials and compositional changes of valuable compounds from banana- A review. *Trends in Food Science & Technology, 79*, 1–9. doi:10.1016/j.tifs.2018.06.016.

Ravi, I., & Mustaffa, M. M. (2013). Starch and amylose variability in banana cultivars. *Indian Journal of Plant Physiology, 18*(1), 83–87. doi:10.1007/s40502-013-0014-2.

Ren, X., Chen, J., Molla, M. M., Wang, C., Diao, X., & Shen, Q. (2016). *In vitro* starch digestibility and *in vivo* glycemic response of foxtail millet and its products. *Food & Function, 7*(1), 372–379. doi:10.1039/C5FO01074H.

Rodriguez-Amaya, D. B., & Kimura, M. (2004). *HarvestPlus handbook for carotenoid analysis*. International Food Policy Research Institute (IFPRI) International Center for Tropical Agriculture (CIAT).

Sahaka, M., Amara, S., Wattanakul, J., Gedi, M. A., Aldai, N., Parsiegla, G., et al., (2020). The digestion of galactolipids and its ubiquitous function in Nature for the uptake of the essential α-linolenic acid. *Food & Function, 11*(8), 6710–6744. doi:10.1039/D0FO01040E.

Shalini, R., Abinaya, G., Saranya, P., & Antony, U. (2017). Growth of selected probiotic bacterial strains with fructans from Nendran banana and garlic. *LWT - Food Science and Technology, 83*, 68–78. doi:10.1016/j.lwt.2017.03.059.

Shirakura, Y., Kikuchi, K., Matsumura, K., Mukai, K., Mitsutake, S., & Igarashi, Y. (2012). 4,8-Sphingadienine and 4-hydroxy-8-sphingenine activate ceramide production in the skin. *Lipids in Health and Disease, 11*(1), 108. doi:10.1186/1476-511X-11-108.

Singh, B., Singh, J. P., Kaur, A., & Singh, N. (2016). Bioactive compounds in banana and their associated health benefits – A review. *Food Chemistry, 206*, 1–11. doi:10.1016/j.foodchem.2016.03.033.

Sreejith, P. E., & Sabu, M. (2017). *Edible bananas of South India: Taxonomy & phytochemistry*. India: Indian Association for Angiosperm Taxonomy (IAAT).

Suman, R., Kalaimathi, K., Palanichamy, S., Sowmiya, R., Vaganan, M. M., Ravi, I., et al., (2018). Anti-cancerous activities of anthocyanins of banana cv. Nendran (Musa sp.) flower bracts against human colon and cervical cancer cell lines. *International Journal of Current Microbiology and Applied Sciences, 7*(12), 2786–2793. doi:10.20546/ijcmas.2018.712.316.

Vilela, C., Santos, S. A. O., Villaverde, J. J., Oliveira, L., Nunes, A., Cordeiro, N., et al., (2014). Lipophilic phytochemicals from banana fruits of several Musa species. *Food Chemistry, 162*, 247–252. doi:10.1016/j.foodchem.2014.04.050.

Younes, H., Levrat, M.-. A., Demigné, C., & Rémésy, C. (1995). Resistant starch is more effective than cholestyramine as a lipid-lowering agent in the rat. *Lipids, 30*(9), 847–853. doi:10.1007/BF02533961.

Food Chemistry Advances 4 (2024) 100700

Contents lists available at ScienceDirect

Food Chemistry Advances

journal homepage: www.elsevier.com/locate/focha

First report on glucocerebrosides from unripe banana peel: Its anti-inflammatory and α-glucosidase inhibition properties

Natakkakath Kaliyathan Raveena [a,c], Sornarani Rajan [b,c], S Priya [a,c], Ravi S. Lankalapalli [b,c,*], M. V. Reshma [a,c,*]

[a] Agro-Processing and Technology Division, CSIR-National Institute for Interdisciplinary Science and Technology (CSIR-NIIST), Thiruvananthapuram 695019, Kerala, India

[b] Chemical Sciences and Technology Division, CSIR-National Institute for Interdisciplinary Science and Technology (CSIR-NIIST), Thiruvananthapuram 695019, Kerala, India

[c] Academy of Scientific & Innovative Research (AcSIR), Ghaziabad 201002, India

ARTICLE INFO

Keywords:
Nendran
Anti-inflammatory
ELISA
RAW 264.7
Valorization
Immunomodulation

ABSTRACT

Banana peel represents a significant waste product of banana processing industries that can yield high-value products. Banana peel contains flavonols, tannins, alkaloids, terpenoids, and various phenolic compounds such as catechin, epicatechin, and catecholamines. Recent studies have demonstrated the immunomodulatory, anti-inflammatory, and antidiabetic potential of these compounds. The current work serves as the first report on the glucocerebroside (GC) consortium from the unripe banana peel *Musa* (AAB) cv. Nendran. Through high resolution mass spectrometry analysis, we have identified eighteen molecular species of GC, containing α- and ω-hydroxy fatty acids. The in vitro anti-inflammation potential of GC consortium was assessed in RAW 264.7 murine macrophage cell line. The GC consortium at a dose of 50 μg/mL, showed a significant reduction in lipopolysaccharide (LPS)-induced nitric oxide (NO) production. The enzyme-linked immunosorbent assay (ELISA) analysis demonstrated GC's immunomodulation potential by showing a reduction in pro-inflammatory cytokines and increase in anti-inflammatory cytokine production. Furthermore, GC exhibited potent α-glucosidase inhibition with an IC_{50} value of 5.12 ± 0.51 μg/mL, significantly lower than standard acarbose (IC_{50} = 87.32 ± 1.99 μg/mL). This research highlights the potential of GC as a promising candidate for therapeutic application due to its anti-inflammatory and α-glucosidase inhibition properties.

1. Introduction

Banana is a tropical crop that belongs to the genus *Musa* of the Musaceae family. Interestingly, one of the most popular varieties of banana is the unripe banana (*Musa* AAB) cv. Nendran, which is famous for its use in making chips. The 'Nendran' has different names in various parts of the world, such as 'Rejeli' in North Indian states, 'French plantain/Horn plantain' in England, 'Hooru plantain' in Denmark, 'Banana cent livers' in France, 'Pisang feige/Hornfeermige' in Germany, 'Pisang candi' in Indonesia, 'Pisang lang/Pisang Nangka/Pisang ton dok' in Malaysia, 'Bhangoaisan' in the Philippines, and 'Kluai nga chang' in Thailand (Sreejith & Sabu, 2017).

In our previous work, we have demonstrated a novel application of unripe Nendran pulp in the form of "banana grit" (Raveena et al., 2022). Notably, the primary byproduct generated during the banana grit production process is the banana peel waste. The banana processing industries, worldwide, generate tons of this waste material every day. Valorization of waste is instrumental for reducing the environmental and economic burden of waste material and transitioning to a circular economy by developing value-added products (Zou et al., 2022). Repurposing banana by-products into valuable commodities could significantly boost agricultural development (Zou et al., 2022). Also, the valorization of banana peel enhances the market viability of banana pulp-based products. Therefore, our study involved the exploration of bioactives in the unripe Nendran peel and the exploration of its biological activity. As lyophilization (freeze drying) involves the removal of water by sublimation under high vacuum, the heat-sensitive compounds retain their original properties and the process extends the shelf life of the matrix (Nowak & Jakubczyk, 2020). This high-end technology is widely used for the preservation of herbs and spices. The unripe

* Corresponding authors.
E-mail addresses: ravishankar@niist.res.in (R.S. Lankalapalli), mvreshma@niist.res.in (M.V. Reshma).

https://doi.org/10.1016/j.focha.2024.100700
Received 20 December 2023; Received in revised form 16 March 2024; Accepted 16 April 2024
Available online 26 April 2024

Nendran peel was lyophilized to retain native compounds and was used for the isolation and characterization of bioactives.

Banana peel, which constitutes a significant percentage of the fruit's weight (35–40 %), is a rich source of phytochemicals such as flavonols, hydroxycinnamic acids, tannins, alkaloids, anthocyanins, terpenoids, and catecholamines, which rationalize its traditional use in treating burns, diarrhoea, diabetes, ulcers, and inflammation (Pereira & Maraschin, 2015; Zaini et al., 2022). Moreover, banana peel has been utilized to improve the nutritional and physicochemical properties of various products. Recent research has shown that mature banana (*Nanica cavendish*) peel can be used to make gluten-free Rissol, while the peel of *Musa cavendish* can be incorporated into bakery products and pasta. Furthermore, *Musa balbisiana* peel powder has been used to enhance the sensory and nutritional quality of chicken sausage (Gomes et al., 2022; Segura-Badilla et al., 2022; Zaini et al., 2020). Nida et al. (2023) utilized it to prepare 3D-printed food package casings and apart from the food sector, banana peel has also found applications in wastewater treatment, biofuel production, bioplastic, and nanocellulose (Alzate Acevedo et al., 2021; Nida et al., 2023). Notably, banana peels find applications across various industries, including cosmetics, medicine, food processing, beverages, textiles, energy production, paper manufacturing, bio-absorbents, biofuel production, and agriculture (Bhavani et al., 2023).

Our previous report on unripe Nendran pulp has revealed the presence of monogalactosyldiacylglycerols, digalactosyldiacylglycerols, acyl steryl glycosides, glucocerebrosides (GCs), and sterylglycoside from the pulp of unripe Nendran (Raveena et al., 2022). Literature data demonstrated the bioactive role of GC with reports on anti-inflammatory potential of GC isolated from *Cordyceps militaris*, an edible fungus (Chiu et al., 2016). Inflammation refers to a complex immunological response that is connected to the gradual release of pro-inflammatory cytokines. Macrophages play a key role in the inflammatory process by providing an immediate defence against foreign agents. When induced by an inflammation stimulus such as LPS, they initiate the production of a variety of pro-inflammatory mediators including TNF-α, IL-6, COX-2, NO, etc. (Geller & Billiar, 1998; Huang et al., 2014). Suppression of these pro-inflammatory cytokines is critical for treating inflammatory diseases. Hence the potential of GCs for the suppression of NO production and its role in the release of pro and anti-inflammatory cytokines were evaluated.

GCs belong to the class of neutral glycosphingolipids, and contains one glucose molecule attached to a ceramide. A ceramide consists of a sphingosine and a long chain fatty acid, connected by an amide linkage (Demir, 2021). The fatty acyl groups of ceramides are typically saturated or monounsaturated with various chain length from 14 to 36 carbons. GC is degraded to produce ceramides by enzymes such as glucosidase, and glucocyl ceramidase (Yang & Chen, 2022). Decreased level of ceramides in the skin barrier often found to be the major reason for many skin disorders. Hence topical application of ceramide through conventional and novel carrier systems have been researched globally (Kahraman et al., 2019). GC is a molecule with numerous applications, it has been incorporated in cosmetics as moisturizing ingredient, and the direct oral intake of GC found to increase the level of epidermal ceramides and reduces skin allergy responses (Kimata, 2006; Spada et al., 2018). This emphasizes the potential of GC in the cosmetic field.

The potential anti-diabetic properties of Nendran peel have garnered significant attention and appreciation traditionally. However, it is crucial to emphasize that, as of the latest available scientific information, these claims lack substantial empirical evidence. The usage of α-glucosidase inhibitors is proven to be the most efficient approach for controlling postprandial hyperglycemia and associated adverse physiological complications, in type 2 diabetes (Hossain et al., 2020). The traditional knowledge regarding banana peel dietary usage for diabetes has led us to examine the α-glucosidase inhibition potential of GCs isolated from Nendran peel.

The identification of bioactive compounds in unripe banana peel, demonstrating dual anti-inflammatory and α-glucosidase inhibition properties, shows the significance of studying this matrix for wider applications. Moreover, considering the versatile benefits, including their potential use in cosmetics, GCs present a promising avenue for both functional foods and skincare formulations.

2. Materials and methods

2.1. General procedures

NMR spectra of isolated compounds were analyzed in CD_3OD, ^1H and ^{13}C NMR were recorded on a Bruker Ascend™ 500 MHz spectrometer at 500 and 125 MHz, respectively. The HR-ESI-MS (High-Resolution Electrospray Ionization Mass Spectrometry) analysis of GC fractions was carried out on a Thermo Scientific Exactive mass spectrometer with an Orbitrap mass analyzer, and an Accela 600 pump system and the ions are given in *m/z*.

2.2. Chemicals and standards

All the solvents used for isolation and purification were of standard analytical grade. The TLC aluminium sheets (silica gel 60 $F_{254,}$ catalogue no. 1.05554.0007) and the silica gel (230–400 mesh, catalogue no. 6.18609) & 100–200 mesh (catalogue no. 6.18608), NMR solvent (CD_3OD, catalogue no.151947–50-SB) and gradient grade methanol (catalogue no. 1.06007) were purchased from Merck Life Science Pvt Ltd, Mumbai, India.

The murine macrophage cell line, RAW 264.7 was procured from the National Centre for Cell Science (NCS), Pune, India. Chemicals and reagents for cell culture studies including Dulbecco's Modified Eagle Medium (DMEM) high glucose medium (catalogue no. AT007–1 L), fetal bovine serum (FBS, catalogue no. RM10432–500ML), antibiotics-100X (with 10,000 U Penicillin, 10 mg streptomycin and 25 μg amphotericin B per ml in 0.9 % normal saline, catalogue no. A002A-5 × 50ML), 3-(4,5-dimethylthiazol-2-yl)−2,5-diphenyl tetrazolium bromide (MTT, catalogue no. TC191–1 G), dimethyl sulfoxide (DMSO, catalogue no. TC349–100ML), bovine serum albumin (BSA, catalogue no. TC548–5 G) were procured from HiMedia, India.

The 3′,5,5′-Tetramethylbenzidine (TMB catalogue no. 555,214) substrate was procured from BD Biosciences, San Diego. Pierce™ BCA protein assay kit (catalogue no. 23,227) and Halt™ protease Inhibitor Cocktail-100X (PIC, catalogue no. 87,786), were purchased from Thermo Scientific, USA. The primary antibodies; tumour necrosis factor-alpha (TNF-α, catalogue no. ITT07014), interleukin-6 (IL-6, catalogue no. ITT06087), interleukin-10 (IL-10, catalogue no. ITT06894), interleukin-13 (IL-13, catalogue no. ITT06813), cyclooxygenase-2 (COX-2, catalogue no. ITT07003), interleukin-1alpha (IL-1α, catalogue no. ITT06893), interferon-gamma (INF-γ, catalogue no. ITT06045), & monocyte chemoattractant protein-1 (MCP-1, catalogue no. ITT07577), and secondary antibody (goat anti-Rabbit IgG/HRP, catalogue no. ITSAH134) were procured from ImmunoTag, USA. LPS from *E. coli* (catalogue no. L6529–1MG), radioimmunoprecipitation assay buffer-10X (RIPA buffer, catalogue no. 20–188), α-glucosidase from *Saccharomyces cerevisiae* (Type 1, lyophilized powder ≥10 units/mg protein, catalogue no. G5003–1KU), *p*-nitrophenyl-α-d-glucopyranoside (pNPG, catalogue no. 487,506–5GM), Griess reagent (catalogue no. G4410–1 G), acarbose (catalogue no. A8980–1 G), and dexamethasone (catalogue no. D4902–100MG) were obtained from Sigma-Aldrich (Darmstadt, Germany), and all the other chemicals were of standard analytical grade.

2.3. Raw material collection for phytochemical analysis

The voucher specimen of 'Nendran' was collected on 15th May 2019 from local organic farmers in Vellayani, Ookode (8°25′54.3″N 77°00′14.8″E) Thiruvananthapuram District, Kerala, India. The specimen was identified and deposited at the Herbarium of Jawaharlal

Nehru Tropical Botanic Garden & Research Institute (TBGT) Thiruvananthapuram, Kerala, India with voucher number 94628 (Raveena et al., 2022).

To conduct the phytochemical exploration studies, mature Nendran infructescence (40.34 kg) was purchased from local organic farmers in Vellayani, Thiruvananthapuram District, Kerala, India. The peel (13.91 kg) and pulp (25.65 kg) were separated. The peel (13.91 kg) was lyophilized using VirTis Genesis-25 EL lyophilizer. The initial freezing was done at −40 °C for 3 h at ambient pressure. For the drying step, the initial shelf temperature was set at −40 °C for 1 hour at 500 mTorr. The temperature was further reduced to −10 °C at a rate of −10 °C reduction in each 2 h. Meanwhile, the pressure was also reduced to 300 mTorr. Then, a holding was given for 2 h at −5 °C at 300 m Torr. Then the temperature was increased to 5 °C and maintained for 2 h at 250 mTorr pressure and further, the temperature increased to 10 °C and maintained for 1 hour 30 min at 200 mTorr pressure. The temperature was finally raised to 25 °C at a rate of increase of 5 °C in each 4 h, and the final applied vacuum was 100 mTorr. The lyophilized peel (1.50 kg) was collected, sealed and stored at −20 °C until further analysis (details of the yield pattern of lyophilization is provided in the supplementary material, Scheme S1).

2.4. Phytochemical exploration studies of banana peel for the isolation of GC

2.4.1. Extraction protocol for isolation of GC

For the isolation of GC, the lyophilized banana peel was subjected to extraction with ethyl acetate, chloroform, and methanol separately. Three solvents with varying polarities, namely chloroform (non-polar), ethyl acetate (mid-polar), and methanol (polar), were selected to assess the extractability of GCs across different polarity ranges.

The lyophilized banana peel was powdered and passed through mesh 10 before extraction and the powdered banana peel (250 g) was extracted with ethyl acetate (1.5 L) for 6 h at 700 rpm using an overhead stirrer (Hei-TORQUE 100, Heidolph, Germany). After 6 h, the extract was collected, kept for settling and filtered through Whatman no. 1 filter paper, fitted with a Buchner funnel, then extracts were concentrated under vacuum in a rotary evaporator (Hei-vap, Heidolph, Germany). This process was repeated twice, and the extracts pooled. The same process was followed in the case of chloroform and methanol extraction of banana peel. The yield of extracts were 11.1 g, 14.09 g, and 12.32 g of ethyl acetate, methanol, and chloroform extracts, respectively (Fig. 1).

2.4.2. Purification of extracts by column chromatography

Before proceeding to the isolation protocols, the TLC pattern of ethyl acetate, chloroform, and methanol extracts were compared with the GC isolated from the banana pulp (Raveena et al., 2022), and the presence of the GC was confirmed in all the three extracts (supplementary material, Figure S1a-S1c). All the three extracts were explored for isolation of GC individually, and the isolation protocol is described below.

2.4.2.1. Exploration of ethyl acetate extract. The ethyl acetate extract (10 g) was loaded on a silica column (230–400 mesh), the column length was 60 cm, and the bed length was 50 cm with an internal diameter of 3.5 cm. The extract was fractionated using the eluents chloroform, and methanol-chloroform in the following ratios 5:95, 10:90, 20:80 & 50:50, respectively, and obtained five fractions. The TLC pattern of these fractions was checked and found that the 20:80 methanol-chloroform fraction (1.13 g) contains GCs along with other compounds and was subjected to the second level of purification. The 20:80 methanol-chloroform fraction was loaded on a silica column (230–400 mesh), the column length was 30 cm and the bed length was 25 cm with an internal diameter of 1 cm, and eluted with 100 % chloroform, 5:95, 10:90, 20:80, 30:70 and 50:50 methanol-chloroform ratios, respectively, which yielded six fractions. The 10:90 methanol-chloroform fraction (109.8 mg) was found to contain GCs with few other categories of compounds; hence, the fraction was further purified using a narrow glass column (0.5 × 20 cm). Three fractions obtained from purification [BP-GC-TT-15–18 (23.7 mg), BP-GC-TT-19–23 (21.7 mg) & BP-GC-TT-24–26 (8.2 mg)] were separately submitted for NMR and HR-ESI-MS analysis as they showed slight difference in Rf and charring pattern. After completion of exploration studies in the ethyl acetate extract, the chloroform and methanol extracts were also explored for the presence of GCs.

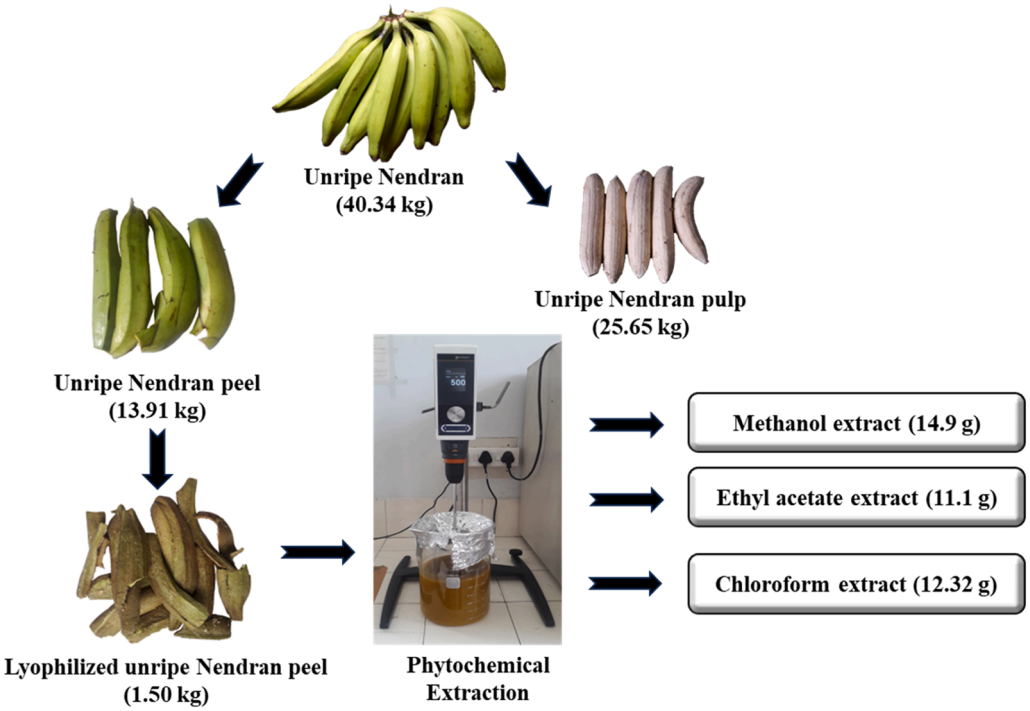

Fig. 1. Schematic representation of processing of unripe banana peel (*Musa* AAB) cv. Nendran for phytochemical exploration studies.

2.4.2.2. Exploration of methanol extract. The purification protocol adopted in the ethyl acetate extract was followed here, which resulted in two fractions: GCs [BP-MeOH-GC-1 (81.30 mg) and BP-MeOH-GC-2 (20.61 mg)]. These two fractions were subjected to HR-ESI-MS analysis for identification of GCs.

2.4.2.3. Exploration of chloroform extract. The chloroform extract was initially fractioned using the eluents chloroform, and methanol-chloroform in the ratios 5:95, 10:90, 20:80 and 50:50 , and obtained five fractions.

In contrast to the ethyl acetate and methanol extracts, the 10:90 methanol-chloroform fraction was found to contain GCs along with other compounds. This fraction was further purified and obtained two fractions of GCs [BP-CHL-GC-1 (45.13 mg) and BP-CHL-GC-2 (169 mg)] and both fractions were subjected to HR-ESI-MS analysis.

2.4.3. HR-ESI-MS analysis of GC fractions

The mobile phase consists of 0.1 % formic acid in water (A) and methanol (B), with an isocratic elution [A(3 %)/B(97 %)] with a flow rate of 150 μL/min for a total runtime of 15 min. Samples were dissolved in gradient-grade methanol with a few drops of chloroform, and the injection volume was 2 μL. The mass range was 100–1500 *m/z*, analyzed in a positive ionization mode.

From the extensive HR-ESI-MS analysis, it was found that the fractions BP-CHL-GC-1 and BP-CHL-GC-2 contain more molecular species of GCs, hence, these fractions were pooled and purified again through a narrow glass column (0.5 × 20 cm), and the resultant GC consortium (103.27 mg) was used for further evaluating in vitro anti-inflammatory, and α-glucosidase inhibition potential.

2.5. Evaluation of immunomodulatory effects of GCs

The immunomodulatory effects of GCs were evaluated in vitro in the murine macrophage cell line, RAW 264.7. In a culture flask (25 cm^2), murine macrophage RAW 264.7 cells were cultured in DMEM high glucose media with 10 % FBS and 5 % antibiotics at 37 °C and 5 % CO_2. The morphology of the cells was observed under a microscope to monitor any changes (Kwon et al., 2018). The sample was dissolved in dimethyl sulfoxide (DMSO) (10 mg/60 μL), and diluted with cell culture medium to obtain the desired concentrations for treatment.

2.5.1. Determination of cell viability by MTT assay

The effect of GCs on the viability of cells was evaluated by assessing the number of metabolically active cells through the reduction of MTT to formazan through a colorimetric assay (Mosmann, 1983). In brief, RAW 264.7 cells (5×10^3 cells/well) were cultured and treated with 5, 10, 25, 50, 100, and 200 μg/mL of GCs, and incubated for 24 h. After the incubation period, MTT solution was added, and cells were incubated for 3 h at 37 °C with 5 % CO_2. Then, the supernatants were withdrawn, DMSO was used for solubilizing the formazan crystals, and absorbance was measured at 570 nm using a multimode reader (Tecan infinite® 200). The cell viability was assessed by following the equation

$$\text{Cell viability } (\%) = \frac{\text{OD of experimental group x 100}}{\text{OD of control group}}$$

2.5.2. Evaluation of NO production by Griess reaction

The amount of NO produced in the cells was determined by measuring the amount of nitrite accumulated in the culture supernatants using the Griess reagent (Green et al., 1982). The RAW 264.7 cells (5×10^3 cells/well) were plated, treated with GC consortium of the following concentrations 5, 10, 25, and 50 μg/mL, and incubated for 4 h. After the incubation period, 1 μg/mL LPS was added to each well and kept for 24 h incubation at 37 °C with 5 % CO_2. Following that, culture supernatants (50 μL) were diluted with equal volumes of the Griess reagent, and incubated for 20 min at room temperature (28 °C) in the dark. The absorbance at 540 nm was measured in a multimode reader (Tecan infinite® 200 PRO). The culture medium was used as blank, and NO concentration in the supernatants was determined from a standard curve generated with sodium nitrite ($NaNO_2$).

2.5.3. Evaluation of pro and anti-inflammatory cytokines production

2.5.3.1. Cell lysate preparation-RIPA method. RAW 264.7 cells at a density of 3×10^5 cells/well were seeded in six-well plates, then treated with GCs of the concentrations 25 and 50 μg/mL, and incubated for 4 h. After incubation, 1 μg/mL LPS was added to each well and kept for 24 h incubation at 37 °C in a 5 % CO_2 atmosphere. After 24 h, media from each well was collected, and the plates were kept on ice. The collected media was centrifuged at 5000 rpm for 10 min at 4 °C, and the supernatant was stored at −80 °C. Adhered cells were washed with 200 μL of ice-cold phosphate buffered saline (PBS), then 200 μL of RIPA lysis buffer (Sigma-Aldrich, catalogue no. 20–188) containing PIC Inhibitors (Thermo Scientific, catalogue no. 87,786), and incubated for 5 min on ice. Cells were scraped, the lysate was transferred to a vial and constant agitation was given at 4 °C for 30 min. The lysate was then sonicated three times at 30 kHz for 1 min each with at least 1 min repose on ice in between. After that, the cell lysate was centrifuged at 12,000 rpm, 4 °C for 20 min. The supernatant was collected and stored at −80 °C (Lakshmi et al., 2021).

2.5.3.2. Determination of protein content. Cellular protein content was determined by bicinchoninic acid (BCA) protein assay (Smith et al., 1985). The cell lysate (10 μL) was mixed thoroughly with 200 μL of freshly prepared BCA working reagent (Reagent A: B, 50:1). The reaction was incubated for 30 min at 37 °C and cooled to room temperature (28 °C). The absorbance was determined at 562 nm using a microplate reader (Tecan infinite® 200 PRO). The cellular protein content was calculated in comparison with the BSA standard curve, and the results were expressed as mg/mL.

2.5.3.3. ELISA. The immuno plate was coated with 100 μL/well of the collected media and incubated at 4 °C for 12 h. Then the media was discarded and wells were gently rinsed with phosphate buffered saline (PBS) containing 0.05 % Tween 20. The antigen coated on the plate was blocked by adding 100 μL/well of blocking buffer (5 % BSA+ 0.5 % Tween 20 in PBS) for 1 hour at 37 °C. After incubation, the blocking buffer was aspirated and gently rinsed with PBS containing 0.05 % Tween 20. After that, 100 μL of the primary antibody solution (TNF-α, IL-1α, INF-γ, IL-6, IL-10, IL-13, MCP-1, COX-2) was added to each well and incubated for 2 h at 4 °C with gentle continuous shaking. The primary antibody was collected after incubation, and the plates were gently rinsed with PBS containing 0.05 % Tween 20. Then 100 μL of horseradish peroxidase-conjugated IgG secondary antibody was added into each well, and incubated for 2 h at 4 °C with gentle shaking. The secondary antibody was recollected and plates were rinsed with PBS containing 0.05 % Tween 20. Then 100 μL/well freshly prepared TMB substrate was added and incubated in the dark for 30 min at room temperature. To that 50 % H_2SO_4 (50 μL/well) was added to terminate the reaction. The absorbance was monitored at 490 nm using a microplate reader (Tecan infinite® 200 PRO) and results were expressed as OD/mg of cell protein (Engvall & Perlmann, 1971; Saranya et al., 2017).

2.6. Evaluation of α-glucosidase inhibition potential of GC

α-Glucosidase assay followed in this study is based on the procedure of Pistia-Brueggeman and Hollingsworth (2011) with slight modifications. Briefly, 20 μL α-glucosidase (1.25 U/mL of 0.05 M potassium phosphate buffer, pH 6.8), 200 μL GC consortium (six different concentrations, 0.88 - 44 μg/mL) was added to vials, and incubated at room temperature for 5 min. Then the hydrolysis process was initiated with

the addition of 200 μL pNPG solution (1 mM) as the substrate. After 20 min, the reaction was terminated by adding 500 μL of 1 M sodium carbonate (Na_2CO_3) and then diluted with 580 μL of distilled water. The absorbance of the solution was recorded at 405 nm (Pistia-Brueggeman & Hollingsworth, 2001) using Biorad multimode microplate reader (BioTek Instruments Inc., Winooski, VT). Acarbose was used as the positive control.

The inhibition rate of the GC was calculated by

$$\%\ \text{Inhibition} = \frac{\text{Absorbance of control} - \text{Absorbance of sample}}{\text{Absorbance of control}} \times 100$$

The IC_{50} value was the concentration of α-glucosidase inhibitor needed to inhibit 50 % of α-glucosidase activity under the assay condition. The same protocol was followed to determine the IC_{50} value of acarbose. The IC_{50} value was obtained by plotting a graph with concentration of test samples in μg/mL along the X-axis against percentage inhibition in the Y-axis.

2.7. Statistical analysis

All the experiments were carried out in triplicates ($n = 3$) and the data were recorded as the mean ± standard error mean (SEM). All the data were statistically analyzed by IBM Statistical Package for Social Science 26 (SPSS Inc., Chicago, USA). One-way analysis of variance (ANOVA) followed by Tukey's post hoc tests was used for multiple comparisons analysis, and $P \leq 0.05$ is considered significant. To compare the means of two samples (IC_{50} value of acarbose and GCs), an independent sample *t*-test was employed.

3. Results and discussion

3.1. Phytochemical exploration studies of banana peel for the isolation of GC

For the study, a total of 40.34 kg of infructescence was procured, from which 13.91 kg of peel was obtained. This substantial peel yield, representing 34 % of the infructescence weight, demonstrates significant potential for peel valorization. When the peel was lyophilized, it resulted in 1.50 kg of peel, indicating that the peel contains around 90 % moisture, and around 10 % dry matter. The lyophilized peel was utilized for the exploration of GCs.

3.1.1. Exploration of ethyl acetate extract

As discussed in Section 2.4.2.1. the column chromatography separation of the ethyl acetate extract yielded three fractions of GC [BP-GC-TT-15–18 (23.7 mg), BP-GC-TT-19–23 (21.7 mg) & BP-GC-TT-24–26 (8.2 mg)]. The ^{1}H, and ^{13}C NMR spectra of these fractions were recorded in CD_3OD (supplementary Fig. S47-S52.). The NMR spectra unambiguously revealed the presence of GCs in the isolated fractions which is in line with our previous studies in the unripe banana pulp (Raveena et al., 2022). Further, the molecular species of GC in each fraction was identified using HR-ESI-MS analysis. The fatty acid composition of the dichloromethane extracts of different parts of the banana plant reported by Oliveira et al. includes saturated, unsaturated, diacid, α- and ω-hydroxy fatty acids (Oliveira et al., 2006). GCs are distinguished by variation in aliphatic acids conjugated as amide. Based on the report from Oliveira et al. (2006), the GC fractions in the present study clearly showed the presence of α- and ω-hydroxy fatty acids from exact mass calculations and HR-ESI-MS analysis. These observations have facilitated an unambiguous identification of eighteen molecular species of GC in the present work (Fig. 2). The identified molecular species of GC conjugated with α-hydroxy fatty acids in the fraction BP-GC-TT-15–18 were 2 and 3, and those conjugated with ω-hydroxy fatty acids were 7, 8, 9, 10, 12, and 16. The fraction BP-GC-TT-19–23 contained molecular species of GC conjugated only with ω-hydroxy fatty acids, which include 7, 8, 9, 10, and 18. Similarly, the fraction BP-GC-TT-24–26 also contained molecular species of GC conjugated only with ω-hydroxy fatty acids viz. 7, 15, and 17 (supplementary Fig. S14-S29).

3.1.2. Exploration of methanol extract

The HR-ESI-MS analysis of the GC fraction BP-MeOH-GC-1 revealed the presence of only one α-hydroxy fatty acid conjugated GC (4), and six

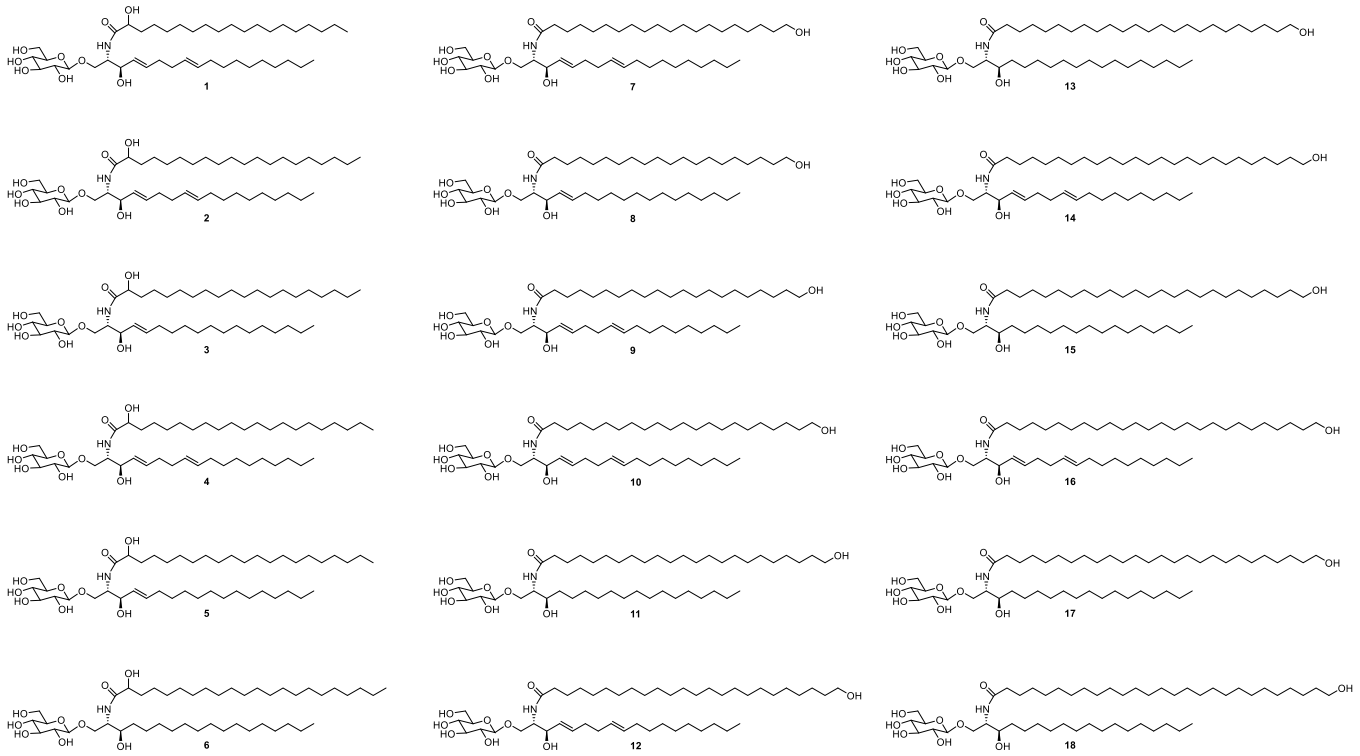

Fig. 2. Structures of molecular species of GCs identified from the unripe banana peel (*Musa* AAB) cv. Nendran.

ω-hydroxy fatty acid conjugated GCs (7, 9, 10, 12, 16, and 17). The fraction BP-MeOH-GC-2 found to contain GC conjugated only with ω-hydroxy fatty acids (7, 9, 10, 12, and 16) (supplementary Fig. S2-S13).

3.1.3. Exploration of chloroform extract

The HR-ESI-MS analysis of the GC fraction BP-CHL-GC-1 showed that it contains GC conjugated with ω-hydroxy fatty acids only (10, 12, 14, and 16). Fraction BP-CHL-GC-2 was found to contain three α-hydroxy fatty acid conjugated GCs (1, 5, and 6), and ten ω-hydroxy fatty acids conjugated GCs (7, 8, 9, 10, 11, 12, 13, 15, 17, and 18). Molecular species 1, 5, and 6 were exclusively present in BP-CHL-GC-2 only (supplementary Fig. S30-S46). As the HR-ESI-MS analysis depicted that the chloroform fractions were most abundant with molecular species of GCs, these two fractions were pooled and purified again through a narrow glass column (0.5 × 20 cm). The resultant GC consortium (103.27 mg) was used for evaluating the in vitro anti-inflammatory, and α-glucosidase inhibition potential of GCs.

3.2. Evaluation of immunomodulatory effects of GCs

3.2.1. Determination of cell viability by MTT assay

The cytotoxicity of GC consortium was assessed using MTT assay by assessing the viability of RAW 264.7 macrophages. Samples of the concentrations 5, 10, 25, 50, 100 & 200 μg/mL were used for assessing the cytotoxicity of the sample, and the results are shown in Fig. 3. As depicted in the figure (Fig. 3), the GCs of concentrations ranging from 5 μg/mL to 50 μg/mL had negligible effects on cell viability, with no significant difference between the control group and the sample-treated group. However, with an increase in concentration to 100 and 200 μg/mL, the viability of RAW 264.7 macrophages significantly decreased to 85.05 ± 0.94 % and 71.44 ± 0.82 %, respectively. Based on this observation, GC consortium of concentrations ranging from 5 to 50 μg/mL were selected for the evaluation of NO production by Griess reaction.

3.2.2. Evaluation of NO production by Griess reaction

Stimulation of macrophages by LPS triggers an overproduction of NO through the breakdown of l-arginine. In the mammalian immune response to inflammatory signals, the generation of NO is controlled by inducible nitric oxide synthase (iNOS) in macrophage cells (Baek et al., 2020). The progression of inflammation is the main cause of many disease conditions, including, Alzheimer's disease and Parkinson's disease. In a comprehensive review by Facchin & team., 2022 on inflammatory biomarkers on an LPS-induced RAW 264.7 cell model points out that measurement of NO levels may be sufficient to screen for possible anti-inflammatory action of a compound in these cells (Facchin et al., 2022). Hence the anti-inflammation potential of the GC consortium was first evaluated by monitoring its role in the suppression of NO production in LPS-induced RAW 264.7 cells.

To assess the influence of GCs in the NO production in macrophages, RAW264.7 cells were stimulated with LPS, and nitrite production was analyzed using the Griess reaction. GCs at concentrations 5, 10, 25 & 50 μg/mL were evaluated for their inhibitory effect on the NO production in LPS-activated RAW264.7 macrophages. The addition of LPS significantly increased the NO production of cells, and the treatment suppressed the NO production in a dose-dependent manner (Fig. 4). Upon treatment with LPS, the NO production increased to 37.70 ± 1.46 μM from the basal level of 6.76 ± 0.40 μM (control) and the positive control dexamethasone significantly reduced the NO production to 10.72 ± 0.47 μM compared to the LPS treated groups. The cells treated with GC consortium of the concentrations 10 & 25 μg/mL showed a significant reduction in the NO production to 25.22 ± 0.40 μM and 17.33 ± 0.70 μM respectively. Whereas GC consortium at a dose of 50 μg/mL showed a reduction in NO production to 10.75 ± 0.58 μM, which is on par with dexamethasone (10.72 ± 0.47 μM) (Fig. 4). Based on assay results, GC of concentrations 25 & 50 μg/mL were selected for further studies.

There are only a few reports discussing the anti-inflammation properties of GC. Literature data demonstrated the anti-inflammatory potential of GC isolated from *Cordyceps militaris*, an edible fungus. GC was able to prevent the accumulation of the pro-inflammatory iNOS protein and thereby reducing the NO production. It also reduced the expression of cyclooxygenase-2 protein in LPS-stimulated macrophages (Chiu et al., 2016). Similarly, the observed reduction in the NO production upon GC treatment may be due to its potential to prevent the accumulation of iNOS.

3.2.3. Effect of GCs on pro and anti-inflammatory cytokines secretion

To study the effects of GCs on the cytokine production in inflamed cells, the ELISA technique was employed. Cytokines play a crucial role in regulating inflammation in the body. Among the doses tested (25 & 50 μg/mL), 50 μg/mL of GC consortium significantly suppressed the production of pro-inflammatory cytokines, including IL-1α, IFN-γ, TNF-α, MCP-1, COX-2, and IL-6, while stimulated the production of anti-inflammatory cytokines IL-10 and IL-13 to a degree that matches to

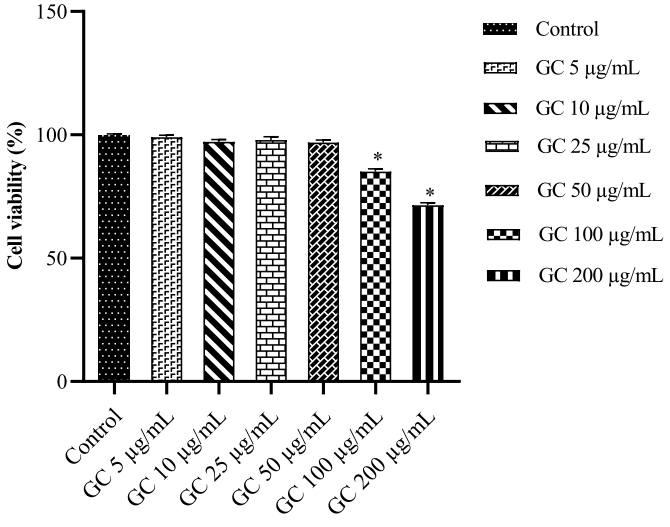

Fig. 3. Effect of GCs on the viability of RAW 264.7 cells. The cells were treated with GC consortium of concentrations ranging from 5 to 200 μg/mL and viability (%) was assessed after 24 h of exposure and significance was determined through ANOVA, $^{*}p \leq 0.05$ (vs. control).

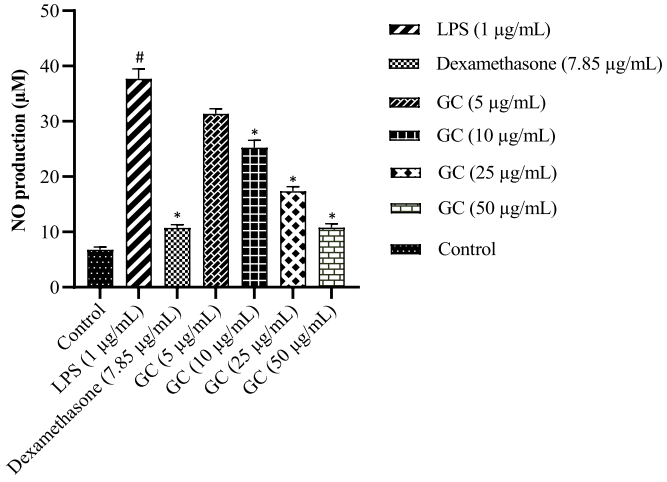

Fig. 4. Effect of GCs on the NO production of RAW 264.7 cells induced by LPS. The cells were treated with GC consortium of concentrations ranging from 5 to 50 μg/mL and NO production (μM) was assessed after 24 h of exposure and significance was determined through ANOVA, $^{\#}p \leq 0.05$ (vs. control), $^{*}p \leq 0.05$ (vs. LPS).

that of dexamethasone (7.85 μg/mL) (Fig. 5a & 5b). It is noteworthy that at the dose of 50 μg/mL, GCs even outperformed dexamethasone by reducing the production of pro-inflammatory cytokines, IL-1α, TNF-α, COX-2, & IL-6, and increasing the production of the anti-inflammatory cytokine IL-10.

Upon LPS stimulation, the activated macrophages primarily produce proinflammatory cytokines, which play a crucial role in triggering inflammatory responses. Proinflammatory cytokines like IL-1β, IL-6, and TNF-α have been implicated in the development of pathological pain, supported by ample evidence. The anti-inflammatory cytokines are a series of immunoregulatory molecules that control the pro-inflammatory cytokine response. Among them, IL-10 stands out for its potent anti-inflammatory properties, by suppressing the expression of inflammatory cytokines such as TNF-α, IL-6 and IL-1 by activated macrophages. Moreover, IL-10 has the ability to up-regulate endogenous anti-cytokines and down-regulate pro-inflammatory cytokine receptors. Thus, it can counter-regulate production and function of pro-inflammatory cytokines at multiple levels (Iyer & Cheng, 2012; Martinez-Espinosa et al., 2021; Zhang & An, 2007). As evident from the ELISA analysis, the increased level of IL-10 upon GC treatment may be the mechanism behind the anti-inflammation potential of GC.

The impact of GCs on immune-mediated disorders has been extensively researched using various animal models. The findings indicate that it possesses remarkable anti-inflammatory, immunomodulatory, and anti-malignant properties. This is primarily achieved by promoting dendritic cells, natural killer T cells, and regulatory T cells. It is noteworthy that the breakdown of GCs to ceramide may significantly contribute to these positive outcomes. (Ilan et al., 2009).

Our study is the first to report the anti-inflammatory benefits of GC extracted from unripe Nendran peel. Our findings suggest that GC can reduce LPS-induced inflammation by decreasing the secretion of pro-inflammatory cytokines and increasing the production of anti-inflammatory agents. Although in vitro studies provide quick results, they are inherently limited in their ability to replicate the intricate complexities of organ systems and the internal environment of the human body. Therefore, these studies warrant additional validation through pre-clinical and clinical studies.

3.3. Evaluation of α-glucosidase inhibition potential of GCs

Due to the incredible therapeutic potential in the treatment of conditions like diabetes, metastatic cancer, HIV infection, and lysosomal storage diseases, glucosidase inhibitors are currently an important area of research (de Melo et al., 2006). Our study extensively evaluated the α-glucosidase inhibition potential of GCs and compared it with the standard drug acarbose (Fig. 6a & 6b). Acarbose and GC consortium demonstrated a dose-dependent α-glucosidase inhibition. However, with GCs, a dose-dependent inhibition pattern is observed within the concentration range of 0.88 μg/mL to 18 μg/mL. At 18 μg/mL concentration, GCs demonstrated nearly 100 % α-glucosidase inhibition. Beyond this range, i.e., from 20 to 44 μg/mL, a plateau is evident in the inhibition curve, as maximum inhibition is achieved at the 18 μg/mL concentration itself.

The study demonstrated that 87.32 ± 1.99 μg/mL of acarbose was

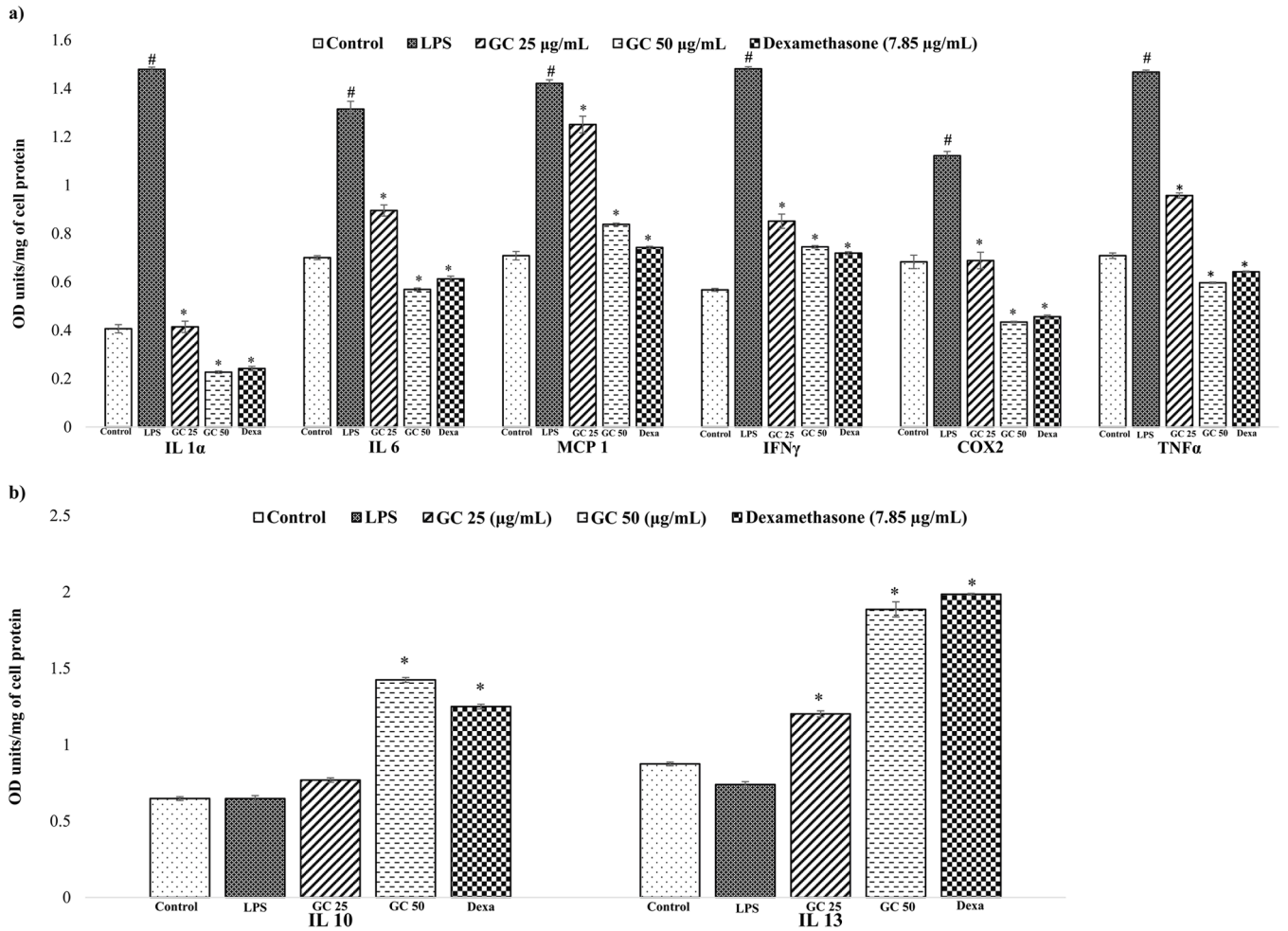

Fig. 5. a) Effect of GCs on the secretion of pro-inflammatory cytokines in the RAW 264.7 macrophage cells induced by LPS. $^{\#}p \leq 0.05$ (vs. control), $^{*}p \leq 0.05$ (vs. LPS) **5b)** Effect of GCs on the secretion of anti-inflammatory cytokines in the RAW 264.7 macrophage cells induced by LPS. $^{*}p \leq 0.05$ (vs. LPS).

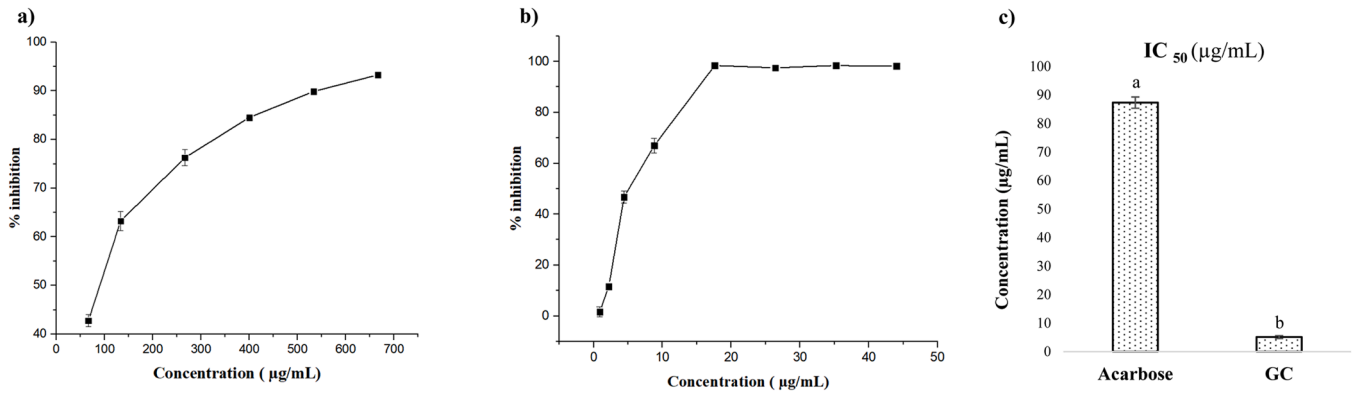

Fig. 6. a) α-glucosidase inhibition potential of acarbose, Fig. 6**b)** α-glucosidase inhibition potential of GCs, Fig. 6**c)** IC_{50} value of acarbose and GC consortium. Standard acarbose is compared with GC consortium and means with different superscript letters in the graph show significant difference at $p \leq 0.05$.

required to inhibit 50 % of α-glucosidase activity where as a remarkably lower amount i.e., 5.12 ± 0.51 µg/mL of GC consortium was only required to exhibit the same effect (Fig. 6c). Acarbose functions by reversibly inhibiting α-glucosidases, which leads to a decrease in the rapid increase of blood glucose levels after a meal, thereby reducing post-prandial hyperglycemia (Martin & Montgomery, 1996). A similar mechanism may be responsible for the α-glucosidase inhibition potential of GC.

It is surprising that there has been no previous literature discussing the α-glucosidase inhibition potential of GC. Even comprehensive reviews discussing the α-glucosidase inhibition potential of various bioactive compounds such as flavonoids, phenolic compounds, polysaccharides, betulinic acid, tannins, steroids, anthocyanins, galangin, procyanidins, hydroxyl-α-sanshool, hydroxyl-β-sanshool, erythritol, ganomycin, saponins, avicularin, oleanolic acids, urasolic acid, etc., also did not include GC in that category (Hossain et al., 2020; Yin et al., 2014). Our preliminary study findings indicate that GC may have the potential to be a potent α-glucosidase inhibitor, which necessitates further evaluation and confirmation.

4. Conclusion

Unripe banana comprises of more than one fourth of its weight as peel. Our study sheds light in the scope for valorisation of the unripe banana peel (*Musa* AAB) cv. Nendran. Present study demonstrates the isolation and characterization of GC molecular species. The study further proves anti-inflammatory potential of the isolated GCs in LPS-induced murine macrophage RAW 264.7 cells by suppressing the NO production and decreasing the secretion of pro-inflammatory cytokines. GC consortium has also shown remarkable α-glucosidase inhibition potential. The in vitro studies, being far away from the normal physiology of the human system, warrant further evaluation to confirm the affirmed results. The isolation of GCs from Nendran peel, showcasing anti-inflammatory and α-glucosidase inhibition potential, reinforces its traditional ethnopharmacological use. GC's versatility extends to cosmetic field also, where it serves as a moisturizing ingredient. The present study being the first report on GCs from banana peel, warrants development of cost-effective and 'green process' for the isolation of GC from the banana peel and its effective utilization. Harnessing the therapeutic qualities of GCs may contribute to the creation of effective and multifaceted products for health and cosmetic applications.

CRediT authorship contribution statement

Natakkakath Kaliyathan Raveena: Data curation, Investigation, Writing – original draft. **Sornarani Rajan:** Investigation, Data curation. **S Priya:** Writing – review & editing, Methodology. **Ravi S. Lankalapalli:** Project administration, Methodology, Investigation, Formal analysis, Data curation, Conceptualization, Supervision, Writing – review & editing. **M.V. Reshma:** Conceptualization, Writing – review & editing, Supervision, Project administration, Data curation, Formal analysis, Funding acquisition, Investigation, Methodology.

Declaration of competing interest

The authors declare that they have no known competing financial interests or personal relationships that could have appeared to influence the work reported in this paper.

Data availability

Data will be made available on request.

Acknowledgments

NKR acknowledges CSIR for providing the CSIR-SRF fellowship support for Ph.D. The financial support from the CSIR Mission project (HCP 35) is gratefully acknowledged.

Supplementary materials

Supplementary material associated with this article can be found, in the online version, at doi:10.1016/j.focha.2024.100700.

References

Alzate Acevedo, S., Díaz Carrillo, Á. J., Flórez-López, E., & Grande-Tovar, C. D (2021). Recovery of banana waste-loss from production and processing: A contribution to a circular economy. *Molecules (Basel, Switzerland), 26*(17), 5282. https://doi.org/10.3390/molecules26175282

Baek, S. H., Park, T., Kang, M. G., & Park, D. (2020). Anti-inflammatory activity and ROS regulation effect of sinapaldehyde in LPS-stimulated RAW 264.7 macrophages. *Molecules (Basel, Switzerland), 25*(18), 4089. https://doi.org/10.3390/molecules25184089

Bhavani, M., Morya, S., Saxena, D., & Awuchi, C. G. (2023). Bioactive, antioxidant, industrial, and nutraceutical applications of banana peel. *International Journal of Food Properties, 26*(1), 1277–1289. https://doi.org/10.1080/10942912.2023.2209701

Chiu, C. P., Liu, S. C., Tang, C. H., Chan, Y., El-Shazly, M., Lee, C. L., et al. (2016). Anti-inflammatory cerebrosides from cultivated *Cordyceps militaris*. *Journal of Agricultural and Food Chemistry, 64*(7), 1540–1548. https://doi.org/10.1021/acs.jafc.5b05931

de Melo, E. B., da Silveira Gomes, A., & Carvalho, I. (2006). α-and β-Glucosidase inhibitors: Chemical structure and biological activity. *Tetrahedron, 62*(44), 10277–10302. https://doi.org/10.1016/j.tet.2006.08.055

Demir, K. (2021). *Chapter ten gangliosides and autoimmunity kenan demir and selim görgün. human autoimmunity and associated diseases, 113*. Cambridge Scholars Publishing.

Engvall, E., & Perlmann, P. (1971). Enzyme-linked immunosorbent assay (ELISA) quantitative assay of immunoglobulin G. *Immunochemistry, 8*(9), 871–874. https://doi.org/10.1016/0019-2791(71)90454-x

Facchin, B. M., Dos Reis, G. O., Vieira, G. N., Mohr, E. T. B., da Rosa, J. S., Kretzer, I. F., et al. (2022). Inflammatory biomarkers on an LPS-induced RAW 264.7 cell model: A

systematic review and meta-analysis. *Inflammation Research, 71*(7), 741–758. https://doi.org/10.1007/s00011-022-01584-0

Geller, D. A., & Billiar, T. R. (1998). Molecular biology of nitric oxide synthases. *Cancer and Metastasis Reviews, 17*, 7–23. https://doi.org/10.1023/a:1005940202801

Gomes, S., Vieira, B., Barbosa, C., & Pinheiro, R. (2022). Evaluation of mature banana peel flour on physical, chemical, and texture properties of a gluten-free Rissol. *Journal of Food Processing and Preservation, 46*(8), e14441. https://doi.org/10.1111/jfpp.14441

Green, L. C., Wagner, D. A., Glogowski, J., Skipper, P. L., Wishnok, J. S., & Tannenbaum, S. R. (1982). Analysis of nitrate, nitrite, and [15N] nitrate in biological fluids. *Analytical Biochemistry, 126*(1), 131–138. https://doi.org/10.1016/0003-2697(82)90118-x

Hossain, U., Das, A. K., Ghosh, S., & Sil, P. C. (2020). An overview on the role of bioactive α-glucosidase inhibitors in ameliorating diabetic complications. *Food and Chemical Toxicology, 145*, Article 111738. https://doi.org/10.1016/j.fct.2020.111738

Huang, H., Hu, G., Wang, C., Xu, H., Chen, X., & Qian, A. (2014). Cepharanthine, an alkaloid from Stephania cepharantha Hayata, inhibits the inflammatory response in the RAW264. 7 cell and mouse models. *Inflammation, 37*, 235–246. https://doi.org/10.1007/s10753-013-9734-8

Ilan, Y., Elstein, D., & Zimran, A. (2009). Glucocerebroside: An evolutionary advantage for patients with Gaucher disease and a new immunomodulatory agent. *Immunology and Cell Biology, 87*(7), 514–524. https://doi.org/10.1038/icb.2009.42

Iyer, S. S., & Cheng, G. (2012). Role of interleukin 10 transcriptional regulation in inflammation and autoimmune disease. *Critical Reviews™ in Immunology, 32*(1). https://doi.org/10.1615/2Fcritrevimmunol.v32.i1.30

Kahraman, E., Kaykın, M., Şahin Bektay, H., & Güngör, S. (2019). Recent advances on topical application of ceramides to restore barrier function of skin. *Cosmetics, 6*(3), 52. https://doi.org/10.3390/cosmetics6030052

Kimata, H. (2006). Improvement of atopic dermatitis and reduction of skin allergic responses by oral intake of konjac ceramide. *Pediatric Dermatology, 23*(4), 386–389. https://doi.org/10.1111/j.1525-1470.2006.00268.x

Kwon, H. K., Jo, W. R., & Park, H. J. (2018). Immune-enhancing activity of *C. militaris* fermented with Pediococcus pentosaceus (GRC-ON89A) in CY-induced immunosuppressed model. *BMC Complementary and Alternative Medicine, 18*, 1–14. https://doi.org/10.1186/s12906-018-2133-9

Lakshmi, S., Renjitha, J., B Sasidhar, S., & Priya, S (2021). Epoxyazadiradione induced apoptosis/anoikis in triple-negative breast cancer cells, MDA-MB-231, by modulating diverse cellular effects. *Journal of Biochemical and Molecular Toxicology, 35*(6), 1–17. https://doi.org/10.1002/jbt.22756

Martin, A. E., & Montgomery, P. A. (1996). Acarbose: An α-glucosidase inhibitor. *American Journal of Health-System Pharmacy, 53*(19), 2277–2290. https://doi.org/10.1093/ajhp/53.19.2277

Martinez-Espinosa, I., Serrato, J. A., & Ortiz-Quintero, B. (2021). Role of IL-10-producing natural killer cells in the regulatory mechanisms of inflammation during systemic infection. *Biomolecules, 12*(1), 4. https://doi.org/10.3390/biom12010004

Mosmann, T. (1983). Rapid colorimetric assay for cellular growth and survival: Application to proliferation and cytotoxicity assays. *Journal of Immunological Methods, 65*(1–2), 55–63. https://doi.org/10.1016/0022-1759(83)90303-4

Nida, S., Moses, J. A., & Anandharamakrishnan, C. (2023). Converting fruit waste to 3D printed food package casings: The case of banana peel. *Circular Economy, 2*(1), Article 100023. https://doi.org/10.1016/j.cec.2022.100023

Nowak, D., & Jakubczyk, E. (2020). The freeze-drying of foods—the characteristic of the process course and the effect of Its parameters on the physical properties of food materials. *Foods, 9*(10), 1488. https://doi.org/10.3390/foods9101488

Oliveira, L., Freire, C., Silvestre, A., Cordeiro, N., Torres, I., & Evtuguin, D. (2006). Lipophilic extractives from different morphological parts of banana plant "Dwarf Cavendish. *Industrial Crops and Products, 23*(2), 201–211. https://doi.org/10.1016/j.indcrop.2005.06.003

Pereira, A., & Maraschin, M. (2015). Banana (*Musa* spp) from peel to pulp: Ethnopharmacology, source of bioactive compounds and its relevance for human health. *Journal of Ethnopharmacology, 160*, 149–163. https://doi.org/10.1016/j.jep.2014.11.008

Pistia-Brueggeman, G., & Hollingsworth, R. I. (2001). A preparation and screening strategy for glycosidase inhibitors. *Tetrahedron, 57*(42), 8773–8778. https://doi.org/10.1016/S0040-4020(01)00877-8

Raveena, N. K., Ingaladal, N., Reshma, M., & Lankalapalli, R. S. (2022). Phytochemical investigation of unripe banana (*Musa* AAB) cv. Nendran and its novel 'Banana Grits. *Food Chemistry Advances, 1*, Article 100063. https://doi.org/10.1016/j.focha.2022.100063

Saranya, J., Shilpa, G., Raghu, K. G., & Priya, S. (2017). *Morus alba* leaf lectin (MLL) sensitizes MCF-7 cells to anoikis by inhibiting fibronectin mediated integrin-FAK signaling through ras and activation of P38 MAPK. *Frontiers in Pharmacology, 8*, Article 220849. https://doi.org/10.3389/fphar.2017.00034

Segura-Badilla, O., Kammar-García, A., Mosso-Vázquez, J., Ávila-Sosa Sánchez, R., Ochoa-Velasco, C., Hernández-Carranza, P., et al. (2022). Potential use of banana peel (*Musa cavendish*) as ingredient for pasta and bakery products. *Heliyon, 8*(10), e11044. https://doi.org/10.1016/j.heliyon.2022.e11044

Smith, P.etal, Krohn, R. I., Hermanson, G., Mallia, A., Gartner, F., Provenzano, Md., et al. (1985). Measurement of protein using bicinchoninic acid. *Analytical Biochemistry, 150*(1), 76–85. https://doi.org/10.1016/0003-2697(85)90442-7

Spada, F., Barnes, T. M., & Greive, K. A. (2018). Skin hydration is significantly increased by a cream formulated to mimic the skin's own natural moisturizing systems. *Clinical, Cosmetic and Investigational Dermatology*, 491–497. https://doi.org/10.2147/ccid.s177697

Sreejith, P., & Sabu, M. (2017). *Edible bananas of south india: Taxonomy & phytochemistry*. India: Indian Association for Angiosperm Taxonomy (IAAT). . ISBN: 81-901637-4-4.

Yang, F., & Chen, G. (2022). The nutritional functions of dietary sphingomyelin and its applications in food. *Frontiers in Nutrition, 9*, Article 1002574. https://doi.org/10.3389/fnut.2022.1002574

Yin, Z., Zhang, W., Feng, F., Zhang, Y., & Kang, W. (2014). α-Glucosidase inhibitors isolated from medicinal plants. *Food Science and Human Wellness, 3*(3–4), 136–174. https://doi.org/10.1016/j.fshw.2014.11.003

Zaini, H. B. M., Sintang, M. D. B., & Pindi, W. (2020). The roles of banana peel powders to alter technological functionality, sensory and nutritional quality of chicken sausage. *Food Science & Nutrition, 8*(10), 5497–5507. https://doi.org/10.1002/2Ffsn3.1847

Zaini, H. M., Roslan, J., Saallah, S., Munsu, E., Sulaiman, N. S., & Pindi, W. (2022). Banana peels as a bioactive ingredient and its potential application in the food industry. *Journal of Functional Foods, 92*, Article 105054. https://doi.org/10.1016/j.jff.2022.105054

Zhang, J. M., & An, J. (2007). Cytokines, inflammation, and pain. *International Anesthesiology Clinics, 45*(2), 27–37. https://doi.org/10.1097/aia.0b013e318034194e

Zou, F., Tan, C., Zhang, B., Wu, W., & Shang, N. (2022). The valorization of banana by-products: Nutritional composition, bioactivities, applications, and future development. *Foods, 11*(20), 3170. https://doi.org/10.3390/foods11203170